LOOP QUANTUM COSMOLOGY

EDITED BY: Guillermo A. Mena Marugán, Francesca Vidotto and Beatriz Elizaga Navascués

PUBLISHED IN: Frontiers in Astronomy and Space Sciences

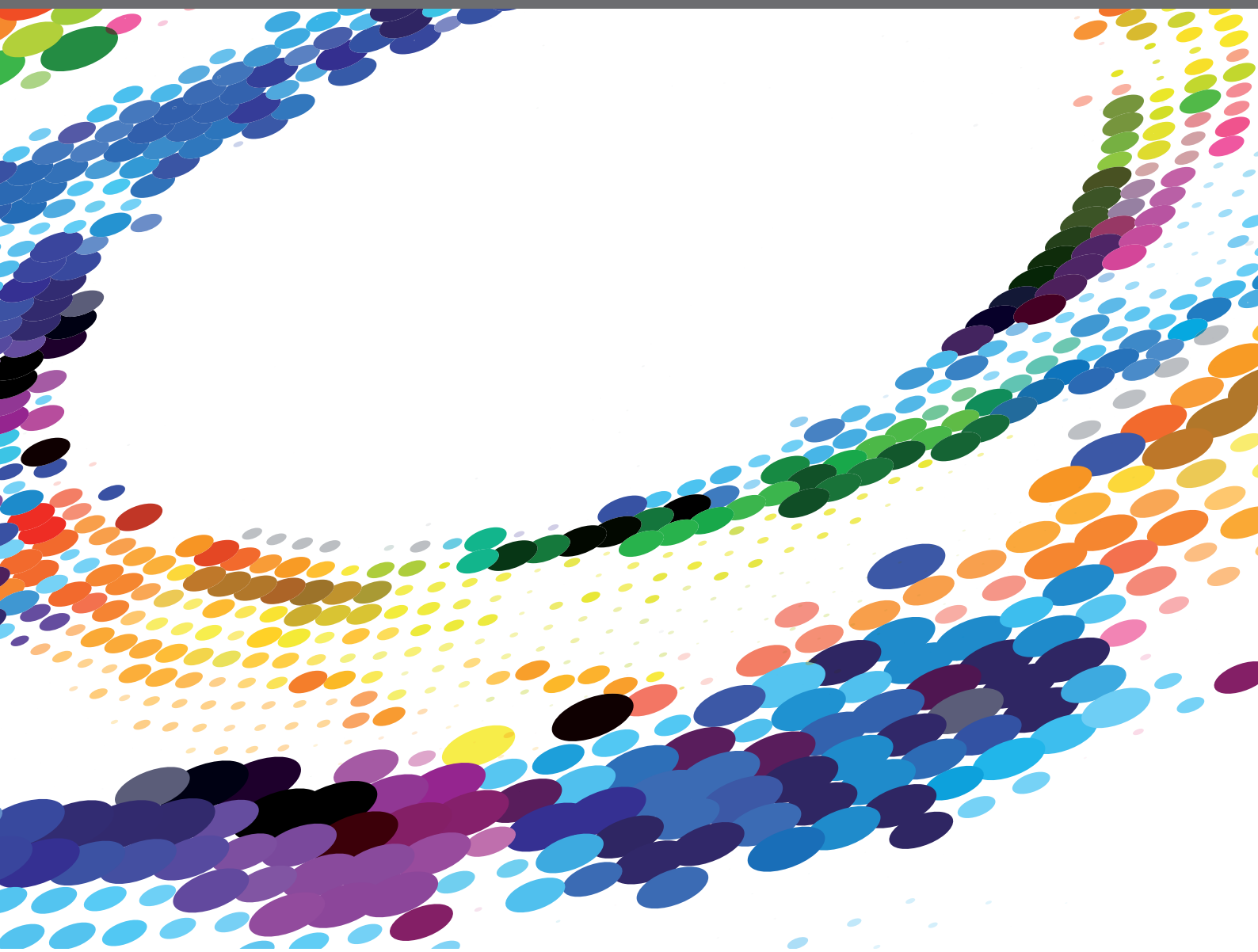

frontiers Research Topics

frontiers

ISSN 1664-8714
ISBN 978-2-88974-338-4
DOI 10.3389/978-2-88974-338-4

About Frontiers

Frontiers is more than just an open-access publisher of scholarly articles: it is a pioneering approach to the world of academia, radically improving the way scholarly research is managed. The grand vision of Frontiers is a world where all people have an equal opportunity to seek, share and generate knowledge. Frontiers provides immediate and permanent online open access to all its publications, but this alone is not enough to realize our grand goals.

Frontiers Journal Series

The Frontiers Journal Series is a multi-tier and interdisciplinary set of open-access, online journals, promising a paradigm shift from the current review, selection and dissemination processes in academic publishing. All Frontiers journals are driven by researchers for researchers; therefore, they constitute a service to the scholarly community. At the same time, the Frontiers Journal Series operates on a revolutionary invention, the tiered publishing system, initially addressing specific communities of scholars, and gradually climbing up to broader public understanding, thus serving the interests of the lay society, too.

Dedication to Quality

Each Frontiers article is a landmark of the highest quality, thanks to genuinely collaborative interactions between authors and review editors, who include some of the world's best academicians. Research must be certified by peers before entering a stream of knowledge that may eventually reach the public - and shape society; therefore, Frontiers only applies the most rigorous and unbiased reviews.
Frontiers revolutionizes research publishing by freely delivering the most outstanding research, evaluated with no bias from both the academic and social point of view. By applying the most advanced information technologies, Frontiers is catapulting scholarly publishing into a new generation.

What are Frontiers Research Topics?

Frontiers Research Topics are very popular trademarks of the Frontiers Journals Series: they are collections of at least ten articles, all centered on a particular subject. With their unique mix of varied contributions from Original Research to Review Articles, Frontiers Research Topics unify the most influential researchers, the latest key findings and historical advances in a hot research area! Find out more on how to host your own Frontiers Research Topic or contribute to one as an author by contacting the Frontiers Editorial Office: frontiersin.org/about/contact

LOOP QUANTUM COSMOLOGY

Topic Editors:
Guillermo A. Mena Marugán, Institute of Structure of Matter, Spanish National Research Council (CSIC), Spain
Francesca Vidotto, Western University, Canada
Beatriz Elizaga Navascués, Japan Society for the Promotion of Science (JSPS), Japan

Citation: Marugán, G. A. M., Vidotto, F., Navascués, B. E., eds. (2022). Loop Quantum Cosmology. Lausanne: Frontiers Media SA. doi: 10.3389/978-2-88974-338-4

Table of Contents

frontiers | Frontiers in Astronomy and Space Sciences

EDITORIAL
published: 26 April 2022
doi: 10.3389/fspas.2022.845459

Editorial: Loop Quantum Cosmology

Beatriz Elizaga Navascués[1]*, *Guillermo A. Mena Marugán*[2] and *Francesca Vidotto*[3,4]

[1]Department of Physics, Waseda University, Tokyo, Japan, [2]Instituto de Estructura de la Materia, IEM-CSIC, Madrid, Spain, [3]Department of Physics and Astronomy, Rotman Institute of Philosophy, University of Western Ontario, London, ON, Canada, [4]Department of Philosophy, Rotman Institute of Philosophy, University of Western Ontario, London, ON, Canada

Keywords: loop quantum cosmology, loop quantum gravity, quantum geometry of black holes, nonperturbative quantum gravity, cosmological perturbations

Editorial on the Research Topic

Loop Quantum Cosmology

Loop Quantum Cosmology is the application to cosmology of the nonperturbative canonical quantization program of General Relativity provided by Loop Quantum Gravity. This has been an active field of investigation for more than 20 years. Most of the work in this research direction is currently devoted to understanding how quantum gravity phenomena affected the primordial perturbations responsible for the anisotropies in the cosmic microwave background (CMB). Loop Quantum Cosmology techniques have also proven themselves useful beyond cosmology, in particular to explore effects of quantum geometry in black hole spacetimes. On the other hand, the advances in the so-called covariant formulation of Loop Quantum Gravity, handling the dynamics within a path integral formalism, have opened new ways to address questions in cosmology. This Research Topic presents different branches that have developed from Loop Quantum Cosmology. It gathers eleven publications that are an excellent sample of their progress, successes and challenges.

Ashtekar et al. have contributed with an article that is addressed both to cosmologists and to the loop quantum gravity community. They revisit the analysis of the CMB data by the Planck collaboration using the standard ΛCDM model with six cosmological parameters. In spite of the success of this model, there exist certain tensions pointing towards the statistical exceptionality of our Universe. These tensions appear in the form of power suppression at large angular scales and in an excessively high value of the lensing amplitude. A new analysis in the light of Loop Quantum Cosmology alleviates these tensions thanks to the connection between the physics of the ultraviolet and the infrared that occurs in the quantum gravitational Universe. This is what the authors call cosmic tango. Moreover, new predictions arise from this revised perspective, opening the possibility of a future confrontation of the proposed formalism with observations.

On related grounds, Agullo et al. have presented a study that shows how a modulation of the primordial power spectrum due to non-Gaussianities in Loop Quantum Cosmology can statistically alleviate some anomalous features that have been observed in the CMB. For this purpose, they provide an introduction to the statistical meaning of these anomalies in the CMB, and explain in what sense they point to the exceptionality of our Universe if it is explained with the ΛCDM model. Then, they describe how non-Gaussian correlations between perturbations with observable and super-Hubble wavelengths can lead to modulations of the angular power spectrum of the CMB. These correlations are studied within the dressed metric formalism of Loop Quantum Cosmology, taking an initial adiabatic state for the perturbations. The resulting non-Gaussian modulation is strongly scale-dependent for large wavelengths, and it is discussed that this property leads to a situation in which the aforementioned features of the CMB, regarded as anomalous within the ΛCDM model, are much more likely to appear in the Loop Quantum Cosmology scenario.

OPEN ACCESS

Edited by:
Lorenzo Iorio,
Ministry of Education, Universities and Research, Italy

Reviewed by:
Abhay Ashtekar,
Institute for Gravitation and the Cosmos, Penn State, United States

***Correspondence:**
Beatriz Elizaga Navascués
w.iac20060@kurenai.waseda.jp

Specialty section:
This article was submitted to Cosmology, a section of the journal Frontiers in Astronomy and Space Sciences

Received: *29 December 2021*
Accepted: *28 February 2022*
Published: *26 April 2022*

Citation:
Elizaga Navascués B, Mena Marugán GA and Vidotto F (2022) Editorial: Loop Quantum Cosmology. Front. Astron. Space Sci. 9:845459. doi: 10.3389/fspas.2022.845459

One of the aspects of Loop Quantum Cosmology that has deserved an increasing amount of attention in recent years is the discussion of possible quantization ambiguities in the Hamiltonian constraint and how they affect the robustness of the predictions for cosmological perturbations. This is the subject of the review presented by Li et al. They consider two alternative quantizations of the standard Hamiltonian of Loop Quantum Cosmology, and compare the predictions for the CMB of these three cases (including the standard quantization). Moreover, two different approaches are analyzed for the description of the quantum geometry effects on the perturbations, namely, the dressed metric and the hybrid approaches. The review also contains a detailed investigation of the viability of different proposals for the choice of a vacuum state of the perturbations. The scalar power spectrum of all the cases under study is calculated selecting some adiabatic vacua. This spectrum shows relevant differences in the infrared, while the ultraviolet sector of the perturbations is rather insensitive to the contemplated changes in the quantization.

Elizaga Navascués and Mena Marugán provide an extensive review of the state of the so-called "hybrid quantization" scheme in Loop Quantum Cosmology. It consists in splitting the homogeneous degrees of freedom and the inhomogeneous ones, that can be thought as additional fields over a background. One can then quantize the former nonperturbatively with the loop techniques, and the latter using the conventional Fock quantization. In this way, this scheme combines tractable constraints with a mathematically robust Fock quantization. It is then possible to study the evolution of cosmological perturbations during the preinflationary and inflationary epochs. In addition, the hybrid quantization has also been applied to Gowdy spacetimes that correspond to a toroidal geometry with linearly polarized gravitational waves. Two aspects of this scheme have particular interest with respect to possible observational predictions: first, the mass of the fields that describe the cosmological perturbations results to have a specific time evolution, that distinguishes the predictions from this framework from other approaches; second, the splitting between homogeneous and inhomogeneous sectors provides a natural way to define a preferred vacuum state.

Schander and Thiemann consider the issue of backreaction in gravity, reviewing the problem of the backreaction between matter and geometric inhomogeneities in cosmology. They first provide a concise summary of concepts and procedures designed to analyze this backreaction by classical means in the late Universe. Then, they comment on semiclassical approaches to cope with the quantum backreaction of the perturbations in earlier epochs, including stochastic gravity in this discussion. Finally, they focus on the more complicated problem of studying backreaction in purely quantum formalisms, applicable to the very early stages of the Universe. Special attention is devoted to Born-Oppenheimer inspired methods in which the perturbations are regarded as fast dynamical degrees of freedom compared with a slowly evolving homogeneous cosmological spacetime. In particular, they review in some detail a formalism introduced by them, which is based on the application and extension to quantum cosmology of space adiabatic perturbation theory.

The extraction of predictions from Loop Quantum Cosmology about the early Universe crucially depends on the choice of vacuum state for the primordial perturbations. Martín-Benito et al. have studied this question when one focuses the attention on the so-called States of Low Energy, which are of Hadamard type and minimize suitably smeared versions of the energy density. Explicitly, they have shown that the shape of the primordial power spectrum resulting from such states depends strongly on the support of the smearing function in the kinetically dominated pre-inflationary regime of Loop Quantum Cosmology. In particular, if this function is only supported on the far future of the bounce, the power spectrum resembles the non-oscillatory one that was previously proposed by Martín de Blas and Olmedo. Furthermore, using the ultraviolet properties of the States of Low Energy, the authors provide a proof that this non-oscillatory vacuum state is of Hadamard type as well.

Gozzini and Vidotto explore the fundamental question of how primordial fluctuations may arise from the spinfoam dynamics of Loop Quantum Gravity. For this purpose, they consider the spinfoam transition amplitude from an empty state to the discretization of certain cosmological, closed, 3-geometries in terms of tetrahedra. This transition amplitude determines a cosmological state, given by a superposition of such closed geometries, which is argued to be the analog to the Hartle-Hawking no-boundary state in the spinfoam formalism. The authors study several properties of this state and show that, even though the average geometry of the state is that of a 3-sphere, it has a large variance and the local correlations between different regions are non-negligible even at large values of the scale factor. Furthermore, the state is highly atypical, as measured with respect to the entanglement entropy of its components. These properties hint towards a quantum gravity mechanism that might solve the horizon problem in cosmology, without the need of inflation.

Marchetti and Oriti similarly consider a quantum cosmological model based on a covariant formulation of the action, but solving its dynamics with the techniques of Group Field Theory. They address, in particular, the question of defining in this context observables in a relational manner. It is interesting then to quantify the quantum fluctuations of the resulting geometrical observables. In order to introduce an observable that plays the function of a physical clock, they include a massless scalar field and study its expectation value. They find that at later time the quantum fluctuations of all observables are suppressed, in agreement with the classical limit, but the fluctuations are important at earlier times, i.e., near the bounce. The appearance of these fluctuations may lead to different interpretations with respect to the validity of a hydrodynamical approximation for the quantum gravitational dynamics; further clarity could be shed on their nature by moving out from the approximation in which Group Field Theory interactions are neglected.

Different ideas and techniques from Loop Quantum Cosmology can be exported to study black hole physics. In this context, García-Quismondo and Mena Marugán investigate the Hamiltonian formulation of the loop quantum model for black holes proposed by Ashtekar, Olmedo and Singh (AOS). The dynamics of its classical version is quite special: it is generated

by the sum of two commuting Hamiltonians, which are related to the mass of the black hole when evaluated on-shell. Loop quantum corrections are introduced in terms of regularization parameters, which the AOS model treats as constant, with values fixed by the black hole mass on each particular solution. This procedure has raised concerns about the validity of the Hamiltonian formulation of the model. García-Quismondo and Mena Marugán explore instead the possibility that these parameters may be functions of the two Hamiltonians, which should be equal to the mass only on-shell. They then show that each Hamiltonian generates dynamical equations that are equivalent to those in the AOS model, but with respect to a time that is different for each of the two Hamiltonians. In the on-shell limit of large black hole masses, both times coincide up to (known) subdominant corrections.

Gambini et al. use a similar regularization to that of the AOS model to study how the central black hole singularity is removed in spherically symmetric Loop Quantum Gravity. The resulting extension of the spacetime through the quantum region that replaces the singularity can be interpreted as a white hole. In their article, the authors investigate whether one can introduce an effective description of this quantum phenomenon by defining semi-classical states: these correspond to an approximate classical geometry with an effective anisotropic fluid coupled to the gravitational field. The resulting framework has the specific advantage of recovering diffeomorphism invariance in the semiclassical limit. This result suggests to use the requirement of small mass fluctuations in the classical limit to select the kind of modifications that the scalar constraint and the observables should inherit at the effective level from the quantization. Interestingly, what is learnt here in the context of black holes can find applications in cosmological models with a local rotational symmetry, such as the toroidal Gowdy spacetime.

It is exciting to see how ideas developed for black holes can be applied to cosmology. Another example of this is given in the paper by Amadei et al. The authors start from an interesting proposal addressing the fate of information in black hole evaporation: information can degrade by being transferred to Planckian degrees of freedom, unaccessible in the approximation for which the gravitational field is described by a smooth manifold. Analogously, cosmological states can be thought as coarse-grained ones where Planckian degrees of freedom that are not accessible to low-energy observers are suitably ignored. In this scenario, the dynamics of a bouncing universe can have a completely unitary description even if these observers experience decoherence. Furthermore, energy conservation implies that the Planckian degrees of freedom do not contribute to the energy balance, even though they are responsible for such decoherence: the energy balance allows for this to happen without the need of a contingent dissipation.

The collection of these eleven papers composes a mosaic of some active research directions in Loop Quantum Cosmology, a part of the lines of research of this exciting field which is still subject to open questions and debate. Cosmology and black hole physics are the most promising windows to observe signatures of (Loop) Quantum Gravity. Hopefully, the ideas in these papers will contribute in sharpening our sight in their search.

AUTHOR CONTRIBUTIONS

BEN, GAMM, and FV are the editors of this Research Topic.

FUNDING

This work was partially supported by Project No. MICINN PID2020-118159GB-C41 from Spain. BE acknowledges financial support from the Standard Program of JSPS Postdoctoral Fellowships for Research in Japan. FV acknowledges financial support from by the Canada Research Chairs Program, the NSERC Discovery Grant "Loop Quantum Gravity: from Computation to Phenomenology", and the QISS JFT grant 61466.

Conflict of Interest: The authors declare that the research was conducted in the absence of any commercial or financial relationships that could be construed as a potential conflict of interest.

frontiers in Astronomy and Space Sciences

BRIEF RESEARCH REPORT
published: 18 February 2021
doi: 10.3389/fspas.2020.629466

Primordial Fluctuations From Quantum Gravity

Francesco Gozzini[1] *and Francesca Vidotto*[2]*

[1]Aix Marseille Univ, Université de Toulon, CNRS, CPT, Marseille, France, [2]University of Western Ontario, London, ON, Canada

We study the fluctuations and the correlations between spatial regions generated in the primordial quantum gravitational era of the universe. We point out that these can be computed using the Lorentzian dynamics defined by the Loop Quantum Gravity amplitudes. We evaluate these amplitudes numerically in the deep quantum regime. Surprisingly, we find large fluctuations and strong correlations, although not maximal. This suggests the possibility that early quantum gravity effects might be sufficient to account for structure formation and solve the cosmological horizon problem.

Keywords: quantum gravity, cosmology, structure formation, spinfoam, spinfoam cosmology, horizon problem, loop quantum gravity

OPEN ACCESS

Edited by:
Antonino Marciano,
Fudan University, China

Reviewed by:
Sayantan Choudhury,
National Institute of Science Education and Research, India
Vyacheslav Ivanovich Dokuchaev,
Institute for Nuclear Research, Russia

***Correspondence:**
Francesca Vidotto
fvidotto@uwo.ca

Specialty section:
This article was submitted to Cosmology, a section of the journal Frontiers in Astronomy and Space Sciences

Received: *14 November 2020*
Accepted: *28 December 2020*
Published: *18 February 2021*

Citation:
Gozzini F and Vidotto F (2021) Primordial Fluctuations From Quantum Gravity. Front. Astron. Space Sci. 7:629466. doi: 10.3389/fspas.2020.629466

1 INTRODUCTION

Standard cosmology–with or without inflation–requires an initial state that exhibits fluctuations and correlations between distinct regions of space. These play a key role, in particular as seeds for structure formation. Here we investigate how these fluctuations and correlations can emerge from a primordial quantum gravitational cosmological phase, using Loop Quantum Gravity (LQG) and a simple model of the early universe.

We consider the quantum transition from an empty state to a 3-geometry. The amplitude of this transition may be relevant in a Big Bang cosmology (Hartle and Hawking, 1983; Halliwell, 1987; Halliwell et al., 2019), as well as in a bouncing cosmology, where it dominates the transition through the bounce (Bianchi et al., 2010; Vidotto, 2011; Bahr et al., 2017). We treat the dynamics of gravity non-perturbatively, using covariant LQG. This calculation does not require a Wick rotation and it is well defined in the Lorentzian theory. The transition generates a quantum state that defines the probability distribution over 3-geometries. This includes correlations between spatially separated regions.

We truncate the degrees of freedom of the gravitational field to a small finite number in addition to the scale factor [cfr (Rovelli and Vidotto, 2008; Borja et al., 2012; Vidotto, 2017)]. Using numerical methods, we obtain four results: 1) The expectation value of the geometric variables at a given value of the scale factor yields precisely (the truncation of) a metric 3-sphere. 2) Contrary to our initial expectation, the variance of these variables is very large: the amplitude of the fluctuations is significant. 3) Correlations between variables in distinct regions–and entanglement entropy between regions–do not vanish with the increase of the scale factor. 4) Entanglement entropy appears to converge to a stable value asymptotically.

All this indicates that the universe emerging from an early quantum era includes fluctuations, homogeneity properties, and large scale correlations, due to the common quantum origin of spatially separated regions. These can be studied theoretically and appear to be compatible with the observed universe. In particular, inflation or a bounce might not be strictly necessary to circumvent the horizon problem. If the initial quantum phase is taken into account, our result suggests that distant regions may have not been causally disconnected in the past, as in classical cosmology.

2 QUANTUM THEORY

We discretize a closed cosmological 3-geometry into five tetrahedra glued to one another, giving an S_3 topology. This is a regular triangulation of a topological 3-sphere, and it corresponds to the boundary of a 4-simplex. The geometry of a flat 4-simplex has twenty degrees of freedom, which capture the gravitational field in this truncation. The result of the transition from nothing to a 3-geometry is described by its covariant LQG Lorentzian amplitude (Vidotto, 2011). The truncation we consider corresponds to the single vertex amplitude, to the first order in the spinfoam expansion (Rovelli and Smerlak, 2012). We take the areas of the faces of the tetrahedra to be equal and use this common value as a proxy for the physical scale factor. The remaining degrees of freedom characterize the shapes of the five tetrahedra. We are interested in the fluctuations of these variables and the correlations between variables in distinct tetrahedra, at different values of the scale factor.

The LQG Hilbert space for this truncation is $\mathcal{H} = L^2[SU(2)^{10}/SU(2)^5]_{\Gamma_5}$, where Γ_5 is the complete graph with five nodes. See (Rovelli and Vidotto, 2015) for the notation and an introduction to the formalism. We label the (oriented) links as $l = 1, \dots, 10$, or alternatively in terms of the two nodes they link: $l = nn'$. The spin network basis in $\mathcal{H}$ is given by the states $|j_l, i_n\rangle$ where the j_l's are spins (half-integer values labeling $SU(2)$ irreps) and the i_n's are a basis in the corresponding intertwiner space $\mathcal{I}_n = (\otimes_{n' \neq n} V_{j_{nn'}})/SU(2)$, where V_j is the spin-j representation space of $SU(2)$. We focus on the subspaces $\mathcal{H}_j$ of $\mathcal{H}$ defined by $j_l = j$. These have the tensorial structure $\mathcal{H}_j = \otimes_n \mathcal{I}_n$, where each $\mathcal{I}_n$ is isomorphic to $(V_j \otimes V_j \otimes V_j \otimes V_j)/SU(2)$. The basis states are tensor states, which we denote as $|j, i_n\rangle = \otimes_n |i_n\rangle$ (by this we mean $|j, i_1, \dots, i_5\rangle = |i_1\rangle \otimes \cdots \otimes |i_5\rangle$). We choose a basis in $\mathcal{I}_n$ fixing a pairing of the links at each node and the basis that diagonalizes the modulus square of the sum of the $SU(2)$ generators in the pair.

The transition amplitude from an empty state to a state $|j, i_n\rangle$ in $\mathcal{H}_j$ is given by the spinfoam amplitude of the boundary state $|j, i_n\rangle$ alone. This is because this transition corresponds to the amplitude of a boundary state that has only one connected component, here interpreted as the future one. To first order in the spinfoam expansion, the amplitude of a boundary state is given by a single vertex. Hence the nothing-to-$|j, i_n\rangle$ amplitude is the vertex amplitude for the boundary state

$$\langle j, i_n | \varnothing \rangle = W(j, i_n) \equiv \langle j, i_n | \psi_o \rangle \tag{1}$$

where $W(j, i_n)$ is the Lorentzian EPRL vertex amplitude (Engle et al., 2008). This implies that we can view the ket $|\psi_o\rangle$ with components $W(j, i_n)$, as the quantum state emerging from the Big Bang. This is the analogue, in (Lorentzian) LQG, of the Hartle-Hawking "no-boundary" initial state in (Euclidean) path-integral quantum gravity (Hartle and Hawking, 1983). This is the state we are interested in. We study the mean geometry it defines and the quantum fluctuations and correlations it incorporates. Specifically, we study the expectation value $\langle A \rangle = \langle \psi_o | A | \psi_o \rangle$, the spread $\Delta A = \sqrt{\langle \psi_o | A^2 | \psi_o \rangle - \langle A \rangle^2}$ and the (normalized) correlations

$$C(A_1, A_2) = \frac{\langle \psi_o | A_1 A_2 | \psi_o \rangle - \langle A_1 \rangle \langle A_2 \rangle}{(\Delta A_1)\,(\Delta A_2)} \tag{2}$$

of local geometry operators $A, A_1, A_2, \dots$ defined on $\mathcal{H}$. We compute also the entanglement entropy $S = -tr(\rho_n \log \rho_n)$ of a node with respect to the rest of the graph, where ρ_n is the reduced density matrix of the state $|\psi_o\rangle$ at any node, all nodes being equivalent by symmetry.

3 QUANTUM GEOMETRY

The spin-network basis states can be viewed as a collection of quantum tetrahedra (Bianchi et al., 2011) glued together by identifying faces. Shared faces have the same area but not necessarily matching shapes, giving rise to a twisted geometry (Freidel and Speziale, 2010). The areas of the faces are eigenvalues of the area operator

$$A_{nl} | i_n \rangle = \sqrt{\vec{E}_{nl} \cdot \vec{E}_{nl}}\, | i_n \rangle = (8\pi\gamma\hbar G) \sqrt{j_l (j_l + 1)}\, | i_n \rangle, \tag{3}$$

written in terms of the flux operators

$$\vec{E}_{nl} = (8\pi\gamma\hbar G) \vec{J}_l \tag{4}$$

entering the node n on link l, where γ is the Barbero-Immirzi constant and $\vec{J}_l$ is the vector of $SU(2)$ generators on link l. The shape of the tetrahedron is measured by the angle operator

$$A_{ab} | i_n \rangle = \cos(\theta_{ab}) | i_n \rangle \tag{5}$$

that gives the cosine of the external dihedral angle between faces a and b, where

$$2 |\vec{J}_a| |\vec{J}_b| A_{ab} = 2 \vec{J}_a \cdot \vec{J}_b = \left(\vec{J}_a + \vec{J}_b \right)^2 - \vec{J}_a^2 - \vec{J}_b^2.$$

Say we use the recoupling basis that pairs links j_a and j_b at node n, and let $|k_n\rangle$ be the intertwiner state at node n. The operator $(\vec{J}_a + \vec{J}_b)^2$ is diagonal on $|k_n\rangle$ with eigenvalue

$$\left(\vec{J}_a + \vec{J}_b \right)^2 | k_n \rangle = k_n (k_n + 1) | k_n \rangle \tag{6}$$

where k_n is the intertwiner spin. Putting together **Eqs 3**, **5**, and **6** we obtain

$$\cos(\theta_{ab}) = \frac{k_n (k_n + 1) - j_a (j_a + 1) - j_b (j_b + 1)}{2 \sqrt{j_a (j_a + 1) j_b (j_b + 1)}} \tag{7}$$

for measuring the dihedral angle $\cos(\theta_{ab})$ of $|k_n\rangle$ in terms of intertwiner spin k_n.

4 NUMERICAL METHODS

The Lorentzian EPRL vertex amplitude $W(j_l, i_n)$ can be written as Speziale (2017)

$$W(j_l, i_n) = \sum_{l_f, k_e} \left(\prod_e (2k_e + 1) B\left(j_l, l_f; i_n, k_e\right) \right) \{15j\}\left(l_f, k_e\right) \quad (8)$$

where f and e label the faces and the half-edges touching the vertex. The symbol $\{15j\}$ is the invariant $SU(2)$ symbol built from contracting the five 4-valent intertwiners at the nodes, and can be expressed as the contraction of five $SU(2)$ $6j$ symbols as

$$\{15j\}\left(l_f, k_e\right) = \sum_x (2x+1)\,(-1)^{\sum_a l_a + \sum_a k_a} \times \begin{Bmatrix} k_1 & l_{25} & x \\ k_5 & l_{14} & l_{15} \end{Bmatrix} \begin{Bmatrix} l_{14} & k_5 & x \\ l_{35} & k_4 & l_{45} \end{Bmatrix} \begin{Bmatrix} k_4 & l_{35} & x \\ k_3 & l_{24} & l_{34} \end{Bmatrix} \times \begin{Bmatrix} l_{24} & k_3 & x \\ l_{13} & k_2 & l_{23} \end{Bmatrix} \begin{Bmatrix} k_2 & l_{13} & x \\ k_1 & l_{25} & l_{12} \end{Bmatrix}. \quad (9)$$

The functions $B(j_l, l_f; i_n, k_e)$ are defined as

$$B\left(j_l, l_f; i_n, k_e\right) = \sum_{p_i} \begin{pmatrix} j_l \\ p_i \end{pmatrix}^{(i_n)} \begin{pmatrix} l_f \\ p_i \end{pmatrix}^{(k_e)} \times \int_0^\infty dr\, \frac{\sinh^2 r}{4\pi} \prod_{i=1}^{4} d^{(\gamma j_i, j_i)}_{j_i l_i p_i}(r). \quad (10)$$

where the factors in front of the integral are $SU(2)$ $4jm$ symbols and the functions $d^{(\gamma j_i, j_i)}_{j_i l_i p_i}(r)$ are boost matrix elements of the Lorentz group. The product in **Eq. 8** is over four of the five half-edges because one redundant factor must be eliminated by gauge-fixing. The sum is over a set of auxiliary spins l_f and auxiliary intertwiners k_e. See Speziale (2017) for more details about this formulation of the EPRL amplitude and the full definition and analysis of all the quantities involved in the previous formulae.

Analytical results show that in the large spin limit this amplitude is generally exponentially suppressed except in two cases (Barrett et al., 2009; Donà et al., 2019). The first case is when the boundary geometry is the geometry of the boundary of a Lorentzian 4-simplex. This case can be naturally related to the semiclassical limit, where spacetime is flat and Lorentzian at scales smaller than the curvature radius. The second case is when the boundary geometry is a vector geometry, which includes the case when the boundary geometry is the geometry of the boundary of a Euclidean 4-simplex. As we shall see below, the mean geometry defined by $|\psi_o\rangle$ is that of a discretized metric 3-sphere i.e., the boundary of a regular Euclidean 4-simplex. Therefore this is a vector geometry. Vector geometries have been considered as a puzzling feature of the theory (Donà et al., 2018): here we can interpret them as a necessary contribution to the primordial quantum cosmological state in order to allow the tunneling from the empty state to the semiclassical 3-sphere geometry.

The form of the amplitude **Eq. 8** is suited for numerical evaluation. The computational steps, in order of increasing complexity and cost, are: 1) evaluation of the $\{15j\}$ symbol; 2) evaluation of the B functions and 3) contraction over all internal and boundary spin labels. We limited our computation to spins (i.e., scale factor) $j \leq 16$ given the time and memory constraints imposed by our computing facility. We used a standard laptop computer for lower spins and a 32-cores server with 196 GBs of RAM for higher spins.

The sum over spins l_f in **Eq. 8** is unconstrained, as $l_f \geq j_l$, where link l corresponds to face f. Hence it is necessary to introduce a cutoff Δs so that $l_f = j_l, j_l + 1, \ldots, j_l + \Delta s$ and the exact value is in the limit $\Delta s \to \infty$. The case with $\Delta s = 0$ has been called the simplified model (Speziale, 2017). Since the computation time is proportional to $(\Delta s + 1)^6$, we are limited to very low values of the cutoff. It can be shown that in the simplified model the Lorentzian part of the amplitude is partially suppressed (Puchta, 2013; Speziale, 2017), and the effect of increasing the cutoff Δs is to gradually enhance the amplitude for Lorentzian configurations. It may seem necessary to reach higher cutoffs in order to match the expected behavior in semiclassical asymptotics of Lorentzian simplices (Donà et al., 2019). However, we found that in our calculation, which spans the space of vector geometries due to the chosen (Euclidean) boundary conditions, the corrections due to higher cutoff values are minor or even negligible, so that the simplified computations effectively suffice to study the model numerically.

All the computations of the present work were carried out using the *sl2cfoam* library (Donà and Sarno, 2018), which is a C library for computing the spinfoam amplitude **Eq. 8** using various optimization strategies. For a complete treatize of all the technical and numerical details that are relevant to this work we refer also to (Gozzetti, 2021[1]), which studies extensions of the model considered here using a recently released version of the library (Gozzetti, 2021[2]).

5 NUMERICAL RESULTS

The results below are given for increasing values of the scale parameter j. In this section we fix the cutoff parameter to $\Delta s = 0$ and the Barbero-Immirzi constant to $\gamma = 1.2$.

(1) The expectation value of the angle operator $A_{ab}|i_n\rangle = \cos(\theta_{ab})|i_n\rangle$ that measures the external dihedral angles between faces punctured by links a and b in any of the boundary tetrahedra (by symmetry all of them are equivalent) results to be

$$\langle A_{ab} \rangle = -0.333 \quad (11)$$

which is precisely the cosine of the external dihedral angle of an equilateral tetrahedron, for any links a, b chosen. This shows that the spatial metric of $|\psi_o\rangle$ averages to that of the 3-boundary of a regular 4-simplex i.e., to that of a 3-sphere in our approximation. The variation of the average with the scale parameter is minor and due entirely to numerical fluctuations (**Figure 1**). The independence of the result from the choice of the links was tested by switching to a different recoupling basis, and also by directly performing the change of basis.

(2) The spread ΔA_{ab} is large and increasing with the scale factor, see **Figure 2**. This suggest that quantum fluctuations in the

[1]Gozzini (2021). High performance lorentzian spin foam numerics. In preparation.
[2]Gozzini (2021). Numerical simulation of the quantum cosmological vacuum with many spin foam vertices. In preparation.

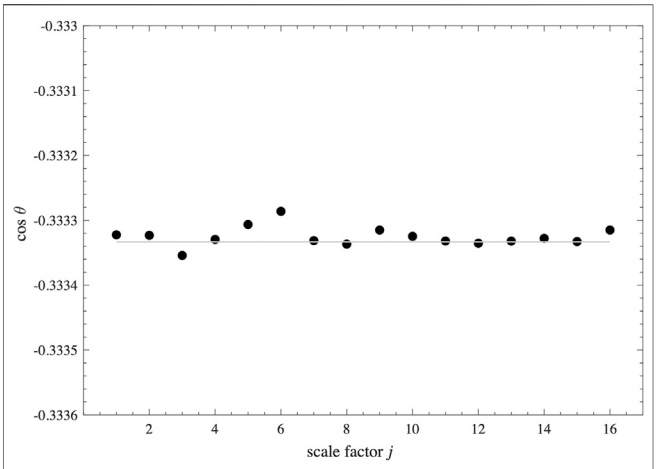

FIGURE 1 | The computed average external dihedral angle of boundary tetrahedra as function of the scale factor. The gray line shows the dihedral angle of a regular tetrahedron.

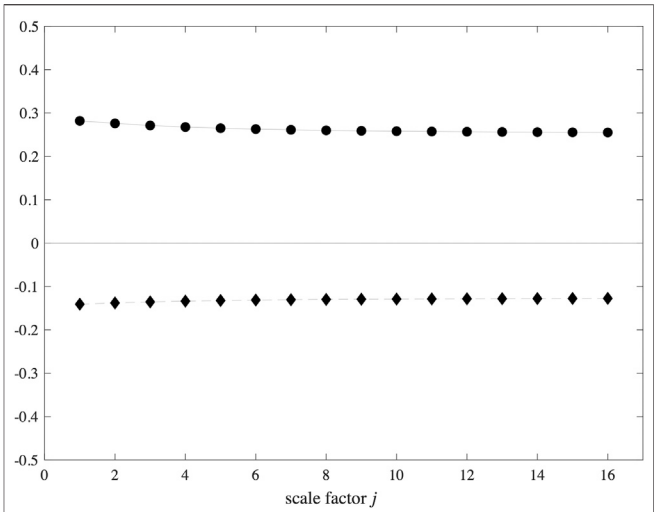

FIGURE 3 | Left: correlations of angle operator $A_{42,43}$ with $A_{23,24}$ (top, positive) and $A_{34,35}$ (bottom, negative). The same plot represents the correlations of $A_{41,45}$ with $A_{14,15}$ (top, positive) and $A_{54,53}$ (bottom, negative).

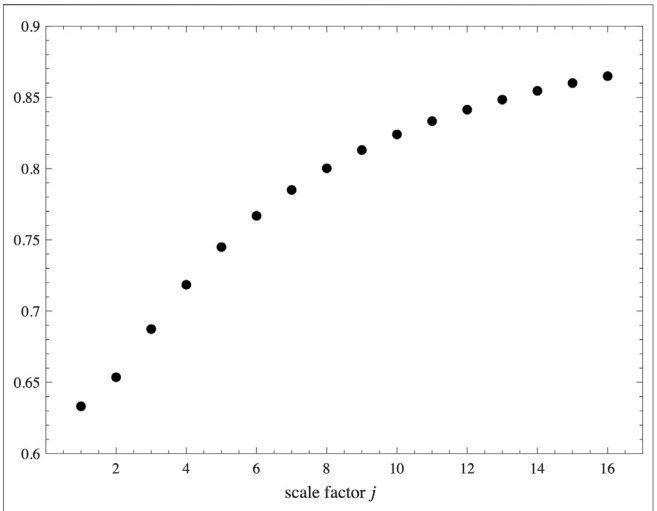

FIGURE 2 | Quantum spread of the cosine of the external dihedral angle of boundary tetrahedra as function of the scale factor.

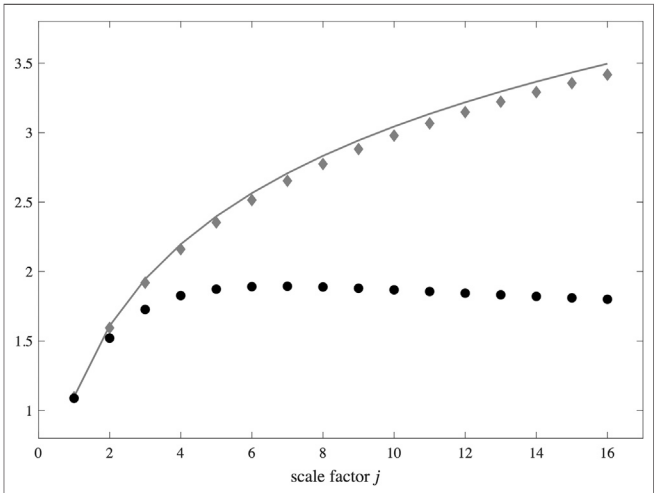

FIGURE 4 | The entanglement entropy of a boundary node with respect to the rest of the graph. Gray continuous line shows the maximum entropy attainable as function of the scale factor parameter. Gray diamonds show the result of Bianchi et al. (2018). Black circles show our result for $|\psi_o\rangle$.

metric are wide and are not suppressed in the large-scale regime.

(3) The correlations between angle operators on different nodes depend on the pairing. We write $A_{nn',nn''}$ for the angle operator A_{ab} at node n, where link a connects n with n' and link b connects n with n''. The correlations are shown in **Figure 3**. For each source node n there are two pairs of correlated—anti-correlated nodes (for $n = 4$ these are $(2, 3)$ and $(1, 5)$). The correlations appear to reach an asymptotic value, hence are not suppressed in the large-scale regime. The 3-metric that comes out from the quantum state $|\psi_o\rangle$ can correlate different spatial patches of the primordial universe, as required for solving the horizon problem of standard cosmology. It would be interesting to verify that in finer triangulations the correlations decay with the distance between non-adjacent faces, as required by local effective field theory.

(4) To quantify the degree of correlation between operators we computed the entanglement entropy between different tetrahedra, viewed as quantum subsystems. A result by Page (Page, 1993) states that, given a splitting $\mathcal{H} = \mathcal{H}_R \otimes \mathcal{H}_{\overline{R}}$ of a Hilbert space $\mathcal{H}$ into subspaces corresponding to a small subsystem R and its complement $\overline{R}$, the typical state in $\mathcal{H}_R$ is found to have an entanglement entropy equal to $S_R \approx \log(\dim \mathcal{H}_R)$ corresponding to a maximally-mixed state. In other words, the vast majority of quantum states of a small

subsystem are close to being, in a broad sense, thermal see Popescu et al. (2006).

We studied the degree of non-typicality of the primordial state $|\psi_o\rangle$ by looking at the entanglement entropy of any tetrahedron as function of the scale factor. The result is shown in **Figure 4**. It indicates that the entropy deviates significantly from the maximally-mixed case, and it appears to get close to an asymptotic value in the limit of large scale factor. We could not push the computations to spins higher than $j = 16$, but the qualitative behavior is clear. For comparison, we show also the maximum entropy $S_{\max}(j) = \log(2j + 1)$ and the result of (Bianchi et al., 2018) on the so-called Bell-network states (Baytaş et al., 2018), which are constructed in the same way as our primordial state $|\psi_o\rangle$ but using the dynamics of the simpler BF theory. See also (Bianchi et al., 2015; Bahr, 2020).

6 CONCLUSION

Summarizing, the quantum state for the primordial universe predicted by the dynamics of Loop Quantum Gravity can be computed in a kinematical truncation and at first order in the vertex expansion. It describes the fluctuating metric of a topologically closed universe in its early quantum regime. Its degrees of freedom encode the shapes of neighboring spatial regions. Their size (area), taken to be equal, is related to the scale factor. We have found that the mean geometry of this state is that of a (truncated) 3-sphere, as we expected by symmetry, but the fluctuations are large. Neighboring regions are correlated and correlations do not vanish as the scale factor increases. This opens the possibility that an inflationary phase may not be needed in order to circumvent the horizon problem, as the primordial quantum phase may introduce stochastic correlations in otherwise causally-independent spatial regions. We also computed the entanglement entropy of a single region viewed as a quantum subsystem of the whole universe. We found that the cosmological state is highly non-typical, showing an entanglement entropy that is apparently reaching an asymptotic value as the scale factor increases. Our work is one of the first explorations of the purely quantum regime of LQG—without resorting to the high-spin semiclassical limit of the theory—and one of the first applications to a concrete physical model of the numerical tools that are recently being developed for covariant Loop Quantum Gravity (Bianchi et al., 2018; Donà and Sarno, 2018; Donà et al., 2019; Dona et al., 2020). Our results indicate that an early quantum phase of the universe may provide an explanation for known puzzling features of the standard cosmological model, such as the horizon problem, possibly even without introducing additional inflationary and/or bouncing phases.

We thank for discussions Pietro Doná, Carlo Rovelli, Giorgio Sarno and Simone Speziale. We thank the Department of Theoretical Physics at UPV/EHU where part of this research was carried, supported by the grant IT956-16 of the Basque Government and by the grant FIS2017-85076-P (MINECO/AEI/FEDER, UE). We acknowledge the Anishinaabek, Haudenosaunee, Lūnaapéewak, and Attawandaron peoples, on whose traditional lands Western University is located.

DATA AVAILABILITY STATEMENT

The raw data supporting the conclusion of this article will be made available upon request by the authors, without undue reservation.

AUTHOR CONTRIBUTIONS

FG contributed to this work writing an original code, performing all the numerical computations, and contributing to the analytical aspects of the computation. FV contributed with the original idea of this paper, devising the computations, supervising their completions, and analysing the results.

REFERENCES

Bahr, B. (2020). Entanglement entropy of physical states in hypercuboidally truncated spin foam quantum gravity. *Class. Quantum Grav.* 37, 094001. doi:10.1088/1361-6382/ab77ea

Bahr, B., Klöser, S., and Rabuffo, G. (2017). Towards a cosmological subsector of spin foam quantum gravity. *Phys. Rev. D.* 96, 086009. doi:10.1103/PhysRevD.96.086009

Barrett, J. W., Dowdall, R. J., Fairbairn, W. J., Gomes, H., and Hellmann, F. (2009). Asymptotic analysis of the engle-pereira-rovelli-livine four-simplex amplitude. *J. Math. Phys.* 50, 112504. doi:10.1063/1.3244218

Baytaş, B., Bianchi, E., and Yokomizo, N. (2018). Gluing polyhedra with entanglement in loop quantum gravity. *Phys. Rev. D.* 98, 026001. doi:10.1103/PhysRevD.98.026001

Bianchi, E., Donà, P., and Speziale, S. (2011). Polyhedra in loop quantum gravity. *Phys. Rev.* 83. doi:10.1103/PhysRevD.83.044035

Bianchi, E., Donà, P., and Vilensky, I. (2018). Entanglement entropy of bell-network states in lqg: analytical and numerical results.

Bianchi, E., Hackl, L., and Yokomizo, N. (2015). Entanglement time in the primordial universe. *Int. J. Mod. Phys.* 24, 1544006. doi:10.1142/S021827181544006X

Bianchi, E., Rovelli, C., and Vidotto, F. (2010). Towards spinfoam cosmology. *Phys. Rev. D.* 82, 084035. doi:10.1103/PhysRevD.82.084035

Borja, E. F., Garay, I., and Vidotto, F. (2012). Learning about quantum gravity with a couple of nodes. *SIGMA* 8. doi:10.3842/SIGMA.2012.015

Donà, P., Fanizza, M., Sarno, G., and Speziale, S. (2019). Numerical study of the Lorentzian Engle-Pereira-Rovelli-Livine spin foam amplitude. *Phys. Rev. D.* 100, 106003. doi:10.1103/PhysRevD.100.106003

Donà, P., Fanizza, M., Sarno, G., and Speziale, S. (2018). Su(2) graph invariants, regge actions and polytopes. *Class. Quantum Grav.* 35, 045011. doi:10.1088/1361-6382/aaa53a

Dona, P., Gozzini, F., and Sarno, G. (2020). Searching for classical geometries in spin foam amplitudes: a numerical method. *Class. Quantum Grav.* 37, 094002. doi:10.1088/1361-6382/ab7ee1

Donà, P., and Sarno, G. (2018). Numerical methods for EPRL spin foam transition amplitudes and lorentzian recoupling theory. *Gen. Relat. Gravit.* 50, 127. doi:10.1007/s10714-018-2452-7

Engle, J., Livine, E. R., Pereira, R., and Rovelli, C. (2008). Lqg vertex with finite immirzi parameter. *Nucl. Phys. B* 799, 136–149. doi:10.1016/j.nuclphysb.2008.02.018

Freidel, L., and Speziale, S. (2010). Twisted geometries: a geometric parametrization of su(2) phase space. *Phys. Rev.* 82, 084040. doi:10.1103/PhysRevD.82.084040

Halliwell, J. J. (1987). Correlations in the wave function of the Universe. *Phys. Rev. D*. 36, 3626–3640. doi:10.1103/PhysRevD.36.3626

Halliwell, J. J., Hartle, J. B., and Hertog, T. (2019). What is the no-boundary wave function of the Universe? *Phys. Rev. D* 99. doi:10.1103/PhysRevD.99.043526

Hartle, J. B., and Hawking, S. W. (1983). Wave function of the universe. *Phys. Rev. D*. 28, 2960–2975. doi:10.1103/PhysRevD.28.2960

Page, D. N. (1993). Average entropy of a subsystem. *Phys. Rev. Lett.* 71, 1291–1294. doi:10.1103/PhysRevLett.71.1291

Popescu, S., Short, A. J., and Winter, A. (2006). Entanglement and the foundations of statistical mechanics. *Nat. Phys.* 2, 754–758. doi:10.1038/nphys444

Puchta, J. (2013). Asymptotic of lorentzian polyhedra propagator.

Rovelli, C., and Smerlak, M. (2012). In quantum gravity, summing is refining. *Class. Quantum Grav.* 29, 055004. doi:10.1088/0264-9381/29/5/055004

Rovelli, C., and Vidotto, F. (2015). *Covariant loop quantum gravity: an elementary introduction to quantum gravity and spinfoam theory*. Cambridge, United Kingdom: Cambridge University Press.

Rovelli, C., and Vidotto, F. (2008). Stepping out of homogeneity in loop quantum cosmology. *Class. Quantum Grav.* 25, 225024. doi:10.1088/0264-9381/25/22/225024

Speziale, S. (2017). Boosting Wigner's nj-symbols. *J. Math. Phys.* 58, 032501. doi:10.1063/1.4977752

Vidotto, F. (2011). Many-node/many-link spinfoam: the homogeneous and isotropic case. *Class. Quantum Grav.* 28, 245005. doi:10.1088/0264-9381/28/24/245005

Vidotto, F. (2017). *Relational quantum cosmology*. Cambridge University Press, 297–316.

Conflict of Interest: The authors declare that the research was conducted in the absence of any commercial or financial relationships that could be construed as a potential conflict of interest.

frontiers in Astronomy and Space Sciences

ORIGINAL RESEARCH
published: 13 May 2021
doi: 10.3389/fspas.2021.604047

Unitarity and Information in Quantum Gravity: A Simple Example

Lautaro Amadei[1], *Hongguang Liu*[1,2] *and Alejandro Perez*[1]*

[1] *Aix Marseille University, Université de Toulon, CNRS, CPT, Marseille, France,* [2] *Institut für Quantengravitation, Universität Erlangen-Nürnberg, Erlangen, Germany*

In approaches to quantum gravity, where smooth spacetime is an emergent approximation of a discrete Planckian fundamental structure, any effective smooth field theoretical description would miss part of the fundamental degrees of freedom and thus break unitarity. This is applicable also to trivial gravitational field (low energy) idealizations realized by the use of Minkowski background geometry which, as with any other spacetime geometry, corresponds, in the fundamental description, to infinitely many different and closely degenerate discrete microstates. The existence of such microstates provides a large reservoir q-bit for information to be coded at the end of black hole evaporation and thus opens the way to a natural resolution of the black hole evaporation information puzzle. In this paper we show that these expectations can be made precise in a simple quantum gravity model for cosmology motivated by loop quantum gravity. Concretely, even when the model is fundamentally unitary, when microscopic degrees of freedom irrelevant to low-energy cosmological observers are suitably ignored, pure states in the effective description evolve into mixed states due to decoherence with the Planckian microscopic structure. Moreover, in the relevant physical regime these hidden degrees of freedom do not carry any "energy" and thus realize, in a fully quantum gravitational context, the idea (emphasized before by Unruh and Wald) that decoherence can take place without dissipation, now in a concrete gravitational model strongly motivated by quantum gravity. All this strengthens the perspective of a quite conservative and natural resolution of the black hole evaporation puzzle where information is not destroyed but simply degraded (made unavailable to low-energy observers) into correlations with the microscopic structure of the quantum geometry at the Planck scale.

Keywords: quantum gravity, quantum cosmology, Planckian discreteness, unitarity, black hole evaporation
PACS numbers: 98.80.Es, 04.50.Kd, 03.65.Ta

OPEN ACCESS

Edited by:
Francesca Vidotto,
Western University, Canada

Reviewed by:
Ivan Agullo,
Louisiana State University, United States
Ana Alonso Serrano,
Max Planck Institute for Gravitational Physics (AEI), Germany

***Correspondence:**
Alejandro Perez
perez@cpt.univ-mrs.fr

Specialty section:
This article was submitted to Cosmology, a section of the journal Frontiers in Astronomy and Space Sciences

Received: *08 September 2020*
Accepted: *15 March 2021*
Published: *13 May 2021*

Citation:
Amadei L, Liu H and Perez A (2021) Unitarity and Information in Quantum Gravity: A Simple Example. Front. Astron. Space Sci. 8:604047. doi: 10.3389/fspas.2021.604047

1. INTRODUCTION

The mathematical models that so far define our successful physical theories are all reversible in the sense that they can predict the future value of the variables they use from their initial values, while conversely the past can be uniquely reconstructed from the values of these variables in the future. The memory of the initial conditions is not lost in the dynamics and their information content remains. This is true for classical mechanics and field theory and it is also true for quantum mechanics and quantum field theory as long as we do not invoke the postulate of the collapse of the wave function (i.e., as long as we do not intervene from the outside via a

measurement[1]). In the quantum mechanical setting, this property boils down to the fact that evolution to the future is given by a unitary operator which can always be undone via its adjoint transformation.

This property of our fundamental models has always troubled naive intuition when faced with situations that appear to be irreversible. For example, what would happen to these words if the computer collapsed at this very moment? What if, after being printed, this paper is burned? Common sense would answer that the information in these pages (if of any relevance) would be lost. However, the physicist, trained to firmly believe in the statement of the previous paragraph, would say that the information in these words is not lost but simply hidden (to the point of becoming unrecoverable) in the humongous number of microscopic variables that would describe the whole system. In the case of burning the paper, these words remain "written" (it would be claimed) in the multiple correlations between the degrees of freedom of the molecules in the gas of the combustion diffusing in the atmosphere while transferring the information to even larger and yet pristine portions of the very large phase space of an unbounded universe. In the case where the computer collapses, a similar story can be told involving the dissipation of the bits into the environment. Of course the physicist cannot prove this; however, it is a consistent story in view of the strongly cherished principle of unitarity.

Such effective irreversibility is clearly captured in the second law of thermodynamics stating that (for suitable situations involving a large number of degrees of freedom) entropy can only increase. At the classical level this clashes at first sight with Liouville's theorem stating that the phase space volume of the support of a probability distribution is preserved by dynamical evolution. However, nothing restricts the shape of this volume to evolve into highly intricate forms that a macroscopic observer might be unable to resolve. More precisely, suitable initial conditions that the observer agent regards as special (for instance the macroscopic configurations of ink particles defining words in this paper before the fire reached them) come with an uncertainty in accordance to the observers limited measurement capabilities. This is idealized by a distribution in phase space occupying an initial phase space volume of a regular shape (this ensemble of points represents the system in what follows). Now as time goes by the apparent phase space volume (not the real volume which remains constant) would seem to grow to the agent just because of its intrinsic inability to separate the points in phase space that the systems occupies from the close neighboring ones where the system is not. The arrow of time (characterizing large systems) is only emergent macroscopically due to the special initial conditions, and the intrinsic coarse graining introduced by a macroscopic observer with its limitations. We will argue that the general lines of this story remain the same when black hole evaporation is considered.

[1]This is not the case in modifications of quantum mechanics where the collapse of the wave function happens spontaneously. In such theories information is actually destroyed (for a discussion of black hole evaporation in such contexts; see Modak et al., 2015; Okon and Sudarsky, 2017, 2018).

General relativity combined with quantum field theory, in a regime where both are expected to be good approximations, imply that large isolated black holes behave like thermodynamical systems in equilibrium. They are objects close to equilibrium at the Hawking temperature that lose energy extremely slowly via Hawking radiation. When perturbed they come back to equilibrium to a new state and the process satisfies the first law of thermodynamics with an entropy equal to 1/4 of the area A of the black hole horizon in Planck units. Under such perturbation (which in particular can also be associated with their slow evaporation), the total entropy of the universe can only increase namely

$$\delta S = \delta S_{\text{matter}} + \frac{\delta A}{4} \geq 0, \tag{1}$$

where δS_{matter} represents the entropy of whatever is outside the black hole (including, for instance, the emitted radiation).

This quasi equilibrium phase—which is extremely long lasting for macroscopic black holes but, at the same time, is only an intermediate situation before complete evaporation—is predicted by general relativity as the result of gravitational collapse taking place for suitable initial conditions. Indeed in order to make a black hole (BH), the past must be special (low entropy) too. Thus, the irreversibility captured by (1) can once more be associated with the same ingredients present in our previous example: the special nature of the initial conditions (low curvature and low densities in the past), high curvature, and huge new phase space regions available in the future; more precisely, in the Planckian regime that the singularity theorems of general relativity predict to develop inside the black hole horizon (the *would-be-singularity* from now on).

Such a perspective resonates with the one emphasized by Penrose (see for instance Penrose, 2005), among others: in full generality (now including gravity) the arrow of time comes from the fact that the universe is special in the past with a spacetime that was well-approximated by a homogeneous geometry and matter distribution (gas and dust) with tiny perturbations that would eventually grow and form galaxies and stars that one day can collapse to form black holes[2]. Before the formation of a black hole, the story of our system exploring larger and larger portions of the available phase space is the usual standard involving molecules, atoms, and fundamental particles. The perspective we put forward here is that the story continues to be the same when black holes form and a new huge portion of phase space is opened by the physics of gravitational collapse. This new channel for entropy growth is opened by the appearance of the internal *would-be-singularity* of the classical description beyond the event horizon. The gravitational collapse ignites interactions with the Planckian regime inside the black hole horizon (see footnote 3), like the lighter setting the paper on fire and thus degrading the ink in the words when burning the paper in our previous discussion. The singularity predicted by general relativity brings the system in contact with the quantum gravity scale, and (as in

[2]To these two specialty conditions one might also have to add one concerning the state of the hypothetical microscopic constituents at the Planck scale if the view we are advocating here and in Perez (2015, 2017) is correct.

the burning paper) this provides the key for resolving the puzzle of information in black hole evaporation.

This perspective, first advocated in Perez (2015, 2017), can be described with the help of **Figure 1** (which applies to the general black hole formation and evaporation background scenario of reference; Ashtekar and Bojowald, 2005). The first assumption in the diagram is that there is evolution across the *would-be-singularity* (predicted by the classical dynamics) inside the black hole. This assumption is intrinsic in the representation in the figure; however, the scenario still makes sense if instead a baby universe is formed, i.e., if the *would-be-singularity* remains causally disconnected from the outside after evaporation. In that case, the correlations established with the baby universe remain hidden forever to outside observers. The virtue of the present scenario in such a case would be to give an identity to the degrees of freedom involved. The idea that the spacetime representation of the situation resembles the one in **Figure 1** comes from the various results in symmetry-reduced models for both cosmology (Bojowald, 2001; Ashtekar et al., 2006) as well as for black holes (Modesto, 2004, 2006; Bojowald, 2005; Bojowald et al., 2005; Gambini and Pullin, 2013; Corichi and Singh, 2016; Ashtekar et al., 2018), and was first pictured in Ashtekar and Bojowald (2005). In such a context, a "scattering theory" representation (where an in-state evolves into an out-state) is possible even though the result (as we will argue) cannot be translated into the language of effective quantum field theory.

But what do we mean by a black hole in this evaporating context? In the asymptotically flat idealization, the black hole region is defined in classical general relativity as the portion of the spacetime $\mathscr{M}$ that is not part of the past of $\mathscr{I}^+$. Such a definition needs to be modified in quantum gravity. In order to do that, we introduce the notion of the semiclassical past $J^-_{\rm C}(\mathscr{I}^+)$ of $\mathscr{I}^+$ as the collection of events in the spacetime that can be connected to $\mathscr{I}^+$ by causal curves along which the Kretschmann scalar $K \equiv R_{abcd}R^{abcd} \leq {\rm C}\ell_p^{-4}$ for some constant C of order unity. The black hole region can then be defined as

$$B \equiv \mathscr{M} - J^-_{\rm C}(\mathscr{I}^+). \tag{2}$$

Its dependence on the constant C is not an important limitation in the discussion about information. Different C would lead to BH regions that coincide with Planckian corrections.

The most clear physical picture emerges from the analysis of the Penrose diagram on the left panel of **Figure 1**, from the point of view of observers at future null infinity $\mathscr{I}^+$. These observers are assumed to be at the center of the mass Bondi frame of the BH formed via gravitational collapse. We also assume that the Bondi mass of the BH is initially $M \gg m_p$ at some delayed time u on $\mathscr{I}^+$ representing the time where the BH has achieved its quasi-equilibrium state and starts evaporating slowly via Hawking radiation, i.e., the BH is initially macroscopic. Under such conditions the evaporation is very slow and we can trust the semiclassical description that suggests that the Bondi mass $M(u)$ will slowly decrease with u from this initial value M until time $u = u_0$ (see figure) with $M(u_0) \gtrapprox m_p$ in a time of the order of M^3 in Planck units. From this time on, the details depend on a full quantum gravity calculation because the curvature around the BH horizon has become Planckian. Nevertheless, independently of such details we can safely say that the spacetime and the matter degrees of freedom encoded on $\mathscr{I}^+$ for $u > u_0$ must be in a superposition of states, all of which are very close to flat spacetime, as far as their geometry is concerned, with matter excitations very close to the vacuum because there is only at best an energy of the order of $E_{\rm late} \approx m_p$ to substantiate both. In addition these excitations must be correlated with the early Hawking radiation with energy $E_{\rm early} \approx M - m_p$ if unitarity is to hold. The late degrees of freedom are often referred to as *purifying degrees of freedom*.

One possibility is to assume that such purifying degrees of freedom are particle excitations coming from what is left of the BH (a remnant). Now, due to the fact that these particles must be extremely low-energy particles as only a total energy of $E_{\rm late} \approx m_p$ is available for purification, a simple estimate of the time (denoted as τ_p) that the process would have to last if this is the main channel for purification yields $\tau_p \approx (M/m_p)^4$. This is the scenario of an extremely long lasting point-particle-like remnant with a huge internal degeneracy which is claimed to be problematic from the point of view of effective quantum field theory (Banks et al., 1993).

Instead we propose a different alternative: if smooth spacetime and matter fields are emergent notions from underlying discrete microscopic physics, then the coarse low-energy notion of classical geometry with smooth fields living on it would correspond in the fundamental Hilbert space to a very large set with (possibly) an infinite number of microscopic states. For instance the Minkowski vacuum unicity in standard quantum field theory would fail in the sense that the requirement that states look *flat* for (coarse-grained) low-energy observers—which are those for which an effective quantum field theory description in terms of smooth fields living on a smooth geometry is a suitable approximation—would still admit a highly degenerate ensemble of microscopic states (all states with total mass indistinguishable from zero by these macroscopic observers). Now, such low-energy modes cannot be identified with effective field theoretical excitations as the infrared excitations of fields mentioned in the previous paragraph (say low-energy photons). Like the molecular structure that escapes the smooth characterization of the Navier-Stokes effective theory of fluids, the degrees of freedom of interest here correspond to defects in the Planckian fabric of quantum gravity bound to be missed by coarse low-energy agents and their effective field theory mathematical models based on smoothness.

Why should information be hidden in the UV but not in the IR modes as in the remnant scenario mentioned above? It is often believed that because the volume inside the black hole actually becomes very large (according to suitable definitions; Christodoulou and De Lorenzo, 2016) then modes that are correlated with the Hawking radiation are redshifted and become highly IR inside. Although this is true for spherically symmetric Hawking quanta in the spherically symmetric Schwarzshild background—where such modes are indeed infinitely redshifted as detected by regular observers when they approach the singularity at $r = 0$—this conclusion fails when one considers no-spherical modes no matter how small the deviation from

spherical symmetry is[3]. Therefore, generically all modes become UV close to the singularity [this is the central weakness of the bag-of-gold scenarios and the perspective proposed in Ashtekar (2020)].

We can draw a formal analogy with the Unruh effect as follows. The Unruh effect arises from the structure of the vacuum state $|0\rangle$ of a quantum field on the Minkowski spacetime when written in terms of the modes corresponding to Rindler accelerated observers with their intrinsic positive frequency notion. The vacuum takes the form

$$|0\rangle = \prod_k \left(\sum_n \exp\left(-n\frac{\pi\omega_k}{a}\right) |n,k\rangle_R \otimes |n,k\rangle_L \right), \qquad (4)$$

where $|n,k\rangle_L$ and $|n,k\rangle_R$ define the particle modes—as viewed by an accelerated observer with uniform acceleration a—on the left and the right of the Rindler wedge (Wald, 1995). Here we see from the form of the previous expansion that even when we are dealing with a pure state (if we define the density matrix $|0\rangle\langle 0|$), the reduced density obtained by tracing over one of the two wedges would produce a thermal state with $T = a/(2\pi)$. The statement in the perspective we propose on the purification of information in BH evaporation can be schematically represented (the following is certainly not a precise equation) by

$$\mathbf{U} \quad \underbrace{|\text{flat}, 0\rangle}_{\text{quantum geometry}} \otimes \overbrace{|\phi\rangle}^{\text{matter fields}}$$

$$= \prod_k \left(\sum_n \exp\left(-\frac{\beta}{2} n\omega_k\right) |\text{flat, n}\rangle \otimes |n,k\rangle \right), \qquad (5)$$

where an initial state of a flat quantum geometry $|\text{flat}, 0\rangle$ tensor product with a state representing initially diluted matter fields $|\phi\rangle$ evolves unitarily via $\mathbf{U}$ into the formation of a BH and the subsequent evaporation (**Figure 1**) which after complete evaporation is written as a superposition of flat quantum geometry states $|\text{flat, n}\rangle$—which are all indistinguishable from $|\text{flat}, 0\rangle$ to low-energy agents and differ among them by quantum numbers n corresponding to quantities that are only measurable if one probes the state down to its Planckian structure—tensor product with normal n-particle excitations of matter fields representing Hawking radiation. As mentioned above, the previous equation is only a schematic. Its main inappropriateness is the fact that the reduced density matrix obtained by tracing over the quantum geometry hidden degrees of freedom would give a thermal state at a fixed temperature T. This is at odds with the expectation that the Hawking radiation should contain a superposition of the thermal radiation emitted at different Hawking temperatures during the long history of the evaporation of the BH. But the point that this equation and the discussion of the previous paragraph should make clear is that the purification mechanism proposed here has nothing to do with the point-like remnant scenario with all its problems associated with a long lasting particle-like remnant. In the present scenario, to the future of the *would-be-singularity* in **Figure 1**, we simply have a quantum superposition of different quantum geometry states that all look flat to low-energy observers. There are no localized remnants hiding in the huge internal degeneracy; there is only a large superposition of states that are inequivalent in the fundamental quantum gravity Hilbert space but seem identical when tested with low-energy probes. Such degrees of freedom cannot be captured by any effective description in terms of smooth fields (EQFT) for the simple reason that they are discrete in their fundamental nature.

Notice that the degrees of freedom, where information would be coded after BH evaporation, do not satisfy the usual Einstein-Planck relationship $E = \hbar\omega$ or equivalently $p = h/\lambda$ (for some "wavelength" λ or "frequency" ω), and this might deceive intuition[4]. These are Planckian defects yet they do not carry Planckian energy. The point is that such a relationship only applies under suitable conditions which happen to be met in many cases but do not need to always be valid. One case is the one of degrees of freedom that can be thought of as waves moving on a preexistent spacetime. This is the case for particle excitations in the Fock space of quantum field theory or effective quantum field theories (both of which are defined in terms of a preexistent spacetime geometry). There is no clear meaning to the above intuitions in the full quantum gravity realm where the present discussion is framed. Even when such relations (linked to the usual uncertainty principle of quantum mechanics) should hold in a suitable sense—if the structure suggested by canonical quantization survives in quantum gravity as it should to a certain degree—they would apply to phase space variables encoding to

[3] In the Schwarzshild background, the frequency measured by a radially freely falling observer normal to the r =constant hypersurfaces goes like

$$\omega^2(r) = \frac{\ell^2}{r^2} + \frac{r}{2M}E^2 + \mathcal{O}\left(\frac{r^2}{M^2}\right), \qquad (3)$$

where $E = -k\cdot\xi$ and $\ell = k\cdot\psi$ are the conserved quantities associated with the massless particle with wave vector k^a, and ξ^a and ψ^a are the stationarity and rotation killing fields of the background. The qualitative behavior approaching $r = 0$ would be the same for any other observer measuring ω (the divergence of ω is observer-independent). Only exactly spherically symmetric modes with $\ell = 0$ would become IR at the singularity. However, this conclusion is no longer true if the BH rotates or if we consider that at the fundamental level, states with exact spherical symmetry inside the BH are of measure zero. Notice that such UV divergence in the non-spherically symmetric Hawking partners implies large deviations from spherical symmetry near the singularity (if their back reaction would be taken into account). This should be kept in mind when modeling the situation with spherically symmetric mini superspace quantum gravity models.

[4] A nice counter example of this intuition is given by the case of a non-relativistic charged particle in a two-dimensional infinite perfect conductor in a uniform magnetic field normal to the conducting plane. The energy eigenvalues are given by the Landau levels $E_n = \hbar\omega_B(n + 1/2)$ where $\omega_B = qB/(mc)$ is the Bohr magneton frequency, but they are infinitely degenerate. There are canonically conjugated variables (P, Q) associated with the particle that are cyclic, i.e., do not appear in the Hamiltonian. In this case, one can produce wave packets that are as "localized" in the variable Q without changing the energy of the system. Interestingly, this is a perfect example of a system where one could have an apparent loss of information of the type we are proposing here (for a more realistic analog gravity model discussing the information paradox along the lines of the present scenario; see Liberati et al., 2019). If one scatters a second particle interacting softly with the charged particle on the plate so that the interaction does not produce a jump between different Landau levels, then correlations with the cyclic variables would be established without changing the energy of the system. This is the perfect model to illustrate the possibility of decoherence without dissipation.

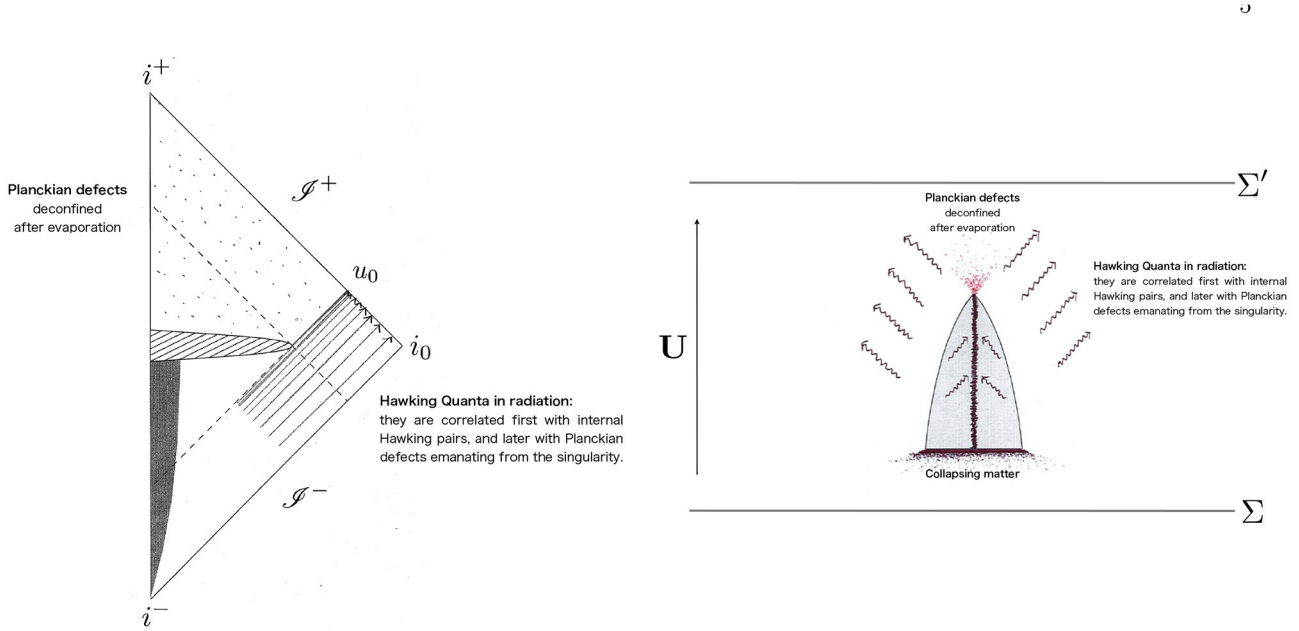

FIGURE 1 | (Left) Penrose diagram illustrating (effectively) the natural scenario, suggested by the fundamental features of LQG, for the resolution of the information puzzle in black hole evaporation (Perez, 2015). The shaded region represents the *would-be-singularity* where high fluctuations in geometry and fields are present and where the low-energy degrees of freedom of the Hawking pairs are forced to interact with the fundamental Planckian degrees of freedom. **(Right)** Same situation as a scattering process from an initial to a final Cauchy hypersurface. This figure contains basically the same information as the Penrose diagram. Its additional merit, if any, is the more intuitive representation of the shrinking black hole as well as the time scales involved (collapse time is very short with respect to the evaporation time). Both these features are absent in the conformal representation on the left. There are limitations to this kind of spacetime representation of a process that is fundamentally quantum and hence only understandable in terms of superpositions of different spacetime geometries.

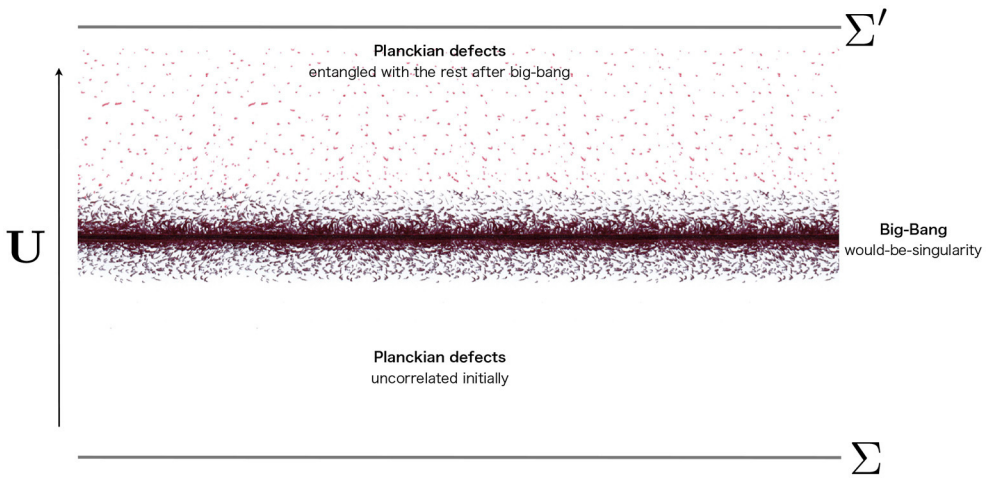

FIGURE 2 | Diagram (effectively) illustrating the natural scenario, suggested by the fundamental features of LQG, for the resolution of the information puzzle in black hole evaporation (Perez, 2015). As in **Figure 1**, one should keep in mind the limitations of this kind of spacetime representation of a process that is fundamentally quantum and hence only understandable in terms of superpositions of different spacetime geometries.

the true degrees of freedom of gravity that we expect (from general covariance) to be completely independent of a preexistent background geometry. We will see that such degrees of freedom with such a peculiar nature actually arise naturally in the toy model of quantum gravity that we analyze in this article.

It is presently hard to prove that such a scenario is viable in a quantum theory of gravity simply because there is no such theoretical framework developed enough for tackling BH formation and evaporation in detail. However, the application of loop quantum gravity to quantum cosmology leads to a

model with similar features, where evolution across the classical singularity is well defined (Bojowald, 2001). The results have been reported in Amadei and Perez (2019). In this article we present the main features of this model in more detail and show that the conclusions of Amadei and Perez (2019), some of which are drawn from some simplified models of matter coupling, are generic and remain true in more physically realistic models.

The results can be described briefly by making reference to **Figure 2** which should be compared with the right panel in **Figure 1**. We will show that the evolution in loop quantum cosmology from a universe in an initially contracting state in the past of the *would-be-singularity* to an expanding universe in its future is perfectly unitary in its fundamental description. Nevertheless, states in the Hilbert space of loop quantum cosmology contain quantum degrees of freedom which are hidden to low-energy coarse-grained observers. If these degrees of freedom are traced out in the initial density matrix then we will see that pure states (in the sense of the reduced density matrix) generically evolve into mixed states across the *would-be-singularity*. Information is lost in correlations with degrees of freedom that are Planckian and thus inaccessible to macroscopic observers. These correlations are established in an inevitable way during the strong curvature phase of evolution across the big bang (just as expected in the BH scenario described above). As energy is conserved (energy is a delicate notion in cosmology but happens to be well-defined in our model as we will see), the defects that purify the final state do not enter into the energy balance which realizes another crucial necessary ingredient of the general scenario (decoherence happens with negligible dissipation; Unruh, 2012).

The paper is organized as follows. In the first part (section 2), we show that the scenario we have described in general terms so far is realized in unimodular quantum cosmology following the standard quantization prescription of loop quantum cosmology. Aside from a different choice of time variable, the model of this section is exactly equivalent to other models studied in the standard literature (Ashtekar and Singh, 2011). In the second part of the paper, we observe that there is natural extension of loop quantum cosmology based on the regularization ambiguity associated with the quantization of the Hamiltonian. This extension provides another interesting realization of our mechanism. Although this second option is not necessary to illustrate our point (already realized in the standard theory in the first part), it gives a different identity to the defects which could lead to independent and thus useful insights. We have included a series of appendices where some calculations are shown. **Appendix D** is especially important because some of the over-simplified model (analytic) calculations in the body of the paper are completed (numerically) using a more physically realistic case of the coupling of gravity with a massless scalar field.

2. UNIMODULAR GRAVITY: FOUR-VOLUME AS TIME

In this section we introduce the basic structure of quantum unimodular gravity in the framework of quantum cosmology. This theory will provide us with a toy model to study the unitary evolution of the state of the universe across the big-bang singularity. We will see that the Hilbert space of loop quantum cosmology contains the type of microscopic degrees of freedom evoked in the general discussion of the introduction. This is a minimalistic model where our scenario can be explicitly realized.

Unimodular gravity as a concept is nearly as old as general relativity itself, it was introduced by Einstein in 1919 (Einstein, 1919) as an attempt to describe nuclear structure geometrically. In his work, Einstein also identified an appealing feature of the theory, which is the fact that the cosmological constant arises as a dynamical constant of motion that needs to be added to the initial values of the theory. In unimodular gravity, the cosmological constant is a constant of integration and not a universal or fundamental constant of nature. Interest in the theory was regained in the late 80's with the observation of Weinberg (1989) that, for the above reason, semiclassical unimodular gravity provides a trivial resolution of the cosmological constant problem as vacuum energy simply does not gravitate. Unimodular gravity is the natural low-energy description that emerges from the formal thermodynamical ideas of Jacobson (1995), and represents the expected low energy regime of the causal set approach (Bombelli et al., 1987).

Another property of unimodular gravity (specially important for us here) is that it completely resolves the problem of time (Unruh, 1989) in the cosmological FLRW context. More precisely, the theory comes with a preferred time evolution and a preferred Hamiltonian (the energy of the universe is well defined and directly linked with the value of the cosmological constant). The quantum theory is described by a Schrodinger-like equation where states of the universe are evolved by a unitary evolution operator. Therefore, unlike the general situation in quantum gravity, the notion of unitarity is unambiguously defined in unimodular quantum cosmology. This is the main reason why unimodular gravity provides the perfect framework for the discussion of the central point of this work.

Here we specialize in homogeneous and isotropic cosmologies that are spatially flat (k = 0), i.e., the spatial manifold Σ is topologically $\mathbb{R}^3$. What follows is the standard construction. For a detailed account of the Hamiltonian analysis in the cosmological framework (see Chiou and Geiller, 2010). The FLRW metric is

$$ds^2 = -N(t)^2 dt^2 + a(t)^2 \underbrace{(dx^2 + dy^2 + dz^2)}_{q_{ab}}, \tag{6}$$

where q_{ab} denotes the fiducial spacial metric. Since Σ is non-compact, some integrals are infrared divergent and are regularized by restricting them to a fixed fiducial cell $\mathcal{V}$ of fiducial volume V_0 with respect to the fiducial spacial metric

$$q_{ab} = e^i_a e^j_b \, \delta_{ij}, \tag{7}$$

where e^i_a denotes a fiducial triad and the physical metric is given by $q_{ab} = a^2(t) q_{ab}$. The action of unimodular gravity in the FLRW mini superspace setup is given by

$$S[a, \dot{a}, \lambda] = \frac{3}{8\pi G} \int_{\mathbb{R}} \left(\frac{V_0 a \dot{a}^2}{N} + \lambda V_0 (N a^3 - 1) \right) dt, \tag{8}$$

where λ is a Lagrange multiplier imposing the unimodular constraint $N = a^{-3}$ (i.e., $\sqrt{|g|} = 1$), and the first term is the Einstein-Hilbert action restricted to the FLRW geometries[5]. In order to use loop quantum cosmology techniques (for a discussion of the quantization in the full loop quantum gravity context; see Smolin, 2009, 2011), one introduces the new canonical variables c and p via the basic Ashtekar-Barbero connection variables A_a^i and E_i^a, namely

$$E_i^a = p\left(e_i^a V_0^{-2/3}\right), \qquad A_a^i = c\left(\omega_a^i V_0^{-1/3}\right), \tag{9}$$

where ω_a^i is a fiducial reference connection. These variables are related to those in (8) via the equations

$$|p| = V_0^{2/3} a^2, \qquad c = V_0^{1/3}\frac{\gamma \dot{a}}{N}. \tag{10}$$

The action becomes

$$S[c,p,\lambda] = \frac{3}{8\pi G}\int_{\mathbb{R}} \gamma^{-1} c\dot{p} - N\gamma^{-2}\sqrt{|p|}c^2 + \lambda(N|p|^{\frac{3}{2}} - V_0)dt, \tag{11}$$

and c and p are canonically conjugated in the sense that

$$\{c,p\} = \frac{8\pi G\gamma}{3}. \tag{12}$$

The unimodular condition $N = a^{-3}$ fixes the lapse to $N = V_0/|p|^{3/2}$ and the unimodular Hamiltonian becomes

$$H = \frac{3V_0}{8\pi G}\frac{c^2}{\gamma^2|p|}. \tag{13}$$

The proportionality of the Hamiltonian with V_0, and the fact that the four-volume bounded by V_0 at two different times is given by $v^{(4)} = V_0\Delta t$, implies that time evolution can be parameterized in terms of the four-volume elapsed from some reference initial slice. The associated Hamiltonian [conjugated to $v^{(4)}/(8\pi G)$] is

$$\Lambda = \frac{3c^2}{\gamma^2|p|}, \tag{14}$$

and corresponds to the cosmological constant.

2.1. Quantization

The loop quantum cosmology quantization uses a non standard representation of the canonical variables where the variable c does not exist as a quantum operator, and the definition of the Hamiltonian requires a special regularization procedure known as the $\bar{\mu}$-scheme (Ashtekar and Singh, 2011). The quantization prescription is greatly simplified by the introduction of new canonically conjugated dynamical variables b and ν defined as (Ashtekar et al., 2008)

$$b \equiv \frac{c}{|p|^{\frac{1}{2}}} \qquad \nu \equiv \mathrm{sign}(p)\frac{|p|^{\frac{3}{2}}}{2\gamma\pi\ell_p^2}, \tag{15}$$

with Poisson brackets[6]

$$\{b,\nu\} = 2\hbar^{-1}. \tag{16}$$

The variable ν corresponds to the physical volume of the fiducial cell divided by ℓ_p^2; it has units of distance. The variable b is simply its conjugate momentum. In terms of these variables the gravitational (unimodular) Hamiltonian (13) integrated in a fiducial cell V becomes

$$H = \frac{3V_0}{8\pi G\gamma^2}b^2. \tag{17}$$

Note the extreme simplicity of the previous expression: the unimodular Hamiltonian is just the analog of that of a free particle in one dimension with a mass parameter of $m = 4\pi\gamma^2/(3V_0)$ and momentum b. In the absence of matter, the Hamiltonian can be quantized in the Wheeler-DeWitt representation where the evolution in unimodular time is unitary and there is no singularity (the classical solutions correspond to De-Sitter geometries with arbitrary but positive cosmological constants). The singularity in the classical theory becomes real when matter is introduced.

In the loop quantum cosmology polymer representation, just as for c, there is no operator corresponding to b but only the operators corresponding to finite ν translations (Ashtekar et al., 2006); from here on referred to as shift operators

$$\exp(i2kb) \triangleright \Psi(\nu) = \Psi(\nu - 4k). \tag{18}$$

For $k = q\sqrt{\Delta}\ell_p$ and $q \in \mathbb{N}$, states that diagonalize the previous shift operators, denoted $|b_0;\Gamma_\Delta^\epsilon\rangle$, are labeled by a real value b_0 and by a graph Γ_Δ^ϵ. The graph is a 1D lattice of points in the real line of the form $\nu = 4n\sqrt{\Delta}\ell_p + \epsilon$ with $\epsilon \in [0, 4\sqrt{\Delta}\ell_p)$ and $n \in \mathbb{N}$. The corresponding wave function is given by $\Psi_{b_0}(\nu) \equiv \langle\nu|b_0;\Gamma_\Delta^\epsilon\rangle = \exp(-i\frac{b_0\nu}{2})\delta_{\Gamma_\Delta^\epsilon}$, where the symbol $\delta_{\Gamma_\Delta^\epsilon}$ means that the wavefunction vanishes when $\nu \notin \Gamma_\Delta^\epsilon$. It follows from (18) that

$$\exp(i2kb) \triangleright |b_0;\Gamma_\Delta^\epsilon\rangle = \exp(i2kb_0)\,|b_0;\Gamma_\Delta^\epsilon\rangle\,. \tag{19}$$

The states $|b;\Gamma_\Delta^\epsilon\rangle$ are eigenstates of the shift operators that preserve the lattice Γ_Δ^ϵ. Notice that the eigenvalues are independent of the parameter ϵ, i.e., they are infinitely degenerate and span a non separable subspace of the quantum cosmology Hilbert space $\mathscr{H}_{lqc}$.

A scale $\bar{\mu}$ is needed in order to define a regularization of (17) representing the Hamiltonian in $\mathscr{H}_{lqc}$. The reason is that there are no operators associated with b but only approximants constructed via the shift operators (18). The so-called $\bar{\mu}$-scheme (Ashtekar and Singh, 2011) introduces a dynamical length scale $\bar{\mu}$ defined as

$$\bar{\mu}^2 = \frac{\ell_p^2\Delta}{|p|}, \tag{20}$$

[5]There is an overall minus sign in the definition action with respect to standard treatments. This is done so that the pure-geometry Hamiltonian is positive definite.

[6]The factor $\hbar^{-1}$ appears on the right hand side of the Poisson brackets due to the introduction of $\hbar$ (via ℓ_p^2) in the definition of the new variable ν. This is done to match standard definitions (Ashtekar and Singh, 2011).

where Δ represents the so-called "area-gap" which plays the role of a UV regulator. It is normally associated with the smallest non-vanishing area quantum in the full theory of loop quantum gravity. For the moment (as in the standard treatment), this is just a fixed parameter[7]. When translated into the variables (15), $\overline{\mu}$ corresponds to considering approximants to b constructed out of shift operators (18) with fixed $k \equiv \sqrt{\Delta}\ell_p$. In terms of these, one obtains the following regularization of the Hamiltonian (17) which is a well-defined self-adjoint operator[8] acting on $\mathscr{H}_{lqc}$

$$H_\Delta \equiv \frac{3V_0}{8\pi G\gamma^2}\frac{1}{\Delta\ell_p^2}\sin^2\left(\Delta^{\frac{1}{2}}\ell_p\, b\right), \tag{21}$$

which coincides with (17) leading to (zero) order in ℓ_p^2. From (14), we obtain an operator associated to the (here dynamical) cosmological constant, namely

$$\Lambda_\Delta \equiv \frac{3}{\gamma^2}\frac{\sin^2\left(\Delta^{\frac{1}{2}}\ell_p\, b\right)}{\Delta\ell_p^2}. \tag{22}$$

In the pure gravity case, the cosmological constant is positive definite and bounded from above by the maximum value $\lambda_{\max} = 1/(\gamma^2\ell_p^2\Delta)$. Negative cosmological constant solutions are possible when matter is added (see **Appendix B**). The states (19) with $k = k_\Delta \equiv \sqrt{\Delta}\ell_p$ diagonalize the Hamiltonian, i.e.,

$$H_\Delta \triangleright |b_0;\Gamma^\epsilon_\Delta\rangle = E_\Delta(b_0)\,|b_0;\Gamma^\epsilon_\Delta\rangle\,, \tag{23}$$

with energy eigenvalues

$$E_\Delta(b_0) = \frac{3V_0}{8\pi G\gamma^2}\frac{1}{\Delta\ell_p^2}\sin^2\left(\Delta^{\frac{1}{2}}\ell_p\, b_0\right). \tag{24}$$

States $|b_0;\Gamma^\epsilon_\Delta\rangle$ are also eigenstates of the cosmological constant with eigenvalue $\lambda_\Delta(b_0) = (8\pi G)E_\Delta(b_0)/V_0$. Notice that the energy eigenvalues do not depend on $\epsilon \in [0, 4\sqrt{\Delta}\ell_p)$. Thus, the energy levels are infinitely degenerate with energy eigenspaces that are non-separable. This is not something peculiar of our model but a general property of the non-standard representation of the canonical commutation relations used in loop quantum cosmology.

2.2. On the Interpretation of the ϵ Sectors

It is customary in the loop quantum cosmology literature to restrict to a fixed value of ϵ in concrete cosmological models, as the dynamical evolution does not mix different ϵ sectors. The terminology *"superselected sectors"* is used in a loose way in discussions. However, these sectors are not superselected in the strict sense of the term because they are not preserved by the action of all the possible observables in the model, i.e., there are non trivial Dirac observables mapping states from one sector to another. The explicit construction of such observables might be very involved in general (as is the usual case with Dirac observables); nevertheless, it is possible to exhibit them directly at least in one simple situation: the pure gravity case. In that case, the shift operator (18) with shift parameter δ commutes with the pure gravity Hamiltonian (the Hamiltonian constraint if we were using standard loop quantum cosmology) and maps the ϵ sector to the $\epsilon - 4\delta$ sector. The analogous Dirac observables in a generic matter model can be formally described with techniques of the type used for the definition of evolving constants of motion (Rovelli, 1991). No matter how complicated this might be in practice, the point is well-illustrated by our explicit example in the matter free case[9].

Thus, different ϵ sectors are not superselected and therefore the infinite degeneracy of the energy eigenvalues of the Hamiltonian (which again we exhibit explicitly in the previous discussion only in the vacuum case) must be taken at face value. How can we understand this large degeneracy from the fact that there would be only a two-fold degeneracy (associated with a contracting or expanding universe) if we had quantized the model using the standard Schrodinger representation or, in other words, the standard Wheeler-DeWitt quantization? The answer is to be found, we claim, in the notion of coarse graining: low-energy observers only distinguish a two-fold degeneracy for energy (or cosmological constant) eigenvalues: one the universe has a given cosmological constant, and two it is expanding or contracting. These are the quantum numbers in the Wheeler-DeWitt quantization which play a role in our context of the low-energy effective quantum field theory formulation. Such coarse observers are declared to be insensitive to the huge additional degeneracy of energy eigenstates encoded in the quantum number ϵ. All these infinitely many states in the quantum cosmology representation must be considered as equivalent to the two-fold degeneracy mentioned above.

In what follows, and for concreteness, we will consider combinations of states with two different values for ϵ only, i.e., on two different lattices. The idea of the previous paragraph will naturally produce a notion of coarse-graining entropy associated with the intrinsic statistical uncertainty due to the inability for a low-energy agent to distinguish these microscopically orthogonal states. Arbitrary superposition with N different ϵ sectors would lead to similar results [the entropy capacity growing with the usual $\log(N)$]. The $N = 2$ case treated here renders some explicit calculations straightforward.

[7] In section 3, we will turn this quantity into a quantum operator acting on the microscopic sector of the Hilbert space that will be introduced.

[8] The Hamiltonian $\hat{H}_0$ (21) is symmetric, that is $\langle\Psi_1, \hat{H}_0\Psi_2\rangle = \langle\hat{H}_0\Psi_1, \Psi_2\rangle$, with respect to the inner product $\langle\Psi_1,\Psi_2\rangle = \sum_\nu \overline{\Psi_1(\nu)}\Psi_2(\nu)$. The action of the Hamiltonian on $\Psi(\nu)$ is given by:

$$\hat{H}_0\Psi(\nu) = -3(2\gamma^2\Delta_s\ell_p^2)^{-1}\left(\Psi(\nu+2\lambda) - 2\Psi(\nu) + \Psi(\nu-2\lambda)\right),$$

with $\lambda = 2\sqrt{\Delta_s}\ell_p$. The key property is $\langle\Psi_1(\nu), \Psi_2(\nu+2\lambda)\rangle = \langle\Psi_1(\nu-2\lambda), \Psi_2(\nu)\rangle$ where ν is in the support of both $\Psi_1(\nu)$ and $\Psi_2(\nu)$. This is the statement of the unitarity of the shift operators $\langle e^{-i2\lambda b}\Psi_1, \Psi_2\rangle = \langle\Psi_1, e^{i2\lambda b}\Psi_2\rangle$. The symmetric nature of the shift operators appearing in H_0 implies the result.

[9] This point was independently communicated to us in the context of Dirac observables for isotropic LQC with a free matter scalar field Madhavan.

2.3. Matter Couplings and a Model Capturing Its Essential Features

Here we discuss two simple matter models in order to isolate the generic features of the influence of matter. At the end of the section, we will define a simple and trivially solvable model capturing these features.

Perhaps the simplest matter model that would serve our purposes is minimal and isotropic coupling to a Dirac fermion defined in de Berredo-Peixoto et al. (2012). After symmetry reduction, the action for matter is

$$S_{\mathrm{F}}(\eta,\bar{\eta}) = V_0 \int_{\mathbb{R}} d\tau \Big[\frac{i}{2} a(\tau)^3 \left(\bar{\eta}\gamma^0 \dot{\eta} - \dot{\bar{\eta}}\gamma^0 \eta \right) - mN(\tau) a(\tau)^3 \bar{\eta}\eta \Big], \tag{25}$$

from which we read the fermionic contribution to the Hamiltonian

$$\begin{aligned} H_{\mathrm{F}} &= mN(\tau)a^3(\tau)\bar{\eta}\eta = -mN(\tau)p_\eta\gamma_0\eta \\ &= \frac{m}{a^3} p_\eta \gamma_0 \eta, \end{aligned} \tag{26}$$

where (Π, Ψ) are the fermionic canonical variables $\Pi \equiv (V_0 a)^{3/2}\psi^\dagger$ and $\Psi \equiv (V_0 a)^{3/2}\psi$ (Thiemann, 2001), and in the second line, we use the unimodular condition $N = V_0^{-1}a^{-3}$. In the quantum theory, the non trivial anti-commutator is $\{\eta, p_\eta\} = \mathbf{1}$ with the rest equal to zero. This is achieved by writing $\eta = \sum_s \left(a_s u^s e^{-imt} + b_s^\dagger v^s e^{imt} \right)$ with non trivial anti-commutation relations for the creation and annihilation of operators $\{a_r, a_s^\dagger\} = \delta_{rs} = \{b_r, b_s^\dagger\}$, with $u^s e^{-imt}$ and $v_s e^{imt}$ as a complete basis of solutions of the Dirac equation for positive and negative frequency, respectively (Peskin and Schroeder, 1995). In our model, we can have either the vacuum state, or one or two fermions which saturate the Pauli exclusion principle. If we assume normal ordering, the contribution to the unimodular energy is

$$H_{\mathrm{F}} = \frac{mn}{a^3}. \tag{27}$$

where $n = 0, 1, 2$ is the occupation number for the fermion. If instead of the condition $N = V_0^{-1}a^{-3}$, we had used $N = 1$ (where time is comoving time) then the energy contribution would have been just m for which we have a clear physical intuition: a single fermion homogeneously distributed in the universe contributes to the Hamiltonian with its total mass. The factor $1/a^3$ in the previous expression comes from the unimodular condition.

In the case of Wheeler-DeWitt quantization, the contribution of the fermion becomes singular at the big bang $a = 0$. In loop quantum cosmology, such a quantity remains bounded above due to loop quantum gravity discreteness. Indeed, using the inverse volume quantization given in reference (Ashtekar and Singh, 2011), one has

$$\hat{H}_{\mathrm{F}} \triangleright |\psi\rangle = -m \sum_\nu |\nu\rangle\, h_{\mathrm{F}}(\nu; \sqrt{\Delta}\ell_p) \Psi(\nu, \eta), \tag{28}$$

where

$$h_{\mathrm{F}}(\nu;\lambda) \equiv \frac{1}{4\lambda^2} \Big(|\nu + 2\lambda|^{\frac{1}{2}} - |\nu - 2\lambda|^{\frac{1}{2}} \Big)^2. \tag{29}$$

We notice that $h_{\mathrm{F}}(\nu; \sqrt{\Delta}\ell_p) < 1$ and decays like $1/\nu$ for $\nu \to \infty$[10]. One could, in principle, add this term to the free Hamiltonian and solve the unimodular time-independent Schrodinger equation

$$(\hat{H}_0 + \hat{H}_{\mathrm{F}}) \triangleright |\psi\rangle = E\,|\psi\rangle\,. \tag{30}$$

Solutions can be interpreted in the sense of scattering theory starting with free wave packets for large ν picked around a value of the cosmological constant (22) or energy (24).

The case of coupling with a scalar field is formally very similar, especially in the simplified case where we assume it to be massless. Following Ashtekar and Singh (2011), and using the unimodular condition $N = a^{-3}$, we get

$$H_\phi = -\frac{p_\phi^2}{8\pi^2\gamma^2\ell_p^4\nu^2}. \tag{31}$$

This leads to

$$\hat{H}_\phi \triangleright |\psi\rangle = -m \sum_\nu |\nu\rangle\, h_\phi(\nu; \sqrt{\Delta}\ell_p) \Psi(\nu, \phi), \tag{32}$$

where

$$h_\phi(\nu;\lambda) \equiv \frac{p_\phi^2}{16\lambda^4} \Big(|\nu + 2\lambda|^{\frac{1}{2}} - |\nu - 2\lambda|^{\frac{1}{2}} \Big)^4. \tag{33}$$

The momentum p_ϕ commutes with the Hamiltonian and thus it is a constant of motion. If we consider an eigenstate of p_ϕ then the problem reduces again to a scattering problem with a potential decaying like $1/\nu^2$ when we consider solving the time-independent Schrodinger equation

$$(\hat{H}_0 + \hat{H}_\phi) \triangleright |\psi\rangle = E\,|\psi\rangle\,. \tag{34}$$

Therefore, both the fermion as well as the scalar field models (which are closer to a possibly realistic scenario) seem tractable with a slight generalization of the standard scattering theory to the discrete loop quantum cosmology setting. However, the main objective in this section is to illustrate an idea in terms of a concrete and simple toy model. With this idea in mind, we will modify the structure suggested by the fermion coupling and the scalar field coupling and simply add an interaction term where the "long-distance interaction" term represented by the function $F(\nu;\lambda)$ is replaced by a short-range analog $F(\nu;\lambda) \propto \delta_{\nu,0}$. The qualitative properties of the scattering will be the same and the model becomes sufficiently trivial for straightforward analytic computations. The results for the more realistic free scalar field model have been dealt with numerically and are presented in **Appendix D**.

For that we consider an interaction that begins at $\nu = 0$:

$$\hat{H} = \hat{H}_0 + \mu \hat{H}_{\mathrm{int}}, \tag{35}$$

[10]There is a great degree of ambiguity in writing the inverse volume operators. Perhaps the simplest is the one introduced in WilsonEwing (2012) that we will actually use in the concrete computations of **Appendix D**. For more discussion on this see Singh and Wilson-Ewing (2014) and references therein.

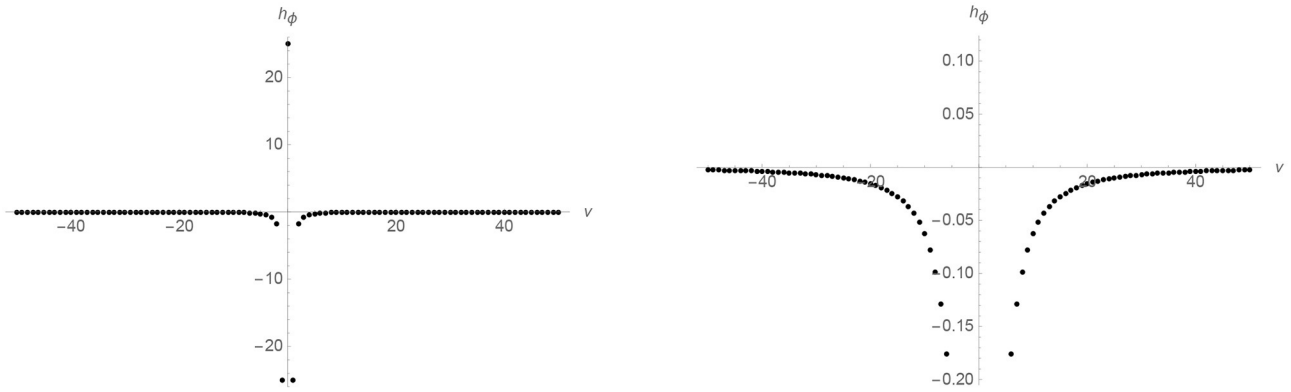

FIGURE 3 | The function $h_\phi(\nu;\lambda)$ evaluated on an ϵ sector containing $\nu = 0$, for $p_\phi = 10$ in natural units and $\lambda = 1/2$ is plotted using two different ranges. On the left, we see that the function is finite near $\nu = 0$. On the right, we can see that it behaves like $-\nu^{-2}$ for large values of ν. This function can be seen as the effective potential where an asymptotically free state of the universe (pure gravity with cosmological constant state or asymptotically de Sitter state) scatters. If the cosmological constant is negative there are bound states whose superposition can be used to define semiclassical universes oscillating in an endless series of big bangs and big crunches (see section B).

where μ is a dimensionless coupling, $\hat{H}_0$ is given in (58), and $\hat{H}_{\rm int}$ is

$$\hat{H}_{\rm int} \triangleright |\psi\rangle \equiv \sum_\nu \left(\ell_p^{-4}\frac{V_0}{\sqrt{\Delta}}\right)|\nu\rangle\,\frac{\delta_{\nu,0}}{\sqrt{\Delta}}\Psi(0). \tag{36}$$

We have added by hand an interaction Hamiltonian that switches on only when the universe evolves through the *would-be-singularity* at the zero volume state. The key feature of the $\hat{H}_{\rm int}$ is that—as its more realistic relatives, matter Hamiltonians (28) and (32)—it breaks translational invariance and thus, it leads to different dynamical evolution for different ϵ sectors.

2.4. Solutions as a Scattering Problem

The scattering problem is very similar to the standard one in one-dimensional quantum mechanics; however, one needs to take into account the existence of the peculiar degeneracy of energy eigenvalues contained in the ϵ sectors; see sections 2.1 and 2.2. We will consider, for simplicity, the superposition of only two states supported on two lattices respectively: the lattice Γ^ϵ_Δ with $\epsilon = 0$ for the first one and the one with $\epsilon = 2\sqrt{\Delta}\ell_p$ for the second one. The degenerate eigenstates of the shift operators (19) with eigenvalues $\exp(i2kb)$ will be denoted as

$$|b,1\rangle \equiv |b;\Gamma^0_\Delta\rangle\,, \quad \text{and} \quad |b,2\rangle \equiv |b;\Gamma^{2\sqrt{\Delta}\ell_p}_\Delta\rangle\,, \tag{37}$$

respectively, while we will denote Γ^1 and Γ^2 as the corresponding underlying lattices. The immediate observation is that states supported on Γ^2 (superpositions of $|b,2\rangle$) will propagate freely because they are supported on a lattice that does not contain the point $\nu = 0$ where the interaction is non trivial. On the other hand, states supported on Γ^1 (superpositions of $|b,1\rangle$) will be affected by the interaction at the big bang. Before and after the big bang, the universe's evolution of the second type of states is well described by the eigenstates of the Hamiltonian (58) described in section 2.1. Such asymmetry of the interaction on different ϵ sectors is not an artifact of the simplicity of the interaction Hamiltonian. This is just a consequence of the necessary breaking of the shift invariance for any realistic matter interaction as we argued in the previous section and we show explicitly in **Appendix D** (see **Figure 3**).

Therefore, the non trivial scattering problem concerns only states on the lattice $\Gamma^1 = \{\nu = 4n\sqrt{\Delta}\ell_p \,|\, n \in \mathbb{Z}\}$ that is preserved by the Hamiltonian and contains the point $\nu = 0$. In order to solve the scattering problem, we consider an in-state of the form

$$|\psi_k\rangle = |\nu\rangle \begin{cases} e^{-i\frac{k}{2}\nu} + A(k)\, e^{i\frac{k}{2}\nu} & (\nu \geq 0) \\ B(k)\, e^{-i\frac{k}{2}\nu} & (\nu \leq 0), \end{cases} \tag{38}$$

where $\nu \in \Gamma^1$, and $A(k)$ and $B(k)$ are coefficients depending on k. For suitable coefficients, such states are eigenstates of the full Hamiltonian (35). Arbitrary solutions (wave packets) can then be constructed in terms of appropriate superpositions of these "plane-wave" states.

We can compute the scattering coefficients $A(k)$ and $B(k)$ from the discrete (finite difference) time-independent Schrodinger equation

$$\left(\hat{H}_0 + \hat{H}_{\rm int}\right) \triangleright |\psi\rangle \;=\; E\,|\psi\rangle \tag{39}$$

which amounts to the following finite difference equation in the ν basis:

$$\sum_\nu \left(-\frac{3V_0}{8\pi G\gamma^2}\frac{1}{2\Delta\ell_p^2}\Big[\Psi(\nu - 4\sqrt{\Delta}\ell_p) + \Psi(\nu + 4\sqrt{\Delta}\ell_p) - 2\Psi(\nu)\Big] + \frac{V_0\mu}{\Delta\ell_p^4}\delta_{\nu,0}\Psi(0) - E(k)\,\Psi(\nu)\right)|\nu\rangle = 0.$$

The matching conditions on $\nu = 0$ are given by:

$$1 + A(k) = B(k)$$
$$-\frac{3}{16\pi G\gamma^2\Delta\ell_p^2}\Big[\Psi(-4\sqrt{\Delta}\ell_p) + \Psi(4\sqrt{\Delta}\ell_p) - 2\Psi(0)\Big]$$
$$+\frac{\mu}{\Delta\ell_p^4}\Psi(0) = \frac{E(k)}{V_0}\Psi(0),$$

where the first equation comes from continuity at $\nu = 0$, the second equation from the time-independent Schrodinger equation. The solution of the previous equations is

$$A(k) = \frac{-i\Theta(k)}{1 + i\Theta(k)}$$
$$B(k) = \frac{1}{1 + i\Theta(k)} \tag{40}$$

where

$$\Theta(k) \equiv \frac{16\pi\gamma^2}{3}\frac{\mu}{\sin(2k\sqrt{\Delta}\ell_p)}. \tag{41}$$

We consider an in-state of the form (valid for early times)

$$|\psi_{in}, t\rangle = \frac{\pi}{\sqrt{2\Delta}\ell_p}\int db\left(\psi(b; b_0, \nu_0)\,|b, 1\rangle + \psi(b; b_0, \nu_0)\,|b, 2\rangle\right)e^{-iE_\Delta(b)t}, \tag{42}$$

where $\psi(b; b_0, \nu_0)$ is a wave function picked at a $b = b_0$ value and $\nu = \nu_0$. Notice that we are superimposing two wave packets supported on lattices Γ^1 and Γ^2, respectively. We can now write the pure in-density matrix

$$\rho_{\rm in}(t) = \frac{\pi^2}{2\Delta\ell_p^2}\int db\, db'\, e^{i[E_\Delta(b) - E_\Delta(b')]t} \tag{43}$$
$$\times\Big[\,|b', 1\rangle\,\psi(b'; b_0, \nu_0) + |b', 2\rangle\,\psi(b'; b_0, \nu_0)\Big]$$
$$\Big[\,\langle b, 1|\,\overline{\psi}(b; b_0, \nu_0) + \langle b, 2|\,\overline{\psi}(b; b_0, \nu_0)\Big] \tag{44}$$

which scatters into the out-density matrix

$$\rho_{\rm out}(t) = \frac{\pi^2}{\Delta\ell_p^2}\int db\, db'\, e^{i[E_\Delta(b) - E_\Delta(b')]t}$$
$$\Big[\,\langle b, 1|\,\overline{\psi}(-b; b_0, \nu_0)\overline{A}(-b) + \langle b, 1|\,\overline{\psi}(b; b_0, \nu_0)\overline{B}(b)$$
$$+\langle b, 2|\,\overline{\psi}(b; b_0, \nu_0)\Big]$$
$$\Big[\,|b', 1\rangle\,\psi(-b')e^{-ib'\overline{\nu}}A(-b') + |b', 1\rangle\,\psi(b')e^{ib'\overline{\nu}}B(b')$$
$$+|b', 2\rangle\,\psi(b'; b_0, \nu_0)\Big].$$

Let us assume that $\psi(b)$ is highly picked at a b_0 so that we can substitute the integration variables b and b' by b_0 and have a finite dimensional representation of the reduced density matrix after the scattering (this step is rather formal, it involves an approximation but it helps when visualizing the result). In the relevant 4×4 sector (with basis elements ordered as $\{|1, b_0\rangle, |1, -b_0\rangle, |2, b_0\rangle, |2, -b_0\rangle\}$), we get the matrix representation

$$\boldsymbol{\rho}_{in} = \begin{pmatrix} \frac{1}{2} & 0 & \frac{1}{2} & 0 \\ 0 & 0 & 0 & 0 \\ \frac{1}{2} & 0 & \frac{1}{2} & 0 \\ 0 & 0 & 0 & 0 \end{pmatrix} \rightarrow \boldsymbol{\rho}_{out}$$
$$= \frac{1}{2}\begin{pmatrix} |B(b_0)|^2 & \overline{A}(-b_0)B(b_0) & B(b_0) & 0 \\ A(-b_0)\overline{B(b_0)} & |A(-b_0)|^2 & A(-b_0) & 0 \\ \overline{B(b_0)} & \overline{A(-b_0)} & 1 & 0 \\ 0 & 0 & 0 & 0 \end{pmatrix}. \tag{45}$$

2.5. Matter Coupling Produces a Coarse-Graining Entropy Jump at the Big Bang

A reduced density matrix encoding the notion of coarse graining associated with the low-energy equivalence of the ϵ sectors is defined by tracing over the discrete degrees of freedom labeling the component of the state in either the Γ_1 or the Γ_2 lattices. In other words, tracing over the two (macroscopically indistinguishable) ϵ sectors, namely

$$\langle b|\,\rho^{\rm R}\,|b'\rangle \equiv \sum_{i=1}^{2}\langle b, i|\,\rho\,|b', i\rangle\,. \tag{46}$$

In other words, the subspace of the Hilbert space we are working with is the one supported on two different ϵ sectors $\mathscr{H}(\Gamma^1) \oplus \mathscr{H}(\Gamma^2) \subset \mathscr{H}_{\rm lqc}$ which, as the two terms are isomorphic $\mathscr{H}(\Gamma^1) \approx \mathscr{H}(\Gamma^2) \approx \mathscr{H}_0$, $\mathscr{H}(\Gamma^1) \oplus \mathscr{H}(\Gamma^2) \subset \mathscr{H}_{\rm lqc}$ can be written as

$$\mathscr{H}_0 \otimes \mathbb{C}^2 \subset \mathscr{H}_{\rm lqc}. \tag{47}$$

The coarse graining is defined by tracing over the $\mathbb{C}^2$ factor. This implies that from the previous 4×4 matrix, we obtain 2×2 reduced density matrices. The reduced density matrix $\boldsymbol{\rho}^{\rm R}_{in}$ remains pure, explicitly

$$\boldsymbol{\rho}^{\rm R}_{in} = \frac{1}{2}\begin{pmatrix} 1 & 1 \\ 1 & 1 \end{pmatrix}. \tag{48}$$

Nevertheless, the reduced density matrix $\boldsymbol{\rho}^{\rm R}_{out}$ is now mixed, namely

$$\boldsymbol{\rho}^{\rm R}_{out} = \frac{1}{2}\begin{pmatrix} 1 + |B(b_0)|^2 & \overline{A}(-b_0)B(b_0) \\ A(-b_0)\overline{B(b_0)} & |A(-b_0)|^2 \end{pmatrix}. \tag{49}$$

We can now compute the entanglement entropy. To first order the cosmological constant, the result is

$$\delta S = \log(2) - \frac{3\Delta\Lambda{\ell_p}^2}{128\pi^2\gamma^2\mu^2} + \mathscr{O}(\Lambda^2\ell_p^4) \tag{50}$$

The behavior as a function of b is shown in **Figure 4**. In **Appendix C1**, we discuss an alternative definition of coarse graining with the same qualitative implications.

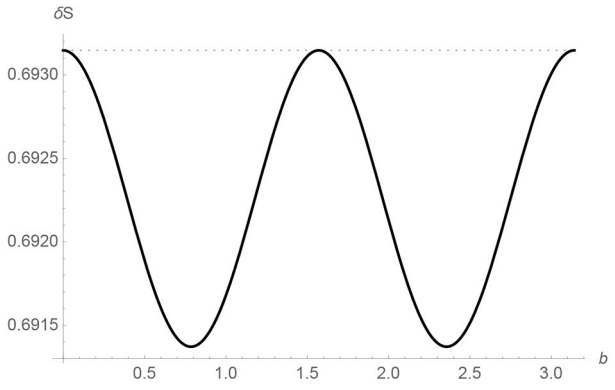

FIGURE 4 | The curve represented by a thin line is the entropy jump δS as a function of b in Planck units for $\gamma = \mu = \Delta = 1$. The small $b\ell_p$ behavior in (93) is apparent. The entropy is periodic for $b\ell_p \in [0, \pi]$ as expected from (86). The dotted line represents the maximum possible entropy which is log[2] in our model.

3. QUANTUM COSMOLOGY ON A SUPERPOSITION OF BACKGROUNDS

In the first part of this paper, we have seen how the fact that the Hilbert space of loop quantum cosmology is vastly larger than the standard Schrodinger representation implies (via coarse graining) that the coarse-graining entropy would rise generically through the evolution across the big bang *would-be-singularity*. In this section, we explore another closely related feature that leads to an apparent non-unitary evolution when dynamics are probed by a low-energy agent. The quantum dynamics in loop quantum cosmology depend on a UV regulator known as the area-gap Δ (section 2.1). We will see here that the loop quantum cosmology model can be extended naturally to admit superpositions of dynamics with different regulators. Such an extension generally leads to the dynamical development of correlations between the macroscopic and the microscopic degrees of freedom. If the microscopic degrees of freedom are assumed to remain hidden to low-energy observers, then such correlations lead to an apparent violation of unitarity in the low-energy description where pure states evolve into mixed states. In other words, the UV data needed to define the quantum dynamics open an independent microscopic channel for information to be degraded.

3.1. The UV Input in Quantum Cosmology: Revisiting the $\bar{\mu}$ Scheme

The $\bar{\mu}$ scheme was designed to avoid an inconsistency in an early model of loop quantum cosmology with the low-energy limit (or large universe limit) of loop quantum cosmology (Green and Unruh, 2004). The problem arises from the effective compactification of the connection variable c due to the polymer regularization of the Hamiltonian with a fixed fiducial scale μ which implies that c and $c + 4\pi/\mu$ are dynamically identified. This leads to anomalous deviations from classical behavior in situations where the variable c is classically expected to be unbounded for large universes. This can be seen clearly in the present situation where the unimodular Hamiltonian (17) is given, in (c, p) variables, by

$$H = \frac{3V_0}{8\pi G}\frac{c^2}{\gamma^2|p|}. \tag{51}$$

For non-vanishing energies (or equivalently non-vanishing cosmological constants), the conservation of the Hamiltonian implies that c grows as $|p| \propto a^2$, i.e., c grows without limits as the universe expands so that no matter how small μ is, anomalous effects due to the compactification of the c become relevant at macroscopic scales (Noui et al., 2005). As no quantum gravity effects seem acceptable in the large universe regime for a model with finitely many degrees of freedom, this anomaly is seen as an inconsistency of the model.

The $\bar{\mu}$ scheme solves this inconsistency by "renormalizing" the regulating scale μ as the universe grows (Equation 20). The interesting thing is that such a renormalization is justified by quantum geometry arguments that link the mini superspace model of loop quantum cosmology to the geometry of a microscopic background state in the full theory. The argument explicitly uses the idea that the low-energy degrees of freedom (dynamical variable of loop quantum cosmology) arise from the coarse graining of the fundamental ones in loop quantum gravity.

Here we review the construction of the $\bar{\mu}$ scheme as described in Ashtekar and Singh (2011). Consider a fundamental quantum geometry state $|s\rangle$ in the Hilbert space of loop quantum gravity, representing a microscopic state on top of which the quantum cosmological coarse-grained dynamics will eventually be defined. Such an underlying fundamental state will have to be approximately homogeneous and isotropic up to a scale of $L > \ell_p$ with respect to the preferred foliation defining the comoving FLRW observers at low energies. If that is the case then such space slices can be divided into (approximately) cubic 3-cells of physical side length L which all have approximately equivalent quantum geometries. The area of a face of such cubic cells in Planck units will be denoted Δ_s so that $L^2 = \ell_p^2\Delta_s$. Note that Δ_s is a property of the underlying microstate: an area eigenstate if the microstate is an eigenstate, or an area expectation value if the state is sufficiently peaked on a quantum geometry and has small fluctuations around it. A simple realization is the one where Δ_s is an area eigenvalue, and the important assumption is that Δ_s is the same for all cells (this encodes the homogeneity of the microscopic state). Consider the area of a large two-dimensional surface (the face of a fiducial cell V), whose area is measured by the low-energy (coarse-grained) quantity p used as the configuration variable in loop quantum cosmology. We naturally would expect that $|p| \gg \ell_p^2$ or alternatively that

$$N\ell_p^2\Delta_s = |p|, \tag{52}$$

where N denotes the number of microscopic cells contained in the coarse-grained surface (a face of V), and $N \gg 1$. The fiducial cell has a fiducial coordinate volume V_0 and hence fiducial side coordinate length $V_0^{1/3}$. Therefore, the fiducial coordinate length

$\bar{\mu}$ of the microscopic homogeneity cells is given by the relation

$$N(\bar{\mu}V_0^{1/3})^2 = V_0^{2/3}. \tag{53}$$

Combining the previous two equations, one recovers Equation (20), namely

$$\bar{\mu}_s^2 \equiv \bar{\mu}^2 = \frac{\ell_p^2 \Delta_s}{|p|}, \tag{54}$$

i.e., the fiducial scale $\bar{\mu}$ is dynamical: as the universe grows (and $|p|$ becomes larger), the underlying fiducial length scale decreases. The fiducial regularization scale (53) depends on the fundamental state $|s\rangle$ via the quantity Δ_s, hence we denote it as $\bar{\mu}_s$. When such a dynamical scale is used in the regularization of the quantum cosmology Hamiltonian, the effective compactification scale for c grows like $|p|$ and the inconsistency previously discussed is avoided. This is transparent in terms of the new canonical pair (b, v). From Equation (15), we can see that $b = c\bar{\mu}_s/(\sqrt{\Delta_s}\ell_p)$, in contrast with c (see 17), remains constant (see 51) in the de Sitter universe. The quantization of the Hamiltonian presented in section 2.1 introduces an effective compactification of the variable b whose dynamical effect is now only relevant when the cosmological constant approaches one in Planck units. This can be seen from (21). The cosmological constant is bounded from above by its natural value in Planck units due to the underlying quantum geometry structure while the anomalous IR behavior is avoided (the problems exhibited in the model studied in Green and Unruh, 2004 are also resolved).

The above is the standard account of the motivation of the $\bar{\mu}$ scheme of Ashtekar et al. (2006) with the little twist (which is very important for us here) that Δ_s need not be the lowest area eigenvalue of loop quantum gravity. In the usual argument, the microscopic state is thought to be built from a special homogeneous spin network (geometry eigenstate) with all spins equal to the fundamental representation. This implies that, in the above construction, $\Delta_s = \Delta_{1/2} \equiv 2\pi\gamma\sqrt{3}$. The observation here is that Δ_s can take different values according to the microscopic properties of the underlying quantum geometry state. One could take for instance all spins equal to the vector representation and then have $\Delta_s = \Delta_1 \equiv 4\pi\gamma\sqrt{2}$ instead, or take j as arbitrary and use $\Delta_s = \Delta_j$. It is important to point out that such a possibility can arise naturally in quantum cosmology models obtained in the group field theory framework (Gielen et al., 2013; Oriti et al., 2016 , 2017).

As we have seen in section 3.1, the field strength regularization, and hence the Hamiltonian, depend on the value Δ_s of the background (approximately homogeneous) spin network state $|s\rangle$ through the dynamical scale $\bar{\mu}_s$. In this way, the dynamics of loop quantum cosmology establish correlations with a microscopic degree of freedom in the underlying loop quantum gravity fundamental state. As such a degree of freedom (the area eigenvalue Δ_s of the minimal homogeneity cells) is quantum, it is natural to model the system by a tensor product Hilbert space $\mathscr{H} \equiv \mathscr{H}_m \otimes \mathscr{H}_{\rm qc}$, where $\mathscr{H}_m$ is the Hilbert space representing the microscopic degree of freedom encoded in the minimal homogeneous cell operator (whose eigenvalues we denote as Δ_s), and $\mathscr{H}_{\rm qc}$ the standard kinematical Hilbert space of loop quantum cosmology.

General states in $\mathscr{H}$ can be expressed as linear combinations of product states $|s\rangle \otimes \psi$ in the respective factor Hilbert spaces. The quantum Hamiltonian has a natural definition on such states and therefore on the whole of $\mathscr{H}$, namely

$$\hat{H} \triangleright (|s\rangle \otimes \psi) = |s\rangle \otimes \hat{H}_{\Delta_s} \triangleright \psi, \tag{55}$$

where $\hat{H}_{\Delta_s}$ is the usual loop quantum cosmology Hamiltonian in the $\bar{\mu}_s$ scheme, which in our particular case is defined in Equation (21) with regulator $\Delta = \Delta_s$.

Notice that the previous extension of the standard loop quantum cosmology framework to the larger Hilbert space $\mathscr{H}$ is also natural from the perspective of the full theory. Indeed, the generally accepted regularization procedure of the Hamiltonian constraint in loop quantum gravity (first introduced by Thiemann, 1998 and further developed in recent analysis—see Ashtekar and Pullin, 2017 and references therein) is state dependent in that the loops defining the regulated curvature of the connection are added on specific nodes of the state where the Hamiltonian is acting upon. This feature finds its analog in the action (55) where the regulating scale Δ_s depends on the state $|s\rangle \in \mathscr{H}_m$.

In order to simplify the following discussion we will restrict states in $\mathscr{H}_m$ even further and consider a subspace $\mathfrak{h} = \mathbb{C}^2 \subset \mathscr{H}_m$, i.e., we will model the situation where the underlying microscopic state is an arbitrary superposition of only two fixed microscopic homogeneous spin-network states. For example we take

$$\mathfrak{h} \equiv \text{span}\Big[\,|+\rangle\,, |-\rangle\,\Big], \tag{56}$$

where $|\pm\rangle \in \mathscr{H}_m$ are two suitable orthogonal background states (these two states will be conveniently picked below). From the infinitely dimensional Hilbert space $\mathscr{H}_m$ we are now selecting a single *q-bit* subspace $\mathbb{C}^2$. The Hilbert space of our model is

$$\mathscr{H} = \mathfrak{h} \otimes \mathscr{H}_{\rm qc}. \tag{57}$$

The factor $\mathfrak{h}$ represents additional microscopic (hidden to low-energy observers) UV degrees of freedom, while $\mathscr{H}_{\rm qc}$ encodes the data that under suitable circumstances (e.g., when the universe is large) represent the low-energy cosmological degrees of freedom.

In this way we see that in addition to the intrinsic degeneracy of energy eigenvalues analyzed in the first part of this paper, there is another candidate for the microscopic degree of freedom associated with the regularization of the Hamiltonian action via the $\bar{\mu}$-scheme. Both mechanisms are correct for the present loop quantum cosmology toy model but reflect generic properties of the full theory of loop quantum gravity. More generally, we expect similar features to be present in any quantum gravity approach where smooth geometry is only emergent from a discrete fundamental theory.

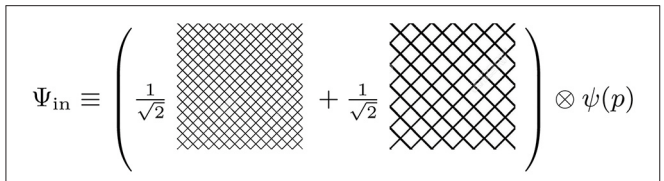

FIGURE 5 | Schematic representation of the state of interest. There are two different UV structures with dynamical implications via the $\bar{\mu}$ scheme. The state represented here has trivial correlations with the microscopic structure and would lead to a zero initial entanglement entropy state as defined by the reduced density matrix where the background state is traced out.

From now on we adopt the convenient notation $|s\rangle$ with $s = \pm$ for such preferred basis elements of $\mathfrak{h}$. With this notation, and using (21), the Hamiltonian (55) becomes

$$\begin{aligned}\hat{H}_0 \triangleright (|s\rangle \otimes |\psi\rangle) &= \frac{3V_0}{8\pi G\gamma^2}\frac{1}{\Delta_s \ell_p^2}\left(\sin(\sqrt{\Delta_s}\ell_p\, b)\right)^2 \triangleright |s\rangle \otimes |\psi\rangle \\ &= -\frac{3V_0}{8\pi G\gamma^2}\sum_\nu \frac{1}{2\Delta_s\ell_p^2}\,|s\rangle \otimes |\nu\rangle \Big[\Psi(\nu \\ &\quad - 4\sqrt{\Delta_s}\ell_p) + \Psi(\nu + 4\sqrt{\Delta_s}\ell_p) - 2\Psi(\nu)\Big],\end{aligned} \tag{58}$$

where $\Psi(\nu) \equiv \langle \nu|\psi\rangle$.

Now, the only special feature of the basis $|\pm\rangle$ is that it is preferred from the perspective of the regularization of the effective (unimodular) loop quantum cosmology Hamiltonian. Consequently, a natural question for the quantum theory is how the dynamics would look if the initial state is arbitrary in factor $\mathfrak{h}$? More precisely, what if we consider the linear combination of two background spin networks $\frac{1}{\sqrt{2}}(|+\rangle + |-\rangle) \in \mathfrak{h}$ times a loop quantum cosmology wave function as depicted in **Figure 5**? To answer this question we consider a special initial state where correlations between the low-energy and the UV degrees of freedom are not present. This will lead to a reduced density matrix—tracing out the microscopic space $\mathfrak{h}$ in (57)—that is *pure* initially, the form of such a state is illustrated in **Figure 5**. At the same time we want to be able to diagonalize the Hamiltonian with such uncorrelated initial states; more precisely this boils down to diagonalizing both H_{Δ_+} and H_{Δ_-} in $\mathscr{H}_{\rm lqc}$. This implies that the factor $\psi(\nu) \in \mathscr{H}_{\rm lqc}$, in **Figure 5**, must be supported on a lattice Γ^ϵ_Δ that is left invariant by the action of both H_{Δ_+} and H_{Δ_-} (left invariant in the sense that the shift operators in the definition of the Hamiltonian only relate to points of Γ^ϵ_Δ and never map points out). This can be achieved by assuming that $\sqrt{\Delta_+} = m\sqrt{\Delta_-}$ for some natural number m. For simplicity we will take $m = 2$ from now on[11]. The parameter ϵ will be taken so that the lattice Γ^ϵ_Δ contains the point $\nu = 0$. This is a standard choice. With all this, the invariant lattice, denoted as Γ_{Δ_-}, is

$$\Gamma_{\Delta_-} \equiv \Gamma^{\epsilon=0}_{k=2\sqrt{\Delta_-}\ell_p}. \tag{59}$$

Note that in the notation described below (37), we have that $\Gamma_{\Delta_-} = \Gamma_1 \cup \Gamma_2$.

The choices made above are not mandatory. One could have chosen a different initial state. The previous choice is particularly interesting here because it would lead to a reduced initial density matrix that is pure and hence initially had vanishing entanglement entropy. Other states would involve correlations and would therefore carry a non vanishing entropy load from the beginning. For the discussion that interests us here and for the analogy with black hole evaporation, it is more transparent to set the entropy to zero initially.

An arbitrary (unimodular) loop quantum cosmology state associated with such a choice of background state can be expressed as:

$$\begin{aligned}\Psi_{\rm in}(\nu, t) &= \langle \nu|\,\frac{1}{\sqrt{2}}\sum_s |s\rangle \otimes |\Psi_{\rm in}(t)\rangle \\ &= \frac{1}{\sqrt{2}}\sum_s |s\rangle \otimes \Big[\delta_{\Gamma_{\Delta_-}}(\nu) \\ &\quad \int_0^{\frac{\pi}{\sqrt{\Delta_-}\ell_p}} dk\, \psi(k; b_0, \nu_0)\exp(-iE_s(k)t)\Big]\end{aligned} \tag{60}$$

where $\psi(k; b_0, \nu_0)$ is a properly normalized function peaked at $k = b_0$ and $\nu = \nu_0$. The initial state in the momentum representation is given by:

$$\begin{aligned}\Psi_{\rm in}(b, t) &= \sum_{\nu\in\Gamma^0_{\Delta_-}} \langle b, 1\cup 2|\nu\rangle\, \langle \nu|\Psi_{\rm in}(t)\rangle \\ &= \frac{\pi}{\sqrt{\Delta_-}\ell_p}\sum_s |s\rangle \otimes \psi(b; b_0, \nu_0)e^{-iE_s(b)t}\end{aligned} \tag{61}$$

Where, in the first line, we used the natural extension of the notation introduced in (37) where $|b, 1\cup 2\rangle$ means an eigenstate of the corresponding shift operators (19) supported on the lattice $\Gamma_{\Delta_-} = \Gamma_1 \cup \Gamma_2$. Notice that we can also write

$$|b, 1\cup 2\rangle = |b, 1\rangle + |b, 2\rangle\,, \tag{62}$$

keeping in mind that terms on the *r.h.s.* are individually eigenstates of the shift operators with twice the lattice spacing of Γ_{Δ_-}. We also used

$$\sum_{\nu\in\Gamma^0_{\Delta_-}} \exp\left(i\frac{b-k}{2}\nu\right) = \frac{\pi}{\sqrt{\Delta_-}\ell_p}\delta(b-k). \tag{63}$$

We can then write

$$\Psi_{\rm in}(t) = \sum_s \int \mathrm{D}b\, |s\rangle \otimes |b, 1\cup 2\rangle\, \psi(b; b_0, \nu_0)e^{-iE_s(b)t}, \tag{64}$$

where

$$\mathrm{D}b \equiv \frac{\pi}{\sqrt{2\Delta_-}\ell_p}db, \tag{65}$$

[11]One might be worried that this is hard to achieve if one sticks to the form of the area spectrum of loop quantum gravity. This is however simply a model and the link with the full theory (remember) must be taken at the heuristic level. Nevertheless, solutions do exist for instance $m = 4$ for $j_+ = 3$ and $j_- = 1/2$.

is the Haar measure on the circle of circumference $\pi/\sqrt{2\Delta_-}\ell_p$. We notice from (64) that even when our initial state contains no correlations between the low energy degrees of freedom represented by b and the microscopic degrees of freedom encoded in $|s\rangle$ at $t = 0$, quantum correlations between the two will develop with time due to the non trivial dependence of the energy spectrum with s. Even when this is quite clear from (64), one can state this fact in an equivalent way by analysing the (pure) density matrix $\rho_{\rm in}(t) \equiv |\Psi_{\rm in}(t)\rangle\langle\Psi_{\rm in}(t)|$, whose matrix elements in the b basis are:

$$\rho_{\rm in}(t) \equiv \sum_{s,s'} \int {\rm D}b\, {\rm D}b' \left(\overline{\psi}(b;b_0,\nu_0)\psi(b';b_0,\nu_0)\, e^{i[E_s(b)-E_{s'}(b')]t}\right) \times |b',1\cup 2\rangle\, |s'\rangle\, \langle b,1\cup 2|\, \langle s|\,. \tag{66}$$

As coarse-grained observers are assumed to be insensitive to the microscopic structure encoded here in the "spin" quantum number s, low-energy physical information is encoded in the reduced density matrix

$$\rho_{\rm inR}(t) \equiv \sum_{s} \int {\rm D}b\, {\rm D}b' \left(\overline{\psi}(b;b_0,\nu_0)\psi(b';b_0,\nu_0)\, e^{i[E_s(b)-E_s(b')]t}\right) \tag{67}$$

$$\times\ |b',1\cup 2\rangle\, |s'\rangle\, \langle b,1\cup 2|\, \langle s|\,, \tag{68}$$

which can be simply be written as

$$\rho_{\rm inR}(t) = \frac{1}{2}\sum_s |\Psi_s(t)\rangle\langle\Psi_s(t)| \tag{69}$$

where

$$|\Psi_s(t)\rangle \equiv \int {\rm D}b\, \psi(b;b_0,\nu_0)\, e^{-iE_s(b)t}\ |b,1\cup 2\rangle\,. \tag{70}$$

Notice that (69) is only pure at $t = 0$ and becomes mixed due to the correlations evoked above as time passes. One can compute the entanglement entropy $S(t) \equiv -{\rm Tr}\left[\rho_{\rm inR}(t)\log(\rho_{\rm inR}(t))\right]$ which turns out to be given by the simple analytic expression (see **Appendix A**)

$$S(t) = -\log\left(1-\frac{\delta}{2}\right) - \frac{\delta}{2}\log\left(\frac{\delta}{1-\frac{\delta}{2}}\right), \tag{71}$$

where

$$\delta(t) \equiv 1 - \left|\int {\rm D}b\, \overline{\psi}(b;b_0,\nu_0)\psi(b;b_0,\nu_0) e^{i[E_+(b)-E_-(b)]t}\right|. \tag{72}$$

For generic wave packets $\psi_s(b)$, the entanglement entropy is a monotonic growing function of time which grows asymptotically to the maximally mixed situation $S_{\rm max} = \log(2)$ (see an example in **Figure 6**).

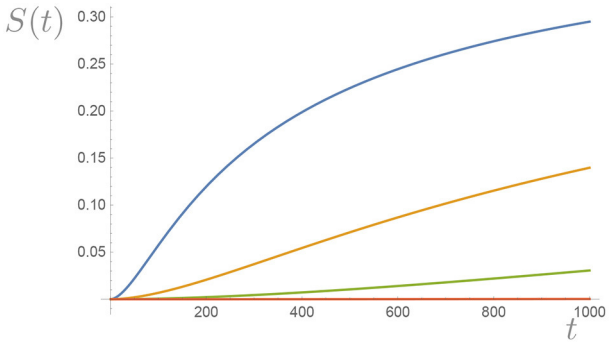

FIGURE 6 | Here we plot $S(t)$ as a function of time for a Gaussian wave packet centered at $b = 2.5\ 10^{-2}$, $b = 5\ 10^{-2}$, $b = 7\ 10^{-2}$, and $b = 10^{-1}$ with width $\sigma = b$, respectively. Numerical integration plus the approximation (73) was used with the assumption that $2(\Delta_+ - \Delta_-)/\gamma^2 = 1$, all in Planck units. As b grows the scalar curvature (the cosmological constant) grows and the rate at which entropy increases grows as well. For $b \ll 1$, an effective unitary evolution is recovered.

A more intuitive picture can be obtained from a suitable expansion of the energy eigenvalues (24) in powers of the label $b\ell_p$

$$E_s(b) = \frac{3V_0}{8\pi G\gamma^2}\frac{1}{\Delta_s\ell_p^2}\left(\sin(\sqrt{\Delta_s}\ell_p b)\right)^2 = \frac{3V_0}{8\pi G\gamma^2}b^2 - \frac{V_0}{8\pi G\gamma^2}\Delta_s\ell_p^2 b^4 + b^2\mathcal{O}(\ell_p^4 b^4). \tag{73}$$

Such an expansion makes sense in that it allows for the identification of the low energy effective Hamiltonian (the one that one would define in a purely Wheeler-DeWitt quantization) plus corrections that involve interactions with the underlying discrete structure of LQG here represented by the spin s degree of freedom. Namely, we can read from the previous expansion that

$$H_{\rm eff} \equiv H^0_{\rm eff}(b) + \Delta H(b,s), \tag{74}$$

where $\hat{H}^0_{\rm eff}(\hat{b}) \equiv \frac{6}{\gamma^2}\hat{b}^2$ is the Wheeler-DeWitt Hamiltonian and the additional term is an interaction with the environment represented by the underlying discrete structure represented by the dependence on s (a hidden degree of freedom from the low-energy continuum perspective). Of course, the hats in the previous equation denote operators in a different representation (the continuum Schrodinger representation) that is not unitarily equivalent to the "fundamental" polymer representation introduced in section 2.1 and used in the LQC setup (recall for instance that the operator $\hat{b}$ does not even exist in the polymer representation).

The lack of purity for $t > 0$ of the reduced density matrix (69) is due to correlations that develop between the low-energy degree of freedom b and the hidden microscopic degree of freedom s via this non trivial interaction Hamiltonian. This means that generically [i.e., for arbitrary initial states $\psi_s(b)$], the fundamental evolution would seem to violate unitarity, from the

perspective of low-energy observers, due to the decoherence with the microscopic quantum geometric structure. Notice however that for states $\psi_s(b)$ picked at sufficiently small $\bar{k}$, i.e., $\bar{k}\sqrt{\Delta_s}\ell_p \ll 1$, we have from (22) that

$$\Lambda(b) \approx 3\gamma^{-2}b^2 \tag{75}$$

and the density matrix (69) is pure at all times.

More precisely, we can translate the criterion for the absence of decoherence with the underlying microscopic discrete structure in terms of the value of the cosmological constant of the given state. For an eigenstate of the Hamiltonian the relation is given by $\Lambda \equiv E_s(b)$. Therefore the criterion for the absence of decoherence in terms of the cosmological constant is

$$\Delta_s \ell_p^2 \gamma^2 \Lambda \approx \ell_p^2 \Lambda \ll 1 \tag{76}$$

Interestingly, for states with low values of the cosmological constant in natural units—equivalent semi-classically to the scalar curvature R in our matter-free model—define a decoherence free subspace. When the cosmological constant does not satisfy condition (76), decoherence with the microscopic structure is turned on and maximized for Λ of order one in Planck units: notice incidentally that due to the polymer quantization the cosmological constant is bounded by

$$\Lambda_{\max} = \frac{3}{\gamma^2 \Delta_{\frac{1}{2}} \ell_p^2}. \tag{77}$$

For low values of Λ, unitarity is recovered in the effective description that ignores the microscopic structure.

Decoherence takes place here due to an interaction between the low-energy coarse degrees of freedom and the microscopic discreteness in the underlying quantum geometry background, but in a way (in our simple model) that the energy and hence the cosmological constant is conserved. However, the presence of decoherence suggests the possibility for a natural deviation of this idealized absence of dissipation: generally decoherence and dissipation often come together. Therefore, a surprising and unexpected consequence of our analysis is the suggestion of a natural channel for the relaxation of a large cosmological constant due to the possibility of dissipative effects associated with the decoherence pointed out here.

Incidentally, all this shows that only in the limit of low values of E (small cosmological constant), the coarse graining that leads from the full theory of loop quantum gravity to the mini superspace description of loop quantum cosmology is well-defined. This is not surprising and only confirms the usual intuition that drives the construction of models of loop quantum cosmology. However, it opens the door for a qualitative understanding of the necessity of decoherence effects in more general situations. For instance, the standard $\bar{\mu}_s$ construction suggests that coarse graining is weaker at the big bang where the Hamiltonian evolution (58) takes the universe through the $\nu = 0$ states. During this high (spacial) curvature phase it is natural to expect that the higher corrections in (73) (describing the interaction with the microscopic Planckian structure) can no longer be neglected.

Interestingly, there is another way to make decoherence disappear. This is due to the asymptotic behavior of the separation of area eigenvalues in loop quantum gravity which imply that for large Δ_s there are states such that $\Delta_s - \Delta_{s'} \approx \Delta_s \exp(-\pi\sqrt{2\Delta_s/3})$ (Fernando Barbero et al., 2018). Therefore, in the continuum limit $\Delta_s - \Delta_{s'} \ll 1$ the dynamical entanglement growth of our model can be made as small as wanted.

3.2. Matter Coupling Produces an Entanglement Entropy Jump at the Big Bang

In the pure gravity case, we can make decoherence as small as needed by choosing states with a cosmological constant that is sufficiently small. Here we show that this is no longer possible once matter is added and that there is a generic development of correlations with the UV degrees of freedom in the evolution across the *would-be-singularity*: an initially pure state (reduced low-energy density matrix) evolves generically into a mixed state (reduced low-energy density matrix) after the big bang.

In order to see this in more detail, we just need to write out the matter Hamiltonians acting in the Hilbert space (57). One needs the natural generalization of the expressions written in section 2.3 for the present context. For instance, for scalar field coupling, Equation (32) becomes

$$\hat{H}_\phi \triangleright (|s\rangle \otimes |\psi\rangle) = -m \sum_{\nu \in \Gamma} |s\rangle \otimes |\nu\rangle \, h_\phi(\nu; \sqrt{\Delta_s}\ell_p)\Psi(\nu, \phi), \tag{78}$$

where

$$h_\phi(\nu; \lambda) \equiv \frac{p_\phi^2}{16\lambda^4}\left(|\nu + 2\lambda|^{\frac{1}{2}} - |\nu - 2\lambda|^{\frac{1}{2}}\right)^4. \tag{79}$$

The momentum p_ϕ commutes with the Hamiltonian and thus is a constant of motion. As before, if we consider an eigenstate of p_ϕ then the problem reduces again to a scattering problem with a potential decaying like $1/\nu^2$ when solving the time-independent Schrodinger equation

$$\hat{H}_0 + \hat{H}_\phi \triangleright (|s\rangle \otimes |\psi\rangle) = E\,(|s\rangle \otimes |\psi\rangle)\,. \tag{80}$$

From the discussion in section 2.3, we can capture the basic qualitative effect of matter interaction by considering a simple solvable model where the matter contribution is concentrated at a single event at the big bang. None of the qualitative conclusions that follow depend on this simplification, and a more realistic free scalar field model can be dealt with (some results are shown in **Appendix D**). With some extra effort one could actually analyze a more realistic model [say the one defined by (78)] but the conclusion will remain the same. Therefore, we consider

$$\hat{H} = \hat{H}_0 + \mu \hat{H}_{\text{int}}, \tag{81}$$

where μ is a dimensionless coupling, $\hat{H}_0$ is given in (58), and $\hat{H}_{\text{int}}$ is the generalization of (36)

$$\hat{H}_{\text{int}} \triangleright (|s\rangle \otimes |\psi\rangle) \equiv \sum_\nu \hat{O}\,|s\rangle \otimes |\nu\rangle \, \frac{\delta_{\nu,0}}{\sqrt{\Delta_s}}\Psi(0) \tag{82}$$

where $\hat{O}$ is a self adjoint operator in $\mathfrak{h} = \mathbb{C}^2$. A natural and simple model for this operator is to choose

$$\hat{O} \equiv \ell_p^{-4} \frac{V_0}{\sqrt{\Delta_s}}. \tag{83}$$

This choice is formulated in the notation introduced below (58) and inspired by the analogy with a spin system. We have added by hand an interaction Hamiltonian that switches on only when the universe evolves through the *would-be-singularity* at the zero volume state. This encodes the idea of the intrinsic uncertainty of the peculiar construction of the mini superspace model of loop quantum cosmology that we discussed in section 3.1. The discrete local degrees of freedom must be important close to the big bang and symmetry reduction must fail in some way that can only be correctly described if a full quantum gravity theory is available. Here we model such unknown dynamics in the simplest fashion available to us here, which consists of including the possibility for the background state $|s\rangle$ (representing in spirit the underlying quantum geometry) to be modified by the dynamics via $\hat{H}_{\rm int}$.

Here we proceed as in section 2.4 while keeping in mind that, in the present case, there are two distinct cases at hand given by the two possible values $\Delta_\pm$. Let us consider an in-state of the form

$$|k, s\rangle = |s\rangle \otimes |\nu\rangle \begin{cases} e^{-i\frac{k}{2}\nu} + A_s(k)\, e^{i\frac{k}{2}\nu} & (\nu \geq 0) \\ B_s(k)\, e^{-i\frac{k}{2}\nu} & (\nu \leq 0), \end{cases} \tag{84}$$

where $A_s(k)$ and $B_s(k)$ are coefficients depending on k and (in contrast with the case in section 2.4) now also on $s = \pm 1$ (with $|\pm\rangle$ the eigenstates of $\hat{S}_z$). For suitable coefficients, such states are eigenstates of the Hamiltonian H_0 as well as the full Hamiltonian (35). Arbitrary solutions (wave packets) can then be constructed in terms of appropriate superpositions of these "plane-wave" states.

$$\begin{aligned} A_s(k) &= \frac{-i\Theta_s(k)}{1 + i\Theta_s(k)} \\ B_s(k) &= \frac{1}{1 + i\Theta_s(k)} \end{aligned} \tag{85}$$

where

$$\Theta_s(k) \equiv \frac{16\pi\gamma^2}{3} \frac{\mu}{\sin(2k\sqrt{\Delta_s}\ell_p)}. \tag{86}$$

One can superimpose the previous eigenstates to produce wave packets (semiclassical states) for the wave function of the universe that are picked at value ν_0 of the rescaled volume (see footnote 6). Wave packets will evolve in time according to the Schrodinger equation which in our case is just a discrete analog of the one corresponding to a free particle in quantum mechanics with an interaction term at the "origin" $\nu = 0$. If we start with a state that is sufficiently picked around ν_0 for $\nu \gg \ell_p$ initially, then the state can be described in terms of the superposition (64) where the explicit values of the coefficients $A_s(b)$ and $B_s(b)$ do not appear. Equation (42) is generalized to

$$\begin{aligned} \Psi_{\rm in}(t \ll 0) = &\int \mathrm{D}b \left(|b,1\rangle\, \psi(b; b_0, \nu_0) \right. \\ &\left. + |b,2\rangle\, \psi(b; b_0, \nu_0) \right) e^{-iE_-(b)t} \\ + &\int \mathrm{D}b \left(|b,1\rangle\, \psi(b; b_0, \nu_0) + |b,2\rangle\, \psi(b; b_0, \nu_0) \right) e^{-iE_+(b)t}. \end{aligned} \tag{87}$$

The coefficients (85) enter the expression of the scattered wave packet at a later time which becomes

$$\begin{aligned} &\Psi_{\rm out}(t \gg 0) = \\ &\int \mathrm{D}b\ |-\rangle \otimes |b, 1 \cup 2\rangle \Big[\psi(-b; b_0, \nu_0) A_-(-b) \\ &+ \psi(b; b_0, \nu_0) B_-(b) \Big] e^{-iE_-(b)t} + \\ &\int \mathrm{D}b\ |+\rangle \otimes \Big[|b,1\rangle \left(\psi(-b; b_0, \nu_0) A_+(-b) \right. \\ &\left. + \psi(b; b_0, \nu_0) B_+(b) \right) + |b,2\rangle\, \psi(b; b_0, \nu_0) \Big] e^{-iE_+(b)t}. \end{aligned} \tag{88}$$

Note that the solution of the scattering problem for the $E_+(b)$ eigenvalues is asymmetric with respect to the components of the in-state supported on Γ_1 and Γ_2. Indeed the states $|b,2\rangle$ are eigenstates of the Hamiltonian directly because they are not supported on $\nu = 0$ and hence they do not "see" the interaction: this is captured by trivial scattering coefficients for this component.

3.3. Entropy Associated With the Entanglement With the UV Degrees of Freedom

From the previous initial state we can calculate [by tracing over the factor $\mathfrak{h}$, see (57)] the initial reduced density matrix

$$\begin{aligned} \rho^{\rm R}_{\rm in}(t) = &\int \mathrm{D}b\, \mathrm{D}b'\, e^{i[E_+(b) - E_+(b')]t} \\ &\times \Big[|b',1\rangle\, \psi(b'; b_0, \nu_0) + |b',2\rangle\, \psi(b'; b_0, \nu_0) \Big] \\ &\Big[\langle b,1|\, \overline{\psi}(b; b_0, \nu_0) + \langle b,2|\, \overline{\psi}(b; b_0, \nu_0) \Big] \\ + &\int \mathrm{D}b\, \mathrm{D}b'\, e^{i[E_-(b) - E_-(b')]t} \\ &\times \Big[|b',1\rangle\, \psi(b'; b_0, \nu_0) + |b',2\rangle\, \psi(b'; b_0, \nu_0) \Big] \\ &\Big[\langle b,1|\, \overline{\psi}(b; b_0, \nu_0) + \langle b,2|\, \overline{\psi}(b; b_0, \nu_0) \Big]. \end{aligned} \tag{89}$$

The reduced density matrix after the big bang is

$$\rho^{\mathrm{R}}_{\mathrm{out}}(t) = \int \mathrm{D}b\,\mathrm{D}b'\, e^{i[E_+(b)-E_+(b')]t}$$
$$\Big[\,\langle b,1|\left(\overline{\psi}(-b;b_0,\nu_0)\overline{A}_+(-b)+\overline{\psi}(b;b_0,\nu_0)\overline{B}_+(b)\right)$$
$$+\,\langle b,2|\,\overline{\psi}(b;b_0,\nu_0)\Big]$$
$$\Big[\,|b,1\rangle\left(\psi(-b';b_0,\nu_0)A_+(-b')+\psi(b';b_0,\nu_0)B_+(b')\right)$$
$$+\,|b,2\rangle\,\psi(b';b_0,\nu_0)\Big]+$$
$$e^{i[E_-(b)-E_-(b')]t}\Big[\,|b',1\cup 2\rangle\,\psi(-b';b_0,\nu_0)A_-(-b')$$
$$+\,|b',1\cup 2\rangle\,\psi(b';b_0,\nu_0)B_-(b')\Big] \qquad (90)$$
$$\times\Big[\,\langle b,1\cup 2|\,\overline{\psi}(-b;b_0,\nu_0)\overline{A}_-(-b)$$
$$+\,\langle b,1\cup 2|\,\overline{\psi}(b;b_0,\nu_0)\overline{B}_-(b)\Big],$$

where $\alpha_+ = 1/4$ and $\alpha_- = 1$ and δ_{s+} is unity when $s = +$ and vanishes when $s = -$. Then the non vanishing entries of the reduced density matrix are

$$\rho^{R\,11}_{out}(b_0,b_0) = \frac{1}{4}\left(|B_+(b_0)|^2+|B_-(b_0)|^2\right)$$
$$\rho^{22}_{out}(b_0,b_0) = \frac{1}{4}\left(1+|B_-(b_0)|^2\right)$$
$$\rho^{R\,12}_{out}(b_0,b_0) = \frac{1}{4}\left(B_+(b_0)+|B_-(b_0)|^2\right) = \overline{\rho^{R\,21}_{out}(b_0,b_0)}$$
$$\rho^{R\,11}_{out}(-b_0,-b_0) = \frac{1}{4}\left(|A_+(-b_0)|^2+|A_-(-b_0)|^2\right)$$
$$\rho^{R\,22}_{out}(-b_0,-b_0) = \frac{1}{4}\left(|A_-(-b_0)|^2\right)$$
$$\rho^{R\,12}_{out}(-b_0,-b_0) = \frac{1}{4}\left(|A_-(-b_0)|^2\right)$$
$$= \overline{\rho^{R\,21}_{out}(-b_0,-b_0)}$$
$$\rho^{R\,11}_{out}(b_0,-b_0) = \frac{1}{4}\left(\overline{A}_+(-b_0)B_+(b_0)+\overline{A}_-(-b_0)B_-(b_0)\right)$$
$$= \overline{\rho^{R\,11}_{out}(-b_0,b_0)}$$
$$\rho^{R\,22}_{out}(b_0,-b_0) = \frac{1}{4}\left(\overline{A}_-(-b_0)B_-(b_0)\right) = \overline{\rho^{R\,22}_{out}(-b_0,b_0)}$$
$$\rho^{R\,21}_{out}(b_0,-b_0) = \frac{1}{4}\left(\overline{A}_+(-b_0)+\overline{A}_-(-b_0)B_-(b_0)\right)$$
$$= \overline{\rho^{R\,12}_{out}(-b_0,b_0)}$$
$$\rho^{R\,12}_{out}(b_0,-b_0) = \frac{1}{4}\left(\overline{A}_-(-b_0)B_-(b_0)\right) = \overline{\rho^{R\,21}_{out}(-b_0,b_0)}. \qquad (91)$$

The matrix ρ^R_{out} is positive definite, $\mathrm{Tr}[\rho^R_{out}] = 1$ and $\rho^R_{out} = \rho^{R\dagger}_{out}$. In the case $b_0\ell_p \ll 1$ we have

$$\Theta_s(b_0) \approx \frac{8\pi\gamma^2\mu}{3}\frac{1}{b_0\sqrt{\Delta_s}\ell_p}. \qquad (92)$$

We can now compute the entanglement entropy jump δS to the first leading order in $b_0\ell_p/\mu$. The result [expressed in terms of the cosmological constant in this regime, namely (75)] is

$$\delta S = \delta_0 S - \frac{3\Delta_-\ell_p^2\log(3)}{128\pi^2\gamma^2\mu^2}\,\Lambda + \mathcal{O}(\Lambda^2\ell_p^4), \qquad (93)$$

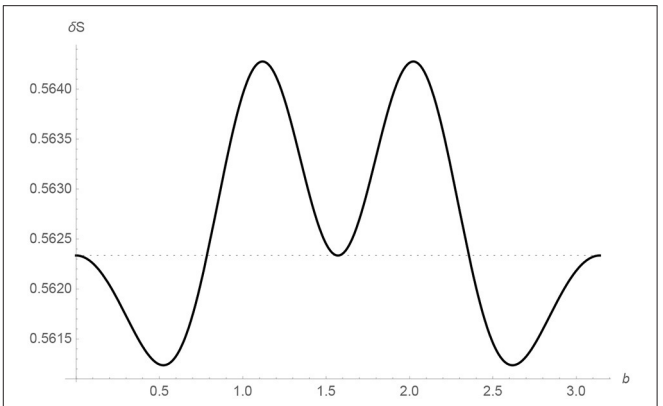

FIGURE 7 | The entropy jump δS as a function of b in Planck units for $\gamma = \mu = \Delta_- = 1$. The small $b\ell_p$ behavior in (93) is apparent. The entropy is periodic for $b\ell_p \in [0,\pi]$ as expected from (86).

where $\delta_0 S = 2\log(2) - \frac{3}{4}\log(3)$. The previous equation shows that the entropy jump is non trivial at crossing the big bang *would-be-singularity*, even in the low cosmological (low-energy) limit where (according to the analysis of the previous section) decoherence with the microscopic Planckian structure can be neglected during the time the universe is large. Information is unavoidably degraded (it seems lost for low-energy observers) during the singularity crossing.

The general entropy jump for arbitrary (not necessarily small) Λ can be computed explicitly. Its value is bounded by log(2) in our model. Finally, the energy is conserved through the big bang and during all the dynamical evolutions for the arbitrary values of b_0. The decoherence and entanglement which can be interpreted as an information loss happens without energy spending as required by the scheme put forward in Perez (2015).

4. DISCUSSION

We have seen that one can precisely realize the scenario put forward in Perez (2015) for the resolution of Hawking's information loss paradox in quantum gravity in the context of loop quantum cosmology. The key feature making this possible is the existence of additional degrees of freedom with no macroscopic interpretation which unavoidably entangle with the macroscopic degrees of freedom during the dynamical evolution and lead to a reduced density matrix whose entropy grows. The fundamental description is unitary but the effective description—that does not take the microscopic degrees of freedom into account and hence is analogous to the QFT description of BH evaporation—evolves pure states into mixed states. The microscopic degrees of freedom in the toy model are not introduced by hand, their existence is intimately related to the peculiar choice of representation of the fundamental phase space variables that leads to singularity resolution (Bojowald, 2001). Moreover, such a representation mimics the one used in the full theory of loop quantum gravity (Lewandowski et al., 2006) where also one expects such extra residual and microscopic degrees of

freedom to exist and remain hidden to low-energy coarse-grained observers describing physics in terms of an effective QFT.

From a more general perspective, we expect this scenario to transcend the framework of loop quantum gravity: in any approach to quantum gravity, where spacetime geometry is emergent[12] from more fundamental discrete degrees of freedom, the effect (precisely illustrated here by our toy model) would generically occur.

These results extrapolated to the context of black hole formation and evaporation suggest a simple resolution of the information paradox that avoids the pathological features of other proposals. For instance, the possible development of firewalls (Almheiri et al., 2013; Braunstein et al., 2013) or the risks of information cloning that the holographic type of scenarios must deal with (Marolf, 2017) are completely absent here. As decoherence in our model takes place without diffusion Unruh (2012), the usual difficulties (Banks et al., 1984) with energy conservation in the purification process are avoided along the lines of Unruh and Wald (1995), Unruh (2012) in a concrete quantum gravity framework (hence without the problems faced by the QFT approach Hotta et al., 2015; Wald, 2019).

We notice that the possibility of decoherence illustrated in the present model also suggests the possibility of diffusion into the underlying Planckian structure, such diffusion might have, in suitable situations, important consequences at large scales as argued in a series of recent papers (Josset et al., 2017; Perez et al., 2018; Perez and Sudarsky, 2019). The present model is very simplistic and realizes an example where such diffusion is not possible due to (unimodular) energy conservation and the fact that the microscopic degrees of freedom do not contribute independently to the Hamiltonian. Nevertheless, one could generalize these models easily in order to include diffusion. This possibility is under current investigation and we plan to report the results elsewhere.

[12]For instance in the causal sets approach (Bombelli et al., 1987), or in the context of Jacobson's ideas about emergence (Jacobson, 1995) (where, incidentally, in both cases unimodular gravity is the natural emergent structure), in causal dynamical triangulations (Ambjorn et al., 2004), and group field theory (Oriti, 2011), etc.

DATA AVAILABILITY STATEMENT

The original contributions presented in the study are included in the article/**Supplementary Material**, further inquiries can be directed to the corresponding author/s.

AUTHOR'S NOTE

This is a toy model of quantum cosmology that illustrates a novel mechanism for the resolution of Hawking's information puzzle for black hole evaporation.

AUTHOR CONTRIBUTIONS

All authors listed have made a substantial, direct and intellectual contribution to the work, and approved it for publication.

ACKNOWLEDGMENTS

We thank P. Martin-Dussaud for finding for outlining useful inequalities in reference (Petz and Ohya, 1993). We thank M. Geiller, C. Rovelli, S. Speziale, M. Varadarajan, and E. Wilson-Ewing for their stimulating discussions and Pietro Donà for the key remark that the notion of coarse-graining entropy that we had initially in mind could be written as standard entanglement entropy. This manuscript has been released as a pre-print at [https://inspirehep.net/literature/1772094] (Perez et al.).

SUPPLEMENTARY MATERIAL

The Supplementary Material for this article can be found online at: https://www.frontiersin.org/articles/10.3389/fspas.2021.604047/full#supplementary-material

REFERENCES

Almheiri, A., Marolf, D., Polchinski, J., and Sully, J. (2013). Black holes: complementarity or firewalls? *JHEP* 1302:062. doi: 10.1007/JHEP02(2013)062

Amadei, L., and Perez, A. (2019). Hawking's information puzzle: a solution realized in loop quantum cosmology. *arXiv*.

Ambjorn, J., Jurkiewicz, J., and Loll, R. (2004). Emergence of a 4-D world from causal quantum gravity. *Phys. Rev. Lett.* 93:131301. doi: 10.1103/PhysRevLett.93.131301

Ashtekar, A. (2020). Black hole evaporation: a perspective from loop quantum gravity. *Universe* 6:21. doi: 10.3390/universe6020021

Ashtekar, A., and Bojowald, M. (2005). Black hole evaporation: a paradigm. *Class. Quant. Grav.* 22, 3349–3362. doi: 10.1088/0264-9381/22/16/014

Ashtekar, A., Olmedo, J., and Singh, P. (2018). Quantum transfiguration of kruskal black holes. *Phys. Rev. Lett.* 121:241301. doi: 10.1103/PhysRevLett.121.241301

Ashtekar, A., Pawlowski, T., and Singh, P. (2006). Quantum nature of the big bang: improved dynamics. *Phys. Rev. D* 74:084003. doi: 10.1103/PhysRevD.74.084003

Ashtekar, A., and Pullin, J. (eds.). (2017). "Quantum dynamics," in *Loop Quantum Gravity: The First 30 Years* (WSP), 69–96. doi: 10.1142/9789813220003_0003

Ashtekar, A., and Singh, P. (2011). Loop quantum cosmology: a status report. *Class. Quant. Grav.* 28:213001. doi: 10.1088/0264-9381/28/21/213001

Ashtekar, A., Taveras, V., and Varadarajan, M. (2008). Information is not lost in the evaporation of 2-dimensional black holes. *Phys. Rev. Lett.* 100:211302. doi: 10.1103/PhysRevLett.100.211302

Banks, T., O'Loughlin, M., and Strominger, A. (1993). Black hole remnants and the information puzzle. *Phys. Rev. D* 47, 4476–4482.

Banks, T., Susskind, L., and Peskin, M. E. (1984). Difficulties for the evolution of pure states into mixed states. *Nucl.Phys. B* 244:125.

Bojowald, M. (2001). Absence of singularity in loop quantum cosmology. *Phys. Rev. Lett.* 86:5227–5230. doi: 10.1103/PhysRevLett.86.5227

Bojowald, M. (2005). Nonsingular black holes and degrees of freedom in quantum gravity. *Phys. Rev. Lett.* 95:061301. doi: 10.1103/PhysRevLett.95.061301

Bojowald, M., Goswami, R., Maartens, R., and Singh, P. (2005). A Black hole mass threshold from nonsingular quantum gravitational collapse. *Phys. Rev. Lett.* 95:091302. doi: 10.1103/PhysRevLett.95.091302

Bombelli, L., Lee, J., Meyer, D., and Sorkin, R. (1987). Space-time as a causal set. *Phys. Rev. Lett.* 59, 521–524.

Braunstein, S. L., Pirandola, S., and Zyczkowski, K. (2013). Better late than never: information retrieval from black holes. *Phys. Rev. Lett.* 110:101301. doi: 10.1103/PhysRevLett.110.101301

Chiou, D.-W., and Geiller, M. (2010). Unimodular loop quantum cosmology. *Phys. Rev. D* 82:064012. doi: 10.1103/PhysRevD.82.064012

Christodoulou, M., and De Lorenzo, T. (2016). Volume inside old black holes. *Phys. Rev. D* 94:104002. doi: 10.1103/PhysRevD.94.104002

Corichi, A., and Singh, P. (2016). Loop quantization of the Schwarzschild interior revisited. *Class. Quant. Grav.* 33:055006. doi: 10.1088/0264-9381/33/5/055006

de Berredo-Peixoto, G., Freidel, L., Shapiro, I. L., and de Souza, C. A. (2012). Dirac fields, torsion and Barbero-Immirzi parameter in Cosmology. *JCAP* 1206:017. doi: 10.1088/1475-7516/2012/06/017

Einstein, A. (1919). *Spielen Gravitationsfelder im Aufbau der Materiellen Elementarteilchen eine Wesentliche Rolle?* Sitzungsber. Berlin: Preuss. Akad. Wiss.

Fernando Barbero, J., Margalef-Bentabol, J., and Villaseñor, E. J. S. (2018). On the distribution of the eigenvalues of the area operator in loop quantum gravity. *Class. Quant. Grav.* 35:065008. doi: 10.1088/1361-6382/aaabf9

Gambini, R., and Pullin, J. (2013). Loop quantization of the Schwarzschild black hole. *Phys. Rev. Lett.* 110:211301. doi: 10.1103/PhysRevLett.110.211301

Gielen, S., Oriti, D., and Sindoni, L. (2013). Cosmology from group field theory formalism for quantum gravity. *Phys. Rev. Lett.* 111:031301. doi: 10.1103/PhysRevLett.111.031301

Green, D., and Unruh, W. G. (2004). Difficulties with closed isotropic loop quantum cosmology. *Phys. Rev. D* 70:103502. doi: 10.1103/PhysRevD.70.103502

Hotta, M., Schützhold, R., and Unruh, W. G. (2015). Partner particles for moving mirror radiation and black hole evaporation. *Phys. Rev. D* 91:124060. doi: 10.1103/PhysRevD.91.124060

Jacobson, T. (1995). Thermodynamics of space-time: the Einstein equation of state. *Phys. Rev. Lett.* 75, 1260–1263.

Josset, T., Perez, A., and Sudarsky, D. (2017). Dark energy as the weight of violating energy conservation. *Phys. Rev. Lett.* 118:021102. doi: 10.1103/PhysRevLett.118.021102

Lewandowski, J., Okolow, A., Sahlmann, H., and Thiemann, T. (2006). Uniqueness of diffeomorphism invariant states on holonomy-ux algebras. *Commun. Math. Phys.* 267, 703–733. doi: 10.1007/s00220-006-0100-7

Liberati, S., Tricella, G., and Trombettoni, A. (2019). The information loss problem: an analogue gravity perspective. *Entropy* 21:940. doi: 10.3390/e21100940

Madhavan, V. Private communication.

Marolf, D. (2017). The Black Hole information problem: past, present, and future. *Rept. Prog. Phys.* 80:092001. doi: 10.1088/1361-6633/aa77cc

Modak, S. K., Ortíz, L., Peña, I., and Sudarsky, D. (2015). Non-paradoxical loss of information in black hole evaporation in a quantum collapse model. *Phys. Rev. D* 91:124009. doi: 10.1103/PhysRevD.91.124009

Modesto, L. (2004). Disappearance of black hole singularity in quantum gravity. *Phys. Rev. D* 70:124009. doi: 10.1103/PhysRevD.70.124009

Modesto, L. (2006). Loop quantum black hole. *Class. Quant. Grav.* 23, 5587–5602. doi: 10.1088/0264-9381/23/18/006

Noui, K., Perez, A., and Vandersloot, K. (2005). On the physical Hilbert space of loop quantum cosmology. *Phys. Rev. D* 71:044025. doi: 10.1103/PhysRevD.71.044025

Okon, E., and Sudarsky, D. (2017). Black holes, information loss and the measurement problem. *Found. Phys.* 47:120. doi: 10.1007/s10701-016-0048-1

Okon, E., and Sudarsky, D. (2018). Losing stuff down a black hole. *Found. Phys.* 48, 411–428. doi: 10.1007/s10701-018-0154-3

Oriti, D. (2011). "The microscopic dynamics of quantum space as a group field theory," in *Proceedings, Foundations of Space and Time: Reections on Quantum Gravity* (Cape Town), 257–320.

Oriti, D., Sindoni, L., and Wilson-Ewing, E. (2016). Emergent Friedmann dynamics with a quantum bounce from quantum gravity condensates. *Class. Quant. Grav.* 33:224001. doi: 10.1088/0264-9381/33/22/224001

Oriti, D., Sindoni, L., and Wilson-Ewing, E. (2017). Bouncing cosmologies from quantum gravity condensates. *Class. Quant. Grav.* 34:04LT01. doi: 10.1088/1361-6382/aa549a

Penrose, R. (2005). *The Road to Reality: A Complete Guide to the Laws of the Universe.* London: Vintage.

Perez, A. (2015). No firewalls in quantum gravity: the role of discreteness of quantum geometry in resolving the information loss paradox. *Class. Quant. Grav.* 32:084001. doi: 10.1088/0264-9381/32/8/084001

Perez, A. (2017). Black holes in loop quantum gravity. *Rept. Prog. Phys.* 80:126901. doi: 10.1088/1361-6633/aa7e14

Perez, A., and Sudarsky, D (2019). Dark energy from quantum gravity discreteness. *Phys. Rev. Lett.* 122:221302. doi: 10.1103/PhysRevLett.122.221302

Perez, A., Sudarsky, D., and Bjorken, J. D. (2018). A microscopic model for an emergent cosmological constant. *Int. J. Mod. Phys. D* 27:1846002. doi: 10.1142/S0218271818460021

Peskin, M. E., and Schroeder, D. V (1995). *An Introduction to Quantum Field Theory.* Reading, PA: Addison-Wesley.

Petz, D., and Ohya, M. (1993). *Quantum Entropy and Its Use.* Springer.

Rovelli, C. (1991). Time in quantum gravity: an hypothesis. *Phys. Rev. D* 43, 442–456.

Singh, P., and Wilson-Ewing, E. (2014). Quantization ambiguities and bounds on geometric scalars in anisotropic loop quantum cosmology. *Class. Quant. Grav.* 31:035010. doi: 10.1088/0264-9381/31/3/035010

Smolin, L. (2009). The Quantization of unimodular gravity and the cosmological constant problems. *Phys. Rev. D* 80:084003. doi: 10.1103/PhysRevD.80.084003

Smolin, L. (2011). Unimodular loop quantum gravity and the problems of time. *Phys. Rev. D* 84:044047. doi: 10.1103/PhysRevD.84.044047

Thiemann, T. (1998). Quantum spin dynamics (QSD). *Class. Quant. Grav.* 15, 839–873.

Thiemann, T. (2001) *Modern Canonical Quantum General Relativity.* New York, NY.

Unruh, W. G. (1989). A unimodular theory of canonical quantum gravity. *Phys. Rev. D* 40:1048. doi: 10.1098/rsta.2012.0163

Unruh, W. G. (2012). Decoherence without dissipation. *Trans. R. Soc. Lond.* 370:4454.

Unruh, W. G., and Wald, R. M. (1995). On evolution laws taking pure states to mixed states in quantum field theory. *Phys. Rev. D* 52, 2176–2182.

Wald, R. M. (1995). *Quantum Field Theory in Curved Space-Time and Black Hole Thermodynamics.* Chicago Lectures in Physics. Chicago, IL: University of Chicago Press.

Wald, R. M. (2019). Particle and energy cost of entanglement of Hawking radiation with the final vacuum state. *Phys. Rev. D* 100:065019. doi: 10.1103/PhysRevD.100.065019

Weinberg, S. (1989). The cosmological constant problem. *Rev. Mod. Phys.* 61, 1–23.

Wilson-Ewing, E. (2012). Lattice loop quantum cosmology: scalar perturbations. *Class. Quant. Grav.* 29:215013. doi: 10.1088/0264-9381/29/21/215013

Conflict of Interest: The authors declare that the research was conducted in the absence of any commercial or financial relationships that could be construed as a potential conflict of interest.

frontiers in Astronomy and Space Sciences

REVIEW
published: 03 June 2021
doi: 10.3389/fspas.2021.624824

Hybrid Loop Quantum Cosmology: An Overview

Beatriz Elizaga Navascués[1]* *and Guillermo A. Mena Marugán*[2]*

[1]*Institute for Quantum Gravity, Friedrich-Alexander University Erlangen-Nürnberg, Erlangen, Germany,* [2]*Instituto de Estructura de la Materia, IEM-CSIC, Madrid, Spain*

Loop Quantum Gravity is a nonperturbative and background independent program for the quantization of General Relativity. Its underlying formalism has been applied successfully to the study of cosmological spacetimes, both to test the principles and techniques of the theory and to discuss its physical consequences. These applications have opened a new area of research known as Loop Quantum Cosmology. The hybrid approach addresses the quantization of cosmological systems that include fields. This proposal combines the description of a finite number of degrees of freedom using Loop Quantum Cosmology, typically corresponding to a homogeneous background, and a Fock quantization of the field content of the model. In this review we first present a summary of the foundations of homogeneous Loop Quantum Cosmology and we then revisit the hybrid quantization approach, applying it to the study of Gowdy spacetimes with linearly polarized gravitational waves on toroidal spatial sections, and to the analysis of cosmological perturbations in preinflationary and inflationary stages of the Universe. The main challenge is to extract predictions about quantum geometry effects that eventually might be confronted with cosmological observations. This is the first extensive review of the hybrid approach in the literature on Loop Quantum Cosmology.

Keywords: loop quantum cosmology, loop quantum gravity, quantum field theory on curved backgrounds, quantum effects in cosmology, primordial perturbations

OPEN ACCESS

Edited by:
Julio Navarro,
University of Victoria, Canada

Reviewed by:
Suddhasattwa Brahma,
McGill University, Canada
Kazuharu Bamba,
Fukushima University, Japan

***Correspondence:**
Beatriz Elizaga Navascués
w.iac20060@kurenai.waseda.jp
Guillermo A. Mena Marugán
mena@iem.cfmac.csic.es

Specialty section:
This article was submitted to Cosmology, a section of the journal Frontiers in Astronomy and Space Sciences

Received: *01 November 2020*
Accepted: *03 May 2021*
Published: *03 June 2021*

Citation:
Elizaga Navascués B and Mena Marugán GA (2021) Hybrid Loop Quantum Cosmology: An Overview. Front. Astron. Space Sci. 8:624824. doi: 10.3389/fspas.2021.624824

1 INTRODUCTION

Modern Physics has two basic pillars in Quantum Mechanics and Einstein's theory of General Relativity (GR). However, the latter is a geometric description of the gravitational field that does not incorporate the principles of Quantum Mechanics. Numerous attempts have been made to construct a quantum theory of the spacetime geometry but, at present, there is still no proposal that the scientific community accepts unanimously as fully satisfactory. One of the proposals for the quantum description of gravity that has reached more impact with a robust mathematical development is Loop Quantum Gravity (LQG) (Ashtekar, 1986; Ashtekar and Lewandowski, 2004; Thiemann, 2007). It is a quantization formalism for globally hyperbolic spacetimes, based on a canonical and non-perturbative formulation of the geometric degrees of freedom. The fundamental novelty with respect to other pre-existing canonical proposals [such as the Wheeler-DeWitt (WdW) quantization, also called quantum geometrodynamics (DeWitt, 1967; Halliwell, 1991)] lies in the use of techniques imported from Yang-Mills gauge theories (Yang and Mills, 1954), known by their success in explaining non-perturbative regimes of the strong and electroweak interactions. In addition, the formulation of LQG is independent of any spacetime background structure and is aimed to respect the general covariance of Einstein's theory (in its canonical formulation). To achieve this goal, LQG adopts the quantization scheme proposed by Dirac for systems with constraints (Dirac, 1964). In

particular, in GR the Hamiltonian is a linear combination of constraints which, via Poisson brackets, generate diffeomorphism transformations, that are the fundamental symmetries of the theory. Dirac's proposal consists in requiring that those constraints are satisfied at the quantum level on the physical states of the system. In more detail, the geometric degrees of freedom in vacuo are described in LQG by pairs of canonical variables that consist of the components of a densitized triad and a gauge connection (Ashtekar and Lewandowski, 2004; Thiemann, 2007). Their respective fluxes through surfaces and holonomies form an algebra under Poisson brackets, which is the algebra that one wants to represent quantum mechanically over a Hilbert space, where the constraints of the theory should finally be imposed.

A major obstacle that the different candidates for a theory of quantum gravity have to face, regardless of their nature, is the extreme difficulty that is found to confront them with experimental data. Most of the possible effects of a quantum spacetime are expected to occur in regimes of very high curvatures or energies. In this sense, the Universe that we observe appears to be very classical, and GR explains it almost perfectly. However, there are observational windows to regimes of the Universe in which traces of a phenomenology that exceeded Einstein's theory might be found. A relevant example is the so-called Cosmic Microwave Background (CMB). This approximately black-body radiation reaches us from regions so far away that provides information about how the Universe was like at the early times when it became transparent. Under certain circumstances, this information might as well contain some details about very previous stages of the Universe when the spacetime geometry could have experienced quantum effects (Di Tucci et al., 2019), especially if the observable Universe had in those epoques a size of the order of the Planck scale. A second obstacle for most of the quantum gravity proposals is the complication to extract concrete predictions about those regimes where quantum effects may have been important. Therefore, from a physical point of view, it is greatly convenient to consider the specialization of those formalisms to more restricted scenarios that, even without contemplating all the phenomena that may be accounted for in the full quantum theory, are able to describe regions of the Universe of particular interest. With this motivation, approximately at the beginning of this century, it was suggested to apply LQG methods to cosmological systems that possess a finite number of degrees of freedom, owing to the presence of certain symmetries. This effort crystallized in the appearance of Loop Quantum Cosmology (LQC) (Ashtekar et al., 2003; Bojowald, 2008; Ashtekar and Singh, 2011), a branch of LQG aimed to deal with the quantum analysis of cosmological systems.

The first cosmologies that were studied in LQC were homogeneous and isotropic universes of the Friedmann-Lemaître-Robertson-Walker (FLRW) type, that classically provide a good approximation to the behavior of the observed Universe in large scales. The quantization of this type of cosmological systems was consistently completed, providing satisfactory results both from a formal and from a physical point of view. Probably the most remarkable of these results is the resolution of the Big Bang cosmological singularity, that is replaced in this formalism with a quantum bounce, usually called the Big Bounce. In addition to these investigations on homogeneous and isotropic spacetimes, other homogeneous cosmologies with a lower degree of symmetry have also been considered in LQC to discuss the role of anisotropies. In particular, a special attention has been devoted to the quantization of Bianchi I models (Chiou, 2007a; Chiou, 2007b; Martín-Benito et al., 2008; Ashtekar and Wilson-Ewing, 2009; Martín-Benito et al., 2009b).

Although homogeneity and isotropy are very successful hypotheses to describe our universe at large scales, it is necessary to give an explanation to the existence and evolution of the observed inhomogeneities. In fact, the temperature of the CMB itself presents anisotropies that contain information about the small inhomogeneities in the geometry and matter content of the primeval Universe. Such inhomogeneities should be ultimately responsible of having given rise to the structures that we observe today (Liddle and Lyth, 2000). As we have pointed out, it has been recently proposed that the power spectrum of the CMB anisotropies might even encode information about quantum effects that were relevant in the very early stages of the Universe, if the scale of the region that we observe nowadays was of the Planck order at that time (Agullo and Morris, 2015; Di Tucci et al., 2019). Other information about those epochs of the Universe with extremely high curvature might be present in non-gaussianities of the CMB, or in the spectrum of tensor cosmological perturbations. Even if the information that we could extract from just one of this kind of observations might be insufficient to falsify the predictions of a candidate theory of quantum cosmology, such as LQC, the combined set of a number of different types of observations might increase the statistical significance of a possible agreement with the predictions (Ashtekar et al., 2020). With this motivation in mind to investigate quantum effects of gravity in realistic cosmological spacetimes, a hybrid strategy was proposed a decade ago in LQC for the quantum description of scenarios that contemplate the presence of inhomogeneities, both geometric and in the matter content. On the one hand, this canonical strategy employs methods inspired by LQC for the representation of the homogeneous sector of the geometry. On the other, it uses Fock representations, typical of Quantum Field Theory (QFT), to describe the rest of degrees of freedom of the system. The combination of both techniques must result in a consistent quantization of the complete system. This formalism for the quantization of inhomogeneous spacetimes implicitly assumes that there is a regime in which the most important quantum gravitational effects are felt by the homogeneous sector of the system, an assumption that seems plausible in the early stages of our universe. In the light of this hybrid approach, the advantages of reaching an evolution of the inhomogeneities that is unitary in the regime of QFT in a curved spacetime, applicable when the behavior of the homogeneous sector can be considered approximately classical, exceed the purely theoretical aspects and appear essential to allow robust physical results, that are not affected by the severe ambiguity that would imply the

consideration of Fock representations that are not even unitarily equivalent among them.

The hybrid quantization approach, using an LQC representation for the homogeneous geometry, was first implemented in one of the Gowdy cosmological models (Martín-Benito et al., 2008; Mena Marugán and Martín-Benito, 2009; Garay et al., 2010; Martín-Benito et al., 2010b). These models describe spacetimes that, even if subject to certain symmetry conditions (the presence of two spatial Killing vectors), still include gravitational inhomogeneities (Gowdy, 1971; Gowdy, 1974). The hybrid quantization was completed for the model with three-torus spatial topology and linearly polarized gravitational waves (Martín-Benito et al., 2008; Martín-Benito et al., 2010a). Although the physical Hilbert space was formally characterized, it is perhaps impossible to find analytically any of these states. Therefore, approximation techniques began to be developed for the operators that appear in the resulting constraints, valid for certain quantum states (Martín-Benito et al., 2014). On these states, the Hamiltonian constraint operator adopted a particularly simple approximate expression, formally corresponding to a homogenous and isotropic cosmology with different types of effective matter content, and possibly with higher-order curvature corrections, once the average volume of the Gowdy universe was identified with the isotropic volume (Elizaga Navascués et al., 2015; Elizaga Navascués et al., 2015).

More interesting from a physical point of view is the application of the hybrid quantization approach to perturbed FLRW spacetimes coupled to a scalar field (Fernández-Méndez et al., 2012; Fernández-Méndez et al., 2013; Fernández-Méndez et al., 2014; Castelló Gomar et al., 2014; Castelló Gomar et al., 2015; Benítez Martínez and Olmedo, 2016; Castelló Gomar et al., 2016; Castelló Gomar et al., 2017). Within the framework of GR, a model of this kind can be employed to describe quite successfully the primordial Universe, including small inhomogeneities that, after undergoing an inflationary stage, are capable of explaining the experimental observations about the anisotropies of the CMB (Mukhanov, 2005). This application of hybrid LQC starts with a classical formulation in which the physical degrees of freedom of the cosmological perturbations are gauge invariants, i.e. quantities that do not vary under a perturbative diffeomorphism (Bardeen, 1980; Sasaki, 1983; Kodama and Sasaki, 1984; Mukhanov, 1988; Castelló Gomar et al., 2015). In fact, one can construct a canonical description of the perturbations that includes such gauge invariants as a subset of the canonical variables (Langlois, 1994; Pinho and Pinto-Neto, 2007; Falciano and Pinto-Neto, 2009; Castelló Gomar et al., 2015). However, the passage to a quantum treatment of the whole cosmological system requires that the homogeneous degrees of freedom, rather than being considered as a fixed background, are also included in this canonical description [see Refs. (Halliwell and Hawking, 1985; Shirai and Wada, 1988) for considerations in WdW]. This is actually possible at least at the lowest non-trivial order of perturbative truncation of the action (Castelló Gomar et al., 2015). In this way, the system is well prepared for its canonical quantization following the hybrid quantization approach.

Despite the attention paid recently to cosmological perturbations in LQC with scalar fields, it is also convenient to introduce other types of matter content that are known to exist in the Universe. This is the case of fermionic fields. The interest of contemplating the presence of these fields in early cosmological epochs goes beyond a formal analysis, because it is necessary to confirm that their inclusion does not affect significantly the quantum evolution of the cosmological scalar and tensor perturbations (which are bosonic in nature).

In summary, the purpose of this work is to review the foundations of hybrid LQC and its application to inhomogeneous cosmological systems, with an emphasis put on the analysis of the possible quantum geometry effects on primordial perturbations. The final goal of the approach would be to extract predictions about modifications with respect to Einstein's theory with the hope that, in this era of precision cosmology, those modifications might be confronted with observations in order to falsify the formalism. We would like to remark that the focus of this review will be exclusively put on the hybrid approach. The literature already contains detailed reviews of homogenous LQC and of several other approaches dealing with inhomogeneities in LQC (Bojowald, 2008; Ashtekar and Singh, 2011; Banerjee et al., 2012; Ashtekar and Barrau, 2015; Rovelli and Vidotto, 2015; Alesci and Cianfrani, 2016; Gielen and Sindoni, 2016; Grain, 2016; Agullo and Singh, 2017; Wilson-Ewing, 2017; Bojowald, 2020). This is the first extensive review specifically devoted to hybrid LQC. We will concentrate our discussion on the results achieved in the hybrid quantization, and we will mention only marginally other approaches in the conclusions, to comment on some distinctive properties of the hybrid proposal. For other strategies to cope with infinite dimensional systems in LQC, the existing reviews provide a fairly complete amount of information that the reader can directly consult.

The paper is organized as follows. We first review the foundations of LQC in **Section 2**. In the first subsection we explain the choice of Ashtekar-Barbero variables and some questions about the construction of the theory of LQG with them. In the remaining subsections of **Section 2** we apply those variables to the study of homogeneous and isotropic universes, discussing their quantization and commenting in special detail the quantum Hamiltonian that one obtains for those models. We then pass to discuss the hybrid approach in LQC, studying in **Section 3** the cosmological system that was first analyzed in this quantization scheme. In the rest of sections, we focus our attention on the more interesting case (from a physical point of view) of a perturbed homogeneous and isotropic spacetime, in order to explore how quantum gravity effects may have affected the cosmological perturbations in the primeval universe. With this aim, we first review in **Section 4** the procedure to construct a canonical formulation for this cosmological system in terms of gauge invariants and gauge constraints for the perturbations, together with their momenta, and of suitable zero modes for the background. In **Section 5** we consider the possible introduction of a Dirac field in the formalism. We then explain in **Section 6** the implementation of the hybrid LQC approach in this canonical system. Next, in **Section 7** we discuss how we can derive modified

propagation equations for the perturbations starting with the quantum Hamiltonian constraint and introducing a convenient ansatz for the quantum states, as well as some plausible approximations. These modified equations for the gauge invariants can be studied to deduce predictions that ultimately might be confronted with observations. In doing this, a key piece of information are the initial conditions that one must choose, both for the background cosmology and for the perturbations, in order to fix their vacuum state. These issues are discussed in **Section 8**. Finally, in **Section 9** we explore the possible determination, or at least restriction, of the viable choices of a vacuum for the gauge invariant perturbations that result from demanding a good behavior in the quantum Hamiltonian operators and the evolution of those perturbations, putting an emphasis on a procedure of asymptotic diagonalization of their Hamiltonians. **Section 10** contains the conclusions. In the rest of this work, we adopt units such that $c = \hbar = 1$, where c is the speed of light in vacuo and $\hbar$ is Planck reduced constant. Nonetheless, we maintain Newton constant explicitly in all our formulas. Owing to these conventions and to some convenient redefinitions of quantities with respect to the notation employed in previous works, special care must be taken when comparing numerical factors in our equations with those appearing in the published literature.

2 LOOP QUANTUM COSMOLOGY

Let us first introduce the formalism of LQC, applied in this work to spacetime systems that in Einstein's theory correspond to homogeneous cosmologies. We will focus our attention on a flat FLRW model, minimally coupled to a homogeneous scalar field. In this section, we will review in detail the case of a massless field, because then the quantum constraints can be solved exactly. Later in our discussion, when we consider inflationary cosmologies, we will introduce a potential in the action of the scalar field, that can be viewed as the inflaton field of the system. An FLRW spacetime is the model typically used to describe the evolution of an expanding homogeneous and isotropic universe in GR. Here, we will study only the case of flat spatial curvature. In the following section we will also generalize our analysis to globally hyperbolic spacetimes (that admit a foliation on compact Cauchy hypersurfaces) of Bianchi I type.

LQC starts from a Hamiltonian formulation of the system under consideration, selecting as canonical variables for the geometry those used in LQG. In the Arnowitt-Deser-Misner (ADM) formulation of GR, given an arbitrary Cauchy hypersurface $\sum$, the dynamical degrees of freedom of the spacetime metric can be captured by the spatial metric induced on $\sum$, h_{ab} (we use lower case letters from the beginning of the alphabet to denote spatial indices), and its variation along the normal surface vector. This variation is called the extrinsic curvature and is given by the tensor $K_{ab} = \mathcal{L}_n h_{ab}/2$, where $\mathcal{L}_n$ is the Lie derivative along the normal vector n. Taking the spatial metric h_{ab} as the configuration variable, a linear function of the extrinsic curvature determines its canonically conjugate momentum. Starting from this canonical pair for the geometry and canonical pairs corresponding to the matter content, if a Legendre transformation is carried out in the Hilbert-Einstein Lagrangian (with suitable boundary terms), one obtains a Hamiltonian that is a linear combination of first-class constraints. Their coefficients are non-dynamical Lagrange multipliers, provided by the lapse function N and the three components of the shift vector N^a. Each of these constraints vanishes on the solutions of GR. They are the generators of the fundamental symmetries of GR: the spacetime difeomorphisms. More specifically, the constraint that is multiplied by the lapse function is called Hamiltonian or scalar constraint, and generates time reparametrizations, modulo a spatial difeomorphism. The three constraints that come multiplied by the components of the shift vector are called momentum constraints, and generate spatial difeomorphisms.

2.1 Ashtekar-Barbero Variables: Holonomies and Fluxes

The Hamiltonian description of GR can be reformulated in terms of geometric canonical variables that, involving a gauge connection, simplify the functional form of the constraints (Ashtekar, 1986). Under the quantization scheme proposed by Dirac, these variables may seem more convenient for developing the quantum theory. In addition, the introduction of a gauge connection allows the controlled use of structures that are well known in group theory, and that can facilitate the construction of a well-defined Hilbert space. These variables can be introduced as follows.

First, in the spatial sections we can make use of triads, which are defined as a local basis of vectors e^a_i of the considered Cauchy hypersurface, and in terms of which the spatial metric can be expressed locally as

$$h_{ab} = e^i_a e^j_b \delta_{ij} \tag{1}$$

where the co-triads e^i_a are the inverse of e^a_i. Since the Kronecker delta is the Euclidean metric in three dimensions, the relationship (**Eq. 1**) is invariant under the transformation of the triadic basis under three-dimensional rotations, at each point of the Cauchy sections. Therefore, the use of co-triads for the description of the spatial metric automatically introduces additional local symmetry into the theory, provided by the group $SO(3)$. Any Cauchy hypersurface is thus supplied with a principal fiber structure of three-dimensional reference systems, with $SO(3)$ as the gauge group (Isham, 1999). We employ lower case Latin letters from the middle of the alphabet for indices corresponding to components in a local triadic basis of orthonormal frames, or equivalently in a basis of the three-dimensional Lie algebra $so(3)$. A section of the bundle is a locally smooth assignment of an element of the group to each point of the manifold. Different choices of triads, related to each other point to point by gauge transformations, can then be understood as different sections of the bundle.

In order to define a notion of horizontality between the different fibers, as well as the associated parallel transport, one introduces a gauge connection, characterized by a one-form on

the spatial hypersurfaces with components that take values in the three-dimensional Lie algebra $so(3)$. We will call this connection Γ_a^i. Of all the possible connections, there is one that is uniquely determined by the densitized triad through the metricity condition

$$^{(3)}\nabla_b E_i^a + \epsilon_j^k \Gamma_b^j E_k^a = 0, \tag{2}$$

where ϵ_{ijk} is the totally antisymmetric Levi-Cività symbol (its indices are raised and lowered using the Kronecker delta), $^{(3)}\nabla_b$ denotes the covariant derivative associated with the Levi-Cività connection compatible with h_{ab}, and $E_i^a = \sqrt{h}e_i^a$ is the densitized triad, with h equal to the determinant of the spatial metric.

In adddition, taking into account that the extrinsic curvature in triadic form

$$K_a^i = K_{ab}e_j^b\delta^{ij} \tag{3}$$

can be understood as a vector of $\mathrm{so}(3)$ with respect to the gauge transformations, as well as a one-form in spacetime, it is possible to consider, instead of Γ_a^i, the so-called Ashtekar-Barbero connection (Barbero, 1995):

$$A_a^i = \Gamma_a^i + \gamma K_a^i. \tag{4}$$

In this definition, γ is a real non-vanishing number, of arbitrary value in principle, which is known as the Immirzi parameter (Immirzi, 1997).

The pair formed by this connection and the densitized triad, the so-called Ashtekar-Barbero variables, turns out to be canonical for GR:

$$\left\{A_a^i\left(\vec{x}\right), E_j^b\left(\vec{y}\right)\right\} = 8\pi G\gamma\delta_a^b\delta_j^i\delta^3\left(\vec{x}-\vec{y}\right), \tag{5}$$

where $\delta^3(\vec{x}-\vec{y})$ is the three-dimensional Dirac delta. LQG starts with these variables in the attempt to construct a quantum theory of gravity.

Actually, in order to allow the coupling to the gravitational field of matter with a half-integer spin, A_a^i is considered as a connection that takes values in the three-dimensional Lie algebra $\mathrm{su}(2)$. That is, in practice the gauge group $SO(3)$ of the principal bundle is replaced by its double cover, $SU(2)$.

In terms of the Ashtekar-Barbero variables, the Hamiltonian constraint $\mathcal{H}$ and the momentum constraints $\mathcal{H}_a$ of GR (in vacuo) take the form (Thiemann, 2007):

$$\mathcal{H} = \frac{1}{16\pi G\sqrt{h}}\left[\epsilon^{ij}{}_k F_{ab}^k - \left(1+\gamma^2\right)\left(K_a^iK_b^j - K_b^iK_a^j\right)\right]E_i^aE_j^b, \tag{6}$$

$$\mathcal{H}_a = \frac{1}{8\pi G\gamma}F_{ab}^iE_i^b, \tag{7}$$

where F_{ab}^i is the curvature of the Ashtekar-Barbero connection:

$$F_{ab}^i = \partial_aA_b^i - \partial_bA_a^i + \epsilon^i{}_{jk}A_a^jA_B^K. \tag{8}$$

Finally, the introduction of an additional gauge symmetry in the theory translates into the appearance of three new constraints, that generate spin rotations in $SU(2)$ (once this is considered as the cover of the group of three-dimensional rotations):

$$\mathcal{G}_i = \frac{1}{8\pi G\gamma}\left[\partial_aE_i^a + \epsilon_{ij}^kA_a^jE_k^a\right]. \tag{9}$$

Owing to their form as a divergence, given by the covariant derivative of the triadic field with respect to the connection A_a^i (Isham, 1999) and contracted in spacetime indices, these three constraints resemble the Gauss law of electromagnetism, and, accordingly, they are usually called the Gauss constraints. For the type of spacetimes with homogeneous spatial surfaces that we want to consider, and with a suitable choice of reference system, the Gauss and the momentum constraints are automatically satisfied, therefore involving no restriction on the system.

From a systematic point of view, the first step in the construction of a quantum theory of gravity, based on the introduced Hamiltonian formalism with a gauge connection, would be to find a representation, as operators on a Hilbert space, of an algebra that captures all the relevant information about the canonical pair (**Eq. 5**). Now, the formulation of the quantum theory must reasonably be such that physical results turn out to be described by quantities that do not depend on the choice of $SU(2)$ gauge. With this purpose, it is convenient that the elements of the algebra of classical variables to be quantized do not vary, or vary as little as possible, under the $SU(2)$ transformations that change the sections of the bundle. A well-known construction in Yang-Mills theories that captures the gauge invariant information about the connection is the holonomy. Given a curve $\tilde{\gamma}$ on a spatial hypersurface $\sum$, the holonomy along it of the connection A_a^i is defined as follows:

$$h_{\tilde{\gamma}} = \mathcal{P}\exp\int_{\tilde{\gamma}}A_a^i\tau_i dx^a, \tag{10}$$

where $\mathcal{P}$ denotes path ordering and τ_i provides a basis of the Lie algebra $\mathrm{su}(2)$. Holonomies determine the parallel transport defined by the Ashtekar-Barbero connection between the $SU(2)$ fibers that are assigned to each point of the manifold. Given any section of the principal bundle and the curve $\tilde{\gamma}$, the holonomy dictates how this curve should be lifted to the fiber so that its tangent vector is parallelly transported (Isham, 1999). Under a change of section, the holonomy is only affected by the gauge transformation evaluated at the end points of the curve. On the other hand, it is clear that its construction does not depend at all on any fixed spacetime structure, nor on the choice of coordinate system. All these properties of the holonomies make them good candidates to be the variables represented quantum mechanically in order to capture the relevant information about the configuration space of Ashtekar-Barbero connections. In LQG, one considers holonomies along edges e, typically piecewise analytic, defined as an embedding of the interval (0,1) in our Cauchy hypersurface (Ashtekar and Lewandowski, 2004). The variables that represent the rest of the phase space must contain the densitized triad E_i^a. Since this triad is a vector density in $\sum$, its Hodge dual can be directly integrated over two-dimensional surfaces S. The result is a flux through them, which again does not depend on any additional spacetime structure nor on the choice of coordinates,

$$E(S,f) = \int_S f^i E^a_i \epsilon_{abc} dx^b dx^c, \tag{11}$$

where f^i is a function that takes values on the algebra $\mathrm{su}(2)$ and can be treated as a vector with respect to gauge transformations. The space of holonomies h_e and fluxes $E(S, f)$ forms an algebra under Poisson brackets that no longer possesses the distributional divergences of the canonical relations (**Eq. 5**). This is the algebra chosen in LQG to represent quantum mechanically the canonical commutation relations of GR.

2.2 Homogeneous Cosmologies: Polymer Quantization

We will now summarize the methodology used in LQC for the quantization of flat FLRW cosmologies, following a strategy inspired by LQG. First, let us recall that the momentum and Gauss constraints are trivial in this homogeneous system, setting at convenience the reference system for the description of the spatial metric h_{ab}, as well as the internal gauge of the triads that determine it (**Eq. 1**). For simplicity, we will choose spatial coordinates adapted to the homogeneity of the spatial sections and homogeneous diagonal triads, proportional to the Kronecker delta δ^a_i. For these triads, the connection Γ^i_a vanishes. We will also assume that the spatial hypersurfaces of the chosen foliation are compact, with a three-torus topology (T^3). This compactness ensures that spatial integrations do not give rise to infrared divergences [in non-compact cases, this problem can be handled by introducing fiducial structures (Ashtekar et al., 2003; Ashtekar and Wilson-Ewing, 2009)]. In addition, restricting the study to compact hypersurfaces is very convenient if these cosmologies provide the homogeneous sector of other more general scenarios, because the application of the hybrid strategy for their quantization would use QFT techniques that are known to be well-posed and robust in the case of compact Cauchy sections.

Taking all these considerations into account, and choosing the compactification period in T^3 of each of the orthogonal directions adapted to homogeneity equal to 2π, the geometric sector of flat FLRW cosmologies can be described using Ashtekar-Barbero variables that adopt for them the specific form

$$A^i_a = \frac{c}{2\pi}\,\delta^i_a, \qquad E^a_i = \frac{p}{4\pi^2}\,\delta^a_i, \qquad \{c,p\} = \frac{8\pi G\gamma}{3}. \tag{12}$$

For any global function of time t, the canonical variables $p(t)$ and $c(t)$ can be classically related with the scale factor $a(t)$, typically used in cosmology, and with its temporal derivative $a(t)$ by the equations

$$|c| = 2\pi\gamma\left|\frac{\dot{a}}{N}\right|, \qquad |p| = 4\pi^2 a^2. \tag{13}$$

Note that the geometric sector of the phase space has a finite dimension (equal to two), a fact that will greatly facilitate its quantum description. Inspired by the methodology of LQG, we construct holonomies that describe the degree of freedom c characterizing the connection. Thanks to the symmetries of the spatial sections, it is sufficient to consider straight edges e_a of length $2\pi\mu$, with $\mu \in \mathbb{R}$, in the three orthogonal directions adapted to the spatial homogeneity (Ashtekar et al., 2006). The holonomies of the connection A^i_a along these edges have the simple expression

$$h_{e_a}(\mu) = \cos\left(\frac{c\mu}{2}\right) I + 2\sin\left(\frac{c\mu}{2}\right)\delta^i_a \tau_i, \tag{14}$$

where I is the identity in SU(2). Similarly, spatial symmetries allow us to restrict all our considerations just to fluxes of the densitized triad through squares, formed by edges along two of the reference orthogonal directions adapted to homogeneity. These fluxes are then completely determined by the variable p, that hence describes the geometric sector of the momentum space. Holonomies, or equivalently their matrix elements, describe the rest of the geometric sector of the phase space. More specifically, the geometric configuration space consists of the algebra formed by functions that depend on the connection through finite linear combinations of the complex exponentials $\mathcal{N}_\mu(c) = \exp(i\mu c/2)$, with $\mu \in \mathbb{R}$. On the other hand, we recall that the mater content of our FLRW cosmology is given by a homogeneous (massless) scalar field ϕ. This scalar field is minimally coupled to the geometry. We will call π_ϕ its canonically conjugate momentum. The canonical algebra that we want to represent has then the following non-trivial Poisson brackets:

$$\{\mathcal{N}_\mu(c), p\} = i\frac{4\pi G\gamma}{3}\mu\mathcal{N}_\mu(c), \qquad \{\phi, \pi_\phi\} = 1. \tag{15}$$

In LQC, the quantum representation of this algebra parallels the strategy adopted in LQG. In that theory, the geometric configuration space is described by means of the so-called cylindrical functions. These are functions that depend on the Ashtekar-Barbero connection through holonomies along graphs that are formed by a finite number of edges. The algebra of cylindrical functions is completed with respect to the supreme norm, obtaining a commutative C^*-algebra with identity element. Gel'fand's theory guarantees that this algebra is isomorphic to an algebra of continuous functions over a certain compact space, called the Gel'fand spectrum, that contains the smooth connections as a dense subspace. The Hilbert space for the representation of the algebra of holonomies and fluxes in LQG is then that of square integrable functions on the Gel'fand spectrum, with respect to a certain measure (Ashtekar and Lewandowski, 2004; Velhinho, 2007).

In the homogeneous and isotropic scenarios that we are considering, on the other hand, the geometric sector of the configuration space, when completed with respect to the supreme norm, is the C^*-algebra of quasi-periodic functions over $\mathbb{R}$. The complex exponentials that describe the holonomies, $\mathcal{N}_\mu : \mathbb{R} \to S^1$, where S^1 is the circumference of unit radius, form a basis in it (Velhinho, 2007). Its Gel'fand spectrum is the Bohr compactification of the real line, $\mathbb{R}_B$, that contains $\mathbb{R}$ as a dense subspace (Rudin, 1962). The space $\mathbb{R}_B$ can be characterized as the set of all homomorphisms between the additive group of real numbers and the multiplicative group of complex unit module numbers. That is, every $x \in \mathbb{R}_B$ is a map $x : \mathbb{R} \to S^1$ such that

$$x(0) = 1, \qquad x(\mu + \mu') = x(\mu)\, x(\mu'), \qquad \forall \mu, \mu' \in \mathbb{R}. \quad (16)$$

This space $\mathbb{R}_B$ admits a compact topological group structure (Velhinho, 2007). All functions $F_\mu : \mathbb{R}_B \to S^1$ such that $F_\mu(x) = x(\mu)$, for any $\mu \in \mathbb{R}$, are continuous with respect to that topology. In addition, since it is a compact group, it admits a unique Haar measure M_H, which is invariant under the group action. The Hilbert space for the representation of the algebra of holonomies and fluxes in homogeneous and isotropic LQC is then $L^2(\mathbb{R}_B, M_H)$. It follows that the set of functions $\{F_\mu, \mu \in \mathbb{R}\}$ are an orthonormal basis of this Hilbert space (Velhinho, 2007), that is therefore not separable. Using Dirac's notation, we will denote this basis as $\{|\mu\rangle, \mu \in \mathbb{R}\}$, where $\langle\mu|\mu'\rangle = \delta_{\mu\mu'}$ is the inner product on $L^2(\mathbb{R}_B, M_H)$. The quantum representation of the algebra (**Eq. 15**) that describes the gravitational sector of the phase space is (Ashtekar et al., 2003; Velhinho, 2007)

$$\widehat{\mathcal{N}}_{\mu'}|\mu\rangle = |\mu + \mu'\rangle, \qquad \widehat{p}|\mu\rangle = \frac{4\pi G\gamma}{3}\mu|\mu\rangle. \quad (17)$$

This representation is often called polymer representation, and its Hilbert space is isomorphic to that of functions over $\mathbb{R}$ that are square summable with respect to the discrete measure. Making use of this isomorphism, it is clear that the states of the polymer Hilbert space must have support only on a countable number of points, and, when this number is finite, they are the direct analogue of the cylindrical functions of LQG. Besides, note that the representation of the basic operators that describe the holonomies is not continuous. As a consequence, the operator that would represent the Ashtekar-Barbero connection is not well defined, a fact that also occurs in LQG.

At this point of our discussion, it may be worth noticing that the construction of $L^2(\mathbb{R}_B, M_H)$ as the Hilbert space of the representation strongly depends on the choice of the Haar measure. In fact, it is possible to find another measure in $\mathbb{R}_B$ that results in a standard Schrödinger representation for the connections and triads (Velhinho, 2007). This alternate representation, unlike the polymer one, is continuous and is employed in the more familiar WdW quantization of this cosmological system (DeWitt, 1967). However, owing to the discrete character of M_H, the two measures, and hence their corresponding quantum theories, are not equivalent. It is therefore not surprising that LQC can provide different predictions than traditional geometrodynamics about the quantum regimes of this cosmological model.

Finally, a standard continuous Schrödinger representation is chosen for the matter sector of the phase space, that can be described by the scalar field and its conjugate momentum. The corresponding Hilbert space is $L^2(\mathbb{R}, d\phi)$, where the scalar field acts by multiplication and its momentum as the derivative $\widehat{\pi}_\phi = -i\partial_\phi$.

2.3 LQC: Hamiltonian Constraint

The Hilbert space obtained by the tensor product of the polymer space and $L^2(\mathbb{R}, d\phi)$ does not necessarily contain the physical states of the quantum theory. They should still satisfy the Hamiltonian constraint, that is the only non-trivial constraint that exists on the system, and which should be imposed à la Dirac quantum mechanically (Dirac, 1964). For this reason, the elements of the considered Hilbert space are often called kinematic states. The next step in our quantization is then the representation of the Hamiltonian constraint as an operator on the kinematic Hilbert space. The gravitational part of this constraint is given by

$$-\frac{\pi^2}{2G\gamma^2\sqrt{h}} E^a_i E^b_j \epsilon^{ij}{}_k F^k_{ab}. \quad (18)$$

Taking into account that the lapse function is homogeneous, we have already considered the integrated version of the constraint over the three spatial directions. In terms of the Ashtekar-Barbero variables introduced before for the geometric sector, the constraint $\mathcal{H}_S$ that we obtain for homogeneous and isotropic cosmologies, including the contribution of the homogeneous massless matter field ϕ, has the following form:

$$\mathcal{H}_S = |p|^{-3/2}\left(\frac{\pi_\phi^2}{2} - \frac{3}{8\pi G\gamma^2}c^2p^2\right). \quad (19)$$

The first evident obstruction for a polymer quantization of this constraint is the absence of an operator to represent the connection. However, this difficulty can be surpassed if the following classical identity is taken into account:

$$F^i_{ab} = -2\lim_{A_\square \to 0} \mathrm{tr}\left(\frac{h_{\square_{ab}}}{A_\square}\tau^i\right), \qquad a \neq b, \quad (20)$$

where the symbol $\mathrm{tr}(\cdot)$ stands for the trace and $h_{\square_{ab}}$ is the holonomy along a certain circuit that encloses a coordinate area $A_\square$. For spacetimes such as flat FLRW and Bianchi I cosmologies, one can consider a rectangular circuit in the plane formed by the directions a and b. Thus, in our specific flat FLRW case, this holonomy can be written as

$$h_{\square_{ab}} = h_{e_a}(\mu) h_{e_b}(\mu) h^{-1}_{e_a}(\mu) h^{-1}_{e_b}(\mu) \quad (21)$$

and the enclosed coordinate area is $A^{FLRW}_\square = 4\pi^2\mu^2$.

If these holonomies are represented polymerically, the limit contained in expression (**Eq. 20**) is not well defined, because neither is the connection operator. Therefore, in LQC, the enclosed coordinate area is not made to tend to zero, but instead one appeals to the existence of a minimum value, characterized by the minimum coordinate length $2\pi\overline{\mu}$ of the edges that enclose it: $A^{FLRW}_{\square_{min}} = 4\pi^2\overline{\mu}^2$. It seems clear then that this prescription for the quantum representation of the curvature introduces a new scale. The arbitrariness in its choice can be fixed by recurring to full LQG, where the geometric area operator has a minimum non-zero eigenvalue Δ. Drawing inspiration from this fact, in LQC one postulates that this value coincides with the geometric physical area corresponding to $A^{FLRW}_{\square_{min}}$.

Recalling the (second) classical relation in (**Eq. 13**), one concludes then that the minimum coordinate length should satisfy (Ashtekar et al., 2006)

$$\overline{\mu} = \sqrt{\frac{\Delta}{|p|}}. \quad (22)$$

Once we have determined the scale $\overline{\mu}$ (now turned into a dynamical variable) that sets the minimum coordinate area in the FLRW cosmological model, we have to represent the classical expression (**Eq. 20**) on the polymer Hilbert space, taking in it the limit $A_{\square}^{FLRW} \to A_{\square_{min}}^{FLRW}$. In practice, this prescription amounts to the replacement of c with the function $\sin(\overline{\mu}c)/\overline{\mu}$ in the classical expression of the Hamiltonian constraint $\mathcal{H}_S$ before one proceeds to its quantum representation. The dependence of the constraint on the connection is thus captured by the complex exponentials $\mathcal{N}_{\pm 2\overline{\mu}}(c)$, that in particular depend on p through $\overline{\mu}$. We must then specify their representation on the polymer Hilbert space, since the classical dependence of $\mathcal{N}_{\pm 2\overline{\mu}}(c)$ on c and p makes their construction ambiguous in terms of the operators that we have taken so far as basic for the FLRW geometry, namely $\widehat{\mathcal{N}}_{\mu}$ and $\widehat{p}$. With this aim, it is useful to introduce first the following operator, constructed by means of the spectral theorem (Reed and Simon, 1980):

$$\widehat{v} = \frac{\widehat{\mathrm{sign}(p)}\widehat{|p|^{3/2}}}{2\pi G\gamma\sqrt{\Delta}}, \qquad \widehat{v}|\mu\rangle = \frac{\mathrm{sign}[p(\mu)]|p(\mu)|^{3/2}}{2\pi G\gamma\sqrt{\Delta}}|\mu\rangle, \tag{23}$$

where $p(\mu)$ is the eigenvalue of $\widehat{p}$ corresponding to the eigenstate $|\mu\rangle$, given in (**Eq. 17**). The direct classical counterpart of this operator is proportional to the physical volume of the FLRW flat and compact Universe. In addition, it has a Poisson bracket with $b = \overline{\mu}c$ equal to minus two. If we relabel the orthonormal basis $\{|\mu\rangle, \mu \in \mathbb{R}\}$ using the eigenvalues v of $\widehat{v}$, the operators $\widehat{\mathcal{N}}_{\pm\overline{\mu}}$ are then defined so that their action is simply a constant translation, namely they simply shift the new label by a constant (Ashtekar et al., 2006):

$$\widehat{\mathcal{N}}_{\pm\overline{\mu}}|v\rangle = |v \pm 1\rangle. \tag{24}$$

The square of these operators defines $\widehat{\mathcal{N}}_{\pm 2\overline{\mu}}$.

The prescription that we have explained in order to represent the elements of holonomies that appear in the Hamiltonian of LQC is commonly called the improved dynamics scheme[1]. However, this scheme alone is not enough to complete the representation of the constraint $\mathcal{H}_S$. The presence of the zero eigenvalue in the spectrum of the operator $\widehat{p}$ creates problems added to those already mentioned. Indeed, the Hamiltonian constraint depends on the inverse of the geometric variable p *via* ratios that involve the determinant of the spatial metric. The quantum representation of this inverse cannot be defined in the kinematic Hilbert space using the spectral theorem, because zero is part of the discrete spectrum of $\widehat{p}$. This difficulty can be circumvented again by appealing to the following classical identity, employed as well in LQG adapted to a more general context (Thiemann, 1996):

$$\frac{\mathrm{sign}(p)}{|p|^{1/2}} = \frac{|p|^{1/2}}{2\pi G\gamma\sqrt{\Delta}}\mathrm{tr}\left(\tau_i \sum_a \delta^i_a h_{e_a}(\overline{\mu})\left\{h^{-1}_{e_a}(\overline{\mu}), |p|^{1/2}\right\}\right). \tag{25}$$

The quantum operators that correspond to inverse powers of the triadic variable p are then defined by representing, on the improved dynamics scheme, the variables appearing on the right-hand side of this equality. In particular, Poisson brackets are represented by $-i$ times the commutator of the corresponding operators. If one follows this quantization procedure, the operator representing the homogeneous Hamiltonian constraint $\mathcal{H}_S$ in LQC is (Martín-Benito et al., 2009a)

$$\widehat{\mathcal{H}}_S = \left[\widehat{\frac{1}{\sqrt{|p|}}}\right]^{3/2} \widehat{H}_S \left[\widehat{\frac{1}{\sqrt{|p|}}}\right]^{3/2}, \tag{26}$$

where we have defined the densitized operator

$$\widehat{H}_S = \frac{\widehat{\pi}_\phi^2}{2} - \frac{\widehat{\Omega}_0^2}{2}. \tag{27}$$

Here

$$\widehat{\Omega}_0 = \frac{3\pi G}{2}\sqrt{|\widehat{v}|}\left[\widehat{\mathrm{sign}}(\widehat{v})\widehat{\sin}(b) + \widehat{\sin}(b)\widehat{\mathrm{sign}}(\widehat{v})\right]\sqrt{|\widehat{v}|}, \tag{28}$$

$$\widehat{\sin}(b) = \frac{1}{2i}\left(\widehat{\mathcal{N}}_{2\overline{\mu}} - \widehat{\mathcal{N}}_{-2\overline{\mu}}\right). \tag{29}$$

In these definitions, we have used a prescription for the factor ordering of the involved operators proposed by Martín-Benito, Mena Marugán, and Olmedo (Martín-Benito et al., 2009a), known with the initials of these authors as the MMO prescription. Its most characteristic feature is the symmetrization of the sign of the orientation of the triad with the holonomy elements in (**Eq. 28**). The operator $\widehat{\mathcal{H}}_S$ defined in this way presents certain interesting properties thanks to its symmetric factor ordering, compared with the quantum constraint obtained with another, frequently adopted prescription, proposed by Ashtekar, Pawlowski, and Singh (APS) (Ashtekar et al., 2006; Ashtekar et al., 2006; Ashtekar et al., 2006). In particular, its action decouples the state of the polymer basis with $v = 0$ from its orthogonal complement. This allows for a neat densitization of the Hamiltonian constraint (Martín-Benito et al., 2009a). Besides, the action of the operator does not mix states with positive and with negative values of v (Martín-Benito et al., 2009a) (namely, it does not change the orientation of the triad). We can then restrict the quantum analysis of the FLRW cosmologies to the linear subspace generated by states $|v\rangle$ with $v \in \mathbb{R}^+$, for example. Actually, the action of the constraint leaves invariant smaller and separable subspaces that are called superselection sectors, and that are simpler with the MMO prescription than in the APS case owing to the separation between sectors of different triad orientation. In more detail, the action of $\widehat{\mathcal{H}}_S$ (or, equivalently, of $\widehat{H}_S$) turns out to preserve every one of the linear subspaces generated by states $|v\rangle$ with v belonging to the semilattice $\mathcal{L}^+_{\overline{\varepsilon}} = \{\overline{\varepsilon} + 4k, k \in \mathbb{N}\}$, entirely characterized by its smallest point $\overline{\varepsilon} \in (0, 4]$. Notice that the value of $\overline{\varepsilon}$ is always strictly positive, and therefore the same is automatically true for the variable v in each of the considered superselection sectors. Finally, a comment is due about the imposition of the (densitized) Hamiltonian constraint $\widehat{H}_S$. Although the kernel of this operator is not a proper subspace of the kinematic Hilbert space, the quantum

[1]An alternate way to define the Hamiltonian constraint operator using a regularized expression for the extrinsic curvature has been explored recently (Yang et al., 2009; Dapor and Liegener, 2018; Assanioussi et al., 2019; García-Quismondo and Mena Marugán, 2019).

constraint can be rigorously imposed in our representation by its adjoint action, allowing in this way generalized solutions that should provide the physical Hilbert space once they are supplied with a suitable inner product, different from the kinematic one.

In fact, it has been possible to characterize the resulting physical Hilbert space, together with complete sets of Dirac observables. The resolution of the constraint is straightforward once one completes the spectral analysis of the operator $\widehat{\Omega}_0^2$. It has been proven that this operator has a non-degenerate absolutely continuous spectrum equal to the positive real line (Martín-Benito et al., 2008; Martín-Benito et al., 2009a). The eigenvalue equation of the operator $\widehat{\Omega}_0^2$ can be regarded as a second-order difference equation. With the MMO prescription adopted in its definition, the generalized eigenfunctions turn out to be entirely determined by their value at $\bar{\varepsilon}$, point from which they can be constructed by solving the eigenvalue equation. Besides, up to a global phase, these eigenfunctions $e_\delta^{\bar{\varepsilon}}(\nu)$ are real, because the second-order difference equation associated with the action of the operator is a real equation. With the eigenfunctions at hand, one easily obtains the solutions to the Hamiltonian constraint, which take the form

$$\xi(\nu,\phi) = \int_0^\infty d\delta\, e_\delta^{\bar{\varepsilon}}(\nu)\left[\xi_+(\delta)e^{i\sqrt{\delta}\,\phi} + \xi_-(\delta)e^{-i\sqrt{\delta}\,\phi}\right]. \tag{30}$$

Therefore, physical states can be identified, for instance, with the positive frequency solutions $\xi_+(\delta)\exp(i\sqrt{\delta}\,\phi)$ that are square integrable over the spectral parameter $\delta \in \mathbb{R}^+$ (Martín-Benito et al., 2009a) (negative frequency solutions provide essentially the same Hilbert space). A complete set of Dirac observables is given by $\widehat{\pi}_\phi$ and $|\widehat{\nu}|_{\phi_0}$, where this latter operator is defined as the action of the operator $\widehat{\nu}$ when the scalar field equals ϕ_0. On the Hilbert space of physical states specified above, these observables are self-adjoint, property that in fact characterizes the inner product on the space of solutions described by the functions $\xi_+(\delta)$.

On the other hand, a numerical analysis of the dynamics, with respect to the homogeneous scalar field, of certain families of states with a semiclassical behavior at large volumes shows that they remain sharply peaked during the quantum evolution (Ashtekar et al., 2006). Actually, the trajectories of their peaks coincide, in the regions of low matter density, with those dictated by Einstein's equations in the considered FLRW cosmology. However, when the matter density reaches values that are comparable to the Planck density ρ_{Planck}, the trajectory of the peak separates from the classical solution and turns to describe a transition from a Universe in contraction to an expanding one (or vice versa) (Ashtekar et al., 2006). In particular, the matter density reaches a critical value when it is equal to $0.41\,\rho_{\text{Planck}}$ [for the value of the Immirzi parameter that leads in LQG to the Bekenstein-Hawking law for the entropy of black holes (Ashtekar et al., 2001; Domagala and Lewandowski, 2004; Meissner, 2004)]. As we explained in the Introduction, this phenomenon of quantum nature that eludes the cosmological singularity of the Big Bang is known by the name of Big Bounce. There is also evidence that it occurs in LQC beyond the context of homogeneous and isotropic cosmologies, with indications that it is present as well in anisotropic cosmologies such as Bianchi I models (Gupt and Singh, 2012), or in inhomogeneous cosmologies such as the linearly polarized Gowdy model with toroidal spatial sections (Tarrío et al., 2013).

3 HYBRID LQC: THE GOWDY MODEL

Historically, hybrid LQC was first developed for the Gowdy linearly polarized cosmological model, with spatial sections with the topology of a three-torus, T^3, and after carrying out a partial gauge fixing that removes all constraints on the system except for the zero mode of the Hamiltonian constraint and of one of the momentum constraints (these zero modes are the average of those constraints on the spatial sections, modulo a constant numerical factor). Gowdy models are inhomogeneous cosmological spacetimes with compact spatial sections and two axial Killing vector fields (Gowdy, 1971; Gowdy, 1974). The case with three-torus spatial topology is the simplest one. The linear polarization restriction on the gravitational wave content of the model amounts to require that the two Killing vectors are hypersurface orthogonal. The Killing symmetries then imply that the physical degree of freedom still present in those gravitational waves can be thought of as varying in only one spatial direction. After the mentioned partial gauge fixing, the phase space of this Gowdy model can be identified with that of a Bianchi I spacetime containing a linearly polarized wave. Furthermore, given the spatial behavior of this wave, we can describe it as a scalar field χ defined on the circle, S^1, that corresponds to the cyclic spatial direction in which the wave propagates. In addition, we couple a massless scalar field Φ with the same symmetries as those of the geometry (Martín-Benito et al., 2010a). The hybrid quantization of this model will therefore be based on the quantization of Bianchi I cosmologies according to the LQC formalism [and the MMO prescription, see Refs. (Martín-Benito et al., 2008; Mena Marugán and Martín-Benito, 2009; Garay et al., 2010; Martín-Benito et al., 2010b)], as well as on a suitable Fock representation of the matter field Φ and of the scalar field χ assigned to the linearly polarized gravitational wave. For convenience, we extract the zero mode ϕ of the matter field, that behaves as a homogeneous scalar field giving a non-trivial matter content to the Bianchi I cosmology, and assume that χ has vanishing zero mode (this assumption is only meant to simplify the discussion and involves no relevant conceptual consequences). The two sectors of the model, namely the homogeneous Bianchi I sector and the inhomogeneous scalar field sector, get mixed in a non-trivial way by the zero mode of the Hamiltonian constraint, that must be imposed on the considered system.

Let us describe the model in more detail. It is most convenient to choose coordinates $\{t,\theta,\sigma,\delta\}$ adapted to the Killing symmetries, such that ∂_σ and ∂_σ are the Killing vectors. Then, the degrees of freedom of the model only depend on the time t and on the cyclic spatial coordinate $\theta \in S^1$. Starting with the canonical formulation of GR, we can then peform a symmetry reduction to take into account the Killing symmetries, as well as a partial gauge fixing that removes the momentum and Hamiltonian constraints except for the zero modes of the latter and of the momentum constraint in the θ-direction

(Mena Marugán and Martín-Benito, 2009). In this way, we get a reduced phase space that is formed by four canonical pairs of degrees of freedom (corresponding to the zero modes of the model), a gravitational field (that describes the linearly polarized gravitational wave of the model, and that we consider devoid of zero mode), and the inhomogeneous part of the massless scalar field. The homogeneous sector, composed of the four pairs of zero modes, coincides with the phase space of a Bianchi I cosmology coupled to a homogeneous massless scalar field ϕ. Besides, using a Fourier transform, we decompose the gravitational and matter scalar fields of the model, χ and Φ respectively, passing to describe them in terms of their Fourier (non-zero) modes. These modes and the corresponding modes of the canonical momenta of the two fields form the inhomogeneous sector of the system. The obtained reduced phase space is subject to two constraints, that were not eliminated in the process of partial gauge fixing. One of them is the zero mode of the momentum constraint in the θ-direction, H_θ. This constraint generates rigid rotations in the circle coordinatized by θ, and imposes a restriction that affects exclusively the inhomogeneous sector. The other constraint that must be imposed is the zero mode H_S of the Hamiltonian constraint of the system. This constraint H_S is the sum of a homogeneous term H_{hom}, that is the Hamiltonian constraint of the Bianchi I model, and an additional term H_{inh}, that couples the homogeneous and inhomogeneous sectors and vanishes when the inhomogeneous sector is not present.

The next step in our analysis consists in describing the Bianchi I cosmologies with three-torus spatial topology in terms of Ashtekar-Barbero variables, in order to quantize them by using LQC techniques. We can adopt a suitable internal gauge and adopt a diagonal form for the triads and connections. In this way, each of the Ashtekar-Barbero variables can be totally characterized by three homogeneous functions, that determine the diagonal components. We will call these functions p_a and c_a, corresponding to the densitized triad and $\mathrm{su}(2)$-connection, respectively, and with $a = \theta, \sigma, \delta$. The only non-trivial Poisson brackets for them are $\{c_a, p_b\} = 8\pi\gamma G\delta_{ab}$, so they form canonical pairs. We call $\mathcal{H}^{\mathrm{BI}}_{\mathrm{kin}} \otimes L^2(\mathbb{R}, d\phi)$ the kinematic Hilbert space for the Bianchi I model in LQC, where $\mathcal{H}^{\mathrm{BI}}_{\mathrm{kin}}$ denotes the polymer representation space of the Bianchi I geometries in LQC and $L^2(\mathbb{R}, d\phi)$ is the space of square integrable functions for the homogeneous scalar field, defined on the real line (Ashtekar and Wilson-Ewing, 2009) With this choice of Hilbert space, we adopt again a standard Schrödinger representation for the zero mode of the matter field, ϕ, so that its canonical conjugate momentum acts as a derivative, $\widehat{\pi}_\phi = -i\partial_\phi$. The construction of $\mathcal{H}^{\mathrm{BI}}_{\mathrm{kin}}$, on the other hand, is similar to that explained for the FLRW geometry in LQC, except for the fact that we now have three pairs of canonically conjugated Ashtekar-Barbero degrees of freedom instead of only one. The inner product on this Hilbert space is discrete, so that the triad operators $\widehat{p}_a$ have a point spectrum equal to the real line. Defining the tensor product $\otimes_a |p_a\rangle$ (with $a = \theta, \sigma, \delta$) of the eigenvectors of each of the triad operators we obtain eigenstates $|p_\theta, p_\sigma, p_\delta\rangle$ that form an orthonormal basis of the Hilbert space $\mathcal{H}^{\mathrm{BI}}_{\mathrm{kin}}$.

On the other hand, we can extend the improved dynamics proposal from the FLRW geometries to the Bianchi I model as proposed in Ref. (Ashtekar and Wilson-Ewing, 2009), introducing in this way minimum coordinate length scales $\overline{\mu}_a$ for each of the spatial directions. Explicitly, these length scales are

$$\overline{\mu}_a = \sqrt{\frac{\Delta\,|p_a|}{|p_b\,p_c|}}, \tag{31}$$

with $a \neq b \neq c$ and $a, b, c \in \{\theta, \sigma, \delta\}$. We then introduce the operators $\widehat{\mathcal{N}}_{\pm\overline{\mu}_a}$ to represent the holonomy elements $\mathcal{N}_{\pm\overline{\mu}_a} = \exp(\pm i\overline{\mu}_a c_a/2)$ along an edge in the a-direction of coordinate length $2\pi\overline{\mu}_a$. These operators appear in the regularization of the curvature operator in the Hamiltonian constraint and are defined in a similar way as we did for the isotropic case in FLRW.

The action of these holonomy operators on the states $|p_\theta, p_\sigma, p_\delta\rangle$ is rather complicated, since each of the length scales $\overline{\mu}_a$ depends not only on p_a, but also on the triad variables in the other directions. To simplify the expressions, it is convenient to relabel these states in the form $|v, \lambda_\sigma, \lambda_\delta\rangle$, where

$$\lambda_a = \mathrm{sign}(p_a)\frac{\sqrt{|p_a|}}{(4\pi G\gamma\sqrt{\Delta})^{1/3}}, \tag{32}$$

$$\mathrm{v} = 2\lambda_\theta\lambda_\sigma\lambda_\delta. \tag{33}$$

Apart from an orientation sign, v is equal to $1/(2\pi G\gamma\sqrt{\Delta})$ multiplied by the physical volume of the Bianchi I Universe, volume that we will often call also the homogeneous volume. The action of the holonomy operators $\widehat{\mathcal{N}}_{\pm\overline{\mu}_\theta}$ just scale λ_θ in such a way that the label v is shifted by the unit (Ashtekar and Wilson-Ewing, 2009). In full detail, we have

$$\widehat{\mathcal{N}}_{\pm\overline{\mu}_\theta}|v, \lambda_\sigma, \lambda_\delta\rangle = |v \pm \mathrm{sign}(\lambda_\sigma\lambda_\delta), \lambda_\sigma, \lambda_\delta\rangle. \tag{34}$$

On the other hand, the holonomy operators $\widehat{\mathcal{N}}_{\pm\overline{\mu}_\sigma}$ and $\widehat{\mathcal{N}}_{\pm\overline{\mu}_\delta}$ additionally produce state-dependent scalings of λ_σ and λ_δ, respectively. For example, we have

$$\widehat{\mathcal{N}}_{\pm\overline{\mu}_\sigma}|v, \lambda_\sigma, \lambda_\delta\rangle = |v \pm \mathrm{sign}(\lambda_\sigma v), v^{-1}[v \pm \mathrm{sign}(\lambda_\sigma v)]\lambda_\sigma, \lambda_\delta\rangle. \tag{35}$$

To complete the ingredients that are needed for the hybrid quantization of the Gowdy model, we have to select a Fock quantization of the inhomogeneous sector. Actually, it has been proven that it is possible to single out a unique Fock quantization (given by a Fock representation and a Heisenberg dynamics for the background independent part of the fields), up to unitary equivalence, by imposing certain natural conditions, that require that the symmetry generated by H_θ and the quantum evolution of the creation and annihilation operators be unitarily implementable (Corichi et al., 2006; Cortez et al., 2007). In particular, this result removes the freedom of choice among the infinite number of inequivalent Fock representations, that may lead to different physics. Besides, the unitarity of the Heisenberg dynamics also imposes a concrete parametrization for the non-zero modes of both the gravitational field χ and the matter field Φ in terms of the background variables (namely the zero modes). Following these criteria, we represent the inhomogeneous sector of our hybrid model in Fock spaces $\mathcal{F}^\alpha$ (with $\alpha = \chi, \Phi$) chosen in Refs. (Corichi et al., 2006; Cortez et al., 2007). An orthonormal basis of each of

these Fock spaces is provided by the n–particle states $|\mathrm{n}^\alpha\rangle = |\cdots, n^\alpha_{-2}, n^\alpha_{-1}, n^\alpha_1, n^\alpha_2, \cdots\rangle$, where n^α_l denotes the occupation number of the field α in the mode $l \in \mathbb{Z} - \{0\}$. Let $\hat{a}^{(\alpha)}_l$ and $\hat{a}^{(\alpha)\dagger}_l$ denote the annihilation and creation operators of that mode, respectively. We can then reach a kinematic Hilbert space for the hybrid quantization of the Gowdy model by taking the tensor product $\mathcal{H}_{\mathrm{kin}} = \mathcal{H}^{\mathrm{BI}}_{\mathrm{kin}} \otimes L^2(\mathbb{R}, d\phi) \otimes \mathcal{F}^\chi \otimes \mathcal{F}^\Phi$. Excluding the zero mode of the matter field temporally from our considerations, an orthonormal basis for the Hilbert space of the rest of the system is formed by the states $|\nu, \lambda_\sigma, \lambda_\delta, \mathrm{n}^\chi, \mathrm{n}^\Phi\rangle$ for all real values of the three first labels and all sets n^χ and n^Φ of integers with a finite number of non-vanishing elements.

Finally, we are in an adequate position to represent the constraints of the system as densely defined operators on this Hilbert space. Choosing normal ordering, the generator of the translations in the circle reads (Martín-Benito et al., 2010a)

$$\hat{H}_\theta = \sum_{l=1}^{\infty} \sum_{\alpha=\chi,\Phi} l\left(\hat{a}^{(\alpha)\dagger}_l \hat{a}^{(\alpha)}_l - \hat{a}^{(\alpha)\dagger}_{-l} \hat{a}^{(\alpha)}_{-l}\right). \tag{36}$$

This constraint leads to the condition

$$\sum_{l=1}^{\infty} \sum_{\alpha=\chi,\Phi} l\left(n^\alpha_l - n^\alpha_{-l}\right) = 0 \tag{37}$$

on n–particle states of the inhomogeneities. Those states that satisfy the condition span a proper Fock subspace $\mathcal{F}_{\mathrm{p}}$ of $\mathcal{F}^\chi \otimes \mathcal{F}^\Phi$. Let us now consider the quantum Hamiltonian constraint. We choose again normal ordering for the creation and annihilation operators of the inhomogeneous sector, while for the part of the constraint that acts on the homogeneous sector we choose a convenient symmetrization inspired by the MMO prescription (Garay et al., 2010). Rational powers of the norm of the triad variables are represented adopting an algebraic symmetrization, which decouples the states of zero homogeneous volume ν from their orthogonal complement. Like in the FLRW cosmology, this fact allows us to remove the states with vanishing homogeneous volume from our kinematic space, therefore eliminating the quantum kinematic analogues of the classical singularities with $\nu = 0$. Moreover, again like in the FLRW model, one finds that the action of the Hamiltonian constraint does not mix states with different orientations of any of the components of the triad or, equivalently, with different signs of the variables ν, λ_σ, and λ_δ. Hence, as far as the constraints of the system are concerned, one can restrict all considerations, e.g., to the sector of strictly positive labels for the homogeneous geometry. Taking this into account, we redefine $\Lambda_a = \ln(\lambda_a)$ for $a = \sigma, \delta$ so that the anisotropy labels continue to take values over the real line.

The Hamiltonian constraint $\hat{H}_S = \hat{H}_{\mathrm{hom}} + \hat{H}_{\mathrm{inh}}$ that one obtains with this hybrid quantization, after performing a densitization similar to that in the FLRW case, has the following form (Garay et al., 2010; Martín-Benito et al., 2010b):

$$\hat{H}_{\mathrm{hom}} = \frac{\hat{\pi}^2_\phi}{2} - \frac{\pi G}{16} \sum_{a \neq b} \sum_b \hat{\Theta}_a \hat{\Theta}_b, \tag{38}$$

$$\hat{H}_{\mathrm{inh}} = 2\pi\left(4\pi G\gamma\sqrt{\Delta}\right)^{2/3} \widehat{e^{2\Lambda_\theta}} \hat{H}_F + \frac{\pi G^{4/3}}{16\left(4\pi\gamma\sqrt{\Delta}\right)^{2/3}} \widehat{e^{-2\Lambda_\theta}} \hat{D}\left(\hat{\Theta}_\delta + \hat{\Theta}_\sigma\right)^2 \hat{D}\hat{H}_I. \tag{39}$$

Here $a, b \in \{\theta, \sigma, \delta\}$. As we have already commented, $\hat{H}_{\mathrm{hom}}$ is the constraint operator for the Bianchi I model with a homogeneous massless scalar field in LQC, according to the MMO prescription (Martín-Benito et al., 2008). On the other hand, the operator $\pi G\gamma\hat{\Theta}_a$ is the representation of $c_a p_a$, which is a constant of motion in the classical theory. We have defined

$$\hat{\Theta}_a = \frac{1}{2i} \widehat{\sqrt{|\nu|}} \left[\left(\hat{\mathcal{N}}_{2\overline{\mu}_a} - \hat{\mathcal{N}}_{-2\overline{\mu}_a}\right) \widehat{\mathrm{sign}(p_a)} + \widehat{\mathrm{sign}(p_a)} \left(\hat{\mathcal{N}}_{2\overline{\mu}_a} - \hat{\mathcal{N}}_{-2\overline{\mu}_a}\right)\right] \widehat{\sqrt{|\nu|}}, \tag{40}$$

similar to the operator $\hat{\Omega}_0$ introduced in the isotropic case (**Eq. 28**). In addition, the operator $\hat{D}$ represents the product of the volume by its inverse [which is regularized in the standard way within LQC; (**Eq. 25**)]. Its action on the basis of volume eigenstates is

$$\hat{D}|\nu\rangle = \nu\left(\sqrt{|\nu+1|} - \sqrt{|\nu-1|}\right)^2 |\nu\rangle. \tag{41}$$

The contribution of the inhomogeneities is captured by $\hat{H}_{\mathrm{F}}$ and $\hat{H}_I$. The operator $\hat{H}_{\mathrm{F}}$ can be understood as a free-field Hamiltonian, that leaves invariant the n–particle states. It is given by

$$\hat{H}_F = \sum_{l=1}^{\infty} \sum_{\alpha=\chi,\Phi} l\left(\hat{a}^{(\alpha)\dagger}_l \hat{a}^{(\alpha)}_l + \hat{a}^{(\alpha)\dagger}_{-l} \hat{a}^{(\alpha)}_{-l}\right). \tag{42}$$

The operator $\hat{H}_I$ may be interpreted as an interaction Hamiltonian that creates and annihilates an infinite collection of pairs of particles, while preserving the momentum constraint $\hat{H}_\theta$. Explicitly,

$$\hat{H}_I = \sum_{l=1}^{\infty} \sum_{\alpha=\chi,\Phi} \frac{1}{l}\left(\hat{a}^{(\alpha)\dagger}_l \hat{a}^{(\alpha)}_l + \hat{a}^{(\alpha)\dagger}_{-l} \hat{a}^{(\alpha)}_{-l} + \hat{a}^{(\alpha)\dagger}_l \hat{a}^{(\alpha)\dagger}_{-l} + \hat{a}^{(\alpha)}_l \hat{a}^{(\alpha)}_{-l}\right). \tag{43}$$

It is worth remarking that the inhomogeneities of both fields contribute to the constraints in exactly the same way.

The action of the Hamiltonian constraint operator $\hat{H}_S$ does not relate all of the states with different values of $\nu \in \mathbb{R}^+$ and $\Lambda_a \in \mathbb{R}$, with $a = \sigma, \delta$. There are invariant subspaces in the Hilbert space spanned by those states. Each of these subspaces provides a superselection sector for the quantum theory. The superselection sectors in the homogeneous volume ν are semilattices of step four, $\mathcal{L}^+_{\bar{\varepsilon}} = \{\bar{\varepsilon} + 4n, n \in \mathbb{N}\}$, determined by the initial point $\bar{\varepsilon} \in (0, 4]$, exactly as in the FLRW model. Note that, again, the homogeneous volume is bounded from below by a strictly positive quantity in each of these sectors. The superselection sectors in Λ_a are more complicated. If we fix some initial data Λ^*_a and $\bar{\varepsilon}$, the values of Λ_a in the corresponding sector (constructed by the repeated action of the Hamiltonian constraint) take the form $\Lambda_a = \Lambda^*_a + \Lambda_{\bar{\varepsilon}}$, where

$\Lambda_{\bar{\varepsilon}}$ is any of the elements of a certain set $\mathcal{W}_{\bar{\varepsilon}}$ that is countable and dense in the real line (Garay et al., 2010):

$$\mathcal{W}_{\bar{\varepsilon}} = \left\{ z\ln\left(\frac{\bar{\varepsilon}-2}{\bar{\varepsilon}}\right) + \sum_{n,m\,\in\,\mathbb{N}} k_m^n \ln\left(\frac{\bar{\varepsilon}+2n}{\bar{\varepsilon}+2m}\right) \right\}. \tag{44}$$

Here, $k_m^n \in \mathbb{N}$ and $z \in \mathbb{Z}$ if $\bar{\varepsilon} > 2$, while $z = 0$ when $\bar{\varepsilon} \leq 2$.

Given that the action of $\widehat{\Theta}_a$ is considerably complicated, it has not been possible to elucidate yet whether this operator is self-adjoint. In spite of this, it is common to assume that $\widehat{H}_{\rm hom}$ is essentially self-adjoint (Ashtekar and Wilson-Ewing, 2009) and that the same applies to $\widehat{H}_S$ (Garay et al., 2010; Martín-Benito et al., 2010b). Regardless of this, one can try to formally solve the constraints of the Gowdy model. The solutions turn out to be completely determined by the data on the section of the v-space defined by $v = \bar{\varepsilon}$. Thanks to this fact, one can characterize the physical Hilbert space as the Hilbert space of such initial data, with an inner product that can be determined by imposing reality conditions on a complete set of observables (Rendall, 1993; Rendall, 1994). In this way, one arrives to the space $\mathcal{H}_{\rm phys} = \mathcal{H}^{\rm BI}_{\rm phys} \otimes L^2(\mathbb{R}, d\phi) \otimes \mathcal{F}_{\rm P}$, where $\mathcal{H}^{\rm BI}_{\rm phys}$ is the physical Hilbert space for Bianchi I cosmologies derived in Ref. (Martín-Benito et al., 2010b).

4 HYBRID LQC: COSMOLOGICAL PERTURBATIONS

After testing the viability of the hybrid quantization strategy in the Gowdy model, the approach was also applied to the discussion of a much more relevant scenario in cosmology, namely the study of primordial cosmological perturbations in the very early stages of the Universe. Using that the inflationary Universe is usually described as an FLRW cosmology that plays the role of a background where the perturbations develop and propagate, the idea was to quantize this background in the framework of LQC and treat the perturbations with the techniques of QFT in a curved spacetime. The hybrid approach then transforms the curved, FLRW classical background into a quantum spacetime with which the quantum field excitations corresponding to the perturbations coexist and interact by means of the gravitational constraints. For simplicity and for a better control of the mathematical techniques of QFT, we will again assume that the spatial sections are compact, with a three-torus topology. On the other hand, in order to isolate the perturbative degrees of freedom that do not depend on a possible perturbative diffeomorphism of the FLRW spacetime, that would result in a new identification of the background geometry, we will adopt a description in terms of perturbative gauge invariants. For cosmological scalar perturbations, one can employ the invariants introduced by Mukhanov and Sasaki (MS) (Sasaki, 1983; Kodama and Sasaki, 1984; Mukhanov, 1988) (considered as a pair of canonical fields). Gauge invariants are also the tensor perturbations, as well as the degrees of freedom of a Dirac field if it is present (Elizaga Navascués et al., 2017) (treating this field entirely as a perturbation). The description of the phase space of the perturbations can be completed with suitable redefinitions of the generators of the perturbative diffeomorphisms and canonical momenta of them. For the hybrid quantization, a piece of information that is most relevant as far as the inhomogeneities are concerned is the choice of a Fock representation for the gauge invariant fields. To restrict this choice and adopt a representation with especially appealing physical properties, we will still adhere to the criterion that the Fock quantization must allow a unitary implementation of the spatial symmetries of the model and of the Heisenberg dynamics associated with the creation and annihilation operators. With these ingredients, we will proceed to construct a hybrid quantum theory for the perturbed system. On this system, we will see that the only non-trivial constraint turns out to be the zero mode of the Hamiltonian constraint. We will then discuss its quantum imposition. Moreover, we will show how to extract from it (with a convenient ansatz and plausible approximations) Schrödinger equations for the perturbations, as well as effective equations to describe the propagation of the perturbations on the FLRW geometry subject to quantum effects. These equations can be used to study modifications to the power spectra of the cosmological perturbations, originated from quantum gravitational effects. The program that we have outlined will be implemented in this and the following five sections.

We start by constructing a convenient canonical description of the system formed by the FLRW cosmology and its perturbations that contains a complete set of gauge invariants. As in the case studied in our introduction to LQC, the FLRW spacetimes that we will consider possess compact sections with the topology of a three-torus. Their geometry can be described by a scale factor a and its canonical momentum π_a (or equivalently by the pair of variables c and p that determine the Ashtekar-Barbero variables in LQC). With the same choice of reference system for this cosmological background that we employed in the previous expositions about LQC, the coordinate volume of the spatial sections equals $8\pi^3$. As before, these spacetimes will contain a homogeneous scalar field, ϕ, responsible of the expansion and that consequently will play the role of an inflaton. This inflaton can be interpreted as the zero mode of a generally inhomogeneous scalar field Φ, interpretation that will be especially useful at the moment of introducing perturbations in the system. On the other hand, the main difference with respect to our previous studies is that we will now allow the possible existence of a potential $\mathcal{V}(\phi)$ for this inflaton.

The FLRW system is subject only to a non-trivial homogeneous Hamiltonian constraint, as we have discussed above. It can be written as $H_0 = 0$ where[2]

$$H_0 = \frac{1}{16\pi^3 a^3}\left(\pi_\phi^2 - \frac{4\pi G}{3}a^2\pi_a^2 + 128\pi^6 a^6 \mathcal{V}(\phi)\right). \tag{45}$$

[2]We reserve the notation H_S for the constraint of the whole perturbed model.

Let us next introduce perturbations in this system, both for the geometry and for the matter scalar field. It is also possible to introduce a Dirac field to describe fermions, regarded as perturbations of the FLRW cosmology (Elizaga Navascués et al., 2017). We postpone the consideration of these fermions to the next section. We can separate the metric and inflaton perturbations into scalar, vector, and tensor, depending on their behavior under the symmetries of the spatial sections (notice that these symmetries provide the Euclidean group in the limit in which the sections become non-compact). In addition, using that the spatial Laplacian (and the Dirac operator) corresponding to the auxiliary Euclidean metric ${}^0h_{ab}$ (with unit determinant) defined on our toroidal sections respect these symmetries, we can expand the different perturbations in eigenmodes of this differential operator. Moreover, since the spatial sections are compact, these modes are discrete. In this way, we can deal with the spatial dependence of the perturbations by considering infinite sequences of modes. For instance, choosing again (orthogonal) spatial coordinates of period equal to 2π, we expand the scalar perturbations of the metric and the matter field in a Fourier basis of sines and cosines,

$$Q^{\vec{k},+}\left(\vec{\theta}\right)=\sqrt{2}\cos\left(\vec{k}\cdot\vec{\theta}\right),\qquad Q^{\vec{k},-}\left(\vec{\theta}\right)=\sqrt{2}\sin\left(\vec{k}\cdot\vec{\theta}\right). \quad (46)$$

Here, the vector notation $\vec{\theta}$ stands for the spatial coordinates (θ,σ,δ), and the Euclidean scalar product has been denoted with a dot symbol. Each mode is characterized by a wavevector $\vec{k}\in\mathbb{Z}^3-\{0\}$, with strictly positive first non-vanishing component. Note that, in this way, we are not including the zero mode, that is part of the degrees of freedom considered in the FLRW background. The eigenvalue of the spatial Laplacian corresponding to $\vec{k}$ is $-\omega_k^2=-\vec{k}\cdot\vec{k}$. Scalar perturbations are described then by the corresponding Fourier coefficients of the scalar field Φ (without the zero mode, namely the inflaton), the trace and traceless scalar parts of the spatial metric h_{ab} (without the FLRW contribution), the lapse N (without its homogeneous part), and the scalar part of the shift N^a.

Similarly, tensor perturbations are described by the Fourier-like coefficients of the tensor part of the spatial metric, with two possible polarizations. These coefficients arise from the expansion in terms of the real tensor harmonics $G_{ab}^{\vec{k},\varepsilon,\pm}$, eigentensors of the spatial Laplacian (Fernández-Méndez, 2014). As above, the tuple $\vec{k}$ can take here any value in $\mathbb{Z}^3-\{0\}$, with positive first non-vanishing component, while ε is the dichotomic label that specifies the polarization, and the superscripts ± indicate whether the harmonic is even or odd under a periodic translation of $\vec{\theta}$, as in the scalar case. Vector perturbations, on the other hand, are described by the remaining parts of the shift and the spatial metric, that can be expanded in Fourier-like coefficients in terms of eigenvectors $S_a^{\vec{k}}$ of the Laplace operator and of tensors obtained from those by spatial covariant derivatives (Halliwell and Hawking, 1985). Here, $\vec{k}$ is again any non-vanishing tuple of integers. It is convenient to parametrize all of these mode coefficients as follows:

$$h_{ab}\left(t,\vec{\theta}\right)=a^2(t)\,{}^0h_{ab}\left(\vec{\theta}\right)\left[1+2\sum_{\vec{k},\pm}a_{\vec{k},\pm}(t)Q^{\vec{k},\pm}\left(\vec{\theta}\right)\right] \quad (47)$$

$$+6a^2(t)\sum_{\vec{k},\pm}b_{\vec{k},\pm}(t)\left[\frac{1}{\omega_k^2}Q^{\vec{k},\pm}_{|ab}\left(\vec{\theta}\right)+\frac{1}{3}{}^0h_{ab}\left(\vec{\theta}\right)Q^{\vec{k},\pm}\left(\vec{\theta}\right)\right]$$

$$+a^2(t)\sum_{\vec{k}}c_{\vec{k}}(t)S^{\vec{k}}_{(a|b)}\left(\vec{\theta}\right)+2\sqrt{6}a^2(t)\sum_{\vec{k},\varepsilon,\pm}d_{\vec{k},\varepsilon,\pm}(t)G_{ab}^{\vec{k},\varepsilon,\pm}\left(\vec{\theta}\right), \quad (48)$$

$$N\left(t,\vec{\theta}\right)=N_0(t)+\frac{6\pi^2}{G}a^3(t)\sum_{\vec{k},\pm}g_{\vec{k},\pm}(t)Q^{\vec{k},\pm}\left(\vec{\theta}\right), \quad (49)$$

$$N_a\left(t,\vec{\theta}\right)=a^2(t)\sum_{\vec{k},\pm}\frac{1}{\omega_k^2}l_{\vec{k},\pm}(t)Q^{\vec{k},\pm}_{|a}\left(\vec{\theta}\right)+a(t)\sum_{\vec{k}}v_{\vec{k}}(t)S^{\vec{k}}_a\left(\vec{\theta}\right), \quad (50)$$

$$\Phi\left(t,\vec{\theta}\right)=\phi(t)+\sqrt{\frac{3}{4\pi G}}\sum_{\vec{k},\pm}f_{\vec{k},\pm}(t)Q^{\vec{k},\pm}\left(\vec{\theta}\right). \quad (51)$$

A vertical bar stands for the spatial covariant derivative with respect to the Euclidean metric ${}^0h_{ab}$, and a parenthesis enclosing two spatial indices indicates symmetrization. Thus, the scalar perturbations are determined by $a_{\vec{k},\pm}$, $b_{\vec{k},\pm}$, $g_{\vec{k},\pm}$, $l_{\vec{k},\pm}$, and $f_{\vec{k},\pm}$, whereas the tensor perturbations are described by the coefficients $d_{\vec{k},\varepsilon,\pm}$, and the vector perturbations by $c_{\vec{k}}$ and $v_{\vec{k}}$. We have normalized some of these coefficients in a convenient way to absorb several factors in the formulas that we will use in our discussion.

Inserting these expressions in the Hilbert-Einstein action minimally coupled to the scalar field Φ (with suitable boundary terms) and truncating the result at quadratic order in the coefficents of the perturbations, it is possible to reach a Hamiltonian formulation for our system (Halliwell and Hawking, 1985; Fernández-Méndez, 2014). In this formulation, the above coefficients for the perturbations either play the role of Lagrange multipliers of some of the constraints, or form a canonical set together with the FLRW scale factor, the inflaton, and suitable momenta for all of them. In other words, at the order of our truncation in the action, the system formed by the FLRW cosmology and its perturbations is a totally constrained system that admits a canonical symplectic structure (Castelló Gomar et al., 2015). It is worth emphasizing that, at the considered truncation order, we are treating exactly the zero modes that determine the FLRW background, so that the perturbations that we have expressed explicitly do not contain zero modes. On the other hand, with the kind of matter content considered in our discussion, it is possible to show that the vector perturbations do not include any physical degree of freedom, but are pure gauge. To simplify our exposition, we will therefore eliminate them from our analysis in the following.

The perturbed system that we have constructed is subject to two types of constraints. On the one hand, the perturbations of the momentum and Hamiltonian constraints lead to a collection of constraints that are linear in the perturbations, and that appear accompanied by Lagrange multipliers that are also linear perturbative factors. Explicitly, the mode $H_{\uparrow 1}^{\vec{k},\pm}$ of the linear perturbative momentum constraint has Lagrange multiplier

given by the coefficient $l_{\vec{k},\pm}$ of the perturbations of the shift vector, while the mode $H_1^{\vec{k},\pm}$ of the linear perturbative scalar constraint adopts as Lagrange multiplier the coefficient $g_{\vec{k},\pm}$ of the perturbation of the lapse. These constraints depend exclusively on the scalar perturbations of the metric, once the vector perturbations have been gauged away. A different type of constraint is the zero mode of the Hamiltonian constraint, which can be considered a global restriction on the system formed by the FLRW cosmology and the perturbations. This constraint has a Lagrange multiplier given by the homogeneous lapse function N_0, and is the sum of two contributions: a term that reproduces what would have been the constraint H_0 of the FLRW cosmology in the absence of perturbations, and an additional term H_2 that contains the perturbative contribution and that is quadratic in the perturbations. This latter term is composed in turn of two parts, ${}^{(s)}H_2$ and ${}^{(T)}H_2$, respectively formed by the contributions of the scalar and the tensor perturbations. In this way, the total Hamiltonian takes the expression

$$H = N_0\,[H_0 + {}^{(s)}H_2 + {}^{(T)}H_2] + \sum g_{\vec{k},\pm}\,H_1^{\vec{k},\pm} + \sum l_{\vec{k},\pm}\,H_{\uparrow 1}^{\vec{k},\pm}. \quad (52)$$

Moreover, the quadratic perturbative contributions to the zero mode of the Hamiltonian constraint can be decomposed as the sum of the contributions of each of the modes of the perturbations as follows:

$${}^{(s)}H_2 = \sum_{\vec{k},\pm} {}^{(s)}H_2^{\vec{k},\pm}, \qquad {}^{(T)}H_2 = \sum_{\vec{k},\varepsilon,\pm} {}^{(T)}H_2^{\vec{k},\varepsilon,\pm}. \quad (53)$$

The variables that we have chosen to describe the perturbative degrees of freedom have the drawback that they do not commute with the linear perturbative constraints, even when the FLRW cosmology is taken as a fixed entity with vanishing Poissson brackets. As a consequence, those variables would change if one performs a perturbative diffeomorphism, that would alter the form of the FLRW background without affecting the physics. To avoid this problem with the physical identification of the background, it is most convenient to use a set of variables that indeed commutes with the linear perturbative constraints when the zero modes are frozen in the computation of Poisson brackets. This leads us to consider gauge invariants for the perturbations. In the case of flat spatial sections, the gauge invariant degrees of freedom of the scalar perturbations are usually described in cosmology employing MS invariants, because they are straightforwardly related to the co-moving curvature perturbations. The variables that we have introduced for the tensor perturbations, on the other hand, are directly gauge invariant, and we will only redefine them linearly to re-express their dynamical contribution to the Hamiltonian in a convenient way.

With this motivation, we are going to introduce a change of variables for the perturbations, from the canonical set that we have been using to a new set formed by the following variables (Langlois, 1994; Castelló Gomar et al., 2015):

- The mode coefficients of the MS gauge invariant field, $v_{\vec{k},\pm}$. Explicitly, they are given by the formula (Fernández-Méndez et al., 2013; Castelló Gomar et al., 2014)

$$v_{\vec{k},\pm} = \sqrt{\frac{6\pi^2}{G}}a\left[f_{\vec{k},\pm} + \sqrt{\frac{3}{4\pi G}}\,\frac{\pi_\phi}{a\pi_a}\left(a_{\vec{k},\pm} + b_{\vec{k},\pm}\right)\right]. \quad (54)$$

We notice that these coefficients mix the scalar perturbations of the metric and the perturbations of the matter scalar field.

- The mode coefficients of the tensor perturbations conveniently rescaled (Benítez Martínez and Olmedo, 2016):

$$\tilde{d}_{\vec{k},\varepsilon,\pm} = \sqrt{\frac{6\pi^2}{G}}a\,d_{\vec{k},\varepsilon,\pm}. \quad (55)$$

This rescaling simplifies the dependence of the Hamiltonian on the tensor perturbations.

- The mode coefficients $\pi_{v_{\vec{k},\pm}}$ and $\pi_{\tilde{d}^{\pm}_{\vec{k},\varepsilon}}$ of the canonical momenta of the above fields, defined also as gauge invariants. There exists a certain ambiguity in the specification of these momenta, since once can always add a contribution that is linear in the configuration fields, multiplied by any function of the FLRW background. A convenient criterion to fix this contribution is to require that the time derivative of each of these momenta, as dictated by Hamilton's equations, is proportional to the corresponding configuration variable. This condition amounts to demand that the Hamiltonian that generates the dynamics of the scalar and tensor perturbations should not contain cross terms between the configuration fields and their momenta, and turns out to determine the latter of these variables completely.
- An Abelianization of the linear perturbative constraints. Actually, at the order of our perturbative truncation in the action, it is possible to modify these constraints on the scalar perturbations with terms that are linear in those perturbations and such that the new constraints that one obtains commute under Poisson brackets among them, as well as with the MS field and its momentum, after freezing the zero modes. To achieve this Abelianization, it suffices to introduce the replacement

$$H_1^{\vec{k},\pm} \to \breve{H}_1^{\vec{k},\pm} = H_1^{\vec{k},\pm} - \frac{18\pi^2}{G}a^3H_0a_{\vec{k},\pm}. \quad (56)$$

This new linear perturbative scalar constraint is used together with $H_{\uparrow 1}^{\vec{k},\pm}$ as additional variables in our canonical set.

- Suitable momenta of the Abelianized linear perturbative constraints. As far as those constraints generate gauge transformations consisting of perturbative diffeomorphisms,

their momenta can be interpreted as variables that parametrize possible gauge fixations for the perturbations. A especially simple choice is

$$\pi_{H_1^{\vec{k},\pm}} = \frac{1}{a\pi_a}\left(a_{\vec{k},\pm} + b_{\vec{k},\pm}\right), \qquad \pi_{H_{\uparrow 1}^{\vec{k},\pm}} = -3b_{\vec{k},\pm}. \tag{57}$$

Remarkably, the introduced change of variables for the scalar and tensor perturbations can be completed into a canonical transformation for the entire system (that is, without freezing the background), at the considered truncation order, by modifying the zero modes with terms that are quadratic in the perturbations (Pinho and Pinto-Neto, 2007; Falciano and Pinto-Neto, 2009; Castelló Gomar et al., 2015). For this, we can proceed as follows. We substitute the old perturbative variables in the Legendre term of the action (or, equivalently, in the symplectic potential) as functions of the new ones and, after several integrations by parts and convenient identifications of factors, we find new zero modes that keep the canonical form of the Legendre term up to perturbative contributions that are negligible in our truncation scheme. The new configuration variables obtained in this way adopt the generic expression

$$\tilde{w}_q^\iota = w_q^\iota + \frac{1}{2}\sum_{m,\vec{k},\pm}\left[X_{q_m}^{\vec{k},\pm}\frac{\partial X_{p_m}^{\vec{k},\pm}}{\partial w_p^\iota} - \frac{\partial X_{q_m}^{\vec{k},\pm}}{\partial w_p^\iota}X_{p_m}^{\vec{k},\pm}\right], \tag{58}$$

where we have called $\{w_q^\iota\} = \{a, \phi\}$ the configuration variables of the zero mode sector, $\{w_\iota^p\}$ are their momenta ($\iota = 1, 2$), and $\{X_{q_m}^{\vec{k},\pm}, X_{p_m}^{\vec{k},\pm}\}$ are the old variables for the scalar and tensor perturbations, each of which is given by a different value of the label m. A tilde on top of any of these canonical quantities indicates its new counterpart, defined according to the above procedure.

In the case of the momentum variables for the zero modes, the change is given by a formula of the same kind, but with a flip of sign in the term that provides the corrections quadratic in the perturbations,

$$\tilde{w}_p^\iota = w_p^\iota - \frac{1}{2}\sum_{m,\vec{k},\pm}\left[X_{q_m}^{\vec{k},\pm}\frac{\partial X_{p_m}^{\vec{k},\pm}}{\partial w_q^\iota} - \frac{\partial X_{q_m}^{\vec{k},\pm}}{\partial w_q^\iota}X_{p_m}^{\vec{k},\pm}\right]. \tag{59}$$

The availability of a canonical set for the entire perturbed system, formed by the FLRW cosmology and the perturbations, is of the greatest importance. In particular, it makes possible an easy implementation of the hybrid strategy following canonical quantization rules. But, in order to proceed to this quantization, we still have to determine the form of the zero mode of the Hamiltonian constraint (the only non-linear perturbative constraint of the system) in terms of the new canonical set, keeping the quadratic truncation order. In order to do this, we notice that, since the change of zero modes is quadratic in the perturbations, an expansion of the FLRW contribution H_0 around the new zero modes leads immediately to the desired constraint if we only include the first derivative contribution. Let us introduce the compact notation

$$\{w^\iota\} = \left\{w_q^\iota, w_\iota^p\right\}, \qquad \{\tilde{w}^\iota\} = \left\{\tilde{w}_q^\iota, \tilde{w}_\iota^p\right\}, \tag{60}$$

$$\left\{\tilde{X}_m^{\vec{k},\pm}\right\} = \left\{\tilde{X}_{q_m}^{\vec{k},\pm}, \tilde{X}_{p_m}^{\vec{k},\pm}\right\}. \tag{61}$$

Then, according to our comments, the expression of the new global scalar constraint at our truncation order is (Castelló Gomar et al., 2015; Benítez Martínez and Olmedo, 2016)

$$H_0 + \sum_\iota (w^\iota - \tilde{w}^\iota)\frac{\partial H_0}{\partial w^\iota} + \sum_{\vec{k},\pm} {}^{(s)}H_2^{\vec{k},\pm} + \sum_{\vec{k},\varepsilon,\pm} {}^{(T)}H_2^{\vec{k},\varepsilon,\pm}, \tag{62}$$

with the phase space dependence of H_0, its derivatives, ${}^{(s)}H_2^{\vec{k},\pm}$, and ${}^{(T)}H_2^{\vec{k},\varepsilon,\pm}$ evaluated directly at $(\tilde{w}^\iota, \tilde{X}_m^{\vec{k},\pm})$. Namely, in (**Eq. 62**), the evaluation of the Hamiltonian functions must be made as if one identified the old and the new set of variables. As a consequence, the contribution of each of the modes of the perturbations to the new global scalar constraint is

$${}^{(s)}\breve{H}_2^{\vec{k},\pm} \sim {}^{(s)}H_2^{\vec{k},\pm} + \sum_\iota {}^{(s)}\Delta\tilde{w}_{\vec{k},\pm}^\iota \frac{\partial H_0}{\partial w^\iota}, \tag{63}$$

$${}^{(T)}\breve{H}_2^{\vec{k},\varepsilon,\pm} \sim {}^{(T)}H_2^{\vec{k},\varepsilon,\pm} + \sum_\iota {}^{(T)}\Delta\tilde{w}_{\vec{k},\varepsilon,\pm}^\iota \frac{\partial H_0}{\partial w^\iota}, \tag{64}$$

where the symbol $\sim$ indicates equality modulo the Abelianized linear constraints and up to the relevant perturbative order in our truncation. Besides, we have called

$$w^\iota - \tilde{w}^\iota = \sum_{\vec{k},\pm} {}^{(s)}\Delta\tilde{w}_{\vec{k},\pm}^\iota + \sum_{\vec{k},\varepsilon,\pm} {}^{(T)}\Delta\tilde{w}_{\vec{k},\varepsilon,\pm}^\iota, \tag{65}$$

where the superscripts (s) and (T) stand for the quadratic contributions of scalar and tensor nature, respectively. It is possible to prove that the sum of contributions in the left-hand side of (**Eq. 63**) gives precisely the MS Hamiltonian (Castelló Gomar et al., 2015), i.e., the Hamiltonian that generates the dynamical evolution (in proper time) of the MS field on the FLRW background. Likewise, the sum ${}^{(T)}\breve{H}_2^{\vec{k},\varepsilon,\pm}$ of the tensor contributions to the constraint provides a dynamical Hamiltonian of harmonic oscillator type for the tensor perturbations on the FLRW cosmological background.

It is worth pointing out that, in the definition of these perturbative Hamiltonians, we can replace the squared momentum of the inflaton with $\pi_\phi^2 - 16\pi^3 a^3 H_0$. This is so because all the new terms proportional to H_0 that are produced in this way are quadratic in the perturbations and can thus be absorbed in a redefinition of the zero mode of the lapse function up to a modification of the total scalar constraint that is at least quartic in those perturbations. Hence, such a modification is negligible at our truncation order. The freedom available in using this replacement can be fixed by requiring that the perturbative contribution to the Hamiltonian constraint be at most linear in the inflaton momentum, because one can always use the commented replacement to decrease the polynomial order

in π_ϕ by two units until one reaches either a linear contribution of the inflaton momentum or a term that is independent of it. The total Hamiltonian of the system then becomes (Castelló Gomar et al., 2015)

$$H = \overline{N}_0 \left[H_0 + \sum_{\vec{k},\pm} {}^{(s)}\breve{H}_2^{\vec{k},\pm} + \sum_{\vec{k}\varepsilon} {}^{(T)}\breve{H}_2^{\vec{k},\varepsilon,\pm} \right] + \sum_{\vec{k},\pm} \breve{g}_{\vec{k},\pm} \breve{H}_1^{\vec{k},\pm} + \sum_{\vec{k},\pm} \breve{l}_{\vec{k},\pm} H_{\uparrow 1}^{\vec{k},\pm}, \tag{66}$$

where $\overline{N}_0$ is the suitably redefined homogeneous lapse function that differs from the original one, N_0, in perturbative terms that are quadratic. Similarly, $\breve{g}_{\vec{k},\pm}$ and $\breve{l}_{\vec{k},\pm}$ are Lagrange multipliers that differ from the original ones, $g_{\vec{k},\pm}$ and $l_{\vec{k},\pm}$ respectively, by linear perturbative contributions. Their explicit expressions can be found in Ref. (Castelló Gomar et al., 2015), but they are not especially relevant for the rest of our discussion.

Notice that this total Hamiltonian, imposed as a collection of constraints on the system, would include backreaction at the considered perturbative order. As we have commented, the contribution of the scalar perturbations to the global Hamiltonian constraint is nothing but the MS Hamiltonian, which is a sum of terms that are quadratic in the MS configuration variables and of quadratic terms in their momenta, but without terms that mix these two types of variables. This is a consequence of our choice of MS momentum field, as we explained when we introduced the new perturbative variables. A similar behavior is found in the contribution of the tensor perturbations to the Hamiltonian constraint. In more detail,

$${}^{(s)}\breve{H}_2^{\vec{k},\pm} = \frac{1}{2\tilde{a}} \left[\left(\omega_k^2 + s^{(s)} + r^{(s)}\pi_{\tilde{\phi}} \right) v_{\vec{k},\pm}^2 + \pi^2_{v_{\vec{k},\pm}} \right], \tag{67}$$

$${}^{(T)}\breve{H}_2^{\vec{k},\varepsilon,\pm} = \frac{1}{2\tilde{a}} \left[\left(\omega_k^2 + s^{(T)} \right) \tilde{d}^2_{\vec{k},\varepsilon,\pm} + \pi^2_{\tilde{d}_{\vec{k},\varepsilon,\pm}} \right]. \tag{68}$$

Here, $s^{(s)} + r^{(s)}\pi_{\tilde{\phi}}$ and $s^{(T)}$ play the role of effective background dependent masses for the scalar and the tensor perturbative modes, respectively. The expressions of these background functions are

$$s^{(s)} = \frac{H_0^2}{32\pi^6\tilde{a}^4} \left(\frac{38\pi G}{3} - 9\frac{H_0^2}{\tilde{a}^2\pi_{\tilde{a}}^2} \right) + \tilde{a}^2 \left(\mathcal{V}''(\tilde{\phi}) - \frac{16\pi G}{3}\mathcal{V}(\tilde{\phi}) \right), \tag{69}$$

$$s^{(T)} = \frac{G}{48\pi^5}\frac{H_0^{(2)}}{\tilde{a}^4} - \frac{16\pi G}{3}\tilde{a}^2\mathcal{V}(\tilde{\phi}), \tag{70}$$

$$r^{(s)} = -12\frac{\tilde{a}}{\pi_{\tilde{a}}}\mathcal{V}'(\tilde{\phi}). \tag{71}$$

The prime symbol denotes de derivative of the potential $\mathcal{V}$ with respect to the inflaton $\tilde{\phi}$, and

$$H_0^{(2)} = \frac{4\pi G}{3}\tilde{a}^2\pi_{\tilde{a}}^2 - 128\pi^6\tilde{a}^6\mathcal{V}(\tilde{\phi}). \tag{72}$$

We notice that

$$s^{(s)} = s^{(T)} + \frac{9H_0^{(2)}}{32\pi^6\tilde{a}^4} \left(\frac{4\pi G}{3} - \frac{H_0^{(2)}}{\tilde{a}^2\pi_{\tilde{a}}^2} \right) + \tilde{a}^2\mathcal{V}''(\tilde{\phi}). \tag{73}$$

In particular, substituting (**Eq. 72**), we see that $s^{(s)} = s^{(T)}$ when the inflaton potential ν vanishes.

In total, after a convenient change of densitization similar to that explained in homogeneous and isotropic LQC (*via* multiplication by the homogeneous physical volume $V = 8\pi^3\tilde{a}^3$), we obtain a Hamiltonian constraint that can be written in the form

$$H_S = \frac{1}{2}\left[\pi_{\tilde{\phi}}^2 - H_0^{(2)} - \Theta_e - \Theta_o\pi_{\tilde{\phi}} \right], \tag{74}$$

where we have introduced the notation

$$\Theta_e = \sum_{\vec{k},\pm} {}^{(s)}\Theta_e^{\vec{k},\pm} + \sum_{\vec{k},\varepsilon,\pm} {}^{(T)}\Theta_e^{\vec{k},\varepsilon,\pm}, \tag{75}$$

$$\Theta_o = \sum_{\vec{k},\pm} {}^{(s)}\Theta_o^{\vec{k},\pm}, \tag{76}$$

$${}^{(s)}\Theta_e^{\vec{k},\pm} = -\left[\left(\vartheta_e\omega_k^2 + {}^{(s)}\vartheta_e^q \right) v_{\vec{k},\pm}^2 + \vartheta_e\pi^2_{v_{\vec{k},\pm}} \right], \tag{77}$$

$${}^{(T)}\Theta_e^{\vec{k},\varepsilon,\pm} = -\left[\left(\vartheta_e\omega_k^2 + {}^{(T)}\vartheta_e^q \right) \tilde{d}^2_{\vec{k},\varepsilon,\pm} + \vartheta_e\pi^2_{\tilde{d}_{\vec{k},\varepsilon,\pm}} \right], \tag{78}$$

$${}^{(s)}\Theta_o^{\vec{k},\pm} = -{}^{(s)}\vartheta_o v_{\vec{k},\pm}^2, \tag{79}$$

that explicitly separates the linear term in the inflaton momentum. Clearly, we have the identities

$${}^{(s)}\vartheta_e^q = \vartheta_e s^{(s)}, \qquad {}^{(T)}\vartheta_e^q = \vartheta_e s^{(T)}, \qquad {}^{(s)}\vartheta_o = \vartheta_e r^{(s)}, \tag{80}$$

with $\vartheta_e = 8\pi^3\tilde{a}^2$.

We note that there is no tensor contribution to Θ_o. It is also worth remarking that all the ϑ-functions are independent of the particular mode that one considers. Besides, the part of the Hamiltonian constraint that contains the perturbative contribution is the same for the scalar and for the tensor perturbations except for the difference in their background dependent mass. This shows up in the appearance of the terms ${}^{(s)}\Theta_o^{\vec{k},\pm}$ and in the difference between ${}^{(s)}\vartheta_e^q$ and ${}^{(T)}\vartheta_e^q$.

5 HYBRID LQC: INCLUSION OF FERMIONS

In the matter content of our cosmological system, we can also include fermionic fields, e.g. a Dirac field. Their pressence does not modify much our treatment if we consider them as perturbations, including the possible fermionic zero modes, so that they do not alter the dynamics of the homogeneous background cosmology in the linearized theory. Since the Dirac action is quadratic in the fermionic field, as a perturbation it couples directly only to the background FLRW geometry, but not to the perturbations of the metric, nor to the matter scalar field (Elizaga Navascués et al., 2017). Moreover, for

the same reason, the fermionic field does not contribute to the linearized perturbative constraints, that arise from the perturbation of the Hamiltonian and momentum constraints. As a consequence, the fermionic field can be treated as a gauge invariant perturbation at the considered order of truncation. This simplifies the formulation considerably.

If we adopt a Weyl representation (D'Eath and Halliwell, 1987), the Dirac field can be described by a pair of two-component spinors of definite chirality. We will call φ^A and $\chi^*_{A'}$ the respective left-handed and right-handed spinors associated with the field. Capital Latin letters from the beginning of the alphabet, both primed and unprimed, take values equal to 1 or 2, corresponding to the two components of the chiral spinors. These indices will be raised and lowered using the antisymmetric symbols ϵ^{AB} and ϵ_{AB} (with e.g., $\epsilon_{12} = 1$) , as well as their counterparts for right-handed chirality. It is most convenient to adopt an internal gauge such that the spatial part of the tetrad has vanishing temporal Lorentz components, namely $e^a_0 = 0$. As a consequence of this gauge fixation on the spin structure in four dimensions, the two-component spinors of the Dirac field can be viewed as families of cross-sections of a spinor bundle defined on the compact spatial sections. On the other hand, the Hamiltonian formalism of the Dirac field is initially complicated by the existence of second-class constraints that relate the field with its momentum. Nevertheless, one can eliminate these constraints and capture the canonical anticommutation relations of the Dirac field in anticommutators of its two-component spinors. To take into full account this anticommuting character, we will treat these components as Grassmann variables (Berezin, 1966).

In a similar way as we did with the metric and the scalar field perturbations, we can decompose the spinors of the Dirac field in modes. Since the spatial differential operator that appears naturally in the dynamical equation of our fermionic field is the Dirac operator constructed with the auxiliary Euclidean triad ${}^0e^a_i$ on the toroidal spatial sections of our model (with ${}^0e^i_a\,{}^0e^j_b\,\delta_{ij} = {}^0h_{ab}$ being the Euclidean metric introduced above), it is logical to treat the spatial dependence of the field by an expansion in eigenmodes of this Dirac operator. The spectrum of this operator is discrete, owing to the compactness of the sections. The eigenvalues are $\pm\,\omega_k$, where $\omega_k^2 = \vec{k}\cdot\vec{k}$ and $\vec{k} \in \mathbb{Z}^3$ is any tuple of integers. We are assuming a trivial spin structure on the spatial sections. Otherwise, the definition of ω_k would include a constant displacement of $\vec{k}$ characteristic of the specific spin structure chosen for the fermions (Friedrich, 1984). Using these modes, we can express the two-component spinors of the Dirac field in the form

$$\varphi_A(x) = \frac{1}{(2\pi)^{3/2}\tilde{a}^{3/2}} \sum_{\vec{k},(\pm)} \left[m_{\vec{k}} w_A^{\vec{k},(+)} + r^*_{\vec{k}} w_A^{\vec{k},(-)} \right], \tag{81}$$

$$\chi^*_{A'}(x) = \frac{1}{(2\pi)^{3/2}\tilde{a}^{3/2}} \sum_{\vec{k},(\pm)} \left[s^*_{\vec{k}} \left(w^{\vec{k},(+)} \right)^*_{A'} + t_{\vec{k}} \left(w^{\vec{k},(-)} \right)^*_{A'} \right]. \tag{82}$$

Here $w_A^{\vec{k},(\pm)}$ are the left-handed Dirac eigenspinors with respective eigenvalue equal to $\pm\,\omega_k$. With our choice of the auxiliary Euclidean triad, and recalling that we have assumed a trivial spin structure, these eigenspinors take the expression

$$w_A^{\vec{k},(\pm)} = u_A^{\vec{k},(\pm)} e^{i\vec{k}\cdot\vec{\theta}}, \tag{83}$$

where the spinors $u_A^{\vec{k},(\pm)}$ are constant and normalized (including a choice of phase) so that

$$\left(u^{\vec{k},(\pm)} \right)^*_{1'} u_1^{\vec{k},(\pm)} + \left(u^{\vec{k},(\pm)} \right)^*_{2'} u_2^{\vec{k},(\pm)} = 1, \tag{84}$$

$$\int d^3\theta\, w_A^{\vec{k}',(+)} \epsilon^{AB} w_B^{\vec{k},(-)} = 0, \tag{85}$$

$$\int d^3\theta\, w_A^{\vec{k}',(\pm)} \epsilon^{AB} w_B^{\vec{k},(\pm)} = 8\pi^3 \delta_{\vec{k}',-\vec{k}}, \tag{86}$$

with $d^3\theta$ denoting the volume element $d\theta d\sigma d\delta$. The two last equations are not valid for zero modes. In that case, one can directly define $u_A^{\vec{0},(\pm)}$ as the spinors with

$$u_1^{\vec{0},(+)} = 1, \qquad u_1^{\vec{0},(-)} = 0, \tag{87}$$

$$u_2^{\vec{0},(+)} = 0, \qquad u_2^{\vec{0},(-)} = 1. \tag{88}$$

On the other hand, the complex conjugate of (**Eq. 83**) provides a basis of right-handed modes, with the chirality of $\chi^*_{A'}$.

Each of the coefficients $m_{\vec{k}}$, $s_{\vec{k}}$, $t_{\vec{k}}$, and $r_{\vec{k}}$ forms a Grassmann canonical pair with its respective complex conjugate (D'Eath and Halliwell, 1987). Furthermore, in this sense they provide a canonical set together with the variables introduced in the previous section for the metric and scalar field perturbations and for the FLRW cosmology, once we have adopted a description of the cosmological perturbations in terms of gauge invariants (Elizaga Navascués et al., 2017). For convenience, in the following we will employ the notation $(x_{\vec{k}}, y_{\vec{k}})$ to refer to any of the ordered pairs of coefficients $(m_{\vec{k}}, s_{\vec{k}})$ or $(t_{\vec{k}}, r_{\vec{k}})$.

As we have already commented, there is no fermionic term in the linear perturbative constraints of our system, so that the only contribution of the Dirac field to the total Hamiltonian is included in the zero mode of the Hamiltonian constraint. This contribution is given by the Dirac Hamiltonian, evaluated at the variables for the cosmological zero modes defined in the previous section and at the fermionic perturbations determined by the variables $(x_{\vec{k}}, y_{\vec{k}})$, as far as the respective dependence on the FLRW cosmology and the Dirac field is concerned. Motivated by previous works on this subject (D'Eath and Halliwell, 1987), the first approach to the treatment of fermions in hybrid LQC was to carry out a change of fermionic variables that produces a diagonalization of the Dirac Hamiltonian. To reach this diagonalization, the change of variables must depend on the FLRW geometry, a situation that is similar to that studied when we introduced gauge invariants to describe the relevant degrees of freedom of the scalar perturbations. This has two consequences, as we know. First, the zero modes have to be corrected to maintain the canonical structure in the set of variables that describe the whole of the cosmological system. Second, the fermionic contribution to the Hamiltonian constraint gets an additional term, up to quadratic order in the perturbations, owing to the background dependence of the change of variables. Even if

this change was designed to diagonalize the Dirac Hamiltonian, it will generally not diagonalize the new fermionic contribution, and therefore the resulting fermionic Hamiltonian will still contain interacting terms. Actually, the new fermionic variables have Poisson brackets of the creation-annihilation type, so that we can view these fermionic interactions as the creation or annihilation of pairs of particles. Finally, we will treat the fermionic zero modes on their own, keeping their description in terms of the original variables $(x_{\vec{0}}, y_{\vec{0}})$ to avoid problems with the particularization of our formulas to a vanishing Dirac eigenvalue (i.e., for $\omega_k = 0$).

Explicitly, and leaving aside those zero modes, the new variables are given by

$$a_{\vec{k}}^{(x,y)} = \sqrt{\frac{\xi_k - \omega_k}{2\xi_k}}\, x_{\vec{k}} + \sqrt{\frac{\xi_k + \omega_k}{2\xi_k}}\, y_{-\vec{k}}^{*},$$
$$\left(b_{\vec{k}}^{(x,y)}\right)^{*} = \sqrt{\frac{\xi_k + \omega_k}{2\xi_k}}\, x_{\vec{k}} - \sqrt{\frac{\xi_k - \omega_k}{2\xi_k}}\, y_{-\vec{k}}^{*}, \tag{89}$$

where

$$\xi_k = \sqrt{\omega_k^2 + M^2\tilde{a}^2}, \tag{90}$$

with M denoting the mass of the Dirac field. Notice that the sum of the square modulus of the coefficients in each of the above linear combinations of the variables $(x_{\vec{k}}, y_{\vec{k}})$ equals the unit. This ensures that the transformation is canonical in the fermionic phase space (Elizaga Navascués et al., 2017). In a Fock representation with a standard interpretation, the operators representing $a_{\vec{k}}^{(x,y)}$ and $b_{\vec{k}}^{(x,y)}$ would annihilate particles and antiparticles, respectively, while their adjoints (representing the complex conjugate variables) would create them.

The fact that our change of fermionic variables depends only on the scale factor implies that we only need to modify the momentum of that background variable in order to recover a canonical set for the entire cosmological system. The modification of the momentum $\pi_{\tilde{a}}$ consists in adding to it the following terms that are quadratic in the fermionic perturbations, obtained in a similar way as it was explained in the previous section for the scalar and tensor perturbations (Elizaga Navascués et al., 2017):

$$-\frac{iM}{2}\sum_{\vec{k}\neq\vec{0},\,(x,y)}\frac{\omega_k}{\xi_k^2}\left[a_{\vec{k}}^{(x,y)}b_{\vec{k}}^{(x,y)} + \left(a_{\vec{k}}^{(x,y)}\right)^{*}\left(b_{\vec{k}}^{(x,y)}\right)^{*}\right]. \tag{91}$$

For simplicity in our notation, we will denote the new momentum of the scale factor with the same symbol as before. From the context, it must be clear in our discussion whether we are referring to the original momentum or to the momentum that has been changed with the addition of fermionic contributions. On the other hand, we also notice that the variables for the scalar and tensor perturbations need not be altered at this stage, because our change of fermionic variables is independent of them.

In terms of this new canonical set, the total Hamiltonian has the same expression (**Eq. 66**) as before except for two things. First, its dependence on $\pi_{\tilde{a}}$ must be evaluated at the new momentum of the FLRW scale factor, which includes the fermionic modification. And second, the zero mode of the Hamiltonian constraint includes one additional contribution ${}^{(F)}H_2$ which is due to fermions,

$$H_0 + {}^{(S)}H_2 + {}^{(T)}H_2 + {}^{(F)}H_2 = 0. \tag{92}$$

In consonance with our comments above, this fermionic contribution is given by the sum of the Dirac Hamiltonian ${}^{(F)}H_D$, once it is expressed in terms of the new fermionic variables, and an interaction term ${}^{(F)}H_I$, arising from the correction to H_0 caused by the change of momentum for the scale factor [like in (**Eq. 62**)]. In detail, their expressions are

$${}^{(F)}H_2 = {}^{(F)}H_D + {}^{(F)}H_I, \tag{93}$$

$${}^{(F)}H_D = {}^{(F)}H_{\vec{0}} + \frac{1}{2\tilde{a}}\sum_{\vec{k}\neq 0,\,(x,y)}\xi_k\left[\left(a_{\vec{k}}^{(x,y)}\right)^{*}a_{\vec{k}}^{(x,y)} - a_{\vec{k}}^{(x,y)}\left(a_{\vec{k}}^{(x,y)}\right)^{*}\right] \tag{94}$$

$$+\frac{1}{2\tilde{a}}\sum_{\vec{k}\neq 0,\,(x,y)}\xi_k\left[\left(b_{\vec{k}}^{(x,y)}\right)^{*}b_{\vec{k}}^{(x,y)} - b_{\vec{k}}^{(x,y)}\left(b_{\vec{k}}^{(x,y)}\right)^{*}\right],$$

$${}^{(F)}H_{\vec{0}} = M\left[s_{\vec{0}}r_{\vec{0}}^{*} + r_{\vec{0}}s_{\vec{0}}^{*} + m_{\vec{0}}t_{\vec{0}}^{*} + t_{\vec{0}}m_{\vec{0}}^{*}\right], \tag{95}$$

$${}^{(F)}H_I = -\frac{i\pi_{\tilde{a}}GM}{12\pi^2\tilde{a}}\sum_{\vec{k}\neq 0,\,(x,y)}\frac{\omega_k}{\xi_k^2}\left[a_{\vec{k}}^{(x,y)}b_{\vec{k}}^{(x,y)} + \left(a_{\vec{k}}^{(x,y)}\right)^{*}\left(b_{\vec{k}}^{(x,y)}\right)^{*}\right]. \tag{96}$$

6 HYBRID QUANTIZATION OF COSMOLOGICAL PERTURBATIONS: IMPLEMENTATION

Once we have at our disposal a canonical set of variables for the description of our perturbed cosmological model in which the variables that describe the perturbations are either gauge invariants, perturbative gauge generators, or associated gauge degrees of freedom, we are in an appropriate situation to face the quantization of the system. We will carry out this quantization adopting the hybrid approach within the framework of LQC. As we have already commented, this hybrid strategy is based on the hypothesis that the most relevant effects of quantum geometry for cosmology are those that affect the FLRW substrate, namely the behavior of the scale factor, while the purely quantum geometric effects on the perturbations can be approximately ignored, and handle the quantum description of those anisotropies and inhomogeneities using techniques directly related with the formalism of QFT in a curved spacetime, generalized to the case in which such a spacetime is quantum mechanical as well. In practice, we quantize the FLRW cosmology using the methods of LQC and the perturbations (essentially) with Fock quantization methods, then combine both types of quantum descriptions by adopting a tensor product representation space for the system, and finally impose on it the diffeomorphism

constraints that are present in the system. We will see that, among them, the only intrincate constraint is the zero mode of the Hamiltonian constraint, that relates in a complicated way the FLRW cosmology with the scalar and tensor gauge invariant perturbations (as well as with the fermionic ones if we also consider a Dirac field). Thus, the hybrid quantization is non-trivial precisely because of the imposition of this constraint.

The linear perturbative constraints obtained from the Abelianization of the perturbations of the diffeomorphism constraints can be imposed straightforwardly by representing them as derivative operators with respect to their canonically conjugate degrees of freedom (or, if one considers an integrated version of these constraints, as operators that displace the values of such canonically conjugate degrees of freedom, resulting in transformations that should be symmetries). With this representation, the states that satisfy such constraints à la Dirac are simply those that are independent of the gauge degrees of freedom $\pi_{\bar{H}_1^{\vec{k},\pm}}$ and $\pi_{H_{\uparrow 1}^{\vec{k},\pm}}$ (**Eq. 57**). In other words, physical states depend only on (a complete set of compatible) zero modes and gauge invariants. Note that this result is obtained without the need to introduce any perturbative gauge fixing. Physical states must still satisfy one constraint, that is the only one remaining at this stage, namely the zero mode of the Hamiltonian constraint, as we anticipated.

The desired quantum formulation is then reached by choosing the representation space of the improved dynamics scheme of homogeneous and isotropic LQC, $\mathcal{H}_{LQC}^{grav}$, for the perturbatively corrected volume and its momentum (namely, the zero modes of the FLRW geometry once they have been suitably modified with terms that are quadratic in the perturbations in order to maintain the canonical symplectic structure of the entire cosmological system). For the perturbatively corrected inflaton and its momentum, we use a standard Schrödinger representation $L^2(\mathbb{R}, d\tilde{\phi})$. On the other hand, for the MS and tensor gauge invariants, we adopt Fock representations $\mathcal{F}_s$ and $\mathcal{F}_T$, chosen within a unique privileged family of unitarily equivalent representations that are characterized by (Castelló Gomar et al., 2012; Cortez et al., 2012):

- The invariance of the vacuum under the symmetries of the spatial hypersurfaces.
- A unitarily implementable Heisenberg evolution of the creation and annihilation operators, in the context of QFT in a curved background. This Heisenberg evolution is determined by the dynamics of the gauge invariant modes that we have picked out for the description of the perturbations.

In addition, if the system contains a Dirac field, viewed as a fermionic perturbation, we employ for it a Fock representation $\mathcal{F}_D$ in the equivalence class of the one that is naturally associated with the previously introduced choice of creation and annihilationlike variables proposed by D'Eath and Halliwell (D'Eath and Halliwell, 1987). This again belongs to a uniquely distinguished class of unitarily equivalent representations characterized by the same two conditions that we have listed above, together with the requirement of recovering a standard notion of particles and antiparticles. It is worth emphasizing that the choice of Fock representation (or of a family of unitarily equivalent representations) does not determine a concrete choice of vacuum state. Any Fock state in our representation is valid for this purpose. Therefore, in order to fix a unique vacuum state, more restrictions are needed, either in the form of additional requirements about the physical properties of the subsequent quantum theory or in the form of conditions on a particular spatial section able to specify the state there.

Let us continue with our hybrid approach, thus adopting as representation space the tensor product $\mathcal{H}_{LQC}^{grav} \otimes L^2(\mathbb{R}, d\tilde{\phi}) \otimes \mathcal{F}_s \otimes \mathcal{F}_T \otimes \mathcal{F}_D$. We construct our quantum representation so that the zero modes commute with the perturbations, as it happens under Poisson brackets in the classical theory, and so that all functions of the inflaton $\tilde{\phi}$ act by multiplication. As we have commented, the zero mode of the Hamiltonian constraint results in a non-trivial coupling between the various factors of our tensor product. The quantization proposed for this constraint is based on the representation adopted in homogeneous LQC[3]. For the FLRW contribution H_0 we adopt the same prescription as in LQC. In particular, we adhere to the improved dynamics proposal, so that quantities that depend on the momentum of the scale factor are represented in terms of holonomies defined employing squares with a fiducial length that guarantees that the physical area enclosed by them coincides with the area gap Δ, determined by the area spectrum of LQG. Using the resulting basic operators of homogeneous LQC, as well as the homogeneous physical volume operator $\widehat{V} = 2\pi G\gamma\sqrt{\Delta}|\widehat{v}|$ and the regularized inverse volume operator obtained from them, we get

$$\widehat{H}_0^{(2)} = \widehat{\Omega}_0^2 - 2\widehat{V}^2\mathcal{V}\left(\tilde{\phi}\right). \tag{97}$$

We recall that $\mathcal{V}(\tilde{\phi})$ is the inflaton potential, and that $\widehat{\Omega}_0$ was defined in (**Eq. 28**).

As for the functions of zero modes of the FLRW cosmology that appear in the perturbative part of the constraint, we adopt a symmetric factor ordering that tries and respects, as far as possible, the assignation of representation from homogeneous and isotropic LQC. In more detail, we adopt the following rules for their quantum representation:

- We symmetrize à la Weyl the representation of the product $\Theta_o\pi_\phi$, to deal with the presence of functions of ϕ in Θ_o that do not commute with the inflaton momentum.
- We adopt an algebraic symmetrization for factors of the form $V^r g(b)$, that are promoted to the operators $\widehat{V}^{r/2}\widehat{g}_{\mathrm{LQC}}\widehat{V}^{r/2}$, where r is any real number and $g(b)$ a function of the variable b, with $\widehat{g}_{\mathrm{LQC}}$ its operator counterpart in the improved dynamics scheme of LQC. This algebraic symmetric factor ordering is adopted as well for powers of the inverse volume.

[3]The quantum constraint that corresponds to the alternate regularization proposed for homogeneous LQC in Ref. (Dapor and Liegener, 2018) and its associated dynamics have been studied in Refs. (Castelló Gomar et al., 2020; García-Quismondo et al., 2020).

- Even powers of $-\tilde{a}\pi_{\tilde{a}}\sqrt{4\pi G/3}$ are promoted to even powers of the operator $\widehat{\Omega}_0$, which represents this quantity in LQC, whereas odd powers, let's say, of order $2z+1$, with z any integer, are represented as $|\widehat{\Omega}_0|^z\widehat{\Lambda}_0|\widehat{\Omega}_0|^z$. Here $|\widehat{\Omega}_0|$ is the square root of the positive operator $\widehat{\Omega}_0^2$, and $\widehat{\Lambda}_0$ is defined exactly as $\widehat{\Omega}_0$, but with holonomies of double length. The result can be obtained by dividing the right-hand side of expression (**Eq. 28**) by 2, and replacing b in that expression with $2b$. The operator $\widehat{\Lambda}_0$ defined in this way only shifts ν in multiples of four units, and hence preserves the superselection sectors of the homogeneous and isotropic geometry.

With these prescriptions, we arrive at the following operator representation of the functions (**Eq. 80**) that appear in the densitized Hamiltonian constraint:

$$\widehat{\vartheta}_e = 2\pi\widehat{V}^{2/3}, \tag{98}$$

$$^{(s)}\widehat{\vartheta}_e^q = \frac{2G}{3}\widehat{\left[\frac{1}{V}\right]}^{1/3}\widehat{H}_0^{(2)}\left(19-18\widehat{\Omega}_0^{-2}\widehat{H}_0^{(2)}\right)\widehat{\left[\frac{1}{V}\right]}^{1/3}+\frac{\widehat{V}^{4/3}}{2\pi}\left(\mathcal{V}'\left(\tilde{\phi}\right)-\frac{16\pi G}{3}\mathcal{V}\left(\tilde{\phi}\right)\right), \tag{99}$$

$$^{(T)}\widehat{\vartheta}_e^q = \frac{2G}{3}\widehat{\left[\frac{1}{V}\right]}^{1/3}H_0^{(2)}\widehat{\left[\frac{1}{V}\right]}^{1/3}-\frac{8G}{3}\widehat{V}^{4/3}\mathcal{V}\left(\tilde{\phi}\right), \tag{100}$$

$$^{(s)}\widehat{\vartheta}_o = 12\sqrt{\frac{G}{3\pi}}\mathcal{V}'\left(\tilde{\phi}\right)\widehat{V}^{2/3}\left|\widehat{\Omega}_0\right|^{-1}\widehat{\Lambda}_0\left|\widehat{\Omega}_0\right|^{-1}\widehat{V}^{2/3}. \tag{101}$$

According to these formulas, the counterpart of relation (**Eq. 73**) between the scalar and tensor background dependent masses is

$$^{(s)}\widehat{\vartheta}_e^q = {}^{(T)}\widehat{\vartheta}_e^q+12G\widehat{\left[\frac{1}{V}\right]}^{1/3}\widehat{H}_0^{(2)}\left(1-\widehat{\Omega}_0^{-2}\widehat{H}_0^{(2)}\right)\widehat{\left[\frac{1}{V}\right]}^{1/3}+\frac{\widehat{V}^{4/3}}{2\pi}\mathcal{V}''\left(\tilde{\phi}\right). \tag{102}$$

It is worth remarking that $^{(s)}\widehat{\vartheta}_o$ is proportional to the derivative of the inflaton potential, so that one expects its contribution to be negligible when the dependence of the potential on the inflaton is not important. The operators representing the phase space functions (**Eq. 75**) can be constructed with the above operators and the Fock representation adopted for the modes of the MS and the tensor gauge invariants. In a completely similar manner, one can construct an operator representation for the fermionic contribution H_F to the densitized zero mode of the Hamiltonian constraint (obtained from the original one by multiplication with the homogeneous volume), that depends only on the FLRW geometry and the Dirac field, but not on the inflaton nor on its momentum. For more details about this fermionic contribution, we refer the reader to Refs. (Castelló Gomar et al., 2015; Elizaga Navascués et al., 2017). In this way, we finally get

$$\widehat{H}_S = \frac{1}{2}\left[\widehat{\pi}_{\tilde{\phi}}^2-\widehat{H}_0^{(2)}-\widehat{\Theta}_e-\frac{1}{2}\left(\widehat{\Theta}_o\widehat{\pi}_{\tilde{\phi}}+\widehat{\pi}_{\tilde{\phi}}\widehat{\Theta}_o\right)+\widehat{H}_F\right]. \tag{103}$$

7 HYBRID LQC: MODIFIED PERTURBATION EQUATIONS

Although we have been able to handle all the constraints of our perturbed model except the zero mode of the Hamiltonian constraint, this constraint is still so intrincate that, in the presented form, it does not seem possible to obtain its general solution analytically. In order to investigate the properties of the physical states, we will now introduce an ansatz that contemplates a situation of special interest. We will consider states in which the dependence on the FLRW geometry and on each of the gauge invariant fields can be separated. In this separation, all parts are allowed to depend on the inflaton. In more detail, from now on we analyze states of the form

$$\xi\left(\nu,\tilde{\phi}\right)\psi_s\left(N_s,\tilde{\phi}\right)\psi_T\left(N_T,\tilde{\phi}\right)\psi_F\left(N_F,\tilde{\phi}\right), \tag{104}$$

where we have adopted the abstract notation N_s, N_T, and N_F to denote the dependence on the degrees of freedom of the corresponding Fock space, via a set of occupation numbers in the respective basis of n-particle states. In addition, $\xi(\nu,\tilde{\phi})$ designates a state in the kinematic Hilbert space of homogeneous and isotropic LQC, such that it is normalized and evolves unitarily with respect to $\tilde{\phi}$ as

$$\xi\left(\nu,\tilde{\phi}\right) = \widehat{U}\left(\nu,\tilde{\phi}\right)\chi(\nu), \tag{105}$$

where $\widehat{U}$ is an evolution operator with generator $\widehat{\tilde{H}}_0$ that is close to the unperturbed one, determined by $\widehat{H}_0^{(2)}$. This last condition can be understood as the requirement that the action of $\widehat{H}_0^{(2)}-(\widehat{\tilde{H}}_0)^2-[\widehat{\pi}_{\tilde{\phi}},\widehat{\tilde{H}}_0]$ on $\xi(\nu,\tilde{\phi})$ be at most of the order of the perturbative contributions when imposing the Hamiltonian constraint. Moreover, in the following, for simplicity, we will assume that this term is actually negligible in the action of the Hamiltonian constraint on the considered state, assumption that can always be checked for consistency once $\xi(\nu,\tilde{\phi})$ is specified.

On this family of states, we still must impose à la Dirac the Hamiltonian constraint operator $\widehat{H}_S$, that couples the FLRW background cosmology with the gauge invariant perturbations. To get solutions in physically relevant regimes, we can employ certain approximations that facilitate the resolution of the constraint. First, we consider regimes in which the transitions in the FLRW geometry mediated by the Hamiltonian constraint can be ignored as negligible on $\xi(\nu,\tilde{\phi})$. In this situation, the relevant part of the Hamiltonian constraint is provided by its expectation value on $\xi(\nu,\tilde{\phi})$ over the FLRW geometry (with the integration measure of the inner product of LQC). This expectation value provides a constraint equation on the gauge invariant perturbations of the form

$$\widehat{\pi}_{\tilde{\phi}}^2\psi+\left(2\langle\widehat{\tilde{H}}_0\rangle_\xi-\langle\widehat{\Theta}_o\rangle_\xi\right)\widehat{\pi}_{\tilde{\phi}}\psi = \left[\langle\widehat{\Theta}_e+\frac{1}{2}\left(\widehat{\Theta}_o\widehat{\tilde{H}}_0+\widehat{\tilde{H}}_0\widehat{\Theta}_o\right)-\widehat{H}_F\rangle_\xi+\frac{1}{2}\langle\left[\widehat{\pi}_{\tilde{\phi}}-\widehat{\tilde{H}}_0,\widehat{\Theta}_o\right]\rangle_\xi\right]\psi, \tag{106}$$

where we have called $\Psi = \psi_s(N_s, \tilde{\phi})\psi_T(N_T, \tilde{\phi})\psi_F(N_F, \tilde{\phi})$. In what follows, we will neglect the perturbative operator $\langle\widehat{\Theta}_o\rangle_\xi$ when compared to $\langle\widehat{\tilde{H}}_0\rangle_\xi$ on the left-hand side of this equation, according to our perturbative scheme.

Suppose for the moment that in (**Eq. 106**) we can also neglect the first term, equal to the second derivative of the wave function of the perturbations with respect to the inflaton. This can be regarded as a kind of Born-Oppenheimer approximation, in the sense that one neglects the variation of certain degrees of freedom of the considered quantum state in comparison with the variation of others. Explicitly, we ignore the variation of the perturbations with respect to the inflaton in favor of the variation of the FLRW state, that is given in average by the expectation value $\langle\widehat{\tilde{H}}_0\rangle_\xi$. Additionally, it is worth noticing that the last term in the constraint (**Eq. 106**) affects only the scalar perturbations, because $\widehat{\Theta}_o$ depends only on them. Let us assume that this term for the scalar perturbations is negligibly small. Taking into account that, in our representation, $\widehat{\pi}_{\tilde{\phi}}$ acts as the derivative with respect to the explicit dependence on the inflaton $\tilde{\phi}$ (multiplied by $-i$), and that $\widehat{\tilde{H}}_0$ has been chosen to be close to the generator of the homogeneous and isotropic quantum dynamics with respect to the inflaton, the term under consideration can be understood as the total derivative of the operator $\widehat{\Theta}_o$ with respect to the inflaton, both in its explicit and in its implicit dependence. Thus, we expect that the analyzed contribution to the scalar perturbations can be ignored when the variation with respect to the inflaton is not significantly relevant. With these two approximations, the studied constraint amounts to the sum of a set of Schrödinger equations, one for each of the considered perturbations (scalar, tensor, and fermionic). Specifically, we get the following equations for the gauge invariant perturbations:

$$\widehat{\pi}_{\tilde{\phi}}\psi_s = \frac{\langle 2^{(s)}\widehat{\Theta}_e + \left(\widehat{\Theta}_o\widehat{\tilde{H}}_0 + \widehat{\tilde{H}}_0\widehat{\Theta}_o\right)\rangle_\xi}{4\langle\widehat{\tilde{H}}_0\rangle_\xi}\psi_s, \tag{107}$$

$$\widehat{\pi}_{\tilde{\phi}}\psi_T = \frac{\langle {}^{(T)}\widehat{\Theta}_e\rangle_\xi}{2\langle\widehat{\tilde{H}}_0\rangle_\xi}\psi_T, \tag{108}$$

$$\widehat{\pi}_{\tilde{\phi}}\psi_F = -\frac{\langle\widehat{H}_F\rangle_\xi}{2\langle\widehat{\tilde{H}}_0\rangle_\xi}\psi_F. \tag{109}$$

Note that the separation of variables can actually be made mode by mode in each of the gauge invariant perturbations, since these modes are not coupled by the Hamiltonian constraint.

Had we not neglected the contribution of $\widehat{H}_0^{(2)} - (\widehat{\tilde{H}}_0)^2 - [\widehat{\pi}_{\tilde{\phi}}, \widehat{\tilde{H}}_0]$, but considered instead that its action on the wave function of the FLRW geometry is of the same order as that of the perturbative contributions, we would have obtained an equation similar to the constraint (**Eq. 106**) although with an additional term, given by the expectation value on $\xi(v, \tilde{\phi})$ of the discussed difference of operators. Then, we should have added to the right-hand side of each Schrödinger equation a backreaction term, which could only depend on the inflaton. The balance between these backreaction terms $C^{(\xi)}(\tilde{\phi})$ would require that

$$\frac{\left\langle\left(\widehat{\tilde{H}}_0\right)^2 - \widehat{H}_0^{(2)} + \left[\widehat{\pi}_{\tilde{\phi}}, \widehat{\tilde{H}}_0\right]\right\rangle_\xi}{2\langle\widehat{\tilde{H}}_0\rangle_\xi} = C_s^{(\xi)}\left(\tilde{\phi}\right) + C_T^{(\xi)}\left(\tilde{\phi}\right) + C_F^{(\xi)}\left(\tilde{\phi}\right), \tag{110}$$

where the subscript on the backreaction tells us whether the term corresponds to the scalar (s), tensor (T), or fermionic (F) contribution. From this balance, we see that the sum of all the backreaction terms gives us information, in mean value and within our approximations, about how much the state $\xi(v, \tilde{\phi})$ departs from an exact solution of the unperturbed homogeneous and isotropic cosmology in LQC.

Moreover, let us return to (**Eq. 106**) and let us assume now *only* that the gauge invariant perturbations admit a direct (effective) counterpart of the Heisenberg dynamics that results for their operator analogs from this Hamiltonian constraint equation, something that seems reasonable because the considered Hamiltonian is quadratic in the perturbative variables. Then, it is immediate to realize that we get a set of modified propagation equations for the MS modes, the tensor perturbations, and the fermionic perturbations. For instance, the modified MS equations are

$$d^2_{\eta_\xi} v_{\vec{k},\pm} = -v_{\vec{k},\pm}\left[\frac{\omega_k^2 + \langle 2^{(s)}\widehat{\vartheta}_e^q + {}^{(s)}\widehat{\vartheta}_o\left({}^{(s)}\widehat{\vartheta}_o\widehat{\tilde{H}}_0 + \widehat{\tilde{H}}_0\,{}^{(s)}\widehat{\vartheta}_o\right) + \left[\widehat{\pi}_{\tilde{\phi}} - \widehat{\tilde{H}}_0, {}^{(s)}\widehat{\vartheta}_o\right]\rangle_\xi}{2\langle\widehat{\vartheta}_e\rangle_\xi}\right], \tag{111}$$

where the conformal time η_ξ is defined by the equation

$$\langle\widehat{\tilde{H}}_0\rangle_\xi d\eta_\xi = \langle\widehat{\vartheta}_e\rangle_\xi d\tilde{\phi}. \tag{112}$$

Therefore, this time depends on the state $\xi(v, \tilde{\phi})$ of the FLRW geometry. Similarly, for the modes of the tensor perturbations we obtain

$$d^2_{\eta_\xi}\tilde{d}_{\vec{k},\varepsilon,\pm} = -\tilde{d}_{\vec{k},\varepsilon,\pm}\left[\omega_k^2 + \frac{\langle {}^{(T)}\widehat{\vartheta}_e^q\rangle_\xi}{\langle\widehat{\vartheta}_e\rangle_\xi}\right]. \tag{113}$$

The conformal time is the same as for the scalar perturbations, thanks to the fact that the operator $\widehat{\vartheta}_e$ that multiplies the squared momenta in the Hamiltonian constraint (and that represents the squared scale factor, up to a constant) coincides both for tensor and scalar gauge invariants and, furthermore, for all the modes of these perturbations. In a similar way, an equation with quantum geometry corrections and in the same conformal time can be obtained as well for the femionic perturbations [see Ref. (Elizaga Navascués et al., 2017)].

In the above propagation equations, the ratio of expectation values on the right-hand side gives the quantum corrected mass for the specific gauge invariant perturbation under consideration. We notice that this corrected mass is actually mode independent, because this is the case for the corresponding operators. Also, note that the equations contain no dissipative term. Much more important, the deduced effective equations are hyperbolic in the ultraviolet regime, regardless of the concrete behavior of the quantum state for the FLRW geometry, provided that our approximations are valid.

In order to extract predictions from the above equations about quantum geometry effects on the primordial perturbations, one needs to compute the expectation values

that give the corrected masses for the MS and tensor perturbations. There are several possible strategies to reach this goal. Let us list three of these strategies, in decreasing order of accuracy but increasingly easier to implement. First, one could compute the quantum expectation values numerically. For this, one may try and ignore the backreaction (checking the validity of this approximation afterwards) and integrate numerically the quantum evolution of the FLRW state with respect to the inflaton. With the FLRW state obtained in this way, one can calculate with numerical methods the desired expectation values at each given value of $\tilde{\phi}$. The more difficult part of this program is the integration of the FLRW dynamics in the presence of non-trivial inflaton potentials. Second, taking into account the commented complication that the potential introduces, one can compute the evolution of the FLRW state not numerically, but in an interaction picture in which the potential (or part of it) is regarded as an interaction added to the homogeneous and isotropic Hamiltonian of LQC (Castelló Gomar et al., 2016), and treated as a perturbation of that Hamiltonian using a Dyson series expansion (Galindo and Pascual, 1990). And third, for suitable FLRW states, one can directly adhere to the effective dynamics description of LQC, integrating numerically only the trajectory of the peak of the state, rather that the quantum dynamics strictly speaking. Furthermore, this integration can be simplified by identifying regimes with universal behavior in the evolution from the bounce for the background solutions of interest in LQC (Agullo and Morris, 2015; Zhu et al., 2017; Zhu et al., 2017; Elizaga Navascués et al., 2018). For instance, the most interesting situations to get quantum geometry corrections on the primordial spectra that can be observed nowadays are found for background solutions that are kinetically dominated around the bounce, so that the potential there has little influence. This allows us to introduce further simplifications in the integration of the FLRW trajectories that, at the end of the day, facilitate the calculation of the quantites that determine the studied masses of the perturbations.

Most of the work in the literature has indeed been done assuming an effective dynamics for the description of the FLRW cosmology in LQC. Even if, with this approximation, the problem of computing the evolution of the primordial perturbations is handleable, the results (and hence the predictions obtained from them) depend critically on the initial conditions that one chooses for the FLRW background in this effective dynamics, as well as on the initial conditions that determine the state of the perturbations subject to the propagation equations that we have derived. We will discuss these issues in the next section.

Let us point out that, adopting this effective dynamics for the description of the FLRW states, it has been proven (Elizaga Navascués et al., 2018) that the corrected mass that appears in the modified propagation equations for the scalar and tensor perturbations is positive around the Big Bounce, at least for the most interesting ranges of energy density contribution of the inflaton potential. Since the Big Bounce is precisely the region where the quantum effects on the geometry are more significant, one would expect that the largest departures from the classical situation described by GR cosmology happen there. This positivity of the quantum corrected mass is important to be able to define adiabatic vacua as initial states around the bounce for all the perturbative modes (Martín de Blas and Olmedo, 2016; Elizaga Navascués et al., 2018; Elizaga Navascués et al., 2018). A negative mass involves a breakdown of the adiabatic approximation around the bounce at least for values of ω_k that are not sufficiently large, invalidating the construction of adiabatic states as natural candidates for a vacuum at frequencies that can be of physical interest, for instance because they cover part of the observed spectrum in the CMB. Moreover, the positivity of the mass at the bounce is not shared by other proposals for the quantization of cosmological perturbations within the framework of LQC, like the so-called dressed metric approach that has been put forward by Agullo, Ashtekar, and Nelson (Agullo et al., 2012; Agullo et al., 2013; Agullo et al., 2013).

Finally, in our discussion above, and owing to the compactness of the spatial sections, the modes that we have considered possessed a discrete spectrum of Laplace eigenvalues, ω_k, that play the role of frequencies in the modified propagation equations for the perturbations even after the introduction of quantum geometry corrections. Nonetheless, it is possible to reach the continuum limit for this set of frequencies in the following form. One first extracts a length scale of reference from the scale factor. All observable quantities are defined with respect to this reference scale, that becomes physically irrelevant. One may choose as such scale the value of the scale factor today, or at the moment of the bounce, for instance. Then, the desired continuum limit is reached as the limit in which we make the reference scale tend to infinity. We refer the reader to Ref. (Elizaga Navascués and Mena Marugán, 2018) for more details.

8 INITIAL CONDITIONS

As we have commented, even if we have succeeded in deriving propagation equations for the primordial perturbations that contain modifications caused by quantum geometry effects and even if we assume FLRW states that can be described within the effective dynamics approach to LQC, in order to extract predictions about the primordial cosmological perturbations we need to specify the particular FLRW effective solution that plays the role of a background and, in addition, the vacuum state that determines the conditions on the perturbations. Both pieces of information can be supplied by giving convenient initial data on a certain spatial section. An appealing possibility is to choose this section precisely at the Big Bounce. We will concentrate our discussion on this case. Other possibilities are equally valid, for instance a section in the asymptotic past, if the effective dynamical evolution previous to the bounce connects with a manageable asymptotic region (Wu et al., 2018).

Let us consider first the initial conditions for the FLRW background, solution to the effective dynamics of LQC. The

FLRW cosmology is described by two pairs of canonical zero modes, namely four variables. But we have chosen to impose initial conditions at the bounce, where the time derivative of the scale factor vanishes, reducing the liberty in one degree of freedom[4]. In addition, the Hamiltonian constraint associated with the effective dynamics reduces the degrees of freedom in one more variable. Moreover, we have also commented that we can employ the value of the scale factor at the bounce as a reference scale, depriving it of physical relevance. In practice, this allows us to set that value equal to the unit, for instance. In total, we see that only one variable must be fixed at the bounce by the initial conditions there. We choose the value of the inflaton as this piece of initial data. On the other hand, we can consider also as free data the parameters that determine the inflaton potential. Focusing our attention on the most studied case of a quadratic potential, we find only one parameter, given by the inflaton mass. From this perspective, the FLRW effective background turns out to be completely fixed if we provide the value of the inflaton at the bounce and the value of the inflaton mass.

Actually, we are only interested in effective solutions that lead to power spectra for the perturbations that are compatible with the observations, but that still retain some quantum geometry corrections. One expects that, if these corrections have survived, they should be present in the region of large angular scales or its nearby region, because it is only in this region that the agreement between GR and observations may not be completely solid (Planck Collaboration, 2016a; Planck Collaboration, 2016b). This requirement determines a relatively narrow interval of values for the initial condition on the inflaton ϕ_B and the inflaton mass m, around $\phi_B = 0.97$ and $m = 1.2 \times 10^{-6}$ (in Planck units). For this latter choice of specific values, we show in **Figure 1** the evolution of the Hubble parameter H multiplied by the scale factor. This rescaled Hubble parameter aH vanishes at the bounce and then increases in a very short superinflationary epoch in which H grows to a value of the Planck order. This happens so fast that the scale factor remains almost constant in the process. Since we have taken the scale factor at the bounce equal to one, then aH at its maximum should be of the order of one as well in Planck units (like H). This maximum sets a scale, that we denote K_{LQC} in terms of wavenumbers, and that should be of Planck order according to our previous arguments. From that moment on, the rescaled Hubble parameter starts to decrease until it reaches a minimum. Besides, the quantum corrections in the effective dynamical equations of the background become negligibly small, and the effective trajectory gets totally adapted to a GR cosmological solution.

For solutions that allow for quantum geometry corrections in the spectra of the perturbations at large scales, the inflaton dynamics around the bounce is dominated by its kinetic energy density, which is of Planck order, with an ignorable contribution of the potential. Since the potential is almost negligible, the effective solution behaves as if the scalar field were massless, situation in which the inflaton momentum is a constant of motion and the kinetic energy density decreases rapidly, as a^{-6}. The kinetic energy density continues to diminish until it becomes of the order of the potential. Given that $\dot{a}$ increases when the potential drives the evolution of the scale factor (both in GR and in the effective dynamics of LQC), the coincidence between the kinetic energy density and the potential of the inflaton occurs approximately when aH reaches its minimum. On the other hand, during the evolution from the bounce to this minimum of aH, the inflaton typically increases only by a few orders of magnitude. As a result, the potential, quadratic in the inflaton, varies as well only in a few orders. Taking this into account, and since the potential at the bounce is $m^2\phi_B^2/2$, with values around 10^{-12} in Planck units, when the kinetic and potential energies coincide we expect a density in the range $(10^{-12}, 10^{-9})$. This energy density determines yet another scale in the system, that we call K_{K-P} expressed as a wavenumber.

In total, the influence of the effective background solution on the perturbations is characterized by two (wavenumber) scales, that we have already mentioned, K_{LQC} and K_{K-P}. In a first approximation to the problem, these scales determine the regions where the quantum geometry effects may cause departures from the standard model of inflation in GR. As we have argued, K_{LQC} is of the order of the unit, because it is related to quantum gravity phenomena. To estimate K_{K-P} in our solutions, note that during the epoch of kinetic dominance, the energy density decreases as a^{-6} from a value of the Planck order to values in the interval $(10^{-12}, 10^{-9})$ as we have pointed out. Recalling the Hamiltonian constraint of effective LQC (or of FLRW cosmology in GR, once one is away from the immediate vecinity of the bounce), one concludes that H^2 must be proportional to the discussed energy density in the considered region, and thus decrease during kinetic dominance also as a^{-6}. Consequently, aH must evolve as a^{-2}, decreasing from the Planck order as the cubic root of the energy density, and hence reaching values in the range $[10^{-4}, 10^{-3}]$. In **Figure 1** we see that wavenumbers larger than K_{LQC} only intersect aH once in the evolution. Note that this intersection is the moment when the associated physical length a/k coincides with the Hubble scale $1/H$, and therefore can be taken as the moment of horizon crossing. For modes between K_{LQC} and K_{K-P}, there exist three intersections. Essentially, the modes exit the horizon immediately after the bounce, reenter in the phase of kinetic dominance, and exit again during the inflationary expansion. We expect these modes to be severely affected by the quantum geometry effects around the bounce, and that their evolution differs considerably from that experienced in GR for a background solution with the same behavior in the classical region. Finally, modes with wavenumbers below K_{K-P} do not exit the horizon during inflation but much before, a fact from which one may expect important departures from the predictions of standard inflation.

After the potential equals the kinetic energy density, the latter rapidly decreases while the potential becomes essentially constant and generates inflation. We are interested in effective background solutions such that the modes that experience quantum geometry effects (roughly, those with wavenumbers between K_{LQC} and

[4]This is only a reflection of the fact that, as it happens in classical FLRW cosmology with homogeneous matter content, one of Hamilton's equations of motion contains redundant information in effective LQC.

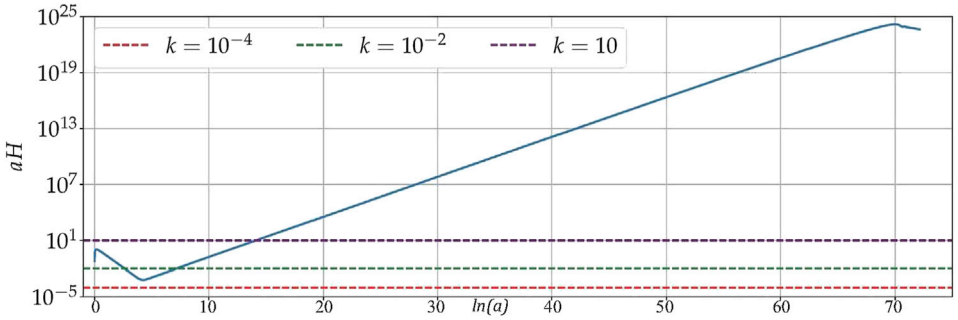

FIGURE 1 | Solution of the rescaled Hubble parameter aH in the effective dynamics of LQC for a matter content given by an inflaton with mass equal to 1.2×10^{-6} and a value at the bounce equal to 0.97 (both quantities in Planck units). The plot shows several wavenumbers to illustrate the different numbers of intersections that are possible.

K_{K-P}) are entering the horizon today. If they had entered much long ago, they would correspond to scales of the power spectra where there is no discrepancy with GR, raising the problem of explaining the absence of departures from the Einsteinian predictions or implying that quantum gravity effects are too tiny to be observable in those circumstances. On the other hand, if they had not entered the horizon again (nor were about to do it), they could not be observed in the power spectra. The interesting situation is when the modes are entering the horizon at present, as we have said. But the effective FLRW backgrounds for which this happens turn out to experience a short-lived inflation. As a consequence, during the first moments of the inflationary expansion, there is still some influence of the kinetic energy density, producing departures from a genuine slow-roll behavior. This will affect the power spectra if the modes that were exiting the horizon at those moments are observed today [see e.g., the discussion of Ref. (Contaldi et al., 2003) in the framework of GR]. Therefore, the slow-roll approximation will not be good, at least, for modes that exited the horizon during those first stages of inflation (Contaldi et al., 2003). Such modes are precisely those close to the scale K_{K-P}. Hence, those modes will experience two types of corrections from a standard inflationary scenario with slow-roll in GR: quantum geometry effects, accumulated around the bounce, and short-lived inflation effects. One of the most important challenges for LQC nowadays is to be able to separate these two kinds of effects and prove that it is possible to identify and falsify the quantum modifications in cosmological observations.

In summary, the LQC modifications in the FLRW background with respect to the standard inflationary solutions of GR may have a relevant influence on modes between the typical scale of the quantum geometry effects and the scale K_{K-P}, close to the onset of inflation. If these include the modes that are now re-entering the horizon, so that the scale of the Universe that we observe today was at the very early stages in the range affected by the quantum effects, some traces of those quantum modifications may have survived in the CMB in spite of the later inflationary expansion, and they might be observable. The fact that the background which those modes feel effectively differs substantially from a de Sitter expanding phase should imply that the natural vacuum for them ought to differ from the standard Bunch-Davies vacuum (Bunch and Davies, 1978). As a result, the power spectra of the perturbations at those scales changes from the conventional predictions based on the choice of a Bunch-Davies state. Suppose that the new vacuum state is related to the standard one by a Bogoliubov transformation that does not mix modes with different values of ω_k, something that is ensured if the invariance under the symmetries of the spatial sections is respected. Let us call α_k and β_k the coefficients of this Bogoliubov transformation, with $|\alpha_k|^2 - |\beta_k|^2 = 1$. Recall that the beta-coefficient determines the antilinear part of the Bogoliubov transformation, i.e., the part that mixes creation and annihilation operators. These coefficients can be determined, e.g., at the initial time chosen in our analysis, if we know there the initial data that specify the two bases of solutions of the gauge invariant field equations, $\{\tilde{\mu}_k\}$ and $\{\mu_k\}$, that characterize respectively the new and the old vacua. Then, if the primordial power spectrum of the standard vacuum is $\mathcal{P}_{\mathcal{R}}(k)$, the power spectrum of the new vacuum state does not need to be calculated from scratch: it is given by the formula

$$\tilde{\mathcal{P}}_{\mathcal{R}}(k) = \left[|\alpha_k|^2 + |\beta_k|^2 + 2|\alpha_k||\beta_k|\cos\left(\phi_k^{\alpha} - \phi_k^{\beta} + 2\phi_k^{\mu}\right)\right]\mathcal{P}_{\mathcal{R}}(k). \tag{114}$$

Here, ϕ_k^{α} and ϕ_k^{β} are the phases of the respective Bogoliubov coefficients, treated as complex numbers, and ϕ_k^{μ} is the phase of the solution μ_k evaluated at the time of computation of the power spectrum (typically by the end of inflation).

The second problem related with the choice of initial data is, therefore, the selection of conditions that determine the vacuum state of the perturbations. Clearly, from the above formula, a change of vacuum state may result in a radical variation of the power spectrum. The predictive power of the formalism is lost unless we have a way to select a vacuum as the preferred state for the gauge invariant perturbations. While, in situations like de Sitter inflation, the high degree of symmetry of the background can help us in picking out a unique state, invariant under the symmetries and with a local Minkowskian behavior, this does not seem possible in more general situations, like those experienced

by the modes affected by quantum geometry effects in the kind of effective backgrounds that appear in LQC. In these circumstances, several proposals have been suggested in order to single out a unique Fock state that could then be viewed as privileged in the system.

Among these proposals, the attempt to use adiabatic states (Parker, 1969; Lüders and Roberts, 1990) has received a considerable attention (Agullo et al., 2013; Agullo et al., 2013; Agullo and Morris, 2015; Martín de Blas and Olmedo, 2016). Nonetheless, their construction may find some obstructions, especially if the effective mass in the propagation equations of the perturbations becomes negative. We have seen that this does not occur in the hybrid approach in the region of important quantum geometry effects, at least for (effective) solutions with kinetic dominance in the energy balance of the inflaton (Elizaga Navascués et al., 2018). Nonetheless, this is not the case for other approaches like the dressed metric quantization if one considers scales that are not sufficiently small (Elizaga Navascués et al., 2018). Besides, the power spectra of adiabatic states, computed numerically, often present large oscillations, and even if these oscillations are averaged, they typically result in an increase of power that does not seem to fit properly with observations if the scales affected by the quantum geometry effects are inside the Hubble horizon today (Agullo and Morris, 2015).

Ashtekar and Gupt have put forward a different proposal for the vacuum state (Ashtekar and Gupt, 2017; Ashtekar and Gupt, 2017). In the region with relevant LQC effects, they have required that the quantum Weyl curvature satisfy a bound which is the lowest value compatible with the uncertainty principle and stable under evolution. This condition selects a ball of states. Among them, the vacuum of the perturbations is chosen by imposing another condition at the end of inflation, ensuring that the dispersion in the field operators be minimized (Ashtekar and Gupt, 2017). In the dressed metric approach, this proposal has been shown to lead to primordial power spectra that, though still highly oscillatory, seem in very good agreement with observations after being averaged (Ashtekar and Gupt, 2017; Ashtekar et al., 2020). Nonetheless, the direct relation of this vacuum with adiabatic states is not known.

Another interesting proposal for a vacuum state is the so-called non-oscillating vacuum, suggested by Martín-de Blas and Olmedo (Martín de Blas and Olmedo, 2016). The proposal is to select the state that minimizes the integral

$$\int_{\eta_0}^{\eta_f} d\overline{\eta} \left| \frac{d\left(|\mu_k|^2\right)}{d\overline{\eta}} \right| \tag{115}$$

in a certain interval of conformal time, usually the interval from the time of the initial spatial section to a time well inside the inflationary regime. For instance, in our typical class of effective backgrounds, this can be a time when the kinetic energy density of the inflaton becomes so negligible that the inflationary expansion is completely driven by the potential. Since the primordial power spectrum for each mode is proportional to the square norm of the associated mode solution μ_k, the proposal picks out a state that minimizes the power oscillations in a definite sense. In general, the determination of this vacuum state needs numerical methods, since the criterion of choice is posed as a variational problem that involves the calculation of an integral. For simple cases, the proposal can be handled analitycally and has been proven to provide a conventional choice of vacuum state. Thus, it selects the Poincaré vacuum for flat spacetime in the presence of a scalar field, either massless or with a quadratic potential. In addition, for de Sitter spacetime, the proposal selects the Bunch-Davies vacuum (Martín de Blas and Olmedo, 2016). The primordial and angular power spectra for this vacuum state have been calculated numerically, both for scalar and tensor perturbations (Benítez Martínez and Olmedo, 2016; Castelló Gomar et al., 2017). The results are compatible with observations, and they even open the possibility of explaining some of the features of the spectra that perhaps may be in tension with GR (Castelló Gomar et al., 2017; Elizaga Navascués et al., 2018), at large angular scales or for multipoles around $l = 20$ (Ade and et al., 2016; Ade and et al., 2016).

9 CHOICE OF VACUUM STATE FOR THE PERTURBATIONS: SPLITTING OF PHASE SPACE VARIABLES

The problem of selecting a vacuum for the perturbations appears in our formalism because the requirements that we have imposed to determine the Fock representation of the gauge invariant perturbations in the hybrid approach at most select a family of representations that are unitarily equivalent, but not a privileged state. Any of those representations, or equivalently any Fock state in the considered family, can be chosen as the vacuum. This leaves a large freedom in the selection of a vacuum for the perturbations, and so in the initial conditions that characterize it. The proposals that we have commented at the end of the previous section are some of the attempts to fix this freedom, but there is yet no general consensus about how to settle the question. Besides, although some of those proposals lead to power spectra that are compatible with observations, they happen to rely on numerical and/or minimization techniques.

In fact, we can consider families of representations related among them by unitary transformations which depend on the background. The Heisenberg dynamics of the creation and annihilation operators associated with each of these representations, even if unitarily implementable as provided by a composition of unitary transformations, would differ between them, given that part of the evolution is removed by assigning it to the background sector of phase space. What is more, by means of this type of unitary transformations with dependence on the background, we can change the splitting of the phase space degrees of freedom between the zero modes that describe the background and the modes of the gauge invariant perturbations. Actually, there exist many ways of separating the phase space into a homogeneous sector and an inhomogeneous one using canonical transformations that mix them. The specific splitting that one adopts determines the properties of the resulting quantization. In particular, the representation of the Hamiltonian constraint and its ultraviolet features strongly depend on this choice.

This fact can be employed to improve the behavior of the field operators that represent the perturbative terms, ameliorating the need for the introduction of regularization procedures typical of QFT. Indeed, as they stand, the actions of the MS, tensor, and fermionic Hamiltonians that appear in the constraint (**Eq. 103**) are ill defined with a standard choice of Fock representation for the corresponding perturbations. Moreover, the backreaction is in general divergent. For instance, by constructing the unitary operator that implements the Heisenberg dynamics of the fermionic variables (in the context of QFT in a quantum mechanically corrected background), one can compute the backreaction of the fermions, $C_F^{(\xi)}(\tilde{\phi})$, and show that it is not absolutely convergent (Elizaga Navascués et al., 2017).

These problems can be solved, or at least alleviated, by introducing new gauge invariants prior to quantization, defined by using canonical transformations that depend on the zero modes. Considering the system as a whole, we have freedom in:

- Changing the dynamical separation between the FLRW geometry and the gauge invariant perturbations via canonical transformations.
- Chosing the Fock vacuum for the perturbations, within the hybrid scheme, regarding this vacuum as the state from which one defines the Fock representation as a cyclic one.

All this ambiguity can be encoded in choices of the form

$$a_{\vec{k},\pm} = f_{\vec{k},\pm}\left(\tilde{a},\pi_{\tilde{a}},\tilde{\phi},\pi_{\tilde{\phi}}\right)\nu_{\vec{k},\pm} + g_{\vec{k},\pm}\left(\tilde{a},\pi_{\tilde{a}},\tilde{\phi},\pi_{\tilde{\phi}}\right)\pi_{\nu_{\vec{k},\pm}} \tag{116}$$

for the MS annihilationlike variables. Here,

$$f_{\vec{k},\pm}\, g^{*}_{\vec{k},\pm} - g_{\vec{k},\pm} f^{*}_{\vec{k},\pm} = -i, \tag{117}$$

so that the introduced variables satisfy, when one freezes the background, canonical commutation relations with the corresponding MS creationlike variables, defined by the complex conjugate of relation (**Eq. 116**). For the tensor variables, on the other hand, one is led to consider analogous families of creation and annihilationlike variables, characterized by two functions $f_{\vec{k},\varepsilon,\pm}$ and $g_{\vec{k},\varepsilon,\pm}$ that satisfy a condition similar to (**Eq. 117**). Generally, one is interested exclusively in canonical transformations of the gauge invariant variables that depend (apart that on the cosmological zero modes) only on the frequency ω_k of the mode, but not on other details about the wavevector $\vec{k}$, nor on the sine or cosine character of the Fourier mode or the polarization of the tensor mode. For those cases, we would adopt the simpler notation f_k and g_k for the functions that define the creation and annihilationlike variables.

In the case of fermions, the ambiguity is captured in the freedom to define annihilationlike variables for particles and creationlike variables for antiparticles as follows:

$$a^{(x,y)}_{\vec{k}} = f_1^{\vec{k}}\left(\tilde{a},\pi_{\tilde{a}},\tilde{\phi},\pi_{\tilde{\phi}}\right)x_{\vec{k}} + f_2^{\vec{k}}\left(\tilde{a},\pi_{\tilde{a}},\tilde{\phi},\pi_{\tilde{\phi}}\right)y^{*}_{-\vec{k}}, \tag{118}$$

$$\left(b^{(x,y)}_{\vec{k}}\right)^{*} = g_1^{\vec{k}}\left(\tilde{a},\pi_{\tilde{a}},\tilde{\phi},\pi_{\tilde{\phi}}\right)x_{\vec{k}} + g_2^{\vec{k}}\left(\tilde{a},\pi_{\tilde{a}},\tilde{\phi},\pi_{\tilde{\phi}}\right)y^{*}_{-\vec{k}}, \tag{119}$$

with

$$f_2^{\vec{k}} = e^{iF_2^{\vec{k}}}\sqrt{1-\left|f_1^{\vec{k}}\right|^2}, \quad g_1^{\vec{k}} = e^{iJ_{\vec{k}}}\left(f_2^{\vec{k}}\right)^{*}, \quad g_2^{\vec{k}} = -e^{iJ_{\vec{k}}}\left(f_1^{\vec{k}}\right)^{*}. \tag{120}$$

In the same spirit that we have commented above, one is usually interested only in cases in which the functions $f_1^{\vec{k}}$, $g_1^{\vec{k}}$, $g_1^{\vec{k}}$, and $g_2^{\vec{k}}$ depend on $\vec{k}$ only *via* ω_k. Notice that the creation and annihilationlike variables (**Eq. 89**) that we used for the fermions in **Sec. 5** were of this kind. We will restrict to this type of cases in the following.

As we already know, a change from the gauge invariant variables that we have adopted for our system to any of the above sets of creation and annihilationlike variables for the perturbations can be completed into a canonical set for the full cosmological model. It suffices to correct again the zero modes with contributions that are quadratic in perturbations in the way that we discussed in **Sec. 4**. In addition, in terms of the new canonical set, the resulting MS, tensor, and fermionic Hamiltonians are the old ones plus some known corrections. These new contributions contain, in general, both diagonal products of annihilation and creationlike variables, and terms that are responsible for the creation and destruction of pairs. The asymptotic behavior of these latter interaction terms when $\omega_k \to \infty$ is what tells us if the quantization of the Hamiltonians is well defined on the vacuum, assuming normal ordering. In all cases $f_k, g_k, f_1^k, f_2^k, g_1^k$, and g_2^k can be chosen so that the dominant powers of ω_k in the interaction terms that prevent a nice behavior of the Hamiltonian operators on Fock space are eliminated.

Moreover, it is possible to remove, order by order in inverse powers of ω_k, all the asymptotic contribution to the interaction terms in the Hamiltonians. For example, let us consider the scalar perturbations. The MS Hamiltonian gets asymptotically diagonalized with (Elizaga Navascués et al., 2019)

$$\omega_k g_k = i f_k\left[1 - \frac{1}{2\omega_k^2}\sum_{n=0}^{\infty}\left(\frac{-i}{2\omega_k}\right)^n \gamma_n\right]. \tag{121}$$

The functions γ_n are determined by the recursion relation

$$\gamma_{n+1} = \tilde{a}\,\{H_0,\gamma_n\} + 4s^{(s)}\left[\gamma_{n-1} + \sum_{l=0}^{n-3}\gamma_l\gamma_{n-(l+3)}\right] - \sum_{l=0}^{n-1}\gamma_l\gamma_{n-(l+1)}, \quad \forall n \geq 0, \tag{122}$$

where $\gamma_0 = s^{(s)} + r^{(s)}\pi_{\tilde{\phi}}$ is just the background dependent mass for the MS field. Creation and annihilationlike variables are then asymptotically fixed, up to a phase, since from the canonical commutation relations it generally follows that

$$2\left|f_k\right|^2 = -\frac{|h_k|^2}{\mathrm{Im}\,(h_k)}, \qquad \text{where} \qquad h_k = \frac{f_k}{g_k}. \tag{123}$$

Similar asymptotic characterizations to diagonalize the field Hamiltonians can be obtained for the tensor perturbations and for the Dirac field (Elizaga Navascués et al., 2019). Actually, in all of these cases, the first few terms in the asymptotic expansion are

enough to construct variables with well-defined Hamiltonians (and finite backreaction contributions to the quantum constraint).

On the other hand, the phases that still remain free in the creation and annihilationlike variables can be determined univocally by means of further physical considerations. Specifically, it seems natural to demand that the background dependence extracted from the dynamics of the original perturbations by our choice of those phases is the minimum allowed, and that the resulting asymptotically diagonal Hamiltonians are positive, as functions of the background.

Given that our analysis has been carried out asymptotically for modes with large wavenumbers, the question arises of what happens for other kinds of modes and, in particular, if the asymptotic expansions provided by the Hamiltonian diagonalization for large ω_k can uniquely specify a choice of creation and annihilationlike variables for all the modes. Let us consider, e.g., the scalar perturbations. In fact, the interaction terms in the Hamiltonian for each possible value of ω_k are completely eliminated if and only if

$$\omega_k^2 + s^{(s)} + r^{(s)}\pi_{\tilde{\phi}} + h_k^2 - \tilde{a}\{h_k, H_0\} = 0. \tag{124}$$

This is a semilinear partial differential equation for which the complex solutions satisfy

$$\mathrm{Im}\,(h_k)^2 = \omega_k^2 + s^{(s)} - \frac{\mathrm{Im}\,(h_k)''}{2\mathrm{Im}\,(h_k)} + \frac{3}{4}\left[\frac{\mathrm{Im}\,(h_k)'}{\mathrm{Im}\,(h_k)}\right]^2, \tag{125}$$

where the prime stands for the operation of taking the Poisson bracket $\tilde{a}\{,H_0\}$. It is worth commenting that, in the linearized context of QFT in curved spacetimes, our asymptotic characterization above can be shown to lead in a unique way to the Minkowski vacuum in the case of constant mass, and to the Bunch-Davies vacuum when the homogeneous background is taken as the de Sitter solution (Elizaga Navascués et al., 2019). Thus, in these linearized contexts, the procedure of asymptotic diagonalization is able to uniquely fix a solution to (**Eq. 124**) for all wavenumbers, and this solution reproduces the natural choice of vacuum state in the considered scenarios. Furthermore, the corresponding asymptotic expansions for the fermionic creation and annihilationlike variables that diagonalize the Hamiltonian have been proven to determine as well a unique choice for all scales in the linearized de Sitter context, even if it is known that those expansions have zero radius of convergence in this case (Elizaga Navascués et al., 2020).

In summary, the asymptotic diagonalization of the Hamiltonian of the perturbations may provide a procedure to determine a vacuum state, and therefore to fix initial conditions for the primordial perturbations in such a way that they are optimally adapted to the dynamics dictated by the Hamiltonian constraint of the total system. Moreover, recent investigations (Elizaga Navascués et al., 2020) support a close analytical relation between the vacuum state that would be selected in this manner and the NO vauum proposed by Martín-de Blas and Olmedo (Martín de Blas and Olmedo, 2016), at least in the context of hybrid LQC.

10 CONCLUSION

In this work, we have reviewed the hybrid approach to LQC. This approach to the quantum description of gravitational systems with local degrees of freedom within the framework of the loop quantization program tries to provide, in a controlled way, a formalism for the study of inhomogeneous cosmological scenarios that, yet, display some symmetries that simplify the physics, or in which the inhomogeneities can be described in a perturbative way over a highly symmetric background. In this way we have been able to analyze linearly polarized gravitational waves in Gowdy cosmologies with toroidal compact sections, and scalar, tensor, and fermionic perturbations at quadratic order in the action around an FLRW spacetime in the presence of an inflaton. In particular, for these cosmological perturbations and at the considered truncation order, we have found a canonical set for the full system composed of gauge invariant perturbations (including the MS field), linear perturbative constraints and gauge variables conjugate to them, and zero modes that contain the relevant information about the background FLRW cosmology. In a hybrid quantization of this canonical system, physical states depend only on the quantum FLRW background and on gauge invariant perturbations. Starting from the zero mode of the Hamiltonian constraint, that couples these perturbations with the FLRW background, and adopting a suitable ansatz for the quantum states of interest, we have been able to derive propagation equations for the perturbations in the primeval stages of the Universe. These equations differ slightly from those of GR by the inclusion of quantum corrections, corrections that we have succeeded to explicitly derive with our hybrid strategy taking fully into account the quantum behavior of the FLRW substrate, and therefore beyond the level of an effective description of this background within homogeneous and isotropic LQC.

In order to quantize differently the system within the framework of LQC, but still adhering to the idea of developing a QFT for the perturbations on a quantum spacetime, one can follow the so-called dressed metric approach, put forward in Refs. (Ashtekar et al., 2009; Agullo et al., 2013; Agullo et al., 2013), instead of the hybrid approach. Indeed, as in the hybrid proposal, the dressed metric approach adopts also the philosophy of combining a loop representation for the homogeneous sector of the (truncated) phase space and a Fock representation for the tensor and MS perturbations (and possible fermionic perturbations, if they are present). Again, in the dressed metric approach one also introduces an ansatz for the quantum states of cosmological interest in which the dependence on the homogeneous geometry and on the perturbations factorizes. In this ansatz, all partial wavefunctions are allowed to depend on the inflaton field ϕ. However, in the dressed metric case there is no Hamiltonian constraint that affects the perturbations, since the whole of the truncated cosmology is not treated as a constrained symplectic system. Instead, one has the Hamiltonian constraint of the homogeneous FLRW model, and the Hamiltonian functions (**Eq. 67**) and (**Eq. 68**) that, classically, generate the dynamics of the perturbations. Consequently, the approach requires that

the homogeneous part of the states be an exact solution of the FLRW model in LQC, and then uses this solution to define the quantum dynamics on the phase space of the gauge invariant perturbations (Agullo et al., 2013; Agullo et al., 2013). In this way, the perturbations behave as test fields that see a dressed metric determined by certain expectation values of operators of the homogeneous geometry, which incorporate the most relevant quantum effects.

In spite of the similarities between the hybrid and the dressed metric approaches, the effective equations that they provide for the propagation of the gauge invariant perturbations are somewhat different even if backreaction is neglected. The discrepancy appears only in the term of the time dependent mass in the propagation equations (Elizaga Navascués et al., 2018). At the end of the day, this can be traced back to the differences in the treatment of the phase space of the perturbed FLRW cosmologies in the hybrid and the dressed metric proposals. As we have emphasized, in the hybrid case the whole phase space is treated as a symplectic manifold, and accordingly it is described in terms of canonical variables. This applies, in particular, to the expression deduced for the time dependent mass. On the contrary, in the dressed metric formalism, one evaluates the time dependent mass directly on the FLRW metric dressed with quantum corrections. For states such that this metric satisfies the effective dynamics of LQC, the time derivatives involved in the corresponding expression of the time dependent mass are then computed along an effective trajectory of homogeneous and isotropic LQC. The difference then arises because of the departure of the standard classical relation between the time derivatives of the scale factor and its canonical momentum (inherent to the hybrid approach) with respect to the alternative effective relation in LQC (employed in the dressed metric case) (Elizaga Navascués et al., 2018). Remarkably, this difference is specially important around the bounce, precisely the region where the quantum corrections on the propagation of the perturbations are expected to be relevant.

Several other approaches have also been suggested for the investigation of cosmological perturbations within LQC. For a comprehensive summary of such approaches, we refer the reader to the reviews listed in Refs. (Banerjee et al., 2012; Ashtekar and Barrau, 2015; Rovelli and Vidotto, 2015; Alesci and Cianfrani, 2016; Gielen and Sindoni, 2016; Grain, 2016; Agullo and Singh, 2017; Wilson-Ewing, 2017). They include the deformed constraint algebra approach (Bojowald et al., 2008; Bojowald et al., 2011; Cailleteau et al., 2014; Barrau et al., 2015), the group field theory models (Gerhardt et al., 2018; Gielen and Oriti, 2018; Gielen, 2019), and the quantum reduced loop gravity scheme (Alesci et al., 2018; Olmedo and Alesci, 2019). Additionally, different ways of addressing backreaction effects of the perturbations on the background within canonical quantum cosmology have been recently explored using techniques from space adiabatic perturbation theory (Schander and Thiemann, 2020). Our attention here has been exclusively put on the hybrid approach in order to fill a gap in the literature, as this is the first extensive review of this proposal that includes a detailed description of the application to primordial perturbations.

A remarkable fact of the hybrid quantization is that, while inhomogeneities and background degrees of freedom are treated as parts of a single constrained system, the imposition of the quantum constraints is consistent and does not give rise to anomalies. This statement holds both in the Gowdy model and for cosmological perturbations. The precise relation of these constraints with the full set of four-dimensional spacetime diffeomorphisms is a different issue that calls for more detailed investigations. As presented in Sec. III, the Gowdy model is not only a symmetry reduction of Einstein gravity, but it is also a partially gauge-fixed system in which only two global constraints remain, namely the zero mode of the Hamiltonian constraint and the zero mode of the momentum constraint in the angular direction on which the metric fields depend[5]. It is worth emphasizing that these are only two constraints, and not two constraints per point (neither of the spatial section nor in the considered angular direction). The aforementioned momentum constraint generates rigid translations in the corresponding angle, while the Hamiltonian one generates global time reparameterizations. These two constraints of the model actually display vanishing Poisson brackets between them and, with the adopted quantization, their corresponding operators commute. For cosmological perturbations, the constraint algebra has to be consistent just up to the order of the perturbative truncation used in our treatment. We have shown that the linear perturbative diffeomorphisms and Hamiltonian constraints admit an Abelianization at this truncation order, and we have represented them directly as part as our canonical elementary variables. The only remaining constraint in the system is a global one, given by the zero mode of the Hamiltonian constraint, that includes contributions from the background and from the perturbations. Notably, its only dependence on the perturbations is via gauge invariants, and therefore commutes with the linear perturbative constraints both classically and in the quantum theory. Indeed, we recall that in the hybrid quantization the Mukhanov-Sasaki and tensor perturbations are represented as operators that commute with the linear perturbative constraints. In other words, at the level of our perturbative truncation and with our hybrid strategy, the algebra of the quantum constraints of our perturbed system does not present anomalies.

The physical relation of these constraints with the four-dimensional diffeomorphisms algebra and the extent to which recent claims about problems with general covariance in LQC (Bojowald, 2020; Bojowald, 2020; Bojowald, 2020) affect the system at the considered perturbative order deserve further study. These claims have been inspired in part by the deformed constraint algebra approach, which in particular predicts processes of effective signature change in high curvature regimes (Bojowald and Mielczarek, 2015; Barrau and Grain, 2016; Schander et al., 2016). In this respect, let us point out, for instance, that some of the perturbative canonical variables used in the hybrid approach are defined with fields that are non-local functions of the spatial metric, inasmuch as they can only be obtained by taking inverse derivatives. This is a common situation

[5]For other alternative quantizations of the Gowdy model developed recently within the framework of LQC, see e.g., Refs. (Bojowald and Brahma, 2015; Martín de Blas et al., 2017).

even in standard cosmological perturbation theory (Bardeen, 1980; Sasaki, 1983; Kodama and Sasaki, 1984; Mukhanov, 1988; Langlois, 1994; Mukhanov, 2005). Moreover, in terms of the background variables employed in our formulation, the metric functions include corrections that are quadratic in the perturbations already at the studied truncation order. A representation of these metric components as quantum operators has yet to be constructed, but it is clear that now issues such as the non-degenerate Lorentzian character of the metric become intrincate questions from a quantum perspective. Even the square scale factor, that in absence of pertubations is *strictly* positive in each superselection sector of homogeneous LQC with the quantization prescription adopted here[6], might in principle turn negative by the effect of the perturbations. Nonetheless, none of these unexplored questions on the quantum geometric structure changes the hyperbolic ultraviolet behavior that we have found for the propagation equations of the perturbative modes.

Even if we have succeeded in deriving such mode equations, that rule the evolution of the primordial perturbations in the hybrid approach, we have seen that this is not yet enough to extract predictions that can be confronted with observations. For this purpose, we also need two types of initial data, namely initial values to fix the FLRW background and conditions to choose a unique vacuum state for the perturbations. With respect to the FLRW cosmology, we have seen that it suffices to provide, e.g., the value of the inflaton at the bounce, apart from the parameters that determine the inflaton potential. In the case of a quadratic potential, we have found values for the inflaton on the bounce section and for the inflaton mass such that the modes affected by quantum geometry effects are those that are re-entering the Hubble horizon nowadays, situation that is the most interesting possibility in terms of observational plausibility in the CMB. Concerning the vacuum state of the perturbations, we have commented on various proposals to select it that lead to power spectra that seem compatible with the observational data.

To go beyond those proposals and find a criterion to select the vacuum that is rooted on the hybrid strategy, that combines loop and Fock representations, we have put an additional emphasis on the choice of splitting between the homogeneous and isotropic sector of phase space and the gauge invariant perturbations. This freedom can be employed to reach a Hamiltonian constraint with nice properties, at least as far as its action on the perturbations is concerned. Requiring such good physical and mathematical properties turns out to restrict the possible quantum dynamics of the perturbative gauge invariants, as well as the Fock representation chosen for them. In turn, this can be regarded as a limitation in the admissible choices of vacuum state. In particular, we have shown that a criterion such as the diagonalization of the Hamiltonian of the gauge invariant perturbations, based on its asymptotic structure, might be able to provide a unique vacuum state, to which one may partcularize in the future the discussion of the effects of quantum geometry in cosmology to extract concrete and distinctive predictions.

AUTHOR CONTRIBUTIONS

The two authors have contributed equally to this review, revisiting the original material, writing the manuscript, and deciding its final redaction.

FUNDING

This work was supported by Grant No. MINECO FIS 2017–86497-C2-2-P from Spain.

ACKNOWLEDGMENTS

The authors want to thank all the researchers that have contributed to the development of Hybrid Loop Quantum Cosmology, a community that includes Laura Castelló Gomar, Jerónimo Cortez, Mikel Fernández-Méndez, Alejandro García-Quismondo, Mercedes Martín Benito, Daniel Martín-de Blas, Javier Olmedo, Santiago Prado, Paula Tarrío, and José M. Velhinho. They also want to thank Abhay Ashtekar, Alejandro Corichi, Kristina Giesel, Jerzy Lewandowski, Hanno Sahlmann, Thomas Thiemann, and Anzhong Wang for inspiration and discussions.

REFERENCES

Agullo, I., Ashtekar, A., and Nelson, W. (2012). A Quantum Gravity Extension of the Inflationary Scenario. *Phys. Rev. Lett.* 109, 251301. doi:10.1103/physrevlett.109.251301

Agullo, I., Ashtekar, A., and Nelson, W. (2013). Extension of the Quantum Theory of Cosmological Perturbations to the Planck Era. *Phys. Rev. D.* 87, 043507. doi:10.1103/physrevd.87.043507

Agullo, I., Ashtekar, A., and Nelson, W. (2013). The Pre-inflationary Dynamics of Loop Quantum Cosmology: Confronting Quantum Gravity with Observations. *Classical Quan. Gravity* 30, 085014. doi:10.1088/0264-9381/30/8/085014

Agullo, I., and Morris, N. A. (2015). Detailed Analysis of the Predictions of Loop Quantum Cosmology for the Primordial Power Spectra. *Phys. Rev. D.* 92, 124040. doi:10.1103/physrevd.92.124040

Agullo, I., and Singh, P. (2017). "Loop Quantum Cosmology," in *100 Years of General Relativity. Loop Quantum Gravity: The First 30 Years*. Editors A. Ashtekar and J. Pullin (Singapore: World Scientific), Vol. 4, 183–240. doi:10.1142/9789813220003_0007

Alesci, E., Barrau, A., Botta, G., Martineau, K., and Stagno, G. (2018). Phenomenology of Quantum Reduced Loop Gravity in the Isotropic Cosmological Sector. *Phys. Rev. D.* 98, 106022. doi:10.1103/physrevd.98.106022

Alesci, E., and Cianfrani, F. (2016). Quantum Reduced Loop Gravity and the Foundation of Loop Quantum Cosmology. *Int. J. Mod. Phys. D.* 25, 1642005. doi:10.1142/s0218271816420050

Ashtekar, A., Baez, J. C., and Krasnov, K. (2001). Quantum Geometry of Isolated Horizons and Black Hole Entropy. *Adv. Theor. Math. Phys.* 4, 1.

Ashtekar, A., and Gupt, B. (2017). Initial Conditions for Cosmological Perturbations. *Classical Quan. Gravity* 34, 035004. doi:10.1088/1361-6382/aa52d4

[6]In fact, this strict positivity is in tension with the assumption inherent in certain representation independent analyses in LQC that the canonical variable describing the densitized triad is supported over the whole real line.

Ashtekar, A., Gupt, B., Jeong, D., and Sreenath, V. (2020). Alleviating the Tension in CMB Using Planck-Scale Physics. *Phys. Rev. Lett.* 125, 051302. doi:10.1103/physrevlett.125.051302

Ashtekar, A., and Gupt, B. (2017). Quantum Gravity in the Sky: Interplay between Fundamental Theory and Observations. *Classical Quan. Gravity* 34, 014002. doi:10.1088/1361-6382/34/1/014002

Ashtekar, A., Kaminski, W., and Lewandowski, J. (2009). Quantum Field Theory on a Cosmological, Quantum Space-Time. *Phys. Rev. D.* 79, 064030. doi:10.1103/physrevd.79.064030

Ashtekar, A., Pawłowski, T., and Singh, P. (2006). Quantum Nature of the Big Bang. *Phys. Rev. Lett.* 96, 141301. doi:10.1103/physrevlett.96.141301

Ashtekar, A., Pawłowski, T., and Singh, P. (2006). Quantum Nature of the Big Bang: An Analytical and Numerical Investigation. *Phys. Rev. D.* 73, 124038. doi:10.1103/physrevd.73.124038

Ashtekar, A., Pawłowski, T., and Singh, P. (2006). Quantum Nature of the Big Bang: Improved Dynamics. *Phys. Rev. D.* 74, 084003. doi:10.1103/physrevd.74.084003

Ashtekar, A., and Wilson-Ewing, E. (2009). Loop Quantum Cosmology of Bianchi Type I Models. *Phys. Rev. D.* 79, 083535. doi:10.1103/physrevd.79.083535

Ashtekar, A., and Barrau, A. (2015). Loop Quantum Cosmology: From Pre-inflationary Dynamics to Observations. *Classical Quan. Gravity* 32, 234001. doi:10.1088/0264-9381/32/23/234001

Ashtekar, A., Bojowald, M., and Lewandowski, J. (2003). Mathematical Structure of Loop Quantum Cosmology. *Adv. Theor. Math. Phys.* 7, 233–268. doi:10.4310/atmp.2003.v7.n2.a2

Ashtekar, A., and Lewandowski, J. (2004). Background Independent Quantum Gravity: A Status Report. *Classical Quan. Gravity* 21, R53–R152. doi:10.1088/0264-9381/21/15/r01

Ashtekar, A. (1986). New Variables for Classical and Quantum Gravity. *Phys. Rev. Lett.* 57, 2244–2247. doi:10.1103/physrevlett.57.2244

Ashtekar, A., and Singh, P. (2011). Loop Quantum Cosmology: A Status Report. *Classical Quan. Gravity* 28, 213001. doi:10.1088/0264-9381/28/21/213001

Assanioussi, M., Dapor, A., Liegener, K., and Pawłowski, T. (2019). Emergent de Sitter epoch of the loop quantum cosmos: A detailed analysis. *Phys. Rev. D.* 100, 084003. doi:10.1103/physrevd.100.084003

Banerjee, K., Calcagni, G., and Martín-Benito, M. (2012). Introduction to Loop Quantum Cosmology. *SIGMA* 8, 016.

Barbero, J. F. (1995). Real Polynomial Formulation of General Relativity in Terms of Connections. *Phys. Rev. D.* 51, 5507.

Bardeen, J. M. (1980). Gauge-invariant Cosmological Perturbations. *Phys. Rev. D.* 22, 1882–1905. doi:10.1103/physrevd.22.1882

Barrau, A., Bojowald, M., Calcagni, G., Grain, J., and Kagan, M. (2015). Anomaly-free Cosmological Perturbations in Effective Canonical Quantum Gravity. *JCAP* 05, 051.

Barrau, A., and Grain, J. (2016). Cosmology without Time: What to Do with a Possible Signature Change from Quantum Gravitational Origin? arXiv: 1607.07589.

Benítez Martínez, F., and Olmedo, J. (2016). Primordial Tensor Modes of the Early Universe. *Phys. Rev. D.* 93, 124008. doi:10.1103/physrevd.93.124008

Berezin, F. A. (1966). *The Method of Second Quantization*. New York: Academic.

Bojowald, M., and Brahma, S. (2015). Covariance in Models of Loop Quantum Gravity: Gowdy Systems. *Phys. Rev. D.* 92, 065002. doi:10.1103/physrevd.92.065002

Bojowald, M., Calcagni, G., and Tsujikawa, S. (2011). Observational Constraints on Loop Quantum Cosmology. *Phys. Rev. Lett.* 107, 211302. doi:10.1103/physrevlett.107.211302

Bojowald, M., Hossain, G. M., Kagan, M., and Shankaranarayanan, S. (2008). Anomaly Freedom in Perturbative Loop Quantum Gravity. *Phys. Rev. D.* 78, 063547. doi:10.1103/physrevd.78.063547

Bojowald, M. (2008). Loop Quantum Cosmology. *Living Rev. Rel.* 11, 4. doi:10.12942/lrr-2008-4

Bojowald, M., and Mielczarek, J. (2015). Some Implications of Signature-Change in Cosmological Models of Loop Quantum Gravity. *JCAP* 08, 052.

Bojowald, M. (2020). No-go Result for Covariance in Models of Loop Quantum Gravity. *Phys. Rev. D.* 102, 046006. doi:10.1103/physrevd.102.046006

Bojowald, M. (2020). Non-covariance of the Dressed-Metric Approach in Loop Quantum Cosmology. *Phys. Rev. D.* 102, 023532. doi:10.1103/physrevd.102.023532

Bojowald, M. (2020). Critical Evaluation of Common Claims in Loop Quantum Cosmology. *Universe* 6, 36. doi:10.3390/universe6030036

Bunch, T. S., and Davies, P. (1978). Quantum field theory in de Sitter space: Renormalization by point splitting. *Proc. R. Soc. Lond. A.* 360, 117.

Cailleteau, T., Linsefors, L., and Barrau, A. (2014). Anomaly-free Perturbations with Inverse-Volume and Holonomy Corrections in Loop Quantum Cosmology. *Classical Quan. Gravity* 31, 125011. doi:10.1088/0264-9381/31/12/125011

Castelló Gomar, L., Cortez, J., Martín-de Blas, D., Mena Marugán, G. A., and Velhinho, J. M. (2012). Uniqueness of the Fock Quantization of Scalar Fields in Spatially Flat Cosmological Spacetimes. *JCAP* 11, 001.

Castelló Gomar, L., Fernández-Méndez, M., Mena Marugán, G. A., and Olmedo, J. (2014). Cosmological Perturbations in Hybrid Loop Quantum Cosmology: Mukhanov–Sasaki Variables. *Phys. Rev. D.* 90, 064015. doi:10.1103/physrevd.90.064015

Castelló Gomar, L., García-Quismondo, A., and Mena Marugán, G. A. (2020). Primordial Perturbations in the Dapor-Liegener Model of Hybrid Loop Quantum Cosmology. *Phys. Rev. D.* 102, 083524. doi:10.1103/physrevd.102.083524

Castelló Gomar, L., Martín-Benito, M., and Mena Marugán, G. A. (2015). Gauge-invariant Perturbations in Hybrid Quantum Cosmology. *JCAP* 06, 045. doi:10.1088/1475-7516/2015/06/045

Castelló Gomar, L., Martín-Benito, M., and Mena Marugán, G. A. (2016). Quantum Corrections to the Mukhanov-Sasaki Equations. *Phys. Rev. D.* 93, 104025. doi:10.1103/physrevd.93.104025

Castelló Gomar, L., Mena Marugán, G. A., Martín de Blas, D., and Olmedo, J. (2017). Hybrid Loop Quantum Cosmology and Predictions for the Cosmic Microwave Background. *Phys. Rev. D.* 96, 103528. doi:10.1103/physrevd.96.103528

Chiou, D. W. (2007a). Effective Dynamics, Big Bounces, and Scaling Symmetry in Bianchi Type I Loop Quantum Cosmology. *Phys. Rev. D.* 76, 124037. doi:10.1103/physrevd.76.124037

Chiou, D. W. (2007b). Loop Quantum Cosmology in Bianchi Type I Models: Analytical Investigation. *Phys. Rev. D.* 75, 024029. doi:10.1103/physrevd.75.024029

Contaldi, C. R., Peloso, M., Kofman, L., and Linde, A. (2003). Suppressing the Lower Multipoles in the CMB Anisotropies. *JCAP* 07, 002.

Corichi, A., Cortez, J., Mena Marugán, G. A., and Velhinho, J. M. (2006). Quantum Gowdy T 3 Model: a Uniqueness Result. *Classical Quan. Gravity* 23, 6301–6319. doi:10.1088/0264-9381/23/22/014

Cortez, J., Mena Marugán, G. A., Olmedo, J., and Velhinho, J. M. (2012). Criteria for the Determination of Time Dependent Scalings in the Fock Quantization of Scalar Fields with a Time Dependent Mass in Ultrastatic Spacetimes. *Phys. Rev. D.* 86, 104003. doi:10.1103/physrevd.86.104003

Cortez, J., Mena Marugán, G. A., and Velhinho, J. M. (2007). Uniqueness of the Fock Quantization of the Gowdy T3 Model. *Phys. Rev. D.* 75, 084027. doi:10.1103/physrevd.75.084027

Dapor, A., and Liegener, K. (2018). Cosmological Effective Hamiltonian from Full Loop Quantum Gravity Dynamics. *Phys. Lett. B.* 785, 506–510. doi:10.1016/j.physletb.2018.09.005

D'Eath, P. D., and Halliwell, J. J. (1987). Fermions in Quantum Cosmology. *Phys. Rev. D.* 35, 1100.

DeWitt, B. S. (1967). Quantum Theory of Gravity. I. The Canonical Theory. *Phys. Rev.* 160, 1113–1148. doi:10.1103/physrev.160.1113

Di Tucci, A., Feldbrugge, J., Lehners, J-L., and Turok, N. (2019). Quantum Incompleteness of Inflation. *Phys. Rev. D.* 100, 063517. doi:10.1103/physrevd.100.063517

Dirac, P. A. M. (1964). *Lectures on Quantum Mechanics*. New York: Belfer Graduate School Monograph Series.

Domagala, M., and Lewandowski, J. (2004). Black-hole Entropy from Quantum Geometry. *Classical Quan. Gravity* 21, 5233–5243. doi:10.1088/0264-9381/21/22/014

Elizaga Navascués, B., Martín de Blas, D., and Mena Marugán, G. A. (2018). Time-dependent Mass of Cosmological Perturbations in the Hybrid and Dressed Metric Approaches to Loop Quantum Cosmology. *Phys. Rev. D.* 97, 043523. doi:10.1103/physrevd.97.043523

Elizaga Navascués, B., Martín-Benito, M., and Mena Marugán, G. A. (2017). Fermions in Hybrid Loop Quantum Cosmology. *Phys. Rev. D.* 96, 044023. doi:10.1103/physrevd.96.044023

Elizaga Navascués, B., Martín-Benito, M., and Mena Marugán, G. A. (2015). Modeling Effective FRW Cosmologies with Perfect Fluids from States of the Hybrid Quantum Gowdy Model. *Phys. Rev. D.* 91, 024028. doi:10.1103/physrevd.91.024028

Elizaga Navascués, B., Martín-Benito, M., and Mena Marugán, G. A. (2015). Modified FRW Cosmologies Arising from States of the Hybrid Quantum Gowdy Model. *Phys. Rev. D.* 92, 024007. doi:10.1103/physrevd.92.024007

Elizaga Navascués, B., and Mena Marugán, G. A. (2018). Perturbations in Hybrid Loop Quantum Cosmology: Continuum Limit in Fourier Space. *Phys. Rev. D.* 98, 103522. doi:10.1103/physrevd.98.103522

Elizaga Navascués, B., Mena Marugán, G. A., and Prado, S. (2019). Asymptotic Diagonalization of the Fermionic Hamiltonian in Hybrid Loop Quantum Cosmology. *Phys. Rev. D.* 99, 063535. doi:10.1103/physrevd.99.063535

Elizaga Navascués, B., Mena Marugán, G. A., and Prado, S. (2020). Non-oscillating Power Spectra in Loop Quantum Cosmology. *Classical Quan. Gravity* 38, 035001.

Elizaga Navascués, B., Mena Marugán, G. A., and Prado, S. (2020). Unique fermionic vacuum in de Sitter spacetime from hybrid quantum cosmology. *Phys. Rev. D.* 101, 123530. doi:10.1103/physrevd.101.123530

Elizaga Navascués, B., Martín de Blas, D., and Mena Marugán, G. (2018). The Vacuum State of Primordial Fluctuations in Hybrid Loop Quantum Cosmology. *Universe* 4, 98. doi:10.3390/universe4100098

Elizaga Navascués, B., Mena Marugán, G. A., and Thiemann, T. (2019). Hamiltonian Diagonalization in Hybrid Quantum Cosmology. *Classical Quan. Gravity* 36, 185010. doi:10.1088/1361-6382/ab32af

Falciano, F. T., and Pinto-Neto, N. (2009). Scalar Perturbations in Scalar Field Quantum Cosmology. *Phys. Rev. D.* 79, 023507. doi:10.1103/physrevd.79.023507

Fernández-Méndez, M., Mena Marugán, G. A., and Olmedo, J. (2014). Effective Dynamics of Scalar Perturbations in a Flat Friedmann-Robertson-Walker Spacetime in Loop Quantum Cosmology. *Phys. Rev. D.* 89, 044041. doi:10.1103/physrevd.89.044041

Fernández-Méndez, M., Mena Marugán, G. A., and Olmedo, J. (2013). Hybrid Quantization of an Inflationary Model: The Flat Case. *Phys. Rev. D.* 88, 044013. doi:10.1103/physrevd.88.044013

Fernández-Méndez, M., Mena Marugán, G. A., and Olmedo, J. (2012). Hybrid Quantization of an Inflationary Universe. *Phys. Rev. D.* 86, 024003. doi:10.1103/physrevd.86.024003

Fernández-Méndez, M. (2014). *Perturbaciones y Dinámica Efectiva de Cosmología Cuántica de Lazos Inhomogénea. PhD Thesis*. Madrid: Universidad Complutense de Madrid. Available at: https://eprints.ucm.es/28962/1/T35905.pdf.

Friedrich, T. (1984). Zur Abhängigkeit des Dirac-operators von der Spin-Struktur. *Colloq. Math.* 48, 57–62. doi:10.4064/cm-48-1-57-62

Galindo, A., and Pascual, P. (1990). *Quantum Mechanics I*. Berlin: Springer-Verlag. doi:10.1007/978-3-642-83854-5

Garay, L. J., Martín-Benito, M., and Mena Marugán, G. A. (2010). Inhomogeneous Loop Quantum Cosmology: Hybrid Quantization of the Gowdy Model. *Phys. Rev. D.* 82, 044048. doi:10.1103/physrevd.82.044048

García-Quismondo, A., and Mena Marugán, G. A. (2019). The Martín-Benito-Mena Marugán-Olmedo Prescription for the Dapor-Liegener Model of Loop Quantum Cosmology. *Phys. Rev. D.* 99, 083505. doi:10.1103/physrevd.99.083505

García-Quismondo, A., Mena Marugán, G. A., and Pérez, G. S. (2020). The Time-dependent Mass of Cosmological Perturbations in Loop Quantum Cosmology: Dapor-Liegener Regularization. *Classical Quan. Gravity* 37, 195003. doi:10.1088/1361-6382/abac6d

Gerhardt, F., Oriti, D., and Wilson-Ewing, E. (2018). The Separate Universe Framework in Group Field Theory Condensate Cosmology. *Phys. Rev. D.* 98, 066011. doi:10.1103/physrevd.98.066011

Gielen, S. (2019). Inhomogeneous Universe from Group Field Theory Condensate. *JCAP* 02, 013.

Gielen, S., and Oriti, D. (2018). Cosmological Perturbations from Full Quantum Gravity. *Phys. Rev. D.* 98, 106019. doi:10.1103/physrevd.98.106019

Gielen, S., and Sindoni, L. (2016). Quantum Cosmology from Group Field Theory Condensates: A Review. *SIGMA* 12, 082.

Gowdy, R. H. (1971). Gravitational Waves in Closed Universes. *Phys. Rev. Lett.* 27, 826–829. doi:10.1103/physrevlett.27.826

Gowdy, R. H. (1974). Vacuum Spacetimes with Two-Parameter Spacelike Isometry Groups and Compact Invariant Hypersurfaces: Topologies and Boundary Conditions. *Ann. Phys.* 83, 203–241. doi:10.1016/0003-4916(74)90384-4

Grain, J. (2016). The Perturbed Universe in the Deformed Algebra Approach of Loop Quantum Cosmology. *Int. J. Mod. Phys. D.* 25, 1642003. doi:10.1142/s0218271816420037

Gupt, B., and Singh, P. (2012). Quantum Gravitational Kasner Transitions in Bianchi-I Spacetime. *Phys. Rev. D.* 86, 024034. doi:10.1103/physrevd.86.024034

Halliwell, J. J. (1991). "Introductory Lectures on Quantum Cosmology," in *Proceedings of the 1990 Jerusalem Winter School on Quantum Cosmology and Baby Universes*. Editors S. Coleman, J. B. Hartle, T. Piran, and S. Weinberg (Singapore: World Scientific), 159–243.

Halliwell, J. J., and Hawking, S. W. (1985). Origin of Structure in the Universe. *Phys. Rev. D.* 31, 1777–1791. doi:10.1103/physrevd.31.1777

Immirzi, G. (1997). Quantum Gravity and Regge Calculus. *Nucl. Phys. B. - Proc. Supplements* 57, 65–72. doi:10.1016/s0920-5632(97)00354-x

Isham, C. J. (1999). *Modern Differential Geometry for Physicists*. 2nd edition. Singapore: World Scientific. doi:10.1142/3867

Kodama, H., and Sasaki, M. (1984). Cosmological Perturbation Theory. *Prog. Theor. Phys. Suppl.* 78, 1–166. doi:10.1143/ptps.78.1

Langlois, D. (1994). Hamiltonian Formalism and Gauge Invariance for Linear Perturbations in Inflation. *Classical Quan. Gravity* 11, 389–407. doi:10.1088/0264-9381/11/2/011

Liddle, A. R., and Lyth, D. H. (2000). *Cosmological Inflation and Large-Scale Structure*. Cambridge, UK: Cambridge University Press. doi:10.1017/cbo9781139175180

Lüders, C., and Roberts, J. E. (1990). Local Quasiequivalence and Adiabatic Vacuum States. *Commun. Math. Phys.* 134, 29–63. doi:10.1007/bf02102088

Martín de Blas, D., and Olmedo, J. (2016). Primordial Power Spectra for Scalar Perturbations in Loop Quantum Cosmology. *JCAP* 06, 029. doi:10.1088/1475-7516/2016/06/029

Martín de Blas, D., Olmedo, J., and Pawłowski, T. (2017). Loop Quantization of the Gowdy Model with Local Rotational Symmetry. *Phys. Rev. D.* 96, 106016. doi:10.1103/physrevd.96.106016

Martín-Benito, M., Garay, L. J., and Mena Marugán, G. A. (2008). Hybrid Quantum Gowdy Cosmology: Combining Loop and Fock Quantizations. *Phys. Rev. D.* 78, 083516. doi:10.1103/physrevd.78.083516

Martín-Benito, M., Martín-de Blas, D., and Mena Marugán, G. A. (2014). Approximation Methods in Loop Quantum Cosmology: From Gowdy Cosmologies to Inhomogeneous Models in Friedmann-Robertson-Walker Geometries. *Classical Quan. Gravity* 32, 075022.

Martín-Benito, M., Martín-de Blas, D., and Mena Marugán, G. A. (2010a). Matter in Inhomogeneous Loop Quantum Cosmology: The Gowdy T3 Model. *Phys. Rev. D.* 83, 084050.

Martín-Benito, M., Mena Marugán, G. A., and Olmedo, J. (2009a). Further Improvements in the Understanding of Isotropic Loop Quantum Cosmology. *Phys. Rev. D.* 80, 104015. doi:10.1103/physrevd.80.104015

Martín-Benito, M., Mena Marugán, G. A., and Pawłowski, T. (2008). Loop Quantization of Vacuum Bianchi I Cosmology. *Phys. Rev. D.* 78, 064008. doi:10.1103/physrevd.78.064008

Martín-Benito, M., Mena Marugán, G. A., and Pawłowski, T. (2009b). Physical Evolution in Loop Quantum Cosmology: The Example of Vacuum Bianchi I. *Phys. Rev. D.* 80, 084038. doi:10.1103/physrevd.80.084038

Martín-Benito, M., Mena Marugán, G. A., and Wilson-Ewing, E. (2010b). Hybrid Quantization: From Bianchi I to the Gowdy Model. *Phys. Rev. D.* 82, 084012. doi:10.1103/physrevd.82.084012

Meissner, K. A. (2004). Black-hole Entropy in Loop Quantum Gravity. *Classical Quan. Gravity* 21, 5245–5251. doi:10.1088/0264-9381/21/22/015

Mena Marugán, G. A., and Martín-Benito, M. (2009). Hybrid Quantum Cosmology: Combining Loop and Fock Quantizations. *Int. J. Mod. Phys. A.* 24, 2820–2838. doi:10.1142/s0217751x09046187

Mukhanov, V. (2005). *Physical Foundations of Cosmology*. Cambridge, UK: Cambridge University Press. doi:10.1017/cbo9780511790553

Mukhanov, V. (1988). Quantum Theory of Gauge-Invariant Cosmological Perturbations. *Zh. Eksp. Teor. Fiz.Sov. Phys. JETP* 67, 1294.

Olmedo, J., and Alesci, E. (2019). Power Spectrum of Primordial Perturbations for an Emergent Universe in Quantum Reduced Loop Gravity. *JCAP* 04, 030.

Parker, L. (1969). Quantized Fields and Particle Creation in Expanding Universes. I. *Phys. Rev.* 183, 1057–1068. doi:10.1103/physrev.183.1057

Pinho, E. J. C., and Pinto-Neto, N. (2007). Scalar and Vector Perturbations in Quantum Cosmological Backgrounds. *Phys. Rev. D.* 76, 023506. doi:10.1103/physrevd.76.023506

Planck Collaboration (2016a). Planck 2015 Results. XX. Constraints on Inflation. *A&A* 594, A20.

Planck Collaboration (2016b). Planck 2015 Results. XIII. Cosmological Parameters. *A&A*, 594, A13.

Reed, M., and Simon, B. (1980). *Methods of Modern Mathematical Physics I: Functional Analysis*. San Diego: Academic Press.

Rendall, A. D. (1994). Adjointness Relations as a Criterion for Choosing an Inner Product. arXiv:gr-qc/9403001.

Rendall, A. D. (1993). Unique Determination of an Inner Product by Adjointness Relations in the Algebra of Quantum Observables. *Classical Quan. Gravity* 10, 2261–2269. doi:10.1088/0264-9381/10/11/009

Rovelli, C., and Vidotto, F. (2015). *Covariant Loop Quantum Gravity: An Elementary Introduction to Quantum Gravity and Spinfoam Theory*. Cambridge, UK: Cambridge University Press.

Rudin, W. (1962). *Fourier Analysis on Groups*. New York: Interscience Publishers.

Sasaki, M. (1983). Gauge-Invariant Scalar Perturbations in the New Inflationary Universe. *Prog. Theor. Phys.* 70, 394–411. doi:10.1143/ptp.70.394

Schander, S., Barrau, A., Bolliet, B., Grain, J., Linsefors, L., and Mielczarek, J. (2016). Primordial Scalar Power Spectrum from the Euclidean Big Bounce. *Phys. Rev. D.* 93, 023531. doi:10.1103/physrevd.93.023531

Schander, S., and Thiemann, T. (2020). Quantum Cosmological Backreactions IV: Constrained Quantum Cosmological Perturbation Theory. arXiv:1909.07271.

Shirai, I., and Wada, S. (1988). Cosmological Perturbations and Quantum Fields in Curved Space. *Nucl. Phys. B.* 303, 728–750. doi:10.1016/0550-3213(88)90428-2

Tarrío, P., Fernández-Méndez, M., and Mena Marugán, G. A. (2013). Singularity Avoidance in the Hybrid Quantization of the Gowdy Model. *Phys. Rev. D.* 88, 084050. doi:10.1103/physrevd.88.084050

Thiemann, T. (2007). *Modern Canonical Quantum General Relativity*. Cambridge, UK: Cambridge University Press. doi:10.1017/cbo9780511755682

Thiemann, T. (1996). Anomaly-free Formulation of Non-perturbative, Four-Dimensional Lorentzian Quantum Gravity. *Phys. Lett. B.* 380, 257–264. doi:10.1016/0370-2693(96)00532-1

Velhinho, J. M. (2007). The Quantum Configuration Space of Loop Quantum Cosmology. *Classical Quan. Gravity* 24, 3745–3758. doi:10.1088/0264-9381/24/14/013

Wilson-Ewing, E. (2017). Testing Loop Quantum Cosmology. *Comptes Rendus Physique* 18, 207–225. doi:10.1016/j.crhy.2017.02.004

Wu, Q., Zhu, T., and Wang, A. (2018). Non-adiabatic Evolution of Primordial Perturbations and Non-gaussinity in Hybrid Approach of Loop Quantum Cosmology. *Phys. Rev. D.* 98, 103528. doi:10.1103/physrevd.98.103528

Yang, C. N., and Mills, R. L. (1954). Conservation of Isotopic Spin and Isotopic Gauge Invariance. *Phys. Rev.* 96, 191–195. doi:10.1103/physrev.96.191

Yang, J., Ding, Y., and Ma, Y. (2009). Alternative Quantization of the Hamiltonian in Loop Quantum Cosmology. *Phys. Lett. B* 682, 1–7. doi:10.1016/j.physletb.2009.10.072

Zhu, T., Wang, A., Kirsten, K., Cleaver, G., and Sheng, Q. (2017). Pre-inflationary Universe in Loop Quantum Cosmology. *Phys. Rev. D.* 96, 083520. doi:10.1103/physrevd.96.083520

Zhu, T., Wang, A., Kirsten, K., Cleaver, G., and Sheng, Q. (2017). Universal Features of Quantum Bounce in Loop Quantum Cosmology. *Phys. Lett. B.* 773, 196–202. doi:10.1016/j.physletb.2017.08.025

Conflict of Interest: The authors declare that the research was conducted in the absence of any commercial or financial relationships that could be construed as a potential conflict of interest.

frontiers in Astronomy and Space Sciences

ORIGINAL RESEARCH
published: 04 June 2021
doi: 10.3389/fspas.2021.685288

Cosmic Tango Between the Very Small and the Very Large: Addressing CMB Anomalies Through Loop Quantum Cosmology

Abhay Ashtekar[1]*, *Brajesh Gupt*[1,2] *and V. Sreenath*[3]

[1]*Institute for Gravitation and the Cosmos and Physics Department, The Pennsylvania State University, University Park, Pennsylvania, PA, United States,* [2]*Texas Advanced Computing Center, The University of Texas at Austin, Austin, TX, United States,* [3]*Department of Physics, National Institute of Technology Karnataka, Surathkal, India*

While the standard, six-parameter, spatially flat ΛCDM model has been highly successful, certain anomalies in the cosmic microwave background bring out a tension between this model and observations. The statistical significance of any one anomaly is small. However, taken together, the presence of two or more of them imply that according to standard inflationary theories we live in quite an exceptional Universe. We revisit the analysis of the PLANCK collaboration using loop quantum cosmology, where an unforeseen interplay between the ultraviolet and the infrared makes the *primordial* power spectrum scale dependent at very small k. Consequently, we are led to a somewhat different ΛCDM Universe in which anomalies associated with large scale power suppression and the lensing amplitude are both alleviated. The analysis also leads to new predictions for future observations. This article is addressed both to cosmology and loop quantum gravity communities, and we have attempted to make it self-contained.

Keywords: CMB, anomalies, loop quantum cosmology (LQC), big bounce, UV-IR interplay

OPEN ACCESS

Edited by:
Guillermo A. Mena Marugán, Instituto de Estructura de la Materia (IEM), Spain

Reviewed by:
Jorge Pullin, Louisiana State University, United States
Mercedes Martin-Benito, Complutense University of Madrid, Spain
Jerónimo Cortez, Universidad Nacional Autónoma de México, Mexico

***Correspondence:**
Abhay Ashtekar
ashtekar.gravity@gmail.com

Specialty section:
This article was submitted to Cosmology, a section of the journal Frontiers in Astronomy and Space Sciences

Received: *24 March 2021*
Accepted: *28 April 2021*
Published: *04 June 2021*

Citation:
Ashtekar A, Gupt B and Sreenath V (2021) Cosmic Tango Between the Very Small and the Very Large: Addressing CMB Anomalies Through Loop Quantum Cosmology. Front. Astron. Space Sci. 8:685288. doi: 10.3389/fspas.2021.685288

1 INTRODUCTION

The quantum geometry effects underlying loop quantum gravity (LQG) lead to a natural resolution of the big bang singularity [see, e.g. Ashtekar and Singh (2004), Agullo and Singh (2017), for reviews]. Therefore, one can hope to meaningfully extend the standard inflationary paradigm to the Planck regime. Over the past decade, several closely related approaches have been used to carry out this task, leading to a striking interplay between theory and observations [see, in particular Agullo et al. (2012), Agullo et al. (2013a), Agullo et al. (2013b), Fernandez-Mendez et al. (2012), Barrau et al. (2014), Linsefors et al. (2013), Ashtekar and Barrau (2015), Agullo and Morris (2015), Agullo (2015), Ashtekar and Gupt (2017a), Ashtekar and Gupt (2017b), Gomar et al. (2017), Agullo et al. (2018), Barrau et al. (2018), Agullo et al. (2020a), Agullo et al. (2020b), Sreenath et al. (2019), Agullo et al. (2021a), Agullo et al. (2021b)]. In this article we will focus on the recent results that shed new light on the anomalous features seen in the cosmic microwave background (CMB). Specifically, we will show that in our approach two of the anomalies seen in the CMB can be accounted for using the pre-inflationary dynamics of loop quantum cosmology (LQC). This phase of dynamics alters the quantum state of cosmological perturbations at the onset of the (relevant part of the) slow roll, leading to revised values of the six parameters that characterize the ΛCDM Universe. The revision alleviates the tension due to two anomalies that have received considerable attention, while leaving the successes of standard inflation intact. Main results were reported in Ashtekar et al. (2020). The

purpose of this paper is to provide details and also present some supplementary material to put the results in a broader context. These results illustrate that LQC has matured sufficiently to lead to testable predictions.

The paper is addressed both to the LQG community and cosmologists. For the benefit of the LQG community, that primarily focuses on mathematical physics, we have included a discussion of the interplay between theory and observations that leads to the six parameter ΛCDM cosmological model. We will summarize the underlying procedure and point out certain subtleties in data analysis. For cosmologists, we will summarize the key features of LQC that lead to new observable predictions. Specifically we will explain how the quantum geometry effects *in the ultraviolet*, that lead to the singularity resolution, have unforeseen and interesting consequences on the dynamics of cosmological perturbations *in the infrared*. It is this 'cosmic tango' between the very small and the very large that alleviates anomalies. Overall, in terms of conceptual flow, we have attempted to make this paper self-contained. In particular, within the page limits of this special issue, we clarify apparently conflicting statements in the LQC literature. In order to make the material accessible to both communities, we will have to briefly review ideas and results that are likely to be well-known in one community but not the other.

The two anomalies we focus on arise as follows. Motivated in large part by inflationary scenarios, the CMB analysis generally begins by assuming that the *primordial* scalar power spectrum has a nearly scale invariant form, characterized by just two parameters, the scalar perturbation amplitude A_s and the scalar spectral index n_s. We will refer to this form as the *standard ansatz (SA)*. A_s, n_s and 4 other parameters (discussed in **Section 2.1**) characterize a specific ΛCDM Universe. Given these six parameters one can evolve the primordial perturbations using known astrophysics and predict the observable power spectra. By varying the values of the 6 parameters, and confronting the theoretical prediction with observations, one finds the posterior probability distributions of the six cosmological parameters. By and large the CMB observations can be well explained using the ΛCDM Universe determined by the marginalized mean values of these parameters. However, one also finds some anomalous features. The first is power suppression at large angular scales: the observed power in the temperature-temperature (TT) spectrum is suppressed for $\ell \lesssim 30$ in the spherical harmonic decomposition, relative to what the theory predicts. The second anomaly we focus on is associated with the so-called lensing amplitude, A_L, associated with gravitational lensing that the CMB photons experience as they propagate from the surface of last scattering to us. The ΛCDM cosmology based on the *SA* assumes $A_L = 1$ while, when it is allowed to vary, A_L prefers a value larger than unity. This tension hints at an internal inconsistency. To alleviate it, one can introduce a positive spatial curvature (Handley, 2019) but then there are inconsistencies with the low z measurements, prompting a recent suggestion (Di Valentino et al., 2019) that this anomaly gives rise to a "possible crisis in cosmology."

As we will see, both the anomalies are simultaneously alleviated in our approach. The key new element is the following: Pre-inflationary dynamics of LQC leads to a *primordial* power spectrum that differs from the *SA*, but only at large angular scales. While it continues to be nearly scale invariant–and essentially indistinguishable from the one given by the *SA*–for $\ell \gtrsim 30$, there is a specific power suppression for $\ell \lesssim 30$. As a result, the best-fit values of the six cosmological parameters change. Interestingly, the change in 5 of the 6 parameters is extremely small, $\lesssim 0.4\%$. But the value of the 6th parameter–the optical depth τ–is increased by $\sim 9.8\%$! We will see that this change then leads to the alleviation of the tension between observations and theoretical predictions based on the *SA*. Note that in spite of this significant change in the value of τ, LQC leaves the highly successful predictions of standard inflation at small angular scales unaffected. In particular, all the finer features of various power spectra predicted by standard inflation for $\ell > 30$—where the observational error bars are small–are present also in the LQC prediction. Thus the LQC analysis provides an explicit example supporting a conclusion of Chowdhury et al. (2019) that *trans*-Planckian effects are not a "threat to inflation".

The paper is organized as follows. **Section 2** summarizes the procedure used in observational cosmology to arrive at the 6 parameter ΛCDM model and explains the two anomalies and their significance in greater detail. **Section 3** summarizes the basic results from LQC that are used in the subsequent analysis. In particular, we explain the origin of the surprising interplay between the ultraviolet and the infrared that is a rather robust feature of the LQC approaches. The main results are presented in **Section 4**. They include a discussion of: 1) the LQC corrected *primordial* power spectrum for scalar perturbations; 2) the TT, temperature-electric polarization (TE), the electric polarization (EE), and the lensing potential ($\phi\phi$) power spectra we predict, and comparisons with those obtained using the *SA* as well as with the observed power spectra reported by the PLANCK team in their final analysis (Aghanim et al., 2020b). As usual these power spectra are presented in terms of the spherical harmonic components C_ℓ of the respective correlation functions; 3) the TT correlation function $C(\theta)$ predicted by LQC and its comparison with the prediction of the *SA* as well as PLANCK observations; 4) the A_L vs. τ plots that show that the observed values fall in the 1σ contour in LQC, but not if one uses the *SA*; and, 5) the power spectrum for BB polarization predicted by LQC and its comparison with that predicted by the *SA*. The detailed calculations underlying these plots were performed using the Starobinsky and quadratic potentials. The first is preferred phenomenologically while the second has been used often because of its simplicity. Close agreement between the two sets of results is an indication of robustness of the LQC results. In **Section 5** we summarize the main results and put them in a broader context.

So far the discrepancy between the results of the SHOES team (Riess et al., 2019) and CMB measurements (Adam et al., 2020) associated with the value of the Hubble parameter has not been systematically addressed in LQC. This is in large part because it is not yet clear whether there is a definitive tension, or if the

discrepancy is primarily due to systematic calibration offsets (Efstathiou, 2020). Observations may decide on this issue in the near future.

2 THEORETICAL PREDICTIONS AND PLANCK OBSERVATIONS

This section is addressed primarily to the LQG community. In **Section 2.1** we summarize the procedure used by the PLANCK team to arrive at the six parameter ΛCDM model and in **Section 2.2** we explain the power suppression and the lensing amplitude anomalies in a bit more detail.

2.1 The 6 Parameter ΛCDM Model

The six parameters that characterize the ΛCDM Universe can be neatly divided in three groups. The first two parameters–the amplitude A_s and the spectral index n_s for scalar modes–feature in the *SA* for the primordial power spectrum:

$$\mathcal{P}_{\mathcal{R}}(k) = A_s \left(\frac{k}{k_\star}\right)^{n_s - 1} \tag{2.1}$$

Here k is the wave number in the Fourier decomposition and $k_\star$ is a pivot scale (set to $k_\star = 0.002\,\mathrm{Mpc}^{-1}$ in the WMAP analysis and $k_\star = 0.05\ \mathrm{Mpc}^{-1}$ in the PLANCK analysis). If we had $n_s = 1$, the primordial spectrum would be scale invariant, i.e., it would be independent of the wave number k of the cosmological perturbation. If n_s is less than 1 (as observations imply) then there is more power at small k, i.e., the power spectrum has a red tilt (One can also consider the possibility of a running n_s, where it has a k dependence but we will not need this generality.) The second set of parameters, the baryonic and cold matter densities $\Omega_b h^2$ and $\Omega_c h^2$, are important for the propagation of cosmological perturbations starting from the end of inflation. The last group of parameters are $100\theta_{MC}$, that characterizes the angular scale of acoustic oscillations, and the optical depth τ that characterizes the reionization epoch. These two parameters govern the propagation of perturbations from the last scattering surface to now. Thus, given these six parameters one can use the known astrophysics to propagate the cosmological perturbations starting from the end of inflation, providing us with the theoretical predictions for power spectra we should observe now.

More precisely, for each choice of the six parameters, one can calculate 4 correlation functions C_ℓ^{TT}, C_ℓ^{TE}, C_ℓ^{EE}, $C_\ell^{\phi\phi}$ that are the spherical harmonic decompositions of the corresponding correlation function $C^{\mathrm{XY}}(\theta)$ (where θ characterizes the angular separation of two points in the sky). These correlation functions can be measured and compared with the theoretical predictions, expressed as functions of the six parameters. The statistical analysis, usually done by employing Markov-Chain Monte Carlo method, then leads to the posterior probability distribution for the six parameters. In particular, the maximum likelihood value of the marginalized probability distributions yield the values of six parameters that determine a ΛCDM Universe. Observations of the PLANCK collaboration provide these values (together with the corresponding 1-sigma spreads); this is the "Universe according to PLANCK" (within the 68% confidence level, characterized by the 1σ contours).

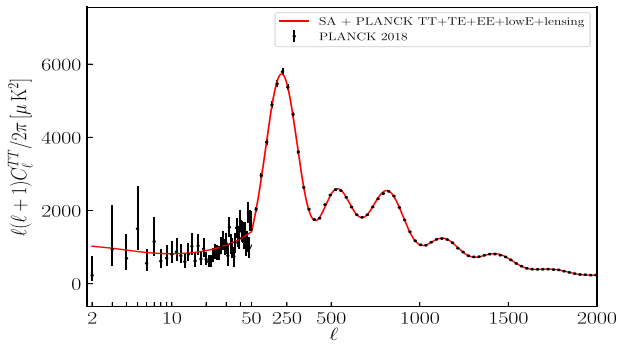

FIGURE 1 | *The TT-power spectrum.* The (red) continuous curve is the theoretical prediction from standard ansatz while the (black) dots with error bars represent the measurements of the PLANCK team reported in 2018. There is excellent agreement between theory and observations for $\ell > 50$ but the observed power is suppressed relative to the theoretical prediction for $\ell \lesssim 30$. As usual, the horizontal axis uses a logarithmic scale for $\ell \lesssim 50$ but a linear scale for $\ell \gtrsim 50$.

Once these parameters are determined, one can calculate additional observable quantities *assuming* that model and, by carrying out measurements, one can subject the model to consistency tests. For example, the lensing amplitude A_L is set to unity in this construction. One can let this parameter vary and test if this value is consistent with observations. Another type of test is provided by the (odd parity) B-modes. In any one model, one can calculate the correlation function C_ℓ^{BB}. As we discuss in **Section 5**, several observational missions will soon measure this correlation function with accuracy that may be sufficient to distinguish one model from another (Matsumura et al., 2014; Delabrouille et al., 2018; Hanany et al., 2019). Similarly, the reionization depth τ will be measured by missions that are unrelated to the CMB (Fialkov and Loeb, 2016). They will constrain τ, providing us with independent checks on the current ΛCDM model.

2.2 Anomalies

As **Figure 1** shows, the TT power spectrum is in excellent agreement with the theoretical predictions using the *SA* at small angular scales ($\ell > 50$). This is especially noteworthy because the instrumental errors are truly minuscule in this range.

However, for $\ell \lesssim 30$ the observed power is lower than the theoretical prediction. This power suppression was evident already in the WMAP data, and is reenforced by the PLANCK findings. Over the years it has been argued (Spergel et al., 2003; Sarkar et al., 2011; Akrami et al., 2019; Schwarz et al., 2016) that this anomaly is brought to forefront if one carries out the comparison using the quantity $S_{1/2} := \int_{-1}^{1/2} [C(\theta)]^2\, \mathrm{d}(\cos\theta)$ that features the physical space TT correlation function $C(\theta)$ in place of the spherical harmonic coefficients C_ℓ. Qualitatively, large angular scales correspond to small ℓ in the spherical harmonic decomposition. However, for any given θ_o the value $C(\theta_o)$

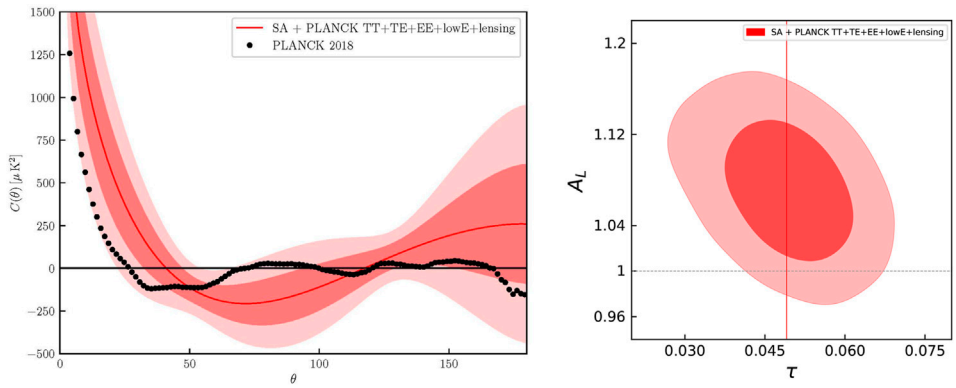

FIGURE 2 | *Left Panel:* *Large scale power anomaly as measured by* $C(\theta)$. The (red) continuous curve is the theoretical prediction from the *SA* with 68 and 95% confidence level contours arising from cosmic variance, while the (black) dots represent the 2018 PLANCK team measurements. The *SA* prediction for $S_{1/2}$ is more than 35 times the observed value. ***Right Panel:*** *Lensing amplitude* A_L *vs. optical depth* τ $A_L = 1$ lies outside the 1 σ contour, signaling the tension between theory and observations.

receives contributions from *all* ℓ. Therefore $S_{1/2}$ is a more *direct* measure of the cumulative power for $\theta \geq 60°$ than the C_ℓ's for low ℓs. Indeed, as the left panel in **Figure 2** vividly shows, the observed $C(\theta)$ (the black, dotted curve) is very close to zero for $\theta > 60°$, in contrast to the theoretical (solid, red) curve. The observed value of $S_{1/2}$ is ~ 1209, while the theoretical prediction from the *SA* is 42, 496.5, some 35 times larger. Since the extent of this discrepancy is not immediate from **Figure 1**, one may wonder why the power spectrum is not reported using $C^{\rm TT}(\theta)$ in place of $C_\ell^{\rm TT}$. The reason is that the $C_\ell^{\rm TT}$ for distinct ℓs are (almost) uncorrelated and can therefore be treated as independent observables, while $C^{\rm TT}(\theta)$ for distinct θ have massive cross-covariance, whence the statistical significance of power suppression is only $2-3\sigma$ in spite of the large deviation seen in the left panel of **Figure 2**. Also, because of these correlations, to obtain the 1 and 2σ contours in this plot one has to take into account a large covariance matrix which in turn requires a detailed understanding of the instruments and the masking procedure near $\theta = 180°$ used in the data analysis to remove the contamination coming from the galactic plane.

The second anomaly is associated with the lensing amplitude A_L depicted in the right panel of **Figure 2**. As it propagates from the last scattering surface at $z \approx 1100$ to us, the CMB is lensed due to inhomogeneities. The lensing potential is nearly Gaussian because there are many lenses along the line of sight. As explained in **Section 2.1**, the six parameter ΛCDM Universe is determined using best fits to *all four* power spectra. Once this is done, one can compare each observed power spectrum, one by one, with the theoretically predicted power spectrum for that specific ΛCDM Universe. Just as this comparison revealed an anomalous suppression of power in $C_\ell^{\rm TT}$ for $\ell < 30$, one finds an anomaly also in the lensing potential power spectrum $C_\ell^{\phi\phi}$: Relative to the prediction of the best-fit ΛCDM model, there is power enhancement in the range $8 \leq \ell \leq 400$ used by the PLANCK collaboration to report the baseline cosmological results (Adam et al., 2020) (In this range, the reconstruction procedure is robust and the impact of systematics is reduced). As a consistency check on the 6-parameter ΛCDM model, one introduces a 7th phenomenological parameter $A_{\rm L}$—the lensing amplitude, normalized so that $A_{\rm L} = 1$ in the 6 parameter ΛCDM model–and allows it to vary. Varying $A_{\rm L}$ can be considered as a conservative way of marginalizing over the systematics of the PLANCK data. Departure of $A_{\rm L}$ from unity signals a tension with predictions based on the standard 6-parameter ΛCDM. One finds that $A_{\rm L}$ is higher than 1 at $\sim 1.9\sigma$ level (Adam et al., 2020). This is the lensing amplitude anomaly and its occurrence has been interpreted as a hint of new physics (Di Valentino and Bridle, 2018). The right panel of **Figure 2** illustrates this tension. Here $A_{\rm L}$ is plotted against the optical depth τ because this plot will be useful when we compare the results from LQC with those from the SA in **Section 4**: Of the six parameters, only τ receives significant corrections from LQC. τ is singled out even within the *SA* by the fact that the relative error (as measured by the ratio of the standard deviation to the mean value) in τ is $\sim 13\%$ while that in the other five ΛCDM parameters are less than 1%. In the plot, the tension is manifested in the fact that the line $A_{\rm L} = 1$ lies outside the 1σ contour. Attempts to alleviate this tension within the standard paradigm based on general relativity (GR)—e.g. changing the background geometry by introducing spatial curvature–are not supported by lensing reconstruction or Baryonic oscillations (BAO) data (since the joint constraint with BAO is consistent with flat Universe, with $\Omega_{\rm K} = 0.001 \pm 0.002$).

As noted in the introduction, while the statistical significance of either of these anomalies is low, together the two imply that the observed Universe will emerge only once in $\sim 10^6$ realizations of the posterior probability distributions. Therefore, as the PLANCK collaboration suggested both in its 2015 and 2018 data releases, alleviation of this tension is of considerable interest especially if the mechanism is rooted in physics beyond GR (Ade et al., 2016; Aghanim et al., 2020a).

3 LOOP QUANTUM COSMOLOGY

This section is addressed primarily to the cosmology community. In **Section 3.1** we briefly recall how quantum geometry effects

underlying LQG lead to a resolution of the big bang singularity, replacing it with a big bounce. Since physical quantities do not diverge anywhere, one can extend the standard inflationary scenario all the way to the bounce. In **Section 3.2**, we discuss the pre-inflationary dynamics of cosmological perturbations, specifically the propagation of quantum fields representing these perturbations on the *quantum* background geometry provided by LQC. In **Section 3.3**, we explain why, contrary to one's initial expectations, this pre-inflationary dynamics can leave observable signatures at large scales in the CMB. We will use this framework in **Section 4** to extract the LQC corrections to the primordial power spectrum. As mentioned in **Section 1**, together with observations, these corrections imply that we live in a somewhat different ΛCDM Universe in which the two anomalies are naturally alleviated.

3.1 The Big Bounce of LQC

Investigations of the early Universe are often carried out assuming that spacetime is well approximated by a spatially flat FLRW background metric of GR, together with first order cosmological perturbations that are described by quantum fields. Consider the inflationary paradigm and, for brevity, let us refer to the time when the pivot mode $k = k_\star$ exits the Hubble horizon simply as 'the onset of inflation'. At this onset, while spacetime curvature is huge by astrophysical standards–some 10^{65} times that at the horizon of a solar mass black hole–it is only $\sim 10^{-12}$ times the Planck scale. Therefore, at the level of accuracy of current interest, it is safe to ignore the quantum gravity effects even at the onset of inflation. Since spacetime geometry is well approximated by a (perturbed) de Sitter metric at this time, one assumes that the quantum fields representing cosmological perturbations are in the Bunch–Davies (BD) vacuum that is selected by the isometries of the de Sitter metric and evolves the perturbations to the future (as curvature decreases further).

However, conceptually it is rather ad-hoc to begin, so to say, 'in the middle' of evolution. If we go further back in the past, curvature attains the Planck scale, and then diverges at the big bang. During this pre-inflationary epoch, spacetime geometry is *not at all* well-approximated by the de Sitter geometry. Why, then, can we assume the state to be the BD at the onset of inflation? Should we not start in the deep Planck regime and check whether the state is in fact in the BD vacuum at this onset? This would require quantum cosmology, where the Friedmann, Lemaître, Robertson, Walker (FLRW) solution of Einstein's equations, characterized by the scale factor $a(t)$ and a matter field $\phi(t)$, is replaced by a quantum state $\Psi(a, \phi)$ subject to an appropriate quantum version of Einstein-matter field equations. Note that reference to the proper time t has disappeared–quantum dynamics is relational, à la Leibnitz: for example, one can use the matter field ϕ as an internal clock, and describe how the scale factor evolves with respect to it. Quantum fields representing cosmological perturbations are now to propagate on a *quantum* FLRW geometry $\Psi(a, \phi)$ which assigns probability amplitudes to various metrics, rather than on a single FLRW spacetime.

While this general viewpoint is common to all quantum cosmologies, LQC has two key features that distinguish it from the older Wheeler–DeWitt (WDW) theory, often called quantum geometrodynamics. First, as explained below, the mathematical framework of LQC descends from the well-developed kinematics of LQG, using a symmetry reduction tailored to homogeneity and isotropy. In the WDW theory one is yet to develop rigorous kinematics for full quantum geometrodynamics; because issues related to the presence of an infinite number of degrees of freedom are generally ignored, the underlying mathematical framework has remained formal. In quantum cosmology, then, one introduces structures like the WDW equation without guidance from a more complete framework. This leads to the second key difference. The LQC quantum Einstein's equation is qualitatively different from the WDW equation, in that it mirrors features of the *quantum* Riemannian geometry of full LQG. As a direct result, strong cosmological singularities–and in particular the big bang–are naturally resolved in LQG (Singh, 2009; Ashtekar and Singh, 2011; Agullo and Singh, 2017).

We will now explain these differences in some detail. As is common in quantum field theories, in full LQG one begins with the Heisenberg algebra $\mathcal{A}$ of basic ('canonically conjugate') observables, called the holonomy-flux algebra (Ashtekar and Isham, 1992; Ashtekar and Lewandowski, 2004; Giesel, 2017). We then have a highly non-trivial result that ensures that $\mathcal{A}$ admits a unique representation by operators of a Hilbert space $\mathcal{H}$ that respects the 'background independence' or 'diffeomorphism covariance' of the theory (Lewandowski et al., 2006; Fleischhack, 2009). This representation underlies the rigorous kinematical framework of LQG. In particular, one finds that geometrical observables are well-defined self-adjoint operators with *discrete* eigenvalues. Of particular interest is the *area gap*–the first non-zero eigenvalue Δ of the area operator. It is a fundamental microscopic parameter of the theory that then governs important macroscopic phenomena in LQC that lead, e.g., to finite upper bounds for curvature.[1] In LQC, one first reduces the holonomy-flux algebra $\mathcal{A}$ used in full LQG to a smaller symmetry reduced algebra $\mathcal{A}_{\rm red}$. Again there is a uniqueness theorem that guarantees that $\mathcal{A}_{\rm red}$ admits a unique representation on a Hilbert space $\mathcal{H}_{\rm LQC}$ that respects the action of the (residual) diffeomorphism group on $\mathcal{A}_{\rm red}$ (Ashtekar and Campiglia, 2012; Engle et al., 2017). This representation is *qualitatively different* (i.e. unitarily inequivalent) from the Schrödinger representation used in the WDW theory. In particular, the *differential* operator representing the gravitational part in the WDW equation is not even defined on $\mathcal{H}_{\rm LQC}$; it is naturally replaced by a certain *difference* operator that explicitly involves the area gap Δ (Ashtekar et al., 2006a; Ashtekar et al., 2006b; Ashtekar and Singh, 2011). One can now start with a quantum state $\Psi(a, \phi)$ that is peaked on the classical dynamical trajectory at a suitably late time when curvature is low, and evolve it *back in time* toward the big bang using either the WDW equation or the LQC evolution equation. Interestingly the wave function

[1]This is because the curvature operator is defined by considering 'Aharanov-Bohm fluxes' across small surfaces S and then shrinking the surface till it has the minimum area Δ.

continues to remain sharply peaked in both cases. In the WDW theory it follows the classical trajectory all the way into the singularity, while in LQC it ceases to follow the classical trajectory once the curvature is about $\sim 10^{-4}$ times the Planck curvature. Then the quantum geometry corrections dominate and the wave function $\Psi(\phi, a)$ bounces when the curvature and matter density attain their upper bounds. In this *backward evolution*, curvature starts decreasing after the bounce and the Universe expands. Once the curvature falls below $\sim 10^{-4}$ times the Planck curvature, the wave function again follows a classical trajectory which is now expanding in the past direction [For details, see Ashtekar et al. (2006b), Ashtekar et al. (2008), Ashtekar and Singh (2011), Agullo and Singh (2017)].

Thus, key differences between LQC and the WDW theory arise from the fact that the WDW theory has no knowledge of the quantum nature of Riemannian geometry that LQC inherits from LQG. Indeed, there is a precise sense in which the LQC evolution equation reduces to the WDW differential equation in the limit in which the area gap goes to zero (Ashtekar et al., 2008). The upper bound of curvature in LQC is given by $\mathrm{curv}_{\mathrm{max}} = [3(24\pi^2)/(2\Delta^3)]\,\ell_{\mathrm{Pl}}^4 \simeq 62\ell_{\mathrm{Pl}}^{-2}$, where, in the last step, we have used the numerical value $\tilde{\Delta} \simeq 5.17\ell_{\mathrm{Pl}}^2$ of the area gap. In any LQC solution $\Psi_{\mathrm{lqc}}(a, \phi)$, the curvature attains its maximum value at the bounce and this value is extremely well approximated by $\mathrm{curv}_{\mathrm{max}}$ if the state is sharply peaked. Note that the upper bound diverges as $\Delta \to 0$, in line with the finding that curvature grows unboundedly as one evolves the WDW state $\Psi_{\mathrm{wdw}}(a, \phi)$ to the past. By contrast, in LQC, while the quantum geometry effects are negligible away from the Planck regime, they become dominant in the Planck regime, creating an effective repulsive force of quantum origin that causes the Universe to bounce.

It is interesting that this force rises and falls extremely rapidly, making the agreement with GR excellent outside the Planck regime. However, it has a very non-trivial global effect, in that physics does not stop at the big bang as in GR. Rather, there is an expanding FLRW Universe to the future of the bounce and a contracting FLRW Universe to the past, joined by a 'quantum bridge'. These qualitatively new features arise without having to introduce matter that violates any of the standard energy conditions, and without having to introduce new boundary conditions, such as the Hartle-Hawking 'no-boundary proposal'; they are consequences just of the quantum corrected Einstein's equations. Thus, the existence of the bounce and the upper bound on curvature and matter density can be directly traced back to quintessential features of quantum geometry. These considerations have been extended beyond the spatially flat FLRW models to include spatial curvature, non-zero cosmological constant, anisotropies [see, e.g. Ashtekar and Singh (2011), Agullo and Singh (2017), and references therein] as well as the simplest inhomogeneities captured by the Gowdy models in GR, and also to the Brans-Dicke theory [see, e.g. Zhang et al. (2013), Elizaga Navascués et al. (2015)]. Taken together, these results bring out the robustness of the LQC bounce.

Since the area gap plays an important role in the LQC dynamics, before concluding this subsection, we will make a small detour to explain how its numerical value $\tilde{\Delta} \simeq 5.17\ell_{\mathrm{Pl}}^2$ is arrived at. Recall, first, that in QCD there is a quantization ambiguity–parametrized by an angle θ–because of the freedom in adding a topological term to the action. One encounters a similar quantization ambiguity in LQG (again associated with the freedom to add a term to the action that does not affect equations of motion), encoded in the so-called Barbero–Immirzi parameter, $\gamma > 0$, which trickles down to the expressions of observables on $\mathcal{H}$, such as the area operator $\widehat{A}_S$. The eigenvalues of $\widehat{A}_S$ are discrete in all γ-sectors. But their numerical values are proportional to γ and vary from one γ sector to another. Observables also have a θ dependence in QCD and the value of θ that Nature has selected is determined experimentally. In LQG, a direct measurement of eigenvalues of geometric operators would determine γ. But of course such a measurement is far beyond the current technological limits. However one can use thought experiments. Specifically, in LQG the number of microstates of a black hole horizon grows exponentially with the area, whence one knows that the entropy is proportional to the horizon area (Ashtekar et al., 1998; Ashtekar et al., 2000). But the proportionality factor depends on the value of γ. Therefore if one requires that the leading term in the statistical mechanical entropy of a spherical black hole should be given by the Bekenstein–Hawking formula $S = A/4\ell_{\mathrm{Pl}}^2$, one determines γ and thus the LQG sector Nature prefers. In this sector the explicit value of the area gap yields $\mathring{\Delta} \simeq 5.17\ell_{\mathrm{Pl}}^2$ (Domagala and Lewandowski, 2004; Meissner, 2004; Barbero and Perez, 2017; Perez, 2017) (and the leading term in the entropy of more general black holes–not necessarily spherical–agrees with the Bekenstein–Hawking formula). This is the value used in LQC calculations.[2]

This concludes our broad-brush overview of how quantum geometry considerations lead to a natural resolution of the big bang singularity in LQC. The resolution has been analyzed in detail in a large number of LQC papers, using Hamiltonian, cosmological-spinfoam and 'consistent histories' frameworks [see, e.g. Ashtekar et al. (2006b), Ashtekar et al. (2009a), Ashtekar et al. (2010), Ashtekar and Singh (2011), Craig and Singh (2013), Agullo and Singh (2017)].

Remark: Recently some concerns have been expressed about the simplicity of the LQC description of the early Universe, and on whether "general physics principles of effective field theory and covariance" have been appropriately incorporated (Bojowald, 2020). Many of the specific technical points were already addressed, e.g., in Ashtekar and Singh (2011), Corichi and Singh (2008), Kaminski and Pawlowski (2010) and in the Appendix of Ashtekar (2009). In addition, we would like to clarify possible confusion on the following points. First, although 'effective equations' are often used in LQC, conceptually they are on a very different footing from those used in effective field theories: One does not integrate out the UV

[2]There are two closely related but technically different ways of characterizing the quantum states of an isolated horizon representing a black hole in equilibrium (Barbero and Perez, 2017). They lead to slightly different values of the Barbero–Immirzi parameter (0.237 and 0.274) and hence of the area gap ($5.17\ell_{\mathrm{Pl}}^2$ and $5.98\ell_{\mathrm{Pl}}^2$). Because the values are very close, our results are not sensitive to these differences. See **Section 4.3**.

modes of cosmological perturbations. The term 'effective' is used in a different sense in LQC: these equations carry some of the leading-order information contained in sharply peaked quantum FLRW geometries $\Psi(a,\phi)$. As we will see in **Section 3.2**, equations satisfied by the cosmological perturbations are indeed covariant. On the issue of simplicity of the LQC description, we note that in the 1980s it was often assumed that the early Universe is irregular at all scales and therefore quite far from being as simple as is currently assumed at the onset of inflation. Yet now observations support the premise that the early Universe is exceedingly simple in that it is well modeled by a FLRW spacetime with first order cosmological perturbations (Chowdhury et al., 2019). Therefore, although a priori one can envisage very complicated quantum geometries, it is far from being clear that they are in fact realized in the Planck regime. Nonetheless, one should keep in mind that, as in other approaches to quantum cosmology, in LQC the starting point is the symmetry reduced, cosmological sector of GR. Difference from the Wheeler-DeWitt theory is that one follows the same systematic procedure in this sector as one does in full LQG. But the much more difficult and fundamental issue of systematically *deriving* LQC from full LQG is still open mainly because dynamics of full LQG itself is still a subject of active investigation. See, e.g., Assanioussi et al. (2018), Olmedo and Alesci (2019) as illustrations of the current status.

3.2 Cosmological Perturbations in the Pre-inflationary Era of LQC

In inflationary paradigms the Mukhanov–Sasaki scalar modes[3] of cosmological perturbations are represented by quantum fields $\widehat{\mathcal{Q}}$ that propagate on a background FLRW metric g_{ab}. The use of a classical background geometry is justified since, as explained above, spacetime curvature is twelve orders of magnitude below the Planck scale even at the onset of inflation. However, to extend the paradigm all the way to the LQC bounce, one has to replace the metric g_{ab} of GR with an LQC wave function $\Psi(a,\phi)$ because assumptions underlying quantum field theory (QFT) on curved spacetimes fail in the Planck regime. At first the task seems daunting: How do you evolve quantum fields when you have only a probability distribution $\Psi(a,\phi)$ for various spacetime geometries rather than a single metric g_{ab}? Fortunately, there is an unexpected simplification (Ashtekar et al., 2009b; Agullo et al., 2012; Agullo et al., 2013b): So long as $\Psi(a,\phi)$ is sharply peaked, and the back reaction of the perturbations $\widehat{\mathcal{Q}}$ on the background quantum geometry Ψ remains negligible, dynamics of quantum fields $\widehat{\mathcal{Q}}$ on Ψ is extremely well-approximated by that of quantum fields $\widehat{\mathcal{Q}}$ propagating on a smooth, quantum corrected FLRW metric $\tilde{g}_{ab}$ which is *constructed in a precise manner* from Ψ. As one would expect, coefficients of $\tilde{g}_{ab}$ depend on $\hbar$. In the literature, $\tilde{g}_{ab}$ is often called the *dressed metric*. It is 'dressed' by certain quantum fluctuations in $\Psi(a,\phi)$ specified below; it carries the information in the quantum geometry $\Psi(a,\phi)$ that the propagation of cosmological perturbations is sensitive to.

The construction of the dressed metric $\tilde{g}_{ab}$ can be summarized as follows. Recall first that in the standard inflationary scenario, the Mukhanov-Sasaki quantum field $\widehat{\mathcal{Q}}$ satisfies a wave equation $(\Box + \mathcal{U}/a^2)\widehat{\mathcal{Q}} = 0$ where $\Box$ is the d'Alembertian w.r.t. to the background FLRW metric g_{ab} (satisfying the unperturbed, zeroth order Einstein's equations) and $\mathcal{U}$ is constructed from the inflationary potential and the background FLRW solution [see, e.g. Agullo et al. (2013b)]. At the classical level, this evolution equation can be derived starting with the full Hamiltonian constraint of GR coupled with the scalar field, and then appropriately truncating it to second order in perturbations (Agullo et al., 2013a). In LQC, the background quantum geometry $\Psi(a,\phi)$ satisfies the zeroth-order LQC Hamiltonian constraint. The scalar mode $\widehat{\mathcal{Q}}$ propagates on this $\Psi(a,\phi)$ and its dynamics is governed by the appropriate second order truncation of the full Hamiltonian constraint. If the state $\Psi(a,\phi)$ is sharply peaked and the back reaction of the perturbation $\widehat{\mathcal{Q}}$ is negligible, then one has the following result (Ashtekar et al., 2009b): Propagation of $\widehat{\mathcal{Q}}$ on the quantum geometry $\Psi(a,\phi)$ is very well approximated by that of a quantum field $\widehat{\mathcal{Q}}$ satisfying $(\tilde{\Box} + \tilde{\mathcal{U}}/\tilde{a}^2)\,\widehat{\mathcal{Q}} = 0$. Here $\tilde{\Box}$ is the d'Alembertian with respect to the dressed metric

$$\tilde{g}_{ab}\mathrm{d}x^a\mathrm{d}x^b \equiv \mathrm{d}\tilde{s}^2 = \tilde{a}^2\Big(-\mathrm{d}\tilde{\eta}^2 + \mathrm{d}\vec{x}^{\,2}\Big) \tag{3.1}$$

with

$$\frac{\tilde{a}^4 = \langle \widehat{H}^{-\frac{1}{2}}\widehat{a}^4(\phi)\,\widehat{H}^{-\frac{1}{2}}\rangle}{\langle \widehat{H}^{-1}\rangle \text{ and } \mathrm{d}\tilde{\eta} = \langle \widehat{H}^{-1/2}\rangle\left(\langle \widehat{H}^{-1/2}\,\widehat{a}^4(\phi)\,\widehat{H}^{-1/2}\rangle\right)^{1/2}\mathrm{d}\phi} \tag{3.2}$$

and $\tilde{\mathcal{U}}(\phi)$ is the dressed effective potential

$$\frac{\tilde{\mathcal{U}}(\phi) = \langle \widehat{H}^{-\frac{1}{2}}\widehat{a}^2(\phi)\widehat{\mathcal{U}}(\phi)\widehat{a}^2(\phi)\,\widehat{H}^{-\frac{1}{2}}\rangle}{\langle \widehat{H}^{-\frac{1}{2}}\widehat{a}^4(\phi)\,\widehat{H}^{-\frac{1}{2}}\rangle\ .} \tag{3.3}$$

All operators and their expectation values refer to the Hilbert space of the background FLRW quantum geometry: the expectation values are taken in the state Ψ, $\widehat{H}$ is the 'free' Hamiltonian in absence of the inflaton potential, and $\widehat{a}(\phi)$ is the (Heisenberg) scale factor operator (Ashtekar et al., 2009b; Agullo et al., 2013b).

At first, the result seems surprising. But physically it can be understood using a simple analogy with propagation of light in a medium such as water. In the full quantum description, individual photons interact with the molecules of the material. However, the key features of propagation can be extracted simply by computing a few macroscopic parameters such as the refractive index and birefringence that can be extracted from the microstructure of the material. Other details of the quantum state of the medium are not important to study propagation. In this analogy, the cosmological perturbation plays the role of light and quantum geometry, the role of the medium. To determine the propagation of $\widehat{\mathcal{Q}}$, one needs to extract only $\tilde{a}$, $\tilde{\eta}$ and $\tilde{\mathcal{U}}$ from the

[3]In the pre-inflationary epoch, the curvature perturbation $\widehat{\mathcal{R}}$ for scalar modes become ill-defined at the turn-around point where $\dot{\phi} = 0$. Therefore, in the LQC literature, one uses the Mukhanov-Sasaki gauge invariant scalar perturbation $\widehat{Q}$ in the pre-inflationary dynamics and converts the result to $\widehat{\mathcal{R}}$ at the end of inflation.

quantum state $\Psi(a,\phi)$. The rest of the very rich information of quantum geometry it contains is not directly relevant (Incidentally, the tensor modes satisfy the wave equation for the *same* dressed metric $\tilde{g}_{ab}$; as in standard inflation, there is no dependence on the potential.)

It is clear from the form of **Eqs 3.2**, **3.3** that the expressions of the dressed metric and the dressed potential could not have been guessed a priori. They resulted from explicit, detailed calculations (Ashtekar et al., 2009b; Agullo et al., 2013b). The observable predictions reported in **Section 4** are obtained by first calculating the dressed metric and the dressed potential starting from the given quantum geometry $\Psi(a,\phi)$ and then evolving the scalar mode using $(\tilde{\Box} + \tilde{\mathcal{U}}/\tilde{a}^2)\,\widehat{\mathcal{Q}} = 0$.

Remarks

1. For clarity, let us spell out the conceptual elements of the procedure used to extract dynamics of cosmological perturbations since there is occasional confusion on this point. The starting point in LQC is the Hamiltonian formulation of GR coupled to the inflaton (albeit in the connection variables used in LQG). One then extracts the sector of full GR that corresponds to the homogeneous isotropic fields (which serve as the background) *together with* first order perturbations. It is this classical theory that is then quantized using LQG techniques (Agullo et al., 2013a). Dynamics of quantum perturbations are governed by the Hamiltonian constraint operator of the truncated sector, where both the background geometry and perturbations are treated quantum mechanically. One does not simply assume that perturbations satisfy linearized equations of GR on a bouncing classical metric. That the dynamics of perturbations is well approximated by quantum field satisfying an evolution equation involving $\tilde{g}_{ab}$ and $\tilde{\mathcal{U}}$ *is a result* that holds under conditions spelled out above. Note also that the equation is covariant w.r.t. $\tilde{g}_{ab}$ and $\tilde{g}_{ab}$ rapidly tends to the classical FLRW metric of GR outside the Planck regime.

2. Initially, analysis of Ashtekar et al. (2009b) suggested that the propagation of $\widehat{\mathcal{Q}}$ on the quantum geometry $\Psi(a,\phi)$ would be exactly the same as that on the corresponding dressed metric **3.1** and potential (**3.3**) for *any* $\Psi(a,\phi)$. However, Kaminski later found (Kamiński, 2012) that there is a subtle infrared problem (that can be missed in numerical simulations since they have to use an infrared cutoff). Kamiński et al. (2020) then showed that, as a result, the implications of Ashtekar et al. (2009b) are not as general; the result would not hold without restrictions on the background quantum geometry $\Psi(a,\phi)$. This situation is qualitatively similar to that, e.g., in quantum electrodynamics which also faces infrared issues in rigorous treatments. However, in QED the ensuing difficulties can be avoided by focusing just on those quantities that are 'infrared safe'. One can adopt a similar strategy in LQC by introducing suitable infrared safe observables through regularization. Furthermore, for states $\Psi(a,\phi)$ that are sufficiently sharply peaked, the regularization ambiguity is completely negligible. Previous calculations of power spectra in LQC [e.g. Agullo et al. (2012), Agullo et al. (2013b), Agullo and Morris (2015), Agullo (2015), Sreenath et al. (2019), Agullo et al. (2021b)], as well as the current investigation, use states that are sufficiently sharply peaked in this sense, whence the use of dressed metric is justified in spite of the infrared difficulties.

3.3 Primordial Spectrum: Why Pre-inflationary Dynamics Matters

A natural question now is whether the pre-inflationary phase of LQC dynamics described in the last two subsections has any observable consequences. Let us therefore focus on the observable modes $\widehat{\mathcal{Q}}_k$. These have co-moving wavenumbers k in the range $\sim (0.1k_\star, 300k_\star)$, where $k_\star = 0.002\mathrm{Mpc}^{-1}$ is the WMAP pivot scale. The evolution equation for these modes implies that, they 'experience' curvature in the background metric $\tilde{g}_{ab}$ only if their *physical* wavelength $\lambda(t) = a(t)/k$ is comparable or larger than the radius of curvature $r_{\mathrm{curv}}(t) = (6/R)^{\frac{1}{2}}$ of $\tilde{g}_{ab}$ corresponding to the scalar curvature R at that time. Let us denote by $t = t_\star$ the time at which the relevant slow roll phase starts; this is our onset of inflation. Therefore, a few e-folds before and after $t_\star$, the observable modes propagate as though they are in flat spacetime and therefore do not get excited by the background geometry. What happens in the distant past? The left panel of **Figure 3** shows the evolution of r_{curv} (blue solid curve) and of λ of observable modes (the gray shaded band), both in GR. Note that in the pre-inflationary epoch r_{curv} is far from being constant whence the spacetime metric is very different from the de Sitter metric. Since the scalar curvature R diverges at the big bang, r_{curv} goes to zero. Because the scale factor a of the classical FLRW metric goes to zero, physical wavelengths λ also goes to zero at the big bang. However, they do not go to zero as fast as r_{curv}. Therefore, as one approaches the big bang in the past evolution, *all* observable modes exit the curvature radius, 'experience' curvature at sufficiently early times and get excited. These excitations have to be delicately fine-tuned for the state to be in the BD vacuum later on, at $t = t_\star$ i.e. at the onset of inflation. Put differently, the Heisenberg state representing the BD vacuum at the onset of inflation is an unnatural choice from the perspective of the Planck regime because it carries certain delicately choreographed excitations there. Of course, one can argue that the quantum field theory in curved spacetime cannot be extrapolated to the Planck regime. But by itself this argument does not provide a justification for using the BD state at $t = t_\star$ either.

In LQC, the situation is quite different. Because the scalar curvature $\tilde{R}$ of the dressed metric $\tilde{g}$ has a finite upper bound $\tilde{R}_{\mathrm{max}} \simeq 62\ell_{\mathrm{Pl}}^{-2}$, reached at the bounce, r_{curv} reaches its minimum value $r_{\mathrm{curv}}^{\mathrm{min}} \simeq 0.31\ell_{\mathrm{Pl}}$, whence it is only those modes which satisfy $\lambda \gtrsim r_{\mathrm{curv}}^{\mathrm{min}}$ at the bounce that experience curvature in their evolution from the bounce to the onset of inflation. In our approach (as discussed below) the background quantum geometry $\Psi(a,\phi)$ is such that only the longest wavelength observable modes satisfy this inequality. This feature is shown in the right panel of **Figure 3**. Therefore, all but the longest wavelength observable modes propagate from the bounce-time to the onset of inflation as though they are in flat spacetime and hence it is natural that they be in the BD vacuum at $t = t_\star$. It is only the longest wavelength modes that will be excited and hence not in the

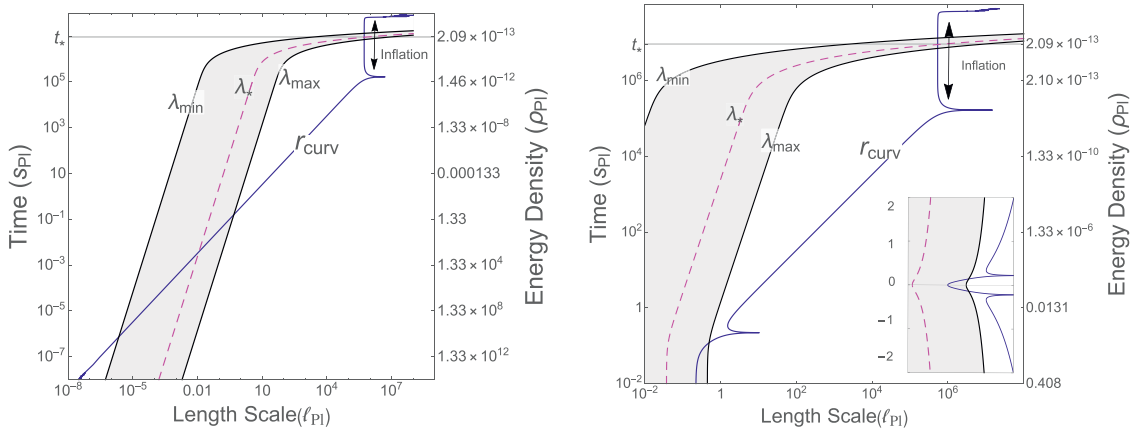

FIGURE 3 | Time dependence of the *physical* wavelengths $\lambda = a/k$ of modes and radius of curvature r_{curv} in the pre-inflationary era, using Starobinsky potential. The left vertical axis shows cosmic time t (in Planck seconds) and right vertical axis shows the energy density (also in Planck units). The shaded bands represent the wavelengths of observable modes and the dashed line denotes the WMAP pivot mode with $\lambda_\star = a(t)/k_\star$. The solid (blue) lines represent the evolution of r_{curv}. ***Left panel:*** *General Relativity.* In the Planck regime near singularity ($t = 0$), *all* observable modes exit the curvature radius and are thus excited. ***Right panel:*** *LQC.* Only the longest wavelength modes in the observable band get excited and fail to be in the BD vacuum at $t = t_\star$. The inset shows dynamics near the bounce. Plots of the quadratic potential are very similar.

BD vacuum. But won't these excitations get just washed away during inflation? The answer is in the negative: because of spontaneous emission, the number density of these excitations remains constant (Agullo and Parker, 2011a; Agullo and Parker, 2011b; Ganc and Komatsu, 2012). As a result, as we will see in **Section 4**, the primordial spectrum does differ from that based on the *SA*, but only at largest angular scales.

Note that there is a deep interplay between the UV and IR in LQC. As we saw in **Section 2.1**, in LQC it is the UV modifications of GR in the Planck regime that tame the big bang singularity and make all physical quantities finite. As a result we have a finite $\tilde{R}_{max}$ and a non-zero $\tilde{r}^{min}_{curv}$. It is then natural for all but the longest wavelength observable modes to be in the BD vacuum at the onset of inflation. While the LQC corrections to the background geometry are significant in the UV, their effect on cosmological perturbations is non-negligible only in the IR. This is the point that was highlighted in the abstract and **Section 1**.

Finally, to obtain specific predictions, one needs a quantum state of geometry $\Psi(a, \phi)$ and a quantum state $\psi(\mathcal{Q}, \phi)$ of scalar modes. At this point, different approaches within LQC make different choices [see, e.g. Agullo et al. (2013b), Fernandez-Mendez et al. (2012), Barrau et al. (2014), Ashtekar and Barrau (2015), Agullo and Morris (2015), Agullo (2015), Gomar et al. (2017), Agullo et al. (2018), Barrau et al. (2018), Agullo et al. (2020a), Agullo et al. (2020b), Sreenath et al. (2019), Agullo et al. (2021a), Agullo et al. (2021b)]. In this paper, we use the procedure introduced in Ashtekar and Gupt (2017a), Ashtekar and Gupt (2017b). Strategy is to select these states by introducing some trial principles that relate properties of quantum geometry in the Planck regime with the late time geometry (which can be taken to be that given by general relativity to an excellent degree of approximation). One can then work out the observable consequences. If any prediction is ruled out by observations, one would return to the drawing board and seek alternate principles that would lead to viable states. If predictions are confirmed by observations, one would build confidence in the general direction and attempt to put the principles on a firmer and more satisfactory footing. The currently used principles are somewhat analogous to the Bohr model of the hydrogen atom in the early days of quantum mechanics. While in retrospect it is naive in some fundamental respects, nonetheless the Bohr model was useful because it captured some essential features of the final, correct description of the hydrogen model.

The first principle constrains $\Psi(a, \phi)$, determining the number of e-folds between the LQC bounce and the CMB surface (i.e., the surface of last scattering) (Ashtekar and Gupt, 2017b). One begins with the observation that the presence of a positive cosmological constant implies that there are cosmological horizons. As a result, given an instant of time there is a maximum value for the radius of a ball that any one observer can see, no matter how long she waits. In the standard ΛCDM model, this radius is ~ 17.29 Mpc at the surface of last scattering. Thus, specification of initial data in this ball determines the entire future of the Universe that is accessible to an 'eternal' observer. As we go to the past, this ball shrinks and, interestingly, at the onset of inflation its physical radius is only $\sim 2.64 \times 10^7 \ell_{Pl}$ for both, the Starobinsky and quadratic potentials. This value is already smaller than the radius of a proton! At the bounce surface of LQC, its radius would be still smaller. From the LQG perspective, it is natural to require that the physical radius of the ball be 6Δ, the minimum value allowed in the spatially flat FLRW quantum geometry. This requirement constrains $\Psi(a, \phi)$ such that the number N_{B-CMB} of e-folds from the bounce to the surface of last scattering to be $\simeq 134$, or the number of e-folds from the bounce to today to be $\simeq 141$.

Finally, the principle that determines the quantum state $\psi(\mathcal{Q}, \phi)$ of scalar modes (Ashtekar and Gupt, 2017b) involves

a quantum generalization of Penrose's Weyl curvature hypothesis (Penrose, 2004) in the Planck regime near the bounce, which physically corresponds to requiring that the state should be 'as isotropic and homogeneous in the Planck regime, as the Heisenberg uncertainty principle allows'.[4] While the first principle sets the scale at which the LQC primordial spectrum ceases to be nearly scale invariant, and thus differs from that given by the *SA*, the second led to the conclusion that there is power suppression with respect to the *SA* rather than power enhancement. Detailed calculations are needed to obtain the precise degree of suppression.

4 RESULTS

In this section we present the main results of this paper, obtained using the LQC summarized in **Section 3**. In terms of more commonly used wavenumbers, the new length scale $r_{\rm cuv}^{\rm min} \sim 0.31\ell_{\rm Pl}$ introduced by LQC provides a new physical scale $k_{\rm LQC} \simeq 3.21\ell_{\rm Pl}^{-1}$, and the primordial spectrum differs from the *SA* for $k_{\rm phy} \lesssim k_{\rm LQC}$ at the bounce. In **Section 4.1** we first discuss these LQC corrections and then their effect on the observed C_ℓ^{XY} correlations (where XY refers to TT, TE, EE and $\phi\phi$). We also present predictions for the value of the optical depth τ and for the BB power spectrum that could potentially be tested using future observations. In **Section 4.2**, we show that the LQC predictions for theC_ℓ^{XY}'s lead to resolution of power suppression and lensing amplitude anomalies. In **Section 4.3**, we will show that the interplay between LQC and observations is a 2-way bridge, in that the CMB observations can also be used to constrain the value of the area gap Δ, the most important of fundamental microscopic parameters of LQG.

4.1 Power Spectra

As we saw at the end of **Section 3**, the physical principle used to select the background quantum geometry implies that the corresponding ΛCDM Universe has undergone approximately 141 e-folds of expansion since the quantum bounce until today (Ashtekar and Gupt, 2017b). Therefore, the characteristic physical scale $k_{\rm LQC}$ at the LQC bounce translates to the co-moving wavenumber $k_o \simeq 3.6 \times 10^{-4}$ Mpc^{-1} which sets the scale below which LQC corrections to the primordial scalar power spectrum become important. In particular, the calculations show that for scales $k \lesssim 10k_o$ the power is suppressed whereas for scales $k \gg k_o$ the power spectrum is essentially scale invariant as in the *SA*.[5] This behavior is captured in following modification to the *SA* for the primordial power spectrum:

$$\mathcal{P}_{\mathcal{R}}^{\rm LQC}(k) = f(k)\, A_s \left(\frac{k}{k_\star}\right)^{n_s - 1} = f(k)\, \mathcal{P}_{\mathcal{R}}^{\rm SA}(k)\,, \qquad (4.1)$$

where $f(k)$ is the correction factor (which is equivalent to the ratio of the power spectra in LQC to that in the *SA*).

The left panel of **Figure 4** shows the correction factor $f(k)$ plotted with respect to the co-moving wavenumber. It is evident from the plot that for both the Starobinsky and quadratic potentials, relative to the prediction of the *SA*, there is power suppression for long wavelength modes corresponding to $k \lesssim 10k_o$. The origin of this difference lies in the fact that, during the pre-inflationary era, the physical wavelength of these modes is sufficiently large to 'experience' the background curvature in the Planck regime near the bounce, leading to excitations over the standard Bunch–Davies (BD) state at the onset of inflation. On the other hand, the physical wavelengths of modes with $k \gg k_o$ are much smaller than the curvature radius throughout the pre-inflationary phase, including the deep Planck regime near the bounce. Therefore their state is practically the same as the standard BD state at the onset of inflation. Note that even for modes with $k \lesssim 10k_o$, LQC corrections are significant only near the bounce. During this epoch the energy density of the scalar field is dominated by the kinetic term. Therefore one would expect the inflationary potentials to have negligible effect on the evolution of the background geometry and perturbations in the deep Planck regime, which is when the LQC corrections are imprinted on the modes of scalar perturbations. This expectation is explicitly borne out in the left panel in **Figure 4**: the primordial spectra for Starobinsky and quadratic potentials are essentially identical. Analytical considerations of (Bhardwaj et al., 2019) suggest that this feature will persist for a large class of inflationary potentials. Finally, note that the LQC primordial spectrum has a turnaround at very large wavelengths whose origin is related to the sudden spike in $r_{\rm curv}$ near the bounce. Although these modes are not in the observable range for CMB, it is of interest to better understand the origin of this growth in power for very small k because, together with large and strongly scale dependent non-Gaussianity (which is expected from the LQC bounce (Agullo et al., 2018; Sreenath et al., 2019) it could lead to a coupling between the long wavelength modes and the modes observable in CMB, resulting in a modulation of the primordial power spectrum of the observable modes. Such a non-Gaussian modulation could explain the dipolar modulation of CMB and preference for odd parity that has been observed in the CMB (Agullo et al., 2021a; Agullo et al., 2021b).

Let us now turn to the LQC predictions for *observable* power spectra. For definiteness, in these plots we work with the Starobinsky potential for the *SA* and LQC theoretical predictions. On the observational side, 'PLANCK 2018' refers to the TT + TE + EE + lowE + lensing 2018 data released by the PLANCK collaboration. In order to obtain constraints on the parameters in LQC and SA models, we used the publicly available software package COSMOMC (Lewis and Bridle, 2002) which supports the likelihood code used in the original 2018 PLANCK analyses. COSMOMC is based on the Markov-Chain-Monte-Carlo (MCMC) procedure for estimation of parameters based on maximum likelihood analysis. For a given theoretical model with

[4]This condition provides a small ball in the space of all quasi-free states and the desired state $\psi(\mathcal{Q}, \phi)$ is the one in this ball that is 'maximally classical' at the end of inflation in a specific, well-defined sense (Ashtekar and Gupt, 2017).

[5]The value of k_o is linear in $k_{\rm LQC}$ and $10k_o \simeq 3.6 \times 10^{-3}$Mpc^{-1} corresponds to $\ell \simeq 30$. Hence if one were to increase (or decrease) $k_{\rm LQC}$ by hand, the LQC effects would manifest themselves in observations at larger (respectively, smaller) values of ℓ.

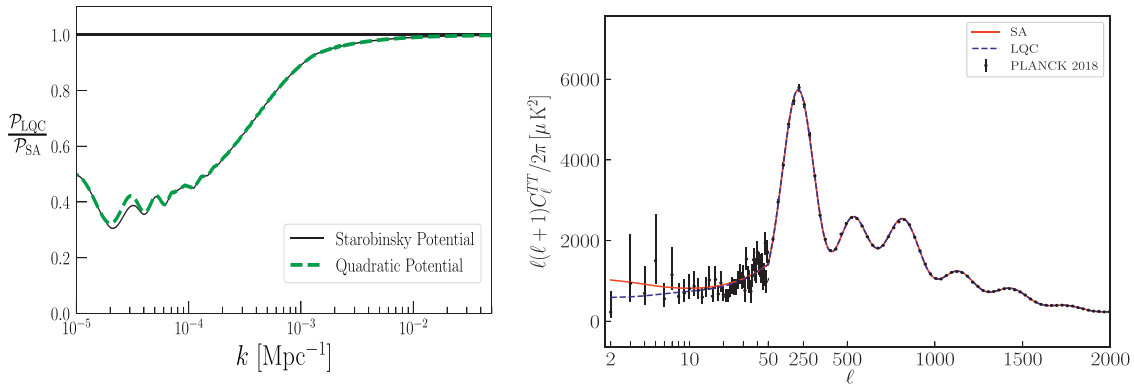

FIGURE 4 | *Left Panel:* *The primordial power spectrum of LQC*: The LQC suppression factor $f(k)$ is less than 1 for $k \lesssim 10k_\circ \simeq 3.6 \times 10^{-3}$ Mpc^{-1} for both the Starobinsky and quadratic potentials. At short wavelengths (large k), or small angular scales, the LQC power spectrum is indistinguishable from the SA i.e. $f(k) = 1$ for $k \gg k_\circ$. ***Right Panel:*** *TT power spectra.* The 2018 PLANCK spectrum (black dots with error bars), the LQC (dashed (blue) line) and the standard ansatz (SA) predictions (solid (red) line). As is usual, on the x-axis we have used a logarithmic scale for $\ell \leq 50$ and linear scale for $\ell > 50$.

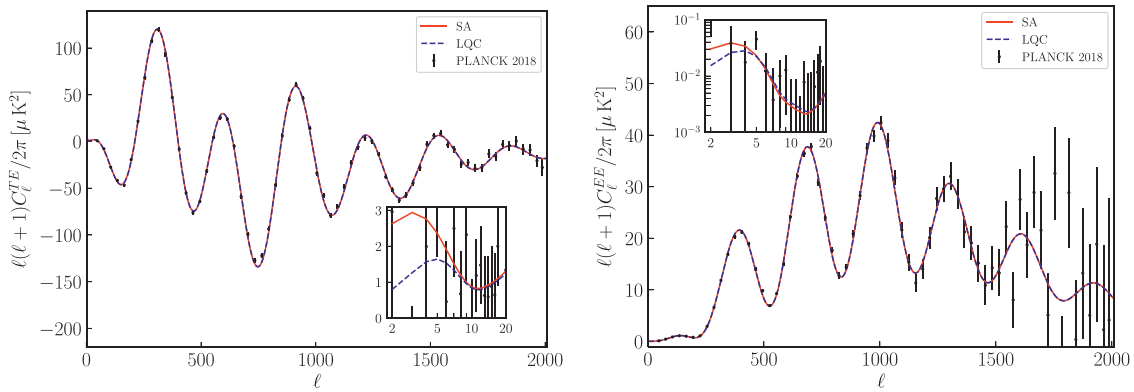

FIGURE 5 | *TE and EE power spectra.* The 2018 PLANCK spectrum (black dots with error bars), the LQC (dashed (blue) line) and the standard ansatz (SA) predictions (solid (red) line). Values of the 6 ΛCDM parameters are fixed to their best fit values shown in **Table 1**.

a number of parameters (here the ΛCDM model with 6 parameters), one builds a Markov chain from randomly sampled parameter values from a space predefined by priors. Each Markov chain begins with a random sample from the prior-constrained parameter space. Subsequent steps in the chain are then selected via Metropolis-Hasting algorithm: a Monte Carlo sample from the parameter space is proposed and then accepted or rejected based on the likelihood function which quantifies the degree of agreement between the theoretical prediction and the experimental data [in this paper we work with the same likelihood function as used in PLANCK 2018 papers (Aghanim et al., 2020b)]. This procedure is repeated until a convergence criteria is satisfied. The chain of accepted values are further trimmed and thinned in order to remove dependence on the initial data point and correlation between subsequent steps. The converged Markov chain thus obtained approximates the posterior distribution of the parameters to be estimated. In order to obtain one-dimensional constraints on (or two-dimensional correlation between) the individual parameters, marginalization procedure is used. For details of the MCMC techniques adapted to cosmological settings see (Lewis and Bridle, 2002).

TABLE 1 | Comparison between the Standard Ansatz (SA) and LQC. The mean values of marginalized probability distributions for the six cosmological parameters, and values of $S_{1/2}$ calculated using $C_\ell^{\rm TT}$.

Parameter	SA	LQC
$\Omega_b h^2$	0.02238±0.00014	0.02239±0.00015
$\Omega_c h^2$	0.1200±0.0012	0.1200±0.0012
$100\theta_{MC}$	1.04091±0.00031	1.04093±0.00031
τ	0.0542±0.0074	0.0595±0.0079
$\ln(10^{10}A_s)$	3.044±0.014	3.054±0.015
n_s	0.9651±0.0041	0.9643±0.0042
$S_{1/2}$	42,496.5	14,308.05
A_L	1.072±0.041	1.049±0.040

The right panel of **Figure 4** shows the theoretical predictions as well as the observed power spectrum, with its error bars. The

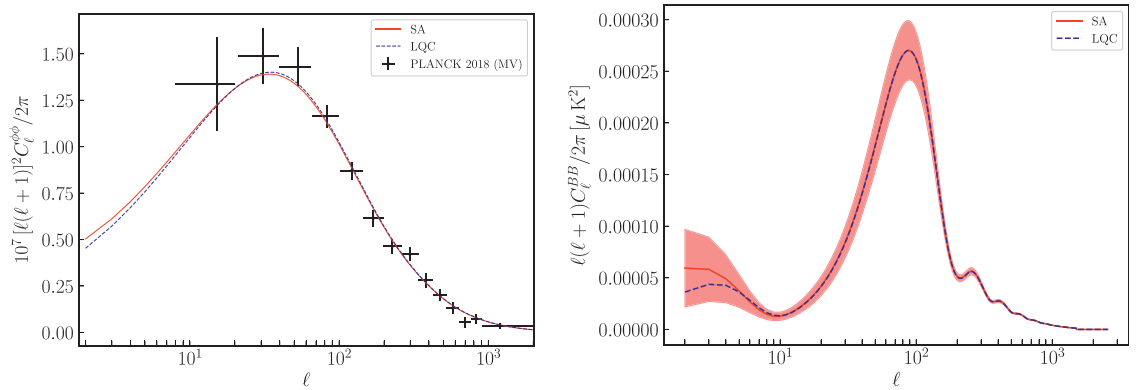

FIGURE 6 | LQC prediction (dashed (blue) line) and the standard ansatz (SA) prediction (solid (red) line). ***Left Panel:*** *Lensing power spectra.* The 2018 PLANCK spectrum (where the black crosses show binning and error bars). ***Right Panel:*** *The theoretical predictions for the BB power spectra.* There is power suppression in LQC for very low ℓ. The shaded region shows the 68% confidence level region.

plots clearly show that the primordial power suppression of LQC for small k leads to power suppression in the TT spectrum for multipoles $\ell < 30$, relative to the predictions from the *SA*. The same primordial power spectrum can also be used to compute the predicted TE and EE correlation spectra. **Figure 5** shows the TE (left panel) and EE (right panel) spectra as observed by Planck 2018, along with those obtained using the best fit ΛCDMmodels with LQC and the *SA*. Note that in the right panel of **Figure 4** and in **Figure 5** the LQC and the *SA* plots are shown for *their corresponding* marginalized mean values of the 6 parameters shown in **Table 1**. By contrast, in (Ashtekar and Gupt, 2017b) both the LQC and the *SA* curves were plotted for the same values of 6 parameters of the ΛCDM model, coming from the *SA*. As **Table 1** shows, the mean value of optical depth τ is > 9% higher in LQC than with the *SA* and electric polarization is quite sensitive to τ. Interestingly, this change in the best fit ΛCDM Universe has the effect of slightly reducing suppression in the passage from the primordial power spectrum to the observed one. As a result, the LQC power suppression in the TT, TE and EE spectra we now find is somewhat less pronounced than it was in Ashtekar and Gupt (2017b).

Finally, the left panel of **Figure 6** shows the lensing correlation spectrum $C_\ell^{\phi\phi}$ reported by the PLANCK collaboration with their 2018 data, along with the LQC and the *SA* predictions. For this figure we have again used the mean marginalized values of the 6 parameters shown in **Table 1**, and the lensing amplitude is fixed to $A_L = 1$, in accordance with the base ΛCDM model. As with the TT, TE and EE spectra, the lensing spectrum also shows suppression at large angular scales corresponding to $\ell < 30$. However, observations are quite sparse for low ℓ. Interestingly, for $30 < \ell < 100$, the LQC prediction for $C_\ell^{\phi\phi}$ is slightly larger than that for SA (This is in fact inevitable; see **Section 5**). This behavior leads the LQC spectrum to fit slightly better with the observed data in the range $30 < \ell < 100$ and hints toward resolving the lensing amplitude anomaly in LQC without having to introduce additional modifications to the standard ΛCDM model. In the next subsection we will see that this possibility is in fact realized.

We will conclude this discussion of observable implications of LQC with predictions for future missions. First, as we noted in **Section 2.2**, currently the optical depth τ is the least accurately measured of the 6 ΛCDM parameters, with a relative error of ~ 13%. The LQC value is some 9.8% higher than that in 'the Universe according to PLANCK'. This prediction will be tested by the future observation of global 21 cm evolution at high redshifts that is estimated to reach a percent level accuracy in the measurement of τ (Fialkov and Loeb, 2016). As for the observable power spectra, to date the PLANCK satellite has provided the best full sky measurement of the CMB anisotropies. However, there is still scope for improvement in the measurement of electric polarization, and the odd-parity magnetic polarization is yet to be detected. Therefore, several space-based mission have been planned to further improve the polarization measurements. In addition to the predictions for the TE and EE power spectra discussed above, our LQC model also makes predictions for the BB power spectrum. The right panel of **Figure 6** provides the prediction for the unlensed BB power spectrum both from the *SA* and in LQC. Recall that the tensor-to-scalar ratio r depends on the potential of the inflationary model. But, being a ratio, it is the same in LQC as from SA (Agullo et al., 2013b). We have set $r = 0.0041$, its value for the Starobinsky potential. As in the case of other four spectra, we observe a relative suppression of power at low multipoles. However, this is also where the reionization bump occurs. Since LQC predicts a larger value of optical depth, the B-B power suppression is lower than what one might have expected from the primordial power suppression (and using the same value of τ for both SA and LQC). Nonetheless, it may be possible to test this prediction against the data from the future B-mode missions such as LiteBIRD (Matsumura and et al., 2014), Cosmic Origins Explorer (Delabrouille and et al., 2018), ECHO[6] or Probe Inflation and Cosmic Origins (PICO) (Hanany et al., 2019) (which should observe the BB spectrum if $r \gtrsim 0.001$).

[6]http://cmb-bharat.in/

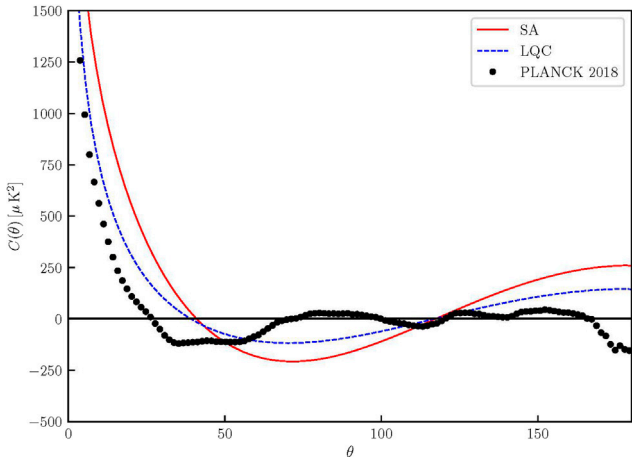

FIGURE 7 | *The temperature-temperature angular power spectrum* $C(\theta)$. The 2018 PLANCK spectrum (thick black dots), the LQC [dashed (blue) line], and the standard ansatz [solid (red) line] predictions. The LQC predictions are closer to the observed Planck 2018 data points.

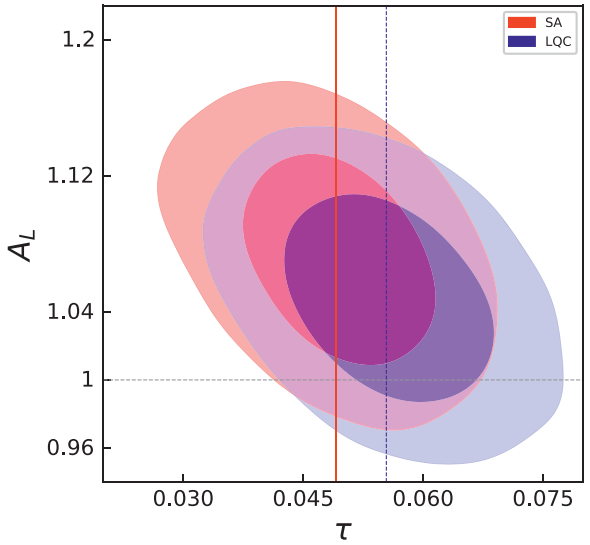

FIGURE 8 | 1σ *and* 2σ *probability distributions in the* $A_L - \tau$ *plane.* Predictions of the *SA* (in red) and LQC (in blue). Vertical lines denote the mean values of τ for the *SA* and LQC. It is evident that $A_L = 1$ is outside the 1σ contour for the *SA* while is restored within 1σ for the LQC model.

4.2 Anomalies Alleviated

As discussed in **Section 2.2**, in our approach the pre-inflationary phase of LQC dynamics enables one to address two CMB anomalies. The first, shown in the left panel of **Figure 2**, is that the observed angular correlation function $C^{\rm TT}(\theta)$ remains close to zero for angles $\theta > 60°$ in contrast to the predictions of the standard ΛCDM model based on the *SA*. Let us now examine the prediction of $C^{\rm TT}(\theta)$ from LQC. This prediction is plotted as the dashed (blue) curve in **Figure 7**, along with the prediction from the *SA* shown as the (red) dashed curve and the $C^{\rm TT}(\theta)$ observed by the 2018 PLANCK mission shown by (black) dots. One sees by inspection that the LQC predictions are closer to the observed values than the *SA* predictions. This behavior can be further quantified by comparing the value of $S_{1/2} := \int_{-1}^{1/2} [C(\theta)]^2\, d(\cos\theta)$ which, as we saw in **Section 2.2**, represents a cumulative total power at large angular scales ($\theta > 60°$):

$$S^{\rm Planck}_{1/2} = 1209.18; \quad S^{\rm SA}_{1/2} = 42496.5; \quad S^{\rm LQC}_{1/2} = 14308.05. \qquad (4.2)$$

The tension between observations and the theoretical prediction from the *SA* is encapsulated by the fact that $S^{\rm SA}_{1/2}$ is almost 35 times larger than $S^{\rm Planck}_{1/2}$. This is the power suppression anomaly. This discrepancy is appreciably reduced in LQC since $S^{\rm LQC}_{1/2}$ is $\sim 1/3$ of $S^{\rm SA}_{1/2}$. As indicted in **Section 2.2**, because $C(\theta)$ for different values of θ are correlated, and because one has to use a masking procedure in the data analysis near $\theta = 180°$, the task of providing the 1σ and 2σ contours around the LQC plots is challenging, requiring manipulations of a large covariance matrix in the data analysis, as well as a detailed understanding of aspects of the instrument. It would be of considerable interest if the CMB experts could provide these plots starting with the LQC TT-power spectrum. Note also that because power is suppressed for $\ell \lesssim 30$, if LQC results were used in the PLANCK analysis, error bars for low ℓ would also be reduced and we would have a sharp measure of the LQC alleviation of this anomaly.

The second anomaly, shown in the right panel of **Figure 2**, is the lensing amplitude anomaly. This anomaly is not directly observed in the $C^{\rm XX}_\ell$ plots or in $C(\theta)$ plots, but arises when one performs a consistency check of the ΛCDM model. Instead of fixing the lensing amplitude to $A_L = 1$ (as is assumed in standard ΛCDM model) one allows it to vary along with the standard 6 parameters, i.e., one now analyzes a 7 parameter model. The anomaly lies in the finding that $A_L = 1$ is beyond 1σ error bar as shown in the right panel of **Figure 2**. This led the authors of Di Valentino et al. (2019) to conclude that there is a possible "crisis in cosmology" because, to alleviate this problem, one would need to introduce spatial curvature which creates significant departures from the observed power spectra as small angular scales. As shown in **Figure 8**, however, repeating the analysis with the LQC power spectrum restores $A_L = 1$ within 1σ contour thereby resolving the lensing amplitude anomaly and avoiding the hint of a potential "crisis".

To summarize, the observed CMB power spectrum has many non-trivial and interesting features at small angular scales and observational error bars are small in this regime. It is remarkable that these features are correctly predicted by the ΛCDM model based on the SA. The LQC corrections could well have led to discrepancies with these successful predictions of the *SA*. That does not happen. Rather, there are departures only *at large angular scales* leading to a suppression of the *primordial* power for small *k*. This difference from the nearly scale invariant standard ansatz (**2.1**) leads to the alleviation of two anomalies in the CMB.

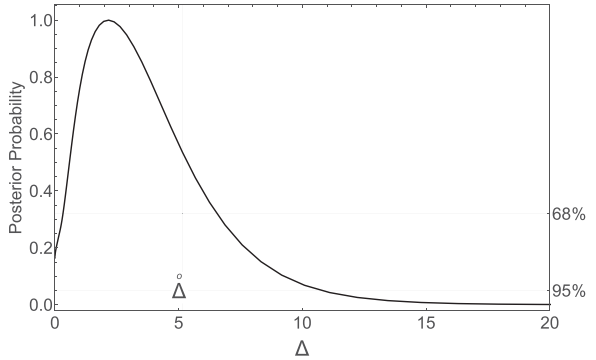

FIGURE 9 | *Marginalized posterior probability distribution for* Δ. The value $\tilde{\Delta} \simeq 5.17\ell_{\rm Pl}^2$ selected by the black hole entropy considerations is denoted by the vertical line. It lies within 1σ of the marginalized mean value $3.86\ell_{\rm Pl}^2$ that lies to the right of the peak. Thus, there is an unforeseen internal consistency.

4.3 From Observations to Fundamental Theory

As we saw in **Section 3**, the area gap Δ is the key microscopic parameter that determines values of important new, macroscopic observables such as the matter density and the curvature at the bounce. Its specific value, $\tilde{\Delta} = 5.17\,\ell_{\rm Pl}^2$, is determined by the statistical mechanical calculation of the black hole entropy in loop quantum gravity [see, e.g. Ashtekar et al. (1998), Ashtekar et al. (2000), Barbero and Perez (2017), Perez (2017)]. Results reported in the last two subsections are based on this value. However, with the CMB observations at hand, we can now, so to say, turn the tables and regard Δ as an additional parameter and *use the CMB observations to constrain its value*.

Thus, let us consider Δ to be a *free parameter* and obtain a posterior probability distribution for its value by letting it vary along with the 6 parameters of the ΛCDM model. Note that this procedure is similar to the self-consistency check that is performed for the lensing amplitude A_L. The ΛCDM Universe determined by the *SA* does not pass that test because, when it is allowed to vary, A_L prefers a value that is greater than 1 and the discrepancy is significant in that the value 1 lies outside the 1σ contour of the best fit value (Adam et al., 2020). Is there perhaps a similar tension here? More precisely, does the value $\tilde{\Delta} \simeq 5.17\ell_{\rm Pl}^2$ obtained from black hole entropy calculations lie within the 68% confidence contour of the value preferred by the CMB observations? If it does not, LQC would fail the self-consistency test at the 1σ level. If it does, there would be an unforeseen coherence between detailed conclusions drawn from very different considerations: the LQG analysis of black hole entropy and the LQC investigation of the very early Universe!

Figure 9 shows the one-dimensional posterior distribution of $\Delta_{\rm B}$. The best-fit value–the peak in the distribution–is at $\Delta = 2.18\,\ell_{\rm Pl}^2$ while the marginalized mean value is $3.86\ell_{\rm Pl}^2$.with the following constraint:

$$1.26\ell_{\rm Pl}^2 < \Delta < 6.47\ell_{\rm Pl}^2 \quad \text{(at 68\% confidence level)} \tag{4.3}$$

Clearly, the value $\tilde{\Delta} \simeq 5.17\ell_{\rm Pl}^2$ chosen in **Section 3.3** and used in this paper, is within 68% (1σ) confidence level of the constraint obtained from Planck 2018. This not only indicates a synergy between the fundamental theoretical considerations and observational data, but also provides internal consistency of the LQC model.

5 DISCUSSION

To determine the six parameter ΛCDM Universe we live in, the PLANCK team began with the standard ansatz (**2.1**) for the primordial spectrum and used known astrophysics to determine the observable power spectra for various values of the six cosmological parameters, $A_s, n_s, \Omega_b h^2, \Omega_c h^2, 100\theta_{MC}$. By comparing these theoretical predictions with observations, they determined the marginalized mean values of the six parameters (together with the error bars corresponding to 68% confidence level). This is the ΛCDM Universe according to PLANCK. This procedure has had tremendous success, especially with the finer features of the power spectra at small angular scales. However, there are also some anomalies. Since they are only at $\sim 2-3\sigma$ level, the statistical significance of any one anomaly is low. However, taken together, two or more anomalies imply that we live in an exceptional realization of the six posterior distributions provided by this procedure.

One can view these anomalies as potential gates to new physics. Indeed, the PLANCK collaboration has emphasized this possibility in its 2015 (Ade et al., 2016) as well as 2018 data releases (Aghanim et al., 2020a). As the second of these papers points out, "...if any anomalies have primordial origin, then their large scale nature would suggest an explanation rooted in fundamental physics. Thus it is worth exploring any models that might explain an anomaly (even better, multiple anomalies) naturally, or with very few parameters." LQC researchers have followed up on this suggestion. In this paper we presented a concrete realization of this idea. Specifically, one begins with the observation that, in the standard procedure summarized above, the theoretical input, beyond known astrophysics, is the *SA*, motivated by the inflationary scenario. It assumes that the primordial spectrum is nearly scale invariant and can be characterized just by two numbers A_s and n_s across *all* wavenumbers k. However, in LQC the resolution of the big bang singularity introduces a new scale $k_{\rm LQC}$ and quantum gravity corrections in the pre-inflationary phase of dynamics appear for $k \lesssim k_{\rm LQC}$. For these small wavenumber modes, the LQC primordial spectrum is no longer nearly scale invariant, whence there is departure from the predictions drawn from the *SA*.

Several closely related approaches have been used in LQC to probe the effects of this pre-inflationary dynamics [see, e.g. Agullo et al. (2012), Agullo et al. (2013a), Agullo et al. (2013b), Fernandez-Mendez et al. (2012), Barrau et al. (2014), Linsefors et al. (2013), Ashtekar and Barrau (2015), Agullo and Morris (2015), Agullo (2015), Ashtekar and Gupt (2017a), Ashtekar and Gupt (2017b), Gomar et al. (2017), Agullo et al. (2018), Barrau et al. (2018), Sreenath et al. (2019), Agullo et al. (2021b)]. Our approach has two main ingredients: 1) the use of sharply peaked quantum states $\Psi(a, \phi)$ for the background *quantum* FLRW geometry, that then enable one

to well-approximate the dynamics of cosmological perturbations on the quantum geometry $\Psi(a,\phi)$ by that on a quantum corrected 'dressed metric' $\tilde{g}_{ab}$ (Ashtekar et al., 2000; Agullo et al., 2013b); and, 2) the use of certain principles to select $\Psi(a,\phi)$ and the quantum state $\psi(\mathcal{Q},\phi)$ of the scalar mode of cosmological perturbations for any given inflationary potential (Ashtekar and Gupt, 2017a; Ashtekar and Gupt, 2017b). For any given inflationary potential, the principle used to select $\Psi(a,\phi)$ limits the number of e-folds during pre-inflationary dynamics, thereby implying that the modes that receive significant LQC corrections in the primordial spectrum correspond to the large angular scales $\ell \lesssim 30$. The principle used to select $\psi(\mathcal{Q},\phi)$ implies that in the primordial spectrum there is power reduction (rather than enhancement) in these modes. This then translates to a power suppression for $\ell \lesssim 30$ in the observed power spectra. For modes with $\ell \gg 30$, the LQC power spectra are indistinguishable from those obtained using the *SA*. Thus, LQC predictions leave the highly successful predictions of standard inflation at small angular scales unaffected, but modify the predictions at large angular scales.

Details of the LQC pre-inflationary dynamics reveal some interesting facts. First, the quantum geometry effects on the background FLRW geometry are dominant only in a short interval around the bounce. Second, it is the modes whose physical wavelength $\lambda_{\rm phy}$ is longer than the curvature radius $r_{\rm curv}$ during the pre-inflationary evolution that fail to be in the BD vacuum at onset of inflation. In the observable band, only the longest wavelength modes are thus affected and they satisfy $\lambda_{\rm phy} \gtrsim r_{\rm curv}$ only for 2–3 e-folds after the bounce. Thus, the background quantum geometry as well as the quantum perturbations Planck receive non-negligible LQC corrections during a *very short duration*. Yet these corrections lead to observable effects in that they alleviate some anomalies. Third, while we did not discuss tensor modes in this paper, their power spectra have the same behavior as that of scalar modes and, given an inflationary potential, the tensor to scalar ratio r does not receive LQC corrections (within accuracies reported here). Finally, there is an unforeseen interplay between the UV and the IR: While it is the *UV modifications* of GR that lead to the singularity resolution and create the new LQC scale $k_{\rm LQC}$, the structure of the evolution equations satisfied by cosmological perturbations is such that it is the *IR modes* with $k \lesssim k_{\rm LQC}$ that are affected during their pre-inflationary evolution. It is this unforeseen cosmic tango between the very small and the very large that is responsible for the alleviation of the two anomalies discussed in this paper.

Given that LQC simultaneously alleviates the power suppression and the lensing amplitude anomalies, it is worth investigating a more general question: Are the two conceptually related? As reported in Ashtekar et al. (2020), the answer is in the affirmative. Since this relation seems not to have been noticed before, we will make a small detour to explain it. Let us begin by assuming that there is *some* mechanism–not necessarily originating in LQC–that provides a primordial power spectrum of the form

$$\mathcal{P}_{\mathcal{R}}^{\rm new}(k) = f(k)\, A_s \left(\frac{k}{k_\star}\right)^{n_s - 1} \tag{5.1}$$

with $f(k) < 1$ for $k < k_\circ$ and $f(k) = 1$ for $k > k_\circ$ for some $k_\circ$, and compare and contrast the new ΛCDM Universe obtained from this modified ansatz with that given by the SA of **Eq. 2.1**. In the first step, we can restrict our analysis only to smaller angular scales ($k \gg k_\circ$). Then, the primordial spectrum in both schemes would be the same, whence we would obtain the same marginalized mean values of the six cosmological parameters. Denote by $\mathring{A}_s$ the marginalized mean value of the scalar amplitude A_s thus obtained. In the second step, let us consider the *full* range of observable modes, including $k \leq k_\circ$. Now, given that the observations show that the TT power is suppressed at large-scales, i.e., for $k \lesssim k_\circ$, if one uses the SA + ΛCDM model the marginalized mean value $A_s^{\rm SA}$ using the *entire* k range will be lower than $\mathring{A}_s$. By contrast if the primordial power spectrum is of the form of **Eq. 5.1**, the initial power is already suppressed by $f(k)$. Therefore, $\mathring{A}_s$ will not have to be lowered as much to obtain the marginalized mean value $A_s^{\rm new}$. Thus, we have

$$\mathring{A}_s > A_s^{\rm new} > A_s^{\rm SA} \tag{5.2}$$

The key point is the last inequality: $A_s^{\rm new} > A_s^{\rm SA}$ (We spelled out the argument because at first it seems counter-intuitive that power suppression leads to a larger $A_s^{\rm new}$. But note that power is suppressed only for low k.). Next, we know that for large k, the product $A_s e^{-2\tau}$ is fixed by observations. Hence, it follows that the best fit values of the optical depth in the two scheme must satisfy $\tau^{\rm new} > \tau^{\rm SA}$. Finally, from the very definition of lensing amplitude, the value of A_L is anti-correlated to the value of A_s. Therefore, it follows that we have the inequality $A_L^{\rm new} < A_L^{\rm SA}$. Thus in any theory that has primordial spectrum of the form (**5.1**), A_s, τ and A_L will have the same *qualitative* behavior as in LQC, and hence the tension with observations would be reduced. What LQC provides is a precise form of the suppression factor $f(k)$ from 'first principles', and hence specific quantitative predictions. Also, recall from **Section 4.1** that in our analysis the LQC $f(k)$ also came with a specific value $k_o \simeq 3.6 \times 10^{-4}\,{\rm Mpc}^{-1}$ for $k_\circ$. Other mechanisms could well lead to a very different value. If so, in the observed power spectra suppression would arise at a very different value of ℓ. Finally, the specific $f(k)$ computed from LQC also leads to other predictions–e.g., for the BB power spectrum discussed in **Section 4.1**—that need not be shared by other mechanisms.

In this respect, it would be of interest to compare the LQC predictions with those that result from effective field theories à la Ginsburg and Landau, where slow roll inflation is generically preceded by a fast roll phase that leads to a suppression of CMB quadrupole (Boyanovsky et al., 2009). This will require a calculation of angular power spectrum $C(\theta)$, and of the measure $S_{1/2}$ of power suppression, using the marginalized posterior probabilities of the 6 cosmological parameters in this effective field theory approach, and a reanalysis of the lensing amplitude along the lines of **Section 4.2**. Yet other mechanisms have been proposed to account for power suppression at large angular scales in the context of GR [see, e.g. Kofman and

Starobinsky (1985), Das and Souradeep (2014), Contaldi et al. (2003), Cline et al. (2003), Jain et al. (2009), Pedro and Westphal (2014), Lello et al. (2014), Cai et al. (2016)]. These are compared and contrasted with LQC in **Section 5** of Ashtekar and Gupt (2017b). Finally power suppression at large angular scales has been studied in the context of other bouncing models. In those discussions the bounce is often just assumed [as in Cai et al. (2009)], or obtained by adding a scalar field with a negative kinetic term which violates standard energy conditions [as in Liu et al. (2012)]. Our approach is different in that: 1) the bounce is a *prediction* of LQC; 2) since the mechanism has its roots in quantum geometry effects underlying LQG, additional scalar fields or violations of energy conditions are not involved; 3) the standard inflationary potentials are used without adjustments to provide a fast roll phase; and, most importantly, 4) our goal is to investigate whether the CMB observations can inform quantum gravity and vice versa.

In our view, the big bounce and the pre-inflationary dynamics of cosmological perturbations are on a robust footing although the discussion would benefit from a further sharpening of the detailed arguments that led us to the dressed metric $\tilde{g}_{ab}$. The part of the analysis that is on a less solid footing concerns the specific principles (Ashtekar and Gupt, 2017a; Ashtekar and Gupt, 2017b) that were used to select the wave function $\Psi_o(a, \phi)$ of the background quantum geometry and the state $\psi(a, \phi)$ of perturbations. Note that these choices are necessary to make predictions in any approach that starts in the Planck regime. Indeed, even in standard inflation one has to assume that the perturbations are in the BD vacuum at the start of slow roll, and as discussed in **Section 3.3**, it is difficult to justify this assumption from first principles. The fact that the principles led us to predictions that not only reproduce the successes of standard inflation, but also alleviate the tension associated with two anomalies, is an indication that they set us on the right track. However, they should be regarded as tentative first steps, to be improved upon and sharpened in future. In particular, the effect of the duration of the reheating epoch is yet to be investigated in detail. Another direction for future work is suggested by a second approach that has been used to alleviate CMB anomalies using pre-inflationary dynamics (Sreenath et al., 2019; Agullo et al., 2021b). The point of departure is the same as in our approach: the bounce sets a new scale and modes with the longer wavelength at the bounce get excited during the pre-inflationary evolution and are no longer in the BD vacuum at the onset of inflation. However, the primordial spectrum does not exhibit power suppression (**4.1**) as in our case. Instead, a key role is played by the superhorizon modes and their non-Gaussian correlations with the longest wavelength modes with those that are observable in the CMB. These correlations enhance the probability of finding certain features in the individual realizations of the primordial probability distribution, thereby alleviating anomalies associated with dipolar asymmetry and power suppression anomalies. It would be of considerable interest to re-examine all CMB anomalies from a perspective that combines strengths of the two approaches. Finally, all approaches to finding observable consequences of LQC in CMB, that we are aware of, assume an inflationary potential. At a certain level of discussion this is justified since a detailed analysis of the criticisms of the inflationary paradigm has concluded that, although important questions remain, the case for inflation has been "strengthened by the PLANCK data" (Chowdhury et al., 2019). However, from a fundamental perspective, introduction of an inflaton and a specific potential is ad-hoc. Now, in full LQG, the Einstein-Hilbert Lagrangian receives higher order (in particular R^2) corrections because the curvature operator is constructed from Planck scale Wilson loops and hence non-local at the fundamental microscopic scale. Therefore it is important to analyze if these corrections would provide a natural basis for inflation purely from gravitational considerations, as in Starobinsky inflation.

DATA AVAILABILITY STATEMENT

Publicly available datasets were analyzed in this study. This data can be found here: Planck Satellite collaboration 2018 Data release.

AUTHOR CONTRIBUTIONS

AA Primary Contribution: Conceptual and Mathematical Framework (Sections 1, 2, 3, 5), BG and VS Primary Contribution: High performance computing to extract observable predictions from LQC (Section 4, and all the plots in the paper).

FUNDING

NSF grants PHY-1806356 and PHY-1505411; Penn State endowment funds associated with the Eberly Chair.

ACKNOWLEDGMENTS

We are grateful to Donghui Jeong for numerous discussions on observational aspects discussed in this paper and for collaboration in Ashtekar et al. (2020). We would like to thank Ivan Agullo, Francois Bouchet, Woiciech Kaminski, Jerzy Lewandowski, Charles Lawrence, Jerome Martin and Patrick Peter for valuable discussions and Pawel Bielewicz for help with **Figure 7**. One of the referee reports led to a clarifying remark at the end of **Section 3**, and another led to corrections of three typos that could have unnecessarily confused non-experts. This work was supported in part by the NSF grants PHY-1505411 and PHY-1806356, and the Eberly research funds of Penn State. Portions of this research were conducted with high performance computing resources provided by Louisiana State University (http://www.hpc.lsu.edu).

REFERENCES

Adam, R., Aghanim, N., Akrami, Y., Ashdown, M., Aumont, J., Baccigalupi, M., et al. Planck Collaboration (2020). Planck 2018 Results VI. Cosmological Parameters. *Astron. Astrophys.* 641, A6.

Ade, P. A. R., Aghanim, N., Akrami, Y., Aluri, P. K., Arnaud, M., Ashdown, J., et al. Planck Collaboration (2016). Planck 2015 Results. XVI. Isotropy and the Statistics of the CMB. *A&A* 594, A16. doi:10.1051/0004-6361/201526681

Aghanim, N., Akrami, Y., Ashdown, M., Aumont, J., Baccigalupi, M., Ballardini, M., et al. Planck Collaboration (2020a). Planck 2018 Results. I. Overview and the Cosmological Legacy of Planck". *Astron. Astrophys.* 641, A1. doi:10.1051/0004-6361/201833880

Aghanim, N., Akrami, Y., Arroja, F., Ashdown, M., Aumont, J., Baccigalupi, M., et al. Planck Collaboration (2020b). Planck 2018 Results. V. CMB Power Spectra and Likelihoods". *Astron. Astrophys.* 641, A5. doi:10.1051/0004-6361/201936386

Agullo, I., Ashtekar, A., and Nelson, W. (2012). A Quantum Gravity Extension of the Inflationary Scenario. *Phys. Rev. Lett.* 109, 251301. doi:10.1103/physrevlett.109.251301

Agullo, I., Ashtekar, A., and Nelson, W. (2013a). Extension of the Quantum Theory of Cosmological Perturbations to the Planck Era. *Phys. Rev.* D87, 043507. doi:10.1103/PhysRevD.87.043507

Agullo, I., Ashtekar, A., and Nelson, W. (2013b). The Pre-inflationary Dynamics of Loop Quantum Cosmology: Confronting Quantum Gravity with Observations. *Class. Quan. Grav.* 30, 085014. doi:10.1088/0264-9381/30/8/085014

Agullo, I., Bolliet, B., and Sreenath, V. (2018). Non-Gaussianity in Loop Quantum Cosmology D97, 066021. doi:10.1103/PhysRevD.97.066021

Agullo, I., Kranas, D., and Sreenath, V. (2021a). Anomalies in the CMB from a Cosmic Bounce. *Gen. Rel. Grav.* 53 (no.2), 17. doi:10.1007/s10714-020-02778-9

Agullo, I., Kranas, D., and Sreenath, V. (2021b). Large Scale Anomalies in the CMB and Non-Gaussianity in Bouncing Cosmologies. *Class. Quant. Grav.* 38 (no.6), 065010. doi:10.1088/1361-6382/abc521

Agullo, I. (2015). Loop Quantum Cosmology, Non-Gaussianity, and CMB Power Asymmetry. *Phys. Rev. D* 92, 064038. doi:10.1103/physrevd.92.064038

Agullo, I., and Morris, N. A. (2015). Detailed Analysis of the Predictions of Loop Quantum Cosmology for the Primordial Power Spectra. *Phys. Rev. D* 92, 124040. doi:10.1103/physrevd.92.124040

Agullo, I., Olmedo, J., and Sreenath, V. (2020a). Observational Consequences of Bianchi I Spacetimes in Loop Quantum Cosmology. *Phys. Rev. D* 102 (no.4), 043523. doi:10.1103/physrevd.102.043523

Agullo, I., Olmedo, J., and Sreenath, V. (2020b). Predictions for the Cosmic Microwave Background from an Anisotropic Quantum Bounce. *Phys. Rev. Lett.* 124 (no.25), 251301. doi:10.1103/physrevlett.124.251301

Agullo, I., and Parker, L. (2011a). Stimulated Creation of Quanta during Inflation and the Observable Universe. *Gen. Rel. Grav.* 43, 2541. doi:10.1007/s10714-011-1220-8

Agullo, I., and Parker, L. (2011b). Non-gaussianities and the Stimulated Creation of Quanta in the Inflationary Universe. *Phys. Rev. D* 83, 063526. doi:10.1103/physrevd.83.063526

Akrami, Y., Ashdown, M., Aumont, J., Baccigalupi, M., Ballardini, M., Banday, A. J., et al. Planck Collaboration (2019). Planck 2018 Results. VII. Isotropy and Statistics of the CMB. arXiv:1906.02552[astro-ph.CO].

Agullo, I., and Singh, P. (2017). "Loop Quantum Cosmology", in *Loop Quantum Gravity: The First 30 Years*, ed. A. Ashtekar and J. Pullin (Singapore: World Scientific).

Ashtekar, A., Baez, J., Corichi, A., and Krasnov, K. (1998). Quantum Geometry and Black Hole Entropy. *Phys. Rev. Lett.* 80, 904–907. doi:10.1103/physrevlett.80.904

Ashtekar, A., Baez, J. C., and Krasnov, K. (2000). Quantum Geometry of Isolated Horizons and Black Hole Entropy. *Adv. Theor. Math. Phys.* 4, 1–94. doi:10.4310/atmp.2000.v4.n1.a1

Ashtekar, A., and Barrau, A. (2015). Loop Quantum Cosmology: From Pre-inflationary Dynamics to Observations. *Class. Quan. Grav.* 32, 234001. doi:10.1088/0264-9381/32/23/234001

Ashtekar, A., Campiglia, M., and Sloan, D. (2009a). Loop Quantum Cosmology and Spin Foams. *Phys. Lett.* B681, 347–352. doi:10.1016/j.physletb.2009.10.042

Ashtekar, A., Campiglia, M., and Sloan, D. (2010). Casting Loop Quantum Cosmology in the Spin Foam Paradigm. *Class. Quant. Grav.* 27, 135020. doi:10.1088/0264-9381/27/13/135020

Ashtekar, A., and Campiglia, M. (2012). On the Uniqueness of Kinematics of Loop Quantum Cosmology. *Class Quant. Grav.* 29, 242001. doi:10.1088/0264-9381/29/24/242001

Ashtekar, A., Corichi, A., and Singh, P. (2008). Robustness of Key Features of Loop Quantum Cosmology. *Phys. Rev. D* 77, 024046. doi:10.1103/physrevd.77.024046

Ashtekar, A., and Gupt, B. (2017a). Initial Conditions for Cosmological Perturbations. *Class. Quan. Grav.* 34, 035004. doi:10.1088/1361-6382/aa52d4

Ashtekar, A., and Gupt, B. (2017b). Quantum Gravity in the Sky: Interplay between Fundamental Theory and Observations. *Class. Quan. Grav.* 34, 014002. doi:10.1088/1361-6382/34/1/014002

Ashtekar, A., Gupt, B., Jeong, D., and Sreenath, V. (2020). Alleviating the Tension in CMB Using Planck-Scale Physics. *Phys. Rev. Lett.* 125, 051302. doi:10.1103/physrevlett.125.051302

Ashtekar, A., and Isham, C. J. (1992). Representations of the Holonomy Algebras of Gravity and Non-abelian Gauge Theories. *Class. Quant. Grav.* 9, 1433–1467. doi:10.1088/0264-9381/9/6/004

Ashtekar, A., Kaminski, W., and Lewandowski, J. (2009b). Quantum Field Theory on a Cosmological, Quantum Spacetime. *Phys. Rev.* D79, 064030.

Ashtekar, A., and Lewandowski, J. (2004). Background Independent Quantum Gravity: A Status Report. *Class Quant. Grav.* 21, R53–R152. doi:10.1088/0264-9381/21/15/r01

Ashtekar, A. (2009). Loop Quantum Cosmology: An Overview. *Gen. Relativ. Gravit.* 41, 707–741. doi:10.1007/s10714-009-0763-4

Ashtekar, A., Pawlowski, T., and Singh, P. (2006a). Quantum Nature of the Big Bang. *Phys. Rev. Lett.* 96, 141301. doi:10.1103/physrevlett.96.141301

Ashtekar, A., Pawlowski, T., and Singh, P. (2006b). Quantum Nature of the Big Bang: Improved Dynamics. *Phys. Rev. D* 74, 084003. doi:10.1103/physrevd.74.084003

Ashtekar, A., and Singh, P. (2004). Loop Quantum Cosmology: A Status Report. *Class. Quant. Grav.* 28, 213001.

Ashtekar, A., and Singh, P. (2011). Loop Quantum Cosmology: A Status Report. *Class. Quant. Grav.* 28, 213001. doi:10.1088/0264-9381/28/21/213001

Assanioussi, M., Dapor, A., Liegener, K., and Pawlowski, T. (2018). Emergent de Sitter Epoch of the Quantum Cosmos from Loop Quantum Cosmology. *Phys. Rev. Lett.* 121 (no.8), 081303. doi:10.1103/physrevlett.121.081303

Barrau, A., Cailleteau, T., Grain, J., and Mielczarek, J. (2014). Observational Issues in Loop Quantum Cosmology. *Class. Quan. Grav.* 31, 053001. doi:10.1088/0264-9381/31/5/053001

Barrau, A., Jamet, P., Martineau, K., and Moulin, F. (2018). Scalar Spectra of Primordial Perturbations in Loop Quantum Cosmology. *Phys. Rev.* D98, 086003.

Bhardwaj, A., Copeland, E. J., and Louko, J. (2019). Inflation in Loop Quantum Cosmology. *Phys. Rev.* D99, 063520.

Bojowald, M. (2020). Critical Evaluation of Common Claims in Loop Quantum Cosmology. *Universe* 6, 36. doi:10.3390/universe6030036

Boyanovsky, D., Destri, C., de Vega, H. J., and Sanchez, N. G. (2009). The Effective Theory of Inflation in the Standard Model of the Universe and the CMB+LSS Data Analysis. *Int. J. Mod. Phys.* A24, 3669–3864. doi:10.1142/s0217751x09044553

Cai, Y. F., Chen, F., Ferreira, E. G. M., and Quintin, J. (2016). New Model of Axion Monodromy Inflation and its Cosmological Implications. *JCAP* 1606, 027. doi:10.1088/1475-7516/2016/06/027

Cai, Y. F., Qiu, T. T., Brandenberger, R., and Zhang, X. M. (2009). A Nonsingular Cosmology with a Scale-Invariant Spectrum of Cosmological Perturbations from Lee-Wick Theory. *Phys. Rev. D* 80, 023511. doi:10.1103/physrevd.80.023511

Chowdhury, D., Martin, J., Ringeval, C., and Vennin, V. (2019). Inflation after Planck: Judgment Day. *Phys. Rev.* D100, 083537.

Cline, J. M., Crotty, P., and Lesgourgues, J. (2003). Does the Small CMB Quadrupole Moment Suggest New Physics? *JCAP* 0309, 010. doi:10.1088/1475-7516/2003/09/010

Contaldi, C. R., Peloso, M., Kofman, L., and Linde, A. D. (2003). Suppressing the Lower Multipoles in the CMB Anisotropies. *JCAP* 307, 002. doi:10.1088/1475-7516/2003/07/002

Corichi, A., and Singh, P. (2008). Is Loop Quantization in Cosmology Unique? *Phys. Rev.* D78, 024034.

Craig, D., and Singh, P. (2013). "Consistent Probabilities in Loop Quantum Cosmology", Class. *Quan. Grav* 30, 205008. doi:10.1088/0264-9381/30/20/205008

Das, S., and Souradeep, T. (2014). Suppressing CMB Low Multipoles with ISW Effect. *JCAP* 1402, 002. doi:10.1088/1475-7516/2014/02/002

Delabrouille, J., de Bernardis, P., Bouchet, F. R., Achúcarro, A., Ade, P. A. R., Allison, R., et al. CORE Collaboration (2018). Exploring Cosmic Origins with CORE: Survey Requirements and Mission Design. *JCAP* 04, 014. doi:10.1088/1475-7516/2018/04/014

Di Valentino, E., and Bridle, S. (2018). Exploring the Tension between Current Cosmic Microwave Background and Cosmic Shear Data. *Symmetry* 10, 585. doi:10.3390/sym10110585

Di Valentino, E., Melchiorri, A., and Silk, J. (2019). Planck Evidence for a Closed Universe and a Possible Crisis for Cosmology. *Nat. Astron* 4 (no.2), 196–203. doi:10.1038/s41550-019-0906-9

Domagala, M., and Lewandowski, J. (2004). Black Hole Entropy from Quantum Geometry. *Class. Quant. Grav.* 21, 5233–5244. doi:10.1088/0264-9381/21/22/014

Efstathiou, G. (2020). A Lockdown Perspective on the Hubble Tension(with Comments from the SH0ES Team). arXiv:2007.10716v2[astro-ph.CO].

Elizaga Navascués, B., Martín-Benito, M., and Mena Marugán, G. A. (2015). Modified FRW Cosmologies Arising from States of the Hybrid Quantum Gowdy Model. *Phys. Rev. D* 92 (no.2), 024007. doi:10.1103/physrevd.92.024007

Engle, J., Hanusch, M., and Thiemann, T. (2017). Uniqueness of the Representation in Homogeneous Isotropic LQC. *Commun. Math. Phys.* 354 (1), 231–246. [erratum: Commun. Math. Phys. 362, no.2, 759-760 (2018)]. doi:10.1007/s00220-017-2881-2

Barbero, F., and Perez, A. (2017). "Quantum Geometry and Black Holes," in *Loop Quantum Gravity: The First 30 Years* ed. A. Ashtekar and J. Pullin (Singapore: World Scientific).

Fernandez-Mendez, M., Mena Marugan, G. A., and Olmedo, J. (2012). Hybrid Quantization of an Inflationary Universe. *Phys. Rev. D* 86, 024003. doi:10.1103/physrevd.86.024003

Fialkov, A., and Loeb, A. (2016). Precise Measurement of the Reionization Optical Depth from the Global 21 Cm Signal Accounting for Cosmic Heating. *Astrophys. J.* 821, 59. doi:10.3847/0004-637x/821/1/59

Fleishchack, C. (2009). Representations of the Weyl Algebra in Quantum Geometry. *Commun. Math. Phys.* 285, 67–140.

Ganc, J., and Komatsu, E. (2012). Scale-dependent Bias of Galaxies and Mu-type Distortion of the Cosmic Microwave Background Spectrum from Single-Field Inflation with a Modified Initial State. *Phys. Rev. D* 86, 023518. doi:10.1103/physrevd.86.023518

Giesel, K. (2017). "Quantum Geometry", in *Loop Quantum Gravity: The First 30 Years* ed. A. Ashtekar and J. Pullin (Singapore: World Scientific).

Gomar, L. C., Mena-Marugan, G. A., De Blas, D. M., and Olmedo, J. (2017). Hybrid Loop Quantum Cosmology and Predictions for the Cosmic Microwave Background. *Phys. Rev.* D96, 103528.

Hanany, S., et al.[NASA PICO Collaboration]. (2019). PICO: Probe of Inflation and Cosmic Origins", arXiv:1902.10541[astro-ph.IM].

Handley, W. (2019). Curvature Tension: Evidence for a Closed Universe arXiv: 1908.09139 [astoph-CO].

Jain, R. K., Chingangbam, P., Gong, J.-O., Sriramkumar, L., and Souradeep, T. (2009). Punctuated Inflation and the Low CMB Multipoles. *JCAP* 0901, 009. doi:10.1088/1475-7516/2009/01/009

Kaminski, W., and Pawlowski, T. (2010). Cosmic Recall and the Scattering Picture of Loop Quantum Cosmology. *Phys. Rev.* D81, 084027. doi:10.1103/PhysRevD.81.084027

Kamiński, W., Kolanowski, M., and Lewandowski, J. (2020). Dressed Metric Predictions Revisited. *Class. Quant. Grav.* 37 (no.9), 095001. doi:10.1088/1361-6382/ab7ee0

Kamiński, W. (2012). The Volume Operator in Loop Quantum Cosmology. *Phys. Rev. D*, 85, 064001

Kofman, L., and Starobinsky, A. A. (1985). Effect of the Cosmological Constant on Large Scale Anisotropies in the Microwave Backbround. *Sov. Astron. Lett.* 11, 271–274. [Pisma Astron. Zh.11,643(1985)].

Lello, L., Boyanovsky, D., and Holman, R. (2014). Pre-slow Roll Initial Conditions: Large Scale Power Suppression and Infrared Aspects during Inflation. *Phys. Rev.* D89, 063533. arXiv:1307.4066. doi:10.1103/PhysRevD.89.063533

Lewandowski, J., Okolow, A., Sahlmann, H., and Thiemann, T. (2006). Uniqueness of Diffeomorphism Invariant States on Holonomy-Flux Algebras. *Commun. Math. Phys.* 267, 703–733. doi:10.1007/s00220-006-0100-7

Lewis, A., and Bridle, S. (2002). Cosmological Parameters from CMB and Other Data: A Monte Carlo Approach. *Phys. Rev. D* 66, 103511. doi:10.1103/physrevd.66.103511

Linsefors, L., Cailleteau, T., Barrau, A., and Grain, J. (2013). Primordial Tensor Power Spectrum in Holonomy Corrected Loop Quantum Cosmology. *P*hys. Rev. D87 (no. 10), 107503

Liu, J., Cai, Y. F., and Li, H. (2012). Evidences for Bouncing Evolution before Inflation in Cosmological Surveys. *J. Theor. Phys.* 1, 1.

Matsumura, T., et al. (2014). Mission Design of LiteBIRD. *J. Low. Temp. Phys.* 176, 733. doi:10.1007/s10909-013-0996-1

Meissner, K. (2004). Black Hole Entropy in Loop Quantum Gravity. *Class. Quant. Grav. Tetbf21*, 5245–5252. doi:10.1088/0264-9381/21/22/015

Olmedo, J., and Alesci, E. (2019). Power Spectrum of Primordial Perturbations for an Emergent Universe in Quantum Reduced Loop Gravity. *JCAP* 04, 030. doi:10.1088/1475-7516/2019/04/030

Pedro, F. G., and Westphal, A. (2014). Low- CMB Power Loss in String Inflation. *JHEP* 04, 034. doi:10.1007/JHEP04(2014)034

Penrose, R. (2004). *The Road to Reality, (section 28.8)*. NY: Alfred A Knopf

Perez, A. (2017). "Black Holes in Loop Quantum Gravity". *Rept. Prog. Phys.* 80, 126901. doi:10.1088/1361-6633/aa7e14

Riess, A. G., Casertano, S., Yuan, W., Macri, L. M., and Scolnic, D. (2019). Large Magellanic Cloud Cepheid Standards Provide a 1% Foundation for the Determination of the Hubble Constant and Stronger Evidence for Physics beyond CDM. *Astrophys. J.* 876 (no.1), 85.

Sarkar, D., Huterer, D., Copi, C. J., Starkman, G. D., and Schwarz, D. J. (2011). Missing Power vs Low-L Alignments in the Cosmic Microwave Background: No Correlation in the Standard Cosmological Model. *Astropart. Phys.* 34, 591. doi:10.1016/j.astropartphys.2010.12.009

Schwarz, D. J., Copi, C. J., Huterer, D., and Starkman, G. D. (2016). CMB Anomalies after Planck. *Class. Quant. Grav.* 33, 184001. doi:10.1088/0264-9381/33/18/184001

Singh, P. (2009). Are Loop Quantum Cosmos Never Singular?, *Class. Quant. Grav.* 26, 125005. doi:10.1088/0264-9381/26/12/125005

Spergel, D. N., et al.[WMAP] (2003). First Year Wilkinson Microwave Anisotropy Probe (WMAP) Observations: Determination of Cosmological Parameters". *Astrophys. J. Suppl.* 148, 175–194. doi:10.1086/377226

Sreenath, V., Agullo, I., and Bolliet, B. (2019). Computation of Non-Gaussianity in Loop Quantum Cosmology. arXiv:1904.01075[gr-qc]

Zhang, X., Ma, Y., and Artymowski, M. (2013). Loop Quantum Brans-Dicke Cosmology. *Phys. Rev. D* 87 (no.8), 084024. doi:10.1103/physrevd.87.084024

Conflict of Interest: The authors declare that the research was conducted in the absence of any commercial or financial relationships that could be construed as a potential conflict of interest.

frontiers in Astronomy and Space Sciences

ORIGINAL RESEARCH
published: 11 June 2021
doi: 10.3389/fspas.2021.647241

Loop Quantum Black Hole Extensions Within the Improved Dynamics

Rodolfo Gambini[1], *Javier Olmedo*[2]* *and Jorge Pullin*[3]

[1]Department of Physics, University of the Republic, Montevideo, Uruguay, [2]Departamento de Física Teórica y Del Cosmos, Universidad de Granada, Granada, Spain, [3]Department of Physics and Astronomy, Louisiana State University, Baton Rouge, LA, United States

We continue our investigation of an improved quantization scheme for spherically symmetric loop quantum gravity. We find that in the region where the black hole singularity appears in the classical theory, the quantum theory contains semi-classical states that approximate general relativity coupled to an effective anisotropic fluid. The singularity is eliminated and the space-time can be continued into a white hole space-time. This is similar to previously considered scenarios based on a loop quantum gravity quantization.

Keywords: loop quantum gravity, black holes, quantum field theory, spin networks, general relativity

OPEN ACCESS

Edited by:
Francesca Vidotto,
Western University, Canada

Reviewed by:
Jibril Ben Achour,
Ludwig-Maximilians-University Munich, Germany
Kristina Giesel,
University of Erlangen Nuremberg, Germany
Ana Alonso Serrano,
Max Planck Institute for Gravitational Physics (AEI), Germany

***Correspondence:**
Javier Olmedo
javolmedo@ugr.es

Specialty section:
This article was submitted to Cosmology, a section of the journal Frontiers in Astronomy and Space Sciences

Received: *29 December 2020*
Accepted: *26 April 2021*
Published: *11 June 2021*

Citation:
Gambini R, Olmedo J and Pullin J (2021) Loop Quantum Black Hole Extensions Within the Improved Dynamics. Front. Astron. Space Sci. 8:647241. doi: 10.3389/fspas.2021.647241

1 INTRODUCTION

In a previous paper (Gambini et al., 2020a) we studied an improved quantization for spherically symmetric loop quantum gravity. Earlier work (Gambini and Pullin, 2013; Gambini et al., 2014; Gambini et al., 2020b) had considered a constant polymerization parameter, similarly to the "μ_0" quantization scheme in loop quantum cosmology, whereas the improved quantization is similar to the "$\bar{\mu}$" quantization scheme (Ashtekar and Singh, 2011). Other approaches involving improved quantizations have also been explored in (Han and Liu, 2020). We observed that the singularity was removed, but we did not analyze in detail what happened to the space-time beyond the region where the singularity used to be. Here we complete that study. We find that in that region there exist semi-classical quantum states for which the theory behaves like a quantum version of general relativity coupled to an effective anisotropic fluid (Cho and Kim, 2019) that violates the dominant energy condition. In the highest curvature region there is a space-like transition surface, something that was unnoticed in (Gambini et al., 2020a). The space-time continues into a white hole geometry, like in Ref. (Ashtekar et al., 2018). However, in this work we consider a different regularization for the parametrized observable associated to the shift function. Its very definition requires the choice of a slicing and the new regularization avoids an undesirable dependence on it in the semiclassical limit.

The organization of this paper is as follows. In **section 2** we discuss the physical sector of the quantum theory, focusing on semiclassical sectors. In **section 3** we introduce a horizon penetrating slicing based on Painlevé–Gullstrand coordinates and show how it can be used to connect to a white hole space-time. We end with a discussion.

2 PHYSICAL SECTOR OF THE QUANTUM THEORY

The physical sector of the theory is obtained after combining Loop Quantum Gravity quantization techniques and the Dirac quantization program for constrained theories. In summary, we start with a kinematical Hilbert space in the loop representation adapted to spherically symmetric spacetimes for

the geometrical sector $[(K\varphi, E^{\varphi}), (K_x, E^x)]$ together with a standard representation for the spacetime mass and its conjugate momentum (M, P_M). A suitable basis of kinematical states is the one provided by spherical symmetric spin networks tensor product with the standard states for the matter sector in the mass representation. Then, we represent the scalar constraint as a well-defined operator in the kinemtical Hilbert space (for the diffeomorphism constraint we rather work with the related finite group of transformations mimicking the full theory).

Following the construction of Ref. (Gambini et al., 2020a), the physical sector of the theory is encoded in physical states (solutions to the scalar constraint) endowed with a suitable inner product and a set of physical observables. This is achieved, for instance, by applying group averaging techniques for both the quantum scalar constraint and the group of finite spatial diffeomorphisms (see also Refs (Gambini and Pullin, 2013; de Blas et al., 2017)). We focus our study to some of the simplest semi-classical states. Quantum states consist of spatial spin networks labeled by the ADM mass M (a Dirac observable) and integer numbers that characterize the radii of spheres of symmetry associated with each vertex of the network k_i. The semi-classical states we are going to consider here are given by superpositions in the mass centered at M_0 and of width δM_0 and are therefore associated with a fixed discrete structure in space (see (Gambini et al., 2020a) for more details). They provide excellent approximations to the classical geometry in regions of small curvature compared to Planck scale. Concretely, we consider the semi-classical states

$$|\psi\rangle = \frac{1}{\delta M_0}\int dM e^{iMP_0/\hbar}\cos\left[\frac{\pi(M-M_0)}{2\delta M_0}\right]\Theta(M-M_0+\delta M_0)\Theta(M_0+\delta M_0-M) \times|M, k_S, \ldots, k_0, \ldots, k_{-S}\rangle \tag{2.1}$$

with $k_0 < k_j$ for all $j \neq 0$, namely, $j = -S, -S+1, \ldots, 1, -1, \ldots, S$, where

$$k_0 = \mathrm{Int}\left[\left(\frac{2GM_0\Delta}{4\pi\ell_{\mathrm{Pl}}^3}\right)^{2/3}\right], \tag{2.2}$$

times the Planck length squared determines the smallest area of the 2-spheres in the theory. This corresponds to the improved quantization, where Δ is the area gap. Besides, we choose $M_0 \gg m_{\mathrm{Pl}}$ and

$$\delta M_0 \leq \frac{3}{2}\left(\frac{4\pi\ell_{\mathrm{Pl}}^3}{2G\Delta}\right)^{2/3} M_0^{1/3}. \tag{2.3}$$

The states in **Eq. 2.1** belong to a family of sharply peaked semiclassical states in the mass and with support on a concrete spin network (states with higher dispersion in the mass will require superpositions of different spin networks). This choice considerably simplifies the analysis of the effective geometries. As we discussed in our previous papers, the quantum theory has additional observables to the ones encountered in classical treatments (Kastrup and Thiemann, 1994; Kuchar, 1994) which are the ADM mass and the time at infinity. These emerge from the discrete nature of the spin network treatment and are associated with the k_i's, which in turn are associated with the value of the areas of the spheres of symmetry connected with each vertex of the spin network. One can also consider states that are a superposition of M's. The analysis will remain the same as long as the states are peaked around a value of M.

In addition to physical states, the physical observables representing space-time metric components will be defined through suitable parametrized observables. They act as local operators on each vertex of the spin network. Furthermore, they involve point holonomies that are chosen to be compatible with the superselection sectors of the physical Hilbert space (see Ref (Gambini et al., 2020a). for more details). Some of the basic parametrized observables are

$$\widehat{E}^x(x_j)|M, \overrightarrow{k}\rangle = \widehat{O}(z(x_j))|M, \overrightarrow{k}\rangle = \ell_{\mathrm{Pl}}^2 k_{j(x_j)}|M, \overrightarrow{k}\rangle, \tag{2.4}$$

$$\widehat{M}|M, \overrightarrow{k}\rangle = M|M, \overrightarrow{k}\rangle, \tag{2.5}$$

where $z(x)$ is a suitable gauge function that codifies the freedom in the choice of radial reparametrizations.

For the components of the space-time metric on stationary slicings we have, for instance, the lapse and shift,[1]

$$\widehat{N}^2(x_j) := \frac{1}{4}\frac{\left([\widehat{E}^x(x_j)]'\right)^2}{\left(\widehat{E}^{\varphi}(x_j)\right)^2}, \qquad \left[\widehat{N}^x(x_j)\right]^2 = \frac{\widehat{E}^x(x_j)}{\left(\widehat{E}^{\varphi}(x_j)\right)^2}\frac{\sin^2\left(\widehat{\overline{\rho}_j K_{\varphi}}(x_j)\right)}{\overline{\rho}_j^2}, \tag{2.6}$$

where

$$\left(\widehat{E}^{\varphi}(x_j)\right)^2 = \frac{\left[\left(\widehat{E}^x(x_j)\right)'\right]^2/4}{1+\frac{\sin^2\left(\overline{\rho}_j K_{\varphi}(x_j)\right)}{\overline{\rho}_j^2} - \frac{2G\widehat{M}}{\sqrt{|\widehat{E}^x(x_j)|}}}, \tag{2.7}$$

where we polymerized K_{φ} with $\overline{\rho}$ the polymerization parameter of the improved quantization,

$$\overline{\rho} = \frac{\Delta}{4\pi\widehat{E}^x}. \tag{2.8}$$

We choose the k's in the one-dimensional spin network in our physical state and the gauge function $z(x)$ such that

$$\widehat{E}^x(x_j) = \ell_{\mathrm{Pl}}^2 \mathrm{Int}\left[\frac{x_j^2}{\ell_{\mathrm{Pl}}^2}\right], \tag{2.9}$$

[1]In Ref (Gambini et al., 2020a). for the shift we adopted the regularization $K_{\varphi}(x_j) \to \sin(2\overline{\rho}_j K_{\varphi}(x_j))/2\overline{\rho}_j$, but it introduces an undesirable slicing dependence that is avoided with the present regularization. Besides, the representation that we adopt here for the square of the shift function as a parametrized observable is compatible with the superselection rules of the quantum numbers ν_j of the kinematical spin networks as it was discussed in Ref. (Gambini et al., 2020a).

$$\left[\widehat{E}^{x}\left(x_j\right)\right]'|M,\overrightarrow{k}\rangle=\frac{\ell_{\rm Pl}^2}{\delta x}\,\mathrm{Int}\left[\frac{\left(x_j+\delta x\right)^2-x_j^2}{\ell_{\rm Pl}^2}\right]|M,\overrightarrow{k}\rangle, \tag{2.10}$$

and with $x_j=\delta x\,|j|+x_0$ and with $j\in\mathbb{Z}$, where

$$x_0=\sqrt{\mathrm{Int}\left[\left(\frac{2GM\Delta}{4\pi}\right)^{2/3}\right]}. \tag{2.11}$$

Besides, we will choose $\delta x=\ell_{\rm Pl}$ as in the first paper (Gambini et al., 2020a), although we will discuss the consequences of the limiting choices (for a uniform lattice) $\delta x=\frac{\ell_{\rm Pl}^2}{2x_0}$ and $\delta x=x_0$. The different spacings δx just mentioned here correspond to different choices of states in the physical space, all of them lead to the same semiclassical behavior but differ in the deep quantum regime close to the singularity, as one would expect. The quantum regime is for the small values of k_i, where if one were to consider a superposition of states, small changes in k_i's would lead to great fluctuations in the properties of the states.

Then, the metric components take the following form in terms of the previous operators

$$\widehat{g}_{tt}\left(x_j\right)=-\left(\widehat{N}^2-\widehat{g}_{xx}\left[\widehat{N}^x\right]^2\right),\quad \widehat{g}_{tx}\left(x_j\right)=\widehat{g}_{xx}\sqrt{\left[\widehat{N}^x\right]^2},$$
$$\widehat{g}_{xx}\left(x_j\right)=\frac{\left(\widehat{E}^{\varphi}\right)^2}{\widehat{E}^{x}},\quad g_{\theta\theta}\left(x_j\right)=\widehat{E}^{x},\quad g_{\phi\phi}\left(x_j\right)=\widehat{E}^{x}\sin^2\theta.$$

Let us restrict the study to the family of stationary slicings determined by the condition

$$\sin^2\left(\widehat{\overline{\rho}_j K_{\varphi}}\left(x_j\right)\right)=\left[\widehat{F}\left(x_j\right)\right]^2 \tag{2.12}$$

where some specific choices of $F(x_j)$ will be studied below. However, any viable choice must be such that $F(x)$ is real and $F(x)\in[-1,1]$. Now, one can easily construct the operators corresponding to the components of the spacetime metric. They are given by

$$\widehat{g}_{tt}\left(x_j\right)=-\left(1-\frac{\widehat{r}_S}{\sqrt{\widehat{E}^x}}\right),\quad \widehat{g}_{tx}\left(x_j\right)=-\sqrt{\frac{\pi}{\Delta}}\,\frac{\left\{\widehat{[E^x]'}\right\}\sqrt{\widehat{E}^2}}{\sqrt{1-\frac{\widehat{r}_S}{\sqrt{\widehat{E}^x}}+\frac{4\pi\widehat{E}^x\widehat{E}^2}{\Delta}}},$$
$$\widehat{g}_{xx}\left(x_j\right)=\frac{\left\{\widehat{[E^x]'}\right\}^2}{4\widehat{E}^x\left(1-\frac{\widehat{r}_S}{\sqrt{\widehat{E}^x}}+\frac{4\pi\widehat{E}^x\widehat{E}^2}{\Delta}\right)},\quad \widehat{g}_{\theta\theta}\left(x_j\right)=\widehat{E}^{x},\quad \widehat{g}_{\phi\phi}\left(x_j\right)=\widehat{E}^{x}\sin^2\theta,$$

with $\widehat{r}_S=2G\widehat{M}$. The effective metric is defined as $g_{\mu\nu}=\langle\widehat{g}_{\mu\nu}\rangle$, where the expectation value is computed on the extended physical state $|\psi\rangle$ we presented above. We will focus on the leading order corrections when the dispersion in the mass can be neglected. In this case, we can just remove the hats in the previous expression and denote this contribution by ${}^{(0)}g_{\mu\nu}(x_j)$. In addition, we will take a continuum limit that was discussed in our first paper. Namely, $x_j=\delta x\,|j|+x_0$ is replaced by $(|x|+x_0)$, with $x\in\mathbb{R}$ and the integer part function $\mathrm{Int}[\cdot]$ will be dropped from all expressions. This continuum limit means that the effective geometries bounce when they reach $x=0$.

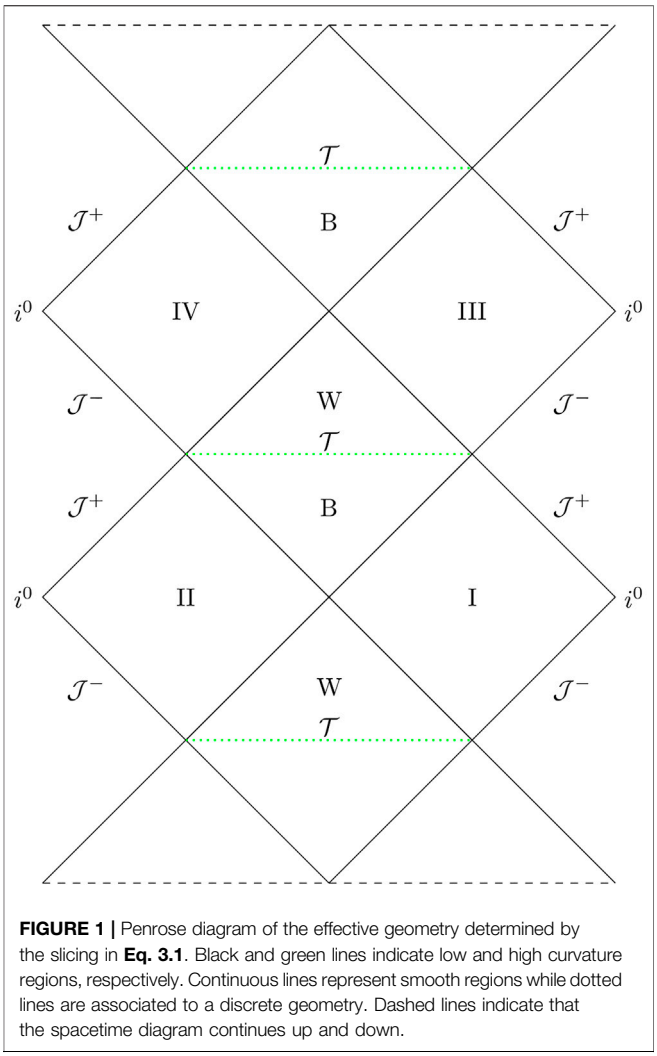

FIGURE 1 | Penrose diagram of the effective geometry determined by the slicing in **Eq. 3.1**. Black and green lines indicate low and high curvature regions, respectively. Continuous lines represent smooth regions while dotted lines are associated to a discrete geometry. Dashed lines indicate that the spacetime diagram continues up and down.

3 PAINLEVÉ-GULLSTRAND COORDINATES: BLACK HOLE TO WHITE HOLE TRANSITION

We are interested in spatial slicings that are horizon penetrating and asymptotically flat. For instance, ingoing Painlevé-Gullstrand coordinates is one of the well-known choices that meet these requirements. Besides, the time coordinate follows the proper time of a free-falling observer. The slicing is defined by the condition $\widehat{F}(x_j)=\widehat{F}_1(x_j)$ where

$$\widehat{F}_1\left(x_j\right)=\overline{\rho}\sqrt{\frac{\widehat{r}_S}{\sqrt{\widehat{E}^x}}}. \tag{3.1}$$

This choice is equivalent to a lapse operator $\widehat{N}(x_j)=\widehat{I}$. Besides, one can easily see that in the semiclassical limit $x_j\to x+x_0$ we have the function $F_1(x)<1$ for all $x\neq 0$, while $F_1(x=0)=1$. This is important since this choice will allow us to completely probe the high curvature region of the effective geometries.

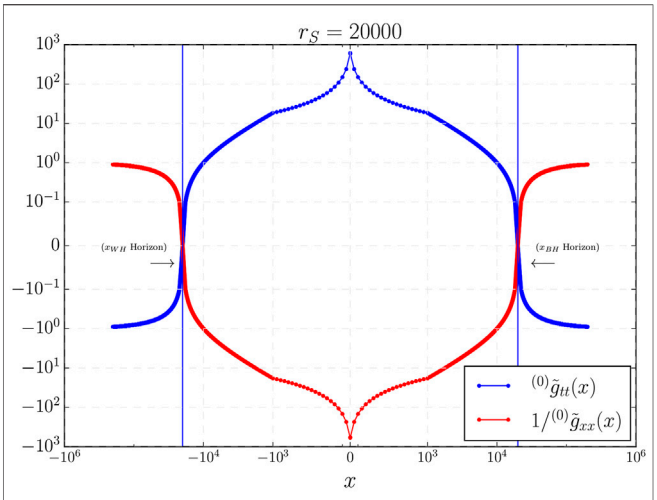

FIGURE 2 | The values of the *tt* component of the metric and the inverse of *xx* for the metric in diagonal form. When the first vanishes, horizons arise. Notice that in the region between the two horizons the discreteness is significant as represented in the separation of the dots (although in the plot we do not show all the points in the lattice but only one out of fifty).

They can be obtained as in (Gambini et al., 2020a). One gets

$$
\begin{aligned}
&{}^{(0)}g_{tt}(x) = -\left(1 - \frac{r_S}{|x| + x_0}\right),\\
&{}^{(0)}g_{tx}(x) = -\mathrm{sign}(x)\sqrt{\frac{r_S}{|x| + x_0}}\left(1 + \frac{\delta x}{2(|x| + x_0)}\right),\\
&{}^{(0)}g_{xx}(x) = \left(1 + \frac{\delta x}{2(|x| + x_0)}\right)^2,\ {}^{(0)}g_{\theta\theta}(x) = (|x| + x_0)^2,\\
&{}^{(0)}g_{\phi\phi}(x) = (|x| + x_0)^2 \sin^2\theta.
\end{aligned}
\tag{3.2}
$$

For this slicing, the low curvature regions occur when $F(x) \simeq 0$ or equivalently at $x \to \pm\infty$. Concretely, at $x \to +\infty$ the effective metric approaches sufficiently fast a classical black hole metric in ingoing Painlevé-Gullstrand coordinates, while for $x \to -\infty$ the effective metric approaches sufficiently fast a classical white hole metric in outgoing Painlevé-Gullstrand coordinates. On the other hand, as we will see below, the curvature reaches its maximum when $F(x) = 1$, namely, at $x = 0$.

In what follows, we refer to **Figure 1** (see the similarities with the Penrose diagram of Ref (Ashtekar et al., 2018)). One can see that the condition ${}^{(0)}g_{tt}(x) = 0$ has two real solutions in x, corresponding to two classical black or white hole horizons, at $x_{BH} > 0$ and $x_{WH} < 0$. In the spacetime regions with $x > x_{BH}$ or $x < x_{WH}$, the surfaces $x =$ const are time-like, and correspond to untrapped regions. In the region right behind the black hole horizon, $x < x_{BH}$, $x =$ const hypersurfaces are space-like. This region is a trapped black hole interior. As we move toward the high curvature region, curvature is maximum at $x = 0$. This space-like hypersurface connects the trapped black hole region with an anti-trapped white hole region. This is the so-called transition surface (Ashtekar et al., 2018). The anti-trapped white hole region extends all the way from $x = 0$ to the white hole horizon $x = x_{WH}$. In all this region, $x =$ const hypersurfaces are still space-like. Once the white hole horizon $x = x_{WH}$ is crossed to the outside region, spacetime is untrapped again and $x =$ const hypersurfaces are again time-like.

In order to illustrate all these properties, it is convenient to first write the effective metric in its diagonal form (It should be noted that although the theory does not recover the full diffeomorphism invariance of the classical theory in the quantum regions, it is a valid mathematical tool to diagonalize a metric nevertheless.) It can be easily obtained by introducing the change of coordinates

$$
dt \to dt + \frac{{}^{(0)}g_{tx}(x)}{{}^{(0)}g_{tt}(x)}dx \tag{3.3}
$$

This transformation amounts to the change

$$
{}^{(0)}g_{xx}(x) \to {}^{(0)}\tilde{g}_{xx}(x) = \frac{\left(1 + \frac{\delta x}{2(|x|+x_0)}\right)^2}{\left(1 - \frac{r_S}{|x|+x_0}\right)}, \quad {}^{(0)}g_{tx}(x) \to {}^{(0)}\tilde{g}_{tx}(x) = 0, \tag{3.4}
$$

while all other components remain as

$$
{}^{(0)}g_{tt}(x) \to {}^{(0)}\tilde{g}_{tt}(x) = -\left(1 - \frac{r_S}{|x| + x_0}\right), \tag{3.5}
$$

$$
\begin{aligned}
{}^{(00)}g_{\theta\theta}(x) \to {}^{(00)}\tilde{g}_{\theta\theta}(x) &= (|x| + x_0)^2,\ {}^{(00)}\tilde{g}_{\varphi\varphi}(x) \to {}^{(00)}\tilde{g}_{\varphi\varphi}(x)\\
&= (|x| + x_0)^2 \sin\theta.
\end{aligned}
\tag{3.6}
$$

In **Figure 2** we show two components of the effective metric in its diagonal form. There where they vanish, a horizon forms and the coordinate system becomes singular. However, we should remember that around $x \simeq x_0$ spacetime is discrete and the continuous line is just an interpolation. Therefore, the metric will be well defined provided the horizons are not located on a vertex of the lattice.

We have also studied the effective stress-energy tensor that encodes the main deviations from the classical theory. It is defined as

$$
T_{\mu\nu} := \frac{1}{8\pi G}G_{\mu\nu}, \tag{3.7}
$$

where $G_{\mu\nu}$ is the Einstein tensor. $T_{\mu\nu}$ is characterized by the effective energy density ρ and radial and tangential pressures densities, p_x and $p_{||}$, respectively. They are defined by means of

$$
\rho^{ext} := T_{\mu\nu}\frac{X^\mu X^\nu}{X^\rho X_\rho}, \tag{3.8}
$$

$$
p_x^{ext} := T_{\mu\nu}\frac{r^\mu r^\nu}{r^\rho r_\rho}, \tag{3.9}
$$

and

$$
p_{||}^{ext} := T_{\mu\nu}\frac{\theta^\mu \theta^\nu}{\theta^\rho \theta_\rho}, \tag{3.10}
$$

where X^μ is the Killing vector field that is time-like in the regions in which $x =$ const hypersurfaces are time-like. r^μ and θ^μ are the vector fields pointing in the radial and θ-angular directions, respectively. When the Killing vector field X^μ is space-like, namely, in the regions in which $x =$ const hypersurfaces are space-like, r^μ becomes time-like. Therefore,

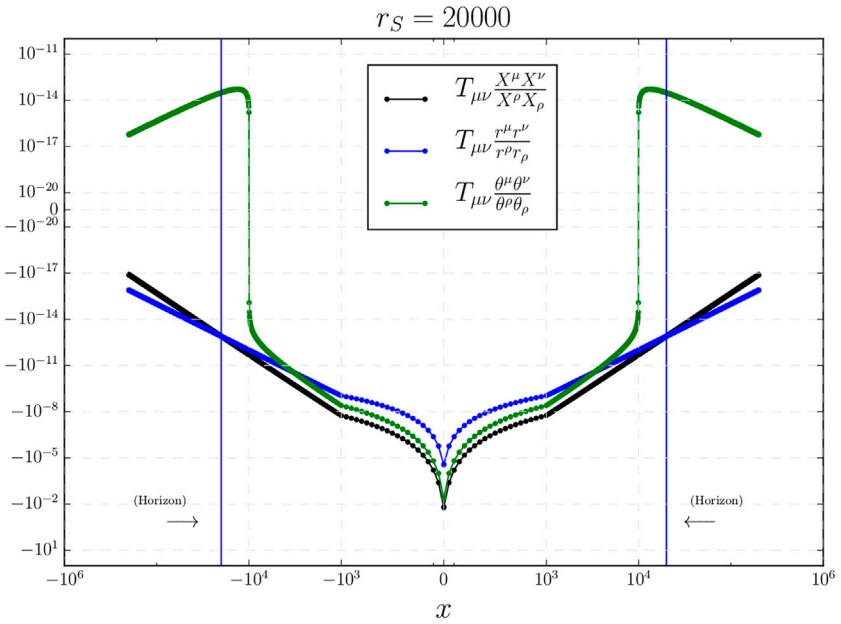

FIGURE 3 | The stress energy tensor of the effective metric ${}^{(0)}\tilde{g}_{\mu\nu}(x)$. This plot corresponds to $\delta x = \ell_{\rm Pl}$, namely, $s = 1$.

$$\rho^{int} := T_{\mu\nu}\frac{r^\mu r^\nu}{r^\rho r_\rho}, \tag{3.11}$$

$$p_x^{int} := T_{\mu\nu}\frac{X^\mu X^\nu}{X^\rho X_\rho}, \tag{3.12}$$

while $p_{||}^{int} = p_{||}^{ext}$ since θ^μ remains space-like. We will assume that these effective space-times can be approximated by a smooth and continuous geometry everywhere, even at the transition surface. This assumption, as we mentioned, fails in the most quantum region. However, we expect that T_μ^ν (a quantity only valid when geometry is smooth) will still give us qualitative hints about quantum geometry corrections there.

In **Figure 3** we show the components of the stress-energy tensor $T_{\mu\nu}$, or equivalently, the components of the Einstein tensor (up to a factor $(8\pi G)$) for the choice $\delta x = \ell_{\rm Pl}$. From them it is easy to extract the energy densities and pressures in each region of these effective space-times.

It is straightforward to compute the value of the energy density and pressures of the stress-energy tensor at the transition surface and in the limit of large mass $r_S \gg \ell_{\rm Pl}$. Actually, their value depend on the choice of spacing δx of the uniform lattice in the radial direction. For instance, for $\delta x = x_0\left(\frac{\ell_{\rm Pl}}{x_0}\right)^s$ with $s = 0, 1, 2$, one can see that[2]

$$\begin{aligned}
\rho^{int}(x=0) &= \frac{2\pi}{\Delta}\times\mathcal{O}\left(\left[\frac{\Delta}{2\pi r_S}\right]^{s/3+2/3}\right),\\
p_x^{int}(x=0) &= -\frac{2\pi}{\Delta}\times\mathcal{O}\left(\left[\frac{\Delta}{2\pi r_S}\right]^{s/3}\right),\\
p_{||}^{int}(x=0) &= -\frac{2\pi}{\Delta}\times\mathcal{O}\left(\left[\frac{\Delta}{2\pi r_S}\right]^{s/3}\right)
\end{aligned} \tag{3.13}$$

Let us note that in the most quantum region,

$$\begin{aligned}
\omega_x(x=0) &= \frac{p_x^{int}(x=0)}{\rho^{int}(x=0)} = -\mathcal{O}\left(\left[\frac{2\pi r_S}{\Delta}\right]^{2/3}\right),\\
\omega_{||}(x=0) &= \frac{p_{||}^{int}(x=0)}{\rho^{int}(x=0)} = -\mathcal{O}\left(\left[\frac{2\pi r_S}{\Delta}\right]^{2/3}\right).
\end{aligned} \tag{3.14}$$

As we see, at the transition surface, the effective stress-energy tensor does not violate the strong energy condition since $\rho^{int}(x=0) \geq 0$. However, it does actually violate the dominant energy condition. Since the dominant energy condition implies that $|\omega_x| \leq 1$ and $|\omega_{||}| \leq 1$, we conclude that this condition is violated since both $|\omega_x(x=0)|$ and $|\omega_{||}(x=0)|$ at the transition quantum spacetime blow up in the limit $r_S \gg \ell_{\rm Pl}$.

One can construct the Penrose diagram of this geometry, together with a possible extension to regions not covered by our slicing.

4 DISCUSSION

There are several comments about the scenario studied in this manuscript. On the one hand, the effective geometries that one can derive in this theory are uniquely determined by the

[2]The choices of δx shown here correspond to the maximum allowed uniform discretization if $s = 0$, while $s = 2$ gives the finest uniform refinement. $s = 1$ is an intermediate choice.

semiclassical physical state and the (parameterized) observables that represent the components of the metric. The quantum corrections on these geometries likewise depend on the minimal area gap Δ and the size of the discretization of the physical states we are considering. Polymer corrections due to the choice of foliation will also contribute if fluctuations of the mass are considered. We are taking for simplicity an element (spin network) of the basis in the physical space of states and ignoring superpositions in different discretizations and masses. Quantum corrections break the covariance, in particular because their dependence on the discretization of the chosen quantum states, but also due to foliation dependent terms. The latter produce $O(\Delta r_S^2/x^2)$ quantum corrections in the (asymptotically flat) external region of the black hole and therefore they are completely unobservable for macroscopic black holes, allowing to recover diffeomorphism invariance. Since different foliations are identified with (observer's) frames of reference, this is equivalent to say that, for physically implementable frames of reference (i.e. physically realizable observers) in the exterior region, quantum corrections will be negligible. Nevertheless, these quantum corrections increase when approaching the high curvature region, reaching maximum values of order $O(\Delta r_S^2/x_0^2)$. For instance, a free-falling observer (as it is the case under consideration in this manuscript) and an accelerated observer will observe there only slightly different corrections, even if its foliation involves accelerations that are Planck order.

Regarding the original choice of shift as parametrized observable adopted in Ref. (Gambini et al., 2020a), we noticed that, as mentioned in (Kelly et al., 2020), the most quantum region showed an inner Cauchy horizon connecting the trapped black hole region with a Planckian size transition space-time where $x =$ const hypersurfaces are time-like. However, strictly speaking, due to this Cauchy horizon, the extension beyond this region is not unique. After the bounce a Cauchy Horizon is traversed and therefore the initial conditions at $\mathcal{I}_-$ that end up producing a black hole are not enough for the determination of the possible extensions beyond the Cauchy horizon. Notice that the Cauchy horizon occurs in a deep quantum region that is in the past of the extension; further non-uniqueness would occur when quantum superpositions are considered. Besides, different foliations capture different extensions. We saw that a choice of foliation (corresponding to an accelerated observer with a Planck order acceleration) leads to an anti de Sitter universe beyond the Cauchy horizon. Similar ambiguities have been noted in classical general relativity (Dafermos and Luk, 2017). One must keep in mind that these ambiguities can be alleviated by considering parametrized observables that correspond to physically implementable frames of reference (i.e. physically realizable observers). We are considering here extrinsic framings corresponding to a choice of polimerization for the functional parameter $K_\varphi(x_j)$. Even though the theory is covariant in the sense that the classical observables become quantum observables in the quantization process, each polimerization corresponds to a different choice of framing. In reference (Gambini and Pullin, 2009) we proved that diffeomorphism invariance of the parametrized observables corresponding to the metric is only preserved for diffeomorphism that do not amplify Planck scale separation to macroscopic scale. The introduction of more realistic intrinsic framings resulting from the inclusion of matter would provide a natural choice of slicing allowing to solve this limitation. For instance, the case of Painlevé-Gullstrand coordinates, that amount to a unit parametrized observable related to the lapse function. The kind of midisuperspace model here considered allows to analyze this issues while most of the minisuperspace scenarios proposed in the literature (see (Bodendorfer et al., 1912; Sartini and Geiller, 2021; Boehmer and Vandersloot, 2007; Campiglia et al., 2008; Ashtekar and Singh, 2011; Cortez et al., 2017; Olmedo et al., 2017; Alesci et al., 2018; Alesci et al., 2019; Assanioussi et al., 2020) for references on hypersurface orthogonal slicings) adopted a particular family of space-time foliations where this issue of slicing dependence did not arise. Other authors have taken the issue of non-covariance to imply that modifications of the constraint algebra are in order, leading to the deformed hypersurface deformation algebra approach (Tibrewala, 2012; Bojowald et al., 2015; Ben Achour et al., 2018).

Summarizing, we have applied an improved quantization scheme for loop quantum gravity in spherical symmetry. The singularity that appears in classical general relativity is eliminated and space-time is continued to a white hole space-time geometry through a transition surface where curvature reaches its maximum value. This is qualitatively similar to scenarios that have been recently proposed (Ashtekar et al., 2018). Our proposal yields effective geometries that are free of undesirable slicing dependencies in the semiclassical limit. Actually, the slicing independence in a precise semiclassical limit of small mass fluctuations can be invoked to restrict polymer modifications of the scalar constraint and the parametrized observables describing the quantum geometry. Finally, it is interesting to note that most of the ideas presented here and in Ref (Gambini et al., 2020a). can be very useful in other situations, like in the vacuum polarized T^3 Gowdy cosmologies with local rotational symmetry (de Blas et al., 2017).

DATA AVAILABILITY STATEMENT

The original contributions presented in the study are included in the article/Supplementary Material, further inquiries can be directed to the corresponding author.

AUTHOR CONTRIBUTIONS

All authors collaborated equally in the research and elaboration of the manuscript.

ACKNOWLEDGMENTS

This work was supported in part by Grant NSF-PHY-1903799, funds of the Hearne Institute for Theoretical Physics, CCT-LSU, Pedeciba, Fondo Clemente Estable FCE_1_2019_1_155865 and Project. No. FIS 2017–86497-C2-2-P of MICINN from Spain. J.O. acknowledges the Operative Program FEDER2014–2020 and the Consejería de Economía y Conocimiento de la Junta de Andalucía.

REFERENCES

Alesci, E., Bahrami, S., and Pranzetti, D. (2018). Quantum Evolution of Black Hole Initial Data Sets: Foundations. *Phys. Rev. D.* 98, 046014. doi:10.1103/physrevd.98.046014

Alesci, E., Bahrami, S., and Pranzetti, D. (2019). Quantum Evolution of Black Hole Initial Data Sets: Foundations. *Phys. Lett. B.* 797, 134908. doi:10.1103/physrevd.98.046014

Ashtekar, A., Olmedo, J., and Singh, P. (2018). Quantum Transfiguration of Kruskal Black Holes. *Phys. Rev. Lett.* 121, 241301. doi:10.1103/physrevlett.121.241301

Ashtekar, A., and Singh, P. (2011). Loop Quantum Cosmology: a Status Report. *Class. Quan. Grav.* 28, 213001. doi:10.1088/0264-9381/28/21/213001

Assanioussi, M., Dapor, A., and Liegener, K. (2020). Perspectives on the Dynamics in a Loop Quantum Gravity Effective Description of Black Hole Interiors. *Phys. Rev. D.* 101, 026002. doi:10.1103/physrevd.101.026002

Ben Achour, J., Lamy, F., Liu, H., and Noui, K. (2018). Polymer Schwarzschild Black Hole: An Effective Metric. *EPL.* 123 (2), 20006. doi:10.1209/0295-5075/123/20006

Bodendorfer, N., Mele, F. M., and Münch, J. (1912). arXiv, 00774.

Boehmer, C. G., and Vandersloot, K. (2007). Spherically Symmetric Loop Quantum Gravity: Analysis of Improved Dynamics. *Phys. Rev.* D76, 1004030. doi:10.1103/PhysRevD.76.104030

Bojowald, M., Brahma, S., and Reyes, J. D. (2015). Covariance in Models of Loop Quantum Gravity: Spherical Symmetry. *Phys. Rev. D.* 92 (4), 045043. doi:10.1103/PhysRevD.92.045043

Campiglia, M., Gambini, R., and Pullin, J. (2008). Loop Quantization of Spherically Symmetric Midi-superspaces : the interior Problem. *AIP Conf. Proc.* 977, 52–63. doi:10.1063/1.2902798

Cho, I., and Kim, H.-C. (2019). Simple Black Holes with Anisotropic Fluid. *Chin. Phys. C.* 43, 025101. doi:10.1088/1674-1137/43/2/025101

Cortez, J., Cuervo, W., Morales-Técotl, H. A., and Ruelas, J. C. (2017). Effective Loop Quantum Geometry of SchwarzsChild Interior. *Phys. Rev. D.* 95, 064041. doi:10.1103/physrevd.95.064041

Dafermos, M., and Luk, J. (2017). The interior of dynamical vacuum black holes I: The C_0-stability of the Kerr Cauchy horizon. arxiv:1710.01722.

de Blas, D. M., Olmedo, J., and Pawłowski, T. (2017). Loop Quantization of the Gowdy Model with Local Rotational Symmetry. *Phys. Rev. D.* 96, 106016. doi:10.1103/physrevd.96.106016

Gambini, R., Olmedo, J., and Pullin, J. (2014). Quantum Black Holes in Loop Quantum Gravity. *Class. Quant. Grav.* 31, 095009. doi:10.1088/0264-9381/31/9/095009

Gambini, R., Olmedo, J., and Pullin, J. (2020a). Spherically Symmetric Loop Quantum Gravity: Analysis of Improved Dynamics. *Class. Quan. Grav.* 37, 205012. doi:10.1088/1361-6382/aba842

Gambini, R., Olmedo, J., and Pullin, J. (2020b). Spherically Symmetric Loop Quantum Gravity: Analysis of Improved Dynamics. *Class. Quant. Grav.* 37, 205012. doi:10.1088/1361-6382/aba842

Gambini, R., and Pullin, J. (2009). Diffeomorphism Invariance in Spherically Symmetric Loop Quantum Gravity. *Adv. Sci. Lett.* 2, 251–254. doi:10.1166/asl.2009.1032

Gambini, R., and Pullin, J. (2013). Loop Quantization of the Schwarzschild Black Hole. *Phys. Rev. Lett.* 110, 211301. doi:10.1103/PhysRevLett.110.211301

Han, M., and Liu, H. (2020). Improved (Mu)over-bar-scheme Effective Dynamics of Full Loop Quantum Gravity. *Phys. Rev. D.* 102 (6), 064061. doi:10.1103/PhysRevD.102.064061

Kastrup, H. A., and Thiemann, T. (1994). Spherically Symmetric Gravity as a Completely Integrable System. *Phys. B.* 425, 665–686. doi:10.1016/0550-3213(94)90293-3

Kelly, J. G., Santacruz, R., and Wilson-Ewing, E. (2020). Effective Loop Quantum Gravity Framework for Vacuum Spherically Symmetric Spacetimes. *Phys. Rev. D.* 102, 106024. doi:10.1103/physrevd.102.106024

Kuchar, K. V. (1994). Geometrodynamics of Schwarzschild Black Holes. *Phys. Rev. D.* 50, 3961–3981. doi:10.1103/PhysRevD.50.3961

Olmedo, J., Saini, S., and Singh, P. (2017). From Black Holes to white Holes: a Quantum Gravitational, Symmetric Bounce. *Class. Quan. Grav.* 34, 225011. doi:10.1088/1361-6382/aa8da8

Sartini, F., and Geiller, M. (2021). Quantum dynamics of the black hole interior in loop quantum cosmology. *Phys. Rev. D.* 103, 066014. doi:10.1103/PhysRevD.103.066014

Tibrewala, R. (2012). Spherically Symmetric Einstein-Maxwell Theory and Loop Quantum Gravity Corrections. *Quant. Grav.* 29, 235012. doi:10.1088/0264-9381/29/23/235012

Conflict of Interest: The authors declare that the research was conducted in the absence of any commercial or financial relationships that could be construed as a potential conflict of interest.

frontiers in Astronomy and Space Sciences

REVIEW
published: 24 June 2021
doi: 10.3389/fspas.2021.701417

Phenomenological Implications of Modified Loop Cosmologies: An Overview

Bao-Fei Li[1,2†], *Parampreet Singh*[1†] *and Anzhong Wang*[3*†]

[1]*Department of Physics and Astronomy, Louisiana State University, Baton Rouge, LA, United States,* [2]*Institute for Theoretical Physics & Cosmology, Zhejiang University of Technology, Hangzhou, China,* [3]*GCAP-CASPER, Department of Physics, Baylor University, Waco, TX, United States*

In this paper, we first provide a brief review of the effective dynamics of two recently well-studied models of modified loop quantum cosmologies (mLQCs), which arise from different regularizations of the Hamiltonian constraint and show the robustness of a generic resolution of the big bang singularity, replaced by a quantum bounce due to non-perturbative Planck scale effects. As in loop quantum cosmology (LQC), in these modified models the slow-roll inflation happens generically. We consider the cosmological perturbations following the dressed and hybrid approaches and clarify some subtle issues regarding the ambiguity of the extension of the effective potential of the scalar perturbations across the quantum bounce, and the choice of initial conditions. Both of the modified regularizations yield primordial power spectra that are consistent with current observations for the Starobinsky potential within the framework of either the dressed or the hybrid approach. But differences in primordial power spectra are identified among the mLQCs and LQC. In addition, for mLQC-I, striking differences arise between the dressed and hybrid approaches in the infrared and oscillatory regimes. While the differences between the two modified models can be attributed to differences in the Planck scale physics, the permissible choices of the initial conditions and the differences between the two perturbation approaches have been reported for the first time. All these differences, due to either the different regularizations or the different perturbation approaches in principle can be observed in terms of non-Gaussianities.

Keywords: modified loop quantum cosmology, initial conditions, cosmic microwave background, power spectrum, big bang singularity resolution

OPEN ACCESS

Edited by:
Guillermo A. Mena Marugán, Instituto de Estructura de la Materia (IEM), Spain

Reviewed by:
Esteban Mato, Universidad de la República, Uruguay
V. Sreenath, National Institute of Technology, Karnataka, India

****Correspondence:***
Anzhong Wang
anzhong_wang@baylor.edu

†These authors have contributed equally to this work

Specialty section:
This article was submitted to Cosmology, a section of the journal Frontiers in Astronomy and Space Sciences

Received: *27 April 2021*
Accepted: *02 June 2021*
Published: *24 June 2021*

Citation:
Li B-F, Singh P and Wang A (2021) Phenomenological Implications of Modified Loop Cosmologies: An Overview. Front. Astron. Space Sci. 8:701417. doi: 10.3389/fspas.2021.701417

1 INTRODUCTION

Despite offering a solution to several fundamental and conceptual problems of the standard big bang cosmology, including the flatness, horizon, and exotic-relic problems, the cosmic inflation in the early Universe also provides a mechanism to produce density perturbations and primordial gravitational waves (PGWs) (Starobinsky, 1980; Guth, 1981; Sato, 1981; Kodama and Sasaki, 1984; Mukhanov et al., 1992; Malik, 2001; Dodelson, 2003; Mukhanov, 2005; Weinberg, 2008; Malik and Wands, 2009; Senatore, 2017). The latter arise from quantum fluctuations of spacetimes and produce not only a temperature anisotropy, but also polarizations in the cosmic microwave background (CMB), a smoking gun of PGWs. However, the inflationary paradigm is incomplete without the knowledge of key elements from quantum gravity. First, it is well-known that the cosmic

inflation is sensitive to the ultraviolet (UV) physics, and its successes are tightly contingent on the understanding of this UV physics (Brandenberger, 1999; Martin and Brandenberger, 2001; Niemeyer and Parentani, 2001; Bergstorm and Danielsson, 2002; Niemeyer and Parentani, 2002; Niemeyer and Parentani, 2003; Easther et al., 2005; McAllister and Silverstein, 2007; Joras and Marozzi, 2009; Ashoorioon et al., 2011; Jackson and Schalm, 2012; Kiefer and Krämer, 2012; Brandenberger and Martin, 2013; Burgess et al., 2013; Chernoff and Tye, 2014; Krauss and Wilczek, 2014; Woodard, 2014; Baumann and McAllister, 2015; Cicoli, 2016; Silverstein, 2016). In particular, if the inflationary phase lasts somewhat longer than the minimal period required to solve the above mentioned problems, the length scales we observe today will originate from modes that are smaller than the Planck length during inflation (Brandenberger, 1999; Martin and Brandenberger, 2001; Niemeyer and Parentani, 2001; Bergstorm and Danielsson, 2002; Niemeyer and Parentani, 2002; Niemeyer and Parentani, 2003; Easther et al., 2005; Joras and Marozzi, 2009; Ashoorioon et al., 2011; Jackson and Schalm, 2012; Brandenberger and Martin, 2013). Then, the treatment of the underlying quantum field theory on a classical spacetime becomes questionable, as now the quantum geometric effects are expected to be large, and the space and time cannot be treated classically any more. This is often referred to as *the trans-Planckian problem* of cosmological fluctuations[1].

The second problem of the inflationary paradigm is more severe. It is well known that inflationary spacetimes are past-incomplete because of the big bang singularity (Borde and Vilenkin, 1994; Borde et al., 2003), with which it is not clear how to impose the initial conditions. This problem gets aggravated for low energy inflation in spatially-closed models which are slightly favored by current observations where the Universe encounters a big crunch singularity and lasts only for a few Planck seconds (Linde, 2014; Linde, 2018).

Another problematic feature of inflation is that one often ignores the pre-inflationary dynamics and sets the Bunch-Davies (BD) vacuum in a very early time. But, it is not clear how such a vacuum state can be realized dynamically in the framework of quantum cosmology (McAllister and Silverstein, 2007; Burgess et al., 2013; Chernoff and Tye, 2014; Baumann and McAllister, 2015; Cicoli, 2016; Silverstein, 2016), considering the fact that a pre-inflationary phase always exists between the Plank and inflation scales, which are about $10^3 \sim 10^{12}$ orders of magnitude difference (Dodelson, 2003; Mukhanov, 2005; McAllister and Silverstein, 2007; Weinberg, 2008; Burgess et al., 2013; Chernoff and Tye, 2014; Baumann and McAllister, 2015; Cicoli, 2016; Silverstein, 2016). While these problems of inflationary paradigm demand a completion from quantum theory of spacetimes, they also open an avenue to overcome one of the main obstacles in the development of quantum gravity, which concerns with the lack of experimental evidences. Thus, understanding inflation in the framework of quantum gravity could offer valuable guidances to the construction of the underlying theory (Weinberg, 1980; Carlip, 2003; Kiefer, 2007; Green et al., 1999; Polchinski, 2001; Johson, 2003; Becker et al., 2007; Ashtekar and Lewandowski, 2004; Thiemann, 2007; Rovelli, 2008; Bojowald, 2011; Gambini and Pullin, 2011; Ashtekar and Pullin, 2017).

In particular, when applying the techniques of loop quantum gravity (LQG) to homogeneous and isotropic Universe, namely loop quantum cosmology (LQC) (Ashtekar and Singh, 2011; Ashtekar and Barrau, 2015; Bojowald, 2015; Agullo and Singh, 2017), it was shown that, purely due to quantum geometric effects, the big bang singularity is generically resolved and replaced by a quantum bounce at which the spacetime curvature becomes Planckian (Ashtekar et al., 2006; Ashtekar et al., 2006; Ashtekar et al., 2010). The robustness of the singularity resolution has been shown for a variety of isotropic and anisotropic spacetimes (Giesel et al., 2020). Interestingly, there exists a reliable effective spacetime description, which has been used to confirm a generic resolution of all strong curvature singularities (Singh, 2009; Singh, 2014). Various phenomenological implications have been studied using this effective spacetime description, whose validity has been verified for isotropic and anisotropic spacetimes (Diener et al., 2014; Diener et al., 2014; Agullo et al., 2017; Diener et al., 2017; Singh, 2018). For low energy inflation models with a positive spatial curvature, the singularity resolution and a successful onset of inflation for classically inadmissible initial conditions have been demonstrated (Dupuy and Singh, 2020; Gordon et al., 2021; Motaharfar and Singh, 2021).

In the last couple of years, several approaches have been proposed, in order to address the impacts of the quantum geometry on the primordial power spectra. These include the approaches of the deformed algebra (Bojowald et al., 2008; Cailleteau et al., 2012; Cailleteau et al., 2012), dressed metric (Agullo et al., 2012; Agullo et al., 2013; Agullo et al., 2013), and hybrid (Fernández-Méndez et al., 2012; Fernández-Méndez et al., 2013; Castelló Gomar et al., 2014; Gomar et al., 2015; Martínez and Olmedo, 2016) [For a recent discussion about similar ideas in anisotropic Bianchi I LQC spacetimes see Refs. (Gupt and Singh, 2012; Gupt and Singh, 2013; Agullo et al., 2020; Agullo et al., 2020) and references therein.]. In particular, the last two approaches have been widely studied and found that they are all consistent with current cosmological observations (Agullo and Morris, 2015; Bonga and Gupt, 2016; Bonga and Gupt, 2016; de Blas and Olmedo, 2016; Ashtekar and Gupt, 2017; Ashtekar and Gupt, 2017; Castelló Gomar et al., 2017; Zhu et al., 2017; Zhu et al., 2017; Agullo et al., 2018; Elizaga Navascués et al., 2018; Navascues et al., 2018; Wu et al., 2018; Zhu et al., 2018). In addition, within the framework of the dressed metric approach recently it has been also shown that some anomalies from the CMB data (Akrami and Planck collaboration, 2020; Akrami and Planck collaboration, 2020; Schwarz et al., 2016) can be reconciled purely due to the quantum geometric effects (Ashtekar et al., 2020; Agullo et al., 2021; Agullo et al., 2021; Ashtekar et al., 2021).

[1]It has been conjectured using models in string theory that the trans-Planckian problem might never arise (Bedroya and Vafa, 2020), which results on severe constraints on various cosmological models [See (Bedroya et al., 2020; Brandenberger, 2021) for more details].

In addition to the standard LQC, in which the Lorentzian term of the classical Hamiltonian constraint is first expressed in terms of the Euclidean term in the spatially flat Friedmann-Lemaître-Robertson-Walker (FLRW) Universe, and then only the quantization of the Euclidean term is considered, the robustness of the singularity resolution with respect to different quantizations of the classical Hamiltonian constraint in the symmetry reduced spacetimes have been extensively studied. Two notable examples are the so-called modified LQC-I (mLQC-I) and modified LQC-II (mLQC-II) models, which were first proposed by Yang, Ding and Ma more than a decade ago (Yang et al., 2009). In a recent study, Dapor and Liegener (DL) (Dapor and Liegener, 2018a; Dapor and Liegener, 2018b) obtained the expectation values of the Hamiltonian operator in LQG using complexifier coherent states (Thiemann, 2001a; Thiemann and Winkler, 2001b; Thiemann, 2006), adapted to the spatially flat FLRW Universe. Using the non-graph changing regularization of the Hamiltonian advocated by Thiemann (Thiemann, 1998a; Thiemann, 1998b; Giesel and Thiemann, 2007), DL obtained an effective Hamiltonian constraint, which, to the leading order, agrees with the mLQC-I model first obtained in (Yang et al., 2009). Sometimes, this model has also been referred to as the DL model or Thiemann regularized LQC. Strictly speaking, when constructing loops in (Dapor and Liegener, 2018a) DL treated the edge length μ as a free parameter, but in (Yang et al., 2009) it was considered as a specific triad dependent function, the so-called $\overline{\mu}$ scheme (Ashtekar et al., 2006), which is known to be the only possible choice in LQC, and results in physics that is independent from underlying fiducial structures used during quantization, and meanwhile yields a consistent infrared behavior for all matter obeying the weak energy condition (Corichi and Singh, 2008). Lately, the studies of (Dapor and Liegener, 2018a) have been extended to the $\overline{\mu}$ scheme (Assanioussi et al., 2018; Assanioussi et al., 2019a; Assanioussi et al., 2019b; Liegener and Singh, 2019).

In the two modified LQC models, mLQC-I and mLQC-II, since different regularizations of the Lorentzian term were used, the resulting equations become the fourth-order and non-singular quantum difference equations, instead of the second-order difference ones obtained in LQC. In these two models the big bang singularity is also generically resolved and replaced by a quantum bounce. In addition, the inflationary phase can naturally take place with a very high probability (Li et al., 2018a; Li et al., 2018b; Saini and Singh, 2019a; Saini and Singh, 2019b; Li et al., 2019). In addition, the dynamics in LQC and mLQC-II is qualitatively similar in the whole evolution of the Universe, while the one in mLQC-I becomes significantly different from LQC (as well as mLQC-II) in the contracting phase, in which an emergent quasi de Sitter space is present. This implies that the contracting phase in mLQC-I is purely a quantum regime without any classical limit[2].

An important question now is what are the effects of these models and approaches on the CMB observations. The answer to this question requires the knowledge of how the quantum fluctuations propagate on a quantum spacetime in LQC and modified loop cosmological models. In particular, in the framework of the dressed metric approach the power spectra of the cosmological perturbations for both mLQC-I and mLQC-II models were investigated (Li et al., 2020c). In the same framework but restricted only to the mLQC-I model, the power spectra of the cosmological perturbations were studied in (Agullo, 2018). More recently, the hybrid approach was applied to mLQC-I (García-Quismondo and Mena Marugán, 2019; Castelló Gomar et al., 2020; García-Quismondo and Mena Marugán, 2020), for which the time-dependent mass of the perturbations was studied in detail (García-Quismondo et al., 2020). The primordial scalar power spectra obtained in the three models, LQC, mLQC-I and mLQC-II, were also investigated in the hybrid approach (Li et al., 2020a), and found that the relative differences in the amplitudes of the power spectra among the three models could be as large as 2% in the UV regime of the spectra, which is relevant to the current observations. Interestingly, in the above work, differences in primordial power spectra were found between the hybrid and dressed metric approaches in the infra-red and oscillatory regimes in mLQC-I.

In this brief review, we shall focus mainly on the states that are sharply peaked along the classical trajectories, so that the description of the "effective" dynamics of the Universe becomes available (Ashtekar and Singh, 2011; Ashtekar and Barrau, 2015; Bojowald, 2015; Agullo and Singh, 2017), and the questions raised recently in (Kamiński et al., 2020) are avoided. This includes the studies of the "effective" dynamics of the homogeneous and isotropic mLQC-I and mLQC-II models, and their cosmological perturbations in the framework of the dressed metric and hybrid approaches. We shall first clarify the issue regarding the ambiguities in the extension of the effective potential for the scalar perturbations across the quantum bounce, and then pay particular attention to the differences among the three models, LQC, mLQC-I and mLQC-II, and possible observational signals. It is important to note that initial conditions are another subtle and important issue not only in LQC but also in mLQCs. This includes two parts: 1) when to impose the initial conditions, and 2) which kind of initial conditions one can impose *consistently*. To clarify this issue, we discuss it at length by showing the (generalized) comoving Hubble radius in each model and in each of the dressed and hybrid approaches. From this analysis, one can see clearly what initial conditions can and cannot be imposed at a chosen initial time.

The outline of this brief overview is as follows. In **Sec. 2** we consider the effective dynamics of mLQC-I and mLQC-II, and discuss some universal features of their dynamics such as the resolution of big bang singularity. In addition, in this section we also show that for states such that the evolution of the homogeneous Universe was dominated initially at the bounce by the kinetic energy of the inflaton, that is, $\dot{\phi}_B^2 \gg V(\phi_B)$, the post-bounce evolution between the bounce and the reheating can be always divided universally into three different phases: *the bouncing, transition, and slow-roll inflation* [cf. **Figure 1**]. During each of these phases the expansion factor $a(t)$ and the

[2]A similar contracting branch is found in certain anisotropic models in the standard regularization of LQC [see for e.g., (Dadhich et al., 2015)].

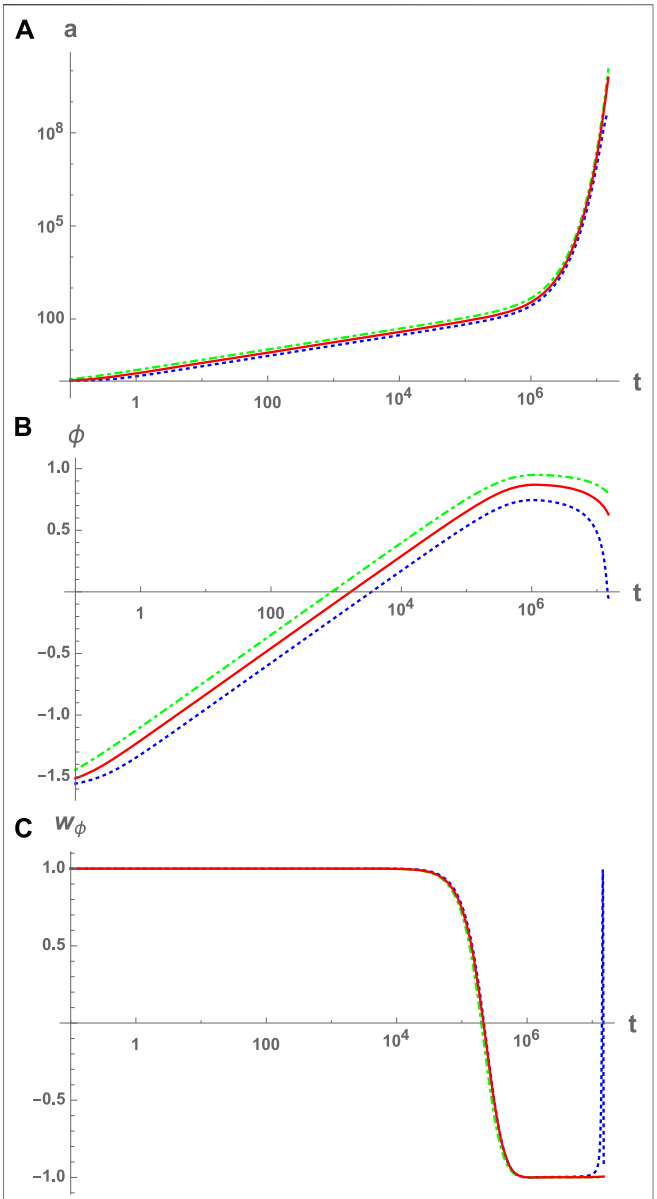

FIGURE 1 | The evolution of the scale factor $a(t)$, the scalar field $\phi(t)$, and the equation w_ϕ of state of the scalar field **(A–C)** in the post-bounce phase are depicted and compared among the three modes, LQC (red solid curves), mLQC-I (blue dotted curves) and mLQC-II (green dot-dashed curves), with the Starobinsky potential. In the last panel, w_ϕ is defined via $w_\phi \equiv P(\phi)/\rho(\phi) = [\dot{\phi}^2 - 2V(\phi)]/[\dot{\phi}^2 + 2V(\phi)]$. The initial condition for the simulation is chosen at the bounce with $\phi_B = -1.6\, m_{pl}, \dot{\phi}_B > 0$(Li et al., 2019).

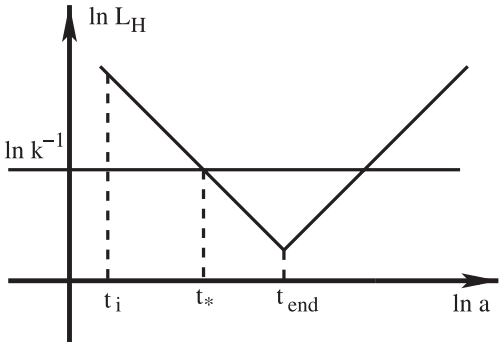

FIGURE 2 | The evolution of the comoving Hubble radius ln (L_H) vs. ln (a) in GR, where t_i denotes the moment of the onset of the slow-roll inflation, t_* the horizon crossing time of a mode with the wavenumber k, and t_{end} the moment that the slow-roll inflation ends.

scalar field $\phi(t)$ can be given analytically. In particular, they are given by **Eqs 2.54–2.55, 2.56–2.57** during the bouncing phase for mLQC-I and mLQC-II, respectively. In this same section, the probabilities of the slow-roll inflation is considered, and shown that it occurs generically. This particular consideration is restricted to the quadratic potential, but is expected to be also true for other cases.

In **Sec. 3**, the cosmological perturbations of mLQC-I and mLQC-II are studied. We discuss initial conditions and the subtle issue of the ambiguity in the choice of the variables π_a^{-2} and π_a^{-1} (present in the effective potential), which correspond to the quadratic and linear inverse of the momentum conjugate to the scale factor. In addition, to understand the issue of initial conditions properly, we first introduce the comoving Hubble radius λ_H^2 and then state clearly how this is resolved in GR [cf. **Figure 2**], and which are the relevant questions in mLQC-I [cf. **Figure 5**] and mLQC-II [cf. **Figure 6**]. From these figures it is clear that the BD vacuum cannot be consistently imposed at the bounce[3], as now some modes are inside the (comoving) Hubble radius while others not. However, the fourth-order adiabatic vacuum may be imposed at this moment for both of these two modified LQC models, as that adopted in LQC (Agullo et al., 2013). In addition, in mLQC-I the de Sitter state given by **Eq. 3.7** [4] can be imposed in the contracting phase as long as t_0 is sufficiently early, so the Universe is well inside the de Sitter phase. On the other hand, in mLQC-II and LQC, the BD vacuum can be imposed in the contracting phase as long as t_0 is sufficiently early, so the Universe becomes so large that the spacetime curvature is very small, and particle creation is negligible. With these in mind, the power spectra obtained in the three models, mLQC-I, mLQC-II and LQC, within the framework of the dressed metric approach were calculated and compared by imposing the initial conditions in the contracting phase. In particular, the spectra can be universally divided into three regimes, the infrared, intermediate and UV. In the infrared and intermediate regimes, the relative differences in the amplitudes of the spectra can be as large as 100% between

[3]It should be noted that anisotropies rise during the contracting phase and generically dominate the earliest stages of the post-bounce of the homogeneous Universe (Gupt and Singh, 2012; Gupt and Singh, 2013; Agullo et al., 2020; Agullo et al., 2020). So, cautions must be taken, when imposing initial conditions at the bounce.

[4]To be distinguished from the BD vacuum described by **Eq. 3.4** we refer to the state described by **Eq. 3.7** as the de Sitter state. The difference between them is due to the term $i/(k\eta)$, which is not negligible in the deep contracting phase of the de Sitter background, as now $|k\eta|$ could be very small. For more details, see the discussions given in **Sec. 3**.A, especially the paragraph after **Eq. 3.9**.

mLQC-I and mLQC-II (the same is also true between mLQC-I and LQC), but in the UV regime such differences get dramatically reduced, which is no larger than 0.1%. Since the modes in the UV regime are the relevant ones to the current observations and also their corresponding power spectra are scale-invariant, so these three models are all consistent with observations.

In **Sec. 4**, the cosmological perturbations of mLQC-I and mLQC-II are studied within the hybrid approach, and the subtleties of the initial conditions are shown in **Figures 8–10**, where **Figures 8, 9** are respectively for the quadratic and Starobinsky potentials in mLQC-I, while **Figure 10** is for the Starobinsky potential in mLQC-II. The case with the quadratic potential in mLQC-II is similar to that of mLQC-I, given by **Figure 8**. From these figures it is clear that imposing the initial conditions now becomes a more delicate issue, and sensitively depends on the potential $V(\phi)$ of the inflaton field. First, in the cases described by **Figures 8**, **9**, all the modes are oscillating during the time $t_i^p < t < t_i$, so one might intend to impose the BD vacuum at the bounce. However, for $t < t_i^p$ the quantity $\Omega_{\rm tot}$ defined in **Eq. 3.9** experiences a period during which it is very large and negative. As a result, particle creation is expected not to be negligible during this period. Then, imposing the BD vacuum at the bounce will not account for these effects, and the resulting power spectra shall be quite different from the case, in which in the deep contracting phase ($t \ll t_B$) the BD vacuum is imposed for mLQC-II and LQC, and the de Sitter state for mLQC-I. On the other hand, in the case described by **Figure 10**, even if the BD vacuum is chosen at the bounce, it may not be quite different from the one imposed in the deep contracting phase, as now in the whole contracting phase all the modes are oscillating, and particle creation is not expected to be important up to the bounce. To compare the results from the three different models, in this section the second-order adiabatic vacuum conditions are chosen in the contracting phase, which is expected not to be much different from the de Sitter state for mLQC-I and the BD vacuum for mLQC-II and LQC, as long as $t_0 \ll t_B$ in all the cases described by **Figures 8–10**. The ambiguities of the choice of π_a^{-2} and π_a^{-1} also occur in this approach, but as far as the power spectra are concerned, different choices lead to similar conclusions (Castelló Gomar et al., 2020). So, in this section only the so-called prescription A is considered. Then, similar conclusions are obtained in this approach regarding the differences among the amplitudes of the power spectra in the three different models. In particular, the relative differences can be as large as 100% between mLQC-I and mLQC-II/LQC, but in the UV regime such differences are reduced to about 2%. A remarkable feature between the two different approaches is also identified: in the infrared and oscillatory regimes, the power spectrum in mLQC-I is suppressed as compared with its counterpart in LQC in the hybrid approach. On the other hand, in the dressed metric approach, the power spectrum in mLQC-I is largely amplified in the infrared regime where its magnitude is as large as of the Planck scale (Agullo, 2018; Li et al., 2020c). The main reason for such differences is that the effective mass in the hybrid approach is strictly positive near the bounce, while it is strictly negative in the dressed metric approach for states that are initially dominated by the kinetic energy of the inflaton (Agullo, 2018; Castelló Gomar et al., 2020; Li et al., 2020c).

The review is concluded in **Sec. 5**, in which we summarize the main conclusions and point out some open questions for future studies.

2 EFFECTIVE QUANTUM DYNAMICS IN MODIFIED LQCS

To facilitate our following discussions, let us first briefly review the standard process of quantization carried out in LQC, from which one can see clearly the similarities and differences among the three models, LQC, mLQC-I and mLQC-II.

2.1 Quantum Dynamics of LQC

The key idea of LQC is to use the fundamental variables and quantization techniques of LQG to cosmological spacetimes, by taking advantage of the simplifications that arise from the symmetries of these spacetimes. In the spatially-flat FLRW spacetime,

$$\begin{aligned} ds^2 &= -N^2(t)dt^2 + q_{ab}(t)dx^a dx^b \\ &\equiv -N^2(t)dt^2 + a^2(t)\delta_{ab}dx^a dx^b, \end{aligned} \tag{2.1}$$

there exists only one degree of freedom, the scale factor $a(t)$, where $N(t)$ is the lapse function and can be freely chosen, given the freedom in reparametrizing t, and $q_{ab}(t)$ denotes the 3-dimensional (3D) spatial metric of the hypersurface $t =$ Constant. In this paper, we shall use the indices $a, b, c, \ldots$ to denote spatial coordinates and $i, j, k, \ldots$ to denote the internal su (2) indices. Repeated indices will represent sum, unless otherwise specified.

In full GR, the gravitational phase space consists of the connection A_a^i and density weighted triad E_i^a. In the present case, the 3D spatial space M has a $\mathbb{R}^3$ topology, from which we can introduce a fiducial cell $\mathfrak{F}$ and restrict all integrations to this cell, in order to avoid some artificial divergences and have a well-defined symplectic structure. Within this cell, we introduce a fiducial flat metric $\mathring{q}_{ab}$ via the relation $q_{ab}(t) = a^2(t)\,\mathring{q}_{ab}$, and then an associated constant orthogonal triad $\mathring{e}_i^a$ and a cotriad $\mathring{\omega}_a^i$. Then, after symmetry reduction A_a^i and E_i^a are given by,

$$A_a^i = c\, v_o^{-1/3}\, \mathring{\omega}_a^i,\ E_i^a = |p|\, v_o^{-2/3} \sqrt{\mathring{q}}\, \mathring{e}_i^a, \tag{2.2}$$

where $|p| = v_o^{2/3} a^2$, $\kappa = 8\pi G/c^4$, v_o denotes the volume of the fiducial cell measured by $\mathring{q}_{ab}$, $\mathring{q}$ is the determinant of $\mathring{q}_{ab}$, and γ is the Barbero-Immirzi parameter whose value can be set to $\gamma \approx 0.2375$ using black hole thermodynamics in LQG (Meissner, 2004). For classical solutions, symmetry reduced connection c is related to time derivative of scale factor as $c = \gamma \dot{a}$, where an over dot denotes a derivative with respect to t for the choice $N = 1$.

The physical triad and cotriad are given by $e_i^a = (\mathrm{sgn\ p})\, |p|^{-1/2} v_o^{1/3}\, \mathring{e}_i^a$ and $\omega_a^i = (\mathrm{sgn\ p})\, |p|^{1/2} v_o^{-1/3}\, \mathring{\omega}_a^i$, where (sgn p) arises because in connection dynamics the phase space contains triads with both orientations. In the following we choose this orientation to be positive and volume of the fiducial cell to be $v_o = 1$. The variables c and p satisfy the communication relation,

$$\{c, p\} = \frac{\kappa\gamma}{3}. \tag{2.3}$$

Then, the gravitational part of the Hamiltonian is a sum of the Euclidean and Lorentzian terms,

$$\mathcal{H}_{\rm grav} = \mathcal{H}^{(E)}_{\rm grav} - (1+\gamma^2)\mathcal{H}^{(L)}_{\rm grav}, \tag{2.4}$$

where, with the choice $N = 1$, these two terms are given, respectively, by

$$\mathcal{H}^{(E)}_{\rm grav} = \frac{1}{2\kappa}\int \mathrm{d}^3x\, \epsilon_{ijk} F^i_{ab} \frac{E^{aj}E^{bk}}{\sqrt{q}}, \tag{2.5}$$

$$\mathcal{H}^{(L)}_{\rm grav} = \frac{1}{\kappa}\int \mathrm{d}^3x\, K^j_{[a} K^k_{b]} \frac{E^{aj}E^{bk}}{\sqrt{q}}, \tag{2.6}$$

where $q = \det(q_{ab}) = a^6\,\mathring{q}$, F^k_{ab} is the field strength of the connection A^i_a, and K^i_a is the extrinsic curvature, given, respectively, by

$$\begin{aligned} F^k_{ab} &\equiv 2\partial_{[a}A^k_{b]} + \epsilon_{ij}{}^k A^i_a A^j_b = c^2 \epsilon_{ij}{}^k\, \mathring{\omega}^i_a\, \mathring{\omega}^j_b, \\ K^i_a &\equiv K_{ab} e^b_i = \frac{e^b_i}{2N}\left(\dot{q}_{ab} - 2D_{(a}N_{b)}\right) = \pm\, \dot{a}\, \mathring{\omega}^i_a. \end{aligned} \tag{2.7}$$

Upon quantization, ambiguities can arise due to different treatments of the Euclidean and Lorentzian terms in the Hamiltonian constraint. In particular, LQC takes the advantage that in the spatially-flat FLRW Universe the Lorentzian part is proportional to the Euclidean part,

$$\mathcal{H}^{(L)}_{\rm grav} = \gamma^{-2}\mathcal{H}^{(E)}_{\rm grav}, \tag{2.8}$$

so that, when coupled to a massless scalar field, the classical Hamiltonian can be rewritten as (Ashtekar et al., 2003; Ashtekar et al., 2006)

$$\begin{aligned} \mathcal{H} &\equiv \mathcal{H}_{\rm grav} + \mathcal{H}_M \\ &= -\frac{1}{2\kappa\gamma^2}\int \mathrm{d}^3x\, \epsilon_{ijk} F^i_{ab} \frac{E^{aj}E^{bk}}{\sqrt{q}} + \mathcal{H}_M, \end{aligned} \tag{2.9}$$

where $\mathcal{H}_M = p_\phi^2/(2\sqrt{q})$, with p_ϕ being the momentum conjugate of ϕ.

The elementary operators in the standard LQC are the triads[5] p and elements of the holonomies given by $\widehat{e^{i\bar{\mu}c/2}}$ of c, where $\bar{\mu} = \sqrt{\Delta l^2_{pl}/|p|}$ with $\Delta \equiv 4\sqrt{3}\pi\gamma$, and Δl^2_{pl} being the minimum non-zero eigenvalue of the area operator, and the Planck length l_{pl} is defined as $l_{pl} \equiv \sqrt{\hbar G}$. However, it is found that, instead of using the eigenket $|p\rangle$ of the area operator p as the basis, it is more convenient to use the eigenket $|v\rangle$ of the volume operator $\hat{v}(\equiv \mathrm{sgn}(p)|p|^{3/2})$, where

$$\hat{v}|v\rangle = \left(\frac{8\pi\gamma}{6}\right)^{3/2}\frac{|v|}{K} l^3_{pl}|v\rangle, \quad \widehat{e^{i\bar{\mu}c/2}}|v\rangle = |v+1\rangle, \tag{2.10}$$

with $K \equiv 2\sqrt{2}\,(3\sqrt{3\sqrt{3}})^{-1}$. Let $\Psi(v,\phi)$ denote the wavefunction in the kinematical Hilbert space of the gravitational field coupled with the scalar field ϕ, we have

$$\begin{aligned} \widehat{\phi}\Psi(v,\phi) &= \phi\Psi(v,\phi), \\ \widehat{p}_\phi\Psi(v,\phi) &= -i\hbar\frac{\partial}{\partial\phi}\Psi(v,\phi), \\ \widehat{|p|^{-3/2}}\Psi(v,\phi) &= \mathcal{B}(v)\Psi(v,\phi), \end{aligned} \tag{2.11}$$

where

$$\begin{aligned} \mathcal{B}(v) &\equiv \left(\frac{6}{8\pi\gamma l^2_{pl}}\right)^{3/2} B(v), \\ B(v) &\equiv \left(\frac{3}{2}\right)^3 K|v|\left||v+1|^{1/3} - |v-1|^{1/3}\right|^3. \end{aligned} \tag{2.12}$$

Then, the equation satisfied by selecting the physical states $\widehat{\mathcal{H}}\Psi(v,\phi) = 0$ can be cast in the form,

$$\begin{aligned} \partial^2_\phi\Psi(v,\phi) = \frac{1}{B(v)}\Big[&C^+(v)\Psi(v+4,\phi) - C^o(v)\Psi(v,\phi) \\ &+ C^-(v)\Psi(v-4,\phi)\Big], \end{aligned} \tag{2.13}$$

where

$$\begin{aligned} C^+(v) &\equiv \frac{3\pi K G}{8}|v+2|\,||v+1| - |v+3||, \\ C^-(v) &\equiv C^+(v-4),\ C^o(v) \equiv C^+(v) + C^-(v). \end{aligned} \tag{2.14}$$

This is the main result of LQC (Ashtekar et al., 2006), which shows that: 1) It is *a second order quantum difference equation with uniform discreteness in volume*, rather than a simple differential equation, a direct consequence of the discrete nature of loop quantum geometry. 2) It provides the evolution of the quantum cosmological wavefunction $\Psi(v,\phi)$, in which *the scalar field serves as a clock*. Thus, once an initial state $\Psi(v,\phi_0)$ is given at the initial moment ϕ_0, the study of the quantum dynamics of LQC can be carried out. It is found that, instead of a big bang singularity, a quantum bounce is generically produced, a result confirmed through extensive numerical simulations (Diener et al., 2014; Diener et al., 2014; Agullo et al., 2017; Diener et al., 2017; Singh, 2018) and an exactly solvable model (Ashtekar et al., 2010). Using this model, one can compute the probability for the quantum bounce which turns out to be unity for an arbitrary superposition of wavefunctions (Craig and Singh, 2013).

For the states sharply peaked around a classical solution, we can obtain "effective" Friedmann and Raychaudhuri (FR) equations, by using the geometric quantum mechanics in terms of the expectation values of the operators $(\widehat{b}, \widehat{v}, \widehat{\phi}, \widehat{p_\phi})$,

$$\dot{b} = \{b, \mathcal{H}\},\ \dot{v} = \{v, \mathcal{H}\}, \tag{2.15}$$

$$\dot{\phi} = \{\phi, \mathcal{H}\},\ \dot{p}_\phi = \{p_\phi, \mathcal{H}\}, \tag{2.16}$$

which take the same forms as their classical ones, but all the quantities now represent their expectation values, $A_I \equiv \langle\widehat{A}_I\rangle$. Then, it was found that the effective Hamiltonian is given by (Ashtekar et al., 2006),

[5]For a modification of LQC based on using gauge-covariant fluxes, see (Liegener and Singh, 2019; Liegener and Singh, 2020).

$$\mathcal{H}_{\text{eff.}} = -\frac{3}{8\pi\gamma^2\overline{\mu}^2 G}|p|^{1/2}\sin^2(\overline{\mu}c) + \frac{1}{2}|p|^{3/2}p_\phi^2, \tag{2.17}$$

which can also be expressed in terms of v and b via the relations $v = |p|^{3/2}$ and $b = c/\sqrt{|p|}$. Then, from **Eqs 2.15**, **2.16** one can find that the "effective" FR equations are given by,

$$H^2 = \frac{8\pi G}{3}\rho\left(1 - \frac{\rho}{\rho_c}\right), \tag{2.18}$$

$$\dot{H} = -4\pi G(\rho + P)\left(1 - \frac{\rho}{\rho_c}\right), \tag{2.19}$$

where

$$H \equiv \frac{\dot{v}}{3v} = \frac{\dot{a}}{a}, \quad \rho_c \equiv \frac{3}{8\pi\lambda a^2\gamma^2 G}, \\ \rho \equiv \frac{\mathcal{H}_M}{v}, \quad P \equiv -\frac{\partial\mathcal{H}_M}{\partial v}, \tag{2.20}$$

and $v = v_o a^3$. Since H^2 cannot be negative, from **Eq. 2.18** we can see that we must have $\rho \le \rho_c$, and at $\rho = \rho_c$ we have $H^2 = 0$, that is, a quantum bounce occurs at this moment. When $\rho \ll \rho_c$, the quantum gravity effects are negligible, whereby the classical relativistic limit is obtained.

For a scalar field ϕ with its potential $V(\phi)$, we have

$$\mathcal{H}_M \equiv \mathcal{H}_\phi = v\left[\frac{p_\phi^2}{2v^2} + V(\phi)\right]. \tag{2.21}$$

Then, from **Eq. 2.16** we find that

$$\dot{\phi} = \frac{p_\phi}{v}, \tag{2.22}$$

$$\dot{p}_\phi = -vV_{,\phi}(\phi). \tag{2.23}$$

In the rest of this review, we shall consider only the states that are sharply peaked around a classical solution, so the above "effective" descriptions are valid, and the questions raised recently in (Kamiński et al., 2020) are avoided.

2.2 Effective Dynamics of mLQC-I

As mentioned in the introduction, an important open issue in LQC is its connection with LQG (Brunnemann and Fleischhack, 2007; Engle, 2007; Brunnemann and Koslowski, 2011). In particular, in LQC the spacetime symmetry is first imposed (in the classical level), before the quantization process is carried out. However, it is well-known that this is different from the general process of LQG (Ashtekar and Lewandowski, 2004; Thiemann, 2007; Rovelli, 2008; Bojowald, 2011; Gambini and Pullin, 2011; Ashtekar and Pullin, 2017), and as a result, different Hamiltonian constraints could be resulted, hence resulting in different Planck scale physics. Though the question of ambiguities in obtaining the Hamiltonian in LQG is still open, based on some rigorous proposals by Thiemann (Thiemann, 1998a; Thiemann, 1998b; Giesel and Thiemann, 2007), various attempts have been carried out, in order to obtain deeper insights into the question.

One of the first attempts to understand this issue was made in (Dapor and Liegener, 2018a), in which the Euclidean and Lorentzian terms given by **Eqs 2.5**, **2.6** are treated differently, by closely following the actual construction of LQG. To be more specific, in the full theory (Ashtekar and Lewandowski, 2004; Thiemann, 2007; Rovelli, 2008; Bojowald, 2011; Gambini and Pullin, 2011; Ashtekar and Pullin, 2017), the extrinsic curvature in the Lorentzian term (2.6) can be expressed in terms of the connection and the volume as

$$K_a^i = \frac{1}{\kappa\gamma^3}\left\{A_a^i, \left\{\mathcal{H}_{\text{grav}}^{(E)}, V\right\}\right\}, \tag{2.24}$$

which once substituted back into **Eq. 2.6** lead to an expression of $\mathcal{H}_{\text{grav}}^{(L)}$ different from that of $\mathcal{H}_{\text{grav}}^{(E)}$ in the standard LQC (see (Yang et al., 2009) for more details). Correspondingly, one is able to obtain the following "effective" Hamiltonian (Yang et al., 2009; Li et al., 2018a),

$$\mathcal{H}_{\text{eff.}}^{\text{I}} = \frac{3v}{8\pi G\lambda^2}\left\{\sin^2(\lambda b) - \frac{(\gamma^2+1)\sin^2(2\lambda b)}{4\gamma^2}\right\} + \mathcal{H}_M. \tag{2.25}$$

Hence, the Hamilton's equations take the form,

$$\dot{v} = \frac{3v\sin(2\lambda b)}{2\gamma\lambda}\left\{(\gamma^2+1)\cos(2\lambda b) - \gamma^2\right\}, \tag{2.26}$$

$$\dot{b} = \frac{3\sin^2(\lambda b)}{2\gamma\lambda^2}\left\{\gamma^2\sin^2(\lambda b) - \cos^2(\lambda b)\right\} - 4\pi G\gamma P, \tag{2.27}$$

where P represents the pressure defined in **Eq. 2.20**. Once the matter Hamiltonian $\mathcal{H}_M$ is specified, together with the Hamiltonian constraint,

$$\mathcal{H} \approx 0, \tag{2.28}$$

Equations 2.26, **2.27** uniquely determine the evolution of the Universe. Using the non-graph changing regularization of the Hamiltonian (Thiemann, 1998a; Thiemann, 1998b; Giesel and Thiemann, 2007), the expectation values of the Hamiltonian operator yield the same "effective" Hamiltonian of **Eq. 2.25** to the leading order (Dapor and Liegener, 2018a).

It has been shown in detail that the big bang singularity is generically replaced by a quantum bounce when the energy reaches its maximum ρ_c^{I} (Yang et al., 2009; Dapor and Liegener, 2018a; Li et al., 2018a; Li et al., 2018b; Li et al., 2019), where

$$\rho_c^{\text{I}} \equiv \frac{\rho_c}{4(1+\gamma^2)}, \tag{2.29}$$

and the Universe is asymmetric with respect to the bounce, in contrast to LQC.

To write **Eqs 2.26**–**2.28** in terms of H, ρ and P, it was found that one must distinguish the pre- and post- bounce phases (Li et al., 2018a). In particular, before the bounce, the modified FR equations take the form (Li et al., 2018a),

$$H^2 = \frac{8\pi G\alpha\rho_\Lambda}{3}\left(1 - \frac{\rho}{\rho_c^{\text{I}}}\right)\left[1 + \left(\frac{1 - 2\gamma^2 + \sqrt{1-\rho/\rho_c^{\text{I}}}}{4\gamma^2\left(1+\sqrt{1-\rho/\rho_c^{\text{I}}}\right)}\right)\frac{\rho}{\rho_c^{\text{I}}}\right], \tag{2.30}$$

$$\frac{\ddot{a}}{a} = -\frac{4\pi\alpha G}{3}\left(\rho + 3P - 2\rho_\Lambda\right) + 4\pi G\alpha P\left(\frac{2 - 3\gamma^2 + 2\sqrt{1-\rho/\rho_c^{\rm I}}}{(1-5\gamma^2)\left(1+\sqrt{1-\rho/\rho_c^{\rm I}}\right)}\right)\frac{\rho}{\rho_c^{\rm I}}$$
$$-\frac{4\pi\alpha G\rho}{3}\left[\frac{2\gamma^2 + 5\gamma^2\left(1+\sqrt{1-\rho/\rho_c^{\rm I}}\right) - 4\left(1+\sqrt{1-\rho/\rho_c^{\rm I}}\right)^2}{(1-5\gamma^2)\left(1+\sqrt{1-\rho/\rho_c^{\rm I}}\right)^2}\right]\frac{\rho}{\rho_c^{\rm I}}, \tag{2.31}$$

where

$$\alpha \equiv \frac{1-5\gamma^2}{\gamma^2+1}, \quad \rho_\Lambda \equiv \frac{\gamma^2\rho_c}{(1+\gamma^2)(1-5\gamma^2)}. \tag{2.32}$$

As $\rho \ll \rho_c^{\rm I}$, **Eqs 2.30**, **2.31** reduce, respectively, to

$$H^2 \approx \frac{8\pi\alpha G}{3}\left(\rho + \rho_\Lambda\right), \tag{2.33}$$

$$\frac{\ddot{a}}{a} \approx -\frac{4\pi\alpha G}{3}\left(\rho + 3P - 2\rho_\Lambda\right). \tag{2.34}$$

These are exactly the FR equations in GR for an ordinary matter field coupled with a positive cosmological constant ρ_Λ, and a modified Newton's constant, $G_\alpha \equiv \alpha G$. For $\gamma \approx 0.2375$, we have $\rho_\Lambda \approx 0.03\rho_{pl}$, which is of the same order as the one deduced conventionally in quantum field theory for the vacuum energy in our Universe. In addition, we also have

$$\left|\frac{G_\alpha}{G} - 1\right|_{\gamma\approx 0.2375} \simeq 0.32 > \frac{1}{8}. \tag{2.35}$$

Finally, we want to emphasize that the minimal energy density of this branch, for which the Hubble rate vanishes, turns out to be negative which can be shown as $\rho_{\rm min} = -\frac{3}{8\pi G\lambda^2} \approx -0.023$. As a result, the necessary condition to generate a cyclic Universe in mLQC-I is the violation of the weak energy condition which is in contrast to the cyclic universes in LQC where the energy density is always non-negative (Li and Singh).

In the post-bounce phase ($t > t_B$), from **Eqs 2.26**–**2.28** we find that (Li et al., 2018a),

$$H^2 = \frac{8\pi G\rho}{3}\left(1 - \frac{\rho}{\rho_c^{\rm I}}\right)\left[1 + \frac{\gamma^2}{\gamma^2+1}\left(\frac{\sqrt{\rho/\rho_c^{\rm I}}}{1+\sqrt{1-\rho/\rho_c^{\rm I}}}\right)^2\right], \tag{2.36}$$

$$\frac{\ddot{a}}{a} = -\frac{4\pi G}{3}\left(\rho + 3P\right) + \frac{4\pi G\rho}{3}\left[\frac{(7\gamma^2+8) - 4\rho/\rho_c^{\rm I} + (5\gamma^2 14 + 8)\sqrt{1-\rho/\rho_c^{\rm I}}}{(\gamma^2+1)\left(1+\sqrt{1-\rho/\rho_c^{\rm I}}\right)^2}\right]\frac{\rho}{\rho_c^{\rm I}}$$
$$+4\pi GP\left[\frac{3\gamma^2 + 2 + 2\sqrt{1-\rho/\rho_c^{\rm I}}}{(\gamma^2+1)\left(1+\sqrt{1-\rho/\rho_c^{\rm I}}\right)}\right]\frac{\rho}{\rho_c^{\rm I}}, \tag{2.37}$$

from which we obtain

$$\dot{H} = \frac{4G\pi\left(P+\rho\right)}{\left(1+\gamma^2\right)}\left(2\gamma^2 + 2\frac{\rho}{\rho_c^{\rm I}} - 3\gamma^2\sqrt{1-\frac{\rho}{\rho_c^{\rm I}}} - 1\right). \tag{2.38}$$

Therefore, regardless of the matter content, the super-inflation (starting at the bounce) will always end at $\rho = \rho_s$, where

$$\rho_s = \frac{\rho_c^{\rm I}}{8}\left(4 - 8\gamma^2 - 9\gamma^4 + 3\gamma^2\sqrt{8 + 16\gamma^2 + 9\gamma^4}\right), \tag{2.39}$$

for which we have $\dot{H}(\rho_s) = 0$.

In the classical limit $\rho/\rho_c^{\rm I} \ll 1$, **Eqs 2.36**, **2.37** reduce, respectively, to

$$H^2 \approx \frac{8\pi G}{3}\rho, \tag{2.40}$$

$$\frac{\ddot{a}}{a} \approx -\frac{4\pi G}{3}\left(\rho + 3P\right), \tag{2.41}$$

whereby the standard relativistic cosmology is recovered.

It is remarkable to note that in the pre-bounce phase the limit $\rho/\rho_c^{\rm I} \ll 1$ leads to **Eqs 2.33**, **2.34** with a modified Newtonian constant G_α, while in the post-bounce the same limits leads to **Eqs 2.40**, **2.41** but now with the precise Newtonian constant G.

2.3 Effective Dynamics of mLQC-II

In LQG, the fundamental variables for the gravitational sector are the su (2) Ashtekar-Barbero connection A_a^i and the conjugate triad E_i^a. When the Gauss and spatial diffeomorphism constraints are fixed, in the homogeneous and isotropic Universe the only relevant constraint is the Hamiltonian constraint, from which we obtain the FR equations, as shown in the previous section. The Hamiltonian in mLQC-II arises from the substitution

$$K_a^i = \frac{A_a^i}{\gamma}, \tag{2.42}$$

in the Lorentzian term (2.6). Then, the following effective Hamiltonian is resulted (Yang et al., 2009),

$$\mathcal{H}_{\rm eff.}^{\rm II} = -\frac{3v}{2\pi G\lambda^2\gamma^2}\sin^2\left(\frac{\lambda b}{2}\right)\left\{1 + \gamma^2\sin^2\left(\frac{\lambda b}{2}\right)\right\} + \mathcal{H}_M, \tag{2.43}$$

from which we find that the corresponding Hamilton's equations are given by,

$$\dot{v} = \frac{3v\sin\left(\lambda b\right)}{\gamma\lambda}\left\{1 + \gamma^2 - \gamma^2\cos\left(\lambda b\right)\right\}, \tag{2.44}$$

$$\dot{b} = -\frac{6\sin^2\left(\frac{\lambda b}{2}\right)}{\gamma\lambda^2}\left\{1 + \gamma^2\sin^2\left(\frac{\lambda b}{2}\right)\right\} - 4\pi G\gamma P = -4\pi G\gamma\left(\rho + P\right). \tag{2.45}$$

It can be shown that the corresponding (modified) FR equations now read (Li et al., 2018b),

$$H^2 = \frac{8\pi G\rho}{3}\left(1 + \gamma^2\frac{\rho}{\rho_c}\right)\left(1 - \frac{(\gamma^2+1)\rho}{\Delta^2\rho_c}\right), \tag{2.46}$$

$$\frac{\ddot{a}}{a} = -\frac{4\pi G}{3}\left(\rho + 3P\right) - \frac{4\pi GP\rho}{\Delta\rho_c}\left[3\left(\gamma^2+1\right) - 2\Delta\right] - \frac{4\pi G\rho^2}{3\Delta^2\rho_c}\left[7\gamma^2 - 1 + \left(5\gamma^2 - 3\right)\left(\Delta - 1\right) - \frac{4\gamma^2\rho}{\rho_c}\right], \tag{2.47}$$

where $\Delta \equiv 1 + \sqrt{1 + \gamma^2\rho/\rho_c}$. From these equations we can see that now the quantum bounce occurs when $\rho = \rho_c^{\rm II}$, at which we have $H = 0$ and $\ddot{a} > 0$, where

$$\rho_c^{\rm II} = 4(\gamma^2 + 1)\rho_c, \tag{2.48}$$

which is different from the critical density ρ_c in LQC as well as the one $\rho_c^{\rm I}$ in mLQC-I. Therefore, the big bang singularity is also resolved in this model, and replaced by a quantum bounce at $\rho = \rho_c^{\rm II}$, similar to LQC and mLQC-I, despite the fact that the bounce in each of these models occurs at a different energy density. However, in contrast to mLQC-I, the evolution of the Universe is symmetric with respect to the bounce, which is quite similar to the standard LQC model.

In addition, similar to the other two cases, now the bounce is accompanied by a phase of super-inflation, i.e., $\dot{H} > 0$, which ends at $\dot{H}(\rho_s) = 0$, but now ρ_s is given by,

$$\rho_s = \frac{\rho_c}{8\gamma^2}\left(3(\gamma^2 + 1)\sqrt{1 + 2\gamma^2 + 9\gamma^4} + 9\gamma^4 + 10\gamma^2 - 3\right). \tag{2.49}$$

For $\gamma = 0.2375$, we find $\rho_s = 0.5132\rho_c^{\rm II}$.

When $\rho \ll \rho_c^{\rm II}$, the modified FR **Eqs 2.46**, **2.47** reduce to,

$$H^2 \approx \frac{8\pi G}{3}\rho, \tag{2.50}$$

$$\frac{\ddot{a}}{a} \approx -\frac{4\pi G}{3}(\rho + 3P), \tag{2.51}$$

which are identical to those given in GR. Therefore, in this model, the classical limit is obtained in both pre- and post-bounce when the energy density ρ is much lower than the critical one $\rho_c^{\rm II}$.

2.4 Universal Properties of mLQC-I/II Models

To study further the evolution of the Universe, it is necessary to specify the matter content $\mathcal{H}_M$. For a single scalar field with its potential $V(\phi)$, the corresponding Hamiltonian takes the form **(2.21)**. As a result, the Hamilton's equations of the matter sector are given by **Eqs 2.22**, **2.23**.

The effective quantum dynamics of LQC, mLQC-I, and mLQC-II were studied in detail recently in (Li et al., 2018b) for a single scalar field with various potentials, including the chaotic inflation, Starobinsky inflation, fractional monodromy inflation, non-minimal Higgs inflation, and inflation with an exponential potential, by using dynamical system analysis. It was found that, while several features of LQC were shared by the mLQC-I and mLQC-II models, others belong to particular models. In particular, in the pre-bounce phase, the qualitative dynamics of LQC and mLQC-II are quite similar, but are strikingly different from that of mLQC-I. In all the three models, the non-perturbative quantum gravitational effects always result in a non-singular post-bounce phase, in which a short period of super-inflation always exists right after the bounce, and is succeeded by the conventional inflation. The latter is an attractor in the phase space for all the three models.

Moreover, similar to LQC (Zhu et al., 2017; Zhu et al., 2017)[6], for the initially kinetic energy dominated conditions,

$$\frac{1}{2}\dot{\phi}_B^2 \gg V(\phi_B), \tag{2.52}$$

it was found that the evolution of the Universe before the reheating is universal. In particular, in the post-bounce phase (between the quantum bounce and the reheating), the evolution can be uniquely divided into three phases: *bouncing, transition and slow-roll inflation*, as shown in **Figure 1** for the Starobinsky potential,

$$V(\phi) = \frac{3m^2}{32\pi G}\left(1 - e^{-\sqrt{16\pi G/3}\phi}\right)^2. \tag{2.53}$$

For other potentials, similar results can be obtained, as long as at the bounce the evolution of the Universe is dominated by the kinetic energy of the inflaton $w(\phi_B) \simeq 1$ (Li et al., 2019; Xiao, 2020).

In each of these three phases, the evolutions of $a(t)$ and $\phi(t)$ can be well approximated by analytical solutions. In particular, during the bouncing phase, they are given by

$$\begin{aligned} a(t) &= \left[1 + 24\pi G\rho_c^{\rm I}\left(1 + \frac{A\gamma^2}{1 + Bt}\right)t^2\right]^{1/6}, \\ \phi(t) &= \phi_{\rm B} \pm \frac{m_{pl}\,\mathrm{arcsinh}\left(\sqrt{24\pi G\rho_c^{\rm I}\left(1 + \frac{C\gamma^2}{1 + Dt}\right)}\,t\right)}{\sqrt{12\pi G\left(1 + \frac{C\gamma^2}{1 + Dt}\right)}}, \end{aligned} \tag{2.54}$$

for mLQC-I model, where the parameters A, B, C and D are fixed through numerical simulations. It was found that the best fitting is provided by (Li et al., 2019),

$$A = C = 1.2, \quad B = 6, \quad D = 2. \tag{2.55}$$

For the mLQC-II model, during the bouncing phase $a(t)$ and $\phi(t)$ are given by

$$\begin{aligned} a(t) &= \left[1 + 24\pi G\rho_c^{\rm II}\left(1 + \frac{A\gamma^2}{1 + Bt}\right)t^2\right]^{1/6}, \\ \phi(t) &= \phi_{\rm B} \pm \frac{m_{pl}\,\mathrm{arcsinh}\left(\sqrt{24\pi G\rho_c^{\rm II}\left(1 + \frac{C\gamma^2}{1 + Dt}\right)}\,t\right)}{\sqrt{12\pi G\left(1 + \frac{C\gamma^2}{1 + Dt}\right)}}, \end{aligned} \tag{2.56}$$

but now with,

[6]In LQC, this universality was first found for the quadratic and Starobinsky potentials (Zhu et al., 2017; Zhu et al., 2017) [see also (Bhardwaj et al., 2019)], and later was shown that they are also true for other potentials, including the power-law potentials (Shahalam et al., 2017; Shahalam, 2018), α-attractor potentials (Shahalam et al., 2018; Shahalam et al., 2020), Monodromy potentials (Sharma et al., 2018), warm inflation (Xiao and Wang, 2020), Tachyonic inflation (Xiao, 2019) and even in Brans-Dicke LQC (Jin et al., 2019; Sharma et al., 2019).

$$A = 2.5, \quad B = 7, \quad C = D = 2. \tag{2.57}$$

In the transition and slow-roll inflationary phases, the functions $a(t)$ and $\phi(t)$ were given explicitly in (Li et al., 2019).

For the initially potential energy dominated cases,

$$\frac{1}{2}\dot{\phi}_B^2 \ll V(\phi_B), \tag{2.58}$$

it was found that such universalities are lost. In particular, for the Starobinsky potential, the potential energy dominated bounce cannot give rise to any period of inflation for both mLQC-I and mLQC-II models, quite similar to what happens in LQC (Bonga and Gupt, 2016; Bonga and Gupt, 2016).

2.5 Probabilities of the Slow-Roll Inflation in mLQC-I/II Models

To consider the probability of the slow-roll inflation in the modified LQC models, let us start with the phase space $\mathbb{S}$ of the modified Friedmann and Klein-Gordon equations, which now is four-dimensional (4D), and consists of the four variables, (v, b) and (ϕ, p_ϕ), from the gravitational and matter sectors, respectively. Using the canonical commutation relations, the symplectic form on the 4D phase space is given by (Singh et al., 2006; Zhang and Ling, 2007; Ashtekar and Sloan, 2011a; Ashtekar and Sloan, 2011b; Corichi and Karami, 2011; Linsefors and Barrau, 2013; Corichi and Sloan, 2014; Chen and Zhu, 2015; Bedic and Vereshchagin, 2019),

$$\Omega = dp_\phi \wedge d\phi + \frac{dv \wedge db}{4\pi G\gamma}. \tag{2.59}$$

However, after taking the effective Hamiltonian constraint into account,

$$\mathcal{C} = 16\pi G\left\{\mathcal{H}_{grav}(v, b) + \frac{p_\phi^2}{2v} + vV(\phi)\right\} \simeq 0, \tag{2.60}$$

where " $\simeq$ " means that the equality holds only on $\overline{\Gamma}$, we can see that the 4D phase space $\mathbb{S}$ reduces to a three-dimensional (3D) hypersurface $\overline{\Gamma}$.

On the other hand, the phase space $\mathbb{S}$ is isomorphic to a 2-dimensional (2D) gauge-fixed surface $\widehat{\Gamma}$ of $\overline{\Gamma}$, which is intersected by each dynamical trajectory once and only once (Ashtekar and Sloan, 2011a; Ashtekar and Sloan, 2011b). From the FR equations, it can be shown that for both mLQC-I and mLQC-II the variable b satisfies the equation (Li et al., 2018a; Li et al., 2018b; Li et al., 2019),

$$\dot{b} = -4\pi G\gamma(\rho + P). \tag{2.61}$$

For any given matter field that satisfies the weak energy condition (Hawking and Ellis, 1973), we have $\rho + P > 0$, so the function b is monotonically decreasing. Then, a natural parameterization of this 2D surface is $b =$ constant, say, b_0. Hence, using the Hamiltonian constraint (2.60) we find

$$p_\phi^{\mathrm{A}} = v\left\{-2\left[\widehat{\mathcal{H}}^{\mathrm{A}}_{grav} + V(\phi)\right]\right\}^{1/2}, \tag{2.62}$$

where A = I, II, and

$$\widehat{\mathcal{H}}^{\mathrm{A}}_{grav} \equiv v^{-1}\mathcal{H}^{\mathrm{A}}_{grav}(v, b_0). \tag{2.63}$$

On the other hand, from **Eqs 2.25**, **2.43** we find that $\widehat{\mathcal{H}}^{\mathrm{A}}_{grav} = \widehat{\mathcal{H}}^{\mathrm{A}}_{grav}(b_0) =$ constant on $\widehat{\Gamma}$. Thus, we find

$$dp_\phi^{\mathrm{A}}|_{\widehat{\Gamma}} = \frac{p_\phi^{\mathrm{A}}}{v}dv - \frac{v^2 V_{,\phi}}{p_\phi}d\phi. \tag{2.64}$$

Inserting this expression into **Eq. 2.59**, we find that the pulled-back symplectic structure $\widehat{\Omega}$ reads

$$\widehat{\Omega}^{\mathrm{A}}\Big|_{\widehat{\Gamma}} = \left\{-2\left[\widehat{\mathcal{H}}^{\mathrm{A}}_{grav}(b_0) + V(\phi)\right]\right\}^{1/2} d\phi \wedge dv, \tag{2.65}$$

from which we find that the Liouville measure $d\widehat{\mu}_L$ on $\widehat{\Gamma}$ is given by

$$d\widehat{\mu}_L^{\mathrm{A}} = \left\{-2\left[\widehat{\mathcal{H}}^{\mathrm{A}}_{grav}(b_0) + V(\phi)\right]\right\}^{1/2} d\phi dv. \tag{2.66}$$

Note that $d\widehat{\mu}_L^{\mathrm{A}}$ does not depend on v, so that the integral with respect to dv is infinite. However, this divergency shall be canceled when calculating the probability, as it will appear in both denominator and numerator. Therefore, the measure for the space of physically distinct solutions can be finally taken as

$$d\omega^{\mathrm{A}} = \left\{-2\left[\widehat{\mathcal{H}}^{\mathrm{A}}_{grav}(b_0) + V(\phi)\right]\right\}^{1/2} d\phi, \tag{2.67}$$

so that the 2D phase space $\widehat{\Gamma}$ is further reduced to an interval $\phi \in (\phi_{\min}, \phi_{\max})$. It should be noted that such a defined measure depends explicitly on b_0, and its choice in principle is arbitrary. However, in loop cosmology there exists a preferred choice, which is its value at the quantum bounce $b_0 = b(t_B)$ (Ashtekar and Sloan, 2011a; Ashtekar and Sloan, 2011b). With such a choice, the probability of the occurrence of an event E becomes

$$P(E) = \frac{1}{\mathcal{D}}\int_{\mathcal{I}(E)}\left\{-2\left[\widehat{\mathcal{H}}^{\mathrm{A}}_{grav}(b_B) + V(\phi)\right]\right\}^{1/2} d\phi, \tag{2.68}$$

where $\mathcal{I}(E)$ is the interval on the ϕ_B-axis, which corresponds to the physically distinct initial conditions in which the event E happens, and $\mathcal{D}$ is the total measure

$$\mathcal{D} \equiv \int_{\phi_{\min}}^{\phi_{\max}}\left\{-2\left[\widehat{\mathcal{H}}^{\mathrm{A}}_{grav}(b_B) + V(\phi)\right]\right\}^{1/2} d\phi. \tag{2.69}$$

Once the probability is properly defined, we can calculate it in different models of the modified LQCs. In LQC (Ashtekar and Sloan, 2011a; Ashtekar and Sloan, 2011b), the calculations were carried out for the quadratic potential. In order to compare the results obtained in different models, let us consider the same potential. Then, for the mLQC-I model it was found that (Li et al., 2019)

$$\sin\left(\lambda b_B^{\mathrm{I}}\right) = \sqrt{\frac{1}{2\gamma^2 + 2}}, \ \sin\left(2\lambda b_B^{\mathrm{I}}\right) = \frac{\sqrt{2\gamma^2 + 1}}{\gamma^2 + 1},$$

$$p_\phi^{\rm I} = \nu\left(2\rho_c^{\rm I} - 2V\right)^{\frac{1}{2}}, \quad d\omega^{\rm I} = \left(2\rho_c^{\rm I} - 2V\right)^{\frac{1}{2}} d\phi, \tag{2.70}$$

so that the probability for the desired slow-roll not to happen is,

$$P^{\rm I}\,(\text{not realized}) \lesssim \frac{\int_{-5.158}^{0.917} d\omega^{\rm I}}{\int_{-\phi_{\rm max}^{\rm I}}^{\phi_{\rm max}^{\rm I}} d\omega^{\rm I}} \simeq 1.12 \times 10^{-5}, \tag{2.71}$$

where $\phi_{\rm max}^{\rm I} = 3.49 \times 10^5\, m_{pl}$.

In mLQC-II, following a similar analysis, it can be shown that the probability for the desired slow-roll not to happen is (Li et al., 2019),

$$P^{\rm II}\,(\text{not realized}) \lesssim 2.62 \times 10^{-6}. \tag{2.72}$$

Note that in LQC the probability for the desired slow roll inflation not to occur is (Ashtekar and Sloan, 2011a; Ashtekar and Sloan, 2011b),

$$P^{\rm LQC}\,(\text{not realized}) \lesssim 2.74 \times 10^{-6}, \tag{2.73}$$

which is smaller than that for mLQC-I and slightly larger than the one for mLQC-II. However, it is clear that the desired slow-roll inflation is very likely to occur in all the models, including the two modified LQC ones.

3 PRIMORDIAL POWER SPECTRA OF MODIFIED LQCS IN DRESSED METRIC APPROACH

As mentioned above, in the literature there exist several approaches to investigate the inhomogeneities of the Universe. Such approaches can be generalized to the modified LQC models, including mLQC-I and mLQC-II. In this section we shall focus ourselves on cosmological perturbations in the framework of mLQCs following the dressed metric approach (Agullo et al., 2012; Agullo et al., 2013; Agullo et al., 2013), while in the next section we will be following the hybrid approach (Fernández-Méndez et al., 2012; Fernández-Méndez et al., 2013; Castelló Gomar et al., 2014; Gomar et al., 2015; Martínez and Olmedo, 2016). We shall restrict ourselves to the effective dynamics, as we did with the homogeneous background in the last section. Such investigations in general include two parts: 1) the initial conditions; and 2) the dynamical evolutions of perturbations. In the framework of effective dynamics, the latter is a second-order ordinary differential equation in the momentum space, so in principle once the initial conditions are given, it uniquely determines the cosmological (scalar and tensor) perturbations.

However, the initial conditions are a subtle issue, which is true not only in LQC but also in mLQCs. This is mainly because that in general there does not exist a preferred initial time and state for a quantum field in an arbitrarily curved space-time (Birrell and Davies, 1982; Wald, 1994; Mukhanov and Winitzki, 2007; Parker and Toms, 2009). If the Universe is sufficiently smooth and its evolution is sufficiently slow, so that the characteristic scale of perturbations is much larger than the wavelengths of all the relevant modes, a well justified initial state can be defined: *the BD vacuum*. This is precisely the initial state commonly adopted in GR at the beginning of the slow-roll inflation, in which all the relevant perturbation modes are well inside *the comoving Hubble radius* (Baumann, 2009) [cf. **Figure 2**].

However, in LQC/mLQCs, especially near the bounce, the evolution of the background is far from "slow," and its geometry is also far from the de Sitter. In particular, for the perturbations during the bouncing phase, the wavelengths could be larger, equal, or smaller than the corresponding characteristic scale, as it can be seen, for example, from **Figure 5**. Thus, it is in general impossible to assume that the Universe is in the BD vacuum state at the bounce (Agullo et al., 2013; Ashtekar and Gupt, 2017; Ashtekar and Gupt, 2017; Zhu et al., 2017; Zhu et al., 2017). Therefore, in the following let us first elaborate in more details about the subtle issues regarding the initial conditions.

3.1 Initial Conditions for Cosmological Perturbations

The initial conditions for cosmological perturbations in fact consists of two parts: when and which? However, both questions are related to each other. In LQC literature, for cosmological perturbations, two different moments have been chosen so far in the dressed and hybrid approaches: 1) the remote past in the contracting phase (Li et al., 2020c) and 2) the bounce (Agullo et al., 2013; Ashtekar and Gupt, 2017; Ashtekar and Gupt, 2017). To see which conditions we need to impose at a given moment, let us first recall how to impose the initial conditions in GR, in which the scalar perturbations are governed by the equation,

$$v_k'' + \left(k^2 - \frac{z''}{z}\right) v_k = 0, \tag{3.1}$$

where k denotes the comoving wave number, and $z \equiv a\dot{\delta\phi}/H$, with $\delta\phi$ being the scalar field perturbations, $\phi = \bar{\phi}(t) + \delta\phi(t, x)$. A prime denotes a derivative with respect to the conformal time η, while an over dot denotes a derivative with respect to the cosmic time t, where $d\eta = dt/a(t)$. The standard choice of the initial sate is the Minkowski vacuum of an incoming observer in the far past, $k \gg aH$ [cf. **Figure 2**]. In this limit, **Eq. 3.1** becomes $v_k'' + k^2 v_k = 0$, which has the solution,

$$v_k \simeq \frac{\alpha_k}{\sqrt{2k}} e^{-ik\eta} + \frac{\beta_k}{\sqrt{2k}} e^{ik\eta}, \tag{3.2}$$

where α_k and β_k are two integration constants, and must satisfy the normalized condition,

$$v_k^* v_k' - v_k^{*\prime} v_k = -i. \tag{3.3}$$

If we further require *the vacuum to be the minimum energy state*, a unique solution exists, which is given by $\alpha_k = 1$, $\beta_k = 0$, that is,

$$\lim_{k \gg aH} v_k \simeq \frac{1}{\sqrt{2k}} e^{-ik\eta}, \tag{3.4}$$

which is often referred to as *the BD vacuum* (Baumann, 2009).

Consider the de Sitter space as the background, we have $a(\eta) = 1/(-\eta H)$, and $z''/z = a''/a = 2/L_H^2$, where $L_H \equiv 1/(aH) = -\eta$ is the corresponding comoving Hubble radius. Then, **Eq. 3.1** reads,

$$v_k'' + \left(\frac{1}{\lambda^2} - \frac{2}{L_H^2}\right)v_k = 0, \tag{3.5}$$

where $\lambda\ (\equiv 1/k)$ denotes the comoving wavelength. The above equation has the following exact solutions,

$$v_k = \frac{\alpha_k}{\sqrt{2k}}e^{-ik\eta}\left(1 - \frac{i}{k\eta}\right) + \frac{\beta_k}{\sqrt{2k}}e^{ik\eta}\left(1 + \frac{i}{k\eta}\right). \tag{3.6}$$

It is clear that on scales much smaller than the comoving Hubble radius ($\lambda \ll L_H$), v_k is oscillating with frequency k and constant amplitude, given by **Eq. 3.2**. Then, setting $(\alpha_k, \beta_k) = (1, 0)$ we find that **Eq. 3.6** reduces to

$$v_k = \frac{1}{\sqrt{2k}}e^{-ik\eta}\left(1 - \frac{i}{k\eta}\right). \tag{3.7}$$

Note that if the initial time t_i is chosen sufficiently small, i.e., $t_i \ll t_{\rm end}$ or $|k\eta| \gg 1$, all the modes are inside the comoving Hubble radius L_H [cf. **Figure 2**], and the BD vacuum (3.4) becomes a natural choice.

However, on the scales much larger than the comoving Hubble radius ($\lambda \gg L_H$), the k^2 term is negligible compared to the squeezing term, z''/z, and as a result, the fluctuations will stop oscillating and the amplitude of v_k starts to increase, yielding

$$v_k \simeq z(\eta). \tag{3.8}$$

As shown in **Figure 2**, if the initial time t_i is chosen to be sufficiently early, all the currently observed modes $k_{\rm ph} \in (0.1, 1000) \times k_0^*$ will be well inside the comoving Hubble radius at $t = t_i$, so the mode function v_k can be well approximately given by **Eq. 3.4**, which is the well-known zeroth order adiabatic state, where $k_0^* = 0.002\ {\rm Mpc}^{-1}$ and $k_{ph}(t) \equiv k/a(t)$ (Bennett et al., 1996; Banday et al., 1996; Komatsu et al., 2011; Larson et al., 2011; Ade and PLANCK Collaboration, 2016; Aghanim and PLANCK Collaboration, 2020).

In modified LQC models, the mode function v_k satisfies the following modified equation,

$$v_k'' + \Omega_{\rm tot}^2(\eta, k)v_k = 0, \tag{3.9}$$

where $\Omega_{\rm tot}^2(\eta, k)$ depends on the homogeneous background and the inflation potential $V(\phi)$, so it is model-dependent. Therefore, the choice of the initial conditions will depend on not only the modified LQC models to be considered but also the moment at which the initial conditions are imposed.

One of the main reasons to choose the remote past in the contracting phase as the initial time for perturbations is that at such time either the background is well described by the de Sitter space (mLQC-I) or the expansion factor $a(t)$ becomes so large that the curvature of the background is negligible (mLQC-II and LQC), so imposing the BD vacuum for mLQC-II and LQC and the de Sitter state given by **Eq. 3.7** for mLQC-I at this moment is well justified. It should be noted that the reason to refer to the state described by **Eq. 3.7** as *the de Sitter state* is the following: In the slow-roll inflation, the homogeneous and isotropic Universe is almost de Sitter, as the Hubble parameter $H \equiv \dot{a}/a$ is almost a constant, so we have $a(\eta) \simeq 1/(-H\eta)$. For $t_i \ll t_{\rm end}$ we have $a(\eta) \ll 1$, and $|\eta k| \simeq |H\eta| \gg 1$, so the choice $(\alpha_k\, \beta_k) = (1, 0)$ will lead **Eq. 3.7** directly to **Eq. 3.4** at the onset of the slow-roll inflation [cf. **Figure 2**]. However, in the deep contracting phase of the same de Sitter space, now the Universe is very large, that is, $a(\eta) \gg 1$, so we must have $|H\eta| \ll 1$ and $|\eta k| \simeq |k/H_\Lambda| a^{-1}(\eta)$, which can be very small in sufficiently early times of the contracting phase, so the terms $i/(k\eta)$ in **Eq. 3.6** now cannot be neglected. To distinguish this case from the one described by **Eq.3.4**, In this review we refer the state described by **Eq. 3.7** with the term $i/(k\eta)$ not being negligible as the de Sitter state, while the state described by **Eq. 3.4** is still called the BD vacuum state, or simply the BD vacuum.

On the other hand, if the initial time is chosen to be at the bounce, cautions must be taken on what initial conditions can be imposed *consistently*. In particular, if at this moment some modes are inside the comoving Hubble radius and others are not, it is clear that in this case imposing the BD vacuum at the bounce will lead to inconsistencies. In addition, there also exist the cases in which particle creation in the contracting phase is not negligible, then it is unclear how a BD vacuum can be imposed at the bounce, after the Universe is contracting for such a long time before the bounce. Thus, in these cases other initial conditions need to be considered, such as the fourth-order adiabatic vacuum (Agullo et al., 2013; Ashtekar and Gupt, 2017; Ashtekar and Gupt, 2017; Zhu et al., 2017; Zhu et al., 2017).

With the above in mind, in the following we turn to consider power spectra of the cosmological perturbations.

3.2 Power Spectra of Cosmological Perturbations

Since the evolutions of the effective dynamics of the homogeneous backgrounds for mLQC-I and mLQC-II are different, in this subsection let us first consider the case of mLQC-I and then mLQC-II. To compare the results with those obtained in LQC, at the end of this subsection, we also discuss the LQC case.

3.2.1 mLQC-I

For mLQC-I, the power spectrum of the cosmological scalar perturbations was first studied in (Agullo, 2018) for the quadratic ϕ^2 potential, and re-examined in (Li et al., 2020c). In the terminology used in (Agullo, 2018), it was found that the corresponding mode function $v_k\ (\equiv q_k/a)$ satisfies **Eq. 3.9** with

$$\begin{aligned} \Omega_{\rm tot}^2 &= k^2 - \frac{a''}{a} + \mathfrak{N}_-, \quad r \equiv \frac{24\pi G\dot{\phi}^2}{\rho}, \\ \mathfrak{N}_- &\equiv a^2\left[V(\phi)r - 2V_{,\phi}(\phi)\sqrt{r} + V_{,\phi\phi}(\phi)\right], \end{aligned} \tag{3.10}$$

where $r = 24\pi G\dot{\phi}^2/\rho$ and $V(\phi)$ denotes the scalar field potential.

It should be noted that, when generalizing the classical expression of the function $\mathfrak{N}_-$ defined in **Eq. 3.10** to its corresponding quantum mechanics operator, there exists ambiguities. In fact, classically $\mathfrak{N}_-$ only coincides with $\Omega_{\rm Q}^2$ in

the expanding phase. The latter is a function of the phase space variables which is explicitly given by (Agullo et al., 2013; Agullo, 2018; Agullo et al., 2018; Li et al., 2020c),

$$\Omega_Q^2 = 3\kappa\frac{p_\phi^2}{a^4} - 18\frac{p_\phi^4}{a^6\pi_a^2} - 12a\frac{p_\phi}{\pi_a}V_{,\phi} + a^2V_{,\phi\phi}, \tag{3.11}$$

where π_a is the moment conjugate to a, and given by one of Hamilton's dynamical equations,

$$\pi_a = -\frac{3a^2}{4\pi G}H, \tag{3.12}$$

with the choice of the lapse function $N = 1$. Therefore, $\pi_a < 0$ ($\pi_a > 0$) corresponds to $H > 0$ ($H < 0$). At the quantum bounce we have $H(t_B) = 0$, so that $\pi_a(t_B) = 0$. Then, Ω_Q^2 defined by **Eq. 3.11** diverges at the bounce. Hence, from the Friedmann equation, $H^2 = (8\pi G/3)\rho$, we find that

$$\frac{1}{\pi_a^2} = \frac{2\pi G}{3a^4\rho}, \quad \frac{1}{\pi_a} = \pm\sqrt{\frac{2\pi G}{3a^4\rho}}, \tag{3.13}$$

where "-" corresponds to $H > 0$, and "+" to $H < 0$. Then, a direct generalization leads to (Li et al., 2020c),

$$\Omega_Q^2 = \begin{cases} \mathfrak{A}_-, & H \geq 0, \\ \mathfrak{A}_+, & H \leq 0, \end{cases} \tag{3.14}$$

where

$$\mathfrak{A}_\pm \equiv a^2\left[V(\phi)r \pm 2V_{,\phi}(\phi)\sqrt{r} + V_{,\phi\phi}(\phi)\right]. \tag{3.15}$$

It should be noted that in (Agullo, 2018) only the function $\mathfrak{A}_-$ was chosen over the whole process of the evolution of the Universe. The same choice was also adopted in (Agullo et al., 2018; Agullo et al., 2021; Agullo et al., 2021).

In addition, $\mathfrak{A}$ defined by **Eq. 3.13** is not continuous across the bounce, as the coefficient $2V_{,\phi}(\phi)\sqrt{r}$ in general does not vanish at the bounce. In (Zhu et al., 2017; Zhu et al., 2017; Navascues et al., 2018) $\mathfrak{A}_-$ appearing in **Eq. 3.10** was replaced by $U(\phi)(\equiv\Omega_+^2)$ over the whole process of the evolution of the homogeneous Universe, where

$$\Omega_\pm^2 \equiv a^2\left[\mathfrak{F}^2V(\phi) \pm 2\mathfrak{F}V_{,\phi}(\phi) + V_{,\phi\phi}(\phi)\right], \tag{3.16}$$

and $\mathfrak{F} \equiv (24\pi G/\rho)^{1/2}\dot{\phi}$.

Another choice was introduced in (Li et al., 2020c), which was motivated from the following considerations. The functions $\Omega_\pm^2$ defined above are not continuous across the bounce, quite similar to $\mathfrak{A}_\pm$. However, if we introduce the quantity Ω^2 as,

$$\Omega^2 = a^2\left[\mathfrak{F}^2V(\phi) + 2\Theta(b)\mathfrak{F}V_{,\phi}(\phi) + V_{,\phi\phi}(\phi)\right], \tag{3.17}$$

to replace $\mathfrak{A}_-$ in **Eq. 3.10**, it could be continuous across the bounce by properly choosing $\Theta(b)$. In particular, the variable $b(t)$ satisfies **Eq. 2.61** (Li et al., 2018a; Li et al., 2018b; Li et al., 2019)[7],

[7]It is interesting to note that **Eq. 2.61** holds not only in mLQC-I, but also in LQC and mLQC-II.

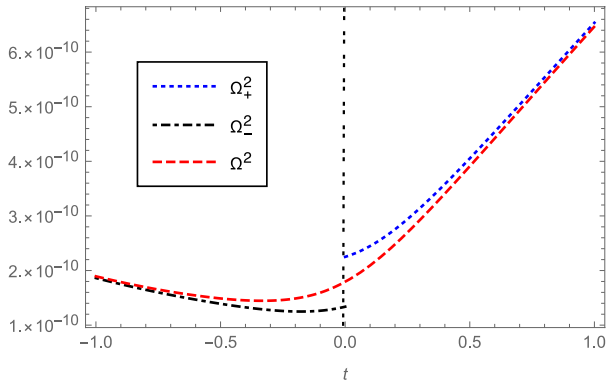

FIGURE 3 | The potential terms Ω_+^2 and Ω_-^2 are compared with their smooth extension Ω^2 across the bounce in mLQC-I for the quadratic potential $V(\phi) = \frac{1}{2}m^2\phi^2$(Li et al., 2020c).

from which we can see that $b(t)$ is always a monotonically decreasing function for any matter that satisfies the weak energy condition (Hawking and Ellis, 1973). Moreover, one can construct a step-like function of b with the bounce as its symmetry axis (Li et al., 2018a; Li et al., 2018b; Li et al., 2019). Therefore, if we define $\Theta(b)$ as

$$\Theta(b) = 1 - 2(1+\gamma^2)\sin^2(\lambda b), \tag{3.18}$$

it behaves precisely as a step function, so that Ω^2 smoothly connects $\Omega_\pm^2$ across the bounce, as shown in **Figure 3**.

In addition to the above choices, motivated by the hybrid approach (Fernández-Méndez et al., 2012; Fernández-Méndez et al., 2013; Castelló Gomar et al., 2014; Gomar et al., 2015; Martínez and Olmedo, 2016), the following replacements for π_a^{-2} and π_a^{-1} in **Eq. 3.11** were also introduced in (Li et al., 2020c),

$$\frac{1}{\pi_a^2} \to \frac{64\pi^2G^2\lambda^2\gamma^2}{9a^4\mathcal{D}}, \tag{3.19}$$

$$\frac{1}{\pi_a} \to -\frac{8\pi G\lambda\gamma\Theta(b)}{3a^2\mathcal{D}^{1/2}}, \tag{3.20}$$

where

$$\mathcal{D} \equiv (1+\gamma^2)\sin^2(2\lambda b) - 4\gamma^2\sin^2(\lambda b). \tag{3.21}$$

Such obtained Ω_Q^2 was referred to as $\Omega_{\rm eff}^2$ in (Li et al., 2020c), and in **Figure 4**, we show the differences among Ω^2, $\Omega_{\rm eff}^2$ and the quantity a''/a, from which one can see that the term a''/a dominates the other two terms over the whole range $t/t_{pl} \in (-8, 10^4)$.

To study the effects of the curvature term, let us first introduce the quantity,

$$k_B^1 = \left(\frac{a''}{a}\right)^{1/2}\Big|_{t=t_B} \approx 1.60, \tag{3.22}$$

which is much larger than other two terms Ω^2 and $\Omega_{\rm eff}^2$, where $\Omega^2(t_B) = 1.75\times10^{-10}$ and $\Omega_{\rm eff}^2(t_B) = 0.006$. Therefore, the differences between Ω^2 and $\Omega_{\rm eff}^2$ near the bounce are highly

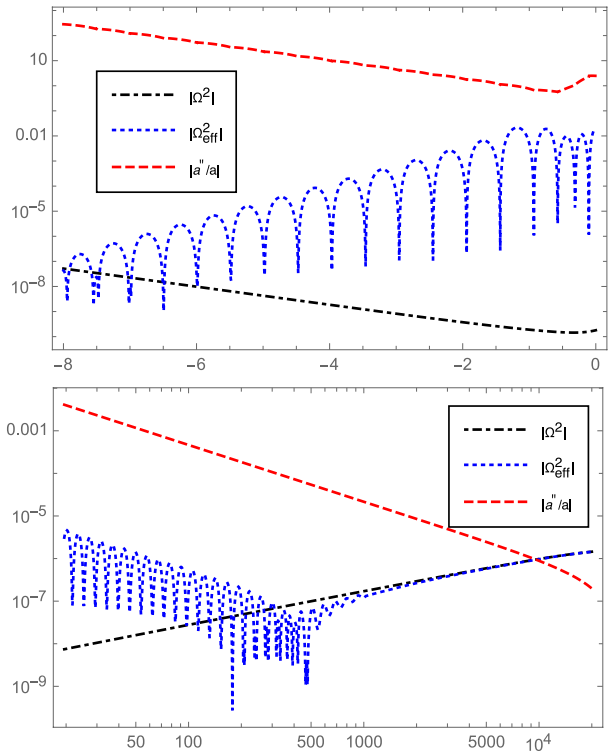

FIGURE 4 | The potential terms Ω^2 and $\Omega^2_{\rm eff}$ are compared with the curvature term a''/a in mLQC-I near the bounce and the preinflationary regime for the quadratic potential $V(\phi) = \frac{1}{2}m^2\phi^2$(Li et al., 2020c).

diluted by the background. On the other hand, in the post-bounce phase, Ω^2 and $\Omega^2_{\rm eff}$ coincide after $t/t_{pl} \simeq 10^4$, while near the onset of the inflation their amplitudes first become almost equal to that of the curvature term, and then quickly exceeds it during the slow-roll inflation, as we can see from **Figure 4**.

From **Figure 4** we can also see that the difference between Ω^2 and $\Omega^2_{\rm eff}$ lies mainly in the region near the bounce. However, as the curvature term a''/a overwhelmingly dominates in this region, it is usually expected that the impact of the different choices of Ω^2 on the power spectrum might not be very large (Agullo et al., 2013; Agullo, 2018; Agullo et al., 2018). However, in (Li et al., 2020c), it was found that the relative difference in the magnitude of the power spectrum in the IR and oscillating regimes could be as large as 10%, where the relative difference is defined as,

$$\mathcal{E} \equiv 2\left|\frac{\mathcal{P}_1 - \mathcal{P}_2}{\mathcal{P}_1 + \mathcal{P}_2}\right|. \tag{3.23}$$

However, the power spectra obtained from Ω^2 and $\Omega^2_{\pm}$ are substantially different even in the UV regime due to the (tiny) difference between $\Omega^2_{\pm}$ at the bounce, see Fig. 14 given in (Li et al., 202c). In fact, the difference is so large that the power spectrum calculated from $\Omega^2_{\pm}$ is essentially already ruled out by current observations.

With the clarification of the ambiguities caused by the quantum mechanical generalization of the function $\mathfrak{N}_-$ defined in **Eq. 3.10**, now let us turn to the issue of the initial conditions, for which we consider only two representative potentials, the quadratic and Starobinsky, given explicitly by

$$V = \begin{cases} \dfrac{1}{2}m^2\phi^2, & \text{quadratic,} \\ \dfrac{3m^2}{32\pi G}\left(1 - e^{-\sqrt{16\pi G/3}\,\phi}\right)^2, & \text{Starobinsky.} \end{cases} \tag{3.24}$$

In mLQC-I, the evolution of the effective (quantum) homogeneous Universe is asymmetric with respect to the bounce (Dapor and Liegener, 2018a; Li et al., 2018a; Li et al., 2018b; Li et al., 2019). In particular, before the bounce ($t < t_B$), the Universe is asymptotically de Sitter, and only very near the bounce (about several Planck seconds), the Hubble parameter H which is negative in the pre-bounce regime suddenly increases to zero at the bounce. Then, the Universe enters a very short super-acceleration phase $\dot{H} > 0$ (super-inflation) right after the bounce, which lasts until $\rho \simeq \rho^{\rm I}_c/2$, where $\dot{H}(t)_{\rho \simeq \frac{1}{2}\rho^{\rm I}_c} = 0$. Afterward, for a kinetic energy dominated bounce $\dot{\phi}^2_B \gg V(\phi_B)$, it takes about $10^4 \sim 10^6$ Planck seconds before entering the slow-roll inflation (Li et al., 2018a; Li et al., 2018b; Li et al., 2019). Introducing the quantity,

$$\lambda^2_H \equiv \frac{a}{a'' - a\mathfrak{N}_-} = -\frac{1}{m_{\rm eff}}, \tag{3.25}$$

where $m_{\rm eff}$ is the effective mass of the modes, from **Eq. 3.10** we find that

$$\Omega^2_{\rm tot} = \frac{1}{\lambda^2} - \frac{1}{\lambda^2_H} = \begin{cases} > 0, & \lambda^2_H > \lambda^2, \\ < 0, & 0 < \lambda^2_H < \lambda^2, \\ > 0, & \lambda^2_H < 0, \end{cases} \tag{3.26}$$

where λ ($\equiv k^{-1}$) denotes the comoving wavelength of the mode k, as mentioned above. Note that such a defined quantity λ^2_H becomes negative when the effective mass is positive. In **Figure 5**, we plot λ^2_H schematically for the quadratic and the Starobinsky potentials with the mass of the inflaton set to $1.21 \times 10^{-6}\, m_{\rm pl}$ and $2.44 \times 10^{-6}\, m_{\rm pl}$ respectively. The initial conditions for the background evolution are set as follows: for the quadratic potential, the inflaton starts with a positive velocity on the right wing of the potential and for the Starobinsky potential the inflaton is released from the left wing of the potential with a positive velocity. For both potentials, the initial conditions are set at the bounce which is dominated by the kinetic energy of the inflaton field. The same mass parameters and similar initial conditions are also used in the following figures where the comoving Hubble radius is plotted schematically. In **Figure 5**, the moments t_H and t_i are defined, respectively, by $a''(t_H) = a''(t_i) = 0$, so t_i represents the beginning of the inflationary phase, and during the slow-roll inflation (Region III), we have $\lambda^2_H \approx L^2_{\rm H}/2 \simeq 1/(2a^2H^2)$, which is exponentially decreasing, and all the modes observed today were inside the comoving Hubble radius at $t = t_i$. Between the times t_H and t_i, λ^2_H is negative, and $\Omega^2_{\rm tot}$ is strictly positive. Therefore, during this period the mode functions are oscillating, while during the epoch between t_B and t_H, some modes ($k^{-2} > k^{-2}_B$) are inside the comoving Hubble radius, and others ($k^{-2} < k^{-2}_B$) are outside it

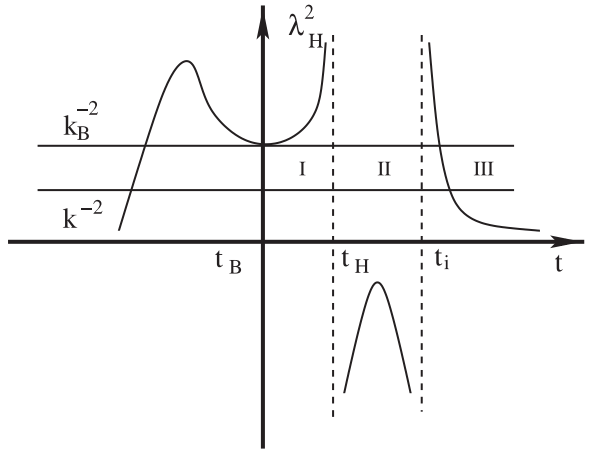

FIGURE 5 | Schematic plot of λ_H^2 defined by **Eq. 3.25** vs. t for mLQC-I in the dressed metric approach for the quadratic and the Starobinsky potentials, where $a''(t_H) = 0$ and $a''(t_i) = 0$ with t_i being the starting time of the inflationary phase. During the slow-roll inflation, we have $\lambda_H^2 \approx L_H^2/2$. In the contracting phase $t < t_B$, the universe is initially de Sitter and we still have $\lambda_H^2 \approx L_H^2/2$, but now it increases exponentially toward bounce $t \to t_B$, as the universe in this phase is exponentially contracting. However, several Planck seconds before the bounce, the universe enters a non-de Sitter state, during which λ_H^2 starts to decrease until the bounce. The qualitative behavior of the comoving Hubble radius is the same for the quadratic and the Starobinsky potentials. Different potentials will change the values of t_H and t_i correspondingly.

right after the bounce, where $k_B \equiv \lambda_B^{-1}(t_B)$. In the contracting phase, when $t \ll t_B$, the Universe is quasi-de Sitter and $\lambda_H^2 \simeq 1/(2a^2H^2)$ increases exponentially toward the bounce $t \to t_B$, as now $a(t)$ is decreasing exponentially. However, several Planck seconds before the bounce, the Universe enters a non-de Sitter state, during which λ_H^2 starts to decrease until the bounce, at which a characteristic Planck scale k_B ($\equiv 1/\lambda_H$) can be well defined. Therefore, for $t \ll t_B$, all the modes are outside the comoving Hubble radius. Then, following our previous arguments, if the initial moment is chosen at $t_0 \ll t_B$, the de Sitter state seems not to be viable. However, when $t_0 \ll t_B$ we have $a(\eta) \simeq 1/(-\eta|H_\Lambda|)$, where $H_\Lambda = -[\lambda(1+\gamma^2)]^{-1}$ and

$$\Omega_{\rm tot}^2 \simeq k^2 - \frac{2}{\eta^2}, \tag{3.27}$$

for which **Eq. 3.9** has the exact solutions given by **Eq. 3.6**. Therefore, at sufficient early times, choosing $\alpha_k = 1$, $\beta_k = 0$ leads us to the de Sitter state (3.7). From the above analysis it is clear that this is possible precisely because of the isometry of the de Sitter space, which is sufficient to single out a preferred state, the de Sitter state (Agullo, 2018).

With the exact solution **(3.7)** as the initial conditions imposed at the moment t_0 ($\ll t_B$) in the contracting phase, it was found that the power spectrum of the cosmological scalar perturbations can be divided into three different regimes: 1) the ultraviolet (UV) ($k > k_{\rm mLQC-I}$); 2) intermediate ($k_i < k < k_{\rm mLQC-I}$); and 3) infrared ($k < k_i$), where $k_{\rm mLQC-I} \equiv a_B\sqrt{R_B/6}$ and $k_i = a_i\sqrt{R_i/6}$, and R_B and R_i are the curvatures given at the bounce and the beginning of the slow-roll inflation, respectively [cf. **Figure 5**]. During the infrared regime, the power spectrum increases as k increases, while in the intermediate regime it is oscillating very fast and the averaged amplitude of the power spectrum is decreasing as k increases. In the UV regime, the spectrum is almost scale-invariant, which is consistent with the current observations. There exists a narrow band, $0.1 \times k_0^* < k < k_{\rm mLQC-I}$, in which the quantum gravitational effects could be detectable by current or forthcoming cosmological observations (Agullo, 2018). Within the dressed metric approach, one of the most distinctive features of the power spectrum in mLQC-I is that its magnitude in the IR regime is of the Planck scale (Agullo, 2018; Li et al., 2020c). This is because those infrared modes are originally outside the Hubble horizon in the contracting phase and thus their magnitudes are frozen as they propagate across the bounce and then into the inflationary phase. Considering that the contracting phase is a quasi de Sitter phase with a Plank-scale Hubble rate, the magnitude of the IR modes is thus also Planckian (Li et al., 2020c).

It should be noted that if the initial conditions are imposed at the bounce, from **Figure 5** we can see clearly that some modes are inside the comoving Hubble radius, and some are not. In addition, in the neighborhood of the bounce, the background is far from de Sitter. So, it is impossible to impose either the BD vacuum or the de Sitter state at the bounce. In this case, one of the choices of the initial conditions is the fourth-order adiabatic vacuum, similar to that in LQC (Agullo et al., 2013; Ashtekar and Gupt, 2017; Ashtekar and Gupt, 2017; Zhu et al., 2017; Zhu et al., 2017).

3.2.2 mLQC-II

In mLQC-II, the evolution of the effective homogeneous Universe is different from that of mLQC-I. In particular, it is symmetric with respect to the bounce and in the initially kinetic energy dominated case at the bounce the solutions can be well approximated by **Eq. 2.56** in the bouncing phase (Li et al., 2018b; Li et al., 2019), similar to that of LQC (Ashtekar and Singh, 2011; Ashtekar and Barrau, 2015; Bojowald, 2015; Agullo and Singh, 2017).

When considering the cosmological perturbations, similar ambiguities in the choices of π_a^{-2} and π_a^{-1} in **Eq. 3.11** exist. In particular, for the choice of **Eq. 3.17** now the function $\Theta(b)$ is replaced by

$$\Theta(b) = \cos\left(\frac{\lambda b}{2}\right), \tag{3.28}$$

which behaves also like a step function across the bounce and picks up the right sign in both contracting and expanding phases, so it smoothly connects $\Omega_\pm$ defined by **Eq. 3.16**.

On the other hand, $\Omega_{\rm eff}^2$ is obtained from **Eq. 3.11** by the replacements,

$$\frac{1}{\pi_a^2} \to \frac{4\pi^2\gamma^2\lambda^2}{9a^4\sin^2(\lambda b/2)\mathcal{D}}, \tag{3.29}$$

$$\frac{1}{\pi_a} \to \frac{-2\pi\gamma\lambda\cos(\lambda b/2)}{3a^2\sin(\lambda b/2)\mathcal{D}^{1/2}}, \tag{3.30}$$

but now with

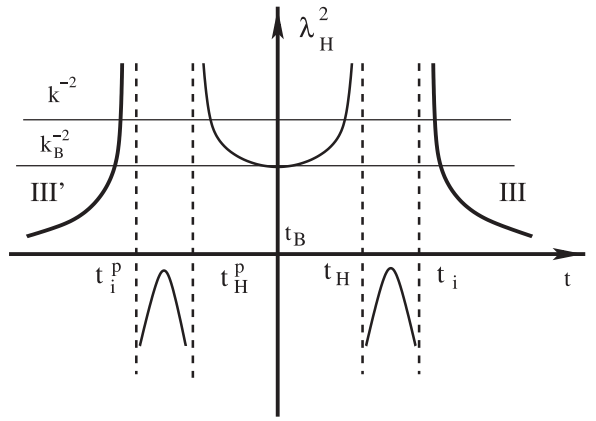

FIGURE 6 | Schematic plot of λ_H^2 defined by **Eq. 3.25** vs. t for mLQC-II in the dressed metric approach for the quadratic and the Starobinsky potentials, where $a''(t_H^p) = a''(t_H) = 0$ and $a''(t_i^p) = a''(t_i) = 0$, and $t = t_i$ denotes the starting time of the inflationary phase, while $t = t_i^p$ is the end time of the deflationary phase in the contracting branch. During the slow-roll inflation, we have $\lambda_H^2 \approx L_H^2/2$. In particular, λ_H^2 is decreasing (increasing) exponentially in Region III (Region III′). The corresponding effective mass near the bounce is always negative. Similar behavior also happens in LQC in the dressed metric approach (Zhu et al., 2017). The bounce is dominated by the kinetic energy of the scalar field, which leads to $t_H^p \approx -t_H$. However, in general we find that $t_i^p \neq -t_i$ due to the effects of the potential energy of the scalar field far from the bouncing point. The comoving Hubble radius has the same qualitative behavior for the quadratic and the Starobinsky potentials, while the values of t_i (t_i^p) and t_H (t_H^p) depend on the type of the potentials and the initial conditions.

$$\mathcal{D} \equiv 1 + \gamma^2 \sin^2\left(\frac{\lambda b}{2}\right). \tag{3.31}$$

Such obtained Ω^2, $\Omega_{\pm}^2$ and $\Omega_{\rm eff}^2$ are quite similar to those given by **Figures 3, 4** in mLQC-I. In particular, at the bounce, we have

$$\Omega^2(t_B) = 1.59 \times 10^{-10}, \quad \Omega_{\rm eff}^2(t_B) = 0.265, \\ k_B^{\rm II} = \left(\frac{a''}{a}\right)^{1/2}\Big|_{t=t_B} \approx 6.84, \tag{3.32}$$

that is, the curvature term a''/a still dominates the evolution near the bounce.

To see how to impose the initial conditions, let us introduce the quantity λ_H^2 defined by **Eq. 3.25** but now $\mathfrak{N}_-$ will be replaced either by Ω^2 or $\Omega_{\rm eff}^2$. The details here are not important, and λ_H^2 is schematically plotted in **Figure 6**, from which we can see that if the initial conditions are chosen to be imposed at the bounce, the BD vacuum (as well as the de Sitter state) is still not available, and the fourth-order adiabatic vacuum is one of the possible choices, similar to the LQC case. However, if the initial conditions are imposed in the contracting phase at $t_0 \ll t_i^p$, the Universe becomes very large $a(t) \gg 1$ and can be practically considered as flat, then the BD vacuum can be chosen.

Certainly, one can choose different initial conditions. In particular, the fourth-order adiabatic vacuum was chosen even in the contracting phase in (Li et al., 2020c). With such a choice, the power spectra from Ω^2 and $\Omega_{\rm eff}^2$ in the region $k \in (5 \times 10^{-6}, 50)$ were studied and found that the relative difference in the magnitude of the power spectra is around 30% in the IR regime and less than 10% in the intermediate regime. In the UV regime, the relative difference can be as small as 0.1% or even less.

3.2.3 LQC

To consider the effects of the ambiguities in the choice of π_a^{-2} and π_a^{-1} in **Eq. 3.11** [8], power spectra of the cosmological perturbations were also studied in the framework of LQC in (Li et al., 2020c). In this case, Ω^2 is obtained from **Eq. 3.17** with

$$\Theta(b) = \cos(\lambda b), \tag{3.33}$$

while $\Omega_{\rm eff}^2$ is obtained from **Eq. 3.11** by the replacements,

$$\frac{1}{\pi_a^2} \to \frac{16\pi^2 G^2 \gamma^2 \lambda^2}{9a^4 \sin^2(\lambda b)}, \tag{3.34}$$

$$\frac{1}{\pi_a} \to \frac{-4\pi\gamma\lambda\cos(\lambda b)}{3a^2 \sin(\lambda b)}. \tag{3.35}$$

As shown explicitly, the term Ω_+^2 is always negligible comparing with the curvature term a''/a in the expression of $\Omega_{\rm tot}^2$ defined in Eq(B.1) by replacing $\mathfrak{N}_-$ with Ω_+^2. So, from **Eq. 3.25** we find that

$$\lambda_H^2 = \frac{1}{a''/a - \Omega_+^2} \simeq \frac{a}{a''}, \tag{3.36}$$

during the bouncing phase $t \in (t_B, t_i)$, and $\lambda_H^2 \simeq a/a''$ was shown schematically by Fig. 18 in (Zhu et al., 2017), which is quite similar to **Figure 6** given above for mLQC-II.

As a result, the initial states of the linear perturbations can be either imposed in the contracting phase at a moment $t_0 \ll t_i^p$ as the BD vacuum, or at the bounce as the fourth-order adiabatic vacuum (Agullo et al., 2013). However, it was shown analytically that such two conditions lead to the same results (Zhu et al., 2017).

To compare the results obtained from the three different models, in (Li et al., 2020c) the fourth-order adiabatic vacuum was chosen even in the contracting phase for LQC. Here, we cite some of the results in **Figure 7**. In particular, it was found that the relative difference in the amplitudes of the power spectra of the scalar perturbations due to the choice of Ω^2 or $\Omega_{\rm eff}^2$ is about 10% in the infrared regime, about 100% in the intermediate regime, and about 0.1% in the UV regime. Since only modes in the UV regime can be observed currently, clearly this difference is out of the sensitivities of the current and forhcoming observations (Abazajian, 2015; Abazajian, 2019).

However, comparing the power spectra obtained from the three different models, even with the same choice of π_a^{-2} and π_a^{-1}, it was found that the relative difference among LQC, mLQC-I and mQLC-II are significant only in the IR and oscillating regimes, while in the UV regime, all three models give quite similar results.

[8] In the framework of LQC, such effects were also studied in (Agullo et al., 2013; Zhu et al., 2017; Zhu et al., 2017; Navascues et al., 2018; Li et al., 2020). In particular, in (Agullo et al., 2018; Li et al., 2020; Agullo et al., 2021; Agullo et al., 2021) the function $\mathfrak{N}_-$ defined in **Eq. 3.15** was chosen over the whole process of the evolution of the Universe.

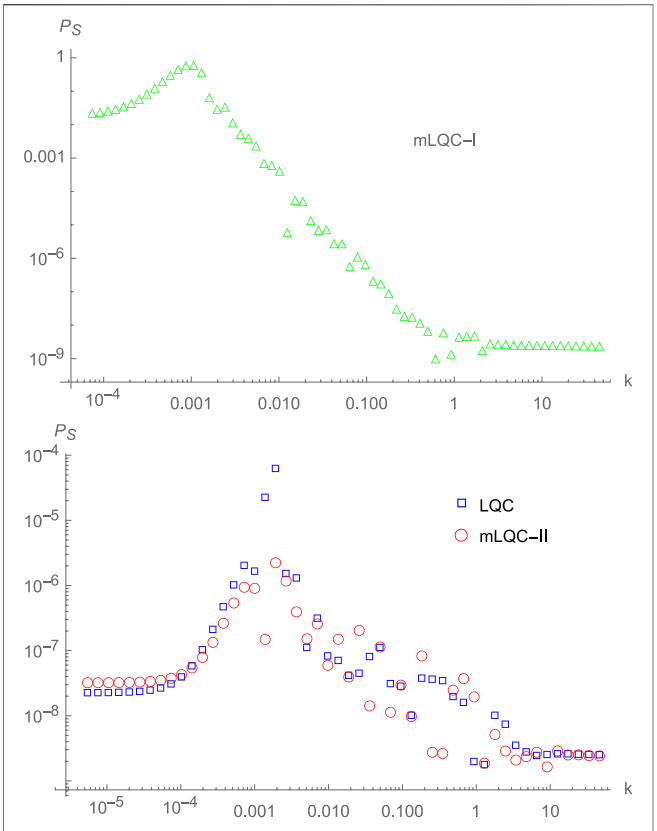

FIGURE 7 | The figure shows the results of the scalar power spectra from three models presented in (Li et al., 2020c) when the potential term is given by $\Omega_{\rm eff}^2$. The inflationary potential is chosen to be the quadratic potential and the e-foldings of the inflationary phases in all three models are chosen to be 72.8. The first panel shows the scalar power spectrum in mLQC-I which is characterized by its unique infrared regime. In the second panel, we compare the scalar power spectra from LQC and mLQC-II.

In particular, with the same regularization of π_a the difference can be as large as 100% throughout the IR and oscillating regimes, while in the UV regime it is about 0.1%.

For the tensor perturbations, the potential term Ω_Q vanishes identically, so no ambiguities related to the choice of π_a exist. But, due to different models, the differences of the power spectra of the tensor perturbations can be still very large in the IR and oscillating regimes among the three models, although they are very small in the UV regime, see, for example, Fig. 12 given in (Li et al., 2020c).

4 PRIMORDIAL POWER SPECTRA OF MODIFIED LQCS IN HYBRID APPROACH

As in the previous section, in this section we also consider the three different models, LQC, mLQC-I, and mLQC-II, but now in the hybrid approach, and pay particular attention to the differences of the power spectra among these models. Since the scalar perturbations are the most relevant ones in the current CMB observations, in the following we shall mainly focus on them, and such studies can be easily extended to the tensor perturbations.

4.1 mLQC-I

Power spectra of the cosmological scalar and tensor perturbations for the effective Hamilton in mLQC-I were recently studied in the hybrid approach (Fernández-Méndez et al., 2013; Castelló Gomar et al., 2014; Gomar et al., 2015). In particular, the mode function v_k of the scalar perturbations satisfies the differential equation (Li et al., 2020b),

$$v_k'' + \left(k^2 + s\right)v_k = 0, \tag{4.1}$$

where

$$\begin{aligned} s =& \frac{4\pi G p_\phi^2}{3\nu^{4/3}}\left(19 - 24\pi G\gamma^2\frac{p_\phi^2}{\pi_a^2}\right)\\ &+\nu^{2/3}\left(V_{,\phi\phi} + \frac{16\pi G\gamma p_\phi}{\pi_a}V_{,\phi} - \frac{16\pi G}{3}V\right)\\ &= -\frac{4\pi G}{3}a^2\left(\rho - 3P\right) + \mathcal{U}, \end{aligned} \tag{4.2}$$

which is the effective mass of the scalar mode, with

$$\begin{aligned} \mathcal{U} \equiv a^2\Bigg[& V_{,\phi\phi} - 12\frac{V_{,\phi}}{\pi_a}\\ &+\frac{64a^6V(\phi)}{\pi G}\left(\rho - \frac{3V(\phi)}{4\pi G}\right)\frac{1}{\pi_a^2}\Bigg]. \end{aligned} \tag{4.3}$$

Note that in (Li et al. 2020a), instead of π_a, the symbol Ω was used. In addition, the cosmological tensor perturbations are also given by **Eqs 4.1**, **4.2** but with the vanishing potential $\mathcal{U} = 0$. Then, we immediately realize that in the hybrid approach quantum mechanically there are also ambiguities in the replacements π_a^{-2} and π_a^{-1}, as mentioned in the last section. So far, two possibilities were considered (Castelló Gomar et al., 2020; García-Quismondo et al., 2020). One is given by the replacements,

$$\frac{1}{\pi_a^2} \to \frac{1}{\Omega_{\rm I}^2}, \qquad \frac{1}{\pi_a} \to \frac{\Lambda_{\rm I}}{\Omega_{\rm I}^2}, \tag{4.4}$$

in **Eq. 4.2**, where

$$\begin{aligned} \Omega_{\rm I}^2 \equiv& -\frac{\nu^2\gamma^2}{\lambda^2}\left\{\sin^2(\lambda b) - \frac{\gamma^2+1}{4\gamma^2}\sin^2(2\lambda b)\right\},\\ \Lambda_{\rm I} \equiv& \nu\frac{\sin(2\lambda b)}{2\lambda}. \end{aligned} \tag{4.5}$$

This is the case referred to as prescription A in (García-Quismondo et al., 2020).

The other possibility is obtained by the replacement of **Eqs 3.34**, **3.35**, which was referred to as Prescription B (García-Quismondo et al., 2020), and showed that the two prescriptions lead to almost the same results. So, in the rest of this section we restrict ourselves only to prescription A.

Then, for the case in which the evolution of the homogeneous Universe was dominated by kinetic energy at the bounce,

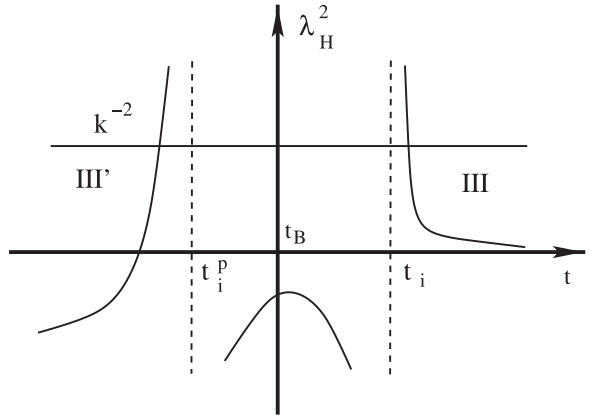

FIGURE 8 | Schematic plot of λ_H^2 defined by **Eq. 4.10** in mLQC-I for the quadratic potential in the hybrid approach, where $s(t_i) = s(t_i^p) = 0$, and $t = t_i$ is the starting time of the inflationary phase. During the slow-roll inflation, we have $\lambda_H^2 \approx L_H^2/2$ (Region III). In the contracting phase, the background is asymptotically de Sitter. The evolution of the universe is asymmetric with respect to the bounce. In particular, λ_H^2 is strictly negative for $t_i^p < t < t_i$, while for $t \simeq t_i^{p-}$ the "generalized" comoving Hubble radius λ_H^2 becomes positive and large. However, as t decreases, λ_H^2 becomes negative again. Although the values of t_i and t_H depend on the initial conditions for the background evolution, for example, when $\phi_B = 1.27\, m_{\rm pl}$ at the bounce, $t_i \approx 7.55 \times 10^4\, t_{\rm pl}$ and $t_H \approx -21.85\, t_{\rm pl}$, the qualitative behavior of the comoving Hubble radius is robust with respect to the choice of the initial conditions as long as the bounce is dominated by the kinetic energy of the scalar field.

$$\dot{\phi}_B^2 \gg 2V(\phi_B), \tag{4.6}$$

it was shown that the effective mass is always positive at the bounce (García-Quismondo et al., 2020). In fact, near the bounce we have (Wu et al., 2018),

$$\begin{aligned} s &= -\frac{4\pi G}{3}a^2(\rho - 3P) + \mathcal{U}(\eta) \\ &\simeq \frac{8\pi G}{3}a^2\rho > 0. \end{aligned} \tag{4.7}$$

Note that in writing the above expression, we have used the fact that during the bouncing phase we have $w_\phi \equiv P/\rho \simeq 1$, and $|\mathcal{U}(\eta)| \ll 1$. On the other hand, in the pre-bounce phase, when $t \ll t_B$ the background is a contracting de Sitter spacetime, so we have (García-Quismondo et al., 2020),

$$\begin{aligned} &s = -\frac{4\pi G}{3}a^2(\rho - 3P) + \mathcal{U}(\eta) \simeq \mathcal{U}(\eta) \simeq 5a^2 V_{,\phi\phi}, \\ &a \simeq a_B e^{H_\Lambda (t - t_B)}, \end{aligned} \tag{4.8}$$

where $H_\Lambda \equiv -\sqrt{8\pi\alpha G\rho_\Lambda/3}$. Thus, the effective mass remains positive in the pre-bounce phase, as long as $V_{,\phi\phi}(t \ll t_B) > 0$. This is the case for both quadratic and Starobinsky potentials. In fact, from **(3.24)**, we find that

$$V_{,\phi\phi} = \begin{cases} m^2, & \text{quadratic}, \\ m^2\left(2 - e^{4\sqrt{\pi G/3}\,\phi}\right)e^{-8\sqrt{\pi G/3}\,\phi}, & \text{Starobinsky}. \end{cases} \tag{4.9}$$

For the case that satisfies the condition (4.6) initially at the bounce, we find that $\phi(t)$ becomes very negative at $t \ll t_B$ for the Starobinsky potential, so $V_{,\phi\phi}(t \ll t_B)$ is positive even in this case. Then, the quantity defined by

$$\lambda_H^2 \equiv -\frac{1}{s}, \tag{4.10}$$

has similar behavior in the post-bounce phases for the case in which the evolution of the homogeneous Universe was dominated by kinetic energy at the bounce, but has different behaviors in the pre-bounce phases, depending specifically on the potentials considered.

In **Figures 8**, **9** we show the comoving Hubble radius for the quadratic and Starobinsky potentials, respectively. From these figures it is clear that for $t_i^p < t < t_i$, λ_H^2 is strictly negative, which implies the effective mass s is positive in this regime. Hence, all the modes assume the oscillatory behavior as the modes inside the Hubble horizon, and we may impose the BD vacuum at the bounce. In addition, when $t \ll t_i^p$, the background is well described by the de Sitter space, so the de Sitter state can be imposed in the deep contracting phase. However, imposing the BD vacuum at the bounce will clearly lead to different power spectra at the end of the slow-roll inflation from that obtained by imposing the de Sitter state in the deep contracting phase. This is because, when the background is contracting to about the moments $t \simeq t_i^{p-}$, the effective mass becomes so large and negative that the mode function v_k will be modified significantly, in comparison with that given at t_0 ($\ll t_i^p$), or in other words, particle creation now becomes not negligible during

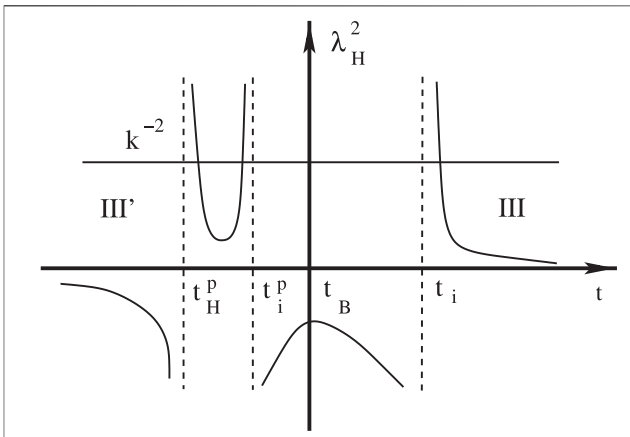

FIGURE 9 | Schematic plot of λ_H^2 defined by **Eq. 4.10** for the Starobinsky potential and mLQC-I in the hybrid approach, where $s(t_i) = s(t_i^p) = s(t_H^p) = 0$, and $t = t_i$ is the starting time of the inflationary phase. During the slow-roll inflation, we have $\lambda_H^2 \approx L_H^2/2$ (Region III). In the contracting phase, the background is asymptotically de Sitter. The evolution of the universe is asymmetric with respect to the bounce. In particular, λ_H^2 is strictly negative for $t_i^p < t < t_i$, while for $t \simeq t_i^{p-}$ it becomes positive and large. However, as t decreases, λ_H^2 becomes negative again. The qualitative behavior of λ_H^2 does not change with the choice of the initial conditions as long as the inflaton initially starts from the left wing of the potential at the kinetic-energy-dominated bounce. However, the exact values of t_i and t_H depend on the initial conditions. For example, when $\phi_B = -1.32\, m_{\rm pl}$, $t_H^p = -7.88\, t_{\rm pl}$, $t_i^p = -4.11\, t_{\rm pl}$ and $t_i = 4.90 \times 10^5\, t_{\rm pl}$.

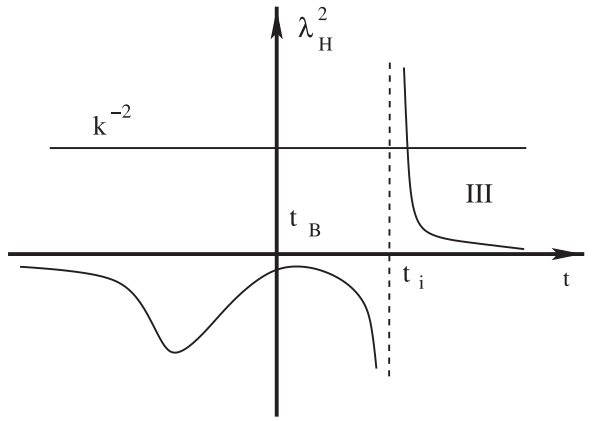

FIGURE 10 | Schematic plot of λ_H^2 defined by **Eq. 4.10** for the Starobinsky potential and mLQC-II in the hybrid approach, where $s(t_i) = 0$, and $t = t_i$ is the starting time of the inflationary phase. During the slow-roll inflation, we have $\lambda_H^2 \approx L_H^2/2$ (Region III) since the contribution from the potential is in general less than a''/a. Again the qualitative behavior of λ_H^2 remains the same as long as the inflaton starts from the left wing of the potential with a positive velocity and the bounce is initially dominated by the kinetic energy of the inflaton field.

the contracting phase. Then, other initial conditions at the bounce may need to be considered.

4.2 mLQC-II

Similar to LQC, the homogeneous Universe of mLQC-II is symmetric with respect to the bounce, and is well described by the analytical solutions given by **Eqs 2.56**, **2.57** for the states that are dominated by kinetic energy at the bounce.

In this model, the cosmological perturbations are also given by **Eqs 4.1**–**4.3** but now with the replacement (Li et al., 2020a),

$$\frac{1}{\pi_a^2} \to \frac{1}{\Omega_{\rm II}^2}, \qquad \frac{1}{\pi_a} \to \frac{\Lambda_{\rm II}}{\Omega_{\rm II}^2}, \tag{4.11}$$

where

$$\Omega_{\rm II}^2 \equiv \frac{4\nu^2}{\lambda^2}\sin^2\left(\frac{\lambda b}{2}\right)\left\{1+\gamma^2\sin^2\left(\frac{\lambda b}{2}\right)\right\}, \qquad \Lambda_{\rm II} \equiv \nu\frac{\sin(\lambda b)}{\lambda}. \tag{4.12}$$

In this case, it can be shown that the effective mass defined by **Eq. 4.2** is always positive in the neighborhood of the bounce, but far from the bounce, the properties of λ_H^2 depend on the potential in the pre-bounce phase, similar to mLQC-I.

In **Figure 10**, we plot λ_H^2 for the Starobinsky potential, while for the quadratic one, it is quite similar to the corresponding one in mLQC-I, given by **Figure 8**. From **Figure 10** we can see that λ_H^2 now is negative not only near the bounce but also in the whole contracting phase, so that all the modes are oscillating for $t < t_i$. Then, one can choose the BD vacuum at the bounce. It is remarkable that for the quadratic potential, this is impossible [cf. **Figure 8**].

Moreover, as $t \to -\infty$, the expansion factor becomes very large, and the corresponding curvature is quite low, so to a good approximation, the BD vacuum can also be chosen in the distant past, not only for the Starobinsky potential but also for other potentials. Due to the oscillating behavior of the mode function over the whole contracting phase, imposing the BD vacuum at the bounce is expected not to lead to significant difference in the power spectra from that in which the same condition is imposed in the deep contracting phase.

4.3 LQC

The evolution of the homogeneous Universe of standard LQC model is also symmetric with respect to the bounce, and is well described by the analytical solutions given in (Zhu et al., 2017; Zhu et al., 2017) for the states that are dominated by kinetic energy at the bounce.

In this model, the cosmological perturbations are also given by **Eqs 4.1.3**.–.**Eqs 4.4.3** but now with the replacement (Li et al., 2020a),

$$\frac{1}{\pi_a^2} \to \frac{1}{\Omega_{\rm LQC}^2}, \qquad \frac{1}{\pi_a} \to \frac{\Lambda_{\rm LQC}}{\Omega_{LQC}^2}, \tag{4.13}$$

where

$$\Omega_{\rm LQC} \equiv \frac{\nu\sin(\lambda b)}{\lambda}, \ \Lambda_{\rm LQC} \equiv \frac{\nu\sin(2\lambda b)}{2\lambda}. \tag{4.14}$$

In this case, it can be shown that the effective mass defined by **Eq. 4.2** is always positive for the states that are dominated by kinetic energy at the bounce (Navascues et al., 2018; Wu et al., 2018), and the quantity λ_H^2 defined by **Eq. 4.10** is negative near the bounce. Again, similar to the mLQC-II case, the modes are oscillating near the bounce. However, in the contracting phase the behavior of λ_H^2 sensitively depends on the inflation potentials. For the Starobinsky one, λ_H^2 behaves similar to that described by **Figure 10**, so the BD vacuum can be imposed either in the deep contracting phase or at the bounce, and such resulted power spectra are expected not to be significantly different from one another. But for the quadratic potential the situation is quite different, and a preferred choice is to impose the BD vacuum in the deep contracting phase ($t_0 \ll t_B$).

4.4 Primordial Power Spectra

As it can be seen that one of the preferred moments to impose the initial conditions for the cosmological perturbations in all these three models is a moment in the contracting phase $t_0 < t_B$. In this phase, we can impose the BD vacuum state as long as the moment is sufficiently earlier, $t_0 \ll t_B$. Certainly, other initial conditions can also be chosen. In particular, in (Li et al., 2020a) the second-order adiabatic vacuum conditions were selected, but it was found that the same results can also be obtained even when the BD vacuum state or the fourth-order adiabatic vacuum is imposed initially.

The nth-order adiabatic vacuum conditions can be obtained as follows: Let us first consider the solution,

$$\nu_k = \frac{1}{\sqrt{2W_k}} e^{-i\int^{\eta} W_k(\bar{\eta})d\bar{\eta}}. \tag{4.15}$$

Then, inserting it into (4.1), one can find an iterative equation for W_k. In particular, it can be shown that the zeroth-order solution is given by $W_k^{(0)} = k$, while the second and fourth order adiabatic solutions are given by,

$$W_k^{(2)} = \sqrt{k^2 + s}, \qquad W_k^{(4)} = \frac{\sqrt{f(s,k)}}{4|k^2 + s|}. \tag{4.16}$$

Here $f(s,k) = 5s'^2 + 16k^4(k^2 + 3s) + 16s^2(3k^2 + s) - 4s''(s + k^2)$. It should be noted that, in order to compare directly with observations, it is found convenient to calculate the power spectrum of the comoving curvature perturbation $\mathcal{R}_k$, which is related to the Mukhanov-Sasaki variable via the relation $\mathcal{R}_k = \nu_k/z$, with $z = a\dot{\phi}/H$. Then, its power spectrum reads

$$\mathcal{P}_{\mathcal{R}_k} = \frac{\mathcal{P}_{\nu_k}}{z^2} = \frac{k^3}{2\pi^2}\frac{|\nu_k|^2}{z^2}. \tag{4.17}$$

In addition, the power spectrum is normally evaluated at the end of inflation, at which all the relevant modes are well outside the Hubble horizon [cf. **Figure 2**].

It should be also noted that the above formula is only applicable to the case where $W_k^{(2)}$ and/or $W_k^{(4)}$ remains real at the initial time. This is equivalent to require $k^2 + s \geq 0$ for $W_k^{(2)}$ and $f(s,k) \geq 0$ for $W_k^{(4)}$. Since the effective mass s in general depends on t, it is clear that the validity of **(4.16)** depends not only on the initial states but also on the initial times.

In addition, in the following only the Starobinsky potential given in **Eq. 3.24** will be considered, as it represents one of the most favorable models by current observations (Bennett et al., 1996; Banday et al., 1996; Komatsu et al., 2011; Larson et al., 2011; Ade and PLANCK Collaboration, 2016; Aghanim and PLANCK Collaboration, 2020). Let us turn to consider the power spectrum of the scalar perturbations in each of the three models. Similar results can be also obtained for the tensor perturbations. In particular, it was found that the scalar power spectra in these three models can be still divided into three distinctive regimes: the infrared, oscillatory and UV, as shown in **Figure 11**.

In the infrared and oscillatory regimes, the relative difference between LQC and mLQC-I can be as large as 100%, while this difference reduces to less than 1% in the UV regime. This is mainly because LQC and mLQC-I have the same classical limit in the post-bounce phase, and as shown in **Figures 5**, **8**, the effective masses in both approaches tend to be the same during the inflationary phase.

However, it is interesting to note that in the infrared and oscillatory regimes, the power spectrum in mLQC-I is suppressed in comparison with that of LQC, which has been found only in the hybrid approach. As a matter of fact, in the dressed metric approach, the power spectrum in mLQC-I is largely amplified in the infrared regime, and its magnitude is of the Planck scale as depicted in **Figure 7** (Agullo, 2018; Li et al., 2020c). The main reason might root in the distinctive behavior of the effective masses in the two approaches, as shown explicitly in **Figures 5**, **8**.

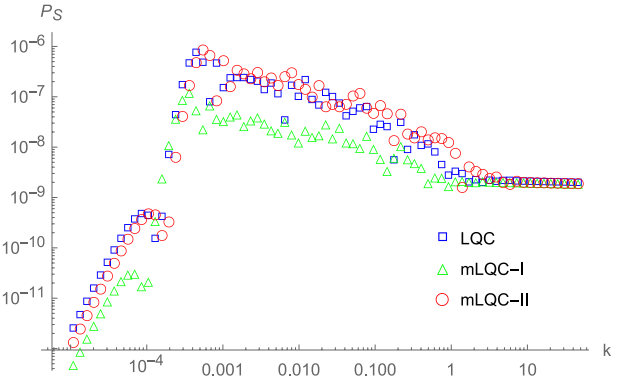

FIGURE 11 | The primordial power spectra of the cosmological scalar perturbations in the hybrid approach with the Starobinsky potential, respectively, for LQC, mLQC-I, and mLQC-II. The mass of the inflaton field is set to $2.44 \times 10^{-6} m_{\rm pl}$. The background evolution is chosen so that the pivot mode is $k_* = 5.15$ in all three models. The initial states are the second-order adiabatic states imposed in the contracting phase at the moment t_0 with $t_0 \ll t_B$(Li et al., 2020a).

On the other hand, the difference of the power spectra between LQC and mLQC-II is smaller than that between LQC and mLQC-I. In particular, in the infrared regime, it is about 50%. The large relative difference (more than 100%) of the power spectra between mLQC-I and mLQC-II also happens in the infrared and oscillatory regimes, while in the UV regime it reduces to about 2%.

To summarize, in the hybrid approach the maximum relative differences of the power spectra among these three different models always happen in the infrared and oscillatory regimes, while in the UV regime, the differences reduce to no larger than 2%, and all the three models predict a scale-invariant power spectrum, and is consistent with the current CMB observations. However, in the hybrid approach, the power spectrum in mLQC-I is suppressed in the infrared and oscillatory regimes. The latter is in a striking contrast to the results obtained from the dressed metric approach, which might be closely related to the fact that the effective masses in these two approaches are significantly different, especially near the bounce and in the prebounce stage.

5 CONCLUSION AND OUTLOOK

In the past 2 decades, LQC has been studied extensively, and several remarkable features have been found (Ashtekar and Singh, 2011; Ashtekar and Barrau, 2015; Bojowald, 2015; Agullo and Singh, 2017), including the generic resolution of the big bang singularity (replaced by a quantum bounce) in the Planckian scale, the slow-roll inflation as an attractor in the post-bounce evolution of the Universe, and the scale-invariant power spectra of the cosmological perturbations, which are consistent with the current CMB observations. Even more interestingly, it was shown recently that some anomalies from the CMB data (Akrami and Planck collaboration, 2020; Akrami and Planck collaboration, 2020; Schwarz et al., 2016) can

be reconciled purely due to the quantum geometric effects in the framework of LQC (Ashtekar et al., 2020; Agullo et al., 2021; Agullo et al., 2021; Ashtekar et al., 2021).

Despite of all these achievements, LQC is still plagued with some ambiguities in the quantization procedure. In particular, its connection with LQG is still not established (Brunnemann and Fleischhack, 2007; Engle, 2007; Brunnemann and Koslowski, 2011), and the quantization procedure used in LQC owing to symmetry reduction before quantization can result in different Hamiltonian constraints than the one of LQG.

Motivated by the above considerations, recently various modified LQC models have been proposed, see, for example (Alesci and Cianfrani, 2013; Alesci and Cianfrani, 2015; Alesci et al., 2017; Oriti, 2017; Oriti et al., 2017; Wilson-Ewing, 2017; Engle and Vilensky, 2018; Gerhardt et al., 2018; Wilson-Ewing, 2018; Baytas et al., 2019; Engle and Vilensky, 2019; Neuser et al., 2019; Olmedo and Alesci, 2019; Schander and Thiemann, 2019; Schander and Thiemann, 2019; Han and Liu, 2020a; Han and Liu, 2020b; Giesel et al., 2020; Giesel et al., 2020; Han et al., 2020; Li et al., 2020b), and references therein. In this brief review, we have restricted ourselves only to mLQC-I and mLQC-II (Yang et al., 2009; Dapor and Liegener, 2018a; Dapor and Liegener, 2018b), as they are the ones that have been extensively studied in the literature not only the dynamics of the homogeneous Universe (Li et al., 2018a; Li et al., 2018b; Saini and Singh, 2019a; Saini and Singh, 2019b; García-Quismondo and Mena Marugán, 2019; Li et al., 2019; García-Quismondo and Mena Marugán, 2020), but also the cosmological perturbations (Agullo, 2018; Castelló Gomar et al., 2020; García-Quismondo et al., 2020; Li et al., 2020a; Li et al., 2020b).

In these two modified LQC models, it was found that the resolution of the big bang singularity is also generic (Li et al., 2018a; Li et al., 2018b; Saini and Singh, 2019a; Saini and Singh, 2019b; Li et al., 2019). This is closely related to the fact that the area operator in LQG has a minimal but nonzero eigenvalue (Ashtekar and Lewandowski, 2004; Thiemann, 2007; Rovelli, 2008; Ashtekar and Singh, 2011; Bojowald, 2011; Gambini and Pullin, 2011; Ashtekar and Barrau, 2015; Bojowald, 2015; Agullo and Singh, 2017; Ashtekar and Pullin, 2017), quite similar to the eigenvalue of the ground state of the energy operator of a simple harmonic oscillator in quantum mechanics. This deep connection also shows that the resolution of the big bang singularity is purely due to the quantum geometric effects. In addition, similar to LQC, the slow-roll inflation also occurs generically in both mLQC-I and mLQC-II (Li et al., 2019). In particular, when the inflaton has a quadratic potential, $V(\phi) = m^2\phi^2/2$, the probabilities for the desired slow-roll inflation not to occur are $\lesssim 1.12 \times 10^{-5}$, $\lesssim 2.62 \times 10^{-6}$, and $\lesssim 2.74 \times 10^{-6}$ for mLQC-I, mLQC-II and LQC, respectively.

When dealing with perturbations, another ambiguity rises in the replacement of the momentum conjugate π_a of the expansion factor a in the effective potential of the scalar perturbations. This ambiguity occurs not only in the dressed metric approach [cf. **Eq. 3.11**] but also in the hybrid approach [cf. **Eq. 4.2**], as it is closely related to the quantization strategy used in LQG/LQC, because now only the holonomies (complex exponentials) of π_a are defined as operators. Several choices have been proposed in the literature (Mena Marugán et al., 2011; Agullo et al., 2013; Agullo, 2018; Agullo et al., 2018; Castelló Gomar et al., 2020; García-Quismondo et al., 2020; Li et al., 2020a; Li et al., 2020b). In **Secs. 3**, **4**, we have shown that for some choices the effects on the power spectra are non-trivial, while for others the effects are negligible. However, even with the same choice, the relative differences in the amplitudes of the power spectra among the three different models can be as large as 100% in the infrared and intermediate regimes of the spectra, while in the UV regime the relative differences are no larger than 2%, and the corresponding power spectra are scale-invariant. Since only the modes in the UV regime are relevant to the current observations, the power spectra obtained in all the three models are consistent with current observations (Bennett et al., 1996; Banday et al., 1996; Komatsu et al., 2011; Larson et al., 2011; Ade and PLANCK Collaboration, 2016; Aghanim and PLANCK Collaboration, 2020).

However, the interactions between the infrared and UV modes appearing in non-Gaussianities might provide an excellent window to observe such effects. This was initially done in LQC (Agullo et al., 2018; Wu et al., 2018; Zhu et al., 2018), and lately generalized to bouncing cosmologies (Agullo et al., 2021; Agullo et al., 2021). It should be noted that in (Agullo et al., 2021; Agullo et al., 2021), the expansion factor $a(t)$ near the bounce was assumed to take the form,

$$a(t) = a_B\left(1 + bt^2\right)^n,$$

where b and n are two free parameters. For example, for LQC we have $n = 1/6$ and $b = R_B/2$, where R_B is the Ricci scalar at the bounce (Zhu et al., 2017; Zhu et al., 2017). But, it is clear that near the bounce $a(t)$ takes forms different from the above expression for mLQC-I/II, as one can see from **Eqs 2.54–2.57**. Thus, it would be very interesting to study such effects in mLQC-I/II, and look for some observational signals.

Moreover, initial conditions are another subtle and important issue not only in LQC but also in mLQCs. As a matter of fact, the initial conditions consist of two parts: the initial time, and the initial conditions. Different choices of the initial times lead to different choices of the initial conditions, or vice versa. To clarify these issues, in **Sections 3**, **4** we have discussed it at length by showing the (generalized) comoving Hubble radius in each model as well as in each of the two approaches, dressed metric and hybrid. From these analyses, we have shown clearly which initial conditions can and cannot be imposed at a given initial time.

In addition, when the Universe changes from contraction to expansion at the bounce, particle and entropy creations are expected to be very large, and it is crucial to keep such creations under control, so that the basic assumptions of the models are valid, including the one that the cosmological perturbations are small and can be treated as test fields propagating on the quantum homogeneous background, as assumed in both the dressed metric and hybrid approaches.

Yet, different initial conditions also affect the amplitudes and shapes of the primordial power spectra, and it would be very interesting to investigate the consistency of such obtained spectra

with current observations, in particular the possible explanations to the anomalies found in the CMB data (Akrami and Planck collaboration, 2020; Akrami and Planck collaboration, 2020; Schwarz et al., 2016), and the naturalness of such initial conditions.

On the other hand, bouncing cosmologies, as an alternative to the cosmic inflation paradigm, have been extensively studied in the literature, see, for example (Wand, 1999; Brandenberger and Peter, 2017), and references therein. However, in such classical bounces, exotic matter fields are required in order to keep the bounce open. This in turn raises the question of instabilities of the models. On the other hand, quantum bounces found in LQC/mLQCs are purely due to the quantum geometric effects, and the instability problem is automatically out of the question. So, it would be very interesting to study bouncing cosmologies in the framework of LQC/mLQCs. The first step in this direction has already been taken (Li et al., 2020b), and more detailed and extensive analyses are still needed.

AUTHOR CONTRIBUTIONS

All authors listed have made a substantial, direct, and intellectual contribution to the work and approved it for publication.

FUNDING

BL and PS are supported by NSF grant PHY-1454832. BL is also partially supported by the National Natural Science Foundation of China (NNSFC) with the Grants No. 12005186.

ACKNOWLEDGMENTS

We are grateful to Robert Brandenberger and David Wands for valuable comments on the manuscript and helpful discussions. We thank Javier Olmedo and Tao Zhu for various discussions related to works presented in this manuscript.

REFERENCES

Abazajian, K. (2019). *CMB-S4 Decadal Survey APC White Paper*. arXiv:1908.01062.

Abazajian, K. N. (2015). Inflation Physics from the Cosmic Microwave Background and Large Scale Structure. *Astropart. Phys.* 63, 55.

Ade, P.PLANCK Collaboration (2016). Planck 2015 Results. XX. Constraints on Inflation. *A&A* 594, A20.

Aghanim, N.PLANCK Collaboration (2020). Planck 2018 Results. X. Constraints on Inflation. *A&A* 641, A10.

Agullo, I., Ashtekar, A., and Gupt, B. (2017). Phenomenology with Fluctuating Quantum Geometries in Loop Quantum Cosmology. *Class. Quan. Grav.* 34, 074003. doi:10.1088/1361-6382/aa60ec

Agullo, I., Ashtekar, A., and Nelson, W. (2013). Extension of the Quantum Theory of Cosmological Perturbations to the Planck Era. *Phys. Rev.* D87, 043507.

Agullo, I., Ashtekar, A., and Nelson, W. (2012). Quantum Gravity Extension of the Inflationary Scenario. *Phys. Rev. Lett.* 109, 251301. doi:10.1103/physrevlett.109.251301

Agullo, I., Ashtekar, A., and Nelson, W. (2013). The Pre-inflationary Dynamics of Loop Quantum Cosmology: Confronting Quantum Gravity with Observations. *Class. Quan. Grav.* 30, 085014. doi:10.1088/0264-9381/30/8/085014

Agullo, I., Bolliet, B., and Sreenath, V. (2018). Non-Gaussianity in Loop Quantum Cosmology. *Phys. Rev.* D97, 066021.

Agullo, I., Kranas, D., and Sreenath, V. (2021). Anomalies in the CMB from a Cosmic Bounce. *Gen. Relativ Gravit.* 53, 17. doi:10.1007/s10714-020-02778-9

Agullo, I., Kranas, D., and Sreenath, V. (2021). Large Scale Anomalies in the CMB and Non-gaussianity in Bouncing Cosmologies. *Class. Quan. Grav.* 38, 065010. doi:10.1088/1361-6382/abc521

Agullo, I., and Morris, N. A. (2015). Detailed Analysis of the Predictions of Loop Quantum Cosmology for the Primordial Power Spectra. *Phys. Rev. D* 92, 124040. doi:10.1103/physrevd.92.124040

Agullo, I., Olmedo, J., and Sreenath, V. (2020). Observational Consequences of Bianchi I Spacetimes in Loop Quantum Cosmology. *Phys. Rev.* D102, 043523.

Agullo, I., Olmedo, J., and Sreenath, V. (2020). Predictions for the Cosmic Microwave Background from an Anisotropic Quantum Bounce. *Phys. Rev. Lett.* 124, 251301. doi:10.1103/physrevlett.124.251301

Agullo, I. (2018). Primordial Power Spectrum from the Dapor-Liegener Model of Loop Quantum Cosmology. *Gen. Relativ Gravit.* 50, 91. doi:10.1007/s10714-018-2413-1

Agullo, I., and Singh, P. (2017). "Loop Quantum Cosmology," in *Loop Quantum Gravity: The First 30 Years*. Editors A. Ashtekar and J. Pullin (Singapore: Wald Scientific).

Akrami, Y.Planck collaboration (2020). Planck 2018 Results. I. Overview and the Cosmological Legacy of Planck. *A&A* 641, A1.

Akrami, Y.Planck collaboration (2020). Planck 2018 Results. VII. Isotropy and Statistics of the CMB. *A&A* 641, A7.

Alesci, E., Botta, G., Cianfrani, F., and Liberati, S. (2017). Cosmological Singularity Resolution from Quantum Gravity: the Emergent-Bouncing Universe. *Phys. Rev.* D96, 046008.

Alesci, E., and Cianfrani, F. (2015). Quantum Reduced Loop Gravity: a Realistic Universe. *Phys. Rev.* D92, 084065.

Alesci, E., and Cianfrani, F. (2013). Quantum-Reduced Loop Gravity: Cosmology. *Phys. Rev.* D87, 083521.

Ashoorioon, A., Chialva, D., and Danielsson, U. (2011). Effects of Nonlinear Dispersion Relations on Non-gaussianities. *J. Cosmol. Astropart. Phys.* 2011, 034. doi:10.1088/1475-7516/2011/06/034

Ashtekar, A., Gupt, B., Jeong, D., and Sreenath, V. (2020). Alleviating the Tension in the Cosmic Microwave Background Using Planck-Scale Physics. *Phys. Rev. Lett.* 125, 051302. doi:10.1103/PhysRevLett.125.051302

Ashtekar, A., Pawlowski, T., and Singh, P. (2006). Quantum Nature of the Big Bang. *Phys. Rev. Lett.* 96, 141301. doi:10.1103/PhysRevLett.96.141301

Ashtekar, A., and Barrau, A. (2015). Loop Quantum Cosmology: From Pre-inflationary Dynamics to Observations. *Class. Quan. Grav.* 32, 234001. doi:10.1088/0264-9381/32/23/234001

Ashtekar, A., Bojowald, M., and Lewandowski, J. (2003). Mathematical Structure of Loop Quantum Cosmology. *Adv. Theor. Math. Phys.* 7, 233–268. doi:10.4310/atmp.2003.v7.n2.a2

Ashtekar, A., Corichi, A., and Singh, P. (2010). Robustness of Key Features of Loop Quantum Cosmology. *Phys. Rev.* D77, 024046.

Ashtekar, A., and Gupt, B. (2017). Initial Conditions for Cosmological Perturbations. *Class. Quan. Grav.* 34, 035004. doi:10.1088/1361-6382/aa52d4

Ashtekar, A., Gupt, B., Jeong, D., and Sreenath, V. (2021). Cosmic Tango between the Very Small and the Very Large: Addressing CMB Anomalies through Loop Quantum Cosmology. *arXiv:2103.14568*.

Ashtekar, A., and Gupt, B. (2017). Quantum Gravity in the Sky: Interplay between Fundamental Theory and Observations. *Class. Quan. Grav.* 34, 014002. doi:10.1088/1361-6382/34/1/014002

Ashtekar, A., and Lewandowski, J. (2004). Background Independent Quantum Gravity: A Status Report. *Class. Quan. Grav.* 21, R53–R152. doi:10.1088/0264-9381/21/15/r01

Ashtekar, A., Pawlowski, T., and Singh, P. (2006). Quantum Nature of the Big Bang: An Analytical and Numerical Investigation. *Phys. Rev. D* 73, 124038. doi:10.1103/physrevd.73.124038

Ashtekar, A., and Pullin, J. (2017). *Loop Quantum Gravity - the First 30 Years*. Singapore: World Scientific.

Ashtekar, A., and Singh, P. (2011). Loop Quantum Cosmology: a Status Report. *Class. Quan. Grav.* 28, 213001. doi:10.1088/0264-9381/28/21/213001

Ashtekar, A., and Sloan, D. (2011a). Probability of Inflation in Loop Quantum Cosmology. *Gen. Relativ. Gravit.* 43, 3619–3655. doi:10.1007/s10714-011-1246-y

Ashtekar, A., and Sloan, D. (2011b). Loop Quantum Cosmology and Slow Roll Inflation. *Phys. Lett. B* 694, 108.

Assanioussi, M., Dapor, A., Liegener, K., and Pawłowski, T. (2018). Emergent de Sitter epoch of the quantum Cosmos from Loop Quantum Cosmology. *Phys. Rev. Lett.* 121, 081303. doi:10.1103/PhysRevLett.121.081303

Assanioussi, M., Dapor, A., Liegener, K., and Pawlowski, T. (2019b). Challenges in Recovering a Consistent Cosmology from the Effective Dynamics of Loop Quantum Gravity. *Phys. Rev.* D100, 106016.

Assanioussi, M., Dapor, A., Liegener, K., and Pawlowski, T. (2019a). Emergent de Sitter epoch of the loop quantum cosmos: A detailed analysis. *Phys. Rev.* D100, 084003.

Banday, K. M. A. J., Bennett, C. L., Hinshaw, G., Kogut, A., Smoot, G. F., and Wright, E. L. (1996). Power Spectrum of Primordial Inhomogeneity Determined from the FOUR-Year [ITAL]COBE[/ITAL] DMR Sky Maps. *ibid* 464, L11–L15. doi:10.1086/310077

Baumann, D., and McAllister, L. (2015). *Inflation and String Theory*. Cambridge: Cambridge Monographs on Mathematical Physics, Cambridge University Press.

Baumann, D. (2009). TASI Lectures on Inflation. *arXiv:0907.5424*.

Baytas, B., Bojowald, M., and Crowe, S. (2019). Equivalence of Models in Loop Quantum Cosmology and Group Field Theory. *Universe* 5, 41.

Becker, K., Becker, M., and Schwarz, J. H. (2007). *String Theory and M-Theory*. Cambridge: Cambridge University Press.

Bedic, S., and Vereshchagin, G. (2019). Probability of Inflation in Loop Quantum Cosmology. *Phys. Rev.* D99 (4), 043512.

Bedroya, A., Brandenberger, R., Loverde, M., and Vafa, C. (2020). Trans-Planckian Censorship and Inflationary Cosmology. *Phys. Rev. D* 101, 103502. doi:10.1103/physrevd.101.103502

Bedroya, A., and Vafa, C. (2020). Trans-Planckian Censorship and the Swampland. *J. High Energ. Phys.* 2020, 123. doi:10.1007/jhep09(2020)123

Bennett, C. L., Banday, A. J., Górski, K. M., Hinshaw, G., Jackson, P., Keegstra, P., et al. (1996). Four-Year [ITAL]COBE[/ITAL] DMR Cosmic Microwave Background Observations: Maps and Basic Results. *Astrophys. J.* 464, L1–L4. doi:10.1086/310075

Bergstorm, L., and Danielsson, U. H. (2002). Can MAP and Planck Map Planck Physics? *J. High Energ. Phys.* 12, 038.

Bhardwaj, A., Copeland, E. J., and Louko, J. (2019). Inflation in Loop Quantum Cosmology. *Phys. Rev.* D99, 063520.

Birrell, N. D., and Davies, P. C. W. (1982). *Quantum fields in Curved Space*. Cambridge: Cambridge University Press.

Bojowald, M. (2011). *Canonical Gravity and Applications: Cosmology, Black Holes, and Quantum Gravity*. Cambridge: Cambridge University Press.

Bojowald, M., Hossain, G. M., Kagan, M., and Shankaranarayanan, S. (2008). Anomaly freedom in Perturbative Loop Quantum Gravity. *Phys. Rev.* D78, 063547.

Bojowald, M. (2015). Quantum Cosmology: a Review. *Rep. Prog. Phys.* 78, 023901. doi:10.1088/0034-4885/78/2/023901

Bonga, B., and Gupt, B. (2016). Inflation with the Starobinsky Potential in Loop Quantum Cosmology. *Gen. Relativ. Grav.* 48, 1. doi:10.1007/s10714-016-2071-0

Bonga, B., and Gupt, B. (2016). Phenomenological Investigation of a Quantum Gravity Extension of Inflation with the Starobinsky Potential. *Phys. Rev.* D93, 063513.

Borde, A., Guth, A. H., and Vilenkin, A. (2003). Inflationary Spacetimes Are Incomplete in Past Directions. *Phys. Rev. Lett.* 90, 151301. doi:10.1103/physrevlett.90.151301

Borde, A., and Vilenkin, A. (1994). Eternal Inflation and the Initial Singularity. *Phys. Rev. Lett.* 72, 3305–3308. doi:10.1103/physrevlett.72.3305

Brandenberger, R. H. (1999). Inflationary Cosmology: Progress and Problems. *arXiv:hep-th/9910410*.

Brandenberger, R. H., and Martin, J. (2013). Trans-Planckian Issues for Inflationary Cosmology. *Class. Quan. Grav.* 30, 113001. doi:10.1088/0264-9381/30/11/113001

Brandenberger, R., and Peter, P. (2017). Bouncing Cosmologies: Progress and Problems. *Found. Phys.* 47, 797–850. doi:10.1007/s10701-016-0057-0

Brandenberger, R. (2021). Trans-Planckian Censorship Conjecture and Early Universe Cosmology. *arXiv:2102.09641*.

Brunnemann, J., and Fleischhack, C. (2007). On the Configuration Spaces of Homogeneous Loop Quantum Cosmology and Loop Quantum Gravity. *arXiv:0709.1621*.

Brunnemann, J., and Koslowski, T. A. (2011). Symmetry Reduction of Loop Quantum Gravity. *Class. Quan. Grav.* 28, 245014. doi:10.1088/0264-9381/28/24/245014

Burgess, C. P., Cicoli, M., and Quevedo, F. (2013). String Inflation after Planck 2013. *J. Cosmol. Astropart. Phys.* 2013, 003. doi:10.1088/1475-7516/2013/11/003

Cailleteau, T., Barrau, A., Grain, J., and Vidotto, F. (2012). Consistency of Holonomy-Corrected Scalar, Vector and Tensor Perturbations in Loop Quantum Cosmology. *Phys. Rev.* D86, 087301.

Cailleteau, T., Mielczarek, J., Barrau, A., and Grain, J. (2012). Anomaly-free Scalar Perturbations with Holonomy Corrections in Loop Quantum Cosmology. *Class. Quan. Grav.* 29, 095010. doi:10.1088/0264-9381/29/9/095010

Carlip, S. (2003). *Quantum Gravity in 2+1 Dimensions*. Cambridge: Cambridge Monographs on Mathematical Physics, Cambridge University Press.

Castelló Gomar, L., Fernández-Méndez, M., Mena Marugan, G. A., and Olmedo, J. (2014). Cosmological Perturbations in Hybrid Loop Quantum Cosmology: Mukhanov-Sasaki Variables. *Phys. Rev.* D90, 064015.

Castelló Gomar, L., García-Quismondo, A., and Mena Marugán, G. A. (2020). Primordial Perturbations in the Dapor-Liegener Model of Hybrid Loop Quantum Cosmology. *Phys. Rev.* D102, 083524.

Castelló Gomar, L., Mena Marugán, G. A., Martín de Blas, D., and Olmedo, J. (2017). Hybrid Loop Quantum Cosmology and Predictions for the Cosmic Microwave Background. *Phys. Rev. D* 96, 103528. doi:10.1103/physrevd.96.103528

Chen, L., and Zhu, J.-Y. (2015). Loop Quantum Cosmology: The Horizon Problem and the Probability of Inflation. *Phys. Rev.* D92, 084063.

Chernoff, D. F., and Tye, S.-H. H. (2014). Inflation, String Theory and Cosmology. *arXiv:1412.0579*.

Cicoli, M. (2016). Recent Developments in String Model-Building and Cosmology. *arXiv:1604.00904*.

Corichi, A., and Karami, A. (2011). Measure Problem in Slow Roll Inflation and Loop Quantum Cosmology. *Phys. Rev. D* 83, 104006. doi:10.1103/physrevd.83.104006

Corichi, A., and Singh, P. (2008). Is Loop Quantization in Cosmology Unique? *Phys. Rev.* D78, 024034.

Corichi, A., and Sloan, D. (2014). Inflationary Attractors and Their Measures. *Class. Quan. Grav.* 31, 062001. doi:10.1088/0264-9381/31/6/062001

Craig, D. A., and Singh, P. (2013). Consistent Probabilities in Loop Quantum Cosmology. *Class. Quan. Grav.* 30, 205008. doi:10.1088/0264-9381/30/20/205008

Dadhich, N., Joe, A., and Singh, P. (2015). Emergence of the Product of Constant Curvature Spaces in Loop Quantum Cosmology. *Class. Quan. Grav.* 32, 185006. doi:10.1088/0264-9381/32/18/185006

Dapor, A., and Liegener, K. (2018b). Cosmological Coherent State Expectation Values in Loop Quantum Gravity I. Isotropic Kinematics. *Class. Quan. Grav.* 35, 135011. doi:10.1088/1361-6382/aac4ba

Dapor, A., and Liegener, K. (2018a). Cosmological Effective Hamiltonian from Full Loop Quantum Gravity Dynamics. *Phys. Lett. B* 785, 506–510. doi:10.1016/j.physletb.2018.09.005

de Blas, D. M., and Olmedo, J. (2016). Primordial Power Spectra for Scalar Perturbations in Loop Quantum Cosmology. *J. Cosmol. Astropart. Phys.* 2016, 029. doi:10.1088/1475-7516/2016/06/029

Diener, P., Gupt, B., Megevand, M., and Singh, P. (2014). Numerical Evolution of Squeezed and Non-gaussian States in Loop Quantum Cosmology. *Class. Quan. Grav.* 31, 165006. doi:10.1088/0264-9381/31/16/165006

Diener, P., Gupt, B., and Singh, P. (2014). Numerical Simulations of a Loop Quantum cosmos: Robustness of the Quantum Bounce and the Validity of Effective Dynamics. *Class. Quan. Grav.* 31, 105015. doi:10.1088/0264-9381/31/10/105015

Diener, P., Joe, A., Megevand, M., and Singh, P. (2017). Numerical Simulations of Loop Quantum Bianchi-I Spacetimes. *Class. Quan. Grav.* 34, 094004. doi:10.1088/1361-6382/aa68b5

Dodelson, S. (2003). *Modern Cosmology*. New York: Academic Press.

Dupuy, J. L., and Singh, P. (2020). Hysteresis and Beats in Loop Quantum Cosmology. *Phys. Rev.* D101, 086016.

Easther, R., Kinney, W. H., and Peiris, H. (2005). Observing Trans-planckian Signatures in the Cosmic Microwave Background. *J. Cosmol. Astropart. Phys.* 2005, 009. doi:10.1088/1475-7516/2005/05/009

Elizaga Navascués, B., Martín de Blas, D., and Mena Marugán, G. (2018). The Vacuum State of Primordial Fluctuations in Hybrid Loop Quantum Cosmology. *Universe* 4, 98. doi:10.3390/universe4100098

Engle, J. (2007). Relating Loop Quantum Cosmology to Loop Quantum Gravity: Symmetric Sectors and Embeddings. *Class. Quan. Grav.* 24, 5777–5802. doi:10.1088/0264-9381/24/23/004

Engle, J., and Vilensky, I. (2018). Deriving Loop Quantum Cosmology Dynamics from Diffeomorphism Invariance. *Phys. Rev.* D98, 023505.

Engle, J., and Vilensky, I. (2019). Uniqueness of Minimal Loop Quantum Cosmology Dynamics. *Phys. Rev. D* 100, 121901. doi:10.1103/physrevd.100.121901

Fernández-Méndez, M., Mena Marugán, G. A., and Olmedo, J. (2013). Hybrid Quantization of an Inflationary Model: The Flat Case. *Phys. Rev.* D88, 044013.

Fernández-Méndez, M., Mena Marugán, G. A., and Olmedo, J. (2012). Hybrid Quantization of an Inflationary Universe. *Phys. Rev.* D86, 024003.

Gambini, R., and Pullin, J. (2011). *A First Course in Loop Quantum Gravity*. Oxford: Oxford University Press.

García-Quismondo, A., and Mena Marugán, G. A. (2020). Dapor-Liegener Formalism of Loop Quantum Cosmology for Bianchi I Spacetimes. *Phys. Rev.* D101, 023520.

García-Quismondo, A., and Mena Marugán, G. A. (2019). Martin-Benito-Mena Marugan-Olmedo Prescription for the Dapor-Liegener Model of Loop Quantum Cosmology. *Phys. Rev.* D99, 083505.

García-Quismondo, A., Mena Marugán, G. A., and Pérez, G. S. (2020). The Time-dependent Mass of Cosmological Perturbations in Loop Quantum Cosmology: Dapor-Liegener Regularization. *Class. Quan. Grav.* 37, 195003. doi:10.1088/1361-6382/abac6d

Gerhardt, F., Oriti, D., and Wilson-Ewing, E. (2018). The Separate Universe Framework in Group Field Theory Condensate Cosmology. *Phys. Rev.* D98, 066011.

Giesel, K., Li, B.-F., and Singh, P. (2020). Revisiting the Bardeen and Mukhanov-Sasaki Equations in the Brown-Kuchar and Gaussian Dust Models. *arXiv: 2012.14443*.

Giesel, K., Li, B.-F., and Singh, P. (2020). Towards a Reduced Phase Space Quantization in Loop Quantum Cosmology with an Inflationary Potential. *Phys. Rev. D* 102, 126024. doi:10.1103/physrevd.102.126024

Giesel, K., and Thiemann, T. (2007). Algebraic Quantum Gravity (AQG): I. Conceptual Setup. *Class. Quan. Grav.* 24, 2465–2497. doi:10.1088/0264-9381/24/10/003

Gomar, L. C., Martín-Benito, M., and Marugán, G. A. M. (2015). Gauge-invariant Perturbations in Hybrid Quantum Cosmology. *J. Cosmol. Astropart. Phys.* 2015, 045. doi:10.1088/1475-7516/2015/06/045

Gordon, L., Li, B.-F., and Singh, P. (2021). Quantum Gravitational Onset of Starobinsky Inflation in a Closed Universe. *Phys. Rev.* D103, 046016.

Green, M. B., Schwarz, J. H., and Witten, E. (1999). *Superstring Theory: Vol.1 & 2*. Cambridge: Cambridge Monographs on Mathematical Physics, Cambridge University Press.

Gupt, B., and Singh, P. (2013). A Quantum Gravitational Inflationary Scenario in Bianchi-I Spacetime. *Class. Quan. Grav.* 30, 145013. doi:10.1088/0264-9381/30/14/145013

Gupt, B., and Singh, P. (2012). Quantum Gravitational Kasner Transitions in Bianchi-I Spacetime. *Phys. Rev.* D86, 024034.

Guth, A. H. (1981). Inflationary Universe: A Possible Solution to the Horizon and Flatness Problems. *Phys. Rev. D* 23, 347–356. doi:10.1103/physrevd.23.347

Han, M., Li, H., and Liu, H. (2020). Manifestly Gauge-Invariant Cosmological Perturbation Theory from Full Loop Quantum Gravity. *arXiv:2005.00883*.

Han, M., and Liu, H. (2020a). Effective Dynamics from Coherent State Path Integral of Full Loop Quantum Gravity. *Phys. Rev.* D101, 046003.

Han, M., and Liu, H. (2020b). Semiclassical Limit of New Path Integral Formulation from Reduced Phase Space Loop Quantum Gravity. *Phys. Rev.* D102, 024083.

Hawking, S. W., and Ellis, G. F. R. (1973). *The Large Scale Structure of Spacetime*. Cambridge: Cambridge University Press.

Jackson, M. G., and Schalm, K. (2012). Model Independent Signatures of New Physics in the Inflationary Power Spectrum. *Phys. Rev. Lett.* 108, 111301. doi:10.1103/physrevlett.108.111301

Jin, W.-J., Ma, Y.-G., and Zhu, T. (2019). Pre-inflationary Dynamics of Starobinsky Inflation and its Generalization in Loop Quantum Brans-Dicke Cosmology. *JCAP* 02, 010.

Johson, C. V. (2003). *D-Branes, Cambridge Monographs on Mathematical Physics*. Cambridge: Cambridge University Press.

Joras, A. E., and Marozzi, G. (2009). Trans-Planckian Physics from a Nonlinear Dispersion Relation. *Phys. Rev.* D79, 023514.

Kamiński, W., Kolanowski, M., and Lewandowski, J. (2020). Dressed Metric Predictions Revisited. *Class. Quan. Grav* 37, 095001. doi:10.1088/1361-6382/ab7ee0

Kiefer, C., and Krämer, M. (2012). Quantum Gravitational Contributions to the Cosmic Microwave Background Anisotropy Spectrum. *Phys. Rev. Lett.* 108, 021301. doi:10.1103/PhysRevLett.108.021301

Kiefer, C. (2007). *Quantum Gravity*. Oxford Science Publications, Oxford University Press.

Kodama, H., and Sasaki, M. (1984). Cosmological Perturbation Theory. *Prog. Theor. Phys. Suppl.* 78, 1–166. doi:10.1143/ptps.78.1

Komatsu, E., Smith, K. M., Dunkley, J., Bennett, C. L., Gold, B., Hinshaw, G., et al.WMAP Collaboration (2011). Seven-year Wilkinson Microwave Anisotropy Probe (Wmap) Observations: Cosmological Interpretation. *ApJS* 192, 18. doi:10.1088/0067-0049/192/2/18

Krauss, L. M., and Wilczek, F. (2014). Using Cosmology to Establish the Quantization of Gravity. *Phys. Rev.* D89, 047501.

Larson, D., Dunkley, J., Hinshaw, G., Komatsu, E., Nolta, M. R., Bennett, C. L., et al.WMAP Collaboration (2011). Seven-year Wilkinson Microwave Anisotropy Probe (Wmap) Observations: Power Spectra and Wmap -Derived Parameters. *ApJS* 192, 16. doi:10.1088/0067-0049/192/2/16

Li, B.-F., Olmedo, J., Singh, P., and Wang, A. (2020a). Primordial Scalar Power Spectrum from the Hybrid Approach in Loop Cosmologies. *Phys. Rev. D* 102, 126025. doi:10.1103/physrevd.102.126025

Li, B.-F., Saini, S., and Singh, P. (2020b). Primordial Power Spectrum from a Matter-Ekpyrotic Bounce Scenario in Loop Quantum Cosmology. *arXiv: 2012.10462*.

Li, B.-F., and Singh, P. Singularity resolution may forbid a cyclic evolution (To Appear).

Li, B.-F., Singh, P., and Wang, A. (2019). Genericness of Pre-inflationary Dynamics and Probability of the Desired Slow-Roll Inflation in Modified Loop Quantum Cosmologies. *Phys. Rev.* D100, 063513.

Li, B.-F., Singh, P., and Wang, A. (2020c). Primordial Power Spectrum from the Dressed Metric Approach in Loop Cosmologies. *Phys. Rev.* D100, 086004.

Li, B.-F., Singh, P., and Wang, A. (2018b). Qualitative Dynamics and Inflationary Attractors in Loop Cosmology. *Phys. Rev.* D98, 066016.

Li, B.-F., Singh, P., and Wang, A. (2018a). Towards Cosmological Dynamics from Loop Quantum Gravity. *Phys. Rev.* D97, 084029.

Liegener, K., and Singh, P. (2020). Gauge-invariant Bounce from Loop Quantum Gravity. *Class. Quan. Grav.* 37, 085015. doi:10.1088/1361-6382/ab7962

Liegener, K., and Singh, P. (2019). New Loop Quantum Cosmology Modifications from Gauge-Covariant Fluxes. *Phys. Rev. D* 100, 124048. doi:10.1103/physrevd.100.124048

Liegener, K., and Singh, P. (2019). Some Physical Implications of Regularization Ambiguities in SU(2) Gauge-Invariant Loop Quantum Cosmology. *Phys. Rev. D* 100, 124049. doi:10.1103/physrevd.100.124049

Linde, A. (2014). Inflationary Cosmology after Planck 2013. *arXiv: 1402.0526*.

Linde, A. (2018). On the Problem of Initial Conditions for Inflation. *Found. Phys.* 48, 1246–1260. doi:10.1007/s10701-018-0177-9

Linsefors, L., and Barrau, A. (2013). Duration of Inflation and Conditions at the Bounce as a Prediction of Effective Isotropic Loop Quantum Cosmology. *Phys. Rev. D* 87, 123509. doi:10.1103/physrevd.87.123509

Malik, K. A. (2001). Cosmological Perturbations in an Inflationary Universe. *arXiv: astro-ph/0101563*.

Malik, K. A., and Wands, D. (2009). Cosmological Perturbations. *Phys. Rep.* 475, 1–51. doi:10.1016/j.physrep.2009.03.001

Martin, J., and Brandenberger, R. H. (2001). Trans-Planckian Problem of Inflationary Cosmology. *Phys. Rev. D* 63, 123501. doi:10.1103/physrevd.63.123501

Martínez, F. B., and Olmedo, J. (2016). Primordial Tensor Modes of the Early Universe. *Phys. Rev. D* 93, 124008. doi:10.1103/physrevd.93.124008

McAllister, L., and Silverstein, E. (2007). String Cosmology: A Review. *Gen. Relativ. Grav.* 40, 565.

Meissner, K. A. (2004). Black-hole Entropy in Loop Quantum Gravity. *Class. Quan. Grav.* 21, 5245–5251. doi:10.1088/0264-9381/21/22/015

Mena Marugán, G. A., Olmedo, J., and Pawlowski, T. (2011). Prescriptions in Loop Quantum Cosmology: A Comparative Analysis. *Phys. Rev. D* 84, 064012. doi:10.1103/physrevd.84.064012

Motaharfar, M., and Singh, P. (2021). *On the Role of Dissipative Effects in the Quantum Gravitational Onset of Warm Starobinsky Inflation in a Closed Universe*. arXiv:gr-qc/2102.09578.

Mukhanov, V., Feldman, H. A., and Brandenberger, R. H. (1992). Theory of Cosmological Perturbations. *Phys. Rep.* 215, 203–333. doi:10.1016/0370-1573(92)90044-z

Mukhanov, V. F., and Winitzki, S. (2007). *Introduction to Quantum Effects in Gravity*. Cambridge: Cambridge University Press.

Mukhanov, V. (2005). *Physics Foundations of Cosmology*. Cambridge: Cambridge University Press.

Navascues, B. E., de Blas, D. M., and Marugan, G. A. M. (2018). Time-dependent Mass of Cosmological Perturbations in the Hybrid and Dressed Metric Approaches to Loop Quantum Cosmology. *Phys. Rev.* D97, 043523.

Neuser, J., Schander, S., and Thiemann, T. (2019). Quantum Cosmological Backreactions II: Purely Homogeneous Quantum Cosmology. *arXiv: 1906.08185*.

Niemeyer, J. C., and Parentani, R. (2002). Corley-Jacobson Dispersion Relation and Trans-planckian Inflation. *Phys. Rev.* D65, 103514.

Niemeyer, J. C., and Parentani, R. (2003). Dependence of the Spectra of Fluctuations in Inflationary Cosmology on Trans-planckian Physics. *Phys. Rev.* D68, 063513.

Niemeyer, J. C., and Parentani, R. (2001). Trans-Planckian Dispersion Relation and Scale Invariance of Inflationary Perturbations. *Phys. Rev.* D64, 101301(R).

Olmedo, J., and Alesci, E. (2019). Power Spectrum of Primordial Perturbations for an Emergent Universe in Quantum Reduced Loop Gravity. *J. Cosmol. Astropart. Phys.* 2019, 030. doi:10.1088/1475-7516/2019/04/030

Oriti, D., Sindoni, L., and Wilson-Ewing, E. (2017). Bouncing Cosmologies from Quantum Gravity Condensates. *Class. Quan. Grav.* 34, 04LT01. doi:10.1088/1361-6382/aa549a

Oriti, D. (2017). The Universe as a Quantum Gravity Condensate. *Comptes Rendus Physique* 18, 235–245. doi:10.1016/j.crhy.2017.02.003

Parker, L., and Toms, D. (2009). *Quantum Field Theory in Curved Spacetime: Quantized Fields and Gravity*. Cambridge: Cambridge University Press.

Polchinski, J. (2001). *String Theory, Vol. 1 & 2*. Cambridge: Cambridge University Press.

Rovelli, C. (2008). *Quantum Gravity*. Cambridge: Cambridge University Press.

Saini, S., and Singh, P. (2019a). Generic Absence of strong Singularities and Geodesic Completeness in Modified Loop Quantum Cosmologies. *Class. Quan. Grav.* 36, 105014. doi:10.1088/1361-6382/ab1274

Saini, S., and Singh, P. (2019b). Von Neumann Stability of Modified Loop Quantum Cosmologies. *Class. Quan. Grav.* 36, 105010. doi:10.1088/1361-6382/ab1608

Sato, K. (1981). First-order Phase Transition of a Vacuum and the Expansion of the Universe. *Monthly Notices R. Astronomical Soc.* 195, 467–479. doi:10.1093/mnras/195.3.467

Schander, S., and Thiemann, T. (2019). Quantum Cosmological Backreactions I: Cosmological Space Adiabatic Perturbation Theory. *arXiv:1906.08166*.

Schander, S., and Thiemann, T. (2019). Quantum Cosmological Backreactions III: Deparametrised Quantum Cosmological Perturbation Theory. *arXiv: 1906.08194*.

Schwarz, D. J., Copi, C. J., Huterer, D., and Starkman, G. D. (2016). CMB Anomalies after Planck. *Class. Quan. Grav.* 33, 184001. doi:10.1088/0264-9381/33/18/184001

Senatore, L. (2017). "Lectures on Inflation," in *New Frontiers in Fields and Strings, Proceedings of the 2015 Theoretical Advanced Study Institute in Elementary Particle Physics, Boulder, Colorado, 1 - 26 June 2015*. Editors J. Polchinski, P. Vieira, and O. DeWolfe (Singapore: World Scientific), 447–543.

Shahalam, M., Al Ajmi, M., Myrzakulov, R., and Wang, A. (2020). Revisiting Pre-inflationary Universe of Family of α -attractor in Loop Quantum Cosmology. *Class. Quan. Grav.* 37, 195026. doi:10.1088/1361-6382/aba486

Shahalam, M. (2018). Preinflationary Dynamics of Power-Law Potential in Loop Quantum Cosmology †. *Universe* 4, 87. doi:10.3390/universe4080087

Shahalam, M., Sami, M., and Wang, A. (2018). Pre-inflationary Dynamics of α-attractor in Loop Quantum Cosmology. *Phys. Rev.* D98, 043524.

Shahalam, M., Sharma, M., Wu, Q., and Wang, A. (2017). Preinflationary Dynamics in Loop Quantum Cosmology: Power-Law Potentials. *Phys. Rev. D* 96, 123533. doi:10.1103/physrevd.96.123533

Sharma, M., Shahalam, M., Wu, Q., and Wang, A. (2018). Preinflationary Dynamics in Loop Quantum Cosmology: Monodromy Potential. *J. Cosmol. Astropart. Phys.* 2018, 003. doi:10.1088/1475-7516/2018/11/003

Sharma, M., Zhu, T., and Wang, A. (2019). Background Dynamics of Pre-inflationary Scenario in Brans-Dicke Loop Quantum Cosmology. *Commun. Theor. Phys.* 71, 1205. doi:10.1088/0253-6102/71/10/1205

Silverstein, E. (2016). TASI Lectures on Cosmological Observables and String Theory. *arXiv:1606.03640*.

Singh, P. (2009). Are Loop Quantum cosmos Never Singular? *Class. Quan. Grav.* 26, 125005. doi:10.1088/0264-9381/26/12/125005

Singh, P. (2018). Glimpses of Space-Time beyond the Singularities Using Supercomputers. *Comput. Sci. Eng.* 20, 26–38. doi:10.1109/mcse.2018.042781324

Singh, P. (2014). Loop Quantum Cosmology and the Fate of Cosmological Singularities. *Bull. Astron. Soc. India* 42, 121.

Singh, P., Vandersloot, K., and Vereshchagin, G. V. (2006). Non-singular Bouncing Universes in Loop Quantum Cosmology. *Phys. Rev.* D74, 043510.

Starobinsky, A. A. (1980). A New Type of Isotropic Cosmological Models without Singularity. *Phys. Lett. B* 91, 99–102. doi:10.1016/0370-2693(80)90670-x

Thiemann, T. (2006). Complexifier Coherent States for Quantum General Relativity. *Class. Quan. Grav.* 23, 2063–2117. doi:10.1088/0264-9381/23/6/013

Thiemann, T. (2001a). Gauge Field Theory Coherent States (GCS): I. General Properties. *Class. Quan. Grav.* 18, 2025–2064. doi:10.1088/0264-9381/18/11/304

Thiemann, T. (2007). *Modern Canonical Quantum General Relativity*. Cambridge: Cambridge University Press.

Thiemann, T. (1998a). Quantum Spin Dynamics (QSD). *Class. Quan. Grav.* 15, 839–873. doi:10.1088/0264-9381/15/4/011

Thiemann, T. (1998b). Quantum Spin Dynamics (QSD): II. The Kernel of the Wheeler - DeWitt Constraint Operator. *Class. Quan. Grav.* 15, 875–905. doi:10.1088/0264-9381/15/4/012

Thiemann, T., and Winkler, O. (2001b). Gauge Field Theory Coherent States (GCS): II. Peakedness Properties. *Class. Quan. Grav.* 18, 2561–2636. doi:10.1088/0264-9381/18/14/301

Wald, R. M. (1994). *Quantum Field Theory Om Curved Spacetime and Black Hole Thermodynamics*. Chicago: The University of Chicago Press.

Wand, D. (1999). Duality Invariance of Cosmological Perturbation Spectra. *Phys. Rev.* D60, 023507.

Weinberg, S. (1980). in *General Relativity, an Einstein Centenary Survey*. Editors S. W. Hawking and W. Israel (Cambridge: Cambridge University Press).

Weinberg, S. (2008). *Cosmology*. Oxford: Oxford University Press.

Wilson-Ewing, E. (2017). Testing Loop Quantum Cosmology. *Comptes Rendus Physique* 18, 207–225. doi:10.1016/j.crhy.2017.02.004

Wilson-Ewing, E. (2018). The Loop Quantum Cosmology Bounce as a Kasner Transition. *Class. Quan. Grav.* 35, 065005. doi:10.1088/1361-6382/aaab8b

Woodard, R. P. (2014). Perturbative Quantum Gravity Comes of Age. *arXiv: 1407.4748*.

Wu, Q., Zhu, T., and Wang, A. (2018). Nonadiabatic Evolution of Primordial Perturbations and Non-gaussinity in Hybrid Approach of Loop Quantum Cosmology. *Phys. Rev. D* 98, 103528. doi:10.1103/physrevd.98.103528

Xiao, K. (2020). Tachyon Field in Loop Cosmology. *Phys. Lett. B* 811, 135859. doi:10.1016/j.physletb.2020.135859

Xiao, K. (2019). Tachyonic Inflation in Loop Quantum Cosmology. *Eur. Phys. J. C* 79, 1019. doi:10.1140/epjc/s10052-019-7538-1

Xiao, K., and Wang, S.-Q. (2020). Pre-inflation Dynamical Behavior of Warm Inflation in Loop Quantum Cosmology. *Mod. Phys. Lett. A.* 35, 2050293. doi:10.1142/s0217732320502934

Yang, J., Ding, Y., and Ma, Y. (2009). Alternative Quantization of the Hamiltonian in Loop Quantum Cosmology. *Phys. Lett. B* 682, 1–7. doi:10.1016/j.physletb.2009.10.072

Zhang, X., and Ling, Y. (2007). Inflationary Universe in Loop Quantum Cosmology. *JCAP* 08, 012.

Zhu, T., Wang, A., Kirsten, K., Cleaver, G., and Sheng, Q. (2017). Pre-inflationary Universe in Loop Quantum Cosmology. *Phys. Rev.* D96, 083520.

Zhu, T., Wang, A., Kirsten, K., Cleaver, G., and Sheng, Q. (2018). Primoridial Non-gaussianity and Power Asymmetry with Quantum Gravitational Effects in Loop Quantum Cosmology. *Phys. Rev.* D97, 043501.

Zhu, T., Wang, A., Kirsten, K., Cleaver, G., and Sheng, Q. (2017). Universal Features of Quantum Bounce in Loop Quantum Cosmology. *Phys. Lett. B* 773, 196–202. doi:10.1016/j.physletb.2017.08.025

Conflict of Interest: The authors declare that the research was conducted in the absence of any commercial or financial relationships that could be construed as a potential conflict of interest.

frontiers in Astronomy and Space Sciences

ORIGINAL RESEARCH
published: 13 July 2021
doi: 10.3389/fspas.2021.701723

Exploring Alternatives to the Hamiltonian Calculation of the Ashtekar-Olmedo-Singh Black Hole Solution

Alejandro García-Quismondo and Guillermo A. Mena Marugán*

Instituto de Estructura de la Materia, IEM-CSIC, Madrid, Spain

In this article, we reexamine the derivation of the dynamical equations of the Ashtekar-Olmedo-Singh black hole model in order to determine whether it is possible to construct a Hamiltonian formalism where the parameters that regulate the introduction of quantum geometry effects are treated as true constants of motion. After arguing that these parameters should capture contributions from two distinct sectors of the phase space that had been considered independent in previous analyses in the literature, we proceed to obtain the corresponding equations of motion and analyze the consequences of this more general choice. We restrict our discussion exclusively to these dynamical issues. We also investigate whether the proposed procedure can be reconciled with the results of Ashtekar, Olmedo, and Singh, at least in some appropriate limit.

Keywords: loop quantum cosmology, loop quantum gravity, black holes, polymer quantization, quantum geometry

OPEN ACCESS

Edited by:
Alvaro De La Cruz-Dombriz, University of Cape Town, South Africa

Reviewed by:
Vyacheslav Ivanovich Dokuchaev, Institute for Nuclear Research, Russia
Wen-Biao Han, Shanghai Astronomical Observatory (CAS), China

****Correspondence:***
Alejandro García-Quismondo
alejandro.garcia@iem.cfmac.csic.es

Specialty section:
This article was submitted to Cosmology, a section of the journal Frontiers in Astronomy and Space Sciences

Received: *28 April 2021*
Accepted: *17 June 2021*
Published: *13 July 2021*

Citation:
García-Quismondo A and Mena Marugán GA (2021) Exploring Alternatives to the Hamiltonian Calculation of the Ashtekar-Olmedo-Singh Black Hole Solution. Front. Astron. Space Sci. 8:701723. doi: 10.3389/fspas.2021.701723

1 INTRODUCTION

Over two years ago, a new model to describe black hole spacetimes in effective loop quantum cosmology was put forward in (Ashtekar et al., 2018a; Ashtekar et al., 2018b; Ashtekar and Olmedo, 2020) by Ashtekar, Olmedo, and Singh (AOS). The work of these authors is set apart from previous related investigations in the literature [see (Ashtekar and Bojowald, 2005a; Ashtekar and Bojowald, 2005b; Cartin and Khanna, 2006; Modesto, 2006; Bojowald et al., 2007; Boehmer and Vandersloot, 2007; Campiglia et al., 2008; Sabharwal and Khanna, 2008; Chiou, 2008a; Chiou, 2008b; Brannlund et al., 2009; Gambini et al., 2014; Gambini and Pullin, 2014; Dadhich et al., 2015; Haggard and Rovelli, 2015; Joe and Singh, 2015; Corichi and Singh, 2016; Campiglia et al., 2016; Saini and Singh, 2016; Cortez et al., 2017; Olmedo et al., 2017; Yonika et al., 2018; Bianchi et al., 2018; Bodendorfer et al., 2019a; Alesci et al., 2019; Bouhmadi-López et al., 2020a; Bojowald, 2020a; Ben Achour et al., 2020; Gambini et al., 2020; Kelly et al., 2020; Gan et al., 2020; Kelly et al., 2021; Bodendorfer et al., 2021a; Bodendorfer et al., 2021b; Daghigh et al., 2021; Münch, 2021), among others] owing to a combination of features. On the one hand, the main focus is placed on black hole related aspects rather than issues central to anisotropic cosmologies. On the other hand, the resulting model is claimed to display neither a dependence on fiducial structures nor large quantum effects on low curvature regions. By virtue of the introduction of quantum geometry (QG)

effects, which is implemented by means of two polymerization parameters[1], the classical singularity at the center of the black hole is replaced with a transition surface that joins a trapped region to its past and an anti-trapped one to its future, extending the Schwarzschild interior to encompass what is interpreted as a white hole horizon. The resulting metric, that we will call effective in the sense that it can be treated classically but incorporates QG modifications, is smooth and its curvature invariants admit upper bounds that do not depend on the mass of the black hole (Ashtekar et al., 2018a; Ashtekar et al., 2018b; Ashtekar and Olmedo, 2020). The model is completed with a description of the exterior region that can be joined smoothly to the interior region, both to its past and its future, resulting in an extension of the whole Kruskal spacetime.

The authors of (Ashtekar et al., 2018a; Ashtekar et al., 2018b; Ashtekar and Olmedo, 2020) emphasize that they adopt a mixed prescription for the implementation of the improved dynamics. Indeed, instead of choosing the relevant polymerization parameters as constants or as arbitrary phase space functions, they claim to fix them to be Dirac observables. However, they do not treat them as such in their Hamiltonian calculation: in practice, the polymerization parameters are regarded as *constants* in that calculation and, once the dynamical equations have been derived and solved, the parameters are set equal to the value of certain functions of the ADM mass of the black hole, which is a Dirac observable itself. This fact was already noted by Bodendorfer, Mele, and Münch in (Bodendorfer et al., 2019b), where they showed that a genuine treatment of the polymerization parameters as constants of motion, which are constant only along dynamical trajectories (i.e., on shell) but not on the whole phase space, would produce an extra phase-space dependent factor in the Hamiltonian equations. The analysis carried out in (Bodendorfer et al., 2019b) exploits the structure of the Hamiltonian constraint of the system, which is composed by the difference of two Dirac observables (the on-shell value of each of which turns out to be the black hole mass), to divide the phase space into two independent subsectors, associated with the degrees of freedom along the radial and angular spatial directions. In each subsector, the dynamics is generated by one of these constants of motion, which can then be regarded as *partial Hamiltonians*. Additionally, in (Bodendorfer et al., 2019b), these Dirac observables play the role of polymerization parameters, in the sense that each of the parameters is taken to be a function only of its associated partial Hamiltonian. On shell, this is equivalent to deal with parameters that are functions of the black hole mass, and at least in this sense one would recover the original proposal of (Ashtekar et al., 2018a; Ashtekar et al., 2018b; Ashtekar and Olmedo, 2020).

Nonetheless, since the two partial Hamiltonians become equal by virtue of the vanishing of the constraint, there is no telling apart which of the two contributes to the on-shell expression of each of the polymerization parameters. Therefore, one may argue that each parameter should be taken as a function of *both* partial Hamiltonians, something that breaks the decoupling of subsectors at the Hamiltonian and dynamical levels. In the following, we focus our discussion exclusively on examining whether there exists an alternative procedure to carry out the Hamiltonian calculation starting from this observation, leaving apart other issues related with the asymptotic behavior of the metric, its physical interpretation, or quantum covariance, that are beyond the scope of this work (for recent criticisms on the AOS viewpoint on these issues, see (Bojowald, 2019; Arruga et al., 2020; Bojowald, 2020b; Bouhmadi-López et al., 2020b). The main purpose of our investigation is to explore the possibility that one can develop an alternative dynamical analysis based on the cross-dependence of the polymerization parameters on the two partial Hamiltonians of the system, and study whether this possibility can reconcile in some sense the derivation of the solution presented in (Ashtekar et al., 2018a; Ashtekar et al., 2018b; Ashtekar and Olmedo, 2020) with a genuine consideration of the parameters as constants of motion.

The rest of this paper is structured as follows. In **Section 2** we explore the consequences of polymerization parameters that are functions of both partial Hamiltonians as regards the derivation of the equations of motion associated with the Hamiltonian constraint of (Ashtekar et al., 2018a; Ashtekar et al., 2018b; Ashtekar and Olmedo, 2020). In **Section 3** we define two time variables that allow us to simplify the form of the dynamical equations and examine whether they can be made equal to each other in general. In **Section 4** we analyze the consistency of imposing this equality on the newly defined time variables at least in the asymptotic limit of large black hole masses, and study their relation for finite values of the mass. Finally, we conclude in **Section 5** with a discussion of our results. Throughout this article, we set the speed of light and the reduced Planck constant equal to one.

2 DYNAMICAL EQUATIONS

In this section, we investigate an alternative avenue in the computation of the equations that govern the modified dynamics of the interior region of a black hole, based on a more general choice of polymerization parameters off shell. With a suitable choice of lapse function of the form (Ashtekar et al., 2018a; Ashtekar et al., 2018b; Ashtekar and Olmedo, 2020)

$$N = \frac{\gamma\delta_b\sqrt{|p_c|}}{\sin\delta_b b}, \tag{1}$$

where γ is the Immirzi parameter. The so-called effective Hamiltonian of the system can be written as (Ashtekar et al., 2018a; Ashtekar et al., 2018b; Ashtekar and Olmedo, 2020)

[1]The term polymerization refers to the name "polymer quantization", which is often employed for the quantization of symmetry reduced models with loop techniques. The motivation for this terminology comes from the 1-dimensional nature of the basic excitations of the gravitational field in the loop quantization, excitations that are localized on the edges of 1-dimensional graphs on which the holonomies are not trivial in the (so-called cylindrical) quantum states, leading to this polymer-like picture of spacetime geometry.

$$NH_{\text{eff}} = \frac{L_o}{G}\,(O_b - O_c), \tag{2}$$

$$O_b = -\frac{1}{2\gamma}\left(\frac{\sin\delta_b b}{\delta_b} + \frac{\gamma^2\delta_b}{\sin\delta_b b}\right)\frac{p_b}{L_o}, \tag{3}$$

$$O_c = \frac{1}{\gamma}\,\frac{\sin\delta_c c}{\delta_c}\,\frac{p_c}{L_o}, \tag{4}$$

where L_o is the length of the edge parallel to the x-direction of the fiducial cell and G is the Newtonian gravitational constant. The canonical variables b, c, p_b, and p_c have the following nonvanishing Poisson brackets:

$$\{b, p_b\} = G\gamma, \quad \{c, p_c\} = 2G\gamma. \tag{5}$$

Furthermore, δ_b and δ_c are the parameters that capture and introduce the QG effects in the system. The classical Hamiltonian of the model within General Relativity is recovered in the limit $\delta_b, \delta_c \to 0$. It is interesting to note that, should δ_b and δ_c be regarded as constants, NH_{eff} is given by the difference of two objects that generate the dynamics in two distinct subsectors of the phase space that are dynamically decoupled. For this reason, we often refer to O_b and O_c as the partial Hamiltonians[2] of the b and c subsectors, respectively. Both O_b and O_c turn out to be Dirac observables, i.e., constant along each dynamical trajectory. The vanishing of the Hamiltonian constraint implies that, on shell, they are equal to the same constant of motion, m, which happens to be proportional to the ADM mass of the black hole.

In the AOS black hole model (Ashtekar et al., 2018a; Ashtekar et al., 2018b; Ashtekar and Olmedo, 2020), the parameters δ_b and δ_c are treated as constants on the whole phase space and then fixed to have the same value as certain functions of the Dirac observable m. The authors of (Bodendorfer et al., 2019b) propose an alternative way to treat these parameters as constants of motion from the very beginning: they take δ_b and δ_c as functions of their respective partial Hamiltonian, $\delta_b = \delta_b(O_b)$ and $\delta_c = \delta_c(O_c)$, so that the parameters remain functions of m on shell. Nonetheless, since both O_b and O_c have the same on-shell value, it can be argued that each of the considered parameters should be assumed to be a function of both partial Hamiltonians: on shell, the contribution of one cannot be told apart from that of the other. In this work, we will follow this line of reasoning and investigate its consequences within the ensuing Hamiltonian calculation.

Thus, let δ_b and δ_c be functions of both partial Hamiltonians

$$\delta_i = f_i(O_b, O_c), \tag{6}$$

with $i = b, c$. This cross-dependence introduces a coupling between the b and c subsectors that was absent in previous works and that will obviously influence the form of the dynamical equations. Let us begin by computing the equations of motion associated with the connection variables b and c, that we will collectively denote with the symbol i (no confusion with the imaginary number will arise in our calculations). We have

$$\partial_t i = s_i\frac{L_o}{G}\big(\{i, O_i\} - \{i, O_j\}\big), \tag{7}$$

where t is the time variable associated with the choice of lapse N, $i, j = b, c$, $j \neq i$, and s_i is a sign defined by

$$s_b = +1, \quad s_c = -1. \tag{8}$$

The Poisson bracket of i with its respective partial Hamiltonian O_i is given by

$$\{i, O_i\} = \{i, p_i\}\frac{\partial O_i}{\partial p_i} + \frac{\partial O_i}{\partial \delta_i}\left(\frac{\partial f_i}{\partial O_i}\{i, O_i\} + \frac{\partial f_i}{\partial O_j}\{i, O_j\}\right). \tag{9}$$

Similarly,

$$\{i, O_j\} = \frac{\partial O_j}{\partial \delta_j}\left(\frac{\partial f_j}{\partial O_i}\{i, O_i\} + \frac{\partial f_j}{\partial O_j}\{i, O_j\}\right). \tag{10}$$

The Poisson brackets of the connection variables with each partial Hamiltonian can be solved for in the system of linear equations formed by **Eqs. 9**, **10**. When rewritten appropriately, this system can be recast in matrix form:

$$\begin{pmatrix} 1-\Delta_{ii} & -\Delta_{ij} \\ -\Delta_{ji} & 1-\Delta_{jj} \end{pmatrix}\begin{pmatrix} \{i, O_i\} \\ \{i, O_j\} \end{pmatrix} = \begin{pmatrix} \{i, p_i\}\dfrac{\partial O_i}{\partial p_i} \\ 0 \end{pmatrix}, \tag{11}$$

where we have defined

$$\Delta_{ij} = \frac{\partial O_i}{\partial \delta_i}\,\frac{\partial f_i}{\partial O_j}. \tag{12}$$

The system **Eq. 11** can be solved if and only if

$$(1-\Delta_{ii})\big(1-\Delta_{jj}\big) - \Delta_{ij}\Delta_{ji} \neq 0. \tag{13}$$

Assuming that this invertibility condition holds,

$$\begin{pmatrix} \{i, O_i\} \\ \{i, O_j\} \end{pmatrix} = \frac{\{i, p_i\}\frac{\partial O_i}{\partial p_i}}{(1-\Delta_{ii})\big(1-\Delta_{jj}\big) - \Delta_{ij}\Delta_{ji}}\begin{pmatrix} 1-\Delta_{jj} \\ \Delta_{ji} \end{pmatrix}. \tag{14}$$

Therefore, by virtue of **Eq. 7**,

$$\partial_t i = \frac{1-\Delta_{jj}-\Delta_{ji}}{(1-\Delta_{ii})\big(1-\Delta_{jj}\big) - \Delta_{ij}\Delta_{ji}}\left[s_i\frac{L_o}{G}\{i, p_i\}\frac{\partial O_i}{\partial p_i}\right], \tag{15}$$

with $i, j = b, c$ and $j \neq i$. Following the same reasoning, the equations of motion associated with the triad variables p_b and p_c turn out to be

$$\partial_t p_i = \frac{1-\Delta_{jj}-\Delta_{ji}}{(1-\Delta_{ii})\big(1-\Delta_{jj}\big) - \Delta_{ij}\Delta_{ji}}\left[-s_i\frac{L_o}{G}\{i, p_i\}\frac{\partial O_i}{\partial i}\right], \tag{16}$$

with $i, j = b, c$ and $j \neq i$.

It is worth noting that the objects in square brackets in **Eqs. 15**, **16** are the dynamical equations that result when δ_b and δ_c are treated as constants on the whole phase space, i.e., those used in (Ashtekar et al., 2018a; Ashtekar et al., 2018b; Ashtekar and Olmedo, 2020). Therefore, if we allow the quantum parameters to

[2]Strictly speaking, the objects that generate the dynamics in each subsector are L_oO_b/G and L_oO_c/G. However, in practice, we will ignore the constant factor L_o/G (which could be reabsorbed through an appropriate redefinition of the lapse function), focus on the more interesting phase space dependent parts, O_b and O_c, and use this terminology to refer to them succinctly.

be functions of both partial Hamiltonians, the equations of motion are modified via a multiplicative phase space dependent factor,

$$C_{ij} = \frac{1 - \Delta_{jj} - \Delta_{ji}}{(1 - \Delta_{ii})(1 - \Delta_{jj}) - \Delta_{ij}\Delta_{ji}}. \tag{17}$$

As expected, this factor reduces to the one found in (Bodendorfer et al., 2019b) when the b and c subsectors are decoupled. Indeed, in that case $\Delta_{ij} = 0$ if $i \neq j$, and C_{ij} reduces to

$$C_{ij} \to C_i = \frac{1}{1 - \Delta_{ii}}, \tag{18}$$

which is identical to what the authors of that reference called F_i^{-1}.

3 TIME REDEFINITIONS

Let $\overrightarrow{v}_{H_0}$ be the Hamiltonian vector field associated with the Hamiltonian H_0 that is identical to NH_{eff} except for the fact that δ_b and δ_c are constant on the whole phase space,

$$\overrightarrow{v}_{H_0} = \left(\frac{\partial H_0}{\partial p_b}, -\frac{\partial H_0}{\partial b}, \frac{\partial H_0}{\partial p_c}, -\frac{\partial H_0}{\partial c}\right) = \left(\overrightarrow{v}_{H_{0,b}}, \overrightarrow{v}_{H_{0,c}}\right). \tag{19}$$

According to the results of the previous section, when the parameters of the model are instead given by functions of both O_b and O_c, the Hamiltonian vector field is given by

$$\overrightarrow{v}_{H_{\text{eff}}} = \left(C_{bc}\overrightarrow{v}_{H_{0,b}}, C_{cb}\overrightarrow{v}_{H_{0,c}}\right). \tag{20}$$

This local rescaling of the Hamiltonian vector field implies that it is possible to introduce a suitable redefinition of the time variable in each subsector such that one can recover the simpler dynamics generated by H_0. However, the fact that C_{ij} is, in general, nonsymmetric means that this change of time is different in the b and c subsectors of the phase space. Indeed, it is immediate to see that, with the appropriate time redefinitions, the dynamical equations become

$$\partial_{\tilde{t}_i} i = s_i \frac{L_o}{G}\{i, p_i\}\frac{\partial O_i}{\partial p_i}, \quad \partial_{\tilde{t}_i} p_i = -s_i \frac{L_o}{G}\{i, p_i\}\frac{\partial O_i}{\partial i}, \tag{21}$$

where the sector-dependent time variable $\tilde{t}_i$ is defined in the following manner:

$$d\tilde{t}_i = C_{ij}dt, \tag{22}$$

with $i, j = b, c$ and $j \neq i$. Hence, we see that the dynamics that we obtain in the b and c subsectors coincides with that of the AOS model (Ashtekar et al., 2018a; Ashtekar et al., 2018b; Ashtekar and Olmedo, 2020) when the corresponding equations of motion **Eqs. 15**, **16** are rewritten in terms of two time variables, $\tilde{t}_b$ and $\tilde{t}_c$, which are in general *different in each subsector*. This observation provides a strategy to solve the dynamical equations obtained in **Section 2**: perform the time redefinitions $t \to \tilde{t}_i$, solve the resulting simpler equations of motion and rewrite the solutions in terms of the original time variable through the integration of **Eq. 22**.

An appealing possibility that we are going to study is whether these time variables can be set to be equal by making use of the freedom that exists off shell. Let us assume that, on shell, $\tilde{t}_b = \alpha\tilde{t}_c$, where α is a real constant. This directly implies that

$$C_{bc}|_{\text{on}} = \alpha C_{cb}|_{\text{on}} \Rightarrow 1 - \Delta_{cc}|_{\text{on}} - \Delta_{cb}|_{\text{on}} = \alpha(1 - \Delta_{bb}|_{\text{on}} - \Delta_{bc}|_{\text{on}}), \tag{23}$$

where the symbol $|_{\text{on}}$ denotes on-shell evaluation, i.e. evaluation on the phase space region where $H_{\text{eff}} = 0$. This requirement constitutes a restriction in the form of the first derivatives of the polymerization parameters with respect to the partial Hamiltonians. In the case $\alpha = 1$ (of direct application to the AOS model), this condition reduces to

$$\Delta_{bb}|_{\text{on}} + \Delta_{bc}|_{\text{on}} = \Delta_{cc}|_{\text{on}} + \Delta_{cb}|_{\text{on}}. \tag{24}$$

We will however consider an arbitrary value of α. Rewriting **Eq. 23** by using the definition of Δ_{ij} (see **Eq. 12**), we obtain that the following condition must be satisfied:

$$1 - \frac{\partial O_c}{\partial \delta_c}\bigg|_{\text{on}}\left(\frac{\partial f_c}{\partial O_c}\bigg|_{\text{on}} + \frac{\partial f_c}{\partial O_b}\bigg|_{\text{on}}\right) = \alpha\left[1 - \frac{\partial O_b}{\partial \delta_b}\bigg|_{\text{on}}\left(\frac{\partial f_b}{\partial O_b}\bigg|_{\text{on}} + \frac{\partial f_b}{\partial O_c}\bigg|_{\text{on}}\right)\right]. \tag{25}$$

Since the two parameters are functions only of the partial Hamiltonians, their evaluation on shell is equivalent to setting $O_b = O_c = m$ in f_i. However, it will prove more useful to rewrite δ_i as functions of the linear combinations

$$\mu_1 = \frac{O_b + O_c}{2}, \quad \mu_2 = \frac{O_b - O_c}{2}, \tag{26}$$

the on-shell values of which are given by $\mu_1|_{\text{on}} = m$ and $\mu_2|_{\text{on}} = 0$. Then, **Eq. 25** can be rewritten as

$$1 - \frac{\partial O_c}{\partial \delta_c}\bigg|_{\text{on}}\frac{\partial f_c}{\partial \mu_1}\bigg|_{\text{on}} = \alpha\left(1 - \frac{\partial O_b}{\partial \delta_b}\bigg|_{\text{on}}\frac{\partial f_b}{\partial \mu_1}\bigg|_{\text{on}}\right). \tag{27}$$

Assuming that the functions f_i are $\mathcal{C}^1$, we can evaluate them on shell first and then compute the derivatives. Thus, for $\tilde{t}_b$ and $\tilde{t}_c$ to be proportional, it must be satisfied on shell that

$$1 - \frac{\partial O_c}{\partial \delta_c}\bigg|_{\text{on}}\frac{\partial f_c(m,0)}{\partial m} = \alpha\left(1 - \frac{\partial O_b}{\partial \delta_b}\bigg|_{\text{on}}\frac{\partial f_b(m,0)}{\partial m}\right). \tag{28}$$

In the rest of our discussion, we will omit the on-shell evaluations in formulas of this kind to simplify our notation. The on-shell restriction will be clear from the context.

The derivatives of the partial Hamiltonians with respect to δ_b and δ_c are

$$\frac{\partial O_b}{\partial \delta_b} = -\frac{1}{2\gamma}\left(1 - \frac{\gamma^2\delta_b^2}{\sin^2\delta_b b}\right)\frac{\delta_b b\cos\delta_b b - \sin\delta_b b}{\delta_b^2}\frac{p_b}{L_o}, \tag{29}$$

$$\frac{\partial O_c}{\partial \delta_c} = \frac{1}{\gamma}\frac{\delta_c c\cos\delta_c c - \sin\delta_c c}{\delta_c^2}\frac{p_c}{L_o}, \tag{30}$$

as can be immediately derived from **Eqs. 3**, **4**. The fact that these derivatives depend on the canonical variables seems in

tension with the requirement that **Eq. 28** must be satisfied on the whole phase space. Since the derivatives $\partial_m f_i(m,0)$ only depend on m (and, therefore, remain constant along each dynamical trajectory), the functions f_i need to be selected so that any phase space dependent contribution is canceled identically.

In order to evaluate these derivatives on shell, it is necessary to identify the independent functional dependences. It is immediate to see that the dependence on the connection variables b and c can be removed in terms of their momenta and the black hole mass. Indeed, the functions of each connection variable can be rewritten in terms of its corresponding partial Hamiltonian and triad variable. Using **Eqs. 3**, **4**, and requiring an acceptable limit for large masses, we obtain

$$\frac{\sin\delta_b b}{\delta_b} = -\frac{\gamma L_o O_b}{p_b}\left(1+\sqrt{1-\frac{p_b^2}{L_o^2 O_b^2}}\right), \tag{31}$$

$$\frac{\sin\delta_c c}{\delta_c} = \frac{\gamma L_o O_c}{p_c}. \tag{32}$$

Hence, the only independent functional dependences that remain on shell are those associated with the triad variables. By means of the above relations, we can recast every function of b and c that appears in **Eqs. 29**, **30** as a function of p_b, p_c, and the partial Hamiltonians, which reduce to m after the on-shell evaluation. After a straightforward computation, we obtain on shell that

$$\frac{\partial O_c}{\partial \delta_c} = \frac{\pm \arcsin\left[\frac{\gamma L_o m f_c(m,0)}{p_c}\right]\sqrt{\frac{p_c^2}{L_o^2}-\gamma^2 m^2 f_c^2(m,0)} - \gamma m f_c(m,0)}{\gamma f_c^2(m,0)}, \tag{33}$$

where the sign $\pm$ corresponds with the sign of $\cos\delta_c c$. A similar, although more complicated expression can be found for the on-shell value of $\partial O_b/\partial\delta_b$. To shorten this expression, we use (exclusively here) the compact notation $\tilde{p}_b = p_b/(L_o m)$:

$$\begin{aligned}\frac{\partial O_b}{\partial \delta_b} = {} & \frac{m}{2\gamma f_b^2(m,0)}\left[1-\tilde{p}_b^2\left(1+\sqrt{1-\tilde{p}_b^2}\right)^{-2}\right] \\ & \times\left\{-\gamma f_b(m,0)\left(1+\sqrt{1-\tilde{p}_b^2}\right)\pm\arcsin\left[\frac{\gamma f_b(m,0)}{\tilde{p}_b}\left(1+\sqrt{1-\tilde{p}_b^2}\right)\right]\right. \\ & \left.\times\sqrt{\tilde{p}_b^2-\gamma^2 f_b^2(m,0)\left(1+\sqrt{1-\tilde{p}_b^2}\right)^2}\right\}.\end{aligned} \tag{34}$$

On the light of these relations, we realize that the condition **Eq. 28** has the following structure:

$$1-F_c(p_c)\frac{\partial f_c(m,0)}{\partial m} = \alpha\left[1-F_b(p_b)\frac{\partial f_b(m,0)}{\partial m}\right], \tag{35}$$

where the functional forms of F_b and F_c are irrelevant for the present argument, except that they are not constant functions. For this condition to hold on the whole phase space, the derivatives of the polymerization parameters must vanish

$$\frac{\partial f_i(m,0)}{\partial m} = 0, \tag{36}$$

and α must be equal to one. As a result, we conclude that, if we demand that $\tilde{t}_b$ and $\tilde{t}_c$ be proportional for all values of the mass, the only possibility is that they are equal and the polymerization parameters are constants. In other words, we cannot reconcile the choice of these parameters as Dirac observables and the dynamics being governed by **Eq. 21** in a single time variable, at least for all values of the mass. The lesson to be drawn from this result is that the appearance of two distinct time variables that simplify the dynamics in the radial and angular subsectors of phase space is a defining feature of the model if we treat the parameters δ_i as proper Dirac observables. The difference between these two times, as well as between them and the coordinate time t, can have consequences on the spacetime geometry, as we will very briefly comment on **Section 5**. In the next section, we will examine whether condition **Eq. 28** can be imposed consistently for black hole masses much larger than the Planck mass.

4 CONSISTENCY IN THE LIMIT OF LARGE BLACK HOLE MASSES

In this section, we investigate whether the dynamics of the AOS model, that results from considering the parameters δ_i as constant numbers in the Hamiltonian calculations, can be recovered at least in the limit of large black hole masses when these parameters are taken instead as constants of motion and one introduces a convenient time redefinition. Let us begin by assuming that it is possible. Then, in the considered limit, the dynamical equations adopt the same form as in (Ashtekar et al., 2018a; Ashtekar et al., 2018b; Ashtekar and Olmedo, 2020), up to subdominant terms that reflect the fact that $\tilde{t}_b$ and $\tilde{t}_c$ cannot be made equal for all values of the mass. Furthermore, according to the argument presented in (Ashtekar et al., 2018a; Ashtekar et al., 2018b; Ashtekar and Olmedo, 2020), the parameters δ_i are found to be given by

$$\begin{aligned}\delta_b &= \left(\frac{\sqrt{\Delta}}{\sqrt{2\pi}\gamma^2 m}\right)^{1/3} + o\left(m^{-1/3}\right), \\ \delta_c &= \frac{1}{2L_o}\left(\frac{\gamma\Delta^2}{4\pi^2 m}\right)^{1/3} + o\left(m^{-1/3}\right),\end{aligned} \tag{37}$$

where the symbol $o(\cdot)$ collectively denotes all the terms that are subdominant with respect to the function inside the parentheses. In these expressions, Δ is the area gap in loop quantum gravity. Therefore, asymptotically,

$$\frac{\partial f_i}{\partial m} = -\frac{1}{3}\frac{\delta_i}{m} + o\left(\frac{\delta_i}{m}\right), \tag{38}$$

with $i = b, c$. Then, the condition **Eq. 28** can be imposed consistently as long as[3]

[3]Should any of the exponents n_i be equal to 4/3, it is straightforward to realize that a further condition on the coefficients of the dominant terms must be met for **Eq. 28** to hold asymptotically.

$$\lim_{m\to\infty}\frac{\partial O_i}{\partial \delta_i}\sim m^{n_i},\quad n_i\leq\frac{4}{3}, \tag{39}$$

with $i = b, c$.

Given the fact that we are working under the assumption that $\tilde{t}_b = \tilde{t}_c = \tilde{t}$ when $m\to\infty$, we obtain from the solutions of (Ashtekar et al., 2018a; Ashtekar et al., 2018b; Ashtekar and Olmedo, 2020) that, in this limit and up to subdominant corrections,

$$\cos\delta_b b(\tilde{t}) = b_o\tanh\left[\frac{1}{2}\left(b_o\tilde{t}+2\tanh^{-1}\frac{1}{b_o}\right)\right], \tag{40}$$

$$\tan\frac{\delta_c c(\tilde{t})}{2} = \frac{\gamma L_o\delta_c}{8m}e^{-2\tilde{t}}, \tag{41}$$

$$p_b(\tilde{t}) = -2\frac{\sin\delta_c c(\tilde{t})}{\delta_c}\frac{\sin\delta_b b(\tilde{t})}{\delta_b}\frac{p_c(\tilde{t})}{\gamma^2+\frac{\sin^2\delta_b b(\tilde{t})}{\delta_b^2}}, \tag{42}$$

$$p_c(\tilde{t}) = 4m^2\left(e^{2\tilde{t}}+\frac{\gamma^2L_o^2\delta_c^2}{64m^2}e^{-2\tilde{t}}\right), \tag{43}$$

where $b_o = \sqrt{1+\gamma^2\delta_b^2}$. Let us now proceed to the computation of the dominant terms of $\partial O_i/\partial\delta_i$.

From **Eq. 43**, it follows immediately that

$$p_c = 4e^{2\tilde{t}}m^2 + o(m^2). \tag{44}$$

The case of the connection variable c and its trigonometric functions is less immediate. Since the solution written above involves the tangent of $\delta_c c/2$, it is useful to employ the identity

$$\cos\delta_c c = \frac{1-\tan^2(\delta_c c/2)}{1+\tan^2(\delta_c c/2)}. \tag{45}$$

Then, by virtue of **Eq. 41**,

$$\cos\delta_c c = 1-\frac{\gamma^2L_o^2}{32e^{4\tilde{t}}}\frac{\delta_c^2}{m^2}+o\left(\frac{\delta_c^2}{m^2}\right). \tag{46}$$

Given that the sum of the squares of the sine and cosine functions is equal to one, we can obtain $\sin\delta_c c$ and $\delta_c c$ from the expression above. In order to do this, it suffices to bear in mind that, according to the conventions of (Ashtekar et al., 2018a; Ashtekar et al., 2018b; Ashtekar and Olmedo, 2020), $b>0$, $c>0$, $p_b\leq 0$, and $p_c\geq 0$. This, together with the fact that $\lim_{m\to\infty}\delta_i = 0$, implies that every relevant trigonometric function is nonnegative.

After a straightforward calculation, we conclude that

$$\frac{\partial O_c}{\partial\delta_c} = -\frac{\gamma^2L_o^2}{48e^{4\tilde{t}}}\frac{\delta_c}{m}+o\left(\frac{\delta_c}{m}\right). \tag{47}$$

The dominant term goes with $m^{-4/3}$ (see **Eq. 37**), which implies that the left hand side of **Eq. 28** tends to one in the limit of large black hole masses. Let us now perform the analogous analysis on the right hand side of **Eq. 28**.

On the light of the form of the solution **Eq. 40** for the connection variable b, it proves useful to employ the identity

$$\tanh(a+b) = \frac{\tanh a+\tanh b}{1+\tanh a\tanh b}, \tag{48}$$

such that, up to subdominant corrections to the leading time-dependent contribution,

$$\cos\delta_b b = \frac{1+b_o\tanh(b_oT)}{1+b_o^{-1}\tanh(b_oT)}, \tag{49}$$

where we have defined $T = \tilde{t}/2$. Rewriting the previous expression as a power series, we get

$$\cos\delta_b b = 1+C_1\delta_b^2+o(\delta_b^2), \tag{50}$$

with a constant C_1 given by

$$C_1 = \gamma^2\frac{\tanh T}{1+\tanh T}. \tag{51}$$

Recasting every function of b that appears in **Eq. 29** as a power series, we find that

$$\left(1-\frac{\gamma^2\delta_b^2}{\sin^2\delta_b b}\right)\frac{\delta_b b\cos\delta_b b-\sin\delta_b b}{\delta_b^2} = -\frac{2}{3}(2C_1+\gamma^2)\frac{C_1}{\sqrt{-2C_1}}\delta_b+o(\delta_b). \tag{52}$$

Lastly, the asymptotic value of p_b can be obtained from **Eq. 42** by introducing the appropriate expansions:

$$-\frac{1}{2}\frac{p_b}{\gamma L_o} = \frac{\sqrt{-2C_1}}{\gamma^2-2C_1}m+o(m). \tag{53}$$

In conclusion, the partial derivative of O_b with respect to δ_b displays the asymptotic behavior

$$\frac{\partial O_b}{\partial\delta_b} = -\frac{2}{3}C_1\frac{\gamma^2+2C_1}{\gamma^2-2C_1}\delta_b m+o(\delta_b m). \tag{54}$$

This, in conjunction with **Eq. 38**, leads to the asymptotic vanishing of $\Delta_{bb}+\Delta_{bc}$. Therefore, the condition **Eq. 28** reduces to $\alpha = 1$ in the asymptotic limit $m\to\infty$. For this value of α, the times $\tilde{t}_b$ and $\tilde{t}_c$ indeed coincide for black holes of asymptotically large masses.

From this result, we conclude that, among all possible choices of $\tilde{t}_b$ and $\tilde{t}_c$ such that they are proportional to each other, only the choice where the proportionality constant is equal to one is admissible in the limit of large black hole masses. Therefore, the AOS solutions can at least be reconciled with the present calculation in this limit. It is important to remark that, although the equations of motion do coincide with those derived in (Ashtekar et al., 2018a; Ashtekar et al., 2018b; Ashtekar and Olmedo, 2020) in the limit of large black hole masses, they are written in a *different time variable* $\tilde{t}$. Thus, the spacetime geometry is modified with respect to the one studied in those works. This opens a door to a different asymptotic behavior of the spacetime metric of the exterior region, which in particular may have a different asymptotic (flat) behavior (Bouhmadi-López et al., 2020b). Additionally, the lapse function associated with $\tilde{t}$ will present a different phase space dependence, that may call for a different re-densitization of the Hamiltonian constraint NH_{eff} with respect to the difference $O_b - O_c$ of what we have called the partial Hamiltonians of the model. We leave these issues for

future studies and, as we declared in the Introduction, restrict our discussion here to the viability of a Hamiltonian derivation of the AOS solution (possibly in an asymptotic sense) treating the polymerization parameters as true constants of motion.

Let us close this section by studying the relation between the time variables $\tilde{t}_b$ and $\tilde{t}_c$ for finite values of the mass. In view of their definitions (see **Eq. 22**) and the fact that the denominator of C_{ij} is symmetric, we obtain that the ratio of the two differential times is

$$\frac{d\tilde{t}_b}{d\tilde{t}_c} = \frac{1-\Delta_{cc}-\Delta_{cb}}{1-\Delta_{bb}-\Delta_{bc}}. \tag{55}$$

On shell, this is equivalent to

$$\frac{d\tilde{t}_b}{d\tilde{t}_c} = \frac{1-\frac{\partial O_c}{\partial \delta_c}\frac{\partial f_c}{\partial m}}{1-\frac{\partial O_b}{\partial \delta_b}\frac{\partial f_b}{\partial m}}. \tag{56}$$

Notice that the numerator (denominator) of the right hand side is a function of $\tilde{t}_c$ ($\tilde{t}_b$). Therefore, by integrating, we obtain an equality between a function of $\tilde{t}_b$ and a function of $\tilde{t}_c$, which provides an implicit relation between the two time variables,

$$\int_{\tilde{t}_b}^{0} d\tilde{t}_b'\left(1-\frac{\partial O_b}{\partial \delta_b}\frac{\partial f_b}{\partial m}\right) = \int_{\tilde{t}_c}^{0} d\tilde{t}_c'\left(1-\frac{\partial O_c}{\partial \delta_c}\frac{\partial f_c}{\partial m}\right), \tag{57}$$

where the choice of integration limits reflects the fact that, according to the conventions of (Ashtekar et al., 2018a; Ashtekar et al., 2018b; Ashtekar and Olmedo, 2020), the time variables are negative in the interior region of the black hole, and their origins coincide. We have already determined that, in the asymptotic limit of large masses, this relation reduces to the identity. However, for finite values of the black hole mass, the difference between both time variables is given by

$$\tilde{t}_b-\tilde{t}_c = \frac{\partial f_b}{\partial m}\int_0^{\tilde{t}_b}\frac{\partial O_b}{\partial \delta_b}d\tilde{t}_b' - \frac{\partial f_c}{\partial m}\int_0^{\tilde{t}_c}\frac{\partial O_c}{\partial \delta_c}d\tilde{t}_c'. \tag{58}$$

Inserting the results obtained in this section,

$$\begin{aligned}\tilde{t}_b-\tilde{t}_c = {}& \frac{\partial f_b}{\partial m}\int_0^{\tilde{t}_b} d\tilde{t}_b'\left[-\frac{2}{3}C_1\left(\tilde{t}_b'\right)\frac{\gamma^2+2C_1\left(\tilde{t}_b'\right)}{\gamma^2-2C_1\left(\tilde{t}_b'\right)}\delta_b m + o\left(\delta_b m\right)\right] \\ & - \frac{\partial f_c}{\partial m}\int_0^{\tilde{t}_c} d\tilde{t}_c'\left[-\frac{\gamma^2 L_o^2}{48e^{4\tilde{t}_c'}}\frac{\delta_c}{m}+o\left(\frac{\delta_c}{m}\right)\right].\end{aligned} \tag{59}$$

Here, we have used that, at the order of approximation needed in the integrals of our expression in the asymptotic limit of large masses, we can identify $\tilde{t}_b = \tilde{t}_c = \tilde{t}$. Since the dominant term of the second integral, which goes as δ_c/m, is already subdominant with respect to that of the first integral, only the b sector contributes to the studied difference at the lowest nontrivial order. We have

$$\tilde{t}_b-\tilde{t}_c = -\frac{4}{3}\gamma^2\frac{\partial f_b}{\partial m}\left[\int_0^{\tilde{t}_b/2}\frac{\tanh T_b\left(1+3\tanh T_b\right)}{1-\tanh^2 T_b}dT_b\right]\delta_b m + o\left(\delta_b^2\right), \tag{60}$$

so that

$$\tilde{t}_c = \tilde{t}_b - \frac{1}{9}\gamma^2\left(-3\tilde{t}_b+3\sinh\tilde{t}_b+\cosh\tilde{t}_b-1\right)\delta_b^2 + o\left(\delta_b^2\right). \tag{61}$$

This equation provides the first-order corrected relation between both time variables, their difference vanishing when $m\to\infty$, as expected. Additionally, this relation reveals another property that was already pointed out in (Bodendorfer et al., 2019b): the difference $\tilde{t}_c-\tilde{t}_b$ also vanishes in the region where quantum effects are negligible, i.e., close to the event horizon. When solving the equations of motion associated with the b sector, the constants of integration were fixed in such a way that the horizon (defined by $b=0$ and $p_b=0$) lies at $\tilde{t}_b=0$ (Ashtekar et al., 2018a; Ashtekar et al., 2018b; Ashtekar and Olmedo, 2020). It is immediate to verify that both time variables are indeed close to each other when $\tilde{t}_b$ approaches zero, since the dominant term of their difference vanishes at least as $\tilde{t}_b^2$ in this limit, when asymptotically large masses are considered.

The dominant-order correction to the difference of times in **Eq. 61** also makes it apparent that the relation between $\tilde{t}_b$ and $\tilde{t}_c$ may become nonmonotonic in general, which allows us to draw yet another parallel with (Bodendorfer et al., 2019b). Indeed,

$$\frac{d\tilde{t}_c}{d\tilde{t}_b} = 1-\frac{1}{9}\gamma^2\left(\sinh\tilde{t}_b+3\cosh\tilde{t}_b-3\right)\delta_b^2+o\left(\delta_b^2\right) \tag{62}$$

is positive in the limit $\tilde{t}_b\to 0$ but may reach a value of $\tilde{t}_b$ where it vanishes and, eventually, changes sign. For the standard value of the Immirzi parameter $\gamma=0.2375$, $\Delta=4\sqrt{3}\pi G\gamma$, and $m=10000m_{\mathrm{Pl}}$ (where m_{Pl} denotes the Planck mass), we obtain that this derivative vanishes at $\tilde{t}_b\approx -9.36t_{\mathrm{Pl}}$ (where t_{Pl} is the Planck time). Therefore, while $\tilde{t}_c$ decreases as $\tilde{t}_b$ decreases near the horizon, this trend is found to be reversed beyond a critical value of $\tilde{t}_b$ at the considered truncation order in the asymptotic expansion. This indicates that there would exist a point along the evolution where the ratio C_{bc}/C_{cb} would cease to be finite. Nonetheless, note that this does not necessarily imply that the invertibility condition in **Eq. 13** would be violated at that point, not even at our truncation order. Actually, the symmetry properties of C_{ij} ensure that only the numerators of C_{bc} and C_{cb} contribute to their ratio. As a result, the nonfiniteness of this ratio at a certain point along the evolution should not be attributed in principle to an ill behavior of the denominator of C_{ij} and, consequently, to a violation of condition **Eq. 13**.

5 CONCLUSION

In this paper, we have examined whether it is possible to construct a Hamiltonian formalism where the polymerization parameters that encode the quantum corrections in black hole spacetimes can be treated as constants of motion. The final identification of these parameters with dynamical constants is one of the ideas of the AOS model, proposed in (Ashtekar et al., 2018a; Ashtekar et al., 2018b; Ashtekar and Olmedo, 2020).

However, instead of incorporating this identification into the Hamiltonian calculation from the beginning, the analysis in those references is carried out ignoring the Poisson brackets of the parameters, treating them as constants on the whole phase space. It is only later on that their value is set equal to certain functions of the black hole mass, which is a Dirac observable of the system under consideration. The authors of (Bodendorfer et al., 2019b) pointed out that the computation of the Hamiltonian equations would change if one takes into consideration those Poisson brackets, regarding the parameters as true constants of motion. To show this, it was noticed in (Bodendorfer et al., 2019b) that, given the form of the Hamiltonian, there are two dynamically decoupled subsectors in phase space, provided that the polymerization parameters do not introduce any cross-dependence. With this caveat, each subsector can be studied separately and its dynamics is generated by one of the two terms that appear in the Hamiltonian constraint (with a suitable choice of lapse). We have referred to these two terms as *partial Hamiltonians*, which turn out to be Dirac observables that reduce to the black hole mass on shell. Imposing that the polymerization parameter associated with each subsector is a function of its corresponding partial Hamiltonian, the equations of motion that one obtains differ from those of the AOS model by a phase space dependent factor that complicates the solutions. However, this factor can be reabsorbed by appropriate time redefinitions, leading to simpler dynamical equations written in two separate time variables, one in each subsector. In (Bodendorfer et al., 2019b), both variables were found to be approximately equal from the event horizon up to a neighborhood of the transition surface where QG effects become important, concluding that the results of the AOS model were approximately valid when restricted to this region of the interior of the black hole.

In the present work, we have extended the aforementioned analysis to take into account the possibility that the polymerization parameters, regarded as constants of motion, depend not only on their corresponding partial Hamiltonian, but on *both* of them. This possibility breaks the decoupling of subsectors that plays a central role in (Bodendorfer et al., 2019b). Indeed, since both partial Hamiltonians coincide with the value of the black hole mass on shell by virtue of the vanishing of the Hamiltonian constraint, one should in principle not be able to tell their contributions apart. A dependence on both of these Dirac observables brings new freedom to the treatment of the polymerization parameters. We have investigated whether this new off-shell freedom can help to derive the AOS model exclusively from a standard Hamiltonian calculation, viewing the parameters as functions of both Dirac observables from the beginning. We have derived in **Section 2** the corresponding equations of motion that govern the dynamics in the interior region. These equations turn out to be corrected by a phase space dependent factor as well, although its functional form is complicated by the fact that the two subsectors no longer decouple dynamically. We have observed that this factor does reduce to the one found in (Bodendorfer et al., 2019b). in the limit where the decoupling is recovered. In **Section 3**, we have written down the time redefinitions that allow us to simplify the dynamics, leading to equations of motion that are identical to those that result from considering constant parameters, although now written in two different time variables. We have then discussed whether these newly defined time variables can be required to be equal to each other. Remarkably, the answer turns out to be in the negative in spite of the commented off-shell freedom, since this condition would imply that the polymerization parameters are necessarily constants on the whole phase space. In **Section 4**, we have verified whether this equality of time variables can be imposed at least in the limit of infinitely large black hole masses, as one would expect to be the case in order to recover the standard results of General Relativity in this asymptotic limit. Indeed, we have proven that one can require this coincidence of times consistently. We have also studied the first-order correction to the relation between both time variables, which has allowed us to draw parallels with previous results obtained in (Bodendorfer et al., 2019b). First, the two time variables are still approximately similar to each other near the event horizon, where the QG effects are not relevant. Second, for finite rather than asymptotically large black hole masses, the dynamical solutions are such that a point in the evolution may generically be reached where the time flow would be reversed, in the sense that the relation between the two time variables would not be monotonic around it.

Our conclusions imply that the results of (Ashtekar et al., 2018a; Ashtekar et al., 2018b; Ashtekar and Olmedo, 2020), which are based on Hamiltonian calculations where the polymerization parameters are treated as constant numbers, can be *partially* reconciled with a treatment where these parameters are regarded as proper constants of motion, at least for black holes with large masses, which on the other hand are the focus of the analysis of those references. The wording "partially" is key here. In particular, one should not forget that the spacetime geometry is modified with respect to that of the AOS model by means of time redefinitions. Even if this apparently slight modification does not alter some of the conclusions of (Ashtekar et al., 2018a; Ashtekar et al., 2018b; Ashtekar and Olmedo, 2020), it may affect, e.g., the rate at which the metric decays at spatial infinity.[4] This matter will constitute the subject of future work.

DATA AVAILABILITY STATEMENT

The original contributions presented in the study are included in the article/Supplementary Material, further inquiries can be directed to the corresponding author.

[4]Although we have not explicitly dealt with the exterior region in this article, the same procedure is applicable to that case.

AUTHOR CONTRIBUTIONS

All authors listed have made a substantial, direct, and intellectual contribution to the work and approved it for publication.

FUNDING

This work has been supported by Project. No. MICINN FIS 2017–86497-C2-2-P from Spain (with extension Project. No. MICINN PID 2020-118159GB-C41 under evaluation). The project that gave rise to these results received the support of a fellowship from "la Caixa" Foundation (ID 100010434). The fellowship code is LCF/BQ/DR19/11740028. Partial funds for open access publication have been received from CSIC.

ACKNOWLEDGMENTS

The authors are very grateful to B. Elizaga Navascués for discussions.

REFERENCES

Alesci, E., Bahrami, S., and Pranzetti, D. (2019). Quantum Gravity Predictions for Black Hole interior Geometry. *Phys. Lett. B* 797, 134908. doi:10.1016/j.physletb.2019.134908

Arruga, D., Ben Achour, J., and Noui, K. (2020). Deformed General Relativity and Quantum Black Holes interior. *Universe* 6, 039. doi:10.3390/universe6030039

Ashtekar, A., and Bojowald, M. (2005). Black Hole Evaporation: A Paradigm. *Class. Quan. Grav.* 22, 3349–3362. doi:10.1088/0264-9381/22/16/014

Ashtekar, A., and Bojowald, M. (2005). Quantum Geometry and the Schwarzschild Singularity. *Class. Quan. Grav.* 23, 391–411. doi:10.1088/0264-9381/23/2/008

Ashtekar, A., and Olmedo, J. (2020). Properties of a Recent Quantum Extension of the Kruskal Geometry. *Int. J. Mod. Phys. D* 29, 2050076. doi:10.1142/s0218271820500765

Ashtekar, A., Olmedo, J., and Singh, P. (2018). Quantum Extension of the Kruskal Spacetime. *Phys. Rev. D* 98, 126003. doi:10.1103/physrevd.98.126003

Ashtekar, A., Olmedo, J., and Singh, P. (2018). Quantum Transfiguration of Kruskal Black Holes. *Phys. Rev. Lett.* 121, 241301. doi:10.1103/physrevlett.121.241301

Ben Achour, J., Brahma, S., Mukohyama, S., and Uzan, J-P. (2020). Towards Consistent Black-To-white Hole Bounces from Matter Collapse. *JCAP* 09, 020. doi:10.1088/1475-7516/2020/09/020

Bianchi, E., Christodoulou, M., D'Ambrosio, F., Haggard, H. M., and Rovelli, C. (2018). White Holes as Remnants: A Surprising Scenario for the End of a Black Hole. *Class. Quan. Grav.* 35, 225003. doi:10.1088/1361-6382/aae550

Bodendorfer, N., Mele, F. M., and Münch, J. (2019). A Note on the Hamiltonian as a Polymerisation Parameter. *Class. Quan. Grav.* 36, 187001. doi:10.1088/1361-6382/ab32ba

Bodendorfer, N., Mele, F. M., and Münch, J. (2021). (b,v)-type Variables for Black to white Hole Transitions in Effective Loop Quantum Gravity. *Phys. Lett. B* 819, 136390, 2021. (in press). doi:10.1016/j.physletb.2021.136390

Bodendorfer, N., Mele, F. M., and Münch, J. (2019). Effective Quantum Extended Spacetime of Polymer Schwarzschild Black Hole. *Class. Quan. Grav.* 36, 195015. doi:10.1088/1361-6382/ab3f16

Bodendorfer, N., Mele, F. M., and Münch, J. (2021). Mass and Horizon Dirac Observables in Effective Models of Quantum Black-To-white Hole Transition. *Class. Quan. Grav.* 38, 095002. doi:10.1088/1361-6382/abe05d

Boehmer, C. G., and Vandersloot, K. (2007). Loop Quantum Dynamics of Schwarzschild interior. *Phys. Rev. D* 76, 1004030. doi:10.1103/PhysRevD.76.104030

Bojowald, M., Cartin, D., and Khanna, G. (2007). Lattice Refining Loop Quantum Cosmology, Anisotropic Models and Stability. *Phys. Rev. D* 76, 064018. doi:10.1103/physrevd.76.064018

Bojowald, M. (2019). *Comment (2) on "Quantum Transfiguration of Kruskal Black Holes"*. University Park: arXiv:1906, 04650.

Bojowald, M. (2020). No-go Result for Covariance in Models of Loop Quantum Gravity. *Phys. Rev. D* 102, 046006. doi:10.1103/physrevd.102.046006

Bojowald, M. (2020). Black-hole Models in Loop Quantum Gravity. *Universe* 6, 125. doi:10.3390/universe6080125

Bouhmadi-López, M., Brahma, S., Chen, C.-Y., Chen, P., and Yeom, D.-h. (2020). A Consistent Model of Non-singular Schwarzschild Black Hole in Loop Quantum Gravity and its Quasinormal Modes. *J. Cosmol. Astropart. Phys.* 2020, 066. doi:10.1088/1475-7516/2020/07/066

Bouhmadi-López, M., Brahma, S., Chen, C.-Y., Chen, P., and Yeom, D.-h. (2020). Asymptotic Non-flatness of an Effective Black Hole Model Based on Loop Quantum Gravity. *Phys. Dark Universe* 30, 100701. doi:10.1016/j.dark.2020.100701

Brannlund, J., Kloster, S., and DeBenedictis, A. (2009). The Evolution of Black Holes in the Mini-Superspace Approximation of Loop Quantum Gravity. *Phys. Rev. D* 79, 084023. doi:10.1103/physrevd.79.084023

Campiglia, M., Gambini, R., and Pullin, J. (2008). Loop Quantization of a Spherically Symmetric Midsuperspaces: The interior Problem. *AIP Conf. Proc.* 977, 52. doi:10.1063/1.2902798

Campiglia, M., Gambini, R., Olmedo, J., and Pullin, J. (2016). Quantum Self-Gravitating Collapsing Matter in a Quantum Geometry. *Class. Quan. Grav.* 33, 18LT01. doi:10.1088/0264-9381/33/18/18lt01

Cartin, D., and Khanna, G. (2006). Wave Functions for the Schwarzschild Black Hole interior. *Phys. Rev. D* 73, 104009. doi:10.1103/physrevd.73.104009

Chiou, D. W. (2008). Phenomenological Dynamics of Loop Quantum Cosmology in Kantowski-Sachs Spacetime. *Phys. Rev. D* 78, 044019. doi:10.1103/physrevd.78.044019

Chiou, D. W. (2008). Phenomenological Loop Quantum Geometry of the Schwarzschild Black Hole. *Phys. Rev. D* 78, 064040. doi:10.1103/physrevd.78.064040

Corichi, A., and Singh, P. (2016). Loop Quantization of the Schwarzschild interior Revisited. *Class. Quan. Grav.* 33, 055006. doi:10.1088/0264-9381/33/5/055006

Cortez, J., Cuervo, W., Morales-Técotl, H. A., and Ruelas, J. C. (2017). On Effective Loop Quantum Geometry of Schwarzschild interior. *Phys. Rev. D* 95, 064041. doi:10.1103/physrevd.95.064041

Dadhich, N., Joe, A., and Singh, P. (2015). Emergence of the Product of Constant Curvature Spaces in Loop Quantum Cosmology. *Class. Quan. Grav.* 32, 185006. doi:10.1088/0264-9381/32/18/185006

Daghigh, R. G., Green, M. D., and Kunstatter, G. (2021). Scalar Perturbations and Stability of a Loop Quantum Corrected Kruskal Black Hole. *Phys. Rev. D* 103, 084031. doi:10.1103/physrevd.103.084031

Gambini, R., Olmedo, J., and Pullin, J. (2014). Quantum Black Holes in Loop Quantum Gravity. *Class. Quan. Grav.* 31, 095009. doi:10.1088/0264-9381/31/9/095009

Gambini, R., Olmedo, J., and Pullin, J. (2020). Spherically Symmetric Loop Quantum Gravity: Analysis of Improved Dynamics. *Class. Quan. Grav.* 37, 205012. doi:10.1088/1361-6382/aba842

Gambini, R., and Pullin, J. (2014). Hawking Radiation from a Spherical Loop Quantum Gravity Black Hole. *Class. Quan. Grav.* 31, 115003. doi:10.1088/0264-9381/31/11/115003

Gan, W.-C., Santos, N. O., Shu, F.-W., and Wang, A. (2020). Properties of the Spherically Symmetric Polymer Black Holes. *Phys. Rev. D* 102, 124030. doi:10.1103/physrevd.102.124030

Haggard, H. M., and Rovelli, C. (2015). Quantum-gravity Effects outside the Horizon Spark Black to white Hole Tunneling. *Phys. Rev. D* 92, 104020. doi:10.1103/physrevd.92.104020

Joe, A., and Singh, P. (2015). Kantowski-Sachs Spacetime in Loop Quantum Cosmology: Bounds on Expansion and Shear Scalars and the Viability of Quantization Prescriptions. *Class. Quan. Grav.* 32, 015009. doi:10.1088/0264-9381/32/1/015009

Kelly, J. G., Santacruz, R., and Wilson-Ewing, E. (2021). Black Hole Collapse and Bounce in Effective Loop Quantum Gravity. *Class. Quan. Grav.* 38, 04LT01. doi:10.1088/1361-6382/abd3e2

Kelly, J. G., Santacruz, R., and Wilson-Ewing, E. (2020). Effective Loop Quantum Gravity Framework for Vacuum Spherically Symmetric Spacetimes. *Phys. Rev. D* 102, 106024. doi:10.1103/physrevd.102.106024

Münch, J. *Causal Structure of a Recent Loop Quantum Gravity Black Hole Collapse Model*. Marseille: arXiv:2103.17112 (2021).

Modesto, L. (2006). Loop Quantum Black Hole. *Class. Quan. Grav.* 23, 5587–5601. doi:10.1088/0264-9381/23/18/006

Olmedo, J., Saini, S., and Singh, P. (2017). From Black Holes to white Holes: a Quantum Gravitational, Symmetric Bounce. *Class. Quan. Grav.* 34, 225011. doi:10.1088/1361-6382/aa8da8

Sabharwal, S., and Khanna, G. (2008). Numerical Solutions to Lattice-Refined Models in Loop Quantum Cosmology. *Class. Quan. Grav.* 25, 085009. doi:10.1088/0264-9381/25/8/085009

Saini, S., and Singh, P. (2016). Geodesic Completeness and the Lack of strong Singularities in Effective Loop Quantum Kantowski-Sachs Spacetime. *Class. Quan. Grav.* 33, 245019. doi:10.1088/0264-9381/33/24/245019

Yonika, A., Khanna, G., and Singh, P. (2018). Von-Neumann Stability and Singularity Resolution in Loop Quantized Schwarzschild Black Hole. *Class. Quan. Grav.* 35, 045007. doi:10.1088/1361-6382/aaa18d

Conflict of Interest: The authors declare that the research was conducted in the absence of any commercial or financial relationships that could be construed as a potential conflict of interest.

frontiers in Astronomy and Space Sciences

REVIEW
published: 23 July 2021
doi: 10.3389/fspas.2021.692198

Backreaction in Cosmology

S. Schander[1,2] *and T. Thiemann*[2]*

[1]Perimeter Institute, Waterloo, ON, Canada, [2]Institute for Quantum Gravity, FAU Erlangen – Nürnberg, Erlangen, Germany

In this review, we investigate the question of backreaction in different approaches to cosmological perturbation theory, and with a special focus on quantum theoretical aspects. By backreaction we refer here to the effects of matter field or cosmological inhomogeneities on the homogeneous dynamical background degrees of freedom of cosmology. We begin with an overview of classical cosmological backreaction which is ideally suited for physical situations in the late time Universe. We then proceed backwards in time, considering semiclassical approaches such as semiclassical or stochastic (semiclassical) gravity which take quantum effects of the perturbations into account. Finally, we review approaches to backreaction in quantum cosmology that should apply to the very early Universe where classical and semiclassical approximations break down. The main focus is on a recently proposed implementation of backreaction in quantum cosmology using a Born–Oppenheimer inspired method.

Keywords: quantum gravity, cosmology, space adiabatic perturbation theory, quantum fields in curved spacetimes, backreaction

OPEN ACCESS

Edited by:
Francesca Vidotto,
Western University, Canada

Reviewed by:
Tomi Sebastian Koivisto,
University of Oslo, Norway
Kazuharu Bamba,
Fukushima University, Japan

***Correspondence:**
T. Thiemann
thomas.thiemann@fau.de

Specialty section:
This article was submitted to Cosmology, a section of the journal Frontiers in Astronomy and Space Sciences

Received: *07 April 2021*
Accepted: *14 June 2021*
Published: *23 July 2021*

Citation:
Schander S and Thiemann T (2021) Backreaction in Cosmology. Front. Astron. Space Sci. 8:692198. doi: 10.3389/fspas.2021.692198

1 INTRODUCTION

The Λ cold dark matter (ΛCDM) concordance model (Cervantes-Cota and Smoot, 2011; Deruelle and Uzan, 2018; Dodelson and Schmidt, 2021), based on the pillars of the Standard Model of particle physics and general relativity, has shaped our current view of the Universe, and has been the driving force behind many of the breakthroughs of modern cosmology, for example the prediction and the discovery of the cosmic microwave background radiation (Aghanim et al., 2019, 2020; Alpher and Herman, 1948a,b; Gamov 1948a,b; Penzias and Wilson 1965). Modeled by only six parameters (Spergel 2015; Aghanim et al., 2020), it features an impressive simplicity while correctly predicting and fitting most of the cosmological data (Aghanim et al., 2019, 2020). One of the most important assumptions within the ΛCDM paradigm is that the Universe is almost spatially homogeneous and isotropic, especially during its earliest phases, but even today when considered on its largest scales. The resulting simplification of Einstein's equations is remarkable as it reduces the ten coupled non-linear partial differential equations in four variables to two ordinary equations in one variable, with solutions known as the Friedmann–Lemaître–Robertson–Walker (FLRW) solutions (Friedman 1922, 1924; Lemaître 1931; Robertson 1933; Walker 1937).

Obviously, a look at the night sky reveals that the Universe is not homogeneous and isotropic, but is characterized by clusters of galaxies and stars, and large voids inbetween (Blumenthal et al., 1984; Cole et al., 2005; Colless et al., 2001; Ross et al., 2020; Zel'dovich et al., 1982). For explanation, the concordance model assumes that smallest quantum fluctuations of the primordial matter and geometry have been stretched to the present time, thereby generating the observable large scale structure. Importantly, these inhomogeneities on any scale smaller than the observable Universe are presumed to evolve following the underlying FLRW background structure, but conversely their evolution does *not* affect the global FLRW evolution. More precisely, it is assumed that effects from

the small scale inhomogeneities onto the largest scales can be neglegted, i.e., there is no substantial backreaction.

Doubts regarding the simplistic nature and the question of backreaction have gained momentum in recent years. In fact, the ΛCDM model, as appealing it may be, leads to the conclusion that approximately 69% of the energy budget of our Universe consists of a yet unknown fluid, dubbed "dark energy," (Aghanim et al., 2020), and which drives the very recent accelerated expansion of the Universe (Riess et al., 1998; Perlmutter et al., 1999; Peebles and Ratra 2003). Most of the remaining 31% of the energy budget is credited to another yet unknown form of cold "dark" matter (Peebles 1982; Blumenthal et al., 1984; Aghanim et al., 2020), which provides an explanation for the characteristic rotation and motion of the remaining 6% of ordinary matter in the Universe. In summary, we are faced with the problem that we are literally in the dark about 94% of the energy and matter content of the observable Universe.

In recent years, these conceptual problems have been accompanied by important tensions in the estimates of certain cosmological parameters as made by different collaborations (Di Valentino et al., 2020a,b; Pesce et al., 2020). The evaluation of the Hubble constant H_0 as performed by the Planck collaboration (explicitely assuming a ΛCDM model) gives a value of $H_0 = (67.27 \pm 0.60)\mathrm{km}/(\mathrm{s}\cdot\mathrm{Mpc})$ (Aghanim et al., 2020), while the SH0ES collaboration finds $H_0 = (74.03 \pm 1.42)\mathrm{km}/(\mathrm{s}\cdot\mathrm{Mpc})$ (Riess et al., 2019), which in turn is based on the measurements of the Hubble Space Telescope. This leads to a tension at the 4.4σ level (Di Valentino et al., 2020a). Furthermore, we point to the (albeit weaker) tensions regarding the measurement of the parameter S_8, a measure for the matter energy density Ω_m and the amplitude of structure growth σ_8 (Aghanim et al., 2020; Di Valentino et al., 2020b).

On the other hand, the theoretical modeling of the early and very early Universe turns out to be a difficult undertaking, in particular the faithful consideration of all interactions within coupled quantum cosmological–matter systems. Since classical cosmological perturbation theory and its various applications to the physics of our Universe (Durrer, 2004; Mukhanov, 2005), represents a successful formalism to model (most of) the cosmological data today, one of the most promising approaches to make progress in the field is to consider an inhomogeneous, but perturbative, *quantum* cosmology, i.e., to establish a quantization of the well-known (possibly) gauge-invariant cosmological perturbation theories (Brandenberger et al., 1993; Brandenberger, 2004; Elizaga Navascués et al., 2016). In fact, there has been tremendous progress in developing such quantum cosmological perturbation theories, for example, in quantum geometrodynamics (Kiefer, 2007; Brizuela and Krämer, 2018), in string cosmology (Erdmenger, 2009), as well as in loop quantum cosmology (LQC) and spinfoam cosmology (Bianchi et al., 2010; Vidotto 2011; Cailleteau et al., 2012; Agullo et al., 2013; Elizaga Navascués et al., 2016), to mention but a few. Unfortunately, the majority of these approaches neglect backreaction effects from the inhomogeneous quantum fields on the homogeneous, dynamical degrees of freedom, or incorporate a series of assumptions which are hard to control, similar to the situation in classical cosmological perturbation theory.

It seems hence very timely to scrutinize and question the various assumptions of the concordance model of cosmology, and to develop suitable formalisms which are able to take interactions in coupled (quantum) cosmological models more realistically and unambigiously into account. In this review, we start by assessing the question of backreaction, i.e., whether cosmological inhomogeneities have an effect on the large scale evolution of the Universe, especially in view of the occurent inconsistencies within the standard model. We consider different aspects of backreaction, in particular we discuss backreaction in classical, semiclassical and quantum mechanical models. Our main focus is on the purely quantum mechanical backreaction and we discuss one recent approach to including backreaction in quantum cosmology in more detail (Schander and Thiemann, 2019a). The structure of the paper is then as follows.

In **Section 2**, we provide an overview of the results in the field of *classical* backreaction, which is particularly relevant for late time cosmological models. In **Section 3**, we consider *semiclassical* backreaction which occurs when considering quantum fields on classical curved space times. **Section 4** gives an overview of *quantum* backreaction, i.e., backreaction that occurs in purely quantum theoretical models. In **Section 5**, we focus on one particular approach to quantum backreaction which uses mathematical tools inspired by the Born–Oppenheimer approximation. **Section 6** provides a final discussion and an outlook.

2 CLASSICAL BACKREACTION

Standard perturbative approaches to cosmological perturbation theory implicitely conjecture that backreaction, i.e., the effects of cosmological inhomogeneities on the global or macroscopic evolution of the Universe can be ignored. For purely classical models of the Universe that are particularly relevant for its late time evolution, this conjecture has generated an intense debate over the last decades. And still, there is no consensus on the question of backreaction in the classical regime , see for example the reviews by Clarkson et al. (2011), Ellis (2011), and Bolejko and Korzynski (2017).

The question of backreaction is closely related to the fitting problem, (Ellis and Stoeger, 1987), and the problem of averaging, (Clarkson et al., 2011). In fact, an intuitive way to access the effects of small inhomogeneities on the macroscopic scales is to construe an averaging procedure that defines new homogeneous variables by integrating the inhomogeneous fields over a certain space time domain, and to compare their properties and dynamics to the assumed FLRW Universe, (Ellis, 2011). However, it is inadmissible to conclude from the validity of Einstein's equations for the inhomogeneous fields on the smallest scales (where they have been excellently checked), that the *averaged* fields satisfy the Einstein equations (Paranjape, 2012). This is because evaluating the Einstein tensor and taking a space (time) average does not commute in general. Hence, the averaging procedure can lead to additional

contributions to Einstein's equations that might be considered as effective source terms for the geometry, see for example (Buchert, 2000, 2001).

As it turns out, the results regarding the form and strength of backreaction depend heavily on the averaging procedure and the matter model being chosen, as well as on the choice of space time volumes to be integrated over. In the non-perturbative regime, the two most discussed averaging procedures are the scalar averaging scheme by Buchert (2008) and the Macroscopic Gravity approach by Zalaletdinov (1997, 2008). Buchert's scheme focuses on building spatial averages of scalar fields and derives effective (scalar) equations of motion for the averaged quantities, for example an improved Raychaudhuri equation for the averaged scale factor that includes a kinematical backreaction term. While being technically easy to implement, the Buchert scheme relies on a system of scalar equations that is not closed (Clarkson et al., 2011), and consequently requires additional information to fix the solution. Besides, the averaging demands to fix suitable spatial domains and hence, a hypersurface slicing. In contrast, the Macroscopic Gravity approach is manifestly covariant but requires to define an auxiliary so–called bi–local transport operator, (Ellis, 2011). Physical applications of these schemes yield a range of different results, ranging from explaining the recent accelerated expansion of the Universe or the H_0-tension (Buchert and Räsänen, 2012; Heinesen and Buchert, 2020), to negligible backreaction effects (Paranjape and Singh, 2007, 2008).

Many of the afore-mentioned approaches (among many others) assume the matter content to be modeled by a fluid, which is likely to be a poor approximation to the true lumpy late time Universe. Models with more realistic matter distributions are for example the Timescape Cosmology by Wiltshire (2009), who separates the Universe into underdense expanding regions bounded by overdense virialized structures, the Swiss Cheese Model (Kantowski, 1969; Tomita, 2000; Biswas and Notari, 2008), or modifications of FLRW Universes that cut spherically symmetric Lemaître–Tolman–Bondi or Szekeres dust space time regions (Marra et al., 2008; Bolejko and Celerier, 2010), to mention but a few. By construction, many of these models follow the evolution of an appropriately fitted FLRW model since they assume a background structure from the beginning. Consequently, they do not attack the backreaction problem outlined before. In contrast, the model by Lindquist and Wheeler (1957) assembles static Schwarzschild regions without relying on any background, and which has been further investigated by Clifton (2011) and Clifton and Ferreira (2009). In both cases, the models provide insights into backreaction effects on light propagation (Krasinski and Bolejko, 2011; Sussman, 2011), which points to another important topic.

In fact, cosmological observations such as the distance–redshift relation or the angular diameter distance rely on measurements of light, traveling along our past lightcone in a very inhomogeneous Universe. The seminal work by Kristian and Sachs (1966) laid out the basis for analyzing backreaction on light propagation. Flanagan (2005), for example, used these ideas to compute the deceleration parameter as measured by comoving observers. Gasperini et al. (2011) define a covariant light–cone average for the backreaction problem, see also (Fanizza et al., 2020) for a more recent generalized proposal. Räsänen (2009) and Räsänen (2010) derives a relationship of the redshift and the angular diameter distance to the average expansion rate for statistically homogeneous and isotropic universes, based on Buchert's approach, and Barausse et al. (2005) and Bonvin et al. (2006) evaluate the distance–redshift relation and the luminosity distance in a perturbative framework. Most recently, Heinesen (2021a), Heinesen (2021b) and Koksbang (2019), Koksbang (2020), Koksbang (2021) investigated the effects of inhomogeneities and averaging on a possible redshift drift.

Many approaches that attempt to make direct contact with cosmological observations restrict their analysis to cosmological perturbation theory in an FLRW Universe, as opposed to the above–mentioned non-perturbative approaches. Most of them consider flat ΛCDM models with Gaussian scalar perturbations as initital conditions. To evaluate backreaction, they compute the deviations to the Hubble expansion rate or similar variables that are caused by backreaction (Brandenberger et al., 2018; Clarkson et al., 2009; Kolb et al., 2010; Kolb et al., 2005; Li and Schwarz, 2008), or give effective Friedmann equations with additional contributions (Paranjape and Singh, 2007; Behrend et al., 2008; Brown et al., 2009; Peebles, 2010; Baumann et al., 2012). The idea is to perform appropriate spatial averages of the perturbed quantities and to use the given statistical information of the perturbation fields in guise of their power spectra. It turns out that due to the smallness of the gravitational potential and the power suppression of modes on large scales, backreaction for the expansion rate is always small. However, the backreaction to the deceleration parameter q and the variance of the Hubble rate depend on an auxiliary UV–cutoff that might lead to large backreaction even if it is set by scales larger than the non-linearity scale (Clarkson et al., 2011). Other approaches to backreaction in the linear regime are (Baumann et al., 2012) who propose a reformulation of perturbation theory that leads to small backreaction on the largest scales but affects the baryon accoustic oscillations, and (Green and Wald, 2011, 2012, 2013, 2014) who claim, using a point limit process, that backreaction can never mimic dark energy and put strong constraints on its strength.

We also point to the quite recent advent of numerical tools that allow to simulate increasingly realistic models of the Universe, including relativistic effects (Löffler et al., 2012; Mertens et al., 2016) and N-body simulations (Adamek et al., 2016; Barrera-Hinojosa and Li, 2020). Using the N-body relativistic code "gevolution," Adamek et al. (2019) find that backreaction on the expansion rate in a ΛCDM and an Einstein–de Sitter Universe remains small if one chooses averaging volumes related to the Poisson gauge, while when choosing comoving gauge backreaction is of the order of 15%. Other works in this respect were done by Macpherson et al. (2019), who also claim that backreaction effects are small, however based on a fluid approximation which breaks down as soon as it comes to shell crossing.

Finally, let us also point to the consideration of backreaction from long wavelength modes of the early Universe. In this respect, early contributions were notably made by Tsamis and Woodard

(1993, 1996), as well as by Abramo et al. (1997) and Mukhanov et al. (1997). The latter works pursue a gauge—invariant formulation of the backreaction problem associated with an effective long wavelength energy momentum tensor, and within a slow–roll inflationary scenario. Unruh (1998) subsequently examined the question of whether this effect is indeed locally measurable, and it was found that such backreaction effects (in single field inflationary theories) can be absorbed by a gauge transformation, (Abramo and Woodard, 2002; Geshnizjani and Brandenberger, 2002). However, backreaction of such fluctuations becomes locally measurable after introducing an additional (subdominant) clock feld, (Geshnizjani and Brandenberger, 2005). This approach was extended by Marozzi et al. (2013) based on the gauge—invariant formalism by Finelli et al. (2011), and secondly by Brandenberger et al. (2018) beyond perturbation theory. Further contributions were made by Losic and Unruh (2005), Losic and Unruh (2008) who support the idea that backreaction represents a real and measurable effect.

3 SEMICLASSICAL BACKREACTION

For considerations of backreaction in models of the very early Universe, the standard model of cosmology suggests that (at least) the matter fields should be studied in a quantum mechanical framework. The implementation of such ideas can be realized via different paths, and we consider here the approaches of semiclassical gravity (Ford 2005; Wald 1977, 1978) and stochastic (semiclassical) gravity (Calzetta and Hu 1987; Hu and Verdaguer 2008; Jordan 1986, 1987). Both approaches rely on the framework of quantum field theory on curved space times (QFT on CST) (Birrell and Davies, 1984; Fulling 1989), which itself takes the effects of the classical curved space times on the quantum matter fields into account but in general *not* the backreaction effects of those quantum fields on the classical background.

The backreaction problem in semiclassical gravity was first brought in by Wald (1977) who considered the backreaction from particle creaction on a gravitational field. The idea of the semiclassical program is to consistently define an improved set of Einstein field equations in which the expectation value of the quantum stress–energy tensor $\boldsymbol{T}_{\mu\nu}$ of the matter fields with respect to an appropriate quantum state of the matter fields ω appears as a source term,

$$R_{\mu\nu} + \frac{1}{2} g_{\mu\nu} R = 8\pi G \omega\big(: \boldsymbol{T}_{\mu\nu} :\big), \tag{1}$$

where the quantization with respect to the matter fields is expressed using bold letters and the dots indicate the normal ordering of the stress–energy tensor. The state ω should be considered as a positive linear functional in the sense of the algebraic approach to quantum field theory (QFT) (Haag 1992; Araki 1999).

The first goal of semiclassical gravity is to define a procedure that leads to a meaningful expression for the expectation value of the stress–energy tensor. In fact, the latter depends on products of operator-valued distributions, even for the simple case of a real-valued Klein–Gordon field, and its expectation value is in general a divergent expression. Wald (1977) gave a set of axioms that are required to hold for a suitable renormalization scheme. Possible proposals are the Hadamard point-splitting method (Brunetti and Fredenhagen, 2000; Hollands and Wald, 2001), and the adiabatic regularization procedure (Fulling and Parker 1974; Fulling et al., 1974; Parker and Fulling, 1974). In either scheme, the result of the regularization procedure is a set of modified "semiclassical" Einstein equations. These equations are substantially harder to solve than the original Einstein equations and many studies restrict to cases of conformally coupled matter to avoid problems regarding the well-posedness and the stability of the solutions (Ford, 2005). Caution is also required regarding the question of self-consistency of the backreaction effects, as has been discussed by Flanagan and Wald (1996).

Many applications of the semiclassical gravity approach to early Universe cosmology have been considered. For example, Fischetti et al. (1979) analyzed the backreaction effects from a conformally invariant matter field in an FLRW Universe with classical radiation, and found that the trace anomaly can soften the cosmological singularity, but not avoid it. Other works in this direction were done by Anderson (1983, 1984, 1985), who also considered the trace effects on the particle horizon. A well-known example of trace anomaly effects from semiclassical gravity is the Starobinsky (1987) cosmological model, which has however not survived the observational scrutiny of the Planck data (Ade et al., 2016).

Another application of semiclassical gravity is the study of backreaction of particle creation on the dynamics of the early Universe, as already conceived by Wald (1977). Grishchuk (1977) as well as Hu and Parker (1977) considered the effect of gravitons around the Planck time in an FLRW Universe with a classical, isotropic fluid. The model leads to a timely non-local (i.e., history-dependent) backreaction effect, (Hu and Verdaguer, 2020). Similar studies were performed for anisotropic FLRW Universes and it was shown that particle production due to the shear anisotropy isotropizes space time (Hu and Parker, 1978; Zel'dovich and Starobinsky, 1972). Regarding the effects of particle creation in a spatially inhomogeneous but isotropic Universe, we refer to the work by Campos and Verdaguer (1994).

We also point to the more recent works by Finelli et al. (2002), Finelli et al. (2004) who specifically consider a slow—roll (almost de Sitter) phase of the very early Universe and compute a(n adiabatically) renormalized energy momentum tensor of quantum inflaton, respectively cosmological scalar fluctuations. In case of the cosmological scalar perturbations, they found that the energy momentum tensor is characterized by a negative energy density which grows during inflation, and also that backreaction is not a mere gauge artifact.

Further contributions to the topic of semiclassical gravity for cosmological situations were notably made by Dappiaggi et al. (2008); Dappiaggi et al. (2010); Eltzner and Gottschalk (2011); Gottschalk and Siemssen (2018); Hack (2013); Matsui and

Watamura (2020); Parker and Raval (1999); Pinamonti (2011), to mention but a few. Most recently, Meda et al. (2020) and Pinamonti and Siemssen (2015) have made progress on the definition of the semiclassical theory for general couplings by proving existence and uniqueness of solutions in flat cosmological space times with a massive quantum scalar field. The idea of relating backreaction effects to the decay of a cosmological constant has for example been promoted by Dymnikova and Khlopov (2001). We also point to the work by Matsui and Watamura (2020) (and references therein) who claim that the approach of semiclassical gravity is not appropriate to describe the early Universe.

The second approach to evaluating backreaction in semiclassical cosmology that we present here, denoted stochastic gravity (Hu and Verdaguer 2020), creates a link to open system concepts and statistical features such as dissipation, fluctuations, noise and decoherence. It employs a so-called closed time path coarse grained effective action (CTP CGEA) (Calzetta and Hu 1987; Jordan 1986, 1987), in order to derive a set of modified semiclassical Einstein equations, denoted as Einstein–Langevin equations. It includes the semiclassical approach but extends it by a stochastic noise term (Hu and Matacz, 1995).

Some of the first applications of the CTP CGEA formalism to the backreaction problem in cosmology were made by Calzetta and Hu (1987, 1989, 1994). Hu and Matacz (1995) derived the Einstein–Langevin equations for the case of a free massive scalar field in a flat FLRW background, as well as for a Bianchi Type-I Universe. The case of a massless conformally coupled field was discussed in (Campos and Verdaguer, 1994). The scope of works includes topics such as stochastic inflation, where quantum fluctuations present in the noise term backreact on the inflaton field (Calzetta and Hu, 1995; Lombardo and Mazzitelli, 1996), as well as studies of the reheating phase in inflationary cosmology (Boyanovsky et al., 1995; Ramsey and Hu, 1997). The formalism was also used by Sinha and Hu (1991) to check the validity of the minisuperspace approximation in quantum cosmology. Further applications can be found in the paper and textbook by Hu and Verdaguer (2008), Hu and Verdaguer (2020).

We also point to one of the most prominent applications of stochastic methods to early Universe cosmology by Starobinsky (1982) and Starobinsky (1988). His stochastic inflationary model evaluates backreaction of small scalar field quantum perturbations on the corresponding long wavelength modes (which are assumed to behave classically) by additional stochastic terms in the long wavelength equations of motion. A slow-roll behavior of the background is assumed. Interestingly, it has been shown that the stochastic and the quantum feld theoretic approaches to perturbations in the early Universe yield the same results, (Starobinsky and Yokoyama, 1994; Finelli et al., 2009; Tsamis and Woodard, 2005). For recent considerations of stochastic inflation beyond the (strict) slow-roll conditions, we refer to the work by Pattison et al. (2019) and references therein.

Both approaches, semiclassical as well as stochastic gravity regard the gravitational field as a classical entity from the start while the matter fields are considered to be of quantum nature. While this represents a seminal progress to incorporating quantum effects of the matter fields in the early Universe, it can and should be questioned whether this somehow incompatible approach (classical and quantum fields treated at the same level) survives the test of future observations, and whether it should be replaced by a more consistent approach - quantum gravity - at least for the earliest moments of the cosmic history.

4 APPROACHES TO QUANTUM BACKREACTION

The question of backreaction in quantum gravity and quantum cosmology encompasses a variety of different approaches and definitions of backreaction. In quantum cosmology, backreaction is usually identified as the effects from the inhomogeneous quantum perturbation fields on the (quantum) homogeneous and isotropic degrees of freedom, which is also the notion of backreaction used in the next section (Schander and Thiemann, 2019c). This approach is tightly related to a perturbative expansion with respect to the inverse Planck mass $m_{\mathrm{Pl}}^{-1} = (G/\hbar)^{1/2}$, where G is Netwon's constant and we set $\hbar \equiv 1$. More precisely, it employs a Born–Oppenheimer type scheme (Born and Oppenheimer, 1927), with respect to m_{Pl}^{-1}. We will thus focus on implementations of the Born–Oppenheimer method to quantum gravity and quantum cosmology.

In fact, the idea that quantum gravity can be considered as a perturbative theory with respect to m_{Pl} was already introduced by Brout (1987). The first investigations of backreaction in quantum gravity that rely on this expansion were performed in the framework of quantum geometrodynamics (Wheeler, 1957; Kiefer, 2007). The idea is to expand the Wheeler–DeWitt equation in terms of the ratio of the Planck mass and the matter field mass (Kiefer and Singh, 1991). A different idea, conceptually similar to the schemes considered here, is to use a Born–Oppenheimer type approach, relying on the same perturbation parameter. Different considerations of the problem (giving rise to similar results) can be found in the works by Bertoni et al. (1996), Brout and Venturi (1989), and Kiefer (1994) (for a summary, see Kiefer, 2007). A review of the ideas of Born and Oppenheimer will be given in the next section, but to understand its use in the given context we present the key ideas.

For simplicity, let Q denote the gravitational and q the matter degrees of freedom. The Born–Oppenheimer scheme employs an ansatz solution for the quantum Hamiltonian and momentum constraint of the form (Kiefer, 2007),

$$\Psi(q, Q) = \sum_n \chi_n(Q)\psi_n(q, Q), \tag{2}$$

where $\{\psi_n(q, Q)\}_n$ is supposed to be a known orthonormal basis of the matter Hilbert space that solves the matter part of

the constraint and Q is to be considered as an external parameter for this eigenvalue problem. Then, one applies the constraints to Ψ and applies some $\psi_k(q, Q)$ from the left (i.e., one considers the inner product of the matter states). This gives rise to constraint equations for the geometric factors $\chi_n(Q)$, which can be seen as an effective quantum problem for the geometric part, including the backreaction effects of the quantum matter system. In this scenario, the Born–Oppenheimer approximation consists in neglecting the contributions that enter with higher orders in m_{Pl}^{-1}.

In order to extract physical results from the formalism, one can additionally employ a semiclassical approximation (which is however *independent* of the Born–Oppenheimer approach). This should yield the semiclassical limit of quantum gravity, i.e., a matter QFT on CST. It is common to employ a WKB ansatz for the geometrical states $\chi_n(Q)$ of the form,

$$\chi_n(Q) = C_n(Q) e^{i m_{\mathrm{Pl}}^2 S[Q]}, \tag{3}$$

where $S[Q]$ stands for the geometric action in the geometrodynamical approach. The perturbative scheme in m_{Pl}^{-1} eventually yields the semiclassical Einstein equations. In this sense, these approaches evaluate the backreaction of the quantum matter fields on the quantum or classical geometry.

One can apply the Born–Oppenheimer and WKB approximations in a different manner. Instead of taking the expectation value with respect to the quantum matter system, one applies the Wheeler–DeWitt constraints on the total Born–Oppenheimer ansatz function and uses the WKB approximation for the geometrical part. Restricting again to the lowest order with respect to the inverse Planck mass, this yields a quantum constraint for the matter wave function which depends on the classical action (through the WKB ansatz), and derivatives with respect to the spatial metric thereof. The idea of the above–cited works (and also of Briggs and Rost, 2000) is to introduce an external time parameter that depends on this derivative, hence giving rise to a Schrödinger equation for the matter system that includes the backreaction of the geometry through the geometry–dependent time derivative. In fact, this gives rise to a notion of time in a formerly background independent framework. Such ideas go back to DeWitt (1967) and have been applied to a variety of cosmological situations (see (Kiefer 2007) and references therein). It is however a different notion of backreaction than the one considered in the next section. Besides, the present approach uses a Born–Oppenheimer approach *plus* a semiclassical WKB approximation while the next section uses the purely quantum mechanical space adiabatic perturbation extension of the Born–Oppenheimer scheme. Applications of the former works to the inflationary paradigm with perturbations and a discussion of the question of unitary evolution of the perturbations can be found in the work by Chataignier and Krämer (2021) and references therein. They also consider cosmological perturbations that include gravitational contributions (i.e., the Mukhanov–Sasaki variables). Similar approaches that do not split the system into geometric and matter parts but include (perturbative) parts of the gravitational degrees of freedom in the fast subsystem and (homogeneous) matter parts in the slow sector were already presented by Halliwell and Hawking (1985) and Vilenkin (1989). This choice is also used in Schander and Thiemann (2019c).

The Born–Oppenheimer approximation was also considered within approaches to quantum gravity with other variable choices. Giesel et al. (2009) aimed at an application of the Born–Oppenheimer methods to loop quantum gravity (LQG) (Thiemann, 2008; Rovelli, 2010), using holonomy–flux variables or connection–flux variables. As it turns out, this choice of variables prevents the use of the Born–Oppenheimer methods since the flux operators are mutually non-commuting (which is a prerequisite for the Born–Oppenheimer scheme). Instead, they use commuting co-triad variables for the gravity sector and a scalar field for the matter sector to derive the semiclassical Einstein equations that take the backreaction of the quantum matter fields via an expectation value into account. Giesel et al. (2009) consider their model on a discrete lattice (as it is common practice for approaches to LQG), and thus formally obtain a lattice QFT on a discrete curved space time. They also point to the possibility of pursuing the formal Born–Oppenheimer scheme and computing *quantum* solutions to the gravity sector with the effective backreaction of the quantum matter fields. Besides, they introduce a hybrid approach (similar to the models we consider here) where the gravitational sector is restricted to FLRW solutions and the fast part of the system is given by the matter quantum fields. They also propose to introduce coherent states for the gravitational subsystem in order to make progress in finding solutions. Due to the complexity of the gravity-matter systems, the focus of this work lies on spelling out the conceptual ideas rather than technically carrying out the program in detail.

More recently, Stottmeister and Thiemann (2016a,b,c) considered similar questions in the context of LQG but employed the more general scheme of space adiabatic perturbation theory (SAPT) (Panati et al., 2003). Since in the latter approach, the variables of the slow, gravitational sector are not required to commute, it is in principle possible to apply the Born–Oppenheimer ideas also to LQG and related theories. The concrete implementation turns however out to be difficult due to the particular structure of the LQG phase space (which relies on a cotangent bundle of a compact Lie group rather than on a vector space) and its quantum represention. Other open issues of their attempts are related to the underlying graph structure of LQG models and the projective limits of finite dimensional truncations of the gravitational phase space that are needed in order to construct a continuum theory (Stottmeister and Thiemann, 2016c). They also point out that a major obstruction to the derivation of a QFT on CST from LQG lies in the inequivalent representations of quantum fields for different gravitational configurations (Stottmeister and Thiemann, 2016c). This problem is a generic feature of background dependent quantum field theories. In this work, we present a (perturbative) solution to this problem which makes the application of space adiabatic methods to quantum cosmology possible (Fernandez-Mendez et al., 2012; Castelló Gomar et al., 2015; Castelló Gomar et al., 2016).

For completeness, we also mention the application of Born–Oppenheimer methods within the spinfoam approach to LQC (Rovelli and Vidotto, 2008) (see Ashtekar et al., 2003; Bojowald, 2008 for the LQC approach), and that Castelló Gomar et al. (2016) consider a conceptually different kind of Born–Oppenheimer approximation in the hybrid approach to LQC. These seminal works make important progress by first considering the problem of backreaction, but must either remain on a rather formal level or include various assumptions which are hard to control. We therefore advocate to employ the SAPT scheme presented in the next section which serves as an unambigious, rigorous and perturbative approach, in principle applicable to any quantum cosmological framework and realizable up to any perturbative order, to taking quantum cosmological backreactions thoroughly into account. The approach applies to a much wider variety of quantum systems in comparison to the Born–Oppenheimer approach (in particular to quantum cosmological perturbation theory), does not rely on the introduction of semiclassical ansatz states and iteratively provides quantum constraints or equations of motion whose solutions approximate the true solutions up to, in principle, indefinitely small errors.

5 QUANTUM BACKREACTION WITH SPACE ADIABATIC METHODS

Computing and including backreaction in (perturbative) quantum cosmology requires an approximation scheme that ideally takes the physical characteristics of the system into account. SAPT as proposed by Panati et al. (2003) and extensions thereof are ideally suited to achieve this goal and to integrate backreaction effects into quantum cosmology (Schander and Thiemann, 2019a; Schander and Thiemann 2019b; Schander and Thiemann 2019c; Neuser et al., 2019).

SAPT is a generalization of the well-known Born–Oppenheimer approximation for non-relativistic molecular systems. Both approaches exploit the small ratio of two internal parameters such as the mass ratio of electrons and nuclei in a molecule to define a perturbation parameter,

$$\varepsilon^2 := \frac{m_\mathrm{e}}{m_\mathrm{n}} \approx 5.46 \times 10^{-4} \ll 1, \tag{4}$$

with the electron mass $m_\mathrm{e} \approx 9.11 \times 10^{-31}$ kg and the nuclei mass $m_\mathrm{n} \approx 1.67 \times 10^{-27}$ kg. In the simplest atom with one nucleus and one electron (although exact solutions are known for this case), the Hamilton function has the form,

$$H(q,P;x,y) = \frac{\varepsilon^2 P^2}{2m_\mathrm{e}} + \frac{y^2}{2m_\mathrm{e}} + V(q;x), \tag{5}$$

where (q,P) and (x,y) are the canonically conjugate pairs of the nucleus and the electron respectively. $V(q;x)$ is a smooth potential, typically a Coulomb potential depending on the distance between nucleus and electron. In this molecular set up, the equipartition theorem states that the kinetic energies of nuclei and electrons are of the same order, and hence, on average, the nuclei move much slower than the electrons with correspondent statistically–averaged velocities, $\langle v_\mathrm{n}\rangle \approx \varepsilon\langle v_\mathrm{e}\rangle$. Born and Oppenheimer used this fact to define suitable ansatz solutions for the quantum mechanical problem: On the typical electronic time scale, the nuclei are at rest and the non-trivial electronic contributions of the Hamilton operator can be considered at fixed nuclei positions $q \in \mathbb{R}$,

$$\boldsymbol{H}_\mathrm{e}(q) := \frac{\boldsymbol{y}^2}{2m_\mathrm{e}} + \boldsymbol{V}(q,\boldsymbol{x}), \tag{6}$$

where the bold letters $\boldsymbol{y}$, $\boldsymbol{x}$ denote momentum and position operators of the electron defined on their respectively dense domains in $L^2(\mathbb{R},\mathrm{d}x)$. Ideally, the operator function $\boldsymbol{H}_\mathrm{e}(q)$ admits a solvable q–dependent eigenvalue problem,

$$\boldsymbol{H}_\mathrm{e}(q)\,\xi_n(q) = E_n(q)\,\xi_n(q), \tag{7}$$

with a discrete q–dependent eigenbasis $\{\xi_n(q)\}_{n\in\mathbb{N}}$ in the *fast* Hilbert space $\mathcal{H}_\mathrm{f} := L^2(\mathbb{R},\mathrm{d}x)$, for which the so–called electronic energy bands $E_n(q)$ are gapped functions, i.e., $E_n(q) - E_m(q) \neq 0$ pointwise for $m \neq n$. One can use this eigenbasis as an ansatz solution for the full Hamilton operator $\widehat{\boldsymbol{H}}$ (the Weyl quantization with respect to the nuclei sector is labeled by hats), and ask whether it provides an approximate solution to the entire problem. Equivalently, we can define for every electronic eigensolution the direct integral operator,

$$\widehat{\boldsymbol{\pi}}_n := \int_{\mathbb{R}}^{\oplus} \mathrm{d}q\,\xi_n(q)\langle\xi_n(q),\cdot\rangle_\mathrm{e} = \int_{\mathbb{R}}^{\oplus} \mathrm{d}q\,\boldsymbol{\pi}_n(q), \tag{8}$$

on the total Hilbert space $\mathcal{H} = L^2(\mathbb{R},\mathrm{d}q)\otimes\mathcal{H}_\mathrm{f}$ and ask whether it commutes with $\widehat{\boldsymbol{H}}$. Of course, the answer is in the negative, but it turns out that the commutator scales like ε,

$$\left[\widehat{\boldsymbol{H}},\widehat{\boldsymbol{\pi}}_n\right] \sim \varepsilon. \tag{9}$$

This is because of the adiabatic relation between the electrons and the nuclei. By construction, the Weyl quantization $\widehat{\boldsymbol{H}}_\mathrm{e}(\hat{q})$ of the electronic Hamiltonian and $\widehat{\boldsymbol{\pi}}_n$ commute. However, the remaining contribution to the Hamilton operator $\widehat{\boldsymbol{H}}$, in particular the kinetic energy of the nucleus, scales like ε^2 and leads hence to the estimate in **Eq. 9**. The Born–Oppenheimer approximation builds on this result and proposes to use the ansatz functions,

$$\Psi(q;x) = \sum_n \psi_n(q)\xi_n(q;x), \tag{10}$$

to solve the full quantum problem. In its simplest version, the scheme neglects any of the contributions that arise from applying the kinetic energy operator of the nucleus to the electronic ansatz functions (as they enter with small ε-factors), and thus results in an effective eigenvalue problem for the nucleus only,

$$\left(\frac{\widehat{P}^2}{2m_\mathrm{n}} + E_n(\hat{q})\right)\psi_n(q) \equiv E\psi_n(q). \tag{11}$$

If this nucleonic eigenproblem can be solved, the scheme leads in fact to viable results for the stationary energy spectra of molecules, which are given by the energy solutions E, and

which include the backreaction of the electrons via the potential energy $E_n(\hat{q})$.

Unfortunately, the Born–Oppenheimer approach comes with some limitations which preclude its application to more complicated systems. Firstly, the scheme explicitely uses that the electronic eigenfunctions depend only on the *configuration* variable of the nucleus. Was the coupling between electrons and nuclei provided by non-commuting slow operators, for example by $\hat{q}$ *and* $\hat{p}$, the scheme would fail since the direct integral construction in **Eq. 8** builds on the commutativity (i.e., the existence of a common spectrum) of the coupling operators. Also one could not define the ansatz functions in **Eq. 10**. Secondly, the scheme does not provide a simple extension to better error estimates. This becomes problematic if one is interested in the dynamical evolution of the system. The interesting dynamics of the nuclei happens on time scales $t_n \sim t_e/\varepsilon$ or larger, but considering the evolution generated by $\hat{\boldsymbol{H}}$ with respect to the above ansatz functions, the scheme cannot lead to trustworthy results due to the commutator relation **Eq. 9**.

It should be possible to do better. In fact, the adiabatic theorem (Teufel, 2003) states that under certain conditions (to be discussed in the sequel), there exists an orthogonal projection operator $\hat{\Pi} \in \mathcal{B}(\mathcal{H})$ in the bounded operators on the total Hilbert space $\mathcal{H}$ such that,

$$\left[\hat{\boldsymbol{H}}, \hat{\boldsymbol{\Pi}}\right] = \mathcal{O}_0(\varepsilon^\infty), \tag{12}$$

where the right hand side means that for all $m \in \mathbb{N}$, there exists a constant $C_m < \infty$ such that $\left\| [\hat{\boldsymbol{H}}, \hat{\Pi}] \right\|_{\mathcal{B}(\mathcal{H})} \leq C_m \varepsilon^m$, in the norm of bounded operators on $\mathcal{H}$. Most importantly, $\hat{\Pi}$ can be constructed by a "semiclassical symbol" function, i.e., an operator-valued ansatz function like the almost–projector function $\boldsymbol{\pi}_n \in C^\infty(\mathbb{R}, \mathcal{B}(\mathcal{H}_f))$ from the simple example above. This symbol function appears as an asymptotic series in the perturbation parameter ε, and–to anticipate the result–the equivalent of $\boldsymbol{\pi}_n(q)$ will serve as the base clause to an iterative ε-scheme to compute better and better approximations to $\hat{\Pi}$. This is the idea of SAPT (Panati et al., 2003).

SAPT uses an ε-scaled phase space (or deformation) quantization scheme (Blaszak and Domanski, 2012) for the slow subsector of the system, while retaining a standard Hilbert space representation for the fast sector. Phase space quantum mechanics is a formulation of quantum mechanics that employs an algebra of phase space functions $\mathcal{A}_Q$ instead of using the standard operator algebra in the Hilbert space representation of quantum mechanics. Quantum mechanical observables are thus represented by real-valued phase space functions. The pullback of the operator product to the phase space algebra gives rise to a non-commutative star product $\star$. Since the star product reduces to the commutative multiplication of phase space functions in the limit $\hbar \to 0$, this formulation of quantum mechanics is also known as deformation quantization. The standard textbooks by Dimassi and Sjöstrand (1999), Folland (1989), and Hörmander (1985a,b) give thorough introductions to the usual *scalar*–valued phase space quantization scheme and pseudodifferential calculus, but the situation here is more subtle. SAPT requires to consider *operator*–valued symbol functions, in particular functions on the slow phase space with values in the operators on the fast Hilbert space. We will thus deal with symbol functions of the form $\boldsymbol{A}(q,p) \in C^\infty(\Gamma_s, \mathcal{B}(\mathcal{H}_f))$ where Γ_s denotes the slow phase space (Teufel, 2003; Appendix A). It is straightforward to map the symbol functions (operator–valued or not) to their operator representatives in the standard Hilbert space approach. The concrete prescription depends of course on the operator ordering that one chooses. In case of the symmetric Weyl quantization prescription, this relation is provided by the Weyl correspondence (Dubin et al., 1980), and a symbol function appears as the kernel of an integral operator that acts on an element of the Hilbert space (Teufel, 2003).

Symbol functions which give rise to admissible operators in the quantum theory can be classified by their asymptotic behavior on the slow phase space. One important class of symbols relevant for SAPT are the semiclassical symbols S^m_ρ, with $m \in \mathbb{R}$ and $0 \geq \rho \geq 1$. An operator–valued function $\boldsymbol{A} \in C^\infty(\mathbb{R}^2, \mathcal{B}(\mathcal{H}_f))$ is in the symbol class $S^m_\rho(\mathcal{B}(\mathcal{H}_f))$ if for every $\alpha, \beta \in \mathbb{N}$, there exists a positive constant $C_{\alpha,\beta}$ such that,

$$\sup_{q \in \mathbb{R}} \left\| \left(\partial_q^\alpha \partial_p^\beta \boldsymbol{A}\right)(q,p) \right\|_{\mathcal{B}(\mathcal{H}_f)} \leq C_{\alpha,\beta} \langle p \rangle^{m-\rho|\beta|}, \tag{13}$$

for every $p \in \mathbb{R}$, and $\langle p \rangle = (1 + |p|^2)^{1/2}$ (Teufel, 2003). For such symbols the Weyl ordering prescription for quantum theory gives rise to a specific star product, and we can finally make sense of the space adiabatic perturbation idea. For two such operator–valued symbols on the slow phase space $\boldsymbol{A} \in S^{m_1}_\rho(\mathcal{B}(\mathcal{H}_f))$, $\boldsymbol{B} \in S^{m_2}_\rho(\mathcal{B}(\mathcal{H}_f))$, their star product is given by,

$$(\boldsymbol{A} \star \boldsymbol{B})(q,P) = \exp\left(\frac{i\hbar}{2}\left(\partial_x \partial_P - \partial_q \partial_D\right)\right) \boldsymbol{A}(x,D)\, \boldsymbol{B}(q,P)\Big|_{x=q, D=P} \in S^{m_1+m_2}_\rho\left(\mathcal{B}(\mathcal{H}_f)\right). \tag{14}$$

We note that the exponential has a series expansion which could be considered as a series with respect to $\hbar$ in the given context. Alluding to the adiabaticity of the system, it is reasonable to define a rescaled momentum operator $p := \varepsilon P$. Replacing P and D by their ε-scaled versions in the star product formula, the new expansion parameter is $\varepsilon\hbar$. Any star product of symbol functions can thus be written in a series expansion in ε. Comparing terms of the same polynomial order in ε, this defines a perturbation theory for quantum mechanical equations which will iteratively solve the eigenvalue problems of interest. The first two orders of the rescaled star product are given by,

$$\begin{aligned}(\boldsymbol{A} \star \boldsymbol{B})(q,p) = {} & (\boldsymbol{A}_0 \cdot \boldsymbol{B}_0)(q,p) + \frac{i\varepsilon\hbar}{2}\{\boldsymbol{A}_0(q,p), \boldsymbol{B}_0(q,p)\} \\ & + \varepsilon(\boldsymbol{A}_0 \cdot \boldsymbol{B}_1 + \boldsymbol{A}_1 \cdot \boldsymbol{B}_0)(q,p) + \mathcal{O}(\varepsilon^2),\end{aligned} \tag{15}$$

where the symbol functions have been expanded with respect to ε according to $\boldsymbol{A} = \sum_k \varepsilon^k \boldsymbol{A}_k$ and $\boldsymbol{B} = \sum_k \varepsilon^k \boldsymbol{B}_k$. Note that the ε-rescaling changes the whole symplectic structure (we now have, $\{q,p\}_s = \varepsilon$), as well as the canonical commutation relations since we obtain,

$$[\widehat{q},\widehat{p}]_{\mathrm{s}} = i\varepsilon\hbar\,\widehat{1}_{\mathrm{s}}. \tag{16}$$

From now on, we will set $\hbar \equiv 1$. Note that in the original Born–Oppenheimer approximation, the perturbative parameter occurs (after an appropriate rescaling) only in the Hamiltonian and the perturbation theory consists in splitting the Hamiltonian (and its spectrum) accordingly, while *here* the quantum algebra is redefined, giving rise to a (n in principle infinite) perturbation series in ε.

5.1 Space Adiabatic Perturbation Theory

SAPT as introduced by Panati et al. (2003) places a set of conditions on the physical system under consideration. These are, in some respects, quite restrictive. However, if one accepts to abandon certain results, such as the convergence of the perturbative series, it is possible to milden the conditions. Here, we present the original conditions introduced by Panati, Spohn and Teufel for a system with d slow and k fast degrees of freedom, and which can be split into four categories:

(C1) **The state space** of the system decomposes as,

$$\mathcal{H} = L^2\left(\mathbb{R}^d\right) \otimes \mathcal{H}_{\mathrm{f}} = L^2\left(\mathbb{R}^d, \mathcal{H}_{\mathrm{f}}\right), \tag{17}$$

where $L^2(\mathbb{R}^d)$ is the state space of the system whose rate of change is by a factor ε^l, $l \in \mathbb{R}^+$, smaller than the rate of change of the (environmental) system $\mathcal{H}_{\mathrm{f}}$. The latter is assumed to be a separable Hilbert space.

(C2) **The quantum Hamiltonian $\widehat{\boldsymbol{H}}$** (may it be an operator or a constraint) is given as the Weyl quantization of a semiclassical symbol $\boldsymbol{H} \in S^m_\rho(\varepsilon, \mathcal{B}(\mathcal{H}_{\mathrm{f}}))$, i.e., $\boldsymbol{H}$ asymptotically approaches an ε-series,

$$\boldsymbol{H}(\varepsilon, z) \asymp \sum_{j=0}^{\infty} \varepsilon^j \boldsymbol{H}_j(z), \tag{18}$$

where $\boldsymbol{H}_j \in S^{m-j\rho}_\rho(\mathcal{B}(\mathcal{H}_{\mathrm{f}}))$ for all $j \in \mathbb{N}$ and $z := (q, P) \in \mathbb{R}^{2d}$. The appropriate notion of convergence is provided by a Fréchet semi–norm in $S^m_\rho(\mathcal{B}(\mathcal{H}_{\mathrm{f}}))$, see (Teufel, 2003) for further details.

(C3) For any fixed $z \in \mathbb{R}^{2d}$, the spectrum $\sigma(z)$ of the principal symbol $\boldsymbol{H}_0(z)$ of $\boldsymbol{H}(\varepsilon, z)$ has isolated parts $\sigma_n(z)$, $n \in \mathbb{N}$. Picking one such $\nu \in \mathbb{N}$ and therefore suppressing any n–dependence in the following, the minimal distance between the elements of $\sigma_\nu(z)$ and the remainder of the spectrum $\sigma_{\mathrm{rem}}(z) := \sigma(z) \backslash \sigma_\nu(z)$ displays a non-vanishing gap. According to its characteristics with varying z, the gap can be classified by means of a parameter γ.

Conditions $(\mathbf{Gap})_\gamma$: Let $f_\pm \in C^0(\mathbb{R}^{2d}, \mathbb{R})$ be two continuous functions with $f_- \leq f_+$.

(G1) **Enclosing interval.** For every $z \in \mathbb{R}^{2d}$ the isolated part of the spectrum $\sigma_n(z)$ is entirely contained in the interval $I(z) := [f_-(z), f_+(z)]$.

(G2) **Gap to the remainder.** The distance between the remainder of the spectrum, $\sigma_{\mathrm{rem}}(z)$ and the enclosing interval $I(z)$ is strictly bigger than zero and increasing for large momenta, i.e.,

$$\mathrm{Dist}\left[\sigma_{\mathrm{rem}}(z), I(z)\right] \geq C_{\mathrm{g}}\left(1 + p^2\right)^{\frac{\gamma}{2}}. \tag{19}$$

(G3) **Boundedness of the interval.** The width of the interval $I(z)$ is uniformly bounded, *i.e.*,

$$\sup_{z \in \mathbb{R}^{2d}} \left| f_+(z) - f_-(z) \right| \leq C_{\mathrm{d}} < \infty. \tag{20}$$

(C4) **Convergence Condition.** If the system satisfies the gap condition $(\mathrm{C3})_\gamma$ for some $\gamma \in \mathbb{R}$, the Hamilton symbol $\boldsymbol{H}$ must be in S^γ_ρ. If $\rho = 0$, also γ must vanish. If $\rho > 0$, γ can be any real number but $\widehat{\boldsymbol{H}}$ must be essentially self–adjoint on $\mathcal{S}(\mathbb{R}^d, \mathcal{H}_{\mathrm{f}})$.

Condition (C4) is not vital in order to perform the formal computations in the following. It ensures however that for considerations on the whole slow phase space Γ_{s}, the error estimates of SAPT are bounded everywhere on Γ_{s}. In particular, the adiabatic decoupling is said to be *uniform*. Note also that the requirement that $\boldsymbol{H}$ has values in the *bounded* operators is violated for many physical systems of interest. In such cases, the space adiabatic scheme cannot be immediately applied and the convergence of the perturbative expansion has to be examined by independent methods (Panati et al., 2003).

Given the conditions (C1)–(C4), the space adiabatic theorem introduces a perturbative construction scheme that is based on iteratively computing three symbol functions: the Moyal projector $\boldsymbol{\pi} \in S^0_\rho$, the Moyal unitary $\boldsymbol{u} \in S^0_\rho$ and an effective Hamiltonian $\boldsymbol{H}_{\mathrm{eff}} \in S^m_\rho$. The Moyal projector serves to identify a subspace of the total Hilbert space which is almost invariant under the dynamics of $\widehat{\boldsymbol{H}}$ and which is associated with one particular quantum number $\nu \in \mathbb{N}$ of the fast sector. The Moyal unitary $\boldsymbol{u}$ is an auxiliary structure which gives rise to a unitary operator that maps the relevant subspace to a much simpler reference subspace. In fact, the original subspace is a technically complicated object and cannot provide us with a simple procedure to derive the (approximated) dynamics in the subspace. The reference subspace is trivial with respect to the fast subsystem and allows to compute the dynamics of the slow sector including the backreaction of the fast degree(s) of freedom. It is used to derive an effective Hamiltonian symbol $\boldsymbol{H}_{\mathrm{eff}}$ whose solutions are approximate solutions to the full Hamilton operator $\widehat{\boldsymbol{H}}$. More precisely.

(S1) There exists a unique formal symbol, $\boldsymbol{\pi} = \sum_{i \geq 0} \varepsilon^i \boldsymbol{\pi}_i$, with $\boldsymbol{\pi}_i \in S^{-i\rho}_\rho(\mathcal{B}(\mathcal{H}_{\mathrm{f}}))$, such that $\boldsymbol{\pi}_0$ is the spectral projection of $\boldsymbol{H}(q,p)$ corresponding to $\sigma_\nu(q,p)$ and with the properties,

$$\text{(S1–1)} : \boldsymbol{\pi} \bigstar_\varepsilon \boldsymbol{\pi} = \boldsymbol{\pi} \qquad \text{(S1–2)} : \boldsymbol{\pi}^\star = \boldsymbol{\pi}$$
$$\text{(S1–3)} : \boldsymbol{H} \bigstar_\varepsilon \boldsymbol{\pi} - \boldsymbol{\pi} \bigstar_\varepsilon \boldsymbol{H} = 0.$$

It can be shown that the Weyl quantization of a resummation of $\boldsymbol{\pi}$, which we denote by $\boldsymbol{\pi}_\varepsilon$ is $\mathcal{O}_0(\varepsilon^\infty)$–close to an operator $\widehat{\boldsymbol{\Pi}}$, i.e., $\widehat{\boldsymbol{\Pi}} = \widehat{\boldsymbol{\pi}}_\varepsilon + \mathcal{O}_0(\varepsilon^\infty)$ and that, $[\widehat{\boldsymbol{H}}, \widehat{\boldsymbol{\Pi}}] = \mathcal{O}_0(\varepsilon^\infty)$.

(S2) Let $\boldsymbol{\pi}_\mathrm{R}$ be the projection on some reference subspace $\mathcal{K}_\mathrm{f} \subseteq \mathcal{H}_\mathrm{f}$. We assume that there exists a symbol $\boldsymbol{u}_0 \in S^0_\rho(\mathcal{B}(\mathcal{H}_\mathrm{f}))$, such that, $\boldsymbol{u}_0 \cdot \boldsymbol{\pi}_0 \cdot \boldsymbol{u}_0^* = \boldsymbol{\pi}_\mathrm{R}$. Then, there is a formal symbol $\boldsymbol{u} = \sum_{i\geq 0}\varepsilon^i \boldsymbol{u}_i$ with $\boldsymbol{u}_i \in S^{-i\rho}_\rho(\mathcal{B}(\mathcal{H}_\mathrm{f}))$ such that,

$$(\mathrm{S2\text{–}1}) : \boldsymbol{u}^* \bigstar_\varepsilon \boldsymbol{u} = 1 \qquad (\mathrm{S2\text{–}2}) : \boldsymbol{u} \bigstar_\varepsilon \boldsymbol{u}^* = 1$$
$$(\mathrm{S2\text{–}3}) : \boldsymbol{u} \bigstar_\varepsilon \boldsymbol{\pi} \bigstar_\varepsilon \boldsymbol{u}^* = \boldsymbol{\pi}_\mathrm{R}.$$

The Weyl quantization of a resummation of $\boldsymbol{u}$, which we denote by $\boldsymbol{u}_\varepsilon$ gives rise to an operator, $\widehat{\boldsymbol{U}} = \widehat{\boldsymbol{u}}_\varepsilon + \mathcal{O}_0(\varepsilon^\infty)$ for which it holds true that, $\hat{U}\,\widehat{\boldsymbol{\Pi}}\,\hat{U} = \widehat{\boldsymbol{\pi}}_\mathrm{R}$.

(S3) There exists a formal, effective Hamilton symbol $\boldsymbol{h}_\mathrm{eff} = \sum_{i\geq 0}\varepsilon^i \boldsymbol{h}_{\mathrm{eff},i}$ defined as,

$$\boldsymbol{h}_\mathrm{eff} := \boldsymbol{u} \bigstar_\varepsilon \boldsymbol{H} \bigstar_\varepsilon \boldsymbol{u}^*.$$

For systems with an external time parameter t and the Weyl quantizations $\widehat{\boldsymbol{u}}$ and $\widehat{\boldsymbol{h}}_\mathrm{eff}$, we have,

$$e^{-i\widehat{H}s} - \widehat{\boldsymbol{u}}^\dagger e^{-i\widehat{h}_\mathrm{eff}s}\,\widehat{\boldsymbol{u}} = \mathcal{O}_0(\varepsilon^\infty|s|). \tag{21}$$

In the next section, we will make these formal definitions and results more explicit and apply the space adiabatic scheme to a simple cosmological model up to second order in the perturbations.

5.2 Backreaction in Quantum Cosmology

As an illustrative example for the space adiabatic scheme, let us consider Einstein general relativity, reduced to spatial homogeneity and isotropy, including a cosmological constant $\Lambda > 0$, and coupled to a spatially homogeneous, isotropic and real Klein–Gordon field ϕ_0 with mass $m_\mathrm{KG} > 0$ and coupling constant $\lambda \in \mathbb{R}$. We assume a globally hyperbolic space time manifold and a metric with Lorentzian signature $(-,+,+,+)$. The only dynamical degree of freedom of the metric is the scale factor $a \geq 0$. The lapse function N is a Lagrange multiplier and will be fixed $N \equiv 1$. We perform a $(3+1)$–split of the manifold into space and time which admits spatial hypersurfaces σ which we fix to be compact, flat three–tori $\mathbb{T}^3$ with side lengths $l \equiv 1$. The cosmological action is,

$$S[a(t), \phi_0(t)] = \int_\mathbb{R} \mathrm{d}t \left(-\frac{1}{\kappa}\left(3\dot{a}^2 a + \Lambda a^3\right) + \frac{1}{2\lambda}\left(\dot{\phi}_0^2 - m^2_\mathrm{KG}\phi_0^2\right)\right), \tag{22}$$

where $\kappa = 8\pi G$ and λ are the gravitational and scalar field coupling constants. If both, (a, ϕ_0) are dimensionless, as we assume, then both coupling constants have the same dimension, and we define the dimensionless ratio,

$$\varepsilon^2 := \frac{\kappa}{\lambda}. \tag{23}$$

Considering typical values of the coupling parameters in the Standard Model, it seems reasonable to assume that this ratio is indeed extremely small. Hence, we identify gravity with the slow sector while the matter field is considered to be the fast subsystem.

The space adiabatic scheme requires a Hamiltonian formulation of the problem. We define the conjugate momenta of a and ϕ_0 as, $p_a := \varepsilon\frac{\partial L}{\partial \dot{a}}$ and $\mu_0 := \frac{\partial L}{\partial \dot{\phi}_0}$, where L is the Lagrange function associated with the action S. The Poisson brackets of the canonical variables evaluate to $\{a, p_a\} = \varepsilon$, and $\{\phi_0, \mu_0\} = 1$. The Legendre transformation generates the Hamilton constraint,

$$C(a, p_a, \phi_0, \pi_0) := -\frac{1}{12}\frac{p_a^2}{a} + \frac{\Lambda}{\lambda\kappa}a^3 + \frac{\mu_0^2}{2a^3} + \frac{1}{2\lambda^2}m^2_\mathrm{KG}a^3\phi_0^2, \tag{24}$$

where for notational reasons, we divided the whole constraint by a constant factor λ. For simplifying the analysis by means of SAPT in the following, we switch to triad–like canonical variables,

$$b := \pm\sqrt{a^3}, \qquad \rho := \frac{2}{3}\frac{p_a}{\sqrt{a}}, \tag{25}$$

which is a double cover of the original phase space and we do not restrict to any of the branches of b. In order to keep the notation as simple as possible, we introduce the following parameters and functions,

$$m_\mathrm{G} := \frac{8}{3}, \qquad \omega^2_\mathrm{G} := \frac{3\Lambda}{4\lambda\kappa}, \qquad \tilde{m}_\mathrm{KG} := b^2, \qquad \omega^2_\mathrm{KG} := \frac{m^2_\mathrm{KG}}{\lambda^2}. \tag{26}$$

These definitions and the new canonical variables give for the Hamilton constraint,

$$C(b, \rho, \phi_0, \mu_0) = -\frac{\rho^2}{2m_\mathrm{G}} + \frac{1}{2}m_\mathrm{G}\omega^2_\mathrm{G}b^2 + \frac{\mu_0^2}{2\tilde{m}_\mathrm{KG}(b)} + \frac{1}{2}\tilde{m}_\mathrm{KG}(b)\omega^2_\mathrm{KG}\phi_0^2. \tag{27}$$

We quantize the system and start by considering the scalar field subsystem using bold operator symbols. The state space is $\mathcal{H}_\mathrm{f} := L^2(\mathbb{R}, \mathrm{d}\phi_0)$, and the scalar field operator and its conjugate momentum satisfy the canonical commutation relation, $[\phi_0, \boldsymbol{\mu}_0]_\mathrm{f} = i\,1_\mathrm{f}$. Similarly, the state space of the geometrical subsystem is $\mathcal{H}_\mathrm{s} := L^2(\mathbb{R}, \mathrm{d}b)$. The quantum operators wear hats and the canonical commutation relation for the geometrical variable and its conjugate momentum are, $[\hat{b}, \hat{\rho}]_\mathrm{s} = i\,\varepsilon\,\hat{1}_\mathrm{s}$. The quantum theory of the coupled system has the tensor product Hilbert space, $\mathcal{H} = \mathcal{H}_\mathrm{s} \otimes \mathcal{H}_\mathrm{f}$. The constraint operator on $\mathcal{H}$ is given by,

$$\widehat{\boldsymbol{C}} = \left(-\frac{\hat{\rho}^2}{2m_\mathrm{G}} + \frac{1}{2}m_\mathrm{G}\,\omega^2_\mathrm{G}\,\hat{b}^2\right) \otimes \mathbf{1}_\mathrm{f} + \frac{1}{2\,\tilde{m}_\mathrm{KG}(\hat{b})} \otimes \boldsymbol{\mu}_0^2 + \frac{1}{2}\tilde{m}_\mathrm{KG}(\hat{b})\,\omega^2_\mathrm{KG} \otimes \boldsymbol{\phi}_0^2. \tag{28}$$

We check the conditions (C1)–(C4) for SAPT. (C1) holds without further ado since the cosmological Hilbert space $\mathcal{H}_\mathrm{s} \otimes \mathcal{H}_\mathrm{f}$ has the required tensor product structure, and $\mathcal{H}_\mathrm{s}$ is an L^2–space and $\mathcal{H}_\mathrm{f}$ is separable. We represent the quantum

constraint as a symbol function $\boldsymbol{C}(\rho, b)$ with values in the linear operators on the Klein–Gordon Hilbert space $\mathcal{H}_{\mathrm{f}}$ by formally quantizing the Klein–Gordon subsystem only,

$$\boldsymbol{C}(b,\rho) = \left(-\frac{\rho^2}{2m_{\mathrm{G}}} + \frac{1}{2} m_{\mathrm{G}} \omega_{\mathrm{G}}^2 b^2 \right) 1_{\mathrm{f}} + \frac{\boldsymbol{\phi}_0^2}{2\,\tilde{m}_{\mathrm{KG}}(b)} + \frac{1}{2} \tilde{m}_{\mathrm{KG}}(b) \omega_{\mathrm{KG}}^2 \boldsymbol{\mu}_0^2. \tag{29}$$

$\boldsymbol{C}(b,\rho)$ is an unbounded operator on $\mathcal{H}_{\mathrm{f}}$ for every $(b,\rho) \in \mathbb{R}^2$. In particular, the operator corresponds to the Hamiltonian of a quantum harmonic oscillator with constant frequency ω_{KG}, b–dependent mass $\tilde{m}_{\mathrm{KG}}(b)$ and an off–set energy. As such, the symbol has for fixed finite (b,ρ) an energy spectrum which is bounded from below but not from above. Besides, $\boldsymbol{C}(b,\rho)$ is an unbounded function with respect to both, b and ρ. According to SAPT, the constraint symbol must however belong to one of the symbol classes $S^m_\rho(\mathcal{B}(\mathcal{H}_{\mathrm{f}}))$ and should therefore have values in the space of *bounded* operators on $\mathcal{H}_{\mathrm{f}}$, be a bounded function with respect to b and grow maximally polynomially in ρ. By means of the standard quantum oscillator eigensolutions $\xi_n \in \mathcal{H}_{\mathrm{f}}$, $n \in \mathbb{N}$ with a b–dependent mass, the correspondent eigenvalue equation has the form,

$$\begin{aligned} \boldsymbol{C}(b,\rho)\,\xi_n(b) &= E_n(b,\rho)\,\xi_n(b), \\ E_n(b,\rho) &= -\frac{\rho^2}{2m_{\mathrm{G}}} + \frac{1}{2} m_{\mathrm{G}} \omega_{\mathrm{G}}^2 b^2 + \omega_{\mathrm{KG}}\left(n + \frac{1}{2}\right) \end{aligned} \tag{30}$$

We emphasize that the b-dependence of the states is purely parametric which allows to define b-dependent projection operators on $\mathcal{H}_{\mathrm{f}}$,

$$\boldsymbol{\pi}_n(b) := \xi_n(b)\,\langle \xi_n(b), \cdot \rangle_{\mathcal{H}_{\mathrm{f}}}, \tag{31}$$

by means of which the Hamilton symbol constraint has the spectral representation,

$$\boldsymbol{C}(b,\rho) = \sum_{n \geq 0} E_n(b,\rho)\,\boldsymbol{\pi}_n(b). \tag{32}$$

In order to respect the conditions for the application of SAPT, it is possible to define an auxiliary Hamilton symbol $\boldsymbol{C}_{\mathrm{aux}}(b,\rho)$ which has values in the bounded operators, is locally a bounded function with respect to b, and which preserves the local structure of the symbol function $\boldsymbol{C}(b,\rho)$ (Panati et al., 2003; Stottmeister, 2015). Since the perturbation scheme is applicable without referring to this auxiliary symbol (if convergence and uniformity of the series expansion do not play a role for the time being), we continue working with the original symbol (32) to illustrate the scheme. Most importantly, the gap condition (C3) is satisfied since the energy functions $E_n(b,\rho)$ are gapped functions on the gravitational phase space. Finally, we formally choose one of the fast energy bands with quantum number $\nu \in \mathbb{N}$ to proceed with the space adiabatic scheme.

Application of Space Adiabatic Perturbation Theory

We start with the perturbative construction of the Moyal projector symbol $\boldsymbol{\pi}$ up to first order in ε. In fact, this will be sufficient to define the effective Hamilton constraint up to *second* order. With the ansatz, $\boldsymbol{\pi}_{(1)} = \boldsymbol{\pi}_0 + \varepsilon \boldsymbol{\pi}_1$, and the natural choice for the base clause,

$$\boldsymbol{\pi}_0 := \xi_\nu(b)\,\langle \xi_\nu(b), \cdot \rangle_{\mathcal{H}_{\mathrm{f}}}, \tag{33}$$

we construct the symbol function $\boldsymbol{\pi}_{(1)}(b,\rho)$ following the construction steps (S1). The first condition (S1–1), $\boldsymbol{\pi} \bigstar_\varepsilon \boldsymbol{\pi} = \boldsymbol{\pi}$, yields that the diagonal contribution to $\boldsymbol{\pi}_1$ vanishes because $\boldsymbol{\pi}_0(b)$ depends solely on b. Regarding the third condition (S1–3), $\boldsymbol{C}_0 \bigstar_\varepsilon \boldsymbol{\pi} - \boldsymbol{\pi} \bigstar_\varepsilon \boldsymbol{C}_0 = 0$, it is straightforward to derive (Teufel, 2003; Neuser et al., 2019), that,

$$\begin{aligned} \boldsymbol{\pi}_1 = &-\frac{i}{2}\,\boldsymbol{\pi}_0 \cdot \left\{ \boldsymbol{\pi}_0, \boldsymbol{C}_0 + E_\nu\, 1_{\mathrm{f}} \right\}_{\mathrm{s}} \cdot \left(\boldsymbol{C}_0^{\perp} - E_\nu\, 1_{\mathrm{f}} \right)^{-1} \cdot \boldsymbol{\pi}_0^{\perp} \\ &-\frac{i}{2} \left(\boldsymbol{C}_0^{\perp} - E_\nu\, 1_{\mathrm{f}} \right)^{-1} \cdot \boldsymbol{\pi}_0^{\perp} \cdot \left\{ \boldsymbol{C}_0 + E_\nu\, 1_{\mathrm{f}}, \boldsymbol{\pi}_0 \right\}_{\mathrm{s}} \cdot \boldsymbol{\pi}_0, \end{aligned} \tag{34}$$

as a determining equation for $\boldsymbol{\pi}_1$, where we defined, $\boldsymbol{C}_0^{\perp} = \boldsymbol{C}_0 \cdot \boldsymbol{\pi}_0^{\perp}$, and $\boldsymbol{\pi}_0^{\perp} := 1_{\mathrm{f}} - \boldsymbol{\pi}_0$. To evaluate the partial derivative $\partial_b \boldsymbol{\pi}_0$ in this equation, we need to evaluate the derivative of the states $\xi_n(b) \in \mathcal{H}_{\mathrm{f}}$ as well as the derivatives of the canonically defined creation and annihilation operators $\boldsymbol{a}^*(b) \in \mathcal{L}(\mathcal{H}_{\mathrm{f}})$ and $\boldsymbol{a}(b) \in \mathcal{L}(\mathcal{H}_{\mathrm{f}})$. Therefore, recall that the initial eigenvalue problem admits the oscillator solutions $\xi_n(b)$. Accordingly, the creation operator $\boldsymbol{a}^*(b)$ can be written in terms of the canonical pair $(\boldsymbol{\phi}_0, \boldsymbol{\mu}_0)$ as,

$$\boldsymbol{a}^*(b) = \sqrt{\frac{\tilde{m}_{\mathrm{KG}}(b)\omega_{\mathrm{KG}}}{2}} \left(\boldsymbol{\phi}_0 - \frac{i}{\tilde{m}_{\mathrm{KG}}(b)\omega_{\mathrm{KG}}} \boldsymbol{\mu}_0 \right), \tag{35}$$

The derivatives of the vacuum state $\xi_0(b)$ and the creation operator are given by,

$$\frac{\partial \xi_0}{\partial b} := \sqrt{2} f(b)\,\xi_2(b), \qquad \frac{\partial \boldsymbol{a}^*(b)}{\partial b} = -2 f(b)\,\boldsymbol{a}(b), \tag{36}$$

where $f(b) := -(\partial_b \tilde{m}_{\mathrm{KG}})/(4\tilde{m}_{\mathrm{KG}}) = -1/(2b)$. We propose the definition of a covariant derivative, or more precisely, a gauge potential $\mathcal{A}$, associated with the b–derivative of the fast oscillator states. Note that this is simply Berry's connection (Berry, 1984). Using the natural basis choice from above, its coefficients with respect to the b–direction on Γ_{s} are given by,

$$\frac{\partial \xi_n(b)}{\partial b} = \mathcal{A}_{bn}^{\;\;n-2}(b)\,\xi_{n-2}(b) + \mathcal{A}_{bn}^{\;\;n+2}(b)\,\xi_{n+2}(b), \tag{37}$$

with, $\mathcal{A}_{bm}^{k}(b) = -\sqrt{n(n-1)} f(b)\,\delta_n^{k+2} + \sqrt{(n+1)(n+2)} f(b)\,\delta_n^{k-2}$. All coefficients $\mathcal{A}_{\rho n}^{\;\;m}$ in the ρ–direction vanish because the fast eigenstates do not depend on ρ. Only the coefficients that connect states differing by two excitations in the b–direction are non-vanishing. Since we have real–valued eigenstates, the connection coefficients are real–valued, too, such that the orthonormality relation between the fast states yields that, $\mathcal{A}_{bn}^{\;\;m} = -\mathcal{A}_{bm}^{\;\;n}$. The b–derivative of the projector symbol $\boldsymbol{\pi}_0$ follows from using Riesz' representation theorem and one can simply write,

$$\frac{\partial \boldsymbol{\pi}_0}{\partial b} = \mathcal{A}_{b\nu}^{\;\;m} \left(\xi_\nu \langle \xi_m, \cdot \rangle_{\mathrm{f}} + \xi_m \langle \xi_\nu, \cdot \rangle_{\mathrm{f}} \right), \tag{38}$$

where ν is still a fixed quantum number while m runs over all natural numbers. To evaluate $\boldsymbol{\pi}_1$, the partial derivative,

$\partial_\rho\,(\boldsymbol{C}_0 + E_\nu \cdot 1_\mathrm{f})$, is simply $(-2\rho/m_\mathrm{G}) \cdot 1_\mathrm{f}$, because only the spectral functions $E_n(b,\rho)$ depend on ρ while the states do not. The functional form of the energy functions also reduces $(\boldsymbol{C}_0^{\perp} - E_\nu \cdot 1_\mathrm{f})$ to a factor $\pm\,(2\omega_\mathrm{KG})^{-1}$, and consequently,

$$\boldsymbol{\pi}_1 = -\frac{i\rho}{2m_\mathrm{G}\omega_\mathrm{KG}}\Big(\mathcal{A}_{b\nu}^{\nu-2}\big(\xi_\nu\langle\xi_{\nu-2},\cdot\rangle_\mathrm{f} - \xi_{\nu-2}\langle\xi_\nu,\cdot\rangle_\mathrm{f}\big) + \mathcal{A}_{b\nu}^{\nu+2}\big(\xi_{\nu+2}\langle\xi_\nu,\cdot\rangle_\mathrm{f} - \xi_\nu\langle\xi_{\nu+2},\cdot\rangle_\mathrm{f}\big)\Big). \quad (39)$$

One can easily check that $\boldsymbol{\pi}_{(1)}$ satisfies all three conditions subsumed under (S1) up to first order in ε, i.e., that it is a projector and commutes with the full Hamilton symbol up to errors of order ε^2. We see that the improved projection symbol mixes adjacent eigenstates of the fast system, and going to higher orders in the perturbative scheme more and more states will be included.

The next step of SAPT consists in constructing the unitary symbol $\boldsymbol{u}_1$ which maps the dynamical subspace related to $\boldsymbol{\pi}_{(1)}$, to a suitable reference subspace $\mathcal{K}_\mathrm{f} \subset \mathcal{H}_\mathrm{f}$. It is convenient to choose one point $(b_0,\rho_0) \in \Gamma_\mathrm{s}$ and define the reference projection as,

$$\boldsymbol{\pi}_\mathrm{R} := \xi_\nu(b_0)\langle\xi_\nu(b_0),\cdot\rangle_\mathrm{f} =: \zeta_\nu\langle\zeta_\nu,\cdot\rangle_\mathrm{f}, \quad (40)$$

where $\zeta_\nu \in \mathcal{H}_\mathrm{f}$ does not depend on the gravitational phase space variables. In a similar fashion, one can define the complete basis $\zeta_n := \xi_n(b_0)$, $n \in \mathbb{N}$ at the point b_0. A natural choice for the unitary operator in line with conditions (S2) at zeroth order is simply,

$$\boldsymbol{u}_0(b) = \sum_{n\geq 0}\zeta_n\langle\xi_n(b),\cdot\rangle_\mathrm{f}. \quad (41)$$

In order to construct $\boldsymbol{u}_1$, the scheme splits the symbol into a hermitian and an antihermitian part. The hermitian part is determined by Eqs. S2-1 and S2-2, namely by requiring that $\boldsymbol{u}\bigstar\boldsymbol{u}^\star = 1_\mathrm{f}$ holds up to first order in ε. Since $\boldsymbol{u}_0$ only depends on the configuration variable b, the hermitian part vanishes trivially. The antihermitian part is determined by restricting **equation (S2S–equation (S3)**, i.e., $\boldsymbol{u}\bigstar\boldsymbol{\pi}\bigstar\boldsymbol{u}^\star = \boldsymbol{\pi}_\mathrm{R}$, to the first order. It yields for $\boldsymbol{u}_1$ (Neuser et al., 2019),

$$\begin{aligned}\boldsymbol{u}_1 &= \big[\boldsymbol{\pi}_\mathrm{R}, \boldsymbol{u}_0\cdot\boldsymbol{\pi}_1^{\mathrm{OD}}\cdot\boldsymbol{u}_0^*\big]_\mathrm{f}\cdot\boldsymbol{u}_0 \\ &= \frac{i\rho}{2\,m_\mathrm{G}\,\omega_\mathrm{KG}}\big[\mathcal{A}_{b\nu}^{\nu-2}\big(\zeta_\nu\langle\xi_{\nu-2},\cdot\rangle_\mathrm{f} + \zeta_{\nu-2}\langle\xi_\nu,\cdot\rangle_\mathrm{f}\big) - \mathcal{A}_{b\nu}^{\nu+2}\big(\zeta_{\nu+2}\langle\xi_\nu,\cdot\rangle_\mathrm{f} + \zeta_\nu\langle\xi_{\nu+2},\cdot\rangle_\mathrm{f}\big)\big]. \quad (42)\end{aligned}$$

Eventually, we are ready to compute the effective Hamiltonian symbol up to second order in the perturbations, and which we restrict to the selected reference space, i.e., we compute, $\boldsymbol{C}_{\mathrm{eff},(2),\mathrm{R}}(b,\rho) := \boldsymbol{\pi}_\mathrm{R}\cdot\boldsymbol{C}_{\mathrm{eff},(2)}(b,\rho)\cdot\boldsymbol{\pi}_\mathrm{R}$. The zeroth order contribution of this symbol is given according to condition (S3) by,

$$\boldsymbol{C}_{\mathrm{eff},0,\mathrm{R}}(b,\rho) = \left(-\frac{\rho^2}{2m_\mathrm{G}} + \frac{1}{2}m_\mathrm{G}\omega_\mathrm{G}^2 b^2 + \omega_\mathrm{KG}\left(\nu+\frac{1}{2}\right)\right)\boldsymbol{\pi}_\mathrm{R}. \quad (43)$$

Thus, the effective constraint symbol for the gravitational degrees of freedom includes the bare gravitational constraint symbol plus an off–set energy which stems from the energy band associated with the quantum number ν of the Klein–Gordon system. This result corresponds to the Born–Oppenheimer approximation. The first order contribution of the effective constraint symbol, $\boldsymbol{C}_{\mathrm{eff},1}(b,\rho)$ contains only off-diagonal terms, such that $\boldsymbol{C}_{\mathrm{eff},1,\mathrm{R}}(b,\rho)$ vanishes identically,

$$\boldsymbol{C}_{\mathrm{eff},1,\mathrm{R}}(b,\rho) = \frac{i}{2}\big\{\boldsymbol{\pi}_\mathrm{R}\cdot\boldsymbol{u}_0, \boldsymbol{C}_0 + E_\nu\,1_\mathrm{f}\big\}_\mathrm{s}\cdot\boldsymbol{u}_0^*\cdot\boldsymbol{\pi}_\mathrm{R} = 0. \quad (44)$$

The same reasoning applies to the computation of the second order contribution $\boldsymbol{C}_{\mathrm{eff},2,\mathrm{R}}(b,\rho)$ giving,

$$\begin{aligned}\boldsymbol{C}_{\mathrm{eff},2,\mathrm{R}} &= \frac{i}{2}\big\{\boldsymbol{\pi}_\mathrm{R}\cdot\boldsymbol{u}_1, \boldsymbol{C}_0 + E_\nu\,1_\mathrm{f}\big\}_\mathrm{s}\cdot\boldsymbol{u}_0\cdot\boldsymbol{\pi}_\mathrm{R} \\ &= \left[\frac{\partial E_n}{\partial\rho}\right]^2\left[\frac{\left(\mathcal{A}_{b\nu}^{\nu-2}\right)^2}{E_\nu - E_{\nu-2}} + \frac{\left(\mathcal{A}_{b\nu}^{\nu+2}\right)^2}{E_\nu - E_{\nu+2}}\right]\boldsymbol{\pi}_\mathrm{R} + \frac{1}{2}\frac{\partial^2 E_n}{\partial\rho^2}\left[\left(\mathcal{A}_{b\nu}^{\nu-2}\right)^2 + \left(\mathcal{A}_{b\nu}^{\nu+2}\right)^2\right]\boldsymbol{\pi}_\mathrm{R}. \quad (45)\end{aligned}$$

Finally, inserting the explicit results for the energy functions and the connection coefficients yields,

$$\boldsymbol{C}_{\mathrm{eff},2,\mathrm{R}}(b,\rho) = -\frac{1}{2\,m_\mathrm{G}}\left(\frac{\rho^2}{m_\mathrm{G}\omega_\mathrm{KG}b^2}\left(\nu+\frac{1}{2}\right) + \frac{1}{2b^2}\left(\nu^2+\nu+1\right)\right)\boldsymbol{\pi}_\mathrm{R}. \quad (46)$$

This proves our statement that besides the trivial Born–Oppenheimer approximation, further backreaction effects arise for the gravitational subsystem. It is now easy to evaluate the action of this symbol on some generic tensor product wave function in $\mathcal{H} = \mathcal{H}_\mathrm{s}\otimes\mathcal{H}_\mathrm{f}$, since the Klein–Gordon tensor factor does not depend on the gravitational degrees of freedom anymore. The problem reduces to a quantum constraint equation on $\mathcal{H}_\mathrm{s}$ only, and can be studied for each ν of interest. Nevertheless, we point out that finding states that are annihilated by the constraint operator $\widehat{\boldsymbol{C}}_{\mathrm{eff},2,\mathrm{R}}$ is not a trivial task as it depends non-polynomially on b. Further details can be found in (Neuser et al., 2019). Finally, the question is how the solutions of **(46)** relate to the solutions of the original problem on $\mathcal{H}$. In fact, one needs to rotate the solutions of $\widehat{\boldsymbol{C}}_{\mathrm{eff},2,\mathrm{R}}$ back to the original Hilbert space using the quantization of the Moyal unitary. It turns out that the resulting solutions are also approximate (orthogonal) solutions to the full Hamilton constraint at the respective perturbative order (Teufel, 2003; Schander and Thiemann, 2019a).

5.3 Backreaction in Inhomogeneous Quantum Cosmology

The purely homogeneous model in the previous section can serve as a showcase for a more realistic inhomogeneous cosmological model. Here, we consider standard cosmological perturbation theory for a gravitational metric field g, a massive real scalar field Φ as the matter content, and a cosmological constant, $\Lambda > 0$. After the split of the relevant degrees of freedom into a homogeneous and an inhomogeneous part, the aim will be to incorporate backreactions from the perturbative degrees of freedom onto the homogeneous and isotropic background degrees of freedom.

As before, the model rests on a four-dimensional globally hyperbolic space time manifold $\mathcal{M}$ that admits the time space split $\mathcal{M} \cong \mathbb{R}\times\sigma$. The metric has Lorentzian signature $(-,+,+,+)$, and the spatial hypersurfaces σ are compact and

flat three-tori $\sigma \cong \mathbb{T}^3$ with side lenghts $l \equiv 1$. The global time parameter $t \in \mathbb{R}$ labels the spatial Cauchy surfaces Σ_t. n^μ is the unit normal vector field to these hypersurfaces, N and N_μ the (standard) lapse and shift functions which parametrize the normal and the tangential part of the foliation. The task of specifying constraints or equations of motion for the metric field g, translates into defining a Cauchy initial value problem for the spatial metric $h_{\mu\nu} = g_{\mu\nu} + n_\mu n_\nu$ induced by g. The extrinsic curvature associated with the time derivative of h is given by $K_{\mu\nu} = h^\rho_\mu h^\lambda_\nu \nabla_\rho n_\lambda$. ∇ is the unique, torsion–free covariant derivative associated with the metric g. After pulling back the tensor fields to $\mathbb{R} \times \mathbb{T}^3$ and denoting spatial indices on the spatial hypersurfaces with lower case latin symbols, $a, b, c, \ldots \in \{1, 2, 3\}$, the Lagrange density is expressed by the sum of the Einstein–Hilbert Lagrange density $\mathcal{L}_{\mathrm{EH}}$ and the scalar field Lagrange density $\mathcal{L}_\Phi$, with,

$$\mathcal{L}_{\mathrm{EH}} = \frac{1}{2\kappa}\sqrt{|h|}N\left(R^{(3)} + K_{ab}K^{ab} - \left(K^a_a\right)^2 - 2\Lambda\right), \tag{47}$$

$$\mathcal{L}_\Phi = \frac{1}{2\lambda}\sqrt{|h|}N\left(-\frac{1}{N^2}\dot{\Phi}^2 + 2\frac{N^a}{N^2}\dot{\Phi}\partial_a\Phi + \left(h^{ab} - \frac{N^aN^b}{N^2}\right)\partial_a\Phi\partial_b\Phi + m^2_\Phi\Phi^2\right). \tag{48}$$

where again, λ is the coupling constant of the scalar field, m_Φ is the mass parameter of the scalar field, and $R^{(3)}$ is the curvature scalar associated with the three–metric h and its Levi–Civita covariant derivative, D. The only degrees of freedom of the spatially homogeneous and isotropic sector are the zeroth order lapse function $N_0(t)$ and the scale factor $a(t)$, associated with the zeroth order spatial metric, ${}^0h(t,x) := a^2(t)\,{}^0\tilde{h}(x)$ with ${}^0\tilde{h}(x)$ being the time-independent metric on the spatial hypersurfaces. A Hamiltonian analysis shows that the lapse function is a Lagrange multiplier with no dynamical features, affirming the arbitrariness of the hypersurface foliation.

We introduce perturbations of the homogeneous degrees of freedom using a decomposition into scalar, vector and tensor parts (Halliwell and Hawking, 1985). Since we make use of their results in a later stage, we will stick to the definition of perturbations used by Castelló Gomar et al. (2015) and Martínez and Olmedo (2016),

$$N(t,x) =: N_0(t) + a^3(t)\,g(t,x) \tag{49}$$

$$N_a(t,x) =: a^2(t)\,D_a\,k(t,x) + a^2(t)\,\epsilon_a^{bc}D_b\,k_c(t,x) \tag{50}$$

$$h_{ab}(t,x) =: a^2(t)\Big[(1+2\alpha(t,x))\,{}^0\tilde{h}_{ab}(x) + 6\left(D_aD_b - \frac{1}{3}\,{}^0\tilde{h}_{ab}(x)D_cD^c\right)\beta(t,x) + 2\sqrt{6}t_{ab}(t,x) + 4\sqrt{3}D_{(a}v_{b)}(t,x)\Big], \tag{51}$$

$$\Phi(t,x) =: \phi(t) + \varphi(t,x). \tag{52}$$

where we introduced the perturbative scalar fields $(g, k, \alpha, \beta, \varphi)$, the vector fields v_a and k_a, and the tensor field perturbations t_{ab}. For notational reasons, we introduce the fields $\check{k} := \Delta k$ and $\check{k}_a := \epsilon_a^{bc}D_bk_c$ as new degrees of freedom associated with the shift.

We perform a Legendre transformation to obtain the Hamilton constraint. We insert the perturbed variables from **Eqs. 49–(52)** into the Lagrange density **(47)**, **(48)**, and expand the Lagrangian and the action functional S up to second order in the perturbations. As the three-torus does not have a boundary, total divergences vanish in the computations. The resulting action does neither depend on the velocities of the lapse variables N_0 and g, nor on the velocities of the shift variables $\check{k}$ and $\check{k}_a$. These Lagrange multipliers will hence be associated with primary constraint equations in the Hamiltonian formalism. In the lines of (Castelló Gomar et al., 2015), we define the conjugate momenta (P_a, P_ϕ) for the homogeneous and isotropic degrees of freedom (a, ϕ) using the Lagrange function $L = \int \mathrm{d}x\,\mathcal{L}$,

$$P_a := \frac{\partial L}{\partial \dot{a}} = -\frac{6}{\kappa N}a\dot{a}, \qquad P_\phi := \frac{\partial L}{\partial \dot{\phi}} = \frac{a^3}{\lambda N}\dot{\phi}. \tag{53}$$

We denote the corresponding phase space by $\Gamma_{\mathrm{hom}} = \Gamma_{\mathrm{s}}$. The perturbation fields $(\alpha, \beta, \varphi, \vartheta_a, t_{ab})$ together with their conjugate momenta $(\pi_\alpha, \pi_\beta, \pi_\varphi, \pi^a_v, \pi^{ab}_t)$ span the perturbative phase space $\Gamma_{\mathrm{pert}} = \Gamma_{\mathrm{f}}$. The momenta are defined as,

$$\pi_\chi := \frac{\partial \mathcal{L}}{\partial \dot{\chi}}, \tag{54}$$

for any field $\chi \in \{\alpha, \beta, \varphi, v_a, t_{ab}\}$. N_0, g, $\check{k}$ and $\check{k}_a$ induce the lapse and shift primary constraints $\Pi_0^{N_0}$, Π_1^g, $\Pi_1^{\check{k}}$ and $\Pi_1^{\check{k}_a,b}$. The Hamiltonian density is eventually given by,

$$\mathcal{H} = N_0\left[\mathcal{H}_0 + \mathcal{H}_2^{\mathrm{s}} + \mathcal{H}_2^v + \mathcal{H}_2^t\right] + g\cdot\mathcal{H}_1^g + \check{k}_a\cdot\mathcal{H}_1^{\check{k}_d,a} + \check{k}\cdot\mathcal{H}_1^{\check{k}} + \lambda_{N_0}\cdot\Pi_0^{N_0} + \lambda_g\cdot\Pi_1^g + \lambda_{\check{k}}\cdot\Pi_1^{\check{k}} + \lambda_{\check{k}_a,b}\cdot\Pi_1^{\check{k}_a,b}. \tag{55}$$

$\mathcal{H}_0$ denotes the Hamiltonian contribution associated with the completely homogeneous and isotropic model. $\mathcal{H}_2^{\mathrm{s}}$, $\mathcal{H}_2^v$ and $\mathcal{H}_2^t$ are of second order in the perturbations and contain only scalar, vector and tensor variables respectively. $\mathcal{H}_1^g$, $\mathcal{H}_1^{\check{k}_d,a}$ and $\mathcal{H}_1^{\check{k}}$ represent first order contributions which factorize with the respective lapse and shift variables. The second line lists the primary constraints associated with lapse and shift and their Lagrange multipliers λ_{N_0}, λ_g, $\lambda_{\check{k}}$ and $\lambda_{\check{k}_a,b}$. The system is completely constrained and we thus perform a Dirac analysis to extract the relevant physics.

Therefore, we identify a suitable set of free variables–in fact, the Dirac analysis will then become a trivial task. We start by noting that the perturbation variables that we introduced are not all gauge–invariant. In the scalar sector, let us employ the gauge–invariant Mukhanov-Sasaki variable ϑ (Mukhanov, 1988, 2005),

$$\vartheta := a\,\varphi + \frac{6\lambda P_\phi}{\kappa P_a}\left(\alpha - \Delta\beta\right) \tag{56}$$

Note that this transformation for the perturbative fields also depends on the homogeneous degrees of freedom. While the original perturbation variables had canonical momenta properly defined by the Legendre transform, the new perturbation variables will break the canonical structure as

they non-trivially depend on the homogeneous degrees of freedom. In order to preserve the canonical structure of the system, it is mandatory to find a suitable transformation for the homogeneous and isotropic variables, too. This appears to be a cumbersome mission. Castelló Gomar et al. (2015) have however shown that it is possible to find a transformation for the homogeneous and isotropic degrees of freedom which preserves the canonical structure of the system up to second order in the cosmological scalar perturbations. The same has been done by Martínez and Olmedo (2016) for the tensor degrees of freedom.

These transformations and the resulting almost–canonical variables in the homogeneous and the perturbative sector lead to a redefinition of the Hamilton constraint. Fortunately, these transformations make the Dirac constraint analysis almost trivial. The secondary constraints that one obtains from requiring the conservation of the primary constraints under the evolution of the Hamiltonian, generate only one single, non-trivial constraint, namely,

$$\mathcal{C} := \mathcal{H}_0 + \tilde{\mathcal{H}}_2^s + \check{\mathcal{H}}_2^t = 0, \tag{57}$$

where $\mathcal{H}_0$ now depends on the transformed homogeneous variables, and $\tilde{\mathcal{H}}_2^s$ and $\check{\mathcal{H}}_2^t$ are second order constraints that depend on the Mukhanov–Sasaki and the tensor perturbations respectively, as well as on the transformed homogeneous variables. Before we give the corresponding expressions, let us perform the typical ε-rescalings of the momenta that will make the space adiabatic scheme work at the technical level. We will simply denote the transformed variables by the original ones, and write,

$$p_a := \varepsilon^2 P_a, \qquad p_\phi := \varepsilon P_\phi. \tag{58}$$

Besides, we perform a canonical rescaling of the inhomogeneous Mukhanov–Sasaki and tensor perturbations, and multiply the constraint by a global ε^2–factor. Then, the total Hamilton constraint, $C = H_0 + \tilde{H}_2^s + \check{H}_2^t = 0$, is given by (Schander and Thiemann, 2019c),

$$H_0 = -\frac{p_a^2}{12a} + \frac{p_\phi^2}{2a^3} + \frac{1}{2}\varepsilon^2 m_\Phi^2 a^3 \phi^2 + \Lambda a^3, \tag{59}$$

$$\tilde{H}_2^s = \frac{1}{2a}\int_{\mathbb{T}^3} \mathrm{d}x \left[\frac{\pi_\vartheta^2}{\sqrt{{}^0\tilde{h}}} + \vartheta\,\varepsilon^4\left[-\sqrt{{}^0\tilde{h}}\,\Delta + m_{\mathrm{MS}}^2\right]\vartheta\right], \tag{60}$$

$$\check{H}_2^t = \frac{1}{2a}\int_{\mathbb{T}^3} \mathrm{d}x \left[\frac{\pi_t^{ab}\pi_{t,ab}}{6\sqrt{{}^0\tilde{h}}} + t^{ab}\varepsilon^4\left[-3\sqrt{{}^0\tilde{h}}\,\Delta + (\varepsilon\, m_{\mathrm{T}})^2\right]t_{ab}\right], \tag{61}$$

with the effective Mukhanov–Sasaki and tensor masses depending on the homogeneous variables,

$$m_{\mathrm{MS}}^2 = \left(-\frac{p_a^2}{18a^2} + \frac{7p_\phi^2}{2a^4} - 12\varepsilon\sqrt{{}^0\tilde{h}}^2\, m_\Phi^2 \frac{a\phi p_\phi}{p_a} - 18\frac{p_\phi^4}{a^6 p_a^2} + \sqrt{{}^0\tilde{h}}^2\, m_\Phi^2 a^2\right)\frac{1}{\sqrt{{}^0\tilde{h}}}, \tag{62}$$

$$(\varepsilon\, m_{\mathrm{T}})^2 = \left(\frac{p_a^2}{6a^2} - 3\varepsilon^2\sqrt{{}^0\tilde{h}}^2\, m_\Phi^2 a^2\phi^2 - 6\sqrt{{}^0\tilde{h}}^2\,\Lambda a^2\right)\frac{1}{\sqrt{{}^0\tilde{h}}}. \tag{63}$$

Now, SAPT requires to quantize the cosmological perturbations. The form of $\tilde{H}_2^s$ and $\check{H}_2^t$ suggests to consider a standard Fock quantization for the Mukhanov–Sasaki and the tensor fields. The quantized fields should satisfy the commutation relations,

$$\begin{aligned}[g(\vartheta), \boldsymbol{\pi}_\vartheta(f)]_{\mathrm{MS}} &= i\int_{\mathbb{T}^3} \mathrm{d}x\, g(x) f(x)\, 1_{\mathrm{MS}},\ [G(\boldsymbol{t}), \boldsymbol{\pi}_t(F)]_{\mathrm{T}} \\ &= i\int_{\mathbb{T}^3} \mathrm{d}x\, G^{ab}(x) F_{ab}(x)\, 1_{\mathrm{T}},\end{aligned}$$

for suitable test functions f, g, G^{ab} and F_{ab} on the three–torus, where 1_{MS} and 1_{T} denote the unities of the quantum algebras. As a basis for the one–particle Hilbert space $L^2(\mathbb{T}^3, \mathrm{d}x)$ it is convenient to choose the plane waves $f_{\overrightarrow{k}}(\overrightarrow{x}) = \exp(i\overrightarrow{k}\overrightarrow{x})$, with $\overrightarrow{k} \in 2\pi\mathbb{Z}$ 0 being discrete. The total perturbative Hilbert space is the tensor product of the correspondent Fock spaces,

$$\mathcal{H}_{\mathrm{f}} = \mathcal{F}_{\mathrm{s,MS}}\left(L^2\left(\mathbb{T}^3, \mathrm{d}x\right)\right) \underset{\tau=\{+,-\}}{\otimes} \mathcal{F}_{\mathrm{s,T},\tau}\left(L^2\left(\mathbb{T}^3, \mathrm{d}x\right)\right), \tag{64}$$

where the index "s" refers to symmetric, and we introduced the label τ which stands for the only two physical degrees of freedom associated with the tensor perturbations (namely their polarizations). The form of the second order contributions to the Hamilton constraint suggest to define the one–particle frequency operators for the Mukhanov–Sasaki and the tensor systems,

$$\omega_{\mathrm{MS}} := \varepsilon^2\sqrt{-\Delta + m_{\mathrm{MS}}^2}, \qquad \omega_{\mathrm{T}} := \varepsilon^2\sqrt{-18\Delta + 6\,(\varepsilon\, m_{\mathrm{T}})^2}. \tag{65}$$

Note that both operators depend on the homogeneous degrees of freedom as they contain the mass functions $m_{\mathrm{MS}}(a, p_a, \phi, p_\phi)$ and $m_{\mathrm{T}}(a, p_a, \phi)$. This implies that the annihilation and creation operators $\boldsymbol{a}(f_{\overrightarrow{k}}) =: \boldsymbol{a}_{\overrightarrow{k}}$, $\boldsymbol{a}^*(f_{\overrightarrow{k}}) =: \boldsymbol{a}^*_{\overrightarrow{k}}$ of the Mukhanov–Sasaki system and the annilation and creation operators of the tensor perturbations $\boldsymbol{b}_\pm(f_{\overrightarrow{k}}) = \boldsymbol{b}_{\overrightarrow{k},\pm}$, $\boldsymbol{b}^*_\pm(f_{\overrightarrow{k}}) = \boldsymbol{b}^*_{\overrightarrow{k},\pm}$, defined in the standard way, depend on the homogeneous degrees of freedom, and so do the natural Fock basis states (Schander and Thiemann, 2019c). In contrast to the cosmological toy model, they depend on the whole set of phase space variables, which represent non-commuting operators in the quantum theory, and which makes the application of SAPT mandatory. The Born–Oppenheimer approach would fail in the given case.

It is most convenient to express the quantum constraint symbol $\boldsymbol{C}(a, p_a, \phi, p_\phi)$ in terms of normal–ordered annihilation and creation operators,

$$\begin{aligned}\boldsymbol{C} = &\left(-\frac{p_a^2}{12a} + \frac{p_\phi^2}{2a^3} + \frac{1}{2}\,\varepsilon^2\, m_\Phi^2 a^3\,\phi^2 + \Lambda\, a^3\right)1_{\mathrm{f}} \\ &+ \frac{1}{a}\sum_{\overrightarrow{k}\in\mathbb{K}} \omega_{\mathrm{MS},\overrightarrow{k}}\, \boldsymbol{a}^*_{\overrightarrow{k}}\, \boldsymbol{a}_{\overrightarrow{k}} + \frac{1}{6a}\sum_{\overrightarrow{K}\in\mathbb{K}} \omega_{\mathrm{T},\overrightarrow{k}}\, \boldsymbol{b}^*_{\overrightarrow{K}}\, \boldsymbol{b}_{\overrightarrow{K}},\end{aligned} \tag{66}$$

where we identify the first contribution as the usual FLRW Hamilton constraint, which we will denote by $E_{\mathrm{hom}}(a, p_a, \phi, p_\phi)$. The label $\overrightarrow{K} := (\overrightarrow{k}, \tau) \in \mathbb{K}$ specifies the mode and the polarization of the tensor perturbations. $\boldsymbol{C}$ admits a discrete spectrum for any point $(a, p_a, \phi, p_\phi) \in \Gamma_{\mathrm{s}}$

because the sums over the wave vectors in the Hamilton constraint are discrete and so is the spectrum of the number operators $\boldsymbol{a}^{\star}_{\overrightarrow{k}}\boldsymbol{a}_{\overrightarrow{k}}$ and $\boldsymbol{b}^{\star}_{\overrightarrow{K}}\boldsymbol{b}_{\overrightarrow{K}}$. Any Fock state $\xi_{(n)} \in \mathcal{H}_{\mathrm{f}}$ with finite energy can be identified with a finite set of non-vanishing quantum numbers $(n) := \{\ldots, n_{\mathrm{MS},\overrightarrow{k}_1}, n_{\mathrm{MS},\overrightarrow{k}_2}, \ldots, n_{\mathrm{T},\tau,\overrightarrow{k}_1}, n_{\mathrm{T},\tau,\overrightarrow{k}_2}, \ldots\}$, where we distinguished between the quantum numbers of the Mukhanov–Sasaki and the tensor perturbations. We introduce degeneracy labels which take the possibility of degenerate eigenstates into account, and we denote them by $b = 1, \ldots, d$ for the Mukhanov–Sasaki system and $b' = 1, \ldots, d'$ for the graviton system. To shorten notation, we integrate the degeneracy labels in $\beta := \{b, b'\}$ and the degeneracy numbers in $\delta := \{d, d'\}$. We write for the set of homogeneous variables, $(q, p) := (a, p_a, \phi, p_\phi)$. The eigenvalue problem for any finite set of quantum numbers $(n)_\beta$ then has the form,

$$\boldsymbol{C}(q,p)\,\xi_{(n)_\beta}(q,p) = E_n(q,p)\,\xi_{(n)_\beta}(q,p), \tag{67}$$

$$E_n(q,p) := E_{\mathrm{hom}}\Big(a, p_a, \phi, p_\phi\Big) + \frac{1}{a}\sum_{\overrightarrow{k}\in\mathbb{K}} n_{\mathrm{MS},\overrightarrow{k},b}\,\omega_{\mathrm{MS},\overrightarrow{k}} + \frac{1}{6a}\sum_{\overrightarrow{K}\in\mathbb{K}} n_{\mathrm{T},\overrightarrow{K},b'}\,\omega_{\mathrm{T},\overrightarrow{K}}.$$

Due to the discreteness of the eigenbasis, it is possible to define non–vanishing energy gaps between the eigenenergy bands of the perturbations, at least for local regions in phase space. In the following, we assume that the relevant energy bands admit such local gaps in the region of interest.

To examine the derivatives of the eigenstates with respect to the homogeneous variables, we need the derivative of the vacuum state and the annihilation operators since any excited state in the Hilbert space $\mathcal{H}_{\mathrm{f}}$ can be constructed from the vacuum state $\Omega(q,p)$ by applying the desired number $(n_{\mathrm{MS},\overrightarrow{k}}, n_{\mathrm{T},\overrightarrow{k},+}, n_{\mathrm{T},\overrightarrow{k},-})$ of creation operators for every wave number $\overrightarrow{k}$. We formally choose one such eigenstate with quantum number(s) $(\nu)_\beta$ given by,

$$\xi_{(\nu)}(q,p) = \prod_{\overrightarrow{K}\in\mathbb{K}} \frac{\left(\boldsymbol{a}^{\star}_{\overrightarrow{k}}\right)^{\nu_{\mathrm{MS},\overrightarrow{k}}}}{\sqrt{\nu_{\mathrm{MS},\overrightarrow{k}}!}} \frac{\left(\boldsymbol{b}^{\star}_{\overrightarrow{K}}\right)^{\nu_{\mathrm{T},\overrightarrow{K}}}}{\sqrt{\nu_{\mathrm{T},\overrightarrow{K}}!}}\,\Omega(q,p) \tag{68}$$

It is useful to write the explicit representation of the Mukhanov–Sasaki wave function and the tensor wave functions as a product,

$$\xi_{(\nu)} =: \xi^{\mathrm{MS}}_{(\nu_{\mathrm{MS}})} \cdot \prod_{\tau} \xi^{\mathrm{T},\tau}_{(\nu_{\mathrm{T}})}. \tag{69}$$

The derivatives of the annihilation operators with respect to $\lambda \in \{q, p\}$, are proportional to the correspondent creation operators,

$$\begin{aligned} \frac{\partial \boldsymbol{a}_{\overrightarrow{k}}(q,p)}{\partial\lambda} &:= f^{\mathrm{MS}}_{\lambda,\overrightarrow{k}}(q,p)\,\boldsymbol{a}^{\star}_{\overrightarrow{k}}(q,p), \\ \frac{\partial \boldsymbol{b}_{\overrightarrow{K}}(q,p)}{\partial\lambda} &:= f^{\mathrm{T}}_{\lambda,\overrightarrow{K}}(q,p)\,\boldsymbol{b}^{\star}_{\overrightarrow{K}}(q,p), \end{aligned} \tag{70}$$

and the explicit expressions of the factors can be found in (Schander and Thiemann, 2019c). The λ-derivative of the vacuum state is then given by,

$$\frac{\partial\Omega(q,p)}{\partial\lambda} = \sum_{\overrightarrow{k}\in\mathbb{K}} f^{\mathrm{MS}}_{\lambda,\overrightarrow{k}}(q,p)\Big(\boldsymbol{a}^{\star}_{\overrightarrow{k}}\,\boldsymbol{a}^{\star}_{\overrightarrow{k}}\,\Omega\Big)(q,p) + \sum_{\overrightarrow{K}\in\mathbb{K}} f^{\mathrm{T}}_{\lambda,\overrightarrow{k}}(q,p)\Big(\boldsymbol{b}^{\star}_{\overrightarrow{K}}\,\boldsymbol{b}^{\star}_{\overrightarrow{K}}\,\Omega\Big)(q,p). \tag{71}$$

The λ-derivative of any excited state $\xi_{(n)}$ is thus uniquely defined by these results and can be expressed as an application of a connection $\mathcal{A}_\lambda \in C^\infty(\Gamma_{\mathrm{s}}, \mathcal{L}(\mathcal{H}_{\mathrm{f}}))$, on the global Hilbert bundle H,

$$\begin{aligned} \frac{\partial\xi_{(n)}(q,p)}{\partial\lambda} &=: \mathcal{A}_\lambda\xi_{(n)} =: \mathcal{A}^{(m)}_{\lambda(n)}\xi_{(m)}, \\ \mathcal{A}^{(m)}_{\lambda(n)}(q,p) &\in C^\infty(\Gamma_{\mathrm{s}}, \mathbb{R}) \qquad \forall (n), (m), \end{aligned} \tag{72}$$

where the summation over (m) includes essentially *all* possible excitation numbers within the Fock space $\mathcal{H}_{\mathrm{f}}$. However, there is only a countable number of (m)'s for which $\mathcal{A}^{(m)}_{\lambda(n)}$ is non-vanishing if (n) is a finite set of non-vanishing excitation numbers. For more details and the explicit calculations, we refer to (Schander and Thiemann, 2019c).

Application of a Space Adiabatic Perturbation Scheme

The construction of the space adiabatic symbols is subject to two different perturbative scalings: ε for the homogeneous scalar field, and ε^2 for the homogeneous gravitational degrees of freedom. The Moyal product for two operator–valued functions $\boldsymbol{f}(q,p) \in S^{m_1}_\rho(\Gamma_{\mathrm{s}}, \mathcal{B}(\mathcal{H}_{\mathrm{f}}))$, $\boldsymbol{g}(q,p) \in S^{m_2}_\rho(\Gamma_{\mathrm{s}}, \mathcal{B}(\mathcal{H}_{\mathrm{f}}))$ has the form,

$$(\boldsymbol{f}\star_\varepsilon\boldsymbol{g})(q,p) \asymp \left[\boldsymbol{f}\exp\left(\frac{i\varepsilon}{2}\left(\overleftarrow{\partial}_\phi\overrightarrow{\partial}_{p_\phi} - \overleftarrow{\partial}_{p_\phi}\overrightarrow{\partial}_\phi\right)\right.\right. - \left.\left.\frac{i\varepsilon^2}{2}\left(\overleftarrow{\partial}_a\overrightarrow{\partial}_{p_a} - \overleftarrow{\partial}_{p_a}\overrightarrow{\partial}_a\right)\right)\boldsymbol{g}\right](q,p) \in S^{m_1+m_2}_\rho\Big(\Gamma_{\mathrm{s}}, \mathcal{B}\Big(\mathcal{H}_{\mathrm{f}}\Big)\Big) \tag{73}$$

As it turns out, the Moyal product with respect to the gravitational degrees of freedom does not contribute to the computations up to second order in the perturbation scheme.

As before, the discrete eigenstate $\xi_{(\nu)_\beta}(q,p) \in \mathcal{H}_{\mathrm{f}}$ with quantum number $(\nu)_\beta$ serves to define the zeroth order Moyal projector symbol,

$$\boldsymbol{\pi}_0(q,p) := \sum_\beta \xi_{(\nu)_\beta}(q,p)\,\langle\xi_{(\nu)_\beta}(q,p), \cdot\,\rangle_{\mathrm{f}}. \tag{74}$$

The only relevant contribution to $\boldsymbol{\pi}_1$ comes from (S1–3). This off–diagonal part $\boldsymbol{\pi}^{\mathrm{OD}}_1$ mixes the adjacent inhomogeneous eigenstates according to,

$$\boldsymbol{\pi}^{\mathrm{OD}}_1 = \frac{i}{2}\sum_{\beta=1}^{\delta}\sum_{(n)\neq(\nu)_\beta} \frac{A_{(\nu)_\beta}(n)}{E_{(\nu)_\beta} - E_{(n)}}\Big(\xi_{(\nu)_\beta}\langle\xi_{(n)}, \cdot\,\rangle_{\mathrm{f}} - \xi_{(n)}\langle\xi_{(\nu)_\beta}, \cdot\,\rangle_{\mathrm{f}}\Big), \tag{75}$$

with

$$A_{(\nu)_\beta (n)} = \mathcal{A}_{\phi(\nu)_\beta}^{\ \ (n)} \frac{\partial\big(E_{(n)} + E_{(\nu)_\beta}\big)}{\partial p_\phi} - \mathcal{A}_{p_\phi (\nu)_\beta}^{\ \ (n)} \frac{\partial\big(E_{(n)} + E_{(\nu)_\beta}\big)}{\partial \phi} + \big(E_{(n)} - E_{(m)}\big)\Big(\mathcal{A}^{(m)}_{p_\phi (\nu)_\beta}\mathcal{A}^{(n)}_{\phi(m)} - \mathcal{A}^{(m)}_{\phi(\nu)_\beta}\mathcal{A}^{(n)}_{p_\phi (m)}\Big). \tag{76}$$

Constructing the unitary symbol $\boldsymbol{\pi}_{(1)}$ requires to choose a simple reference space $\mathcal{K}_\mathrm{f}$, and as before, $\mathcal{H}_\mathrm{f}$ itself is a convenient choice. Its basis is determined by fixing a set of numbers $(q_0, p_0) \in \Gamma_\mathrm{s}$ giving $\{\zeta_{(n)} := \xi_{(n)}(q_0, p_0)\}_{(n)}$. The zeroth order contribution to the Moyal unitary and the reference projector can be chosen as,

$$\boldsymbol{u}_0(q,p) := \sum_{(n)} \zeta_{(n)} \langle \xi_{(n)}(q,p), \cdot \rangle_\mathrm{f}, \quad \boldsymbol{\pi}_\mathrm{R} := \sum_{\beta=1}^{\delta} \zeta_{(\nu)_\beta} \langle \zeta_{(\nu)_\beta}, \cdot \rangle_\mathrm{f}. \tag{77}$$

The hermitian part of $\boldsymbol{u}_1(q,p)$ is determined by evaluating (S2-1) and (S2-2) up to first order in the perturbations,

$$\boldsymbol{u}_1^\mathrm{h}(q,p) = \sum_{(n),(m),(k)} \Big(\mathcal{A}^{(m)}_{\phi(n)}\mathcal{A}^{(k)}_{p_\phi(m)} - \mathcal{A}_{p_\phi(n)}^{\ \ (m)}\mathcal{A}_{\phi(m)}^{\ \ (k)}\Big)\zeta_{(n)} \langle \zeta_{(k)}, \cdot \rangle_\mathrm{f}. \tag{78}$$

Since the sum runs over all possible combinations of quantum numbers, it is clear that the two contributions are equal and cancel each other. We thus have that $\boldsymbol{u}_1^\mathrm{h} = 0$. The antihermitian part of $\boldsymbol{u}_1$ results from employing the result for $\boldsymbol{\pi}_1^\mathrm{OD}$ in the well–known expression from the toy model example,

$$\boldsymbol{u}_1^\mathrm{ah} = \big[\boldsymbol{\pi}_\mathrm{R}, \boldsymbol{u}_0 \cdot \boldsymbol{\pi}_1^\mathrm{OD} \cdot \boldsymbol{u}_0{}^\star\big]_\mathrm{f} \cdot \boldsymbol{u}_0. \tag{79}$$

We evaluate the effective Hamilton constraint symbol according to, $\boldsymbol{C}_\mathrm{eff} = \boldsymbol{u} \bigstar_\varepsilon \boldsymbol{C} \bigstar_\varepsilon \boldsymbol{u}^\star$, and restrict our interest directly to the reference space, i.e., to $\boldsymbol{C}_{\mathrm{eff,R}} = \boldsymbol{\pi}_\mathrm{R} \cdot \boldsymbol{C}_\mathrm{eff} \cdot \boldsymbol{\pi}_\mathrm{R}$. At zeroth order, this yields,

$$\boldsymbol{C}_{\mathrm{eff},0,\mathrm{R}} = \sum_{b,b'=1}^{d,d'} \Bigg[E_\mathrm{hom}\big(a, p_a, \phi, p_\phi\big) + \frac{1}{a} \sum_{\vec{k} \in \mathbb{K}} \nu_{\mathrm{MS},\vec{k},b}\,\omega_{\mathrm{MS},\vec{k}} + \frac{1}{6a} \sum_{\vec{K} \in \mathbb{K}} \nu_{\mathrm{T},\vec{K},b'}\,\omega_{\mathrm{T},\vec{K}} \Bigg] \cdot \zeta_{(\nu)_\beta} \langle \zeta_{(\nu)_\beta}, \cdot \rangle_\mathrm{f}, \tag{80}$$

which includes the standard zeroth order Hamilton constraint for an FLRW Universe $E_\mathrm{hom}(a, p_a, \phi, p_\phi)$, and the bare energy contributions from the relevant energy band $\xi_{(\nu)_a}$. These additional terms are finite since the quantum numbers $\{\nu_{\mathrm{MS},\vec{k},b}, \nu_{\mathrm{T},\vec{k},b'}\}$ are non-vanishing for only a finite number of wave vectors $\vec{k}$. Te first order contribution to the effective Hamiltonian vanishes identically within the subspace of interest.

The second order effective Hamilton symbol includes several contributions but only one of them is of second order in the perturbative parameter, and hence relevant. The occurence of terms that actually enter at higher orders in ε stems from the fact that the perturbative Mukhanov–Sasaki and graviton contributions to $\boldsymbol{C}$ are by definition of second order in ε. It was necessary to include them to make the space adiabatic scheme work at the technical level. We refer again to (Schander and Thiemann 2019c) for more details and only state the final result,

$$\boldsymbol{C}_{\mathrm{eff},2,\mathrm{R}}\big(a, p_a, \phi, p_\phi\big) = -\sum_{b=1}^{d} \sum_{\vec{k} \in \mathbb{K}} \frac{1}{\big(\vec{k}^2 + m^2_\mathrm{MS}\big)^{5/2}} \Big(\nu_{\mathrm{MS},\vec{k},b} + \frac{1}{2}\Big) \frac{9}{2} \frac{m_\Phi^4 p_\phi^4}{a^3 p_a^2}\, \zeta_{(\nu)_b} \langle \zeta_{(\nu)_b}, \cdot \rangle_\mathrm{f}. \tag{81}$$

This second order effective Hamiltonian symbol together with the zeroth order contribution **Eq. 80**, provides after Weyl quantization a constraint operator for the homogeneous sector of quantum gravity which includes, most importantly, the backreaction from the inhomogeneous modes. A similar result was obtained for a quantum cosmological model with scalar field perturbations and a deparametrizing dust particle (Schander and Thiemann, 2019b). The next step of the scheme consequently consists in Weyl quantizing the full effective constraint symbol and in finding physical quantum states on the homogeneous Hilbert space that are annihilated by it. A thorough discussion of the above results will be given in the next and final section.

6 DISCUSSION AND OUTLOOK

This review provides an introduction to the backreaction problem in classical, semiclassical and quantum cosmology, as well as a detailed overview of the current state of research in the respective fields. We have particularly focused on approaches to the backreaction problem in (perturbative) quantum cosmology that are inspired by Born–Oppenheimer methods. The main part of this paper is dedicated to a program which uses SAPT as due to Panati et al. (2003), and which extends the latter scheme to quantum field theoretical models. Thereby, it is possible to compute the backreaction effects from the quantum cosmological perturbations on the homogeneous and isotropic quantum background (Schander and Thiemann, 2019b; Schander and Thiemann, 2019c). We have advocated this framework here as it represents an unambigious and straighforward formalism in order to incorporate the yet neglected backreaction effects in quantum cosmology in a perturbative and rigorous way.

The extension of the SAPT methods actually requires some care. The first issue is related to a violation of the Hilbert–Schmidt condition in QFT on CST. In fact, it is well–known from standard QFT that Klein–Gordon fields with different masses give rise to unitarily inequivalent representations of the field algebra (Haag, 1992). Since here, the effective masses of the Klein–Gordon and tensor fields depend on the homogeneous FLRW background, the theory prevents unitarily equivalent quantum field theories for different background configurations.

This would evidently impede the quantization of the homogeneous sector. Schander and Thiemann (2019a,c) show that it is possible to circumvent these problems by considering transformations of the whole system that are canonical up to second order in the cosmological perturbations (Castelló Gomar et al., 2015; Martínez and Olmedo, 2016; Schander and Thiemann, 2019b).

Another point is that the mass squared functions of the perturbative quantum fields $m^2_{\mathrm{MS}}(a, p_a, \phi, p_\phi)$ and $(\varepsilon m_{\mathrm{T}})^2(a, p_a, \phi)$ in **Eqs. 62** and **63** are indefinite, and which leads to tachyonic instabilities. In (Schander and Thiemann, 2019a), several solutions are propsed, for example to revise the almost–canonical transformations that have actually led to these indefinite mass functions. A second proposal is to restrict the homogeneous phase space of the theory to regions in which the mass functions are positive. This can be made manifest by performing coordinate transformations in the slow sector. This is exemplified for the model with gauge–invariant perturbations in (Radzikowski, 2008; Schander and Thiemann, 2019a).

With the identification and solutions to these initial problems, it was possible to successfully apply the methods of SAPT to the backreaction problem in quantum cosmology. We stated the results for a cosmological, homogeneous and isotropic toy model, and for a fully-fledged perturbative quantum cosmology with gauge-invariant perturbations (Schander and Thiemann, 2019c; Neuser et al., 2019). In the first case, this effective Hamilton constraint includes the backreaction of the homogeneous scalar field; in the second case, the backreactions of the perturbative degrees of freedom on the homogeneous background are taken into account. Here, results up to second order in the adiabatic ε-scheme are presented. The effective Hamiltonian symbol eventually needs to be quantized with respect to the slow sector and the goal is to find admissible solutions. This has been done for an oscillator toy model in (Neuser et al., 2019). One can proceed here in the same way but analytic solutions are harder to find due to the non-polynomial structure of the result, and which requires an in depth analysis of their dense domain. For simplicity, we chose a Weyl quantization scheme and a Schrödinger representation following the original work by Panati et al. (2003). Instead, one could consider the representation underlying LQC which could be of advantage regarding the domain issues (Bojowald, 2008). Due to the peculiarities of that representation (especially the strong discontinuity of the Weyl elements), and in agreement with certain superselection structures of the dynamics, one would need to discretize the labels of the Weyl elements in one of the conjugate variables. This would effectively replace the gravitational slow phase space $T^*\mathbb{R}$ by $T^*(S^1)$ for which the Weyl quantization in application to LQC has been discussed in (Stottmeister and Thiemann, 2016b).

Focusing on the second order contribution to the perturbative model, **Eq. 81**, one might be worried about the infinite sums. Note that the result splits into two parts, namely the one including the finite number of non–vanishing relevant quantum numbers $\nu_{\mathrm{MS},\vec{k},b}$ for different degeneracy labels b, and the contributions which do not depend on these quantum numbers and hence include any summand of the wave vector sum. The first part has only a finite number of contributions and is manageable, while the second includes in principle an infinite sum. Fortunately, the wave vector square enters with an exponent of $-5/2$ which makes the sum a priori a convergent sum. But the effective Mukhanov–Sasaki mass squared $m^2_{\mathrm{MS}}(a, p_a, \phi, p_\phi)$ in the denominator is an *indefinite* function on the homogeneous phase space. This will be cured as soon as a positive definite sector of the mass squared functions has been found.

We emphasize again that the issue of convergence of the perturbation series in the SAPT approach has not been addressed here. We point to easily implementable strategies (Panati et al., 2003; Stottmeister, 2015), that allow to define auxiliary Hamiltonian symbols that capture the relevant physics of the model under consideration and whose perturbation series is safely convergent.

Finally, we stress that there is an obvious connection between backreaction and decoherence (Schlosshauer, 2007). Indeed, in decoherence, one aims at finding an effective description of what we call the slow sector using the reduced density matrix approach, tracing over the fast degrees of freedom (Kiefer, 1987; Paz and Sinha, 1991, 1992) (and references therein), and computing its effective dynamics, e.g., by solving associated Lindblad equations (Manzano, 2020). Using the tensor product structure of the full Hilbert space, the connection to our approach would be to construct the reduced density matrix from a density matrix on the full Hilbert space that can be formed from the eigenstates of the Hamiltonian (constraint) corresponding to a given energy band. Details will be given elsewhere.

AUTHOR CONTRIBUTIONS

SS and TT both contributed to all aspects of the present review.

ACKNOWLEDGMENTS

We thank Kasia Rejzner for helpful references and information on the backreaction problem within the algebraic approach to QFT. The work of SS is supported by Perimeter Institute for Theoretical Physics. Research at Perimeter Institute is supported in part by the Government of Canada through the Department of Innovation, Science and Economic Development and by the Province of Ontario through the Ministry of Colleges and Universities.

REFERENCES

Abramo, L. R. W., Brandenberger, R. H., and Mukhanov, V. F. (1997). Energy-momentum Tensor for Cosmological Perturbations. *Phys. Rev. D* 56, 3248–3257. arXiv: gr-qc/9704037. doi:10.1103/physrevd.56.3248

Abramo, L. R., and Woodard, R. P. (2002). No One Loop Back Reaction in Chaotic Inflation. *Phys. Rev. D* 65, 063515. arXiv: astro-ph/0109272. doi:10.1103/PhysRevD.65.063515

Adamek, J., Clarkson, C., Daverio, D., Durrer, R., and Kunz, M. (2019). Safely Smoothing Spacetime: Backreaction in Relativistic Cosmological Simulations. *Class. Quan. Grav.* 36, 014001. arXiv: 1706.09309 [astro-ph.CO]. doi:10.1088/1361-6382/aaeca5

Adamek, J., Daverio, D., Durrer, R., and Kunz, M. (2016). Gevolution: a Cosmological N-Body Code Based on General Relativity. *J. Cosmol. Astropart. Phys.* 2016, 053. arXiv: 1604.06065 [astro-ph.CO]. doi:10.1088/1475-7516/2016/07/053

Ade, P. A. R., Aghanim, N., Arnaud, M., Ashdown, M., Aumont, J., Baccigalupi, C., et al. (2016). Planck 2015 Results. XIV. Dark Energy and Modified Gravity. *Astron. Astrophys.* 594, À14. arXiv: 1502.01590 [astro-ph.CO].

Aghanim, N., Arroja, F., Ashdown, M., Aumont, J., Baccigalupi, C., Ballardini, M., et al. (2019). Planck 2018 Results. I. Overview and the Cosmological Legacy of Planck. Available at: arXiv: 1807.06205 [astro-ph.CO].

Aghanim, N., Akrami, Y., Ashdown, M., Aumont, J., Baccigalupi, C., Ballardini, M., et al. (2020). Planck 2018 Results. VI. Cosmological Parameters. Available at: arXiv: 1807.06209 [astro-ph.CO].

Agullo, I., Ashtekar, A., and Nelson, W. (2013). Extension of the Quantum Theory of Cosmological Perturbations to the Planck Era. *Phys. Rev. D* 87 (4), 043507. arXiv: 1211.1354 [gr-qc]. doi:10.1103/physrevd.87.043507

Alpher, R. A., and Herman, R. (1948a). Evolution of the Universe. *Nature* 162, 774–775. doi:10.1038/162774b0

Alpher, R. A., and Herman, R. C. (1948b). On the Relative Abundance Of the Elements. *Phys. Rev.* 74, 1737–1742. doi:10.1103/physrev.74.1737

Anderson, P. (1983). Effects of Quantum fields on Singularities and Particle Horizons in the Early Universe. *Phys. Rev. D* 28, 271–285. doi:10.1103/physrevd.28.271

Anderson, P. R. (1984). Effects of Quantum fields on Singularities and Particle Horizons in the Early Universe. II. *Phys. Rev. D* 29, 615–627. doi:10.1103/physrevd.29.615

Anderson, P. R. (1985). Effects of Quantum fields on Singularities and Particle Horizons in the Early Universe. III. The Conformally Coupled Massive Scalar Field. *Phys. Rev. D* 32, 1302–1315. doi:10.1103/physrevd.32.1302

Araki, H. (1999). *Mathematical Theory of Quantum fields*. New York: Oxford University Press.

Ashtekar, A., Bojowald, M., and Lewandowski, J. (2003). Mathematical Structure of Loop Quantum Cosmology. *Adv. Theor. Math. Phys.* 7, 233–268. arXiv: gr-qc/0304074. doi:10.4310/atmp.2003.v7.n2.a2

Barausse, E., Matarrese, S., and Riotto, A. (2005). Effect of Inhomogeneities on the Luminosity Distance-Redshift Relation: Is Dark Energy Necessary in a Perturbed Universe?. *Phys. Rev. D* 71, 063537, 2005 . arXiv: astro-ph/0501152. doi:10.1103/PhysRevD.71.063537

Barausse, E., Matarrese, S., and Riotto, A. (2005). *The Effect Of Inhomogeneities on the Luminosity Distance-Redshift Relation: Is Dark Energy Necessary in a Perturbed Universe*? *Phys. Rev. D* 71, 063537. arXiv: astro-ph/0501152. doi:10.1103/physrevd.71.063537

Barrera-Hinojosa, C., and Li, B. (2020). GRAMSES: a New Route to General Relativistic N-Body Simulations in Cosmology. Part I. Methodology and Code Description. *J. Cosmol. Astropart. Phys.* 2020, 007. arXiv: 1905.08890 [astro-ph.CO]. doi:10.1088/1475-7516/2020/01/007

Baumann, D., Nicolis, A., Senatore, L., and Zaldarriaga, M. (2012). Cosmological Non-Linearities as an Effective Fluid. *J. Cosmol. Astropart. Phys.* 2012, 051. arXiv:1004.2488 [astro-ph.CO]. doi:10.1088/1475-7516/2012/07/051

Behrend, J., Brown, I. A., and Robbers, G. (2008). Cosmological Backreaction from Perturbations. *J. Cosmol. Astropart. Phys.* 2008, 013, 2008. arXiv: 0710.4964 [astro-ph]. doi:10.1088/1475-7516/2008/01/013

Berry, I. V. (1984). Quantal Phase Factors Accompanying Adiabatic Changes. *Proc. R. Soc. Lond. A.* 392, 45–57. doi:10.1098/rspa.1984.0023

Bertoni, C., Finelli, F., and Venturi, G. (1996). The Born - Oppenheimer Approach to the Matter - Gravity System and Unitarity. *Class. Quan. Grav.* 13, 2375–2383. arXiv: gr-qc/9604011. doi:10.1088/0264-9381/13/9/005

Bianchi, E., Rovelli, C., and Vidotto, F. (2010). Towards Spinfoam Cosmology. *Phys. Rev. D* 82, 084035. arXiv:1003.3483 [gr-qc]. doi:10.1103/physrevd.82.084035

Birrell, N. D., and Davies, P. C. W. (1984). "Quantum Fields in Curved Space," in *Cambridge Monographs on Mathematical Physics*. Cambridge, UK: Cambridge Univ. Press.

Biswas, T., and Notari, A. (2008). 'Swiss-cheese' Inhomogeneous Cosmology and the Dark Energy Problem. *J. Cosmol. Astropart. Phys.* 2008, 021, 2008. arXiv: astro-ph/0702555. doi:10.1088/1475-7516/2008/06/021

Blaszak, M., and Domanski, Z. (2012). Phase Space Quantum Mechanics. *Ann. Phys.* 327, 167–211. doi:10.1016/j.aop.2011.09.006

Blumenthal, G. R., Faber, S. M., Primack, J. R., and Rees, M. J. (1984). "Formation of Galaxies and Large-Scale Structure with Cold Dark Matter," in *Nature* 311. Editor M. A. Srednicki, pp. 517–525. doi:10.1038/311517a0

Bojowald, M. (2008). Loop Quantum Cosmology. *Living Rev. Relativ.* 11, 4. doi:10.12942/lrr-2008-4

Bolejko, K., and Célérier, M.-N. (2010). Szekeres Swiss-cheese Model and Supernova Observations. *Phys. Rev. D* 82, 103510. arXiv: 1005.2584 [astro-ph.CO]. doi:10.1103/physrevd.82.103510

Bolejko, K, and Korzyński, M. (2017). Inhomogeneous Cosmology and Backreaction: Current Status and Future Prospects. *Fourteenth Marcel Grossmann Meet.* 14, (1), 602–621. arXiv: 1612.08222 [gr-qc]. doi:10.1142/9789813226609_0033

Bolejko, K., and Korzyński, M. (2017). "Inhomogeneous Cosmology and Backreaction: Current Status and Future Prospects, *Int. J. Mod. Phys. D*, 26". In: Int. J. Mod. Phys. D *26.06*. Ed. by M. Bianchi, R. T. Jantzen, and R. Ruffini, p. 1730011, 2017 . arXiv: 1612.08222 [gr-qc]. doi:10.1142/S0218271817300117

Bonvin, C., Durrer, R., and Gasparini, M. A. (2006). "Erratum: Fluctuations of the Luminosity Distance [Phys. Rev. D73, 023523 (2006)]". In: [Erratum: *Phys. Rev. D* 85,029901, 2006 (2012)], p. 023523. arXiv: astro-ph/0511183. doi:10.1103/PhysRevD.85.029901

Brandenberger, R., Graef, L. L., Marozzi, G., and Vacca, G. P. (2018). Backreaction of Super-hubble Cosmological Perturbations beyond Perturbation Theory. *Phys. Rev. D* 98, 103523. arXiv: 1807.07494. doi:10.1103/PhysRevD.98.103523

Bonvin, C., Durrer, R., and Gasparini, M. (2006). Fluctuations of the Luminosity Distance. *Phys. Rev. D* 73, 023523. arXiv: astro-ph/0511183. doi:10.1103/physrevd.73.023523

Born, M., and Oppenheimer, R. (1927). Zur Quantentheorie der Molekeln. *Ann. Phys.* 389, 457–484. doi:10.1002/andp.19273892002

Boyanovsky, D., D'Attanasio, M., de Vega, H. J., Holman, R., and Lee, D.-S. (1995). Linear versus Nonlinear Relaxation: Consequences for Reheating and Thermalization. *Phys. Rev. D* 52, 6805–6827. arXiv: hep-ph/9507414. doi:10.1103/physrevd.52.6805

Brandenberger, R., Graef, L. L., Marozzi, G., and Vacca, G. P. (2018). Backreaction of Super-Hubble Cosmological Perturbations beyond Perturbation Theory. *Phys. Rev. D* 98, 103523. arXiv: 1807.07494 [hep-th]. doi:10.1103/physrevd.98.103523

Brandenberger, R. H., Feldman, H., and Mukhanov, V. F. (1993). "Classical and Quantum Theory of Perturbations in Inflationary Universe Models," in 37th Yamada Conference: Evolution of the Universe and its Observational Quest. Available at: arXiv: astro-ph/9307016.

Brandenberger, R. H. (2004). "Lectures on the Theory of Cosmological Perturbations," in *Lecture Notes in Physics, The Early Universe and Observational Cosmology 646*. Editors N. Breton, J. L. Cervantes-Cota, and M. Salgado, pp. 127–167. arXiv: hep-th/0306071. doi:10.1007/978-3-540-40918-2_5

Briggs, J. S., and Rost, J. M. (2000). Time *Dependence in Quantum Mechanics*. *Eur. Phys. J. D* 10, 311. arXiv: quant-ph/9902035. doi:10.1007/s100530050554

Brizuela, D., and Krämer, M. (2018). Quantum-Gravitational Effects on Primordial Power Spectra in Slow-Roll Inflationary Models. *Galaxies* 6 (1), 6. doi:10.3390/galaxies6010006

Brout, R. (1987). On the Concept Of Time and the Origin Of the Cosmological Temperature. *Found. Phys.* 17 (6), 603–619. doi:10.1007/bf01882790

Brout, R., and Venturi, G. (1989). Time in Semiclassical Gravity. *Phys. Rev. D* 39, 2436–2439. doi:10.1103/physrevd.39.2436

Brown, I. A., Robbers, G., and Behrend, J. (2009). Averaging Robertson-Walker Cosmologies. *J. Cosmol. Astropart. Phys.* 2009, 016. arXiv: 0811.4495 [gr-qc]. doi:10.1088/1475-7516/2009/04/016

Brunetti, R., and Fredenhagen, K. (2000). Microlocal Analysis and Interacting Quantum Field Theories: Renormalization on Physical Backgrounds. *Commun. Math. Phys.* 208, 623–661. arXiv: math- ph/9903028. doi:10.1007/s002200050004

Buchert, T. (2008). Dark Energy from Structure: A Status Report. *Gen. Relativ Gravit.* 40, 467–527. arXiv: 0707.2153 [gr-qc]. doi:10.1007/s10714-007-0554-8

Buchert, T. (2000). On Average Properties of Inhomogeneous Fluids in General Relativity: Dust Cosmologies. *Gen. Relativ. Gravitation* 32, 105–125. arXiv: gr-qc/9906015. doi:10.1023/a:1001800617177

Buchert, T. (2001). On Average Properties of Inhomogeneous Fluids in General Relativity: Perfect Fluid Cosmologies. *Gen. Relativ. Gravitation* 33, 1381–1405. arXiv: gr-qc/0102049. doi:10.1023/a:1012061725841

Buchert, T., and Räsänen, S. (2012). Backreaction in Late-Time Cosmology. *Annu. Rev. Nucl. Part. Sci.* 62, 57–79. arXiv: 1112.5335 [astro-ph.CO]. doi:10.1146/annurev.nucl.012809.104435

Cailleteau, T., Mielczarek, J., Barrau, A., and Grain, J. (2012). Anomaly-free Scalar Perturbations with Holonomy Corrections in Loop Quantum Cosmology. *Class. Quan. Grav.* 29, 095010. arXiv: 1111.3535 [gr-qc]. doi:10.1088/0264-9381/29/9/095010

Calzetta, E., and Hu, B. L. (1987). Closed-time-path Functional Formalism in Curved Spacetime: Application to Cosmological Back-Reaction Problems. *Phys. Rev. D* 35, 495–509. doi:10.1103/physrevd.35.495

Calzetta, E., and Hu, B. L. (1989). Dissipation of Quantum fields from Particle Creation. *Phys. Rev. D* 40, 656–659. doi:10.1103/physrevd.40.656

Calzetta, E., and Hu, B. L. (1994). Noise and Fluctuations in Semiclassical Gravity. *Phys. Rev. D* 49, 6636–6655. arXiv: gr-qc/9312036. doi:10.1103/physrevd.49.6636

Calzetta, E., and Hu, B. L. (1995). Quantum Fluctuations, Decoherence of the Mean Field, and Structure Formation in the Early Universe. *Phys. Rev. D* 52, 6770–6788. arXiv: gr-qc/9505046. doi:10.1103/physrevd.52.6770

Campos, A., and Verdaguer, E. (1994). Semiclassical Equations for Weakly Inhomogeneous Cosmologies. *Phys. Rev. D* 49, 1861–1880. arXiv: gr-qc/9307027. doi:10.1103/physrevd.49.1861

Castelló Gomar, L., Martín-Benito, M., and Mena Marugán, G. A. (2015). Gauge-invariant Perturbations in Hybrid Quantum Cosmology. *J. Cosmol. Astropart. Phys.* 2015, 045, 2015. arXiv: 1503.03907 [gr-qc]. doi:10.1088/1475-7516/2015/06/045

Castelló Gomar, L., Mena Marugán, G. A., and Martín-Benito, M. (2016). Quantum Corrections to the Mukhanov-Sasaki Equations. *Phys. Rev. D* 93, 2016, 104025. arXiv:1603.08448 [gr-qc]. doi:10.1103/physrevd.93.104025

Cervantes-Cota, J. L., and Smoot, G. (2011). Cosmology Today - A Brief Review. *AIP Conf. Proc.* 1396 (1), 28–52. arXiv: 1107.1789 [astro-ph.CO].

Clarkson, C., Ellis, G., Larena, J., and Umeh, O. (2011). Does the Growth of Structure Affect Our Dynamical Models of the Universe? the Averaging, Backreaction, and Fitting Problems in Cosmology. *Rep. Prog. Phys.* 74, 112901. arXiv: 1109.2314 [astro-ph.CO]. doi:10.1088/0034-4885/74/11/112901

Clifton, T. (2011). Cosmology without Averaging. *Class. Quan. Grav. Class. Quant. Grav.*, 28, 164011, 2011. arXiv: 1005.0788 [gr-qc]. doi:10.1088/0264-9381/28/16/164011

Chataignier, L., and Krämer, M. (2021). Unitarity of Quantum-Gravitational Corrections to Primordial Fluctuations in the Born-Oppenheimer Approach. *Phys. Rev. D* 103 (6), 066005. arXiv: 2011. 06426 [gr-qc]. doi:10.1103/physrevd.103.066005

Clarkson, C., Ananda, K., and Larena, J. (2009). The Influence of Structure Formation on the Cosmic Expansion. *Phys. Rev. D* 80, 083525. arXiv: 0907.3377 [astro-ph.CO]. doi:10.1103/physrevd.80.083525

Clarkson, C., Ellis, G., Larena, J., and Umeh, O. (2011). Does the Growth of Structure Affect Our Dynamical Models of the Universe? The Averaging, Backreaction, and Fitting Problems in Cosmology. *Rep. Prog. Phys.* 74, 112901. arXiv: 1109.2314 [astro-ph.CO]. doi:10.1088/0034-4885/74/11/112901

Clifton, T., and Ferreira, P. G. (2009). Archipelagian Cosmology: Dynamics and Observables in a Universe with Discretized Matter Content. Erratum: Phvs.Rev.D 84, 109902 (2011)]. *Phys. Rev. D* 80, 103503. [arXiv: 0907.4109 [astro-ph.CO]. doi:10.1103/physrevd.80.103503

Cole, S., Percival, W. J., Peacock, J. A., Norberg, P., Baugh, C. M., Frenk, C. S., et al. (2005). The 2dF Galaxy Redshift Survey: Power-Spectrum Analysis of the Final Data Set and Cosmological Implications. *Mon. Not. Roy. Astron. Soc.* 362, 505–534. arXiv: astro- ph/0501174. doi:10.1111/j.1365-2966.2005.09318.x

Colless, M., Dalton, G. B., Maddox, S. J., Sutherland, W. J., Norberg, P., Cole, S., et al. (2001). The 2dF Galaxy Redshift Survey: Spectra and Redshifts. *Mon. Not. Roy. Astron. Soc.* 328, 1039. arXiv: astro-ph/0106498. doi:10.1046/j.1365-8711.2001.04902.x

Dappiaggi, C., Fredenhagen, K., and Pinamonti, N. (2008). Stable Cosmological Models Driven by a Free Quantum Scalar Field. *Phys. Rev. D* 77, 104015. arXiv: 0801.2850 [gr-qc]. doi:10.1103/physrevd.77.104015

Dappiaggi, C., Hack, T.-P., Möller, J., and Pinamonti, N. (2010). Dark Energy from Quantum Matter. Available at: arXiv: 1007. 5009 [astro-ph.CO] (Accessed July 28, 2010).

Deruelle, N., and Uzan, J.-P. (2018). *Relativity in Modern Physics*. Oxford: Oxford University Press.

DeWitt, B. S. (1967). Quantum Theory of Gravity. I. The Canonical Theory. *Phys. Rev.* 160, 1113–1148. doi:10.1103/physrev.160.1113

Di Valentino, E., Anchordoqui, L. A., Akarsu, O., Ali-Haimoud, Y., Amendola, L., Arendse, N., et al. (2020a). Cosmology Intertwined II: The Hubble Constant Tension. Available at: arXiv: 2008.11284 [astro-ph.CO] (Accessed August 25, 2020).

Di Valentino, E., Anchordoqui, L. A., Akarsu, O., Ali-Haimoud, Y., Amendola, L., Arendse, N., et al. (2020b). Cosmology Intertwined III: $F\sigma_8$ and S_8. Available at: arXiv: 2008.11285 [astro-ph.CO] (Accessed August 25, 2020).

Dimassi, M., and Sjöstrand, J. (1999). *Spectral Asymptotics in the Semi-Classical Limit*. Cambridge: Cambridge University Press.

Dodelson, S., and Schmidt, F. (2021). *Modern Cosmology*. Second Edition. Amsterdam: Elsevier - Academic Press.

Dubin, D. A., Hennings, M. A., and Smith, T. B. (1980). *Mathematical Aspects of Weyl Quantization and Phase*, Vol. 1. Singapore: World Scientific Publishing.

Durrer, R. (2004). "2 Cosmological Perturbation Theory," in *Lecture Notes in Physics 653*. Editor E. Pa- pantonopoulos, 31–69. arXiv: astro-ph/0402129. doi:10.1007/978-3-540-31535-3_2

Dymnikova, I., and Khlopov, M. (2001). "Decay of Cosmological Constant in Self-Consistent Inflation," *Eur. Phys. J. C Decay of Cosmological Constant in Selfconsistent Inflation* (Eur. Phys. J. C), 20, 139–146. doi:10.1007/s100520100625

Ellis, G. F. R. (2011). Inhomogeneity Effects in Cosmology. *Class. Quan. Grav.*, 28, , 2011 164001. arXiv: 1103.2335 [astro-ph.CO]. doi:10.1088/0264-9381/28/16/164001

Ellis, G. F. R., and Stoeger, W. (1987). The 'fitting Problem' in Cosmology. *Class. Quan. Grav.*, 4, 1697–1729. doi:10.1088/0264-9381/4/6/025

Elizaga Navascués, B., Martín-Benito, M., and Mena Marugán, G. A. (2016). Hybrid Models in Loop Quantum Cosmology. *Int. J. Mod. Phys. D* 25, 1642007, 2016. arXiv: 1608.05947 [gr-qc]. doi:10.1142/s0218271816420074

Eltzner, B., and Gottschalk, H. (2011). Dynamical Backreaction in Robertson-Walker Spacetime. *Rev. Math. Phys.* 23, 531–551. arXiv: 1003.3630 [math-ph]. doi:10.1142/s0129055x11004357

J. Erdmenger (Editor) (2009). *String Cosmology: Modern String Theory Concepts from the Big Bang to Cosmic Structure*. Hoboken: Wiley.

Fanizza, G., Gasperini, M., Marozzi, G., and Veneziano, G. (2020). Generalized Covariant Prescriptions for Averaging Cosmological Observables. *J. Cosmol. Astropart. Phys. JCAP 02*, 2020, 017. arXiv: 1911.09469 [gr-qc]. doi:10.1088/1475-7516/2020/02/017

Fernández-Méndez, M., Mena Marugán, G. A., Olmedo, J., and Velhinho, J. M. (2012). Unique Fock Quantization of Scalar Cosmological Perturbations. *Phys. Rev. D* 85, 103525. arXiv: 1203.2525 [gr-qc]. doi:10.1103/physrevd.85.103525

Finelli, F., Marozzi, G., Starobinsky, A. A., Vacca, G. P., and Venturi, G. (2009). Generation of Fluctuations during Inflation: Comparison of Stochastic and Field-Theoretic Approaches. *Phys. Rev. D* 79, 044007. arXiv: 0808.1786 [hep-th]. doi:10.1103/physrevd.79.044007

Finelli, F., Marozzi, G., Vacca, G. P., and Venturi, G. (2002). Energy-momentum Tensor of Field Fluctuations in Massive Chaotic Inflation. *Phys. Rev. D* 65, 103521. arXiv: gr-qc/0111035. doi:10.1103/physrevd.65.103521

Finelli, F., Marozzi, G., Vacca, G. P., and Venturi, G. (2011). Backreaction during Inflation: A Physical Gauge Invariant Formulation. *Phys. Rev. Lett.* 106, 121304. arXiv: 1101.1051 [gr-qc]. doi:10.1103/PhysRevLett.106.121304

Finelli, F., Marozzi, G., Vacca, G. P., and Venturi, G. (2004). Energy-momentum Tensor of Cosmological Fluctuations during Inflation. *Phys. Rev. D* 69, 123508. arXiv: gr-qc/0310086. doi:10.1103/PhysRevD.69.123508

Fischetti, M. V., Hartle, J. B., and Hu, B. L. (1979). Quantum Effects in the Early Universe. I. Influence of Trace Anomalies on Homogeneous, Isotropic, Classical Geometries. *Phys. Rev. D* 20, 1757–1771. doi:10.1103/physrevd.20.1757

Flanagan, É. É. (2005). Can Superhorizon Perturbations Drive the Acceleration of the Universe? *Phys. Rev. D* 71, 103521. arXiv: hep-th/0503202. doi:10.1103/physrevd.71.103521

Flanagan, E. E., and Wald, R. M. (1996). Does Back Reaction Enforce the Averaged Null Energy Condition in Semiclassical Gravity? *Phys. Rev. D* 54, 6233–6283. arXiv: gr-qc/9602052. doi:10.1103/physrevd.54.6233

Folland, G. B. (1989). *Harmonic Analysis in Phase Space*. Princeton: Princeton University Press.

Ford, L. H. (2005). "Spacetime in Semiclassical Gravity," in *100 Years of Relativity : Space-Time Structure: Einstein and beyond.* Editor A. Ashtekar, pp. 293–310. arXiv: gr-qc/0504096. doi:10.1142/9789812700988_0011

Friedman, A. (1922). Uber die Krümmung des Raumes. *Z. Physik* 10, 377–386. doi:10.1007/bf01332580

Friedmann, A. (1924). Uber die Möglichkeit einer Welt mit konstanter negativer Krümmung des Raumes. *Z. Physik* 21, 326–332. doi:10.1007/bf01328280

Fulling, S. A., Parker, L., and Hu, B. L. (1974). Conformal Energy-Momentum Tensor in Curved Spacetime: Adiabatic Regularization and Renormalization. *Phys. Rev. D* 10, 3905–3924. doi:10.1103/physrevd.10.3905

Fulling, S. A., and Parker, L. (1974). Renormalization in the Theory of a Quantized Scalar Field Interacting with a Robertson-walker Spacetime. *Ann. Phys.* 87, 176–204. doi:10.1016/0003-4916(74)90451-5

Fulling, S. A. (1989). *London Mathematical Society Student Texts*. Cambridge: Cambridge University Press, 7.

Gamov, G. (1948a). The Evolution of the Universe. *Nature* 162, 680–682.

Gamov, G. (1948b). The Origin of Elements and the Separation of Galaxies. *Phys. Rev.* 74, 505.

Gasperini, M., Marozzi, G., Nugier, F., and Veneziano, G. (2011). Light-cone Averaging in Cosmology: Formalism and Applications. *J. Cosmol. Astropart. Phys.* JCAP *07*, 2011, 008. arXiv: 1104.1167 [astro-ph.CO]. doi:10.1088/1475-7516/2011/07/008

Geshnizjani, G., and Brandenberger, R. (2002). Back Reaction and the Local Cosmological Expansion Rate. *Phys. Rev. D* 66, 123507. arXiv: gr-qc/0204074. doi:10.1103/PhysRevD.66.123507

Geshnizjani, G., and Brandenberger, R. (2005). Back Reaction of Perturbations in Two Scalar Field Inflationary Models JCAP *04*, 006. arXiv: hep-th/0310265. doi:10.1088/1475-7516/2005/04/006

Giesel, K., Tambornino, J., and Thiemann, T. (2009). Born-Oppenheimer Decomposition for Quantum fields on Quantum Spacetimes. Available at: arXiv: 0911.5331 [gr-qc] (Accessed November 27, 2009).

Gottschalk, H., and Siemssen, D. (2018). The Cosmological Semiclassical Einstein Equation as an Infinite-Dimensional Dynamical System. Available at: arXiv: 1809.03812 [math-ph] (Accessed September 11, 2018).

Green, S. R., and Wald, R. M. (2011). A New Framework for Analyzing the Effects of Small Scale Inhomogeneities in Cosmology. *Phys. Rev. D* 83, 084020. arXiv: 1011.4920 [gr-qc]. doi:10.1103/physrevd.83.084020

Green, S. R., and Wald, R. M. (2013). Examples of Backreaction of Small-Scale Inhomogeneities in Cosmology. *Phys. Rev. D* 87, 124037. arXiv: 1304.2318 [gr-qc]. doi:10.1103/physrevd.87.124037

Green, S. R., and Wald, R. M. (2014). How Well Is Our Universe Described by an FLRW Model? *Class. Quan. Grav.* 31, 234003. arXiv:1407.8084 [gr-qc]. doi:10.1088/0264-9381/31/23/234003

Green, S. R., and Wald, R. M. (2012). Newtonian and Relativistic Cosmologies. *Phys. Rev. D* 85, 063512. arXiv: 1111.2997 [gr-qc]. doi:10.1103/physrevd.85.063512

Grishchuk, L. P. (1977). Graviton Creation in the Early Universe. *Ann. NY Acad. Sci.* 302, 439–444. doi:10.1111/j.1749-6632.1977.tb37064.x

Haag, R. (1992). *Local Quantum Physics: Fields, Particles, Algebras*. Berlin: Springer-Verlag.

Hack, T.-P. (2013). The Lambda CDM Model in Quantum Field Theory on Curved Spacetime and Dark: Radiation. Available at: arXiv: 1306.3074 [gr-qc] (Accessed June 13, 2013).

Halliwell, J. J., and Hawking, S. W. (1987). "The Origin of Structure in the Universe," in *Adv. Ser. Astrophys. Cosmol. 3*. Editors L. Z. Fang and R. Ruffini, pp. 277–291.

Halliwell, J. J., and Hawking, S. W. (1985). "Origin of Structure in the Universe. *Phys. Rev. D*" in *The Origin of Structure in the Universe*. Li-Zhi Fang and R. Ruffini Editors, 31, 1777–1791. doi:10.1103/PhysRevD.31.1777

Heinesen, A. (2021a). Multipole Decomposition of Redshift Drift - Model Independent Mapping of the Expansion History of the Universe. *Phys. Rev. D* 103.2, 023537. arXiv: 2011.10048 [gr-qc]. doi:10.1103/physrevd.103.023537

Heinesen, A. (2021b). Redshift Drift as a Model Independent Probe of Dark Energy. *Phys. Rev. D* 103, L081302. arXiv: 2102.03774 [gr-qc]. doi:10.1103/PhysRevD.103.L081302

Heinesen, A., and Buchert, T. (2020). Solving the Curvature and Hubble Parameter Inconsistencies through Structure Formation-Induced Curvature. *Class. Quan. Grav.* 37 (16), 164001, 2020. arXiv: 2002.10831 [gr-qc]. doi:10.1088/1361-6382/ab954b

Heymans, C., Tröster, T., Asgari, M., Blake, C., Hildebrandt, H., Joachimi, B., et al. (2021). KiDS-1000 Cosmology: Multi-Probe Weak Gravitational Lensing and Spectroscopic Galaxy Clustering Constraints. *Astron. Astrophys.* 646, A140, 2021. arXiv: 2007.15632 [astro-ph.CO]. doi:10.1051/0004-6361/202039063

Hollands, S., and Wald, R. M. (2001). Local Wick Polynomials and Time Ordered Products of Quantum Fields in Curved Spacetime. *Commun. Math. Phys.* 223, 289–326. arXiv: gr-qc/0103074. doi:10.1007/s002200100540

Hörmander, L. (1985a). *The Analysis of Linear Partial Differential Operators II: Differential Operators with Constant Coefficients*. Berlin, Heidelberg: Springer-Verlag.

Hörmander, L. (1985b). *The Analysis of Linear Partial Differential Operators III: Pseudo Differential Operators*. Berlin, Heidelberg: Springer-Verlag.

Hu, B. L., and Matacz, A. (1995). Back Reaction in Semiclassical Gravity: The Einstein-Langevin Equation. *Phys. Rev. D* 51, 1577–1586. arXiv: gr-qc/9403043. doi:10.1103/physrevd.51.1577

Hu, B. L., and Parker, L. (1978). Anisotropy Damping through Quantum Effects in the Early Universe. *Phys. Rev. D* 17, 933–945. [Erratum: Phys.Rev.D 17, 3292 (1978)]. doi:10.1103/physrevd.17.933

Hu, B. L., and Parker, L. E. (1977). Effect of Gravitation Creation in Isotropically Expanding Universes. *Phys. Let. A.* 63 (3), 214–220. doi:10.1016/0375-9601(77)90880-5

Hu, B. L., and Verdaguer, E. (2008). Stochastic Gravity: Theory and Applications. *Living Rev. Relativ.* 11, 3. 2008. arXiv: 0802.0658 [gr-qc]. doi:10.12942/lrr-2008-3

Hu, B. L., and Verdaguer, E. (2020). "Semiclassical and Stochastic Gravity: Quantum, Field Effects on Curved Spacetime," in *Cambridge Monographs on Mathematical Physics* (Cambridge: Cambridge University Press).

Jordan, R. D. (1987). Stability of Flat Spacetime in Quantum Gravity. *Phys. Rev. D* 36, 3593–3603. doi:10.1103/physrevd.36.3593

Jordan, R. (1986). Effective Field Equations for Expectation Values. *Phys. Rev. D* 33, 444454. doi:10.1103/physrevd.33.444

Kantowski, R. (1969). Corrections in the Luminosity-Redshift Relations of the Homogeneous Fried-Mann Models. *ApJ* 155, 89. doi:10.1086/149851

Kiefer, C. (1987). Continuous Measurement of Mini-Superspace Variables by Higher Multipoles. *Class. Quan. Grav.* 4, 1369–1382. doi:10.1088/0264-9381/4/5/031

Kiefer, C., and Singh, T. P. (1991). Quantum Gravitational Corrections to the Functional Schrödinger Equation. *Phys. Rev. D* 44, 1067–1076. doi:10.1103/physrevd.44.1067

Kiefer, C. (2007). *Quantum Gravity*. Second Edition. Oxford: Oxford University Press.

Kiefer, C. (1994). "The Semiclassical Approximation to Quantum Gravity," in *Lect. Notes Phys. 434*. Editors J. Ehlers and H. Friedrich, pp. 170–212. arXiv: gr-qc/9312015.

Kiefer, C. (1994). " The Semiclassical Approximation to Quantum Gravity". In: Lect. Notes Phys. *434*. Ed. by H. J. Ehlers Friedrich, pp. 170–212. arXiv: gr- qc/9312015. doi:10.1007/3-540-58339-4_19

Kolb, E. W., Marra, V., and Matarrese, S. (2010). Cosmological Background Solutions and Cosmological Backreactions. *Gen. Relativ Gravit.* 42, 1399–1412. arXiv: 0901.4566 [astro-ph.CO]. doi:10.1007/s10714-009-0913-8

Kolb, E. W., Matarrese, S., Notari, A., and Riotto, A. (2005). The Effect of Inhomogeneities on the Expansion Rate of the Universe. *Phys. Rev. D* 71, 023524. arXiv: hep-ph/0409038. doi:10.1103/physrevd.71.023524

Koksbang, S. M. (2019). Another Look at Redshift Drift and the Backreaction Conjecture. *J. Cosmol. Astropart. Phys.* JCAP *10*, 2019, 036. arXiv: 1909.13489 [astro-ph.CO]. doi:10.1088/1475-7516/2019/10/036

Koksbang, S. M. (2020). Observations in Statistically Homogeneous, Locally Inhomogeneous Cosmological Toy Models without FLRW Backgrounds. *Mon. Not. Roy. Astron. Soc.* 498, L135–L139. arXiv: 2008.07108 [astro-ph.CO]. doi:10.1093/mnrasl/slaa14610.1093/mnrasl/slaa146

Koksbang, S. M. (2021). Searching for Signals of Inhomogeneity Using Multiple Probes of the Cosmic Expansion Rate H(z). *Phys. Rev. Lett.* 126, 231101. arXiv: 2105. 11880 [astro-ph.CO]. doi:10.1103/PhysRevLett.126.231101

Krasinski, A., and Bolejko, K. (2011). Redshift Propagation Equations in the β' = 0 Szekeres Models. *Phys. Rev. D* 83, 083503. arXiv: 1007.2083 [gr-qc].

Kristian, J., and Sachs, R. K. (1966). Observations in Cosmology. *ApJ* 143, 379–399. doi:10.1086/148522

Lemaître, A. G. (1931). A Homogeneous Universe of Constant Mass and Increasing Radius Accounting for the Radial Velocity of Extra-galactic Nebulae. *Monthly Notices R. Astronomical Soc.* 91 (5), 483–490.

Li, N., and Schwarz, D. (2008). Scale Dependence of Cosmological Backreaction. *Phys. Rev. D* 78, 083531. arXiv: 0710.5073 [astro-ph]. doi:10.1103/physrevd.78.083531

Lindquist, R. W., and Wheeler, J. A. (1957). Dynamics of a Lattice Universe by the Schwarzschild-Cell Method. *Rev. Mod. Phys.* 29 (3), 432–443. doi:10.1103/revmodphys.29.432

Löffler, F., Faber, J., Bentivegna, E., Bode, T., Diener, P., Haas, R., et al. (2012). The Einstein Toolkit: A Community Computational Infrastructure for Relativistic Astrophysics. *Class. Quan. Grav.* 29, 115001. arXiv: 1111.3344 [gr-qc]. doi:10.1088/0264-9381/29/11/115001

Lombardo, F., and Mazzitelli, F. D. (1996). Coarse Graining and Decoherence in Quantum Field Theory. *Phys. Rev. D* 53, 2001–2011. arXiv: hep-th/9508052. doi:10.1103/physrevd.53.2001

Losic, B., and Unruh, W. G. (2008). Cosmological Perturbation Theory in Slow-Roll Spacetimes. *Phys. Rev. Lett.* 101, 111101. arXiv: 0804.4296 [gr-qc]. doi:10.1103/PhysRevLett.101.111101

Losic, B., and Unruh, W. G. (2005). Long-wavelength Metric Backreactions in Slow-Roll Inflation. *Phys. Rev. D* 72, 123510. arXiv: gr-qc/0510078. doi:10.1103/PhysRevD.72.123510

Marozzi, G., Vacca, G. P., and Brandenberger, a. R. H. (2013). Cosmological Backreaction for a Test Field Observer in a Chaotic Inflationary Model. *J. Cosmol. Astropart. Phys. JCAP 02*, 2013, 027. arXiv: 1212.6029 [hep-th]. doi:10.1088/1475-7516/2013/02/027

Matsui, H., and Watamura, N. (2020). Quantum Spacetime Instability and Breakdown of Semiclassical Gravity. *Phys. Rev. D* 101.2, 025014. arXiv: 1910. 02186 [gr-qc]. doi:10.1103/physrevd.101.025014

Macpherson, H., Price, D., and Laskv, P. (2019). Einstein's Universe: Cosmological Structure Formation in Numerical Relativity. *Phys. Rev. D* 99 (6), 063522. arXiv: 1807.01711 [astro-ph.CO].

Manzano, D. (2020). A Short Introduction to the Lindblad Master Equation. *AIP Adv.* 10, 025106. doi:10.1063/1.5115323

Marra, V., Kolb, E. W., and Matarrese, S. (2008). Light-cone Averages in a Swiss-Cheese Universe. *Phys. Rev. D* 77, 023003. arXiv: 0710.5505 [astro-ph]. doi:10.1103/physrevd.77.023003

Martínez, F. B., and Olmedo, J. (2016). Primordial Tensor Modes of the Early Universe. *Phys. Rev. D* 93, 124008. arXiv:1605.04293 [gr-qc]. doi:10.1103/physrevd.93.124008

Matsui, H., and Watamura, N. (2020). Quantum, Spacetime Instability and Breakdown of Semiclassical Gravity. *Phys. Rev. D* 101 (2), 025014. arXiv: 1910.02186 [gr-qc]. doi:10.1103/physrevd.101.025014

Meda, P., Pinamonti, N., and Siemssen, D. (2020). Existence and Uniqueness of Solutions of the Semiclassical, Einstein Equation in Cosmological Models. Available at: arXiv: 2007.14665 [math-ph] (Accessed July 29, 2020).

Mertens, J. B., Giblin, J. T., and Starkman, G. D. (2016). Integration of Inhomogeneous Cosmological Spacetimes in the BSSN Formalism. *Phys. Rev. D* 93, 124059. arXiv: 1511.01106 [gr-qc]. doi:10.1103/physrevd.93.124059

Mukhanov, V. F. (2005). *Physical Foundations of Cosmology*. Cambridge: Cambridge University Press.

Mukhanov, V. F. (1988). Quantum, Theory of Gauge Invariant Cosmological Perturbations. *Sov. Phys. JETP* 67, 1297–1302.

Mukhanov, V. F., Abramo, L. R. W., and Brandenberger, R. H. (1997). Backreaction Problem for Cosmological Perturbations. *Phys. Rev. Lett.* 78, 1624–1627. arXiv: gr-qc/9609026. doi:10.1103/physrevlett.78.1624

Neuser, J., Schander, S., and Thiemann, T. (2019). Quantum Cosmological Backreactions II: Purely Homogeneous Quantum Cosmology. Available at: arXiv: 1906.08185 [gr-qc] (Accessed June 19, 2019).

Panati, G., Spohn, H., and Teufel, S. (2003). Space-Adiabatic Perturbation Theory. *Adv. Theor. Math. Phys.* 7, 145–204. arXiv: math-ph/0201055. doi:10.4310/atmp.2003.v7.n1.a6

Paranjape, A. (2012). "Averaging the Inhomogeneous Universe," in *Vignettes in Gravitation and Cosmology*, 77–113. doi:10.1142/9789814322072_0004

Paranjape, A., and Singh, T. P. (2008). Cosmic Inhomogeneities and Averaged Cosmological Dynamics. *Phys. Rev. Lett.* 101, 181101. 2008. arXiv: 0806.3497 [astro-ph]. doi:10.1103/physrevlett.101.181101

Paranjape, A., and Singh, T. P. (2007). The Spatial Averaging Limit of Covariant Macroscopic Gravity: Scalar Corrections to the Cosmological Equations. *Phys. Rev. D* 76, 044006, 2007. arXiv: gr-qc/0703106. doi:10.1103/physrevd.76.044006

Parker, L. E., and Raval, A. (1999). Nonperturbative Effects of Vacuum Energy on the Recent Expansion of the Universe, [Erratum: Phvs. Rev. D 67, 029901 (2003)]. *Phys. Rev. D* 60, 063512. arXiv: gr-qc/9905031. doi:10.1103/physrevd.60.063512

Parker, L., and Fulling, S. A. (1974). Adiabatic Regularization of the Energy-Momentum Tensor of a Quantized Field in Homogeneous Spaces. *Phys. Rev. D* 9, 341–354. doi:10.1103/physrevd.9.341

Pattison, C., Vennin, V., Assadullahi, H., and Wands, D. (2019). Stochastic Inflation beyond Slow Roll. *J. Cosmol. Astropart. Phys.* JCAP *07*, 2019, 031. arXiv: 1905.06300 [astro-ph.CO]. doi:10.1088/1475-7516/2019/07/031

Paz, J. P., and Sinha, S. (1992). Decoherence and Back Reaction in Quantum Cosmology: Multidimensional Minisuperspace Examples. *Phys. Rev. D* 45, 2823–2842. doi:10.1103/physrevd.45.2823

Paz, J. P., and Sinha, S. (1991). Decoherence and Back Reaction: The Origin of the Semiclassical Einstein Equations. *Phys. Rev. D* 44, 1038–1049. doi:10.1103/physrevd.44.1038

Peebles, P. J. E. (1982). Large Sclae Background Temperature and Mass Fluctuations Due to Scale- Invariant Primeval Perturbations. *Astrophys. J.* 263, L1. doi:10.1086/183911

Peebles, P. J. E., Alimi, J.-M., and Fuözfa, A. (2010). Phenomenology of the Invisible Universe. *AIP Conf. Proc.* 1241, 175182. arXiv: 0910.5142 [astro-ph.CO]. doi:10.1063/1.3462631

Peebles, P. J. E. (2010). "Phenomenology of the Invisible Universe," in AIP Conference Proceedings. 1241, 175–182. arXiv: 0910.5142 [astro-ph.CO].

Peebles, P. J. E., and Ratra, B. (2003). "The Cosmological Constant and Dark Energy," in *Rev. Mod. Phys.* 75. Editor J-P. Hsu and D. Fine, pp. 559–606. arXiv: astro-ph/0207347. doi:10.1103/revmodphys.75.559

Penzias, A. A., and Wilson, R. W. (1965). A Measurement of Excess Antenna Temperature at 4080 Mc/s. *ApJ* 142, 419–421. doi:10.1086/148307

Perlmutter, S., Aldering, G., Goldhaber, G., Knop, R. A., Nugent, P., Castro, P. G., et al. (1999). Measurements of Ω and Λ from 42 High-Redshift Supernovae. *ApJ* 517, 565–586. arXiv: astro-ph/9812133. doi:10.1086/307221

Pesce, D. W. T., Braatz, J. A., Reid, M. J., Riess, A. G., Scolnic, D., Condon, J. J., et al. (2020). The Megamaser Cosmology Project. XIII. Combined Hubble Constant Constraints. *Astrophys. J. Lett.* 891 (1), L1. arXiv: 2001.09213 [astro-ph.CO]. doi:10.3847/2041-8213/ab75f0

Pinamonti, N. (2011). On the Initial Conditions and Solutions of the Semiclassical Einstein Equations in a Cosmological Scenario. *Commun. Math. Phys.* 305, 563–604. arXiv: 1001.0864 [gr-qc]. doi:10.1007/s00220-011-1268-z

Pinamonti, N., and Siemssen, D. (2015). Global Existence of Solutions of the Semiclassical Einstein Equation for Cosmological Spacetimes. *Commun. Math. Phys.* 334 (1), 171–191. arXiv: 1309. 6303 [math-ph]. doi:10.1007/s00220-014-2099-5

Radzikowski, λ. I. J. (2008). Stable, Renormalizable, Scalar Tachyonic Quantum, Field Theory with, Chronology Protection. Available at: arXiv: 0804.4534 [math-ph] (Accessed April 29, 2008).

Ramsey, S. A., and Hu, B. L. (1997). Nonequilibrium Inflaton Dynamics and Reheating: Back Reaction of Parametric Particle Creation and Curved Spacetime Effects, [Erratum: Phys. Rev. D 57, 3798 (1998)]. *Phys. Rev. D* 56, 678–705. arXiv: hep-ph/9706207. doi:10.1103/physrevd.56.678

Riess, A. G., Casertano, S., Yuan, W., Macri, L. M., and Scolnic, D. (2019). Large Magellanic Cloud Cepheid Standards Provide a 1% Foundation for the Determination of the Hubble Constant and Stronger Evidence for Physics beyond ΛCDM. *Astrophys. J.* 876 (1), 85, 2019. arXiv: 1903.07603 [astro-ph.CO].

Riess, A. G., Filippenko, A. V., Challis, P., Clocchiatti, A., Diercks, A., Garnavich, P. M., et al. (1998). Observational Evidence from Supernovae for an Accelerating Universe and a Cosmological Constant. *Astron. J.* 116, 1009–1038. arXiv: astro-ph/9805201. doi:10.1086/300499

Robertson, H. P. (1933). Relativistic Cosmology. *Rev. Mod. Phys.* 5, 62–90. doi:10.1103/revmodphys.5.62

Räsänen, S. (2009). Light Propagation in Statistically Homogeneous and Isotropic Dust Universes. *J. Cosmol. Astropart. Phys.* JCAP *02*, 2009, 011. arXiv: 0812.2872 [astro-ph]. doi:10.1088/1475-7516/2009/02/011

Räsänen, S. (2010). Light Propagation in Statistically Homogeneous and Isotropic Universes with General Matter Content. *J. Cosmol. Astropart. Phys.* JCAP *03*, 2010, 018. arXiv: 0912.3370 [astro-ph.CO]. doi:10.1088/1475-7516/2010/03/018

Ross, A. J., Bautista, J., Tojeiro, R., Alam, S., Bailey, S., Burtin, E., et al. (2020). The Completed SDSS-IV Extended Baryon Oscillation Spectroscopic Survey: Large-Scale Structure Catalogues for Cosmological Analysis. *Mon. Not. Roy. Astron. Soc.* 498 (2), 2354–2371. arXiv: 2007.09000 [astro-ph.CO]. doi:10.1093/mnras/staa2416

Rovelli, C., and Vidotto, F. (2008). Stepping Out of Homogeneity in Loop Quantum Cosmology. *Class. Quan. Grav.* 25, 225024. arXiv: 0805.4585 [gr-qc]. doi:10.1088/0264-9381/25/22/225024

Rovelli, C. (2010). "Quantum Gravity," in *Cambridge Monographs on Mathematical Physics*. Cambridge: Cambridge University Press.

Schander, S., and Thiemann, T. (2019a). Quantum Cosmological Backreactions I: Cosmological Space Adiabatic Perturbation Theory. Available at: arXiv: 1906.08166 [gr-qc] (Accessed June 19, 2019).

Schander, S., and Thiemann, T. (2019b). Quantum, Cosmological Backreactions III: Deparametrized Quantum, Cosmological Perturbation Theory. Available at: arXiv: 1906.08194 [gr-qc] (Accessed June 19, 2019).

Schander, S., and Thiemann, T. (2019c). Quantum, Cosmological Backreactions IV: Constrained Quantum, Cosmological Perturbation Theory. Available at: arXiv: 1909.07271 [gr-qc] (Accessed September 16, 2019).

Schlosshauer, M. A. (2007). *Decoherence and the Quantum-To-Classical Transition*. Berlin, Heidelberg: Springer-Verlag.

Sinha, S., and Hu, B. L. (1991). Validity of the Minisuperspace Approximation: An Example from Interacting Quantum Field Theory. *Phys. Rev. D* 44, 1028–1037. doi:10.1103/physrevd.44.1028

Spergel, D. N. (2015). The Dark Side of Cosmology: Dark Matter and Dark Energy. *Science* 347, 1100–1102. doi:10.1126/science.aaa0980

Starobinsky, A. A. (1987). "A New Type of Isotropic Cosmological Models without Singularity," in *Quantum Cosmology, Advanced Series in Astrophysics and Cosmology* 3. Editors I. M. Khalatnikov and V. P. Mineev, pp. 130–133.

Starobinsky, A. A. (1982). "Dynamics of Phase Transition in the New Inflationary Universe Scenario and Generation of Perturbations". In: *Phys. Lett. B* 117, 175–178.

Starobinsky, A. A. (1988). "Stochastic de Sitter (inflationary) stage in early Universe". In: *Field Theory, Quantum Gravity and Strings. Lecture Notes in Physics*. Editors H. J. de Vega and N. Sánchez. Springer, Berlin, Heidelberg.

Starobinsky, A. A., and Yokoyama, J. i. (1994). Equilibrium state of a self-interacting scalar field in the de Sitter background. *Phys. Rev. D* 50, 6357–6368. arXiv: astro-ph/9407016. doi:10.1103/physrevd.50.6357

Stottmeister, A. (2015). On the Embedding of Quantum, Field Theory on Curved Spacetimes into Loop Quantum Gravity. PhD thesis. Nürnberg: Friedrich-Alexander-Universität Erlangen.

Stottmeister, A., and Thiemann, T. (2016a). Coherent States, Quantum Gravity, and the Born-Oppenheimer Approximation. I. General Considerations. *J. Math. Phys.* 57 (6), 063509. arXiv: 1504.02169 [math-ph]. doi:10.1063/1.4954228

Stottmeister, A., and Thiemann, T. (2016b). Coherent States, Quantum Gravity, and the Born- Oppenheimer Approximation. II. Compact Lie Groups. *J. Math. Phys.* 57, 073501. arXiv: 1504.02170 [math-ph]. doi:10.1063/1.49548037

Stottmeister, A., and Thiemann, T. (2016c). Coherent States, Quantum Gravity, and the Born-Oppenheimer Approximation. III.: Applications to Loop Quantum Gravity. *J. Math. Phys.* 57, 083509. arXiv: 1504.02171 [math-ph]. doi:10.1063/1.4960823

Sussman, R. A. (2011). Back-reaction and Effective Acceleration in Generic LTB Dust Models. *Class. Quan. Grav.* 28, 235002. arXiv: 1102.2663 [gr-qc]. doi:10.1088/0264-9381/28/23/235002

Teufel, S. (2003). "Adiabatic Perturbation Theory in Quantum Dynamics," in *Lecture Notes in Mathematics*. Berlin: Springer-Verlag, 1821.

Thiemann, T. (2008). *Modern Canonical Quantum General Relativity*. Cambridge: Cambridge University Press.

Tomita, K. (2000). Distances and Lensing in Cosmological Void Models. *Astrophys. J.* 529, 38. arXiv: astro-ph/9906027.

Tsamis, N. C., and Woodard, R. P. (1993). Relaxing the Cosmological Constant. *Phys. Lett. B* 301, 351–357. doi:10.1016/0370-2693(93)91162-G

Tsamis, N. C., and Woodard, R. P. (1996). Quantum Gravity Slows Inflation. *Nucl. Phys. B* 474, 235–248. arXiv: hep-ph/9602315. doi:10.1016/0550-3213(96)00246-5

Tsamis, N. C., and Woodard, R. P. (2005). Stochastic Quantum Gravitational Inflation. *Nucl. Phys. B* 724, 295–328. arXiv: gr-qc/0505115. doi:10.1016/j.nuclphysb.2005.06.031

Unruh, W. G. (1998). " Cosmological Long Wavelength Perturbations". In: arXiv: astro-ph/9802323.

Vidotto, F. (2011). Spinfoam Cosmology. *J. Phys. Conf. Ser.* 314, 012049, 2011 . arXiv: 1011.4705 [gr-qc]. doi:10.1088/1742-6596/314/1/012049

Vilenkin, A. (1989). Interpretation of the Wave Function of the Universe. *Phys. Rev. D* 39, 1116–1122. doi:10.1103/physrevd.39.1116

Wald, R. M. (1977). The Back Reaction Effect in Particle Creation in Curved Spacetime. *Commun. Math. Phys.* 54, 1–19. doi:10.1007/bf01609833

Wald, R. M. (1978). Trace Anomaly of a Conformally Invariant Quantum Field in Curved Spacetime. *Phys. Rev. D* 17, 1477–1484. doi:10.1103/physrevd.17.1477

Walker, A. G. (1937). On Milne's Theory of World-Structure. *Proc. Lond. Math. Soc.* s2-42 (1), 90–127. doi:10.1112/plms/s2-42.1.90

Wheeler, J. A. (1957). On the Nature of Quantum Geometrodynamics. *Ann. Phys.* 2, 604–614. doi:10.1016/0003-4916(57)90050-7

Wiltshire, D. L. (2009). Average Observational Quantities in the Timescape Cosmology. *Phys. Rev. D* 80, 123512. arXiv: 0909.0749 [astro-ph.CO]. doi:10.1103/physrevd.80.123512

Zalaletdinov, R. (1997). Averaging Problem in General Relativity, Macroscopic Gravity and Using Einstein's Equations in Cosm,ol,ogy. *Bull. Astron. Soc. India* 25, 401–416. arXiv: gr-qc/9703016.

Zalaletdinov, R. (2008). The Averaging Problem in Cosmology and Macroscopic Gravity. *Int. J. Mod. Phys. A.* 23, 1173–1181. arXiv: 0801.3256 [gr-qc]. doi:10.1142/s0217751x08040032

Zel'dovich, Y., Einasto, J., and Shandarin, S. (1982). Giant Voids in the Universe. *Nature* 300, 407–413.

Zel'dovich, Y., and Starobinsky, A. A. (1972). Particle Production and Vacuum Polarization in an Anisotropic Gravitational Field. *Sov. Phys. JETP* 34, 1159–1166.

Conflict of Interest: The authors declare that the research was conducted in the absence of any commercial or financial relationships that could be construed as a potential conflict of interest.

frontiers in Astronomy and Space Sciences

ORIGINAL RESEARCH
published: 26 July 2021
doi: 10.3389/fspas.2021.683649

Quantum Fluctuations in the Effective Relational GFT Cosmology

L. Marchetti[1,2,3] *and D. Oriti*[4]*

[1]Dipartimento di Fisica, Università di Pisa, Pisa, Italy, [2]Arnold Sommerfeld Center for Theoretical Physics, Ludwig-Maximilians-Universität München, München, Germany, [3]Istituto Nazionale di Fisica Nucleare sez. Pisa, Pisa, Italy, [4]Arnold Sommerfeld Center for Theoretical Physics, Ludwig-Maximilians-Universität München, München, Germany

We analyze the size and evolution of quantum fluctuations of cosmologically relevant geometric observables, in the context of the effective relational cosmological dynamics of GFT models of quantum gravity. We consider the fluctuations of the matter clock observables, to test the validity of the relational evolution picture itself. Next, we compute quantum fluctuations of the universe volume and of other operators characterizing its evolution (number operator for the fundamental GFT quanta, effective Hamiltonian and scalar field momentum). In particular, we focus on the late (clock) time regime, where the dynamics is compatible with a flat FRW universe, and on the very early phase near the quantum bounce produced by the fundamental quantum gravity dynamics.

Keywords: quantum gravity, cosmology: theory, loop quantum cosmology, group field theory, emergent spacetime, relational dynamics

OPEN ACCESS

Edited by:
Guillermo A. Mena Marugán, Instituto de Estructura de la Materia, Spain

Reviewed by:
Etera Livine, Université de Lyon, France
Herman J. Mosquera Cuesta, Departamento Administrativo Nacional de Ciencia, Tecnologia e Innovacion, Colciencias, Colombia
Hanno Sahlmann, Friedrich Alexander University Erlangen-Nuremberg, Germany

***Correspondence:**
D. Oriti
daniele.oriti@physik.lmu.de

Specialty section:
This article was submitted to Cosmology, a section of the journal Frontiers in Astronomy and Space Sciences

Received: *21 March 2021*
Accepted: *14 June 2021*
Published: *26 July 2021*

Citation:
Marchetti L and Oriti D (2021) Quantum Fluctuations in the Effective Relational GFT Cosmology. Front. Astron. Space Sci. 8:683649. doi: 10.3389/fspas.2021.683649

1 INTRODUCTION

Three closely related challenges have to be overcome by fundamental quantum gravity approaches, especially those based on discrete or otherwise non-geometric, non-spatiotemporal entities, in order to make contact with General Relativity and observed gravitational physics, based on effective (quantum) field theory. The first is the continuum limit/approximation leading from the fundanental entities and their quantum dynamics to an effective continuum description of spacetime and geometry, with matter fields living on it (Oriti et al., 2017). This requires a mixture of renormalization analysis of the fundamental quantum dynamics and of coarse-graining of its states and observables. The second is a classical limit/approximation of the sector of the theory corresponding to (would-be) spacetime and geometry, to show that indeed an effective classical dynamics compatible with General Relativity and observations emerges, once in the continuum description (Oriti et al., 2017). The third is a definition of suitable observables that can, on the one hand, give a physical meaning to both continuum and classical approximations in terms of spacetime geometry and gravity, and, on the other hand, allow to make contact with phenomenology (Marchetti and Oriti, 2021). In particular, suitable observables are needed to recast the dynamics of the quantum gravity system, in the same continuum and classical approximations, at least, in more customary local evolutionary terms, i.e. in the form of evolution of local quantities with respect to some notion of time (Giddings et al., 2006; Tambornino, 2012). This, in fact, is the language of effective field theory used in gravitational and high energy physics. The first two challenges are standard in any quantum many-body system, but are made more difficult in the quantum gravity context by the necessary background (and spacetime) independence of the fundamental theory, which requires adapting non-trivially standard renormalization, coarse-graining and classical approximation techniques. The same background independence, closely related at the formal level to the diffeomorphism invariance of General Relativity (Giulini, 2007), makes the third

challenge a peculiar difficulty in quantum gravity. Locality or temporal evolution cannot be defined with respect to any manifold point or direction and generic configurations (classical and even less quantum) of the gravitational field (or what replaces it at the fundamental level) do not single out any such notions either. Beside special situations (e.g. in the presence of asymptotic boundaries) local and temporal geometric observables can be understood as relational quantities, i.e. defined as a relation between geometry and other dynamical matter degrees of freedom, that provide a notion of local regions and temporal direction when used as physical reference frames. In other words, and restricting to the issue of time (Isham, 1992; Kuchař, 2011), the relational perspective holds that the absence of preferred, external or background notions of time in generally relativistic quantum theories does not mean that there is no quantum evolution, but only that evolution should be defined with respect to internal, physical degrees of freedom (Höhn et al., 1912; Tambornino, 2012).

From the perspective of "Quantum General Relativity" theories (Rovelli, 2004; Thiemann, 2007), in which the fundamental entities remain (quantized) continuum fields, the relational strategy to define evolution boils down to either the selection of a relational clock at the classical level, in terms of which the remaining subsystem is canonically quantized ("tempus ante quantum" (Isham, 1992; Anderson, 2012)) or the definition of an appropriate clock-neutral quantization (e.g., Dirac quantization) and the representation of classical complete (i.e., relational) observables (Rovelli, 2002; Dittrich, 2006; Dittrich, 2007; Tambornino, 2012) on the physical Hilbert space resulting from such quantization ("tempus post quantum" (Isham, 1992; Anderson, 2012)). Of course, while the first approach (deparametrization) is technically easier, when possible, the second one is in principle preferable because manifestly "clock covariant," since it treats all the quantum degrees of freedom on the same footing, thus allowing in principle to switch from one relational clock to another (see (Bojowald et al., 2011a; Bojowald et al., 2011b; Hoehn et al., 2011; Hoehn and Vanrietvelde, 2018) for more details).

In "emergent quantum gravity" theories, in which the fundamental degrees of freedom are pre-geometric and non-spatiotemporal, and not identified with (quantized) continuum fields, the situation has an additional layer of complications (Marchetti and Oriti, 2021). Any kind of continuum notion in such theories is expected to emerge in a proto-geometric phase of the theory from the collective behavior of the fundamental entities, i.e. only at an effective and approximate level. Among such continuum notions there is any notion of relational dynamics, as we understand it from the generally relativistic perspective.

In the tensorial group field theory formalism (TGFT) for quantum gravity (see (Krajewski, 2011; Oriti, 2011; Carrozza, 2016; Gielen and Sindoni, 2016) for general introductions), comprising random tensor models, tensorial field theories and group field theories (closely related to canonical loop quantum gravity, and providing a reformulation of lattice gravity path integrals and spin foam models), we are in this last emergent spacetime situation (Oriti, 1807).

The issue of the continuum limit is tackled adapting standard renormalization group (Carrozza, 2016) and statistical methods for quantum field theories, leading also to several results concerning the critical behavior of a variety of models. In the more quantum geometric group field theory (GFT) models (Magnen et al., 2009; Baratin et al., 2014; Ben Geloun et al., 2016; Carrozza et al., 2017; Carrozza and Lahoche, 2017; Geloun et al., 2018) (see also (Finocchiaro and Oriti, 2004) and references therein), one can take advantage of the group theoretic data and of their discrete geometric interpretation to give tentative physical meaning to suitable quantum states and to specific regimes of approximation of their quantum dynamics (Oriti et al., 2015). Specifically, the hydrodynamic regime of models of 4d quantum geometry admits a cosmological interpretation and has been analyzed in some detail for simple condensate states (Gielen et al., 2014; Gielen and Sindoni, 2016; Oriti et al., 2016). The corresponding effective dynamics has been recast in terms of cosmological observables both via the relational strategy and by a deparametrization with respect to the added matter degrees of freedom (Gielen and Sindoni, 2016; Oriti et al., 2016; Oriti, 2017; Pithis and Sakellariadou, 2019; Wilson-Ewing, 2019; Marchetti and Oriti, 2021). Among many results (Gielen and Menéndez-Pidal, 2005; Gielen, 2014; Pithis et al., 2016; Pithis and Sakellariadou, 2017; Adjei et al., 2018; Gielen and Polaczek, 2020), the correct classical limit in terms of a flat FRW universe has been obtained rather generically for large expectation values of the volume operator at late relational (clock) times (Oriti et al., 2016; Gielen and Polaczek, 2020; Marchetti and Oriti, 2021), and the big bang singularity is resolved, with a similar degree of generality (Oriti et al., 2016; Gielen and Polaczek, 2020), and replaced with a quantum bounce. In addition, the fundamental quantum gravity interactions seem to be able produce (at least for some regime of parameters) an accelerated cosmological expansion, possibly long-lasting, without introducing additional matter (e.g. inflaton) fields (de Cesare et al., 2016).

The above results have been obtained looking at the expectation values of interesting cosmological observables in (the simplest) GFT condensate states. A careful analysis of quantum fluctuations of the same observables is then important to test the validity of the hydrodynamic description in terms of expectation values, in particular in the large volume limit when one expects classical GR to be valid, but also close to the big bounce regime where one expects them to be strong but still controllable if the bouncing scenario is to be trustable at all. Moreover, the relational evolution relies on the chosen physical (matter) degrees of freedom to behave nicely enough to serve as a good clock, and this would not be the case if subject to strong quantum fluctuations. This analysis of quantum fluctuations is what we perform in this paper.

The precise context in which we perform the analysis is that of the effective relational dynamics framework developed in (Marchetti and Oriti, 2021).

This construction is motivated by the argued usefulness and conceptual importance of effective approaches to relational dynamics (Bojowald et al., 2009; Bojowald and Tsobanjan, 2009; Bojowald et al., 2011a; Bojowald et al., 2011b; Bojowald,

2012), and it was suggested a general framework in which the latter is realized in a "tempus post quantum" approach, but only at a proto-geometric level, i.e. after some suitable coarse graining, the one provided by the GFT hydrodynamic approximation (or its improvements).

Besides its conceptual motivations, this effective relational framework improves on previous relational constructions in GFT cosmology providing a mathematically more solid definition of relational observables, allowing the explicit computation of quantum fluctuations, which will be one the main objectives of the present work.

This improved effective relational dynamics was obtained by the use of "Coherent Peaked States" (CPSs), in which the fundamental GFT quanta collectively (and only effectively) reproduce the classical notion of a spacelike slice of a spacetime foliation labeled by a massless scalar field clock. For this effective foliation to be meaningful quantum flctuations of the clock observables should be small enough (e.g. in the sense of relative variances). When this is the case, the relevant physics is captured by averaged relational dynamics equations for the other observables of cosmological interest, like the universe volume or the matter energy density or the effective Hamiltonian. The purpose of this paper is to explore under which conditions this averaged relational dynamics is meaningful and captures the relevant physics, checking quantum fluctuation for both clock observables and cosmological, geometric ones.

2 EFFECTIVE RELATIONAL FRAMEWORK FOR GFT CONDENSATE COSMOLOGY

The GFT condensate cosmology framework is based on three main ingredients (see e.g. (Gielen and Sindoni, 2016) for a review):

1. The identification of appropriate states which admit an interpretation in terms of (homogeneous and isotropic) cosmological 3-geometries;
2. The construction of an appropriate relational framework allowing to describe e.g. the (averaged) geometric quantities (in the homogeneous and isotropic case, the volume operator) as a function of a matter field (usually a minimally coupled massless scalar field);
3. The extraction of a mean field dynamics from the quantum equations of motion of the microscopic GFT theory, which in turn determines the relational evolution of the aforementioned (averaged) volume operator.

In this section, we will review the concrete realization of the first two steps and of the first part of the third step (i.e. the extraction of a mean field dynamics), in order to prepare the ground for the calculation of expectation values, first, and the quantum fluctuations of geometric observables of cosmological interest. More precisely, the first step will be reviewed in **Section 2.1**, while the second and the first part of the third one will be discussed in **Sections 2.2**, **Sections 2.3**, respectively. The second part of the last step, which requires the detailed computations of expectation values performed in **Section 4.1**, will be instead discussed in **Section 4.2**.

2.1 The Kinematic Structure of GFT Condensate Cosmology

In the Group Field Theory (GFT) formalism (Krajewski, 2011; Oriti, 2011; Carrozza, 2016; Gielen and Sindoni, 2016), one aims at a microscopic description of spacetime in terms of simplicial building blocks (Reisenberger and Rovelli, 2001). The behavior of the fundamental "atoms" that spacetime has dissolved into is described by a (in general, complex) field $\varphi : G^d \to \mathbb{C}$ defined on d copies of a group manifold, $\varphi(g_I) \equiv \varphi(g_1, \ldots, g_d)$. By appropriate choices of the dimension d, of the group manifold G, of the combinatorial pairing of field arguments in the action, and of course its functional form, the perturbative expansion of the theory produces amplitudes that can be seen as a simplicial gravity path-integral (Baratin and Oriti, 2012), with the group-theoretic data entering as holonomies of a discrete gravitational connection. Concretely, most 4d gravity models use $d = 4$ (i.e., the spacetime dimension), and $G = \mathrm{SL}(2,\mathbb{C})$ (local gauge group of gravity), its Euclidean version, $\mathrm{Spin}(4)$, or $\mathrm{SU}(2)$, once an appropriate embedding into $\mathrm{SL}(2,\mathbb{C})$ or $\mathrm{Spin}(4)$ is specified. This latter choice allows for an explicit connection of the GFT quantum states with those in the kinematical Hilbert space of LQG (Gielen and Sindoni, 2016; Oriti, 2016). From now on, therefore, we will specialize to $d = 4$ and $G = \mathrm{SU}(2)$.

Indeed, in this case, the fundamental quanta of the field, assuming it satisfies the "closure" condition $\varphi(g_I) = \varphi(g_I h)$ for each $h \in G$, can be interpreted as 3-simplices (tetrahedra) whose faces are decorated with an equivalence class of geometrical data $[\{g_I\}] = \{\{g_I h\}, h \in G\}$ or, in the dual picture, as open spin-networks, i.e., nodes from which four links are emanating, each of which is associated to group-theoretical data. From this dual perspective, the closure condition becomes the imposition of invariance under local gauge transformations which act on the spin-network vertex.

2.1.1 The GFT Fock Space

The Fock space of such "atoms of space" can be constructed in terms of the field operators $\hat{\varphi}(g_I)$ and $\hat{\varphi}^\dagger(g_I)$ subject to the following commutation relations:

$$\left[\hat{\varphi}(g_I), \hat{\varphi}^\dagger\left(g'_I\right)\right] = \|_G\left(g_I, g'_I\right), \tag{1a}$$

$$\left[\hat{\varphi}(g_I), \hat{\varphi}\left(g'_I\right)\right] = \left[\hat{\varphi}^\dagger(g_I), \hat{\varphi}^\dagger\left(g'_I\right)\right] = 0, \tag{1b}$$

together with a vacuum state $|0\rangle$ annihilated by $\hat{\varphi}$, so that the action of $\hat{\varphi}^\dagger(g_I)$ on $|0\rangle$ creates a "quantum of space" with (an equivalence class of) geometric data $\{g_I\}$. The right-hand-side of **Eq. 1a** represents the identity in the space of gauge-invariant (i.e., right diagonal invariant) fields (Gielen et al., 2014).

GFT "$(m+n)$-body operators" $\hat{O}_{n+m}$

$$\hat{O}_{n+m} \equiv \int (\mathrm{d}g_I)^m (\mathrm{d}h_I)^n O_{m+n}\left(g_I^1, \ldots, g_I^m, h_I^1, \ldots, h_I^n\right) \times \prod_{i=1}^{m} \hat{\varphi}^\dagger\left(g_I^i\right) \prod_{j=1}^{n} \hat{\varphi}\left(h_I^j\right), \tag{2}$$

are then constructed from the matrix elements O_{m+n}, whose form can be determined from simplicial geometric or canonical approaches like Loop Quantum Gravity (LQG) (Ashtekar and Lewandowski, 2004; Rovelli, 2004; Thiemann, 2007). The same kind of construction can of course be performed in any representation of the relevant Hilbert space. We will work with explicit examples of such operators (number operator, volume operator, massless scalar field operator, etc.) in the cosmological context.

Coupling to a Massless Scalar Field

Following (Marchetti and Oriti, 2021; Oriti et al., 2016), a scalar field is minimally coupled to the discrete quantum geometric data, with the purpose of using it as a relational clock at the level of GFT hydrodynamics. This is done by adding to the GFT field and action the degree of freedom associated to a scalar field in such a way that the GFT partition function, once expanded perturbatively around the Fock vacuum, can be identified with the (discrete) path-integral of a model of simplicial gravity minimally coupled with a free massless scalar field (or, equivalently, with the corresponding spin-foam model)[1] (Oriti et al., 2016). Therefore, the field operator changes as follows:

$$\hat{\varphi}(g_I) \quad \rightarrow \quad \hat{\varphi}(g_I, \chi), \tag{3}$$

meaning that the one-particle Hilbert space is now enlarged to $L^2(\mathrm{SU}(2)^4/\mathrm{SU}(2) \times \mathbb{R})$. So, each GFT atom can carry (in the appropriate basis) a value of the scalar field, which is "discretized" on the simplicial structures associated to GFT states and (perturbative) amplitudes (Li et al., 2017). This implies that the commutation relations in (**Eq. 1a**) need to be modified consistently, obtaining

$$[\hat{\varphi}(g_I, \chi), \hat{\varphi}^\dagger(h_I, \chi')] = \mathbb{I}_G(g_I, h_I)\delta(\chi - \chi'). \tag{4}$$

and that operators (**Eq. 2**) in the second quantization picture now involve integrals over the possible values of the massless scalar field (Oriti et al., 2016; Marchetti and Oriti, 2021).

2.1.2 GFT Condensate Cosmology: Kinematics

The Fock space construction described above proves technically very useful in order to address the problem of extraction of continuum physics from GFTs. In particular, in previous works (Gielen, 2014; Oriti et al., 2016), this was exploited to build quantum states that, in appropriate limits, can be interpreted as continuum and homogeneous 3-geometries, thus paving the way to cosmological applications of GFTs. Such states are characterized by a single collective wavefunction, defined over the space of geometries associated to a single tetrahedron or, equivalently (when some additional symmetry conditions are imposed on the wavefunction) over the minisuperspace of homogeneous geometries (Gielen, 2014). For such condensate states then, classical homogeneity is lifted at the quantum level by imposing 'wavefunction homogeneity'. Among the many possible condensate states (characterized by different "gluing" of the fundamental GFT quanta one to another) satisfying the above wavefunction homogeneity, most of the attention was directed toward the simplest GFT coherent states, i.e.,

$$|\sigma\rangle = N_\sigma \exp\Big[\int d\chi \int dg_I \sigma(g_I, \chi)\hat{\phi}^\dagger(g_I, \chi)\Big]|0\rangle, \tag{5}$$

where

$$N_\sigma \equiv e^{-\|\sigma\|^2/2}, \tag{6a}$$

$$||\sigma||^2 = \int \mathrm{d}g_I \mathrm{d}\chi |\sigma(g_I, \chi)|^2 \tag{6b}$$

They satisfy the important property

$$\hat{\varphi}(g_I, \chi)|\sigma\rangle = \sigma(g_I, \chi)|\sigma\rangle, \tag{7}$$

i.e., they are eigenstates of the annihilation operator.

In order to make contact with cosmological geometries, one typically also imposes isotropy on the wave function, requiring the associated tetrahedra to be equilateral. This results in the following condensate wavefunction (Oriti et al., 2016)

$$\sigma(g_I, \chi) = \sum_{j=0}^{\infty} \sigma_{j, \overrightarrow{m}, \iota_+} \mathcal{I}^{jjjj, \iota_+}_{n_1 n_2 n_3 n_4} \sqrt{d^4(j)} \prod_{i=1}^{4} D^j_{m_i n_i}(g_i),$$

where

$$\sigma_{\{j, \overrightarrow{m}, \iota_+\}}(\chi) = \sigma_j(\chi)\overline{\mathcal{I}}^{jjjj, \iota_+}_{m_1 m_2 m_3 m_4}.$$

and where $d(j) = 2j + 1$, j are spin labels, D^j_{mn} are Wigner representation matrices, $\mathcal{I}$ are intertwiners, and $\mathcal{I}^{jjjj, \iota_+}_{m_1 m_2 m_3 m_4}$ is an eigenvector of the LQG volume operator with the largest eigenvalue (Oriti et al., 2016). After imposition of isotropy, σ_j becomes the quantity effectively encoding the physical properties of the state.

2.2 Effective Relational Dynamics Framework and its Implementation in GFT Condensate Cosmology

In (Marchetti and Oriti, 2021), a procedure for extracting an effective relational dynamics framework was proposed for the cosmological context, when one is interested in describing the evolution of some geometric operators with respect of some scalar matter degree of freedom. Since our analysis of quantum fluctuations will take place within such effective relational framework, let us summarize how it is obtained and under which conditions it is expected to be meaningful. In the following, we will analyze also the limits of validity of such conditions.

2.2.1 Effective Relational Evolution of Geometric Observables with Respect to Scalar Matter Degrees of Freedom

The fundamental observables one is interested in are: a "scalar field operator" $\hat{\chi}$, a set of "geometric observables"[2] $\{\widehat{O}_a\}_{a \in S}$ and a

[1]This procedure can in fact be seen as a discrete version of what would be done in a 3rd quantized framework for quantum gravity; indeed, GFT models (like matrix models for 2d gravity) are a discrete realization of the 3rd quantization idea (Gielen and Oriti, 2011).

[2]For instance, in a cosmological context in which one is interested only to homogeneous and isotropic geometries, the volume operator is expected to capture all the geometric properties of the system. In this case, therefore, one only includes this volume operator among the geometric observables of interest.

"number operator" $\widehat{N}$, counting the number of fundamental "quanta of space." Since one is assuming that the theory, at this pre-geometric level, is entirely clock-neutral (and so are all the operators above), the effective relational dynamics is realized through an appropriate choice of a class of states $|\Psi\rangle$ having both an intepretation in terms of continuum geometries[3] (and thus possibly characterizing a proto-geometric phase of the theory) and also carrying a notion of relationality. More precisely, they should allow for the existence of an Hamiltonian operator $\widehat{H}$ such that, for each geometric observable $\widehat{O}_a$,

$$i\frac{\mathrm{d}}{\mathrm{d}\langle\widehat{\chi}\rangle_\Psi}\langle\widehat{O}_a\rangle_\Psi = \left\langle\left[\widehat{H},\widehat{O}_a\right]\right\rangle_\Psi, \tag{8a}$$

at least locally and far enough from singular turning points of the scalar field clock[4]. In order to interpret this evolution as truly relational with respect to the scalar field used as a clock, all the moments of $\widehat{H}$ and of the scalar field momentum $\widehat{\Pi}$ on $|\Psi\rangle$ should be equal. In particular, this implies that the averages of these two operators on $|\Psi\rangle$ should be equal,

$$\langle\widehat{H}\rangle_\Psi = \langle\widehat{\Pi}\rangle_\Psi\,. \tag{8b}$$

This equality was investigated in (Marchetti and Oriti, 2021) in the context of GFT cosmology, and we will discuss it further below.

A further condition that is necessary in order to interpret **Eq. 8a** as a truly relational dynamics involves the smallness of the quantum fluctuations on the matter clock. In (Marchetti and Oriti, 2021), this was imposed by requiring the relative variance of $\widehat{\chi}$ on $|\Psi\rangle$ to be much smaller than one, and to have the characteristic many-body $\langle\widehat{N}\rangle^{-1}$ behavior, i.e.,

$$\delta^2_\chi \ll 1, \qquad \delta^2_\chi \sim \langle\widehat{N}\rangle^{-1}, \tag{9}$$

where the relative variance on $|\Psi\rangle$ is defined as

$$\delta^2_O = \frac{\langle\widehat{O}^2\rangle_\Psi - \langle\widehat{O}\rangle^2_\Psi}{\langle\widehat{O}\rangle^2_\Psi}\,.$$

This is of course formally correct only when one is assuming that the expectation value of $\widehat{\chi}$ is non-zero, as we will discuss further below. When this is not the case, one should define some thresholds which the relative variances should be smaller than (Marchetti and Oriti, 2021).

Let us also notice, that, strictly speaking, one would have to require that all the moments of the scalar field operator higher than the first one are much smaller than one in order to guarantee a negligible impact of quantum fluctuations of the clock on the relational framework. However, one also expects that, being the system fundamentally a many-body system (for which the second condition in (**Eq. 9**) is satisfied), moments higher than the second one get also suppressed in the large N limit which we will be mainly interested in, forming a hierarchy of less and less important quantum effects (typically, in many-body systems, relative moments of order n are suppressed by $\langle N\rangle^{-(n-1)}$, with $n>1$). In the asymptotic $N\to\infty$ regime, therefore, one should be allowed to characterize quantum fluctuations essentially by the behavior of relative variances. This might not be the case, on the other hand, in intermediate regimes of smaller N, where indeed there is no good reason to believe such a hierarchy to be realized. In such cases the impact of quantum fluctuations has to be studied more carefully.

2.2.2 Implementation in GFT Condensate Cosmology: CPSs

The strategy to realize the above framework in the context of GFT condensate cosmology in (Marchetti and Oriti, 2021) made use of Coherent Peaked States (CPSs). These states are constructed so that they can provide, under appropriate approximations, "bona fide" leaves of a relational χ-foliation of spacetime. Given the proto-geometric nature of the states (**Eq. 5**) the idea is to look for a subclass of them characterized by a given value of the relational clock, say χ_0, so that the GFT quanta collectively conspire to the approximate reconstruction of a relational leaf of spacetime labeled by χ_0 itself. Since, in the condensate states (**Eq. 5**) the information about the state is fully encoded in the condensate wavefunction, in (Marchetti and Oriti, 2021) relational proto-geometric states are chosen among those where this wavefunction has a strong peaking behavior:

$$\sigma_\epsilon(g_I,\chi) \equiv \eta_\epsilon(g_I;\chi-\chi_0,\pi_0)\tilde{\sigma}(g_I,\chi)\,, \tag{10}$$

where η_ϵ is the so-called peaking function around χ_0 with a typical width given by ϵ. For instance, one can choose a Gaussian form

$$\eta_\epsilon(\chi-\chi_0,\pi_0) \equiv \mathcal{N}_\epsilon \exp\left[-\frac{(\chi-\chi_0)^2}{2\epsilon}\right]\exp\left[i\pi_0(\chi-\chi_0)\right], \tag{11}$$

where $\mathcal{N}_\epsilon$ is a normalization constant and where it was assumed that the peaking function does not depend on the group variables g_I (the dependence on quantum geometric data is therefore fully encoded in the remaining contribution to the full wavefunction). Further, the reduced wavefunction $\tilde{\sigma}$ was assumed not to spoil the peaking properties[5] of η_ϵ (Marchetti and Oriti, 2021). Since the reduced wavefunction is determined dynamically (see **Section 2.3** below), this constrains the space of admissible solutions to the dynamical equations. However, in the cosmological case, this will not result on discarding any solution, since the most general one (see **Eq. 19b**) has the desired property.

In order for the average clock value to be really meaningful in defining a relational evolution, it is necessary for the width ϵ of the peaking function to be small, $\epsilon\ll 1$. However, as remarked in (Marchetti and Oriti, 2021) and as we will see explicitly below, taking the limit $\epsilon\to 0$, would of course make quantum

[3]In this sense, the operators $\widehat{\chi}$ and $\{\widehat{O}_a\}_{a\in O}$ are expected to have an interpretation in terms of scalar field and geometric quantities respectively, only when averaged on such states.

[4]The above equation is however expected to hold globally if the clock is a minimally coupled massless scalar field, which is going to be the only case we will consider here.

[5]For instance, a reduced wavefunction (whose modulus is) behaving as $\exp[\chi^n]$ with $n\geq 2$ would certainly destroy any localization property of the wavefunction σ_ϵ. On the other hand, any function (whose modulus is) characterized by polynomial or exponential $\exp\chi$ behavior would be an admissible candidate for the reduced condensate wavefunction.

fluctuations on the momentum of the massless scalar field clock to diverge, thus making the clock highly quantum even in regimes in which we expect to reach some kind of semi-classicality. Moreover, even by considering a small but finite ϵ, there is no guarantee in principle for quantum fluctuations in the scalar field momentum to become controllable in the same semi-classical regime. This can be ensured, however, by imposing the additional condition

$$\epsilon\pi_0^2 \gg 1\,. \tag{12}$$

For more remarks and comments on this particular class of states we refer to (Marchetti and Oriti, 2021).

2.3 Reduced Wavefunction Dynamics and Solutions

Since the relational approach discussed in the previous section is by its very nature effective and approximate, following (Marchetti and Oriti, 2021) we will only extract an effective mean field dynamics from the full quantum equations of motion. In other words, we will only consider the imposition of the quantum equations of motion averaged on the states that we consider to be relevant for an effective relational description of the cosmological system:

$$\left\langle \frac{\delta S[\widehat{\varphi},\widehat{\varphi}^\dagger]}{\delta\widehat{\varphi}^\dagger(g_I,\chi_0)} \right\rangle_{\sigma_\epsilon;\chi_0,\pi_0} \equiv \left\langle \sigma_\epsilon;\chi_0,\pi_0 \middle| \frac{\delta S[\widehat{\varphi},\widehat{\varphi}^\dagger]}{\delta\widehat{\varphi}^\dagger(g_I,\chi_0)} \middle| \sigma_\epsilon;\chi_0,\pi_0 \right\rangle = 0\,, \tag{13}$$

where $|\sigma_\epsilon;\chi_0,\pi_0\rangle$ is the isotropic CPS with wavefunction (10) and with peaking function (**Eq. 11**). The quantity S is the GFT action. As we have mentioned at the beginning of **Section 2.1**, its form is chosen so that the GFT partition function expanded around the Fock vacuum matches the spin-foam model one wants to reproduce. Following (Oriti et al., 2016), this would be an EPRL Lorentzian model with a minimally coupled massless scalar field, described in terms of the SU(2) projection of the Lorentz structures entering in the original definition of the model. The action includes a quadratic kinetic term and a quintic (in powers of the field operator) interaction term, $S = K + U + \overline{U}$.

For cosmological applications, there are typically two assumptions that are done on the GFT action. The first is that the classical field symmetries of the action of a minimally coupled massless scalar field (invariance under shift and reflection) are respected by the GFT action as well. This greatly simplifies the form of the interaction and kinetic terms, which read (Oriti et al., 2016; Marchetti and Oriti, 2021)

$$\begin{aligned} K &= \int \mathrm{d}g_I \mathrm{d}h_I \int \mathrm{d}\chi \mathrm{d}\chi' \overline{\varphi}(g_I,\chi) \\ &\quad \times \mathcal{K}\Big(g_I, h_I; \big(\chi-\chi'\big)^2\Big)\varphi\big(h_I,\chi'\big), \\ U &= \int \mathrm{d}\chi \int \left(\prod_{a-1}^{5} \mathrm{d}g_I^a\right) \mathcal{U}\big(g_I^1,\ldots,g_I^5\big) \prod_{a-1}^{5} \varphi\big(g_I^a,\chi\big)0 \end{aligned}$$

The details about the EPRL model are encoded in the specific form of the kinetic and interaction kernels $\mathcal{K}$ and $\mathcal{U}$ above. In particular, it is $\mathcal{U}$ that carries information about the specific Lorentzian embedding of the theory.

The second assumption usually made in cosmological applications, however, is that one is interested in a "mescocopic regime" where these interactions are assumed to be negligible (though see (Pithis et al., 2016; Pithis and Sakellariadou, 2017), for some phenomenological studies including interactions). Under these two assumptions and imposing isotropy on the condensate wavefunction (see **Section 2.1.2**), the above quantum equations of motion reduce to two equations for the modulus ρ_j and the phase θ_j of the reduced wavefunction $\tilde{\sigma}_j \equiv \rho_j \exp[i\theta_j]$ of the CPS for each spin j (Marchetti and Oriti, 2021),

$$0 = \rho_j''(\chi_0) - \frac{Q_j^2}{\rho_j^3(\chi_0)} - \mu_j^2\rho_j(\chi_0)\,, \tag{14a}$$

$$\theta_j'(\chi_0) = \tilde{\pi}_0 + \frac{Q_j}{\rho_j^2(\chi_0)}\,, \tag{14b}$$

where

$$\mu_j^2 = \frac{\pi_0^2}{\epsilon\pi_0^2-1}\left(\frac{2}{\epsilon\pi_0^2} - \frac{1}{\epsilon\pi_0^2-1}\right) + \frac{B_j}{A_j}\,, \tag{15a}$$

$$\tilde{\pi}_0 = \frac{\pi_0}{\epsilon\pi_0^2-1}\,, \tag{15b}$$

Q_j are integration constants and (Oriti et al., 2016)

$$\begin{aligned} A_j &= \sum_{\vec{n},\iota} \left[\mathcal{K}^{(2)}\right]^{jjjj,\iota}_{n_1n_2n_3n_4} \overline{\mathcal{I}}^{jjjj_+}_{n_1n_2n_3n_4} \mathcal{I}^{jjjj_+}_{n_1n_2n_3n_4} \overline{\alpha}^\iota_j \alpha^\iota_j, \\ B_j &= -\sum_{\vec{n},\iota} \left[\mathcal{K}^{(0)}\right]^{jjjj,\iota}_{n_1n_2n_3n_4} \overline{\mathcal{I}}^{jjjj_+}_{n_1n_2n_3n_4} \mathcal{I}^{jjjj_+}_{n_1n_2n_3n_4} \overline{\alpha}^\iota_j \alpha^\iota_j. \end{aligned}$$

Here, $\mathcal{K}^{(2n)}$ denotes the $2n$ -th derivative of the kineric kernel with respect to its scalar field argument evaluated at 0, while α^ι_j are determined by

$$\mathcal{I}^{jjjj,\iota_+}_{n_1n_2n_3n_4} = \sum_\iota \alpha^\iota_j \mathcal{I}^{jjjj,\iota}_{n_1n_2n_3n_4}.$$

Eq. 14a can be immediately integrated once to obtain

$$\mathcal{E}_j = \left(\rho_j'\right)^2 + \frac{Q_j^2}{\rho_j^2} - \mu_j^2\rho_j^2\,, \tag{16}$$

where the constants $\mathcal{E}_j$ are integration constants[6]. This equation can be then combined with **Eq. 14a** in order to obtain a linear equation in terms of $\rho_j^2(\chi_0)$. In fact, since $(\rho_j^2)'' = 2(\rho_j')^2 + 2\rho_j\rho_j''$, combining **Eq. 14a** (multiplied by ρ_j) and **Eq. 16**, we obtain

$$\left(\rho_j^2\right)'' = 2\left(\mathcal{E}_j + 2\mu_j^2\rho_j^2\right). \tag{17}$$

[6]It is interesting to notice that the above equation is equivalent to the equation of motion of a conformal particle (de Alfaro et al., 1976) with a harmonic potential, which is a system characterized by a conformal symmetry. Since there are some interesting examples of systems whose dynamics can be can be mapped into a Friedmann one exactly in virtue of their conformal symmetry, (see e.g. (Lidsey, 1802; Ben Achour and Livine, 2019)), the above equation alone would already suggest a connection between the effective mean field dynamics discussed here and a cosmological one.

The most general solution can be written as

$$\rho_j^2 = -\frac{\mathcal{E}_j}{2\mu_j^2} + A_j e^{2\mu_j \chi_0} + B_j e^{-2\mu_j \chi_0}. \tag{18}$$

Of course we can find some relations between the constants A_j and B_j and the constants of integration Q_j and $\mathcal{E}_j$, so that we can choose a different way to parametrize the solution. Indeed, we first notice that since for $\chi_0 \to +\infty$ the term with A_j dominates, while for $\chi_0 \to -\infty$ the term with B_j dominates, this means that both A_j and B_j are non-negative. Then, by defining $\chi_{0,j}$ as the point at which $(\rho_j^2)'(\chi_{0,j}) = 0$, we see that

$$\sqrt{A_j B_j} = \pm \frac{\sqrt{\mathcal{E}_j^2 + 4\mu_j^2 Q_j^2}}{4\mu_j^2}, \qquad \sqrt{A_j / B_j} = e^{-2\mu_j \chi_{0,j}}.$$

Thus our solution becomes

$$\rho_j^2 = -\frac{\mathcal{E}_j}{2\mu_j^2} + \frac{\sqrt{\mathcal{E}_j^2 + 4\mu_j^2 Q_j^2}}{2\mu_j^2} \cosh\big(2\mu_j(\chi_0 - \chi_{0,j})\big), \tag{19a}$$

where we have chosen only the positive solution because $\rho_j^2 \geq 0$. Equivalently, we can write

$$\rho_j^2 = -\frac{\alpha_j}{2} + \frac{\sqrt{\alpha_j^2 + 4\beta_j^2}}{2} \cosh\big(2\mu_j(\chi_0 - \chi_{0,j})\big), \tag{19b}$$

where we have defined

$$\alpha_j \equiv \mathcal{E}_j / \mu_j^2, \qquad \beta_j^2 \equiv Q_j^2 / \mu_j^2. \tag{20a}$$

The solution is now only parametrized by μ_j, α_j, β_j, and $\chi_{0,j}$. This is our fundamental equation, representing a general solution of (**Eq. 14a**).

For the following discussion, it will be useful to derive some bounds on the modulus of the derivatives of ρ_j^2 divided by ρ_j^2 itself. In order to study these bounds explicitly, it is helpful to define

$$x_j \equiv 2\mu_j(\chi_0 - \chi_{0,j}), \qquad r_j \equiv \beta_j^2 / \alpha_j^2. \tag{20b}$$

Then, denoting $[\rho_j^2]^{(n)}$ the n-th derivative of ρ_j^2 with respect to χ_0, we have

$$\frac{\left|[\rho_j^2]^{(n)}\right|}{\rho_j^2} = (2\mu_j)^n \frac{\sqrt{1+4r_j}}{-\mathrm{sgn}(\alpha_j) + \sqrt{1+4r_j}\cosh x_j} \times \begin{cases} \sinh x_j, & n \text{ odd.} \\ \cosh x_j, & n \text{ even.} \end{cases} \tag{21}$$

In the following sections we will discuss in more detail under which conditions the above states indeed implement a notion of relational dynamics, as defined in **Section 2.2.1**.

3 AVERAGES AND FLUCTUATIONS: GENERALITIES

In this section we compute expectation values of relevant operators in the effective relational GFT cosmology framework (i.e., the number operator $\hat{N}$, the volume operator $\hat{V}$, the momentum operator $\hat{\Pi}$, the Hamiltonian operator $\hat{H}$ and the massless scalar field operator $\hat{X}$), and their relative variances on CPS states, in order to characterize the behavior of the first moments of the relevant operators and with the ultimate purpose of trying to deduce some information about the impact of quantum fluctuations on the effective relational framework discussed so far (**Section 5**).

We express these expectation values and relative variances in terms of the modulus of the reduced wavefunction only, possibly using **Eq. 14b** in order to trade any dependency on the phase of the reduced wavefunction for its modulus. In **Section 4**, instead, we use the explicit solution (**Eq. 19a**, **Eq. 19b**) to considerably simplify the equations obtained in the following two subsections.

3.1 Expectation Value of Relevant Operators

First, let us compute the expectation value of the relevant operators, whose definitions are reviewed below.

Number and Volume Operators

The simple case of the number operator allows us to discuss the prototypical computation that we are going to perform frequently in the following. Its definition is (Oriti, 2017; Marchetti and Oriti, 2021)

$$\hat{N} \equiv \int \mathrm{d}\chi \int \mathrm{d}g_I \hat{\varphi}^\dagger(g_I, \chi)\varphi(g_I, \chi). \tag{22}$$

Its expectation value on a isotropic CPS is therefore given by

$$N(\chi_0) \equiv \langle \hat{N} \rangle_{\sigma_\epsilon; \chi_0, \pi_0} = \sum_j \int \mathrm{d}\chi \rho_j^2(\chi) |\eta_\epsilon(\chi - \chi_0; \pi_0)|^2$$

In order to evaluate this quantity, one can expand the function ρ_j^2 around $\chi = \chi_0$, given the fact that the function η_ϵ is strongly peaked around that point. As a result, the relevant integral to be computed is

$$\rho_j^2(\chi_0) \int \mathrm{d}\chi |\eta_\epsilon(\chi - \chi_0; \pi_0)|^2 \times \left[1 + \sum_{n=1}^{\infty} \frac{(\chi - \chi_0)^n}{n!} \frac{[\rho_j^2]^{(n)}(\chi_0))}{\rho_j^2(\chi_0)}\right]$$

By normalizing η_ϵ so that the integral of its modulus squared is unitary, we see that

$$\int \mathrm{d}\chi (\chi - \chi_0)^{2m} |\eta_\epsilon(\chi - \chi_0; \pi_0)|^2 = \epsilon^m \frac{(2m)!}{4^m m!}, \tag{23}$$

giving zero, instead, for odd powers. In conclusion, one finds

$$N(\chi_0) = \sum_j \rho_j^2(\chi_0) \left[1 + \sum_{n=1}^{\infty} \frac{[\rho_j^2]^{(2n)}(\chi_0))}{\rho_j^2(\chi_0)} \frac{\epsilon^n}{4^n n!}\right] \tag{24}$$

Similar computations hold for the volume operator, counting the volume contributions of all tetrahedra in a given GFT state and defined as (Oriti et al., 2016; Marchetti and Oriti, 2021)

$$\hat{V} = \int \mathrm{d}\chi \int \mathrm{d}g_I \mathrm{d}g_I' \hat{\varphi}^\dagger(g_I, \chi) V(g_I, g_I') \hat{\varphi}(g_I', \chi), \tag{25}$$

in terms of matrix elements $V(g_I, g_I')$ of the first quantized volume operator in the group representation. Indeed, one has (Marchetti and Oriti, 2021)

$$V(\chi_0) \equiv \langle \widehat{V} \rangle_{\sigma_\epsilon;\chi_0,\pi_0} = \sum_J V_j \int \mathrm{d}\chi \rho_j^2(\chi) |\eta_\epsilon(\chi - \chi_0; \pi_0)|^2,$$

where V_j represents the volume contribution of each equilateral tetrahedron whose faces have area determined by the quantum number j. The situation is the same as before, and one therefore concludes that

$$V(\chi_0) = \sum_j V_j \rho_j^2(\chi_0) \left[1 + \sum_{n=1}^{\infty} \frac{\left[\rho_j^2\right]^{(2n)}(\chi_0))}{\rho_j^2(\chi_0)} \frac{\epsilon^n}{4^n n!} \right] \tag{26}$$

In particular, when higher order derivatives can be neglected, we notice that we can write

$$N(\chi_0) \simeq \sum_J \rho_j^2(\chi_0), \qquad V(\chi_0) \simeq \sum_J V_j \rho_j^2(\chi_0), \tag{27}$$

for the expectation value of the number and of the volume operator. We will see in **Section 4.1** that this will be indeed the case when these quantities are evaluated on solutions of the dynamical equations and under some fairly general conditions on the parameters characterizing the dynamics.

Momentum and Hamiltonian Operator

Similar results hold for the scalar field momentum and the hamiltonian operators. The effective[7] Hamiltonian operator $\widehat{H}$ can be defined as a Hermitean operator whose action on a CPS is given by (Marchetti and Oriti, 2021)

$$\widehat{H} \left| \sigma_\epsilon; \chi_0, \pi_0 \right\rangle \equiv -i \left(\frac{N'(\chi_0)}{2} + \int \mathrm{d}g_I \int \mathrm{d}\chi \hat{\varphi}^\dagger(g_I, \chi) \partial_\chi \eta_\epsilon(\chi - \chi_0, \pi_0) \right.$$
$$\left. \tilde{\sigma}(g_I, \chi) \right) \left| \sigma_\epsilon; \chi_0, \pi_0 \right\rangle. \tag{28}$$

Such an operator generates by construction translations with respect to χ_0, and thus, in the regime in which the relational picture is well-defined, it is the operator generating relational evolution of expectation values of geometric operators.

Defining $\overline{\widehat{H}}$ the operator whose action on the CPSs is given by the second term in the round brackets in **Eq. 28**, we see that its expectation value on an isotropic CPS is

$$\langle \overline{\widehat{H}} \rangle_{\sigma_\epsilon;\chi_0,\pi_0} = \pi_0 \int \mathrm{d}g_I \int \mathrm{d}\chi |\eta_\epsilon(\chi - \chi_0, \pi_0)|^2 \rho^2(g_I, \chi) + \frac{i}{2} N'(\chi_0)$$

By definition of $N(\chi_0)$ we can write

$$\langle \overline{\widehat{H}} \rangle_{\sigma_\epsilon;\chi_0,\pi_0} = \pi_0 N(\chi_0) + \frac{i}{2} N'(\chi_0),$$

so that, in conclusion we obtain, for $\widehat{H}$,

$$\langle \widehat{H} \rangle_{\sigma_\epsilon;\chi_0,\pi_0} = \langle \overline{\widehat{H}} \rangle_{\sigma_\epsilon;\chi_0,\pi_0} - i \frac{N'(\chi_0)}{2} = \pi_0 N(\chi_0). \tag{29}$$

[7]We remark that this is an "effective" operator since its construction is always subject to a prior choice of appropriate states; in this case, CPSs (see (Marchetti and Oriti, 2021) for a more detailed discussion).

The situation for the momentum operator is similar. By definition

$$\widehat{\Pi} = \frac{1}{i} \int \mathrm{d}g_I \int \mathrm{d}\chi \left[\hat{\varphi}^\dagger(g_I, \chi) \left(\frac{\partial}{\partial \chi} \hat{\varphi}(g_I, \chi) \right) \right] \tag{30}$$

and one has

$$\begin{aligned} \langle \widehat{\Pi} \rangle_{\sigma;\chi_0,\pi_0} &= \frac{1}{i} \int \mathrm{d}\chi \sum_J \overline{\sigma}_{\epsilon,j}(\chi; \chi_0, \pi_0) \partial_\chi \sigma_{\epsilon,j}(\chi; \chi_0, \pi_0) \\ &= \sum_j \int \mathrm{d}\chi \rho_j^2(\chi) \left(\theta'_j(\chi) + \pi_0 \right) |\eta_\epsilon(\chi - \chi_0; \pi_0)|^2 \\ &= \pi_0 \left[\frac{1}{\epsilon \pi_0^2 - 1} + 1 \right] \sum_j \int \mathrm{d}\chi \rho_j^2(\chi) |\eta_\epsilon(\chi - \chi_0; \pi_0)|^2 \\ &\quad + \sum_j Q_j \\ &= \pi_0 \left(\frac{1}{\epsilon \pi_0^2 - 1} + 1 \right) N(\chi_0) + \sum_j Q_j. \end{aligned} \tag{31}$$

From this explicit form, we notice that the evaluation of both the expectation value of $\widehat{H}$ and $\widehat{\Pi}$ essentially reduces to an evaluation of the averaged number operator.

Now, in the approximation $\epsilon \pi_0^2 \gg 1$, the two expectation values coincide, as required by the effective relational dynamics framework, for any values of χ_0, as long as $\sum_j Q_j = 0$. It is however interesting to notice that, as the number of GFT quanta increases, the impact of the second term above becomes decreasingly important. As a consequence, in the asymptotic regime $N \to \infty$, the equality between the expectation values of the Hamiltonian and the momentum operator is satisfied to any degree of accuracy required, regardless of the strict imposition of $\sum_j Q_j = 0$. So, if one was interested only to the implementation of an effective relational framework in the thermodynamics regime $N \to \infty$, or at large condensate densities (which become large universe volumes), one might be formally dispensed from imposing the condition $\sum_j Q_j = 0$. On the other hand, if one wants to describe mesoscopic intermediate regimes through the same formalism, then such a requirement needs to be imposed. In order to take into account these different possibilities, from now on we retain any $\sum_j Q_j$ term, setting it to zero only when necessary.

Massless Scalar Field Operator

The massless scalar field operator is defined as (Oriti et al., 2016; Marchetti and Oriti, 2021)

$$\widehat{X} \equiv \int \mathrm{d}g_I \int \mathrm{d}\chi \, \chi \hat{\varphi}^\dagger(g_I, \chi) \hat{\varphi}(g_I, \chi), \tag{32}$$

so its expectation value on an isotropic CPS is given by

$$\langle \widehat{X} \rangle_{\sigma_\epsilon;\chi_0,\pi_0} = \sum_j \int \mathrm{d}\chi \, \chi \rho_j^2(\chi) |\eta_\epsilon(\chi - \chi_0; \pi_0)|^2. \tag{33}$$

Notice, however, that this operator is extensive (with respect to the GFT number of quanta, thus indirectly with respect to the universe volume), so it can not be directly related (not even in expectation value) to an intensive quantity such as the massless scalar field. This identification, however, can be meaningful for the rescaled operator $\widehat{\chi} \equiv \widehat{X} / \langle \widehat{N} \rangle_{\sigma_\epsilon;\chi_0,\pi_0}$, at least when the average on a CPS $\left| \sigma_\epsilon; \chi_0, \pi_0 \right\rangle$ is considered.

The evaluation of $\langle\widehat{X}\rangle_{\sigma_\epsilon;\chi_0,\pi_0}$ follows the lines described above: one has to first expand the integrand around χ_0, and then integrates the expansion. As before, only terms with even number of derivatives survive the integration, so we can write the above quantity as

$$\langle\widehat{X}\rangle_{\sigma_\epsilon;\chi_0,\pi_0} = \chi_0\sum_j\rho_j^2(\chi_0)\int \mathrm{d}\chi|\eta_\epsilon(\chi-\chi_0;\pi_0)|^2\left\{1+\sum_{n=1}^{\infty}\left[\frac{\left[\rho_j^2\right]^{(2n)}(\chi_0)}{\rho_j^2(\chi_0)} +2n\frac{\left[\rho_j^2\right]^{(2n-1)}(\chi_0)}{\rho_j^2(\chi_0)\chi_0}\right]\frac{(\chi-\chi_0)^{2n}}{(2n)!}\right\}$$

As a result of the integration one obtains

$$\langle\widehat{X}\rangle_{\sigma_\epsilon;\chi_0,\pi_0} = \chi_0\sum_j\rho_j^2(\chi_0)\times\left\{1+\sum_{n=1}^{\infty}\left[\frac{\left[\rho_j^2\right]^{(2n)}(\chi_0)}{\rho_j^2(\chi_0)} + 2n\frac{\left[\rho_j^2\right]^{(2n-1)}(\chi_0)}{\rho_j^2(\chi_0)\chi_0}\right]\frac{\epsilon^n}{4^n n!}\right\}. \tag{34}$$

The first terms in squared brackets are the same that appear in the expectation value of the number operator. The second terms in square brackets are new. And these terms are in fact crucial: when they are not negligible, the expectation value $\langle\widehat{X}\rangle_{\sigma_\epsilon;\chi_0,\pi_0}$ can not be written anymore as $\chi_0 N(\chi_0)$, which means that the expectation value of the intrinsic massles scalar field operator $\widehat{\chi}$ is not χ_0 anymore.

More precisely, in the most general case, by defining

$$\Delta X(\chi_0) \equiv \sum_j\sum_{n=1}^{\infty}2n\frac{\left[\rho_j^2\right]^{(2n-1)}(\chi_0)}{\chi_0}\frac{\epsilon^n}{4^n n!}, \tag{35}$$

we see that this leads to an expectation value of the "intrinsic" massless scalar field operator of the form

$$\langle\widehat{\chi}\rangle_{\sigma_\epsilon;\chi_0,\pi_0}\equiv\frac{\langle\widehat{X}\rangle_{\sigma_\epsilon;\chi_0,\pi_0}}{N(\chi_0)} = \chi_0\left(1+\Delta X(\chi_0)\big/N(\chi_0)\right), \tag{36}$$

and when the second term satisfies $\left|\Delta X(\chi_0)\right|/N(\chi_0)\gtrsim 1$, the CPS parameter χ_0 is not anymore the expectation value of the intrinsic massless scalar field operator and thus the χ_0 - evolution of averaged geometric operators cannot be interpreted as a relational dynamics. How larger is the second term with respect to 1 depends clearly on two features of the state: i) the impossibility of peaking precisely the clock value, i.e. sending $(\epsilon\to 0)$, and ii) the possibility for N^{-1} to be large in the regime of small number of particles.

Given that the reason why we can not take the limit $\epsilon\to 0$ is related to quantum fluctuations, and that, generally speaking, these are expected to become important when $N\ll 1$, the term $\Delta X/N$ encodes a first interplay between relationality and quantum properties of the clock.

3.2 Relative Variances

According to the requirements specified in **Section 2.2.1**, it is fundamental to check the behavior of clock quantum fluctuations in order to understand whether the relational framework is truly realized at an effective level.

Having done that, this analysis should be extended to all the relevant geometric operators in terms of which we write the emergent cosmological dynamics; this is true in particular for the volume operator, whose averaged dynamics was shown in (Marchetti and Oriti, 2021) to reproduce, "at late times" and under some additional assumptions, a Friedmann dynamics. In order for this "late time regime" to be truly interpreted as a classical one, quantum fluctuations of the volume operator (and possibly also of the other physically interesting operators) should be negligible.

We now proceed to study the behavior of these fluctuations, limiting ourselves here only to relative variances. The explicit computations of these quantum fluctuations can be found in **Supplementary Appendix A**.

Number Operator

As before, we start from the number operator. Its relative variance can be easily found to be

$$\delta_N^2 = N^{-1}(\chi_0), \tag{37a}$$

thus decreasing as the number of atoms of space increases, as expected. When the lowest order saddle point approximation is justified, one can write the above expression as

$$\delta_N^2 \simeq \left[\sum_j\rho_j^2(\chi_0)\right]^{-1}. \tag{37b}$$

Volume Operator

For the volume operator the computations are similar. One finds

$$\delta_V^2 = \frac{\sum_j V_j^2\rho_j^2\left[1+\sum_{n=1}^{\infty}\frac{\left[\rho_j^2\right]^{(2n)}(\chi_0)}{\rho_j^2(\chi_0)}\frac{\epsilon^n}{4^n(n)!}\right]}{\left\{\sum_j V_j\rho_j^2\left[1+\sum_{n=1}^{\infty}\frac{\left[\rho_j^2\right]^{(2n)}(\chi_0)}{\rho_j^2(\chi_0)}\frac{\epsilon^n}{4^n(n)!}\right]\right\}^2}. \tag{38a}$$

If one can neglect higher order derivatives, then

$$\delta_V^2 \simeq \frac{\sum_j V_j^2\rho_j^2}{\left(\sum_j V_j\rho_j^2\right)^2}. \tag{38b}$$

Hamiltonian Operator

The relative variance of the Hamiltonian operator, instead, is given by

$$\delta_H^2 \simeq N^{-1}(\chi_0)\left[1+\left(2\epsilon\pi_0^2\right)^{-1}\right] \simeq N^{-1}(\chi_0), \tag{39}$$

which is under control in the regime $\epsilon\pi_0^2\gg 1$ with a large number of GFT quanta and, in this limit, behaves as the relative variance of the number operator.

Momentum Operator

Next, we discuss the variance of the momentum operator. The computations are a little more involved, but under the assumption that $\epsilon\pi_0^2\gg 1$ one finds

$$\delta^2_{\Pi} = \frac{1}{\left(\pi_0 N + \sum_j Q_j\right)^2}\left\{\sum_j\left(Q_j + \mathcal{E}_j\right) + \sum_j\left[\frac{1}{\epsilon} + \mu_j^2 + \pi_0^2\right]\rho_j^2(\chi_0)\left[1 + \sum_{n=1}^{\infty}\frac{\left[\rho_j^2\right]^{(2n)}(\chi_0)}{\rho_j^2(\chi_0)}\frac{\epsilon^n}{n!4^n}\right] - \sum_j\frac{\rho_j^2(\chi_0)}{2\epsilon}\left(1 + \sum_{n=1}^{\infty}\frac{\left[\rho_j^2\right]^{(2n)}(\chi_0)}{\rho_j^2(\chi_0)}\frac{\epsilon^n}{n!4^n}(2n+1)\right)\right\}.$$

From the explicit form of δ^2_{Π} above we deduce that:

- In the formal limit $\epsilon \to 0$, $\delta^2_{\Pi} \to \infty$, i.e. that the system is subject to arbitrarily large quantum fluctuations. This is of course a consequence of the Heisenberg uncertainty principle when "clock time" localization of the condensate wavefunction is enhanced;
- By taking the limit[8] $\pi_0 \to 0$, the expectation value of $\hat{\Pi}$ on a CPS becomes $\sum_j Q_j$, while one can see that $\delta\Pi^2_{\sigma_\epsilon;\chi_0,\pi_0}$ has a contribution growing essentially as N (see **Supplementary Appendix A**). In this case, therefore, quantum fluctuations become extremely large in the $N \to \infty$ regime, which is certainly an undesired feature, since we expect that in this limit some kind of semi-classical spacetime structure is recovered. On the other hand, as we will see below, when condition (**Eq. 12**) is assumed, in the limit $N \to \infty$ quantum fluctuations are suppressed.

Massless Scalar Field Operator

Finally, we discuss the variance of the massless scalar field operator. Its quantum fluctuations are given by

$$\delta X^2_{\sigma_\epsilon;\chi_0,\pi_0} = \chi_0^2\sum_j\rho_j^2(\chi_0)\left\{1 + \sum_{n=1}^{\infty}\left[\frac{\left[\rho_j^2\right]^{(2n)}(\chi_0)}{\rho_j^2(\chi_0)} + 4n\frac{\left[\rho_j^2\right]^{(2n-1)}(\chi_0)}{\chi_0\rho_j^2(\chi_0)} + 2n(2n-1)\frac{\left[\rho_j^2\right]^{(2n-2)}(\chi_0)}{\chi_0^2\rho_j^2(\chi_0)}\right]\frac{\epsilon^n}{4^n n!}\right\}. \tag{40}$$

which, once divided by (**Eq. 34**) squared, gives the relative variance of $\hat{\chi}$. Notice, in the above equation, that even though the coefficients in the square brackets grow as n for the second term and as n^2 for the third one, the behavior of the overall coefficients of these terms (i.e., by taking into account also the factor $(4^n n!)^{-1}$) is decreasing with n. As we will see in the next section, this implies that in the evaluation of this variance on the specific solutions (19b) it is enough to consider the lowest non-trivial order. The only difference with respect to the expectation value of the massless scalar field, is that in this case odd and even derivatives of the ρ_j^2 function are at the same perturbative order. In particular, for $n = 1$ the last term becomes dominant when $\epsilon/(2\chi_0)^2 \gg 1$, i.e., when $|\chi_0| \ll \sqrt{\epsilon/2}$. Now, suppose that $|\pi_0|^{-1} \ll |\chi_0| \ll \sqrt{\epsilon/2}$ (this region is allowed because $\epsilon\pi_0^2 \gg 1$), so that the computations carried out for the expectation value are still valid, but this last term is indeed important in the evaluation of the fluctuations. We see that this $n = 1$ term gives a contribution to the relative variance of the form

$$\frac{\epsilon}{2\chi_0^2}\frac{\sum_j\rho_j^2(\chi_0)}{\left[\sum_j\rho_j^2(\chi_0)^2\right]^2} \simeq \frac{\epsilon}{2\chi_0^2}N^{-1}(\chi_0).$$

The prefactor on the right-hand-side is by assumption large, but it can be suppressed by the factor $N^{-1}(\chi_0)$, assuming it is large enough.

So, already from this example we can deduce that, in the limit of arbitrarily large N, the only point which has to formally be excluded from the analysis because clock fluctuations become too large is $\chi_0 = 0$. In this point the prefactor is formally divergent, regardless of any large value of N we are considering. This is of course a consequence of using relative variances: if we are interested in the physics at $\chi_0 = 0$, as already argued, e.g., in (Ashtekar et al., 2005), one should set a precise threshold on δX^2, rather than using relative variances.

4 AVERAGES AND FLUCTUATIONS: EXPLICIT EVALUATION

Having obtained the expectation values and the relative variances of relevant operators in the effective relation GFT cosmology frameowork in terms of the modulus of the reduced wavefunction (and possibily of its derivatives), we can now further simplify the obtained expressions by means of **Eq. 19b**.

4.1 Expectation Values

The explicit evaluation of the expectation values of operators, as shown above, involves an infinite number of derivatives of the modulus of the reduced wavefunction. However, it is interesting to notice that

$$1 + \frac{\left[\rho_j^2\right]''}{\rho_j^2}\frac{\epsilon}{4} = \frac{-\mathrm{sgn}\left(\alpha_j\right) + \sqrt{1+4r_j}\cosh x_j\left(1+\epsilon\mu_j^2\right)}{-\mathrm{sgn}\left(\alpha_j\right) + \sqrt{1+4r_j}\cosh x_j} \simeq 1, \tag{41}$$

since

$$\mu_j^2\epsilon = \frac{\epsilon\pi_0^2}{\epsilon\pi_0^2 - 1}\left(\frac{2}{\epsilon\pi_0^2} - \frac{1}{\epsilon\pi_0^2 - 1}\right) + \epsilon\frac{B_j}{A_j} \ll 1, \tag{42}$$

under our working assumption $\epsilon\pi_0^2 \gg 1$ and by further assuming[9] $|B_j/A_j| \ll \epsilon^{-1}$. Moreover, since, in general, one has

$$\frac{\left[\rho^2\right]^{(n+2)}}{\left[\rho^2\right]^{(n)}} = 4\mu_j^2, \qquad n \geq 1, \tag{43}$$

[8]As we have mentioned above, the result above was obtained using the condition $\epsilon\pi_0^2 \gg 1$ (see Eq. 60), which is certainly not justified in this case. However, one can explicitly check, by using the full result in terms of $\tilde{\pi_0}$ and π_0, that the conclusions below are still valid.

[9]Notice that under this assumption, which seems natural given the smallness of ϵ required by the CPS construction, the details of the underlying GFT model become effectively unimportant for the derivation of the results discussed below.

we see that terms with $n > 1$ are negligible with respect to the $n = 1$ term, thus implying that *all* even derivatives in the sums (**Eqs. 24**, **26**) can be neglected. As a result, we can write

$$N(\chi_0) \simeq \sum_j \rho_j^2(\chi_0), \qquad V(\chi_0) \simeq \sum_j V_j \rho_j^2(\chi_0), \tag{44}$$

the first equation above also determining the expectation values of $\widehat{\Pi}$ and $\widehat{H}$, according to **Eqs. 29**, **31**.

Similarly, the natural hierarchy of derivatives obtained from **Eqs. 43**, **42** is present also in the sum over n in **Eq. 35**. For the same reasons as above, therefore, we can write

$$\Delta X(\chi_0) \simeq \sum_j \frac{\left[\rho_j^2\right]'(\chi_0)}{\chi_0} \frac{\epsilon}{2},$$

so that

$$\frac{|\Delta X|}{N} \simeq \left| \sum_j \frac{\left[\rho_j^2\right]'(\chi_0)}{\chi_0} \frac{\epsilon}{2} \right| \left[\sum_j \rho_j^2(\chi_0) \right]^{-1}. \tag{45}$$

However, determining whether these higher derivative terms become important in the expectation values of operators like $\widehat{N}$, $\widehat{V}$, $\widehat{\Pi}$ and $\widehat{H}$ is quite different from determining whether $\Delta X/N$ is important in the expectation value of $\widehat{\chi}$, basically because, as we can clearly see from the above expression, ΔX involves odd derivatives and it explicitly depends on χ_0.

As we have already mentioned, the smallness of the factor $\Delta X/N$ is crucial for a consistent interpretation of χ_0 as the expectation value of the massless scalar field $\widehat{\chi}$, to be used in a relational picture. In general, whenever $|\Delta X|/N \ll 1$, such an interpretation is allowed.

Whether this condition is actually satisfied, though, drastically depends on the properties of the solution ρ_j^2 for each j and hence on the precise set of free parameters $\{\alpha_j, \beta_j, \chi_{0,j}\}$. It is obvious from **Eq. 34** together with the above expression, that as long as

$$1 + \frac{\left[\rho_j^2\right]'}{\rho_j^2 \chi_0} \frac{\epsilon}{2} \simeq 1, \tag{46}$$

this interpretation is allowed. Following the same steps of (**Eq. 41**), we see that the above condition is satisfied as long as

$$\epsilon \mu_j^2 \frac{\left|\tanh x_j\right|}{\left|x_j + x_j^o\right|} \ll 1, \qquad \forall j$$

where $x_j^o \equiv 2\mu_j \chi_{0,j}$, and where we have neglected an unimportant factor 2. This condition is certainly satisfied in two simple (though interesting) cases:

1. First, since $\left|\tanh x_j\right| \leq 1$, we see that when $\left|x_j + x_j^o\right| \equiv 2\mu_j \left|\chi_0\right| \gg (\epsilon \mu_j^2)^{-1}$, i.e., again, neglecting unimportant factors 2, when

$$\left|\chi_0\right| \gg \epsilon \mu_j \sim \pi_0^{-1}, \tag{47}$$

condition (**Eq. 46**) is actually satisfied. Notice also that since $\pi_0^{-1} \ll \sqrt{\epsilon}$, by requiring $\left|\chi_0\right| \gg \sqrt{\epsilon}$ the above condition is also satisfied. It is interesting to notice that $\sqrt{\epsilon}$ actually quantifies the impossibility to perfectly localize the condensate wavefunction around χ_0. If χ_0 is of order or smaller than this quantity, it is clear that any desired localization property is lost in this irreducible uncertainty.

2. Second, notice that if all the $x_j^o \geq 0$ (resp. $x_j^o \leq 0$) the above condition is always satisfied for all $\chi_0 \geq 0$ (resp. for all $\chi_0 \leq 0$). In the case only a single spin is considered, say j_o, this means that the evolution of the modulus of the condensate wavefunction with respect to χ_0 can be interpreted as an evolution with respect to the expectation value of $\widehat{\chi}$ from the minimum of the former, at $x_{j_o}^o \geq 0$ (resp. $x_{j_o}^o \leq 0$) to arbitrarily large positive (negative) values of χ_0. We will discuss this single spin case in more detail in **Section 5.2.3**.

More generally, instead, the value of $h_j(x_j) \equiv \left|\tanh x_j\right| / \left|x_j + x_j^o\right|$ is determined by two scales: $x_j + x_j^o \equiv \kappa_j^{(1)} \equiv 2\mu_j \chi_0$, and $x_j^o / \kappa_j^{(1)} \equiv \kappa_j^{(2)}$. These two quantities acquire a clear physical meaning in a single spin scenario with $j = j_o$ discussed in **Section 5.2.3**. In that case, $\kappa_{j_o}^{(1)}$ basically measures the amount of evolution experienced by $\rho_{j_o}^2$ from $\chi_0 = 0$, while $\kappa_{j_o}^{(2)}$ measures how large is the amount of evolution elapsed since $\chi_0 = 0$ with respect to the moment at which $\rho_{j_o}^2$ has reached its minimum. Since only a single spin is excited, the expectation value of the volume operator and $\rho_{j_o}^2$ are in a one-to-one correspondence (see **Eq. 44**), which gives to the above statements about $\kappa_k^{(1)}$ and $\kappa_j^{(2)}$ a straightforward physical meaning.

Of course, the desired condition (**Eq. 46**) is satisfied for $\left|\kappa_j^{(1)}\right| \gtrsim 1$ (late evolution for ρ_j^2) or for $\left|\kappa_j^{(1)}\right| \ll 1$ and $\left|\kappa_j^{(2)}\right| \lesssim 1$ (early evolution for ρ_j^2, but still later than when the minimum of ρ_j^2 happened), as reviewed in **Table 1**. In the remaining cases, $\left|\kappa_j^{(1)}\right| \ll 1$ and $\left|\kappa_j^{(2)}\right| \gg 1$ (very early evolution for ρ_j^2), instead, we have

$$h_j(x_i) \sim \begin{cases} \left|\kappa_j^{(1)}\right|^{-1}, & \left|\kappa_j^{(1)}\right| \left|\kappa_j^{(2)}\right| \gtrsim 1 \\ \left|\kappa_j^{(2)}\right|, & \left|\kappa_j^{(1)}\right| \left|\kappa_j^{(2)}\right| \ll 1 \end{cases},$$

so, while in the first case the condition $\epsilon \mu_j^2 h_j \ll 1$ becomes the condition already encountered in (**Eq. 47**), $\left|\chi_0\right| \gg \epsilon \mu_j$, in the second case the situation is different. We see that when

$$\epsilon \mu_j^2 \times \begin{cases} \left|\kappa_j^{(1)}\right|^{-1} \ll 1, & \left|\kappa_j^{(1)}\right| \left|\kappa_j^{(2)}\right| \gtrsim 1 \\ \left|\kappa_j^{(2)}\right| \ll 1, & \left|\kappa_j^{(1)}\right| \left|\kappa_j^{(2)}\right| \ll 1 \end{cases},$$

for all js, then we can write $\langle \widehat{X} \rangle_{\sigma_\epsilon; \chi_0, \pi_0} \simeq \chi_0 \sum_j \rho_j^2(\chi_0) \simeq \chi_0 N(\chi_0)$, and conclude that χ_0 is indeed the expectation value of the intrinsic massless scalar field operator $\widehat{\chi}$. See **Tables 1**, **2** for a summary of the results.

4.2 Fluctuations

The arguments exposed above can be used straightforwardly to compute relative variances of operators.

Number, Hamiltonian and Volume

For the relative variances of the number, Hamiltonian and volume operators, we have

$$\delta_H^2 \simeq \delta_N^2 = N^{-1} \simeq \left[\sum_j \rho_j^2\right]^{-1} \tag{48a}$$

$$\delta_V^2 \simeq \sum_j V_j^2 \rho_j^2 \Big/ \left[\sum_j V_j \rho_j^2\right]^2. \tag{48b}$$

Momentum

For the momentum operator, given that we require $\epsilon\mu_j^2 \ll 1$, we can safely only retain the first terms of the expansions appearing in (A). Moreover, since $\mu_j^2 \sim (\epsilon\pi_0)^{-2}$, $\mu_j^2\pi_0^2 \sim (\epsilon\pi_0^2)^{-2}$, and since $\epsilon\pi_0^2 \gg 1$, both the first two terms in squared brackets in the first line of (A), as well as the whole first term in the second line of equation (A) are negligible with respect to the term

$$\pi_0^2 \sum_j \mathcal{N}_\epsilon^2 \int \mathrm{d}\chi \rho_j^2 e^{-\frac{(\chi-\chi_0)^2}{\epsilon}} = \pi_0^2 N(\chi_0).$$

As a result, we finally have

$$\delta\Pi^2_{\sigma_\epsilon;\chi_0,\pi_0} \simeq \pi_0^2 N(\chi_0) + \sum_j \left(\mathcal{E}_j + Q_j\right).$$

Now, we recall that in order to have an identification between the first moments of the Hamiltonian and the momentum operator one needs to have either $\sum_j Q_j = 0$ or to be in the asymptotic limit in which $\sum_j Q_j$ is negligible with respect to $\pi_0 N$. Since $|\pi_0| > 1$ this implies that when this identification is true, then we can also neglect the $\sum_j Q_j$ term in the above equation. As a consequence, we have a relative variance

$$\begin{aligned}\delta_\Pi^2 &\simeq N^{-1}(\chi_0) + N^{-2}(\chi_0)\frac{\sum_j \mathcal{E}_j}{\pi_0^2} \\ &\simeq N^{-1} + N^{-2}\sum_j \mu_j^2 \alpha_j.\end{aligned}$$

So, we see that the first term of the relative variance behaves as σ_N^2, while the second is new, and because of its behavior $\sim N^{-2}$ it might become dominant in the regime in which $N \ll 1$.

Also, let us notice that $\delta\Pi^2_{\sigma_\epsilon;\chi_0,\pi_0}$ is indeed always positive under our assumptions. In fact, we see that we can write

$$\delta\Pi^2_{\sigma_\epsilon;\chi_0,\pi_0} = \pi_0^2 \sum_j \rho_j^2 \left[1 + \frac{\sum_{j\in P}\alpha_j\left(\mu_j^2/\pi_0^2\right)}{\sum_j \rho_j^2} - \frac{\sum_{j\in N}|\alpha_j|\left(\mu_j^2/\pi_0^2\right)}{\sum_j \rho_j^2}\right],$$

where $P \equiv \{j \in J | \alpha_j \geq 0\}$, and $N \equiv J - P$, J being the total set of spins over which the sum is performed[10].

Let us estimate how large is the last term in square brackets. Since $\mu_j^2/\pi_0^2 \sim (\epsilon\pi_0^2)^{-2}$, we can bring it out of the sum and just study

$$\frac{\sum_{j\in N}|\alpha_j|}{\sum_j \rho_j^2} \leq \frac{\sum_{j\in N}|\alpha_j|}{\sum_{j\in N}\rho_j^2} \leq 1,$$

since, for each $j \in N$,

[10]We will formally assume that the set J is finite, either because there is an explicit cut-off Λ on the allowed spins, or because, after a certain spin Λ on, all the ρ_js become dynamically subdominant.

TABLE 1 | Validity of the condition (**Eq. 46**) depending on the scales $\kappa_j^{(1)}$ and $\kappa_j^{(2)}$. The case $|\kappa_j^{(1)}| \ll 1$ and $|\kappa_j^{(2)}| \gg 1$ is studied in **Table 2** below.

$\lvert\kappa_j^{(2)}\rvert$ \ $\lvert\kappa_j^{(1)}\rvert$	$\ll 1$	~ 1	$\gg 1$
$\ll 1$	✓	✓	✓
~ 1	✓	✓	✓
$\gg 1$	?	✓	✓

$$\rho_j^2 = |\alpha_j|\left(1 + \sqrt{1 + 4r_j}\cosh x_j\right)\Big/ 2 \geq |\alpha_j|.$$

Thus, generally speaking, we have

$$\delta\Pi^2_{\sigma_\epsilon;\chi_0,\pi_0} \geq \pi_0^2 \sum_j \rho_j^2 \left[1 + \frac{\sum_{j\in P}\alpha_j\left(\mu_j^2/\pi_0^2\right)}{\sum_j \rho_j^2} - \frac{1}{\left(\epsilon\pi_0^2\right)^2}\right],$$

and the right-hand-side is of course positive because $(\epsilon\pi_0^2) \gg 1$. Moreover, since

$$\delta\Pi^2_{\sigma_\epsilon;\chi_0,\pi_0} \leq \pi_0^2 \sum_j \rho_j^2 \left[1 + \frac{\sum_{j\in P}\alpha_j\left(\mu_j^2/\pi_0^2\right)}{\sum_j \rho_j^2}\right],$$

we see that in this limit we can approximately write

$$\delta\Pi^2_{\sigma_\epsilon;\chi_0,\pi_0} \simeq \pi_0^2 N(\chi_0)\left[1 + N^{-1}(\chi_0)\sum_{j\in P}\alpha_j\left(\mu_j^2/\pi_0^2\right)\right],$$

so that the relative variance becomes

$$\delta_\Pi^2 \simeq N^{-1}(\chi_0) + N^{-2}(\chi_0)\sum_{j\in P}\alpha_j\left(\mu_j^2/\pi_0^2\right). \tag{48d}$$

Massless Scalar Field

Instead, about the relative variance of the massless scalar field operator, we have

$$\begin{aligned}\delta_\chi^2 &\simeq \frac{\epsilon}{2N\chi_0^2}\frac{1}{(1+\Delta X/N)^2} + \frac{N+2\Delta X}{(N+\Delta X)^2} \\ &\lesssim \frac{1}{N}\left(1 + \frac{\epsilon}{2\chi_0^2}\frac{1}{(1+\Delta X/N)^2}\right)\end{aligned} \tag{48e}$$

Let us make two remarks about this quantity:

1. First, in order for (**Eq. 40**) to be non-negative, we need to impose that

$$\Delta X/N \geq -1/2 - \epsilon\Big/\left(4\chi_0^2\right).$$

Contrarily to what happens for the momentum operator, this is actually a feature that we must impose "by hand" on our solutions. We will assume it to be true from now on.

2. Second, the divergence in the above variance at the point $\Delta X/N = 1$ is again due to our choice of using relative variances, and, as already mentioned above, a more careful choice would be to define an appropriate threshold on the quantity $\delta X^2_{\sigma_\epsilon;\chi_0,\pi_0}$ (Ashtekar and Lewandowski, 2004; Marchetti and Oriti, 2021). The precise identification of this threshold is usually demanded to observational constraints, which are not available in our case. As a consequence, we

TABLE 2 | Validity of the condition (**Eq. 46**) depending on the scales $\kappa_j^{(1)}$ and $\kappa_j^{(2)}$, assuming $|\kappa_j^{(1)}| \ll 1$ and $|\kappa_j^{(2)}| \gg 1$.

$(\epsilon\mu_j)^2/\lvert\kappa_j^{(1)}\rvert$ \ $\lvert\kappa_j^{(1)}\kappa_j^{(2)}\rvert$	$\ll 1$	$\gtrsim 1$
$\ll 1$	X	✓
$\gtrsim 1$	X	X

$(\epsilon\mu_j)^2\lvert\kappa_j^{(2)}\rvert$ \ $\lvert\kappa_j^{(1)}\kappa_j^{(2)}\rvert$	$\ll 1$	$\gtrsim 1$
$\ll 1$	✓	X
$\gtrsim 1$	X	X

just consider relative variances, and avoid the point in which they might diverge.

The scaling of all the relative variances (**Eq. 48e**, **48a**, **48b**, **48d**) is essentially determined by $N \simeq \sum_j \rho_j^2$, so it is interesting to study separately situations in which $N \gg 1$ and $N \lesssim 1$.

4.2.1 Large Number of GFT Quanta

We will first consider the case of large number of GFT quanta, $N \gg 1$. Generally speaking, this situation might be realized in two different ways:

1. There exists at least one of the ρ_j^2 s which is much larger than one.
2. All the ρ_j^2 s are $\lesssim 1$, but their sum is still much larger than 1.

While for the number and the Hamiltonian operators variances are smaller than one by assumption, for the momentum, the volume and the massless scalar field operator, the situation is more complicated, so it is useful to discuss them by distinguishing between the two cases above.

First Case

When at least one of the ρ_j^2 s is much larger than one, it is useful to distinguish between two sets, $L \equiv \{j \in J \big| \rho_j^2 \gg 1\}$, $S \equiv J - L$.

δ_Π^2: While the first term of the variance of the momentum operator is certainly much smaller than one, in order to evaluate the second term one should know exactly the values of all the α_j s for each $j \in P$. Nonetheless, since $\mu_j^2/\pi_0^2 \sim (\epsilon\pi_0^2)^{-2}$, the second term is actually neglgible as long as

$$\sum_{j\in P} \alpha_j \ll \left[N(\chi_0)/(\epsilon\pi_0^2)\right]^2,$$

which is certainly satisfied for a large class of initial conditions, given the large value of the right-hand-side. For instance, notice that for $r_j \gtrsim 1$ for each $j \in P$, we have that

$$\sum_{j\in P} \alpha_j \lesssim \sum_{j\in P} \rho_j^2 \lesssim N \ll N^2(\chi_0)/(\epsilon\pi_0^2)^2.$$

Also, notice that when $P = \varnothing$, $\sigma_\Pi^2 \sim N^{-1} \ll 1$ under our assumptions.

δ_V^2: About the volume operator, we have the following set of inequalities:

$$\begin{aligned}\delta_V^2 &= \frac{\sum_{j\in L} V_j^2\rho_j^2}{\left(\sum_j V_j\rho_j^2\right)^2} + \frac{\sum_{j\in S} V_j^2\rho_j^2}{\left(\sum_j V_j\rho_j^2\right)^2} \\ &\ll \frac{\sum_{j\in L} V_j^2\rho_j^4}{\left(\sum_j V_j\rho_j^2\right)^2} + \frac{\sum_{j\in S} V_j^2\rho_j^2}{\left(\sum_j V_j\rho_j^2\right)^2} \\ &\ll 1 + \frac{\sum_{j\in S} V_j^2\rho_j^2}{\left(\sum_j V_j\rho_j^2\right)^2} \leq 1 + \frac{\sum_{j\in S} V_j^2\rho_j^2}{\left(\sum_{j\in L} V_j\rho_j^2\right)^2} \\ &\ll 1 + (V^2)_S/(V^2)_L,\end{aligned}$$

where $(V^2)_{S,L} = \sum_{j\in(S,L)} V_j^2$. For $(V^2)_S/(V^2)_L \sim 1$, the variance of the volume operator is always much smaller than a quantity of order 1 and thus it is negligible. In particular, when $L = J$, it follows that $\delta_V^2 \ll 1$. Then the volume behaves classically, since *all* the moments of the volume operator are negligible, as one can easily see by following the same steps taken for the variance.

δ_χ^2: As for the massless scalar field operator, we see that, when $|\Delta X|/N \ll 1$, the relative variance is negligible as long as $\chi_0^2 \gg \epsilon/N$ (neglecting unimportant factors 2). When, on the other hand this quantity is of order 1, fluctuations on the massless scalar field operator might become important. Again, by definition, the point $\chi_0 = 0$ is a point where relative quantum fluctuations become uncontrollable.

On the other hand, let us consider the situation in which $|\Delta X|/N \gtrsim 1$ (though not very close to $\Delta X/N = -1$ leading to the unphysical singularity on the relative variance discussed above). In such a situation, we can consider the factor $1/|1 + \Delta X/N| \equiv 1/\lambda \lesssim 1$. The condition for having small fluctuations in this case becomes

$$|\chi_0| \gg \sqrt{\epsilon/(\lambda N)}, \tag{49}$$

again neglecting unimportant factors 2. It is interesting to notice that, depending on how large the factor $(\epsilon\pi_0^2)/\lambda^2 N^2$ is, two different situations may be realized.

1. When $(\epsilon\pi_0^2)/\lambda^2 N^2 \gtrsim 1$, we have that $\sqrt{\epsilon/(\lambda N)} \gtrsim \pi_0^{-1}$, and so the condition (49) in turns implies that $|\chi_0| \gg \pi_0^{-1}$. This condition, as shown in the above subsection, in turns implies that χ_0 can be interpreted as the expectation value of the massless scalar field operator.
2. When instead $(\epsilon\pi_0^2)/\lambda^2 N^2 \ll 1$, it may be that

$$\sqrt{\epsilon/(\lambda N)} \ll |\chi_0| \ll \pi_0^{-1},$$

thus leading to a small relative variance of the massless scalar field operator but to the impossibility of identifying χ_0 as a relational parameter after all.

Second Case

The arguments exposed in the first case about the variances of all the operators besides the volume operator (which after all just

made reference to N, which is still $\gg 1$), are still valid. On the other hand, the inequalities used for the volume operator become inadequate in this case. Still, it is clear that we have

$$\rho^2_{j,min} f_\Lambda \leq \sigma^2_V \leq \rho^{-4}_{j,min} f_\Lambda \,,$$

where $\rho^2_{j,min} \equiv \min_{j\in J} \rho^2_j$ and

$$f_\Lambda \equiv \frac{\sum^\Lambda_{j=0} V^2_j}{\left(\sum^\Lambda_{j=0} V_j\right)^2} = \frac{\sum^\Lambda_{j=0} j^3}{\left(\sum^\Lambda_{j=0} j^{3/2}\right)^2} \simeq 3.56\Lambda^{-3.49},$$

where the last approximate equality has been obtained by an explicit fit. Notice that, since $N \simeq \sum_j \rho^2_j \gg 1$, we must have

$$\Lambda \rho_{j,min} \leq N \leq \Lambda \,,$$

which are however not particularly helpful in extracting tighter bounds. As a conclusion, by defining $a = 3.56$ and $b = 3.49$, we see that, when

$$a\rho^2_{j,min} \Big/ \Lambda \gtrsim 1 \,,$$

fluctuations on the volume operator are certainly large, while when

$$a\rho^{-4}_{j,min} \Lambda^{-b} \ll 1 \,,$$

the relative volume variance is certainly negligible. This is of course the case when all the ρ^2_js are of order one, since $\Lambda \gg 1$.

4.2.2 Number of GFT quanta of order of or smaller than one

When the number of GFT quanta is $N \lesssim 1$, the situation is far more complicated. In fact, not only all the relative variances computed so far can be large, but in this case one does not expect a hierarchy of moments of quantum operators, so that considering only relative variances in order to asses the possible quantum effects is no more enough. Furthermore, one expects also that in this regime a hydrodynamic approxiamtion cannot capture anymore the quantum dynamics of the fundamental "atoms of spacetime", which can only be consistently determined by solving all the Schwinger-Dyson equations of the theory and which is however pre-geometric and not in principle relational (as we intend it from the classical perspective).

In such a case, therefore, not only we expect the CPSs not to define a notion of relational dynamics, but we expect averaged results not to capture all the relevant physics of the system. Hence, we will leave the study of this specific regime to some future work.

5 EFFECTIVE RELATIONAL DYNAMICS: THE IMPACT OF QUANTUM EFFECTS

Let us now recapitulate our results and draw some conclusions from them.

In order for the cosmological CPS construction to fit in an effective relational framework, a certain number of conditions, proposed in (Marchetti and Oriti, 2021) and reviewed in **Section 2.2.1**, should be satisfied. Here, we summarize in which regimes they are satisfied, ensuring the reliability of the cosmological evolution obtained in (Marchetti and Oriti, 2021), with its classical Friedmann-like late times dynamics and singularity resolution into a bounce.

As mentioned in **Section 2.2.1**, variances are not in general enough to characterize the properties of operators in a fully quantum regime (see also **Section 4.2.2**), except when there is a clear hierarchy among operator moments, with the higher ones being suppressed by higher powers of the number of quanta. If we try to quantify quantum fluctuations in terms of relative variances, as we will mostly do here, we must be careful not to assume that certain features characterizing the behavior of relative variances are true also for higher moments, since in certain regimes, variances may be indeed small but higher moments become relevant. Still, as we have mentioned, we do expect that there exists a regime in which the aforementioned hierarchy among moments is indeed present: it is the case in which the number of GFT quanta is large.

While in mesoscopic regimes it is not possible to determine under which conditions the hydrodynamic and the effective relational approximations are satisfied only by studying relative variances, large variances can however be taken as a clear evidence that one, or possibly both the above approximations are not adequate.

5.1 Quantum Effects in the Effective Relational CPS Dynamics

First, therefore, let us discuss the form that the conditions in II B 1 take in the CPS cosmology framework, focusing on the volume operator. Then **Eq. 8a** is satisfied by the CPS construction (Marchetti and Oriti, 2021) provided that.

1. The Expectation Value of the (Intrinsic) Massless Scalar Field Operator Is χ_0

We have already mentioned that in general this is not exactly the case, essentially because we can not take the limit $\epsilon \to 0$ in order to avoid divergences in quantum fluctuations of the massless scalar field momentum. Hence, this issue is a consequence of the quantum properties of the chosen relational clock.

Also, in order to interpret the evolution generated by $\widehat{H}$ as a truly relational one, we want its moments to coincide with those of $\widehat{\Pi}$. Imposing this condition as an exact relation for the first moment and for any values of χ_0 requires $\sum_j Q_j = 0$, while this is not formally required in a large N regime where the condition is satisfied approximately.

A similar situation happens for the relative variance. Indeed, again in the large N regime, $\delta^2_\Pi = \delta^2_H = N^{-1}$ to any degree of accuracy required[11].

On the other hand, let us notice that imposing the equality between (48a) and (48d) for smaller N, and so for mesoscopic

[11]While a formal proof would be needed that similar results extend to even higher moments, it seems likely that this is the case.

intermediate regimes, would impose another constraint on the initial conditions, requiring that all the α_js with $j \in P$ are zero. In turns, this implies that at least one of the α_js with $j \in J$ must be negative, in order not to have only trivial solutions. This means, from **Eq. 44**, that the expectation value of the volume never vanishes, which might have important consequences for the volume evolution.

Next, according to the general discussion in (Marchetti and Oriti, 2021) and in Subsection II B 1, one has to be sure that the clock variable is not "too quantum," which, in our framework can be phrased as the requirement that.

2. Relative Quantum Fluctuations of $\widehat{\chi}$ Must Be Much Smaller Than One

As usual, we can get some information about the behavior of clock quantum fluctuations from the form of δ^2_χ obtained above. From the explicit expression in **Eq. 48e**, we notice that besides the general behavior $\sim N^{-1}$, there is an additional irreducible contribution to quantum fluctuations parametrized by ϵ. From the computations in the above subsection we conclude that in this case the smallness of the relative variance is dictated by a non-trivial interplay between ϵ, χ_0 and N, contrarily to what happens for the other observables. This might make it more difficult to try to extrapolate general features of even higher moments in a mesoscopic regime from those that we observe from the relative variance.

Conditions 1 and 2 are the two necessary conditions that need to be satisfied in order to qualify the framework constructed so far as a truly relational one.

Further, the evolution of the expectation value of the volume operator is a good enough characterization of the universe evolution (in the homogeneous and isotropic context) if.

3. Quantum Fluctuations (Encoded in Moments Higher than the First One) of the Volume Operator are Negligible

Also for this operator, as in the massless scalar field case, the existence of a hierarchy of moments is in general far from being trivial, since the relative variance is already strictly dependent on the possible spin cut-off scale.

However, even when satisfying condition 3, the resulting system might be highly non-classical, depending on the value of quantum fluctuations for the remaining operators $\widehat{N}$, $\widehat{\Pi}$ and $\widehat{H}$. A necessary condition for a classicalization of the system to happen is therefore that.

4. Quantum Fluctuations (Encoded in Moments Higher than the First One) of all the Relevant Operators (N, χ, Π, H, V) are Negligible.

Therefore, in order for a classical relational regime to be realized at late enough times in the CPS framework, both conditions 5.1 (together with the identification of the moments of H and Π) and 4 should be satisfied. In particular, large variances of any of these operators actually signal a breakdown of the hydrodynamic approximation underlying **Eq. 13**.

5.2 Effective Relational Volume Dynamics with CPSs

In light of the above conditions it is interesting to examine the relational evolution of the average of the volume operator, since, in GFT cosmology, it is at this level that the comparison with the Friedmann dynamics is usually performed. We will review this below, in **Section 5.2.1**, emphasizing two main regimes of its evolution: a possible bounce and a Friedmann-like late evolution. In **Section 5.2.2**, instead, we will draw some general conclusions on the relationality and classicality of these two phases in light of the results obtained in the previous sections.

5.2.1 General Properties of the Volume Evolution

Let us start from the general expression (**Eq. 26**)

$$V(\chi_0) = \sum_j V_j \rho_j^2(\chi_0)\left[1 + \sum_{n=1}^{\infty} \frac{\left[\rho_j^2\right]^{(2n)}(\chi_0))}{\rho_j^2(\chi_0)} \frac{\epsilon^n}{4^n n!}\right].$$

We see that $V(\chi_0)$ is always positive and never reaches zero, at least as long as one of the β_js (equivalently, one of the Q_j) is different from zero. Also, from the above expression, we see that

$$V' = \sum_j V_j C_j \mu_j \sinh\left(2\mu_j\left(\chi_0 - \chi_{0,j}\right)\right), \tag{50a}$$

$$V'' = 2\sum_j V_j C_j \mu_j^2 \cosh\left(2\mu_j\left(\chi_0 - \chi_{0,j}\right)\right), \tag{50b}$$

where

$$C_j = |\alpha_j|\sqrt{1 + r_j}\left(1 + \sum_{n=1}^{\infty} \frac{\left(\epsilon\mu_j^2\right)^n}{n!}\right).$$

Since $V' \to \pm\infty$ when $\chi_0 \to \pm\infty$, it has to cross zero[12], and since $V'' > 0$ always, we see that V' is monotone, so it has only one zero. This means that there is only one turning point. Were this evolution truly relational, the scenario would be that of a bouncing universe, increasing monotonically as the bounce happens, lately behaving as a Friedmann universe, as already suggested in (Oriti et al., 2016). Let us discuss this two features in more detail.

Bounce

The bounce happens at a relational time $\overline{\chi_0}$ which is $\min_{j\in J}\chi_{0,j} \le \overline{\chi}_0 \le \max_{j\in J}\chi_{0,j}$. Indeed, $V'(\chi_0)|_{\max_{j\in J}\chi_{0,j}} > 0$, while $V'(\chi_0)|_{\min_{j\in J}\chi_{0,j}} < 0$. By continuity and monotonicity, the value of the bounce must be included among these two points. In addition, we notice from **Eqs. 44**, **19b** that when at least one of the r_js is different from zero, or at least one of the α_js is strictly negative, the volume never reaches zero. So, in these cases, the classical singularity is resolved into a bounce with non-zero volume[13].

[12]Here we are assuming $\mu_j > 0$; if $\mu_j < 0$ the limits are opposite, but the result is the same.

[13]See (Oriti et al., 2016; Marchetti and Oriti, 2021) for a comparison with LQG effective bouncing dynamics and (Battefeld and Peter, 2015) for a review of bouncing models.

Friedmann Regime

When $2|\mu_j(\chi_0 - \chi_{0,j})| \gg 1$ (for each j), the hyperbolic functions can be approximated as simple exponentials. In that case, then, assuming μ_j is independent of j, (or that at least it is mildly dependent on it) one obtains

$$\left(\frac{V'}{3V}\right)^2 = \left(\frac{2}{3}\mu_j\right)^2, \qquad V''\Big/V = 4\mu_j^2, \tag{51}$$

which are indeed the flat space ($k = 0$) Friedmann equations, upon imposing that $\mu_j^2 = \mu^2 = 3\pi\tilde{G}$ ($\tilde{G}$ being the dimensionless gravitational constant) (Marchetti and Oriti, 2021) (see **Supplementary Appendix B**, Eq. 65). Notice that the same equations can be obtained also when one of the js is dominating the volume evolution, and its corresponding μ_j is then taken to be proportional to the (effective) Newton constant (Wilson-Ewing, 2019).

5.2.2 Effective Relational Volume Dynamics with CPS: The Impact of Quantum Effects

Let us now characterize better these two phases of the evolution of the average volume in terms of their relationality and quantumness.

Friedmann Dynamics and Classical Regime

The Friedmann regime is selected by the condition $|x_j| \gg 1$ for each j. Notice that this condition does not necessarily imply that $\rho_j^2 \gg 1$, but it does imply that

$$\sum_{j\in P}\alpha_j \ll \sum_{j\in P}\rho_j^2 \lesssim N\,.$$

As the parameter x_j grows, eventually it will be far enough from each single x_j^o to make the factor $|\Delta X|/N \ll 1$, and, eventually also making N arbitrarily large. From these conditions we see that all the fluctuations on the relevant operators become negligible, and the parameter χ_0 becomes the expectation value of the massless scalar field operator $\hat{\chi}$. Therefore, all the conditions from 1 to 4 (including the matching of all the moments of $\hat{H}$ and $\hat{\Pi}$) are satisfied. As a result.

Statement 1: *For the chosen approximation of the underlying GFT dynamics, a classical regime in which the volume evolution with respect to χ_0 can be interpreted as a relational flat space Friedmann dynamics with respect to a massless scalar field clock is always realized, independently of the initial conditions.*

Let us remark that the approximations involving the underlying GFT dynamics that we used to extract an effective mean field dynamics (see **Section 2.3**) may be very important for the validity of the above statement. For instance, among those, a crucial one was the approximation of negligible interactions[14]. These, however, are supposed to become relevant as the average number of GFT quanta become very large, which is the asymptotic regime in which conditions 1 and 4 are expected to be satisfied. When interactions become important it is certainly possible that some of the above arguments do not hold anymore, but it is also possible that non-zero interactions do not modify substantially the conclusions above, but they change the effective matter content of the Friedmann system, possibly including now a dark sector (see e.g. (Pithis et al., 2016; Pithis and Sakellariadou, 2017; Oriti and Pang, 2105)).

Bounce

The situation concerning the bounce is much more complicated, essentially because it is not an asymptotic regime, and thus the value of initial conditions turns out to be important. It is less obvious whether the bounce can be interpreted as a relational dynamics result, or if the averaged evolution is overwhelmed by quantum fluctuations, thus making us question also the validity of the hydrodynamic approximation in (**Eq. 13**).

In general, it might happen that both the conditions 1 and 2 are not satisfied. For instance, this is the case if the bounce happens at $\overline{\chi_0} = 0$ with initial conditions such that $N(0) \lesssim 1$. Similarly, it might happen that only one of the two conditions above is satisfied. This is the case, for instance, of having a bounce $\overline{\chi_0}$ such that

$$\sqrt{\epsilon/(\lambda N)} \ll \left|\overline{\chi_0}\right| \ll \pi_0^{-1}\,,$$

with arbitrarily large values of $N(\overline{\chi_0})$, so that essentially the bounce happens already in a 'large volume' regime. In this case quantum fluctuations of all the relevant operators are negligible but the interpretation of $\overline{\chi_0}$ as expectation value of the massles scalar field operator is not allowed. Or, the other way around, it might be that indeed $\overline{\chi_0} \gg \pi_0^{-1}$, thus allowing to interpret $\overline{\chi_0}$ as expectation value of $\hat{\chi}$ but $N(\overline{\chi_0}) \lesssim 1$, making fluctuations possibly very large for all the relevant operators.

On the other hand, there are regimes in which a bounce can satisfy all the conditions from 5.1 to 5.1. For instance, let us consider the case in which all the $\chi_{0,j} \equiv \overline{\chi_0}$, which therefore marks the bounce. Also, let us assume that $\rho_j^2(\overline{\chi_0}) \gg 1$ for each $j \in J$, so that $N(\overline{\chi_0}) \gg 1$ too. Let us fix $\overline{\chi_0} > 0$, in particular with $\overline{\chi_0} \gg \sqrt{\epsilon/N(\overline{\chi_0})}$. Lastly, let us also assume that $r_j \gtrsim 1$ for each $j \in P$. Then we know that $\Delta X/N$ is negligible for each $\chi_0 \gtrsim \overline{\chi_0}$, and that relative variances are negligibly small. More precisely, relative variances of σ_N^2, σ_V^2 and σ_H^2 are small because of $\rho_j^2(\overline{\chi_0}) \gg 1$, σ_Π^2 is small because of $N(\overline{\chi_0}) \gg 1$ and $r_{j\in P} \gtrsim 1$, while σ_χ^2 is small because of $N(\overline{\chi_0}) \gg 1$ and $\overline{\chi_0} \gg \sqrt{\epsilon/N(\overline{\chi_0})}$. If we could rest assured that all moments higher than the second one are negligible as well and that the effective equality between $\hat{\Pi}$ and $\hat{H}$ is guaranteed, then we could conclude that the bouncing scenario would be not only reliable and truly relational, but that it could also admit an effective classical description (in terms of some modified gravity theory, with an interesting possibility being mimetic gravity (de Cesare, 2019)). Notice also, that under the above conditions, the dynamics is indeed relational from the point $\overline{\chi_0}$ on. In practice, therefore, when these conditions are realized, one could follow the volume evolution from the bouncing point to the Friedmann regime and on toward infinite values of χ_0.

[14]Let us also mention, however, that another important role is played by the assumption $|B_j/A_j| \ll \epsilon^{-1}$, see footnote 42.

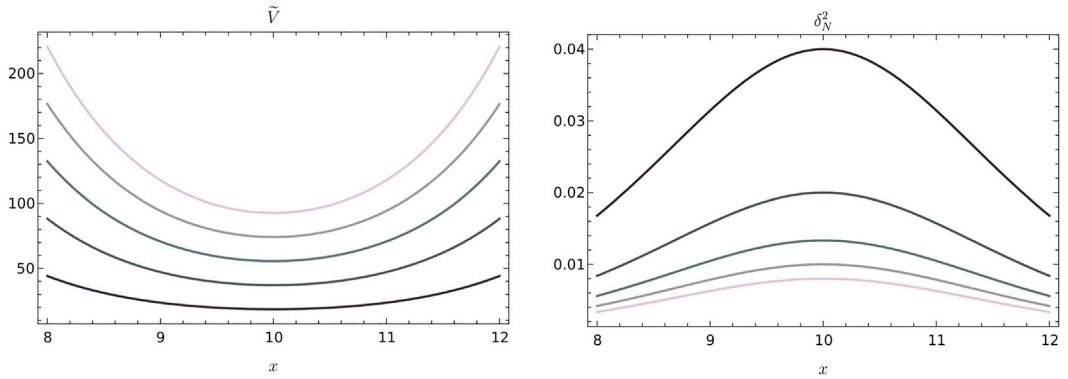

FIGURE 1 | Plots of the dimensionless volume operator $\tilde{V} \equiv V/L_{\mathrm{Pl}}$ and of the relative variance of the number operator δ_N^2 as functions of $x = 2\mu\chi_0$ in a two-spin scenario with $j_1 = 1/2$ and $j_2 = 1$. The plots are obtained with $\mu_{j_1} = \mu_{j_2} = \mu$, $r_{j_1} = r_{j_2} = 0$, $x_{0j_1} = x_{0j_2} = 2\mu\overline{\chi}_0 = 10$, and $\alpha_{j_1} = -10c$, $\alpha_{j_2} = -15c$, with c varying from 1 to 5 in integer steps. Darker (lighter) lines correspond to smaller (higher) values of c.

The relevant quantities for a simplified two-spin scenario like the one described above with $j_1 = 1/2$, $j_2 = 1$, $\mu_{j_1} = \mu_{j_2} = \mu$, $\epsilon\mu^2 \ll 1$, $r_{j_1} = r_{j_2} = 0$, and $\alpha_j < 0$, $|\alpha_j| \gg 1$ for $j \in \{j_1, j_2\}$ are plotted in Figures[15] 1, 2 and 3 as functions of $x \equiv 2\mu\chi_0$. The value of the bounce $\chi_{0,j_1} = \chi_{0,j_2} = \overline{\chi}_0$ is taken to be far enough from $\chi_0 = 0$, so to avoid any unphysical singularity in the quantities represented. In **Figure 1**, we vary the values of α_j from lower to higher values (darker to lighter colors in the plots). In the left panel, we represent the dimensionless volume operator $\tilde{V} = V/L_{\mathrm{Pl}}^3$ (Oriti et al., 2016) (i.e., such that $\tilde{V}_j \sim j^{3/2}$), while on the right panel, we represent the variance of the number operator. As the values of α_j are increased, the minimum value of the averaged volume becomes larger, while δ_N^2 becomes less and less important at the bounce. This behavior is shared also by δ_χ^2 and δ_V^2, since δ_N^2 sets the scaling of the relative variances of all the operators. Indeed, as we can see from **Figure 2**, they are of the same order of magnitude. Actually, one notices that fluctuations in $\widehat{\chi}$ and in $\widehat{N}$ (dashed dark line and lighter solid line respectively) are very close to each other, with differences only of order 10^{-5}-10^{-6} in the range plotted. This is due to the smallness of the quantity $\Delta X/N$, which is plotted in **Figure 3** for increasing values of $\overline{\chi}_0$, as we see from **Eq. 48e**. From both **Figures 2**, **3**, we notice that all the variances and $\Delta X/N$ go to zero at large positive x (where the Friedmann regime is expected to kick in). In any case, we should remark that, since we currently have little control on moments higher than the second ones, one can take the above example only as an indication of the existence of the singularity resolution into a bounce.

In general, therefore, we can draw the following conclusion:

Statement 2: *The bouncing scenario is not a universal feature of the model, meaning that it is not realized under arbitrary choices of the initial conditions. However, if i) there exists at least one $\alpha_j < 0$ or at least one $r_j \neq 0$, ii) all the quantities in **Eqs. 45**, **48e**, **48b** are much less than one when the averaged volume attains its (non-zero) minimum, and iii) all the higher moments of the volume and massless scalar field are negligible, the initial singularity is indeed resolved into a bounce[16].*

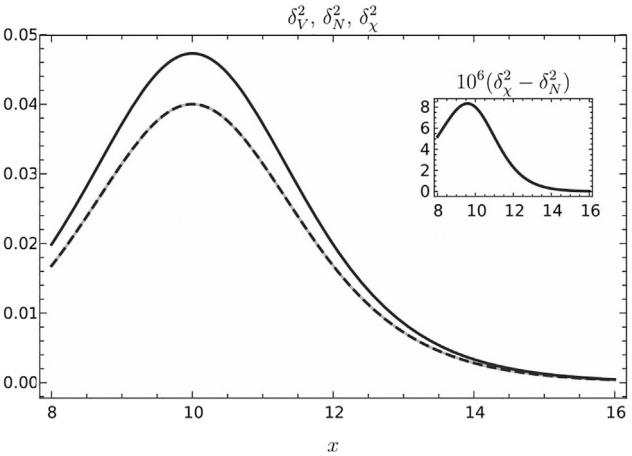

FIGURE 2 | Plot of δ_V^2 (dark solid line), δ_χ^2 (dark dashed line) and δ_N^2 (light solid line) as functions of $x \equiv 2\mu\chi_0$ around the bounce $\overline{x} = 10$ for $\mu_{j_1} = \mu_{j_2} = \mu$, $r_{j_1} = r_{j_2} = 0$, $x_{0j_1} = x_{0j_2} = 2\mu\overline{\chi}_0 = 10$, and $\alpha_{j_1} = -10$, $\alpha_{j_2} = -15$. In the inset plot, instead, is represented $10^6\,(\delta_\chi^2 - \delta_N^2)$ for the same choice of the relevant parameters.

We remark again that this lack of universality is due to the possible role of quantum fluctuations, in particular higher moments, which may make the relational evolution unreliable, while the bouncing dynamics of the average universe volume is in fact general (but not necessarily with a non-zero minimum value). In other words, whether or not the dynamics of the

[15]Indeed, under these assumptions expectation values and variances of $\widehat{\Pi}$ and $\widehat{H}$ are determined by N.

[16]Notice that the requirements (ii) and (iii) correspond to conditions from 1 to 3 being satisfied. The first two of them qualify the framework as relational, while the third one guarantees that the expectation value of the volume operator captures in a satisfactory way the relational evolution of the homogeneous and isotropic geometry.

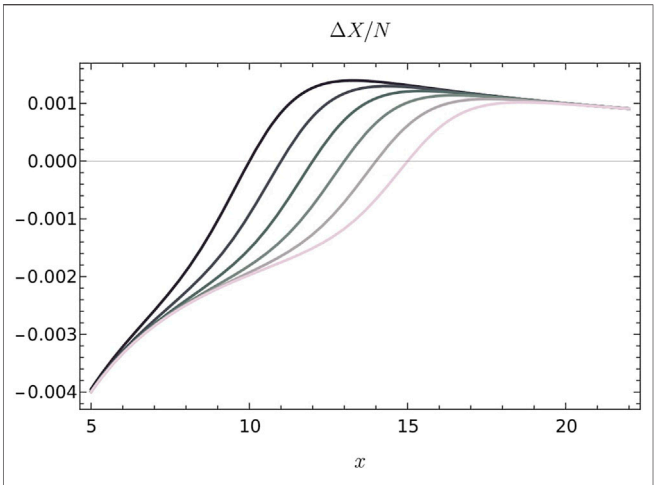

FIGURE 3 | Plot of $\Delta X/N$ as a function of x with $\mu_{j_1} = \mu_{j_2} = \mu$, $r_{j_1} = r_{j_2} = 0$, $\alpha_{j_1} = -10$, $\alpha_{j_2} = -15$ and $\epsilon\mu^2 = 10^{-2}$, but with different values of the bounce, given by $x_{j_1} = x_{j_2} = (1 + 0.1c)10$ for c going from 0 to 5 in integer steps. Darker (lighter) lines correspond to smaller (higher) values of c.

volume is relational and entirely captured by the lowest moment strongly depends on the initial conditions.

5.2.3 An Example: Single Spin Condensate

As an explicit and fairly simple (though possibly very physically relevant (Gielen, 2016)) example of the arguments exposed above, let us consider the case in which only one spin among those in J is excited, say j_o, so that all the sums characterizing the collective operators above are not present anymore. For instance, we now have

$$N(\chi_0) \simeq \rho^2_{j_o}(\chi_0), \qquad V(\chi_0) \simeq V_{j_o}\rho^2_{j_o}(\chi_0), \tag{52}$$

where

$$\rho^2_{j_o}(\chi_0) = \frac{|\alpha_{j_o}|}{2}\left(-\operatorname{sgn}(\alpha_{j_o}) + \cosh x_{j_o}\right), \tag{53}$$

where we have imposed the condition $\sum_j Q_j = 0$, i.e., $Q_{j_o} = 0$, or $\beta_{j_o} = 0$, since we would like to have a relational framework even in intermediate regimes.

Let us study in detail under which conditions a resolution of the initial singularity into a bouncing universe, assuming that indeed quantum effects are effectively encoded into relative variances (so that we can neglect the impact on the system of moments of relevant operators higher than the second one). From **Eqs. 52**, **53**, we deduce that a bounce with a non-zero value of the (average) volume happens only when $\alpha_{j_o} < 0$. We also recall that in this case one has an equality between the second moments of the Hamiltonian and the momentum operator. So, in the following, we will specialize to this case. The situation in this case simplifies considerably: for instance, we have

$$\delta^2_N = \delta^2_V = \sigma^2_H = \delta^2_\Pi = N^{-1} \tag{54}$$

Before proceeding with further considerations, it is interesting to remark that the single spin case mirrors the situation appearing in Loop Quantum Cosmology (LQC) (Bojowald, 2008; Ashtekar and Singh, 2011), where one considers a LQG fundamental state corresponding to a graph constructed out of a large number of nodes and links with the latter being associated all to the same spin. This similarity can be also observed in fluctuations. Indeed, from the above equation we see that in this case the quantity governing quantum fluctuations is exactly the average number of particles, with variances suppressed as N^{-1} for large N. In LQC, the quantity setting the scale of quantum fluctuations is V_0 (Rovelli and Wilson-Ewing, 2014), the coordinate volume of the fiducial homogenous patch under consideration. In a graph interpretation of the LQC framework, $V_0 = N\ell_0$, with ℓ_0 being a fundamental coordinate length, adding another interesting "phenomenological" connection besides those already presented in (Gielen and Oriti, 2014; Oriti et al., 2016; Marchetti and Oriti, 2021) between these two approaches.

Going back to **Eq. 54**, we see that, in order for the bounce to have any hope of being classical, we also need to require $|\alpha_{j_o}| \gg 1$. For the moment, therefore, the two conditions that we have imposed on α_{j_o} are

$$\alpha_{j_o} < 0, \qquad |\alpha_{j_o}| \gg 1. \tag{55}$$

What is left to check are the values of $\Delta X/N$ and σ^2_χ, which are required to be small in order to have a meaningful relational dynamics.

$\Delta X/N$: About $\Delta X/N$, the computation is straightforward: we have

$$\frac{|\Delta X|}{N} = \frac{\left|\left(\rho^2_{j_o}\right)'(\chi_0)\right|}{|\chi_0|}\frac{1}{\rho^2_{j_o}(\chi_0)}\frac{\epsilon}{2} = \frac{|\sinh x_{j_o}|}{\left|x_{j_o} + x^o_{j_o}\right|}\frac{1}{1+\cosh x_{j_o}}\epsilon\mu^2_{j_o}.$$

So, we conclude that for each $x^o_{j_o} \geq 0$ (i.e., for each $\chi_{0,j_o} \geq 0$) the above quantity is always $\ll 1$ for each $\chi_0 \geq 0$.

δ^2_χ: About the relative variance of the massless scalar field operator, assuming $\chi_{0,j_o} \geq 0$, we have

$$\sigma^2_\chi = N^{-1} + \frac{\epsilon}{2N\chi^2_0}.$$

Since the first term is always much smaller than 1 under our assumptions, the relative variance of the massless scalar field operator is negligible as long as $\epsilon/(2N\chi^2_0)$ is negligible as well. This is satisfied for each $\chi_0 \geq \chi_{0,j_o}$ as long as $(\chi_{0,j_o})^2 \gg \epsilon/(2|\alpha_j|)$.

Notice that the assumption of $\chi_{0,j_o} \geq 0$ ($\chi_{0,j_o} \leq 0$) is necessary if one wants to have a relational picture extending from today to the bounce among positive (negative) values of the massless scalar field. Indeed, if the bounce had happened at, say $\chi_{0,j_o} < 0$ (today being at positive values of the massless scalar field), we should have crossed the point $\chi_0 = 0$, which is however a point in which relative quantum fluctuations formally diverge and the clock may become not classical anymore. In conclusion, by further assuming that

$$\chi_{0,j_o} \geq 0\,, \qquad \left(\chi_{0,j_o}\right)^2 \gg \epsilon \Big/ \left(2|\alpha_{j_o}|\right), \tag{56}$$

the singularity is indeed replaced by a bounce (again assuming $\chi_0^{\text{today}} > 0$). Notice that the second inequality above does not impose a very strict constraint on χ_{0,j_o}, since by construction of the CPSs ϵ is assumed to be a very small quantity.

To sum up, a classical bounce that can be understood within the effective relational framework discussed above and in (Marchetti and Oriti, 2021), can be obtained in this single spin case for instance by requiring that.

1. $Q_{j_o} = 0$, guaranteeing equality between the expectation value of $\widehat{\Pi}$ and $\widehat{H}$;
2. Conditions (**Eq. 55**) are satisfied, the first of which guarantees that the expectation value of the volume operator reaches a non-zero minimum before bouncing, and the second of which guarantees small relative variances of the operators $\widehat{N}$, $\widehat{V}$, $\widehat{H}$ and $\widehat{\Pi}$;
3. Assuming that $\chi_0^{\text{today}} > 0$, conditions (**Eq. 56**) are satisfied[17]. The first of them guarantees that χ_0 can be interpreted as the expectation value of the (intrinsic) scalar field operator, while the second one guarantees that its relative quantum fluctuations stay small during the whole Universe's evolution from the bounce until today.

Under these assumptions, the relational time elapsed from the bounce would be

$$\begin{aligned} x_{j_o}^{\text{today}} &\simeq \log\left[\frac{V_{\text{today}}}{V_{j_o}}\frac{2}{|\alpha_{j_o}|} - 1\right] \\ &\simeq \log\left[\frac{V_{\text{today}}}{V_{j_o}}\frac{2}{|\alpha_{j_o}|}\right] = \log\frac{V_{\text{today}}}{V_{j_o}} - \log\frac{|\alpha_{j_o}|}{2}\,, \end{aligned}$$

where we have assumed the term −1 to be negligible with respect to the first contribution. If we further assume that the right-hand-side of the last equality is dominated by the first term, we get

$$x_{j_o}^{\text{today}} \simeq \log\frac{V_{\text{today}}}{V_{j_o}} \sim 252 - \frac{3}{2}\log j_o\,, \tag{57}$$

where the last line is just the result of a crude estimate obtained from $V_{\text{today}} \sim H_0^{-3} \simeq (9.25h \times 10^{25}\ \text{m})^3$, with $h \simeq 0.71$ and $V_{j_o} \simeq (L_P)^3 j_o^{3/2}$.

6 CONCLUSION

We have analyzed the size and evolution of quantum fluctuations of cosmologically relevant geometric observables (in the homogeneous and isotropic case), in the context of the effective relational cosmological dynamics of quantum geometric GFT models of quantum gravity. We considered first of all the fluctuations of the matter clock observables, to test the validity of the relational evolution picture itself. Next, we studied quantum fluctuations of the universe volume and of other operators characterizing its evolution, like the number operator for the fundamental GFT quanta, the effective Hamiltonian and the scalar field momentum (which is expected to contribute to the matter density). In particular, we focused on the late (clock) time regime (see Statement 1, **Section 5.2.2**), where the dynamics of volume expectation value is compatible with a flat FRW universe, and on the very early phase near the quantum bounce. We found that the relative quantum fluctuations of all observables are generically suppressed at late times, thus confirming the good classical relativistic limit of the effective QG dynamics. Near the bounce, corresponding to a mesoscopic regime in which the average number of fundamental GFT quanta can not be arbitrarily large, the situation is much more delicate (see Statement 2, **Section 5.2.2**). Depending on the specific choice of parameters in the fundamental dynamics and in the quantum condensate states, relational evolution as implemented by the CPSs strategy may remain consistent or become unreliable, due to fluctuations of the clock itself and to possible issues with "synchronization" of the fundamental GFT quanta. Even when the relational evolution picture remains valid, quantum fluctuations of the geometric observables may become large, depending again on the precise values of the various parameters. When this happens, this could signal simply a highly quantum regime, but one that is still describable within the hydrodynamic approximation in which the effective cosmological dynamics has been obtained; or it could be interpreted as a signal of a breakdown of the same hydrodynamic approximation, calling for a more refined approximation of the underlying quantum gravity dynamics of the universe.

The analysis will have now to be extended to the case in which GFT interactions are not negligible. We expect such interactions to be most relevant at late clock times and largish universe volume (i.e. largish GFT condensate densities) (Oriti et al., 2016; Marchetti and Oriti, 2021), thus it is unclear whether they should be expected to modify much the behavior of quantum fluctuations, since the are suppressed in the same regime. However, GFT interactions also modify the underlying dynamics of the volume itself, possibly causing a recollapsing phase (de Cesare et al., 2016), thus they may as well enhance quantum fluctuations in such cases. Another important extension would be of course the inclusion of anisotropies (de Cesare et al., 2018), but this is something we need to control much better already at the level of expectation values of geometric observables, in order to be confident about the resulting physical picture. Finally, quantum fluctuations should be considered in parallel with thermal fluctuations, which we can now compute as well using the recently developed thermofield double formalism for GFTs (Assanioussi and Kotecha, 2003; Kotecha and Oriti, 2018; Assanioussi and Kotecha, 2020).

Thus, much more work is called for. It is clear, however, that we now have a solid context to tackle cosmological physics from within full quantum gravity, also for what concerns quantum fluctuations. While we move toward the analysis of cosmological perturbations (Gielen and Oriti, 2018; Gielen, 2019) and the associated quantum gravity phenomenology, these results will

[17] If $\chi_0^{\text{today}} < 0$ the first condition in (**Eq. 56**) would read $\chi_{0,j_o} \leq 0$.

help to control better the viability of the picture of the evolution universe we are going to obtain.

DATA AVAILABILITY STATEMENT

The raw data supporting the conclusion of this article will be made available by the authors, without undue reservation.

AUTHOR CONTRIBUTIONS

All authors listed have made a substantial, direct, and intellectual contribution to the work and approved it for publication.

ACKNOWLEDGMENTS

Financial support from the Deutsche Forschunggemeinschaft (DFG) is gratefully acknowledged. LM thanks the University of Pisa and the INFN (section of Pisa) for financial support, and the Ludwig-Maximilians-Universität Munich for the hospitality.

SUPPLEMENTARY MATERIAL

The Supplementary Material for this article can be found online at: https://www.frontiersin.org/articles/10.3389/fspas.2021.683649/full#supplementary-material

REFERENCES

Adjei, E., Gielen, S., and Wieland, W. (2018). Cosmological Evolution as Squeezing: a Toy Model for Group Field Cosmology. *Class. Quan. Grav.* 35, 105016. doi:10.1088/1361-6382/aaba11

Anderson, E. (2012). *The Problem of Time in Quantum Gravity*. arXiv:1009.2157, 2157.

Ashtekar, A., Bombelli, L., and Corichi, A. (2005). Semiclassical States for Constrained Systems. *Phys. Rev. D* 72, 025008. doi:10.1103/physrevd.72.025008

Ashtekar, A., and Lewandowski, J. (2004). Background Independent Quantum Gravity: A Status Report. *Class. Quan. Grav.* 21, R53–R152. doi:10.1088/0264-9381/21/15/r01

Ashtekar, A., and Singh, P. (2011). Loop Quantum Cosmology: A Status Report. *Class. Quan. Grav.* 28, 213001. doi:10.1088/0264-9381/28/21/213001

Assanioussi, M., and Kotecha, I. (2003). *Thermal Quantum Gravity Condensates in Group Field Theory Cosmology*, 01097.

Assanioussi, M., and Kotecha, I. (2020). Thermal Representations in Group Field Theory: Squeezed Vacua and Quantum Gravity Condensates. *J. High Energ. Phys.* 2020, 173. doi:10.1007/jhep02(2020)173

Baratin, A., Carrozza, S., Oriti, D., Ryan, J., and Smerlak, M. (2014). Melonic Phase Transition in Group Field Theory. *Lett. Math. Phys.* 104, 1003–1017. doi:10.1007/s11005-014-0699-9

Baratin, A., and Oriti, D. (2012). Group Field Theory and Simplicial Gravity Path Integrals: A Model for Holst-Plebanski Gravity. *Phys. Rev. D* 85, 044003. doi:10.1103/physrevd.85.044003

Battefeld, D., and Peter, P. (2015). A Critical Review of Classical Bouncing Cosmologies. *Phys. Rep.* 571, 1–66. doi:10.1016/j.physrep.2014.12.004

Ben Achour, J., and Livine, E. R. (2019). *Cosmology As a CFT^1*. *JHEP* 12, 031.

Ben Geloun, J., Martini, R., and Oriti, D. (2016). Functional Renormalisation Group Analysis of Tensorial Group Field Theories on. *Phys. Rev. D* 94, 024017. doi:10.1103/physrevd.94.024017

Bojowald, M., Höhn, P. A., and Tsobanjan, A. (2011). An Effective Approach to the Problem of Time. *Class. Quan. Grav.* 28, 035006. doi:10.1088/0264-9381/28/3/035006

Bojowald, M., Höhn, P. A., and Tsobanjan, A. (2011). Effective Approach to the Problem of Time: General Features and Examples. *Phys. Rev. D* 83, 125023. doi:10.1103/physrevd.83.125023

Bojowald, M. (2008). Loop Quantum Cosmology. *Living Rev. Relativ.* 11, 4. doi:10.12942/lrr-2008-4

Bojowald, M. (2012). Quantum Cosmology: Effective Theory. *Class. Quan. Grav.* 29, 213001. doi:10.1088/0264-9381/29/21/213001

Bojowald, M., Sandhofer, B., Skirzewski, A., and Tsobanjan, A. (2009). Effective Constraints for Quantum Systems. *Rev. Math. Phys.* 21 (111), 0804. doi:10.1142/s0129055x09003591

Bojowald, M., and Tsobanjan, A. (2009). Effective Constraints for Relativistic Quantum Systems. *Phys. Rev. D* 80, 125008. doi:10.1103/physrevd.80.125008

Carrozza, S. (2016). Flowing in Group Field Theory Space: a Review. *SIGMA* 12, 070.

Carrozza, S., and Lahoche, V. (2017). Asymptotic Safety in Three-Dimensional SU(2) Group Field Theory: Evidence in the Local Potential Approximation. *Class. Quan. Grav.* 34, 115004. doi:10.1088/1361-6382/aa6d90

Carrozza, S., Lahoche, V., and Oriti, D. (2017). Renormalizable Group Field Theory beyond Melonic Diagrams: an Example in Rank Four. *Phys. Rev. D* 96, 066007. doi:10.1103/physrevd.96.066007

de Alfaro, V., Fubini, S., and Furlan, G. (1976). Conformal Invariance in Quantum Mechanics. *Nuov. Cim. A* 34, 569–612. doi:10.1007/bf02785666

de Cesare, M. (2019). Limiting Curvature Mimetic Gravity for Group Field Theory Condensates. *Phys. Rev. D* 99, 063505. doi:10.1103/physrevd.99.063505

de Cesare, M., Oriti, D., Pithis, A. G. A., and Sakellariadou, M. (2018). Dynamics of Anisotropies Close to a Cosmological Bounce in Quantum Gravity. *Class. Quan. Grav.* 35, 015014. doi:10.1088/1361-6382/aa986a

de Cesare, M., Pithis, A. G. A., and Sakellariadou, M. (2016). Cosmological Implications of Interacting Group Field Theory Models: Cyclic Universe and Accelerated Expansion. *Phys. Rev.* D94, 064051.

Dittrich, B. (2006). Partial and Complete Observables for Canonical General Relativity. *Class. Quan. Grav.* 23, 6155–6184. doi:10.1088/0264-9381/23/22/006

Dittrich, B. (2007). Partial and Complete Observables for Hamiltonian Constrained Systems. *Gen. Relativ Gravit.* 39, 1891–1927. doi:10.1007/s10714-007-0495-2

Oriti, D. (2017). "Group Field Theory and Loop Quantum Gravity," in *Loop Quantum Gravity: The First 30 Years*. Editor A. Ashtekar and J. Pullin (WSP). 125–151. doi:10.1142/9789813220003_0005

Finocchiaro, M., and Oriti, D. (2004). *Renormalization of Group Field Theories for Quantum Gravity: New Scaling Results and Some Suggestions*, 07361.

Geloun, J. B., Koslowski, T. A., Oriti, D., and Pereira, A. D. (2018). Functional Renormalization Group Analysis of Rank-3 Tensorial Group Field Theory: The Full Quartic Invariant Truncation. *Phys. Rev. D* 97, 126018. doi:10.1103/physrevd.97.126018

Giddings, S. B., Marolf, D., and Hartle, J. B. (2006). Observables in Effective Gravity. *Phys. Rev. D* 74, 064018. doi:10.1103/physrevd.74.064018

Gielen, S. (2016). Emergence of a Low Spin Phase in Group Field Theory Condensates. *Class. Quan. Grav.* 33, 224002. doi:10.1088/0264-9381/33/22/224002

Gielen, S. (2019). Inhomogeneous Universe from Group Field Theory Condensate. *J. Cosmol. Astropart. Phys.* 2019, 013. doi:10.1088/1475-7516/2019/02/013

Gielen, S., and Menéndez-Pidal, L. (2005). *Singularity Resolution Depends on the Clock*, 05357.

Gielen, S., and Oriti, D. (2018). Cosmological Perturbations from Full Quantum Gravity. *Phys. Rev. D* 98, 106019. doi:10.1103/physrevd.98.106019

Gielen, S., and Oriti, D. (2011). "Discrete and Continuum Third Quantization of Gravity," in *Quantum Field Theory and Gravity: Conceptual and Mathematical Advances in the Search for a Unified Framework, 2*, 1102.

Gielen, S., and Oriti, D. (2014). Quantum Cosmology from Quantum Gravity Condensates: Cosmological Variables and Lattice-Refined Dynamics. *New J. Phys.* 16, 123004. doi:10.1088/1367-2630/16/12/123004

Gielen, S., Oriti, D., and Sindoni, L. (2014). Homogeneous Cosmologies as Group Field Theory Condensates. *JHEP* 06, 013.

Gielen, S., and Polaczek, A. (2020). Generalised Effective Cosmology from Group Field Theory. *Class. Quan. Grav.* 37, 165004. doi:10.1088/1361-6382/ab8f67

Gielen, S. (2014). Quantum Cosmology of (Loop) Quantum Gravity Condensates: An Example. *Class. Quan. Grav.* 31, 155009. doi:10.1088/0264-9381/31/15/155009

Gielen, S., and Sindoni, L. (2016). Quantum Cosmology from Group Field Theory Condensates: a Review. *SIGMA* 12, 082.

Giulini, D. (2007). Remarks on the Notions of General Covariance and Background Independence. *Lect. Notes Phys.* 721, 105–120. doi:10.1007/978-3-540-71117-9_6

Hoehn, P. A., Kubalova, E., and Tsobanjan, A. (2011). Effective Relational Dynamics of a Nonintegrable Cosmological Model. *Phys. Rev. D - Particles, Fields, Gravitation Cosmology* 86.

Hoehn, P. A., and Vanrietvelde, A. (2018). *How to Switch between Relational Quantum Clocks*. arXiv.

Höhn, P. A., Smith, A. R., and Lock, M. P. (1912). *The Trinity of Relational Quantum Dynamics*, 00033.

Isham, C. J. (1992). "Canonical Quantum Gravity and the Problem of Time," in *Integrable Systems, Quantum Groups, and Quantum Field Theories* (Springer), 157.

Kotecha, I., and Oriti, D. (2018). Statistical Equilibrium in Quantum Gravity: Gibbs States in Group Field Theory. *New J. Phys.* 20, 073009. doi:10.1088/1367-2630/aacbbd

Krajewski, T. (2011). *Group Field Theories*. arXiv:1210.6257, 005.

Kuchař, K. V. (2011). Time and Interpretations of Quantum Gravity. *Int. J. Mod. Phys. D* 20, 3.

Li, Y., Oriti, D., and Zhang, M. (2017). Group Field Theory for Quantum Gravity Minimally Coupled to a Scalar Field. *Class. Quan. Grav.* 34, 195001. doi:10.1088/1361-6382/aa85d2

Lidsey, J. E. (1802). *Inflationary Cosmology*. Diffeomorphism Group of the Line and Virasoro Coadjoint Orbits, 09186.

Magnen, J., Noui, K., Rivasseau, V., and Smerlak, M. (2009). Scaling Behavior of Three-Dimensional Group Field Theory. *Class. Quan. Grav.* 26, 185012. doi:10.1088/0264-9381/26/18/185012

Marchetti, L., and Oriti, D. (2021). Effective Relational Cosmological Dynamics from Quantum Gravity. *JHEP* 05, 025.

Oriti, D. (2016). Group Field Theory as the Second Quantization of Loop Quantum Gravity. *Class. Quan. Grav.* 33, 085005. doi:10.1088/0264-9381/33/8/085005

Oriti, D. (1807). *Levels of Spacetime Emergence in Quantum Gravity*, 04875.

Oriti, D., and Pang, X. (2105). *Phantom-like Dark Energy from Quantum Gravity*, 03751.

Oriti, D., Pranzetti, D., Ryan, J. P., and Sindoni, L. (2015). Generalized Quantum Gravity Condensates for Homogeneous Geometries and Cosmology. *Class. Quan. Grav.* 32, 235016. doi:10.1088/0264-9381/32/23/235016

Oriti, D., Sindoni, L., and Wilson-Ewing, E. (2016). Emergent Friedmann Dynamics with a Quantum Bounce from Quantum Gravity Condensates. *Class. Quan. Grav.* 33, 224001. doi:10.1088/0264-9381/33/22/224001

Oriti, D. (2011). "The Microscopic Dynamics of Quantum Space as a Group Field Theory," in *Foundations of Space and Time: Reflections on Quantum Gravity*, 257–320.

Oriti, D. (2017). The Universe as a Quantum Gravity Condensate. *Comptes Rendus Physique* 18, 235–245. doi:10.1016/j.crhy.2017.02.003

Pithis, A. G. A., and Sakellariadou, M. (2019). Group Field Theory Condensate Cosmology: An Appetizer. *Universe* 5, 147. doi:10.3390/universe5060147

Pithis, A. G. A., and Sakellariadou, M. (2017). Relational Evolution of Effectively Interacting Group Field Theory Quantum Gravity Condensates. *Phys. Rev. D* 95, 064004. doi:10.1103/physrevd.95.064004

Pithis, A. G., Sakellariadou, M., and Tomov, P. (2016). Impact of Nonlinear Effective Interactions on Group Field Theory Quantum Gravity Condensates. *Phys. Rev. D* 94, 064056. doi:10.1103/physrevd.94.064056

Reisenberger, M. P., and Rovelli, C. (2001). Spacetime as a Feynman Diagram: the Connection Formulation. *Class. Quan. Grav.* 18, 121–140. doi:10.1088/0264-9381/18/1/308

Rovelli, C. (2002). *A Note on the Foundation of Relativistic Mechanics*. arXiv:gr-qc/0202079.

Rovelli, C. (2004). "Quantum Gravity," in *Cambridge Monographs on Mathematical Physics* (Cambridge, UK: Cambridge University Press). doi:10.1017/CBO9780511755804

Rovelli, C., and Wilson-Ewing, E. (2014). Why Are the Effective Equations of Loop Quantum Cosmology So Accurate? *Phys. Rev. D* 90, 023538. doi:10.1103/physrevd.90.023538

Tambornino, J. (2012). Relational Observables in Gravity: a Review. *SIGMA* 8, 017.

Thiemann, T. (2007). "Modern Canonical Quantum General Relativity," in *Cambridge Monographs on Mathematical Physics* (Cambridge University Press). doi:10.1017/CBO9780511755682

Wilson-Ewing, E. (2019). A Relational Hamiltonian for Group Field Theory. *Phys. Rev.* D99, 086017.

Conflict of Interest: The authors declare that the research was conducted in the absence of any commercial or financial relationships that could be construed as a potential conflict of interest.

Publisher's Note: All claims expressed in this article are solely those of the authors and do not necessarily represent those of their affiliated organizations, or those of the publisher, the editors and the reviewers. Any product that may be evaluated in this article, or claim that may be made by its manufacturer, is not guaranteed or endorsed by the publisher.

frontiers in Astronomy and Space Sciences

ORIGINAL RESEARCH
published: 17 August 2021
doi: 10.3389/fspas.2021.702543

Non-Oscillatory Power Spectrum From States of Low Energy in Kinetically Dominated Early Universes

Mercedes Martín-Benito [1], Rita B. Neves [1] and Javier Olmedo [2]*

[1]Departamento de Física Teórica and IPARCOS, Universidad Complutense de Madrid, Madrid, Spain, [2]Departamento de Física Teórica y Del Cosmos, Universidad de Granada, Granada, Spain

Recently, States of Low Energy (SLEs) have been proposed as viable vacuum states of primordial perturbations within Loop Quantum Cosmology (LQC). In this work we investigate the effect of the high curvature region of LQC on the definition of SLEs. Shifting the support of the test function that defines them away from this regime results in primordial power spectra of perturbations closer to those of the so-called Non-oscillatory (NO) vacuum, which is another viable choice of initial conditions previously introduced in the LQC context. Furthermore, through a comparison with the Hadamard-like SLEs, we prove that the NO vacuum is of Hadamard type as well.

OPEN ACCESS

Edited by:
Francesca Vidotto, Western University, Canada

Reviewed by:
Jorge Pullin, Louisiana State University, United States
Sayantan Choudhury, National Institute of Science Education and Research (NISER), India

***Correspondence:**
Mercedes Martín-Benito
m.martin.benito@ucm.es

Specialty section:
This article was submitted to Cosmology, a section of the journal Frontiers in Astronomy and Space Sciences

Received: *29 April 2021*
Accepted: *28 July 2021*
Published: *17 August 2021*

Citation:
Martín-Benito M, Neves RB and Olmedo J (2021) Non-Oscillatory Power Spectrum From States of Low Energy in Kinetically Dominated Early Universes. Front. Astron. Space Sci. 8:702543. doi: 10.3389/fspas.2021.702543

Keywords: loop quantum cosmology, inflation, primordial perturbations, power spectra, quantum field theory in curved spacetimes, states of low energy, non-oscillatory vacuum state

1 INTRODUCTION

In a previous work (Martín-Benito et al., 2021), we have proposed the States of Low Energy (SLEs) introduced in (Olbermann, 2007) as viable candidates for the vacuum state of cosmological perturbations in Loop Quantum Cosmology (LQC). We were motivated by the fact that they were proven to be Hadamard states that minimized the regularized energy density when smeared along the time-like curve of an isotropic observer via a test function. Furthermore, they had been shown to provide a qualitative behavior in the ultraviolet (UV) and infrared regimes of the primordial power spectra of scalar and tensor perturbations that agrees with observations in models where a period of kinetic dominance precedes inflation (Banerjee and Niedermaier, 2020), which is the case in LQC. However, in (Martín-Benito et al., 2021) we have only considered test functions that could be seen as natural choices within LQC, namely, ones with support on the high curvature regime. As long as this is the case, we have shown that the ambiguity in the introduction of the test function is surpassed in this context, in the sense that the resulting SLE and power spectra seem to be very insensitive to its shape and support, provided it is wide enough.

In this work, we investigate the effect of shifting the test function away from the high curvature regime. Firstly, this provides a more complete analysis of the SLEs and the ambiguity of the test function. Secondly, this allows us to distinguish in the primordial power spectra the consequences coming directly from LQC corrections and those related to having a period of kinetic dominance prior to inflation, which can also be obtained in a classical scenario. We will show that if the test function ignores the Planckian region, the effect in the resulting SLE is appreciable. Furthermore, in the power spectra the oscillations that were previously found for lower wave numbers are now dampened.

This motivates us to compare our results with those found in the LQC literature that adopts as initial conditions for the perturbations the so-called non-oscillatory (NO) vacuum state (de Blas and

Olmedo, 2016; Castelló Gomar et al., 2017). As the name suggests, this state is precisely defined to minimize mode by mode the amplitude of the oscillations of the primordial power spectra in a given time interval. It turns out that this minimization in time is reflected in a minimization of oscillations in the k domain of the power spectra. This NO prescription has been motivated as well as a good candidate for the vacuum of the perturbations (Elizaga Navascués et al., 2020). One question that so far remained unanswered is whether this NO vacuum is or not of Hadamard type. In this work, by comparing with SLEs, we show that indeed this is the case. To do so, we resort to their UV expansions, obtained for SLEs in (Banerjee and Niedermaier, 2020) and for the NO vacuum in (Elizaga Navascués et al., 2020).

This manuscript is organized as follows. In **Section 3** we review the application of SLEs in LQC as presented in (Martín-Benito et al., 2021). In **Section 4** we explore the consequence of excluding the high curvature regime from the test function, computing the corresponding SLEs and power spectra at the end of inflation. **Section 5** is devoted to a proof that the NO vacuum is Hadamard, based on the comparison with SLEs in the UV limit. Finally, we conclude in **Section 6** with a discussion and closing remarks.

Throughout we adopt Planck units $c = \hbar = G = 1$ for numerical computations, keeping factors of G in expressions.

2 COSMOLOGICAL PERTURBATIONS AND STATES OF LOW ENERGY IN LQC

In this section we will briefly review the dynamics of cosmological perturbations in LQC through its hybrid approach, as well as the definition of SLEs in this context, as exposed in (Martín-Benito et al., 2021). Let us start by considering the spatially flat FLRW model with scale factor a, minimally coupled to the scalar field ϕ subject to the potential $V(\phi)$, which will drive inflation. Cosmological perturbations are usually described by scalar and tensor gauge invariant perturbations $\mathcal{Q}$ and $\mathcal{T}^I$ respectively, where I denotes the two possible polarizations of tensor perturbations. Expanding in Fourier modes $\mathcal{Q}_k$ and $\mathcal{T}^I_k$, we can write the equation of motion for each mode with wave number $k = |k|$ as.

$$\ddot{\mathcal{Q}}_k + 3H(t)\dot{\mathcal{Q}}_k + \left(\omega_k^{(s)}(t)\right)^2 \mathcal{Q}_k = 0, \tag{1}$$

$$\ddot{\mathcal{T}}^I_k + 3H(t)\dot{\mathcal{T}}^I_k + \left(\omega_k^{(t)}(t)\right)^2 \mathcal{T}^I_k = 0, \tag{2}$$

where the dot denotes derivative with respect to cosmological time t, and $H = \dot{a}/a$ is the Hubble parameter. As we will discuss further ahead, the form of the terms ω_k depends on the quantization. It is common to work with the rescaled fields $u = a\mathcal{Q}$, $\mu^I = a\mathcal{T}^I$, and in conformal time η, such that $d\eta = dt/a$. Then, we find the equations of motion of the Fourier modes of these fields, u_k and μ_k respectively, to be.

$$u_k''(\eta) + \left(k^2 + s^{(s)}(\eta)\right)u_k(\eta) = 0, \tag{3}$$

$$\left(\mu_k^I(\eta)\right)'' + \left(k^2 + s^{(t)}(\eta)\right)\mu_k^I(\eta) = 0, \tag{4}$$

where the prime denotes derivative with respect to conformal time η and $s^{(s)}(\eta)$ and $s^{(t)}(\eta)$ are the time-dependent mass terms of scalar and tensor modes respectively. From the hybrid approach to LQC, one can write these as functions of the background variables a, ρ (inflaton energy density), P (inflaton pressure) and the inflaton potential $V(\phi)$ as (Elizaga Navascués et al., 2018a):

$$s^{(t)} = -\frac{4\pi G}{3}a^2(\rho - 3P), \qquad s^{(s)} = s^{(t)} + \mathcal{U}, \tag{5}$$

where

$$\mathcal{U} = a^2\left[V_{,\phi\phi} + 48\pi G V(\phi) + 6\frac{a'\phi'}{a^3\rho}V_{,\phi} - \frac{48\pi G}{\rho}V^2(\phi)\right]. \tag{6}$$

To simplify notation, in the following we will use $s(\eta)$ to refer generically to both of them, as our comments apply equally to both scalar and tensor modes. When doing so, for simplicity, we will refer only to u as everything is analogous for μ^I. It is easy to find that $s(\eta)$ can be related to ω_k^2, now written in terms of conformal time, through

$$\omega_k^2(\eta) = \frac{1}{a^2(\eta)}\left[k^2 + s(\eta) + \frac{a''(\eta)}{a(\eta)}\right]. \tag{7}$$

Generally, there are no analytical solutions to such equations of motion, and results have to be obtained numerically, given initial conditions $u_k(0)$, $u_k'(0)$. These can be parametrized up to a phase through

$$u_k(0) = \frac{1}{\sqrt{2D_k}}, \qquad u_k'(0) = \sqrt{\frac{D_k}{2}}(C_k - i), \tag{8}$$

where D_k is a positive function and C_k any real function. Once defined, the perturbations can be evolved until a time η_{end} during inflation when all the scales of interest have crossed the horizon. The primordial power spectra of the comoving curvature perturbation $\mathcal{R}_k = u_k/z$ (where $z = a\dot{\phi}/H$) and tensor perturbations $\mathcal{T}$, defined as

$$\mathcal{P}_{\mathcal{R}}(k) = \frac{k^3}{2\pi^2}\frac{|u_k|^2}{z^2}, \qquad \mathcal{P}_{\mathcal{T}}(k) = \frac{32k^3}{\pi}\frac{|\mu_k^I|^2}{a^2}, \tag{9}$$

are evaluated at $\eta = \eta_{\text{end}}$. The choice of initial conditions amounts to a choice of vacuum state for the perturbations. In this context, there is no notion of a unique natural vacuum. Indeed, several proposals have been made of initial vacua within the LQC framework (Agullo et al., 2015; de Blas and Olmedo, 2016; Ashtekar and Gupt, 2017; Elizaga Navascués et al., 2020) that result in primordial power spectra compatible with observations. In these analyses, initial conditions are set at the LQC bounce where the scale factor of the geometry reaches a minimum, and then it starts expanding. At this bounce, the spacetime curvature reaches a maximum value of the order of the Planck scale. The work of (Martín-Benito et al., 2021) applied the SLE construction defined in (Olbermann, 2007) to this context. These are defined as the states that minimize the energy density smeared along a time-like curve, specified by a test function f. In the following we summarize this procedure, adapted to our notation (namely working with u and μ and in conformal

time). For further details we refer the reader to (Olbermann, 2007; Martín-Benito et al., 2021). Given a fiducial solution v to the equation of motion (3), the SLE associated to the test function $f(\eta)$ is found through the Bogoliubov transformation

$$u_k = \alpha(k)v_k + \beta(k)\bar{v}_k, \tag{10}$$

where the Bogoliubov coefficients $\alpha(k)$ and $\beta(k)$ are found uniquely (up to a phase) to be.

$$\beta(k) = \sqrt{\frac{c_1(k)}{2\sqrt{c_1^2(k) - |c_2^2(k)|}} - \frac{1}{2}}, \tag{11}$$

$$\alpha(k) = -e^{-i\mathrm{Arg}[c_2(k)]}\sqrt{\frac{c_1(k)}{2\sqrt{c_1^2(k) - |c_2^2(k)|}} + \frac{1}{2}}. \tag{12}$$

with.

$$c_1(k) := \frac{1}{2}\int d\eta f^2(\eta)a\left[\left|\left(\frac{v_k}{a}\right)'\right|^2 + \omega_k^2\left|\frac{v_k}{a}\right|^2\right], \tag{13}$$

$$c_2(k) := \frac{1}{2}\int d\eta f^2(\eta)a\left[\left(\left(\frac{v_k}{a}\right)'\right)^2 + \omega_k^2\,\frac{v_k^2}{a^2}\right], \tag{14}$$

Note that these quantities carry a dependence on the test function f. Indeed, as remarked, **Eq. 10** defines the SLE associated to this f. This introduces an ambiguity in the procedure, which has been explored within the LQC approach in (Martín-Benito et al., 2021). In that work, only natural choices for f within this framework were considered, whose support thus included the bounce of LQC. In this current investigation, we will consider test functions that exclude it.

3 EFFECT OF THE BOUNCE IN SLES

In (Martín-Benito et al., 2021) we have shown that there are two families of test functions that can be seen as natural choices for the smearing function within LQC, and that provide SLEs that are very insensitive to their particular form. Namely, we have found that for a test function supported around the bounce of LQC the resulting SLE does not qualitatively depend on its shape or support, as long as it is wide enough. In the case of a test function supported on the expanding branch only, from the bounce onward, in (Martín-Benito et al., 2021) only the case of a steep (but smooth) step function was investigated, in order to fully retain the contributions coming from the bounce. In this case, the SLE remains insensitive to the size of the support as long as it is wide enough. The resulting power spectrum inherits this independence on the choice of test function, and coincidentally shows good agreement with the one of a second order adiabatic vacuum state.

In this section we explore the consequences of not including the bounce in the support of the test function. This way we will be able to study also the effect of the shape of the test function when supported only on the expanding branch away from the high-curvature regime. This will allow us to provide a comparison with an analogous classical scenario of an FLRW model with a period of kinetic dominance prior to inflation.

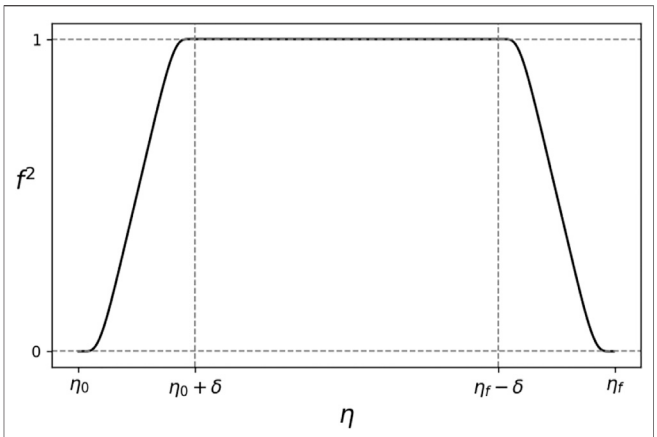

FIGURE 1 | The smooth step function defined in **(15)**, represented in terms of its parameters: initial and final points, η_i and η_f respectively, and δ, which controls the ramping up.

Let us start by considering the smooth step function f^2 plotted in **Figure 1**, supported in the interval $\eta \in [\eta_0, \eta_f]$, as defined in (Martín-Benito et al., 2021):

$$f^2(\eta) = \begin{cases} S\left(\dfrac{\eta - \eta_0}{\delta}\pi\right) & \eta_0 \le \eta < \eta_0 + \delta, \\ 1 & \eta_0 + \delta \le \eta \le \eta_f - \delta, \\ S\left(\dfrac{\eta_f - \eta}{\delta}\pi\right) & \eta_f - \delta < \eta \le \eta_f, \end{cases} \tag{15}$$

where δ determines the ramping up, with a smaller δ resulting in a steeper step, and S is the auxiliary function:

$$S(x) = \frac{1 - \tanh[\cot(x)]}{2}. \tag{16}$$

Figure 2 shows the initial conditions, parametrized through (8), corresponding to the SLE obtained for scalar perturbations when considering the test function (15), with $\eta_0 = 0$, 1, 10 and 100 Planck seconds after the bounce, with η_f fixed at the onset of inflation, and for a sharp step of $\delta \sim 0.06$. The case of $\eta_0 = 0$ corresponds to the one analysed in (Martín-Benito et al., 2021). The effect of excluding the bounce is immediately noticed as soon as the support of the test function is moved one Planck second into the expanding branch. If we push the initial time further into the future, the change is gradually decreased, and for $\eta_0 = 100$ we see some convergence. The corresponding figure for tensor modes is omitted since the initial conditions are essentially the same, as discussed in (Martín-Benito et al., 2021). Within this family of test functions that exclude the bounce, we have also investigated the consequences of changing their shape. In all these cases, we find that, as the starting point moves further away from the bounce, the SLE becomes more insensitive to the shape of the test function. For this reason, below, we will focus our comments on the four step functions defined above, as they already show the different qualitative behaviors one may obtain from different test functions in this scenario.

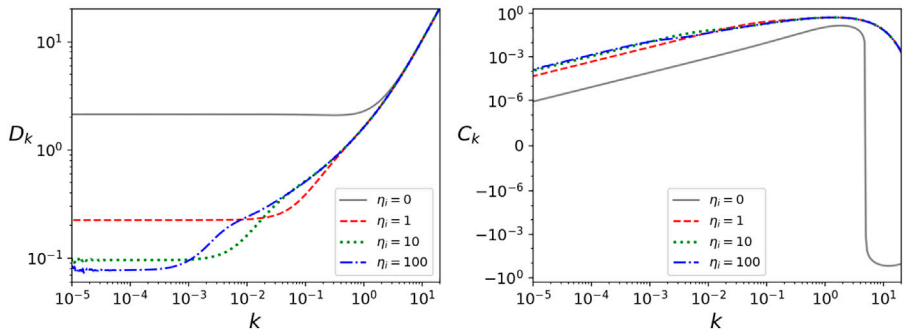

FIGURE 2 | Initial conditions in terms of D_k and C_k, as constructed in **(8)**, for scalar modes at the bounce corresponding to the SLEs obtained with the window function (**Eq. 15**) covering the expanding branch until the onset of inflation with starting points: $\eta_0 = 0$ (solid gray line), $\eta_0 = 1$ (dashed red line), $\eta_0 = 10$ (dotted green line) and $\eta_0 = 100$ (dotted-dashed blue line). The scale of k is in Planck units. All computations were performed for a quadratic potential $V(\phi) = m^2\phi^2/2$, with $m = 1.2 \times 10^{-6}$ and with the value of the scalar field at the bounce fixed to $\phi_B = 1.225$ (toy value). For tensor modes, the resulting SLE at the bounce shows no significant qualitative differences.

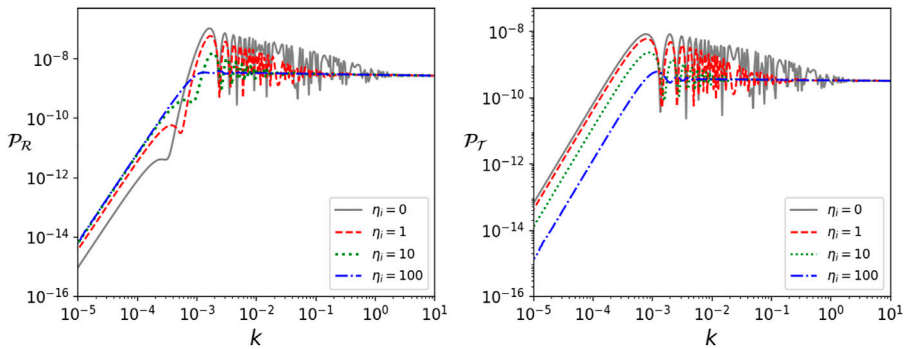

FIGURE 3 | Power spectra of the comoving curvature perturbation $\mathcal{P}_\mathcal{R}$ and tensor perturbation $\mathcal{P}_\mathcal{T}$ corresponding to the SLEs obtained with the window function (**Eq. 15**) covering the expanding branch until the onset of inflation with starting points: $\eta_0 = 0$ (solid gray line), $\eta_0 = 1$ (dashed red line), $\eta_0 = 10$ (dotted green line) and $\eta_0 = 100$ (dotted-dashed blue line). The scale of k is in Planck units. All computations were performed for a quadratic potential $V(\phi) = m^2\phi^2/2$, with $m = 1.2 \times 10^{-6}$ and with the value of the scalar field at the bounce fixed to $\phi_B = 1.225$ (toy value).

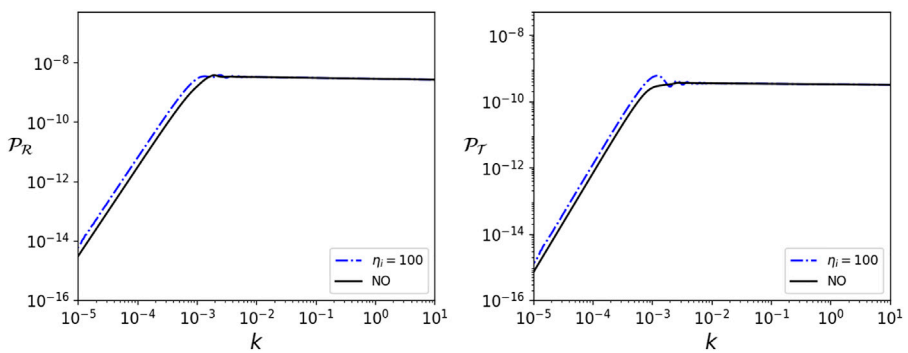

FIGURE 4 | Comparison between the power spectra of the comoving curvature perturbation $\mathcal{P}_\mathcal{R}$ and tensor perturbation $\mathcal{P}_\mathcal{T}$ corresponding to the SLE obtained with $\eta_0 = 100$ (dotted-dashed blue line) and to the NO vacuum (solid black line). The scale of k is in Planck units. All computations were performed for a quadratic potential $V(\phi) = m^2\phi^2/2$, with $m = 1.2 \times 10^{-6}$ and with the value of the scalar field at the bounce fixed to $\phi_B = 1.225$ (toy value).

Figure 3 shows the corresponding primordial power spectra for scalar and tensor perturbations, computed through (9). Here, the effect of removing the bounce is evident. As the support of the test function is pushed further away from the high curvature regime, the oscillations in the power spectra are gradually dampened. It is interesting to note that, in fact, as **Figure 4**

shows, the power spectra are pushed towards those obtained from the non-oscillatory (NO) vacuum state defined in (de Blas and Olmedo, 2016), which is constructed by minimizing the oscillations in time of the power spectrum of perturbations for the whole expanding branch, including the bounce. We further note that the case where the support of the test function starts at $\eta_0 = 100$ will essentially correspond to that obtained by using the SLE as the vacuum state of primordial perturbations in a classical FLRW model with a period of kinetic dominance prior to inflation. However, for smaller η_0, SLEs show oscillations in k at and below scales comparable to those of the curvature at that initial time. Then we can conclude that the oscillations that appear in the power spectra when including the high curvature region (for instance the bounce of LQC) in the support of the test function open an interesting observational window.

For completion, we added an appendix where we apply the SLE and NO vacuum prescriptions in a classical Universe dominated by the kinetic energy of the scalar field. We discuss the situations in which they agree with the natural choice for vacuum state considered in (Contaldi et al., 2003).

4 COMPARISON BETWEEN SLE AND NO VACUUM

One remarkable property of the SLEs that is usually not explicitly proven for other vacua proposals is that they are of Hadamard type (Olbermann, 2007; Banerjee and Niedermaier, 2020). This guarantees that computations such as that of the expectation value of the renormalized stress-energy tensor will be well defined. On the other hand, the NO vacuum has only been proven to behave in the ultraviolet (UV) asymptotic regime as a high order adiabatic state, at least of fourth order (Elizaga Navascués et al., 2018b). Indeed, considering two adiabatic states of orders n and m, one can compute the β coefficient of the Bogoliubov transformation between the two:

$$\beta = i\left[u_k^n \left(u_k^m\right)' - u_k^m \left(u_k^n\right)'\right], \tag{17}$$

and find that in the UV $|\beta|$ decays with k^{-l-2}, where $l = \min(n, m)$. In the case of the comparison of the NO vacuum with an nth-order adiabatic one, it was found that $|\beta| \sim k^{-2-n}$ at least up to $n = 4$, which shows that the NO vacuum is the highest order one of the two. As a Hadamard type vacuum is an infinite order adiabatic state, this is an indication that the NO vacuum might be as well, though a stronger proof would be desirable. In this section, we will provide one, through a comparison with the (Hadamard-like) SLEs.

To simplify the comparison, let us write the UV expansions of both the SLE and the NO state as

$$u_k(\eta) \sim \frac{1}{\sqrt{2F_k(\eta)}} e^{-i\int d\eta F_k(\eta)}, \tag{18}$$

where $\sim$ means the behavior in the large k regime. The NO vacuum state has recently been analysed analytically in (Elizaga Navascués et al., 2020). In particular, that work has found that the state admits the UV asymptotic expansion (18) with:

$$F_k^{NO}(\eta) = -\mathrm{Im}\left(h_k(\eta)\right), \tag{19}$$

where

$$k h_k^{-1} \sim i\left[1 - \frac{1}{2k^2}\sum_{n=0}^{\infty}\left(\frac{-i}{2k}\right)^n \gamma_n\right], \tag{20}$$

and the γ_n coefficients are given by the iterative relation

$$\gamma_{n+1} = -\gamma_n' + 4s(\eta)\left[\gamma_{n-1} + \sum_{m=0}^{n-3}\gamma_m\gamma_{n-(m+3)}\right] - \sum_{m=0}^{n-1}\gamma_m\gamma_{n-(m+1)}, \tag{21}$$

with $\gamma_0 = s(\eta)$ and $\gamma_{-n} = 0$ for all $n > 0$. With this expansion, we are able to compute the NO state up to any order in $1/k$ easily. Actually, one can check by direct inspection that

$$F_k^{NO}(\eta) \sim k\left\{1 + \sum_{n\geq 1}\frac{(-1)^n}{k^{2n}} G_n(\eta)\right\}^{-1}, \tag{22}$$

where the G_n are determined recursively by

$$G_n(\eta) = \sum_{m,l\geq 0, m+l=n-1}\left\{\frac{1}{4}G_m G_l'' - \frac{1}{8}G_m' G_l' + \frac{1}{2}s(\eta)G_m G_l\right\} - \frac{1}{2}\sum_{m,l\geq 1, m+l=n} G_m G_l, \tag{23}$$

with $G_0 = 1$. Remarkably, in (Banerjee and Niedermaier, 2020), the SLEs are found to have the same asymptotic expansion (22), regardless of the choice of the test function.

Therefore, the β coefficients of the Bogoliubov transformation between the SLE and NO vacuum are identically zero in the UV. Thus, we conclude that the NO vacuum is of Hadamard type since it displays exactly the same short-distance structure as the SLEs.

5 CONCLUSION AND DISCUSSION

SLEs have recently been proposed as a suitable choice for the vacuum state of perturbations in LQC (Martín-Benito et al., 2021), where the dependence of the state on the test function was explored. For that investigation, only test functions that included the bounce of LQC were analysed, as they are natural choices within this framework. In this work, we investigate the effect of pushing the support of the test function away from the bounce and indeed from the high curvature regime. In addition to offering a more complete analysis of SLEs within LQC, this allows us to disentangle the effects coming from quantum corrections to the dynamics, which are important in the high curvature regime, from those that arise from having only a period of kinetic dominance prior to inflation, which can be found also in classical inflationary models, and is not a direct consequence of the quantum nature of geometry.

We have found that whether the support of the test function includes the high curvature regime or not has a greater influence on the resulting SLE than any other parameter of the test function that has been studied previously. Indeed, in (Martín-Benito et al., 2021), we had already shown that as long as the support of the test

function includes the high curvature regime and it is wide enough, the SLE is very insensitive to its shape and support. In this work, we have shown that as soon as the test function is pushed away from the bounce, the SLE suffers a big shift, which then converges as the test function is pushed further away from the high curvature regime. We have also found that in this case, when convergence with respect to the support is reached, the SLE is again insensitive to the shape of the test function. Furthermore, through the computation of the power spectra of perturbations at the end of inflation, we see that as the test function is shifted away from the high curvature region the oscillations found for lower modes (scales comparable to those of the curvature at initial time) are gradually dampened, and the spectra are pushed to those of the NO vacuum state introduced in (de Blas and Olmedo, 2016). Then it is safe to conclude that these oscillations are in fact a consequence of the corrections coming from LQC, which opens an interesting observational window into signatures from LQC in observations of the CMB. For instance, the enhancement of power at super-Hubble scales in the primordial power spectrum of scalar perturbations has been proposed, together with large scale non-Gaussianities, as a mechanism to explain several anomalies in the CMB (Agullo et al., 2021a; Agullo et al., 2021b). From this perspective, the power spectrum provided by SLEs prescription when including the bounce is physically relevant. On the other hand, the NO-like power spectra show a lack of power at large scales of primordial origin that can, on the one hand, alleviate some tensions in the CMB (Ashtekar et al., 2020; Ashtekar et al., 2021), and on the other hand, ease the *trans*-Planckian issues on these scenarios (Brandenberger and Martin, 2013; Ashtekar and Gupt, 2017). See (Li et al., 2021) for a recent comparison on further details about different proposals in LQC. However, a detailed analysis of all this requires a rigorous investigation that we leave for future work.

Finally, the fact that SLEs are proven to be Hadamard is a great advantage that most proposals don't enjoy. Typically, this property is difficult to prove explicitly. One strategy, that may be enough for practical purposes, is to compare a state with an adiabatic one of increasing (finite) order, and show, through the β coefficients of the Bogoliubov transformation between the two states, that the state in question is always of higher order than the adiabatic one considered. This shows that it is at least a very high order adiabatic state, and since a Hadamard state is an adiabatic state of infinite order, then most likely so is the proposed state. However, we now have a family of states, namely SLEs, that are explicitly Hadamard. Therefore, the β coefficients of the transformation between any Hadamard state and any SLE should decrease faster than any power of the wave number. We have applied this reasoning to the NO vacuum state, that had previously been shown to be at least of fourth order (Elizaga Navascués et al., 2018b). We find that, in the ultraviolet limit of large wave numbers, the asymptotic expansion that the NO vacuum satisfies (found in (Elizaga Navascués et al., 2020)) agrees exactly with that of the SLE (Banerjee and Niedermaier, 2020) (no matter the test function chosen to define it). As a consequence, the β coefficients of the transformation between the two will be identically zero in the ultraviolet. In other words, the NO vacuum has the same short-distance structure than the SLEs, which proves that the NO vacuum is of Hadamard type as well.

DATA AVAILABILITY STATEMENT

The original contributions presented in the study are included in the article/**Supplementary Material**, further inquiries can be directed to the corresponding author.

AUTHOR CONTRIBUTIONS

All authors listed have made a substantial, direct, and intellectual contribution to the work and approved it for publication.

FUNDING

This work is supported by the Spanish Government through the projects FIS2017-86497-C2-2-P and PID2019-105943GB-I00 (with FEDER contribution). RN acknowledges financial support from Fundação para a Ciência e a Tecnologia (FCT) through the research grant SFRH/BD/143525/2019. JO acknowledges the Operative Program FEDER2014-2020 Junta de Andalucía-Consejería de Economía y Conocimiento under project E-FQM-262-UGR18 by Universidad de Granada.

ACKNOWLEDGMENTS

The authors would like to thank Beatriz Elizaga Navascués and Guillermo Mena Marugán for useful discussions.

SUPPLEMENTARY MATERIAL

The Supplementary Material for this article can be found online at: https://www.frontiersin.org/articles/10.3389/fspas.2021.702543/full#supplementary-material

REFERENCES

Agullo, I., Nelson, W., and Ashtekar, A. (2015). Preferred Instantaneous Vacuum for Linear Scalar fields in Cosmological Space-Times. *Phys. Rev. D* 91, 064051. doi:10.1103/PhysRevD.91.064051

Agullo, I., Kranas, D., and Sreenath, V. (2021). Anomalies in the CMB from a Cosmic Bounce. *Gen. Relativ Gravit.* 53, 17. doi:10.1007/s10714-020-02778-9

Agullo, I., Kranas, D., and Sreenath, V. (2021). Large Scale Anomalies in the CMB and Non-gaussianity in Bouncing Cosmologies. *Class. Quan. Grav.* 38, 065010. doi:10.1088/1361-6382/abc521

Ashtekar, A., Gupt, B., and Sreenath, V. (2021). *Cosmic Tango between the Very Small and the Very Large: Addressing CMB Anomalies through Loop Quantum Cosmology*.

Ashtekar, A., and Gupt, B. (2017). Initial Conditions for Cosmological Perturbations. *Class. Quan. Grav.* 34, 035004. doi:10.1088/1361-6382/aa52d4

Ashtekar, A., Gupt, B., Jeong, D., and Sreenath, V. (2020). Alleviating the Tension in the Cosmic Microwave Background Using Planck-Scale Physics. *Phys. Rev. Lett.* 125, 051302. doi:10.1103/PhysRevLett.125.051302

Banerjee, R., and Niedermaier, M. (2020). Bonus Properties of States of Low Energy. *J. Math. Phys.* 61, 103511. doi:10.1063/5.0019311

Brandenberger, R. H., and Martin, J. (2013). Trans-Planckian Issues for Inflationary Cosmology. *Class. Quan. Grav.* 30, 113001. doi:10.1088/0264-9381/30/11/113001

Castelló Gomar, L., Mena Marugán, G. A., Martín de Blas, D., and Olmedo, J. (2017). Hybrid Loop Quantum Cosmology and Predictions for the Cosmic Microwave Background. *Phys. Rev. D* 96, 103528. doi:10.1103/PhysRevD.96.103528

Contaldi, C. R., Peloso, M., Kofman, L., and Linde, A. (2003). Suppressing the Lower Multipoles in the CMB Anisotropies. *J. Cosmol. Astropart. Phys.* 2003, 002. doi:10.1088/1475-7516/2003/07/002

de Blas, D. M., and Olmedo, J. (2016). Primordial Power Spectra for Scalar Perturbations in Loop Quantum Cosmology. *J. Cosmol. Astropart. Phys.* 2016, 029. doi:10.1088/1475-7516/2016/06/029

Elizaga Navascués, B., Martin de Blas, D., and Mena Marugán, G. A. (2018). Time-dependent Mass of Cosmological Perturbations in the Hybrid and Dressed Metric Approaches to Loop Quantum Cosmology. *Phys. Rev. D* 97, 043523.

Elizaga Navascués, B., Marugán, G. A. M., and Prado, S. (2020). Non-oscillating Power Spectra in Loop Quantum Cosmology. *Class. Quant. Grav.* 38, 035001. doi:10.1088/1361-6382/abc6bb

Elizaga Navascués, B., Martín de Blas, D., and Mena Marugán, G. (2018). The Vacuum State of Primordial Fluctuations in Hybrid Loop Quantum Cosmology. *Universe* 4, 98. doi:10.3390/universe4100098

Li, B.-F., Singh, P., and Wang, A. (2021). Phenomenological Implications of Modified Loop Cosmologies: an Overview. *Front. Astron. Space Sci.* 8, 701417. doi:10.3389/fspas.2021.701417

Martín-Benito, M., Neves, R. B., and Olmedo, J. (2021). *States of Low Energy in Bouncing Inflationary Scenarios in Loop Quantum Cosmology*.

Olbermann, H. (2007). States of Low Energy on Robertson-Walker Spacetimes. *Class. Quan. Grav.* 24, 5011–5030. doi:10.1088/0264-9381/24/20/007

Conflict of Interest: The authors declare that the research was conducted in the absence of any commercial or financial relationships that could be construed as a potential conflict of interest.

Publisher's Note: All claims expressed in this article are solely those of the authors and do not necessarily represent those of their affiliated organizations, or those of the publisher, the editors and the reviewers. Any product that may be evaluated in this article, or claim that may be made by its manufacturer, is not guaranteed or endorsed by the publisher.

frontiers in Astronomy and Space Sciences

ORIGINAL RESEARCH
published: 18 August 2021
doi: 10.3389/fspas.2021.703845

Anomalies in the Cosmic Microwave Background and Their Non-Gaussian Origin in Loop Quantum Cosmology

Ivan Agullo[1]*, *Dimitrios Kranas*[1] and *V. Sreenath*[2]

[1]Department of Physics and Astronomy, Louisiana State University, Baton Rouge, LA, Unites States, [2]Department of Physics, National Institute of Technology Karnataka, Surathkal, India

Anomalies in the cosmic microwave background (CMB) refer to features that have been observed, mostly at large angular scales, and which show some tension with the statistical predictions of the standard ΛCDM model. In this work, we focus our attention on power suppression, dipolar modulation, a preference for odd parity, and the tension in the lensing parameter A_L. Though the statistical significance of each individual anomaly is inconclusive, collectively they are significant, and could indicate new physics beyond the ΛCDM model. In this article, we present a brief, but pedagogical introduction to CMB anomalies and propose a common origin in the context of loop quantum cosmology.

Keywords: cosmic microwave background, loop quantum cosmology, anomalies, early universe, quantum cosmology

OPEN ACCESS

Edited by:
Francesca Vidotto, Western University, Canada

Reviewed by:
Susanne Schander, Perimeter Institute for Theoretical Physics, Canada
Herman J. Mosquera Cuesta, Departamento Administrativo Nacional de Ciencia, Tecnologia e Innovacion, Colciencias, Colombia

***Correspondence:**
Ivan Agullo
agullo@lsu.edu

Specialty section:
This article was submitted to Cosmology, a section of the journal Frontiers in Astronomy and Space Sciences

Received: *30 April 2021*
Accepted: *21 July 2021*
Published: *18 August 2021*

Citation:
Agullo I, Kranas D and Sreenath V (2021) Anomalies in the Cosmic Microwave Background and Their Non-Gaussian Origin in Loop Quantum Cosmology. Front. Astron. Space Sci. 8:703845. doi: 10.3389/fspas.2021.703845

I INTRODUCTION

Observations of the cosmic microwave background (CMB) by the Planck satellite have revealed that the ΛCDM model together with the inflationary scenario checks nearly all the right boxes (Aghanim, 2018a; Akrami, 2018; Aghanim, 2020)—in the sense that it provides a detailed fit to the CMB spectrum based on a few free parameters (Aghanim, 2018a; Aghanim, 2019). The nearly scale-invariant power spectrum predicted by slow-roll inflation has been confirmed with a significance of more than 7σ (Aghanim, 2018b; Akrami, 2018). Further, observations are consistent with the near Gaussian nature of the primordial perturbations predicted by slow-roll inflation (Akrami, 2020).

But in spite of this success, several open questions remain. A prominent one concerns the past incompleteness of the inflationary scenario. As it is well known, general relativity, on which the inflationary scenario rests, breaks down as we approach the Planck regime. Loop quantum cosmology (LQC) uses the principles of loop quantum gravity to address this issue (Bojowald, 2001; Ashtekar et al., 2003; Mena Marugan, 2010; Ashtekar and Singh, 2011; Banerjee et al., 2012; Agullo et al., 2014; Agullo et al., 2017a). In LQC, the big bang singularity is replaced by a bounce (Ashtekar et al., 2006a; Ashtekar et al., 2006b; Ashtekar et al., 2007; Szulc, 2007; Szulc et al., 2007; Bentivegna and Pawlowski, 2008; Martin-Benito et al., 2008; Ashtekar and Wilson-Ewing, 2009a; Ashtekar and Wilson-Ewing, 2009b; Garay et al., 2010; Wilson-Ewing, 2010; Pawlowski and Ashtekar, 2012) which is triggered by quantum gravitational effects. This bounce by itself is not able to generate the primordial perturbations though, and it must be complemented with another mechanism. A natural strategy is to maintain the inflationary phase in the post-bounce era. In such a scenario, the goal of the bounce is, in addition to overcoming the difficulties arising from classical general relativity, to bring the Universe to an inflationary phase. Interestingly, although the inflationary phase is responsible for the primordial perturbations, certain features from the pre-

inflationary bounce may survive if the inflationary era is not too long, and be imprinted in the CMB. Numerous studies have examined the way the bounce predicted by LQC modifies the primordial power spectra of scalar and tensor perturbations (Bojowald et al., 2009; Bojowald and Calcagni, 2011; Agullo et al., 2012; Agullo et al., 2013a; Agullo et al., 2013b; Fernández-Méndez et al., 2013; Fernández-Méndez et al.,2014; Agullo and Morris, 2015; Barrau et al., 2015; de Blas and Olmedo, 2016; Martínez and Olmedo, 2016; Ashtekar and Gupt, 2017; Agullo et al., 2017b; Castelló Gomar et al., 2017; Zhu et al., 2017; Agullo, 2018; Agullo et al., 2020a; Agullo et al., 2020b; Li et al., 2020a; Li et al., 2020b; Ashtekar et al., 2020; Navascués et al., 2020; Navascués and Mena Marugán, 2020; Martín-Benito et al., 2021) and the non-Gaussianity (Agullo, 2015; Agullo et al., 2018; Zhu et al., 2018; Sreenath et al., 2019) at large angular scales, and showed that at smaller scales in the CMB the predictions are indistinguishable from those of standard inflation with Bunch-Davies initial conditions. Hence, if at all early Universe scenarios such as LQC were to leave any imprints on the CMB, they would be expected at the longest observable scales, or equivalently, at the lowest angular multipoles.

It is for this reason that certain puzzling signatures which have been recently observed at large angular scales in the CMB become relevant (Akrami et al., 2019). These signatures, generically known as CMB anomalies, are features that are in conflict with the almost scale invariance predicted by inflation, or with the statistical isotropy and homogeneity assumed in the ΛCDM. In more detail, the anomalies observed by Planck include a lack of two-point correlations at large angular scales, a dipolar asymmetry, a preference for odd parity, alignment of low multipoles, a cold spot, etc. In addition, the Planck analysis has also found a preference for a larger value of the lensing parameter (Aghanim, 2018b) than it is expected. Some of these anomalies were already observed by the WMAP satellite and even by COBE. Hence, the consensus is that these signals are not due to unaccounted systematics. Put it simply, there is no debate about the fact that these are real features in the CMB [see e.g., (Schwarz et al., 2016)]. However, the statistical significance with which these features depart from the predictions of the ΛCDM model is, though non-negligible, inconclusive, and the debate is rather whether any of these features are significant enough to require the introduction of new physics. Recall that the ΛCDM only makes statistical predictions, and therefore none of these features are actually incompatible with ΛCDM. But if we accept the ΛCDM model, the observed features imply that we live in an uncommon realization of the underlying probability distribution. Another possibility is that some or all these features are signatures of new physics, and they are in fact expected signals in a suitable extension of the ΛCDM theory.

In recent work (Agullo et al., 2021a; Agullo et al., 2021b) we proposed that a cosmic bounce before inflation naturally changes the primordial probability distribution in such a way that, in a statistical sense, the observed features are not anomalous. The core of the idea is that a cosmic bounce generates strong correlations (non-Gaussianities) between the longest modes we observe in the sky and longer, super-horizon modes. We cannot observe directly these correlations since some of the modes involved have wave-lengths larger than the Hubble radius today. But these correlations produce indirect effects in observable modes, which can account for the observed anomalies. The goal of this article is to apply the general ideas introduced in (Agullo et al., 2021a; Agullo et al., 2021b) to LQC. We will also take the opportunity to provide a succinct and pedagogical introduction to CMB anomalies and the phenomenon of non-Gaussian modulation, addressed to the quantum cosmology community. See (Agullo and Morris, 2015; de Blas and Olmedo, 2016; Ashtekar and Gupt, 2017; Agullo et al., 2020a; Ashtekar et al., 2020; Agullo et al., 2020b) for other ideas to account for some of the features observed in the CMB within LQC. In particular, the companion article (Ashtekar et al., 2021) in this special issue, provides an interesting set of complementary ideas and perspectives on the way LQC can account for the CMB anomalies.

The plan of this article is as follows. In the next section, we discuss the basic principles behind quantifying temperature anisotropy and discuss the implications of statistical homogeneity and isotropy for CMB anisotropies. Then, we describe some of the anomalies observed by the Planck satellite, which point to a violation of the underlying assumption of statistical homogeneity and isotropy. In **section III**, we describe the mechanism behind the phenomenon of non-Gaussian modulation. In **section IV**, we provide a quick description of the evolution of perturbations in LQC and discuss the power spectrum and bispectrum generated therein. We then apply non-Gaussian modulation to LQC in **section V** and present our results. In this section, we describe how the presence of non-Gaussian modulation in LQC makes these anomalous features more likely to occur, in a way that they are no longer anomalous. Finally, in **section VI**, we conclude with a discussion of our results, its short comings, and future directions.

II INTRODUCTION TO CMB ANOMALIES

The temperature $T(\hat{n})$ of the CMB as a function of the direction $\hat{n}$ is nearly uniform, making it convenient to split $T(\hat{n})$ into an isotropic part, the mean temperature $\overline{T} = \frac{1}{4\pi}\int \mathrm{d}\Omega\, T(\hat{n})$, and the anisotropic deviation from it

$$\delta T(\hat{n}) \equiv \frac{T(\hat{n}) - \overline{T}}{\overline{T}} = \sum_{\ell m} a_{\ell m}\, Y_{\ell m}(\hat{n}), \tag{2.1}$$

where in the last equality we have decomposed the function $\delta T(\hat{n})$ in spherical harmonics $Y_{\ell m}$. [see, for instance, (Durrer, 2008; Weinberg, 2008)]. The mean temperature $\overline{T}$ is a free parameter of the Λ*CDM* model, which is determined by observations. Our best measurement of $\overline{T}$ comes from the FIRAS instrument in the COBE satellite, and is measured $\overline{T} = 2.7260 \pm 0.0013\, K$ (Fixsen, 2009).

The Λ*CDM* model predicts only the statistical properties of the temperature map $\delta T(\hat{n})$ or, equivalently, of the coefficients $a_{\ell m}$. Therefore, the quantities we want to extract from observations are the moments: $\langle a_{\ell m} a_{\ell' m'}\rangle$, $\langle a_{\ell m} a_{\ell' m'} a_{\ell'' m''}\rangle$, etc. There are

theoretical reasons, further supported by observations, to argue that the probability distribution we are after is very close to Gaussian, in which case the simplest non-zero moment, $\langle a_{\ell m} a_{\ell' m'} \rangle$, is all we need (recall that a Gaussian distribution is completely characterized by the mean and the variance). Furthermore, the assumption of statistical homogeneity and isotropy, on which the ΛCDM model rests, implies that $\langle a_{\ell m} a^*_{\ell' m'} \rangle$ must be diagonal in ℓ and m, and m-independent

$$\langle a_{\ell m}\, a^*_{\ell' m'} \rangle \;=\; C_\ell\, \delta_{\ell \ell'}\, \delta_{m m'}. \tag{2.2}$$

In other words, homogeneity and isotropy imply that all information contained in the second moments can be codified in the m-independent coefficients C_ℓ, for $\ell = 1, 2, 3, \ldots$. C_ℓ is known as the angular power spectrum.

The equivalent statement in angular space is that the second moments of $\delta T(\hat{n})$, $C(\theta) \equiv \langle \delta T(\hat{n})\, \delta T(\hat{n}') \rangle$ can only depend on the angle θ between the two directions $\hat{n}$ and $\hat{n}'$:

$$C(\theta) \;\equiv\; \langle \delta T(\hat{n})\, \delta T(\hat{n}') \rangle \;=\; \frac{1}{4\pi} \sum_\ell (2\,\ell + 1)\, C_\ell\, P_\ell(\cos\theta). \tag{2.3}$$

If the assumptions of statistical homogeneity and isotropy break down, then the simple characterization of the two-point correlations in terms of the simple quantity C_ℓ or $C(\theta)$ becomes insufficient, and one would have to work with the full covariance matrix of $a_{\ell m}$ or $\delta T(\hat{n})$.

The angular power spectrum C_ℓ is measured by averaging the data from satellites. But, what is the correct notion of average? Ideally, one would like to have different realizations of the probability distribution (that is, different universes) and take averages on them, which is closer to the way averages are measured in quantum systems. Another possibility is to take averages over the CMB temperature map observed from different locations in the Universe. The ergodic theorem relates both averages. Unfortunately, none of these two strategies is available at the practical level. Rather, what is done in practice is to take advantage of the m-independence of the power spectrum C_ℓ, and obtain it by averaging over its value obtained from individual m's (we actually observe $\delta T(\hat{n})$, but a simple computer code can translate the data to values of $a_{\ell m}$). The limitation of this strategy is clear: we have $2\ell + 1$ values of m for each multipole ℓ, and consequently the uncertainty about the value of C_ℓ obtained in this way will be large for small values of ℓ. This uncertainty is known as cosmic variance, and it is quantified by $\pm \sqrt{2/(2\ell + 1)}\, C_\ell$. It is not difficult to translate this uncertainty to angular space, and the result is $\pm\, \sigma(C(\theta))$, with

$$\sigma^2\,(C(\theta)) \;=\; \frac{1}{8\,\pi^2} \sum_\ell (2\,\ell + 1)\, C_\ell^2\, P_\ell^2(\cos\theta). \tag{2.4}$$

Cosmic variance is an intrinsic limitation of cosmological observations, and cannot be overcome by building more precise instruments. Therefore, in making predictions for C_ℓ or $C(\theta)$, one needs to keep in mind this inherent uncertainty.

We now discuss the anomalous features that have been observed in CMB. The Planck team has carried out several tests to check the statistical isotropy of the CMB (Ade, 2014; Ade, 2016a; Akrami et al., 2019). The CMB is a spherical shell of radiation, which captures a spherical sample of the density perturbations at the time of decoupling in the early Universe. Hence, deviations from isotropy in the CMB sphere will signal deviation from statistical homogeneity or isotropy in the early Universe. Since, as emphasized above, the predictions from the ΛCDM model are statistical, a key aspect of the analysis is to quantify the statistical significance of any observed departure from the theory. In statistical parlance, this is known as hypothesis testing, wherein a null hypothesis, which in this case is the ΛCDM model, is compared with observations. The departure from the null hypothesis is often quantified in terms of the so called p-value. Given a null hypothesis, the p-value is the probability with which a certain phenomenon can occur. If the p-value of an observed feature is zero, the null hypothesis is automatically considered as incorrect. A very small value of the p-value, would rather rule out the hypothesis with a statistical significance given by $1 - p$. The concept is visually illustrated in **Figure 1**: the p-value corresponds to the area of the shaded region.

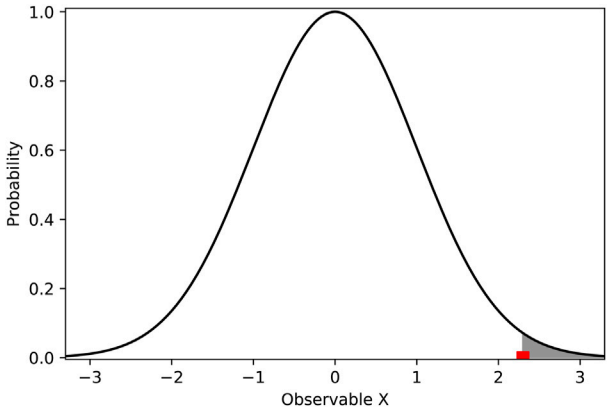

FIGURE 1 | Illustration of the concept of p-value. The figure shows the probability distribution of a certain observable X according to the null hypothesis in black. The value of X that is actually observed is shown in red. Although the expected value of X is zero, the observation is not incompatible with the theoretical prediction, given the statistical character of the later. The shaded area gives us the p-value of the observed value of X. As it is evident from the figure, a smaller p-value implies a larger departure from the null hypothesis.

In order to quantify an anomaly, the first step is to choose an observable of interest, which will serve as the indicator of the anomaly. Rather than analytically deriving the probability distribution of the chosen observable out of the theory, a task that may be difficult for some observables, in practice it is often more convenient to estimate the p-value numerically. This can be done by simulating a large number of random realizations of the CMB temperature map from the probability distribution of the ΛCDM model—using the best fit for the free parameters—and computing the p-value of the chosen observable from them. This is the way the Planck collaboration has evaluated the p-value of the anomalies discussed below (Ade, 2014; Ade, 2016b). For

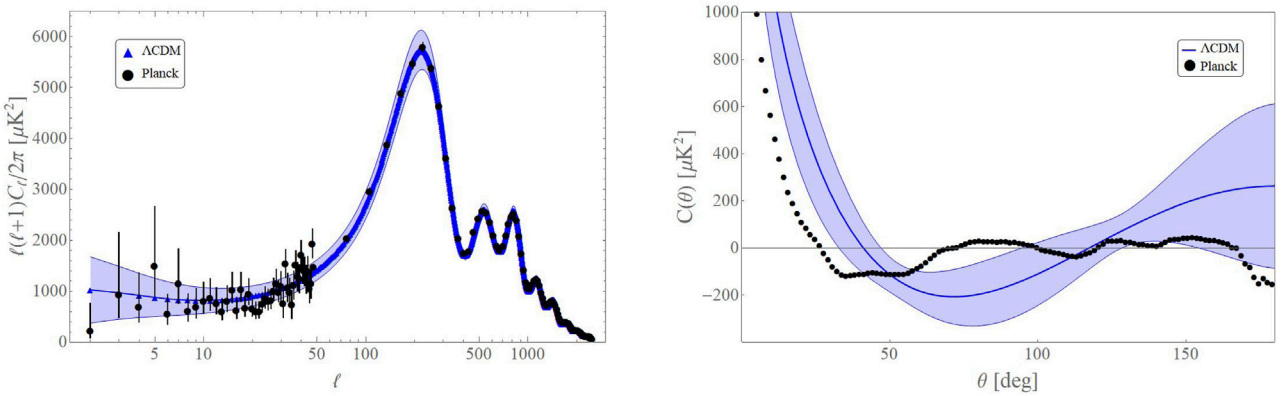

FIGURE 2 | The *TT* power spectrum in the multipole **(A)** and angular space **(B)** generated in the standard model corresponding to the best fit parameters provided by Planck. The blue shaded region indicates the uncertainty due to cosmic variance. The black dots with error bars are the data from Planck. Note that the observed quadrupole is quite low compared to the prediction from the standard model, although it is compatible with the prediction within 1σ when we account for cosmic variance. The lack of power at large angular scales is more evident in the angular power spectrum, where the power is considerably low for angular scales greater than 60°. Furthermore, the amplitude of the predicted power is larger than the observed one by more than 1σ for the largest angular scales and for angles between ≈60° and 80°.

example, if only five simulations out of a thousand lead to a value of an observable which is at least as extreme as the observed value, they would report a p-value of 0.005 for that observation, or equivalently 0.5%. The anomalies considered in this article have p-value ≤ 1% (Schwarz et al., 2016). In the remaining part of this section, we briefly describe the anomalies that we consider in this article.

A Power Suppression

Data from the satellites COBE (Hinshaw et al., 1996), WMAP (Bennett et al., 2003) and Planck (Akrami et al., 2019), have consistently found a lack of two-point correlations at low multipoles, or at large angular scales, compared to what is expected in the ΛCDM model. Visually, this lack of correlations is evident in the real space two-point correlation function $C(\theta)$, shown in the right panel of **Figure 2**: for angles larger than 60°, the two-point function is surprisingly low. The WMAP team had come up with an appropriate observable to quantify this lack of power (Spergel et al., 2003). It is defined by

$$S_{1/2} = \int_{-1}^{1/2} C(\theta)^2 \, \mathrm{d}(\cos\theta). \tag{2.5}$$

Its physical meaning is obvious: it captures the total amount of correlations squared (to avoid cancellations between positive and negative values of $C(\theta)$) in angles $\theta > 60°$. The ΛCDM model predicts $S_{1/2} \approx 42000\,\mu K^4$, while the Planck satellite has reported a measured value[1] of $S_{1/2} = 1{,}209.2\,\mu K^4$ (Akrami et al., 2019), which corresponds to a p-value less than 1% [≤0.5% according to (SchwarzSchwarz et al., 2016)]. Put in simpler terms, this p-value tells us that if we were able to observe one thousand universes ruled out by the ΛCDM model, only about a handful will show such a low value of $S_{1/2}$.

[1]The value of $S_{1/2}$ varies a bit depending on the choice of map and the mask used.

B Dipolar Modulation Anomaly

A second important anomaly that has been also observed by multiple satellites, is the presence of a dipolar modulation of the entire CMB signal (Akrami et al., 2019). This dipole should not be confused with the multipole $\ell = 1$. Rather, the anomaly makes reference to correlations between multipoles ℓ and $\ell + 1$, which can be explained by a modulation of dipolar character, as we further discuss below.

Such modulation was first modeled mathematically in (Gordon et al., 2005), by adding a simple dipole to the temperature map as follows

$$T(\hat{n}) = T_0(\hat{n})\left[1 + A_1\,\hat{n}\cdot\hat{d}\right], \tag{2.6}$$

where $T_0(\hat{n})$ is the unmodulated (statistically isotropic) temperature field, A_1 is the amplitude of the modulation, and $\hat{d}$ its direction. It is easy to check that such modification affects not only the $\ell = 1$ angular multipole, but actually all multipoles equally, and for this reason it is known as a scale-independent dipolar modulation. Its main effect is to create correlations between multipoles ℓ and $\ell + 1$. Such correlations, as mentioned above, violate isotropy [see Appendix B of (Agullo et al., 2021b) for further details].

The Planck team has carried out a likelihood analysis of such modulation of the CMB, and arrived at constraints on the amplitude and direction of the dipolar modulation in different bins of multipoles ℓ. Surprisingly, the analysis has revealed a non-zero amplitude of the dipolar modulation only for low multipoles, in the bin $\ell \in [2, 64]$. The amplitude reported in this bin is $A_1 \approx 0.07$ (Ade, 2016a), and the significance of the detection is greater than 3σ. This reveals, not only a significant deviation of the ΛCDM model, but also that the dipolar modulation is scale-dependent, since it only appears for low multipoles. Therefore, the simple model (**Eq. 2.6**) is insufficient to account for the observed modulation. Finding

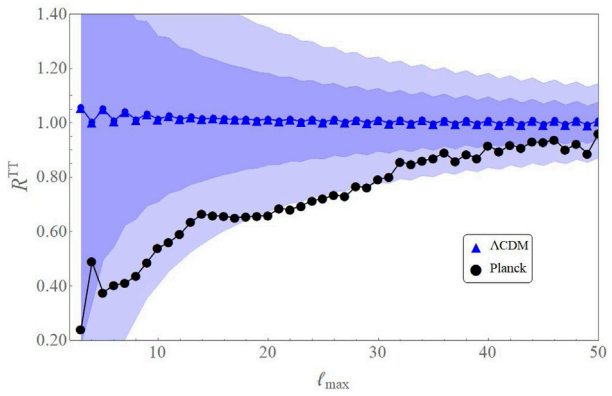

FIGURE 3 | $R^{TT}(\ell_{max})$ generated in the standard model (blue) along with 2σ shaded contours arising from cosmic variance. Black points are the observations by Planck. The observed value of $R^{TT}(\ell_{max})$ for most points is lower than the predictions of the standard model by more than 1σ.

a mechanism to generate a scale-dependent dipolar modulation, without introducing other undesired effects, has challenged the imagination of theorists during the last decade (Dai et al., 2013).

C Parity Anomaly

Observations from both WMAP and Planck have found a preference for odd parity two-point correlations, as opposed to the predictions of the standard ΛCDM model, which predicts that the primordial perturbations generated in our Universe are parity neutral. The parity of the primordial perturbations can be studied by analyzing the multipoles in the range [2, 50], known as the Sachs-Wolfe plateau. This range of multipoles corresponds to long wavelength perturbations which entered the horizon in the recent past, and hence have been relatively unmodified by late time physics. The asymmetry in the parity can be quantified using the estimator

$$R^{TT}(\ell_{\max}) = \frac{D_+(\ell_{\max})}{D_-(\ell_{\max})}, \tag{2.7}$$

where $D_\pm(\ell_{\max})$ quantify the sum of power contained in even (+) or odd (−) multipoles, up to ℓ_{max}. More specifically, $D_\pm(\ell_{\max})$ are defined as

$$D_\pm(\ell_{\max}) = \frac{1}{\ell^\pm_{tot}} \sum_{2,\ell_{max}}^{\pm} \frac{\ell(\ell+1)}{2\pi} C_\ell \tag{2.8}$$

where the + or − signs on the right refer to the fact that we include only even or odd multipoles in the sum, respectively, and $\ell^\pm_{tot}$ refers to the total number of multipoles in the sum. **Figure 3** illustrates that CMB data in the multipole range of [2, 50] shows a clear preference for odd parity compared to the parity neutral, i.e., $R^{TT}(\ell_{max}) = 1$, prediction of the standard model. Although this anomaly, as well as the anomaly in the lensing amplitude discussed in the next subsection, are not as severe as the previous ones due to their lower statistical significance ($\lesssim 2\sigma$), we will later argue that they may be related to the power suppression.

D Lensing Amplitude Anomaly

The cosmic microwave background radiation undergoes lensing by the intervening distribution of matter, as it propagates from the surface of last scattering to us. An important observable in the CMB, in addition to temperature and polarization, is the lensing potential. From the CMB maps, Planck has reconstructed the lensing potential and computed its power spectrum (Aghanim, 2018b). The effect of lensing is the smoothing of CMB power spectrum at small angular scales. The amount of smoothing observed in the CMB angular power spectrum should be consistent with the smoothing derived from the power spectrum of the lensing potential. In order to check this consistency, (Aghanim, 2018a), considered a test-parameter, known as the lensing parameter A_L, that multiplies the lensing power spectrum. Theoretically, the value of lensing parameter should be $A_L = 1$, and in fact Planck assumes this value during the process of parameter estimation. However, if A_L is left as a free parameter, along with the six parameters of the ΛCDM model, in the Markov Chain Monte Carlo (MCMC) analysis, one finds that $A_L = 1.243 \pm 0.096$ for *PlanckTT + lowE* data, which is more than 2σ away from one. If the reconstructed lensing data is also used, along with Planck *EE* and *TE* data, then the lensing parameter is consistent with 1 within 2σ.

A key feature of the anomalies discussed above, except perhaps for the lensing anomaly, is that they appear clearly associated with the largest angular scales we can observe. This suggests a common origin in primordial physics for these diverse set of anomalies. The next section introduces a proposal for a mechanism that can provide such common origin, namely the phenomenon of non-Gaussian modulation. Together with the scale dependence introduced by the quantum bounce of LQC, this mechanism constitutes a promising candidate for the origin of the anomalies we have just described.

III NON-GAUSSIAN MODULATION

Temperature anisotropies in the CMB are a consequence of the evolution of photons and other constituents of the Universe in a perturbed spacetime. Since the observed anisotropies are small, $\delta T/\overline{T} \sim 10^{-5}$, perturbation theory is an appropriate tool. If the primordial perturbations in the metric generated in the early Universe were exactly linear,[2] then only those perturbations with wavelengths smaller than the radius of the Hubble horizon today would be able to affect the CMB. On the contrary, non-linear effects, generically known as non-Gaussianity, couple modes of different wavelengths, and make it possible that primordial perturbations with wavelengths larger than the Hubble radius today can impact what we observe in the CMB (Schmidt and Kamionkowski, 2010; Jeong and Kamionkowski, 2012; Dai et al., 2013; Schmidt and Hui, 2013; Agullo, 2015; Adhikari et al., 2016). We will refer to

[2]Strong non-linearities are important at late times in the Universe during structure formation, but not to explain the CMB.

this phenomenon as non-Gaussian modulation of the CMB. Since long wavelength, super-horizon modes do not evolve with time, we could treat them as spectator modes, whose role is to influence, or bias, sub-horizon modes.

Primordial perturbations are random variables with zero mean and a variance characterized by the two-point correlations discussed in the previous section. We will show that one consequence of the coupling between super-horizon and sub-horizon wavelengths is to modify the two-point correlation functions (Schmidt and Hui, 2013; Agullo, 2015; Adhikari et al., 2016). Though the mean value of the primordial perturbations is not modified, the variance is, in such a way that certain features in the CMB are more likely to be observed than in the absence of non-Gaussian correlations, and consequently they should not be considered as anomalous. In this section, we will describe the essential features of the mechanism of non-Gaussian modulation. We will split the discussion in two parts: in the first one, we will discuss the modulation of the primordial power spectrum due to non-Gaussian correlations with a spectator mode, and in the second part, we describe the effect of such a modulation on the CMB *TT* angular power spectrum.

A Non-Gaussian Modulation of Primordial Perturbations

We are interested in computing the two-point correlation function of the curvature perturbation $\mathcal{R}_{\vec{k}}$ for a mode $\vec{k}$ that is observable in the CMB, in the presence of a longer wavelength mode $\mathcal{R}_{\vec{q}}$, when both modes are correlated.

A convenient and general way to model the effects of non-Gaussian correlations, is to write the curvature perturbations at a given time t in terms of a Gaussian field $\mathcal{R}^G$ as follows (Schmidt and Kamionkowski, 2010)

$$\mathcal{R}_{\vec{k}}(t) = \mathcal{R}^G_{\vec{k}}(t) + \frac{1}{2}\int \frac{d^3q}{(2\pi)^3} f_{\rm NL}(\vec{q},\vec{k}-\vec{q})\,\mathcal{R}^G_{\vec{q}}(t)\,\mathcal{R}^G_{\vec{k}-\vec{q}}(t). \tag{3.1}$$

The convolution in the integral is the Fourier transform of a quadratic combination of $\mathcal{R}^G$ in position space, and is the source of the non-Gaussian character of $\mathcal{R}_{\vec{k}}(t)$, and the function $f_{\rm NL}(\vec{k}_1, \vec{k}_2)$ contains the information about the strength and details of the non-Gaussianity. The goal of this equation is simply to parameterize the non-Gaussianity in a simple and tractable way, while the form of the function $f_{\rm NL}(\vec{k}_1, \vec{k}_2)$ is expected to come from a concrete microscopic model of the early Universe.

Statistical isotropy and homogeneity implies that the function $f_{\rm NL}(\vec{k}_1, \vec{k}_2)$ depends only on the modulus of the two wavenumbers involved, $k_1 \equiv |\vec{k}_1|$ and $k_2 \equiv |\vec{k}_2|$, and on the (cosine of the) angle between them, μ: $f_{\rm NL}(\vec{k}_1, \vec{k}_2) = f_{\rm NL}(k_1, k_2, \mu)$. From it, the three-point correlation function is given by $\langle \mathcal{R}_{\vec{k}_1}\mathcal{R}_{\vec{k}_2}\mathcal{R}_{\vec{k}_3}\rangle = (2\pi)^3\,\delta(\vec{k}_1+\vec{k}_2+\vec{k}_3)\,B_{\mathcal{R}}(\vec{k}_1,\vec{k}_2,\vec{k}_3)$, where the bispectrum $B_{\mathcal{R}}(\vec{k}_1,\vec{k}_2,\vec{k}_3)$ is

$$B_{\mathcal{R}}(\vec{k}_1,\vec{k}_2,\vec{k}_3) = f_{\rm NL}(\vec{k}_1,\vec{k}_2)\,[P_{\mathcal{R}}(\vec{k}_1)P_{\mathcal{R}}(\vec{k}_2) + P_{\mathcal{R}}(\vec{k}_2)P_{\mathcal{R}}(\vec{k}_3) + P_{\mathcal{R}}(\vec{k}_3)P_{\mathcal{R}}(\vec{k}_1)], \tag{3.2}$$

and $P_{\mathcal{R}}(\vec{k})$ is the power spectrum of $\mathcal{R}^G$, defined as

$$\langle \mathcal{R}^G_{\vec{k}_1}\mathcal{R}^{G*}_{\vec{k}_2}\rangle = (2\pi)^3\,\delta(\vec{k}_1-\vec{k}_2)\,P_{\mathcal{R}}(\vec{k}_1). \tag{3.3}$$

The dimensionless power spectrum is defined as $\mathcal{P}_{\mathcal{R}}(\vec{k}) = k^3\,P_{\mathcal{R}}(\vec{k})/2\pi^2$.

Our goal is to compute the two-point function of $\mathcal{R}_{\vec{k}}$ in the presence of the spectator mode $\mathcal{R}_{\vec{q}}$. Using (**Eq. 3.1**), one obtains

$$\begin{aligned}\langle \mathcal{R}_{\vec{k}_1}\mathcal{R}^*_{\vec{k}_2}\rangle|_{\mathcal{R}_{\vec{q}}} = \langle \mathcal{R}^G_{\vec{k}_1}\mathcal{R}^{G*}_{\vec{k}_2}\rangle &+ \frac{1}{2}\int \frac{d^3q'}{(2\pi)^3} f_{\rm NL}(\vec{q}',\vec{k}_2-\vec{q}')\\ &\times \langle \mathcal{R}^G_{\vec{q}'}\mathcal{R}^G_{\vec{k}_1-\vec{q}'}\mathcal{R}^{G*}_{\vec{k}_2}\rangle + \frac{1}{2}\int \frac{d^3q'}{(2\pi)^3} f_{\rm NL}(\vec{q}',\vec{k}_2-\vec{q}')\\ &\times \langle \mathcal{R}^G_{\vec{k}_1}\mathcal{R}^{G*}_{\vec{q}'}\mathcal{R}^{G*}_{\vec{k}_2-\vec{q}'}\rangle + \mathcal{O}(f^2_{\rm NL}).\end{aligned} \tag{3.4}$$

In order to evaluate the impact of the spectator modes $\mathcal{R}^G_{\vec{q}}$, it must be taken out of the statistical average

$$\begin{aligned}\langle \mathcal{R}_{\vec{k}_1}\mathcal{R}^*_{\vec{k}_2}\rangle|_{\mathcal{R}_{\vec{q}}} &= (2\pi)^3\,\delta(\vec{k}_1-\vec{k}_2)\,P_{\mathcal{R}}(\vec{k}_1)\\ &+ f_{\rm NL}(\vec{k}_1,-\vec{k}_2)\,\frac{1}{2}\left(P_{\mathcal{R}}(\vec{k}_1)+P_{\mathcal{R}}(\vec{k}_2)\right)\mathcal{R}_{\vec{q}} + \cdots.\end{aligned} \tag{3.5}$$

where the trailing dots indicate terms that are higher order in non-Gaussianity, and will be subdominant.

It is interesting to note the following facts about the above expression. First of all, non-Gaussianity leads to a modulation of the primordial power spectrum, and the strength of modulation depends on both the size and shape of $f_{\rm NL}(\vec{k}_1, \vec{k}_2)$, as well as the size of the spectator mode $\mathcal{R}_{\vec{q}}$. Secondly, statistical isotropy and homogeneity constrain the wavenumber of the spectator mode to be $\vec{q} = \vec{k}_1 - \vec{k}_2$. In other words, this is the only mode that can affect the two-point correlation function between $\vec{k}_1$ and $\vec{k}_2$. Additionally, the effect of the modulation is to introduce "non-diagonal" elements in the two-point function, i.e., terms not proportional to $\delta(\vec{k}_1 - \vec{k}_2)$. But recall that such non-diagonal terms break homogeneity and isotropy. It is not surprising that we see deviations from these fundamental symmetries, since we are not averaging over the spectator mode: such average would make those terms disappear, since $\langle \mathcal{R}^G_{\vec{q}}\rangle = 0$. But, as it happens for the magnitude of the temperature anisotropies, the quantity that is more interesting for observations is the typical value of such term, and not only its statistical average.

B Non-Gaussian Modulation of CMB

The primordial perturbations $\mathcal{R}_{\vec{k}}$ are related to the CMB multipole coefficients $a_{\ell m}$ through the relation

$$a_{\ell m} = 4\pi \int \frac{d^3k}{(2\pi)^3}\,(-i)^\ell\,\Delta_\ell(k)\,Y^*_{\ell m}(\hat{k})\,\mathcal{R}_{\vec{k}}, \tag{3.6}$$

where $\Delta_\ell(k)$ are the CMB temperature transfer functions, which encode the post-inflationary evolution of the perturbations from

the re-entry of perturbations into the horizon during late radiation domination till today. From this equation, one can compute the covariance matrix

$$\langle a_{\ell m} a^*_{\ell' m'} \rangle = (4\pi)^2 \int \frac{d^3k_1}{(2\pi)^3} \int \frac{d^3k_2}{(2\pi)^3} \; (-i)^{\ell-\ell'} \; \Delta_\ell(k_1)\, \Delta_{\ell'}(k_2) \; Y^*_{\ell m}(\hat{k}_1)\, Y_{\ell' m'}(\hat{k}_2)\, \langle \mathcal{R}^*_{\vec{k}_1} \mathcal{R}^*_{\vec{k}_2} \rangle |_{\mathcal{R}_{\vec{q}}}, \tag{3.7}$$

which is obtained from the two-point functions of the curvature perturbations given in (**Eq. 3.5**). Upon expanding $f_{\rm NL}$ in terms of Legendre polynomials, $f_{\rm NL}(k_1, q, \mu) = \sum_L G_L(k_1, q)\, \frac{2L+1}{2}\, P_L(\mu)$, and using the multipole expansion $\mathcal{R}^G_{\vec{q}} = \sum_{L'M'} \mathcal{R}^G_{L'M'}(q)\, Y_{L'M'}(\hat{q})$, one can write (**Eq. 3.7**) as (Agullo et al., 2021b)

$$\langle a_{\ell m} a^*_{\ell' m'} \rangle = C_\ell\, \delta_{\ell\ell'} \delta_{mm'} + (-1)^{m'} \sum_{LM} A^{LM}_{\ell\ell'}\, C^{LM}_{\ell m \ell' -m'}. \tag{3.8}$$

The above expression consists of two terms. The first term is the usual temperature power spectrum that is diagonal in ℓ and m. The second term arises from the non-Gaussian modulation and, as before, introduces non-diagonal terms. $C^{LM}_{\ell m \ell' m'}$ are Clebsch-Gordan coefficients, and the information about the primordial non-Gaussianity is encoded in the coefficients

$$A^{LM}_{\ell\ell'} = \frac{4}{(2\pi)^3} \int dk_1\, k_1^2\, dq\, q^2\; (-i)^{\ell-\ell'}\; \Delta_\ell(k_1)\, \Delta_{\ell'}(k_1)\, P_{\mathcal{R}}(k_1)\; G_L(k_1, q)\, \mathcal{R}^G_{LM}(q) \times C^{L0}_{\ell 0 \ell' 0} \sqrt{\frac{(2\ell+1)(2\ell'+1)}{4\pi\,(2L+1)}}. \tag{3.9}$$

These coefficients are known as bipolar spherical harmonic (BipoSH) coefficients (Hajian and Souradeep, 2003; Joshi et al., 2010). As we shall see, the BipoSH coefficients provide a convenient way to organize the effects of the non-Gaussian modulation.

The Clebsch-Gordan coefficients present in the above expressions enforce certain properties on the BipoSH coefficients. In particular, Clebsch-Gordan coefficients $C^{LM}_{\ell_1, m_1, \ell_2, m_2}$ are nonzero only if $\ell_1 + \ell_2 \geq L \geq |\ell_1 - \ell_2|$ and if $M = m_1 + m_2$. This, together with properties of the Clebsch-Gordan coefficient $C^{L0}_{\ell 0 \ell' 0}$, implies that, if

i. $L = 0$, then $\ell_1 = \ell_2$
ii. $L = 1$, then $|\ell_1 - \ell_2| = 1$
iii. $L = 2$, then $|\ell_1 - \ell_2| = 0, 2$, etc.

Thus, a non-zero value of $A^{LM}_{\ell\ell'}$ for $L = 0$ can be absorbed in the diagonal angular power spectrum C_ℓ. A non-zero value of $A^{LM}_{\ell\ell'}$ for $L = 1$ induces correlations between multipoles ℓ and $\ell + 1$, or in other words, a dipolar modulation. $L = 2$ induces a quadrupolar modulation, etc. The presence of a large dipolar or higher multipole modulation would appear in the CMB as correlations between multipoles ℓ and $\ell + 1$, which implies a departure from isotropy, as described in **section II**. This departure from isotropy is a consequence of the concrete realization of the spectator mode $\mathcal{R}_{\vec{q}}$ in our local Universe. One would need to average among the observation of the CMB from distant places in the cosmos to conclude that such violation of isotropy is not fundamental, but rather the imprint of strong correlations with super-horizon modes $\mathcal{R}_{\vec{q}}$.

Two remarks are in order now.

i. The strength of non-Gaussian modulation is dictated by the size of $f_{\rm NL}(k_1, q, \mu)$. But it is the dependence of $f_{\rm NL}$ on μ, the cosine of the angle between $\vec{k}_1$ and $\vec{q}$, what determines the relative size of the BipoSH coefficients for different L's, i.e., the "shape" of the modulation. On the other hand, the dependence of $f_{\rm NL}$ on the moduli k_1 and q determines the ℓ-dependence of the modulation. The two multipoles should not be confused: the L-dependence dictates the shape of the modulation, while the ℓ-dependence controls the variation of the amplitude of the modulation at different angular scales in the CMB. The non-Gaussianity generated in slow-roll inflation is small and nearly scale-invariant. Hence, the strength of modulation generated is also quite small. Since the anomalies observed in the CMB are scale dependent, we need a scenario with a strongly scale-dependent and large non-Gaussianity. Such scale dependence is also needed to explain why we have not observed non-Gaussian correlations directly in the CMB, since a strong scale dependence can make these correlations large only when at least one super-horizon mode is involved. In such situation, we could only observe the indirect effects that the non-Gaussian correlations induce in the CMB.

ii. $A^{LM}_{\ell\ell'}$ given in (**Eq. 3.9**) depend on the mode $\mathcal{R}^G_{\vec{q}}$. Since, $\mathcal{R}^G_{\vec{q}}$ is a random variable, we cannot predict the exact value of $A^{LM}_{\ell\ell'}$. We can only compute the standard deviation of the BipoSH coefficients, i.e.

$$\sqrt{\langle |A^{LM}_{\ell\ell'}|^2 \rangle} = \left[\frac{1}{2\pi} \int dq\, q^2\, P_{\mathcal{R}}(q)\, |\mathcal{C}^L_{\ell\ell'}(q)|^2 \right]^{1/2} \times C^{L0}_{\ell 0 \ell' 0} \sqrt{\frac{(2\ell+1)(2\ell'+1)}{4\pi\,(2L+1)}}, \tag{3.10}$$

where

$$\mathcal{C}^L_{\ell\ell'}(q) \equiv \frac{2}{\pi} \int dk_1\, k_1^2\; (i)^{\ell-\ell'}\; \Delta_\ell(k_1) \Delta_{\ell'}(k_1)\, P_{\mathcal{R}}(k_1)\, G_L(k_1, q). \tag{3.11}$$

These are the typical values that the BipoSH coefficients are expected to take in the sky. If these values are large, the effects they entail should be expected in the CMB or, more precisely, they would have a large p-value and should not be considered anomalous.

IV LOOP QUANTUM COSMOLOGY

LQC describes the spacetime geometry in the quantum language of loop quantum gravity. As discussed before, we consider in this paper an early Universe sourced by a scalar field, which drives the Universe to an inflationary phase after the bounce. The bounce introduces a new physical scale to the problem, which can be defined either from the value of the energy density or from the Ricci scalar at the bounce. Perturbations, both scalar and tensor,

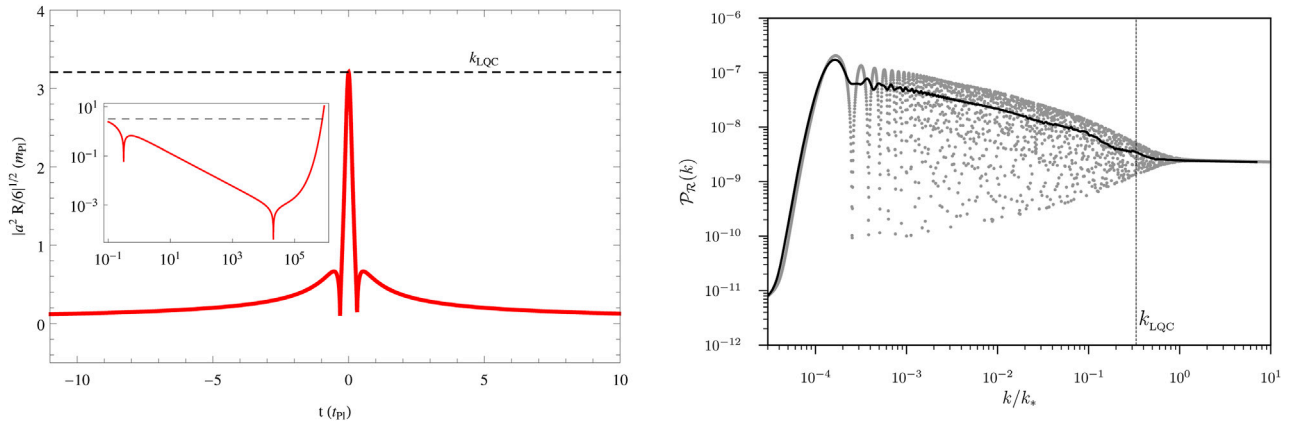

FIGURE 4 | Left: Evolution of the Ricci scalar in LQC. This plot corresponds to a solution of the effective equations with 71 *e*-folds of expansion between the bounce and the end of inflation. Right: Primordial power spectrum of perturbations starting in an adiabatic initial state before the bounce in LQC. The gray dots correspond to numerically-obtained data for individual values of k, while the continuous black line is the average of the grey dots. This plot is obtained for the background geometry showed in the left panel.

are sensitive to this new scale, and their propagation across the bounce amplifies them, for the same reason that propagation across the inflationary phase does. As a consequence, perturbations reach the onset of inflation in an excited and non-Gaussian state, rather than the Bunch-Davies vacuum commonly postulated. These excitations lead to a strongly scale-dependent power spectrum and bispectrum of primordial perturbations. In this section, we will briefly review some of the essential features of perturbations generated in LQC, and in the next section we will describe how these features can account for the anomalous signals observed in the CMB. For further details, see (Ashtekar et al., 2006b; Agullo et al., 2012; Agullo et al., 2013a; Agullo et al., 2013b; Agullo and Morris, 2015; Agullo, 2018).

A Background Dynamics and Free Evolution of Perturbations

Consider a spatially flat Friedmann-Lemaitre-Robertson-Walker spacetime. We shall describe the perturbations following the dressed metric approach. This approach has been discussed in (Agullo et al., 2012; Agullo et al., 2013a; Agullo et al., 2013b; Agullo and Morris, 2015; Agullo et al., 2018) [for a recent review, see (Agullo et al., 2017a)] and we refer the reader to these references for details omitted here. For the purpose of this article, it suffices to say that we consider perturbations as test fields propagating on the background described by the effective equations of LQC (Taveras, 2008; Ashtekar and Singh, 2011; Agullo et al., 2017a). The essential features of perturbations generated in LQC can be summarized using **Figure 4**. The left panel of this figure plots $a\sqrt{|R/6|}$ as a function of time, where a refers to the scale factor and R is the Ricci scalar. In making this plot, we have worked with a scalar field governed by a quadratic potential, and minimally coupled to gravity. Similar results are obtained for other potentials (Bonga and Gupt, 2016a; Bonga and Gupt, 2016b; Zhu et al., 2017). Different solutions to the effective equations of LQC with a scalar field as the dominant source are parameterized by the value of the scalar field at the bounce. As we further discuss below, different choices of this quantity translate to different amounts of cosmic expansion from the bounce to the end of inflation. The Ricci scalar attains its largest value at the bounce, and its maximum value sets a characteristic scale in LQC denoted by $k_{LQC} \equiv a(t_B)\sqrt{R(t_B)/6} \approx a(t_B)\sqrt{\kappa\rho_B}$, where t_B indicates the time of the bounce and ρ_B is the energy density of the scalar field at the time of the bounce. As the inset in the plot shows, inflation occurs at late time, when $a\sqrt{|R/6|}$ grows exponentially fast. Regarding scalar perturbations, they are in an adiabatic regime before the bounce, and we choose them to start in an adiabatic vacuum at those early times [see e.g., (Agullo, 2015; Agullo and Morris, 2015; de Blas and Olmedo, 2016; Ashtekar and Gupt, 2017; Elizaga Navascués et al., 2019; Navascués et al., 2020; Martín-Benito et al., 2021) for other choices of initial state]. As perturbations evolve across the bounce, modes with wavenumbers $k \lesssim k_{LQC}$ are excited. These excitations get further amplified as they cross the curvature scale during inflation. Wavenumbers that are ultraviolet compared to k_{LQC}, $k > k_{LQC}$, are not excited during the bounce, and remain in the adiabatic vacuum at the onset of inflation. Hence, only for those modes one recovers the familiar Bunch-Davies vacuum at the onset of inflation, while more infrared modes keep memory of the bounce. Consequently, as shown in **Figure 4**, the power spectrum of curvature perturbations shows a strong scale dependence at infrared scales, while approaches the more familiar scale-invariant shape for large k's. In particular, we see that the power spectrum for infrared modes $k \lesssim k_{LQC}$ is enhanced and oscillatory. In the extreme infrared limit, modes are neither excited during bounce nor during inflation, and this leads to a power spectrum which scales as k^2. The scale at which these effects appear in the CMB depends on the physical size of the mode k_{LQC} today, compared to the Hubble scale [recall that the physical wavenumber scales with time as $k_{LQC}/a(t)$]. This depends on the expansion accumulated—i.e., the number of *e*-folds N—from the time of the bounce until the end of inflation.

This is a free parameter in LQC. In this article, we investigate whether there is a value of N for which this model can explain the origin of the anomalies in the CMB.

B Generation of Primordial Non-gaussianity

The dressed metric approach was extended beyond linear perturbation theory in (Agullo, 2018), and we provide here a short summary. Primordial curvature perturbations whose wavenumbers are comparable to or smaller than k_{LQC} not only get excited, as described above, but also become non-Gaussian as they cross the bounce. The non-Gaussianity thus generated is further enhanced as the perturbations cross the horizon during inflation. Equal-time three-point functions are computed using time dependent perturbation theory, generalizing the pioneering calculations in (Maldacena, 2003) to bouncing geometries:

$$\begin{aligned}&\langle 0|\widehat{\mathcal{R}}_{\vec{k}_1}(t_e)\,\widehat{\mathcal{R}}_{\vec{k}_2}(t_e)\,\widehat{\mathcal{R}}_{\vec{k}_3}(t_e)|0\rangle\\ &= i\int_{t_i}^{t_e} \mathrm{d}t'\,\langle 0|\left[\widehat{\mathcal{R}}_{\vec{k}_1}(t)\,\widehat{\mathcal{R}}_{\vec{k}_2}(t)\,\widehat{\mathcal{R}}_{\vec{k}_3}(t),\,\widehat{\mathcal{H}}_{int}(t')\right]|0\rangle,\end{aligned} \tag{4.1}$$

where $\widehat{\mathcal{H}}_{int}$ is the interaction Hamiltonian [whose lengthy expression can be found in (Agullo et al., 2018)], t_i refers to the time at which initial conditions are imposed and t_e is the time at which the correlation is evaluated. Usually, t_e is chosen at the end of inflation, after all the three modes have crossed the Hubble radius. With the knowledge of the background dynamics and the initial conditions, we can exactly evaluate the three-point function and hence obtain the function $f_{\rm NL}(\vec{k}_1, \vec{k}_2)$ which characterizes the non-Gaussianity. Our exact computations reveal that the non-Gaussianity generated in LQC is strongly scale-dependent, large and oscillatory, similar to the power spectrum. As for the power spectrum, the non-Gaussianity quickly approaches the inflationary result for wave numbers $k > k_{LQC}$ (Agullo, 2018; Sreenath et al., 2019), and in particular they become negligibly small when the moduli of the three wave numbers $\vec{k}_1$, $\vec{k}_2$ and $\vec{k}_1 - \vec{k}_2$ are larger than k_{LQC}, in such a way that they are too small to be observed directly in the CMB. However, the non-Gaussianity becomes large when at least one of the modes involved is infrared, $k < k_{LQC}$, or equivalently, when one of the modes has wavelength larger than the Hubble radius today. These are the correlations which can account for the CMB anomalies, as we argue in the next section.

The strong oscillatory character of the non-Gaussianity generated in LQC, makes it computationally difficult to obtain an exact evaluation of (**Eq. 3.10**). For this reason, in this work, rather than working with the exact numerically-evaluated non-Gaussianity, we shall work with an analytical approximation derived in (Agullo, 2018)

$$f_{\rm NL}(k_1, k_2, k_3) \simeq \mathfrak{f}_{\rm NL}\, e^{-\alpha\,(k_1+k_2+k_3)/k_{LQC}}, \tag{4.2}$$

where $\alpha = 0.647$, $\mathfrak{f}_{\rm NL} \approx 2750$, and $k_3 = k_1\sqrt{1+\frac{k_2^2}{k_1^2}+2\mu\frac{k_2}{k_1}}$. The value of α is determined from the behavior of the scale factor around the time of the bounce, while the amplitude $\mathfrak{f}_{\rm NL}$ is determined from numerical simulations (Agullo, 2018). As showed in (Agullo, 2018), this expression provides a good approximation for the non-Gaussianity generated in LQC, and is significantly easier to manipulate. This approximation, however, neglects the oscillatory nature of $f_{\rm NL}(k_1, k_2, \mu)$ with k_1 and k_2. The oscillations will generically reduce the size of the effects we describe below. Therefore, the numbers obtained in the next section should be understood as an upper bound for the predictions of LQC, rather than an exact result. This is the main technical limitation of our analysis, and it arises from the highly oscillatory nature of the perturbations.

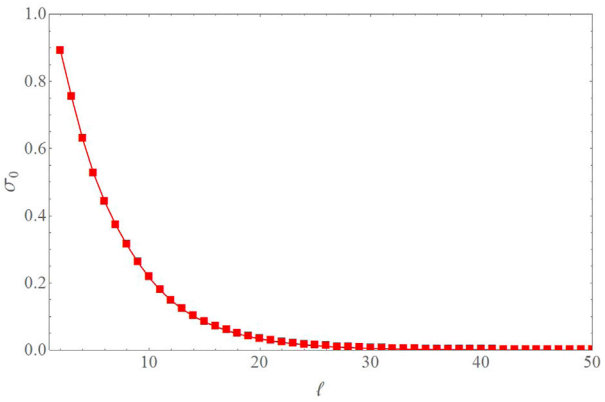

FIGURE 5 | Root-mean-square of the monopolar modulation $\sigma_0(\ell)$ generated in LQC. Note the dependence of σ_0 on ℓ. The scale dependence introduced by the bounce in LQC makes the effects of the modulation significant only for $\ell \lesssim 30$.

V RESULTS

In this section, we shall put the previous results together and compute the root mean square value of the BipoSH coefficients generated in LQC from (**Eq. 3.10**). We will show that the BipoSH coefficients generated in this model are non-zero and have the appropriate magnitude and scale dependence as demanded by observations.

A Monopolar Modulation–Power Suppression

We first consider the monopolar term ($L = 0$). The properties of the Clebsch-Gordan coefficients for $L = 0$ impose the constraints $\ell = \ell'$ and $m = -m'$. Therefore, the monopolar modulation introduces an isotropic shift in the value of C_ℓ, although the shift can be different for different values of ℓ. More concretely, the modulated power spectrum C_ℓ^{mod} is given by

$$C_\ell^{mod} = C_\ell\left(1 - \frac{(-1)^\ell}{C_\ell}\,\frac{A^{00}_{\ell\,\ell}}{\sqrt{2\,\ell+1}}\right). \tag{5.1}$$

Note that $A^{00}_{\ell\,\ell}$ can be either positive or negative, leading to an enhancement or suppression of C_ℓ^{mod} with respect to C_ℓ. As explained before, we cannot predict the exact value of $A^{00}_{\ell\,\ell}$. The interesting quantity is rather the root-mean-square value of the modulation:

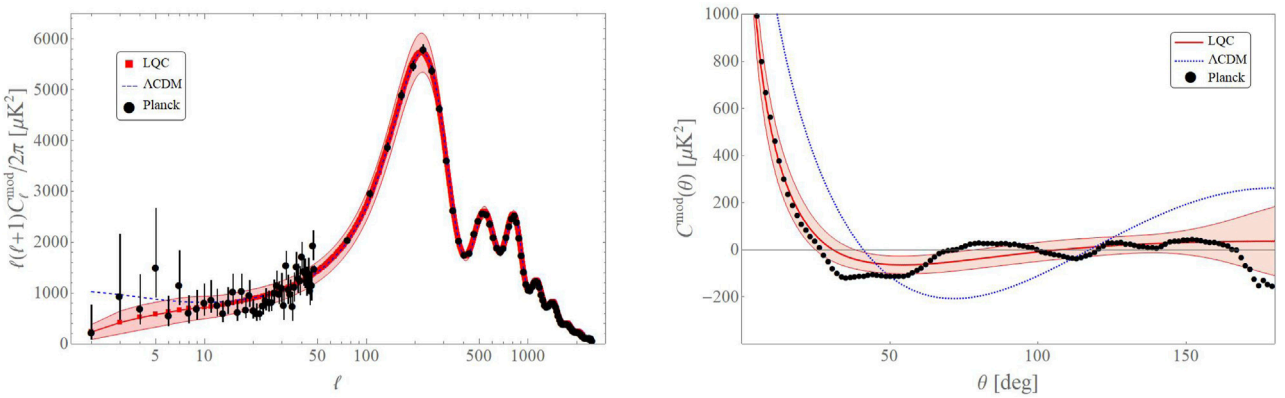

FIGURE 6 | Form of the modulated power spectrum for a typical value of the suppression. The figure shows that the monopolar modulation can account for the suppression of power at multipoles lower than $\ell \approx 30$ **(A)**. In the **(B)**, we also see that the suppression translates to a very low real space power spectrum $C(\theta)$ for $\theta \geq 60°$. The shaded region shows cosmic variance, and the black dots data from Planck.

$$\sigma_0^2(\ell) = \frac{1}{C_\ell^2}\frac{\langle|A_{\ell\,\ell}^{00}|^2\rangle}{2\,\ell+1} = \frac{1}{C_\ell^2}\frac{1}{8\pi^2}\int dq\, q^2\, P_{\mathcal{R}}(q)\,|\mathcal{C}_{\ell\ell}^0(q)|^2, \tag{5.2}$$

where $C_{\ell\ell}^0(q)$ was defined in (**Eq. 3.11**). This quantity determines the typical size and scale dependence of the monopolar modulation expected in the CMB. A large value of σ_0 would make deviations from the unmodulated power spectrum, C_ℓ more likely to be observed in the CMB. The result of our calculations, using the power spectrum and the form of $f_{\rm NL}(k_1, q, \mu)$ described in the previous section, is plotted in **Figure 5**.

We will assume that the probability distribution for the modulation is well approximated by a Gaussian, and hence completely characterized by $\sigma_0(\ell)$. This is a reasonable approximation, since the deviations are expected to be of second order in non-Gaussianity, and therefore very small. With this probability distribution for the monopolar modulation, we can now investigate the connection with the power suppression observed in the CMB. In particular, we want to answer the following question: what is the p-value given the observed value of $S_{1/2}$? We obtain that the probability to find $S_{1/2} \leq 1{,}209.2$ once the non-Gaussian modulation is taken into account is approximately 16%. This is equivalent to saying that the observed suppression is around one standard deviation from the mean. **Figure 6** shows the form of the T-T power spectrum for a simulation for which the monopolar modulation produces $S_{1/2}$ in agreement with observation, along with the 1σ confidence contour arising from cosmic variance. For comparison, we provide the corresponding quantities arising from the standard model, as well as data from Planck (Aghanim, 2019).

These results show that, in presence of the LQC bounce occurring before inflation, a power suppression as the one we observe in the CMB should not be considered anomalous. It is important to emphasize the precise sense in which the suppression is explained: not because the theory predicts that we should observe a suppression in the CMB, but rather because the probability of observing such a suppression is much larger than in the standard ΛCDM model with Bunch-Davies initial conditions. In this sense, the resolution of the anomaly has precisely the same character as its origin: probabilistic.

An important check is to confirm that the non-Gaussian effects are not large enough to jeopardize the validity of the perturbative expansion on which the calculations rest. This question was explored in detail in Ref. (Agullo, 2018), confirming that, in LQC, perturbation theory does not break down when non-Gaussianity is included. Regarding the non-Gaussian modulation discussed in this paper, we find that the correction to the unmodulated angular power spectrum is not small, and it is in fact a significant fraction of the final result, particularly for the smallest multipoles. The relative contribution is, however, smaller than one in all our calculations. In quantitative terms, the relative contribution of the non-Gaussian modulation is of order $\mathfrak{f}_{\rm NL}\sqrt{\mathcal{P}_{\mathcal{R}}}$, which is smaller than one for $\mathfrak{f}_{\rm NL} \sim 10^3$. More importantly, higher order corrections introduce additional powers of the power spectrum $\mathcal{P}_{\mathcal{R}} \ll 1$. So the next-to-leading-order correction to the non-Gaussian modulation is of order $\mathfrak{f}_{\rm NL}(\mathcal{P}_{\mathcal{R}})^{3/2}$, which is negligible due to the smallness of $\mathcal{P}_{\mathcal{R}}$. Therefore, our results are robust under the addition of higher perturbative corrections.

B Dipolar Modulation

Next, we discuss the effects of the $L = 1$, dipolar modulation, induced by the BipoSH coefficients, $A_{\ell\ell+1}^{1M}$, and compare the results with those reported by Planck. As discussed in **section IIB**, the Planck team quantifies the dipolar modulation in terms of a scale-dependent amplitude $A_1(\ell)$ (Ade, 2016a), which can be related with the BipoSH coefficients $A_{\ell\ell+1}^{1M}$ as follows. First, define from $A_{\ell\ell+1}^{1M}$ the multipole coefficients m_{1M} by

$$A_{\ell\ell+1}^{1M} \equiv m_{1M}\, G_{\ell\ell+1}^1, \qquad \text{where}$$
$$G_{\ell\ell+1}^1 \equiv (C_\ell + C_{\ell+1})\sqrt{\frac{(2\ell+1)\,(2\ell+3)}{4\pi\,3}}\,C_{\ell,0,\ell+1,0}^{10} \tag{5.3}$$

is called a form factor. The $m_{1M}(\ell)$ defined above can take three values corresponding to $M = -1$, 0, +1, and in general, they

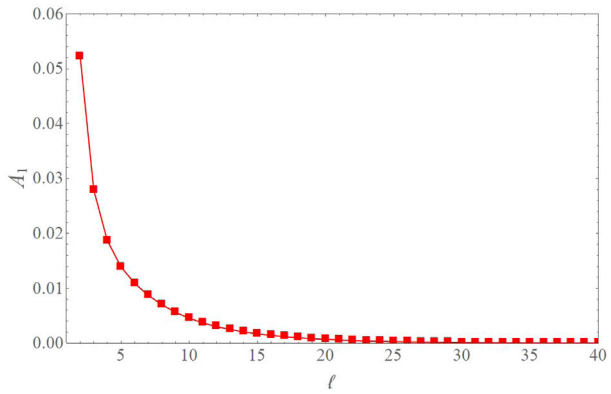

FIGURE 7 | The dipole amplitude $A_1(\ell)$ generated in LQC. Planck reports a value of $A_1 \approx 0.07$ in the multipole bin $\ell \in [2, 64]$.

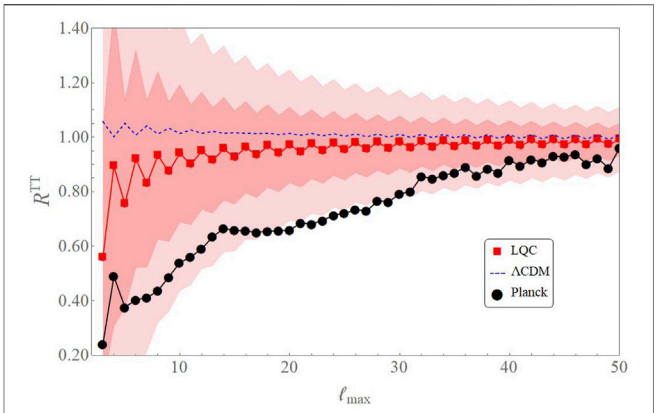

FIGURE 8 | $R^{TT}(\ell_{max})$ for the modulated spectrum generated in LQC (solid red). $R^{TT}(\ell_{max})$ predicted in LQC shows a preference for odd parity for low multipoles, unlike the one in the standard model (dashed, blue).

depend on ℓ. From them, the amplitude of the dipolar modulation is defined as

$$A_1(\ell) \equiv \frac{3}{2}\sqrt{\frac{1}{3\pi}\left(|m_{1\,-1}|^2 + |m_{1\,0}|^2 + |m_{1\,1}|^2\right)}. \qquad (5.4)$$

Hence, from the value of the root-mean-square of $A^{1M}_{\ell\ell+1}$ we can obtain the root-mean-square of $A_1(\ell)$. It is given by the expression

$$A_1(\ell) = \frac{3}{2}\frac{1}{\sqrt{\pi}}\frac{1}{C^{\rm mod}_\ell + C^{\rm mod}_{\ell+1}}\sqrt{\frac{1}{2\pi}\int dq\, q^2\, P_{\mathcal{R}}(q)\,|\mathcal{C}^1_{\ell\ell+1}(q)|^2}, \qquad (5.5)$$

where we have used the modulated (i.e., suppressed) $C^{\rm mod}_\ell$ since, as emphasized in (Ade, 2016a), the dipole amplitude must be evaluated relative to the observed angular power spectrum. Hence, the fact that the observed $C^{\rm mod}_\ell$ are smaller than the ones predicted by ΛCDM, increases the amplitude of the observed dipole. In this sense, the power suppression and the dipolar modulation are not completely independent. However, the amplitude of the dipole is ultimately dictated from the angular μ-dependence of the primordial non-Gaussianity $f_{\rm NL}(k_1, k_2, \mu)$.

The result for $A_1(\ell)$ is plotted in **Figure 7**. We find that the dipolar modulation is strongly scale-dependent, as a consequence of the scale-dependent nature of the non-Gaussianity. Although Planck observations for $A_1(\ell)$ are limited, in the sense that only its mean value in the range $\ell \in [2, 64]$ is reported, the order of magnitude and scale dependence agree with our results.

We have also checked that higher order multipolar modulations, $L = 2, 4, \ldots$ have amplitudes significantly smaller than the dipolar one (Agullo et al., 2018), and therefore additional modulations are not expected in the CMB according to LQC, in agreement with observations. Hence, interestingly, the form of $f_{NL}(k_1, k_2, \mu)$ derived from LQC produces a hierarchy in the amplitude of the modulations which is dominated by a monopole, and a smaller dipole.

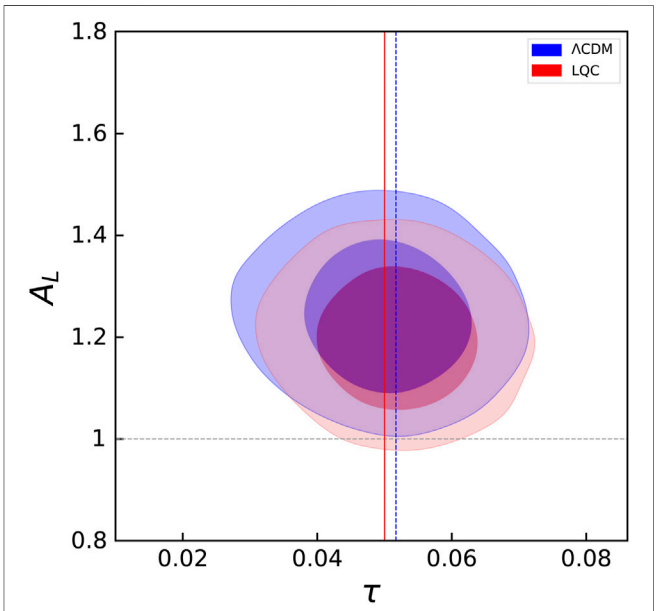

FIGURE 9 | Marginalised joint probability distribution of τ and A_L obtained from MCMC simulation for the standard model and modulated LQC. As we can see, $A_L = 1$ lies within the 2σ contour for the modulated model, thus bringing the lensing parameter closer to one.

C Parity and Lensing Anomalies

In this subsection we briefly discuss the results for the parity and lensing anomalies. As discussed in previous sections, the statistical evidence for these two features is weaker than the power suppression and the dipolar anomaly. Nevertheless, it is interesting to see what the predictions of LQC are.

We find that the monopolar modulation induces also a preference for odd parity multipoles ℓ, in agreement with observations. After inspection, this fact is not surprising, and it is a consequence of the simple fact that, in a power suppressed angular power spectrum, the sum of $\frac{\ell(\ell+1)}{2\pi} C^{\rm mod}_\ell$ starting from

$\ell = 2$ is larger for odd multipoles, precisely because the sum starts at an even multipole—it would have been otherwise if the sum starts at $\ell = 1$. Therefore, we find that in LQC there is a preference for odd-parity multipoles ℓ, as measured by $R^{TT}(\ell_{\max})$, and the result is a consequence of the power suppression. We report our result in **Figure 8**. For comparison, we provide the corresponding values obtained in the ΛCDM model and the observations made by Planck (Aghanim, 2019). Although the result for $R^{TT}(\ell_{\max})$ from LQC is closer to the data, the value of $R^{TT}(\ell_{\max})$ observed by Planck is smaller than what we find in LQC, but the significance of the deviation is modest. In the absence of a better estimator for the parity anomaly, it is not possible for us to make a more precise comparison.

Yet another effect of the power suppression caused by the monopolar modulation is the alleviation of the lensing tension. The relation between a power suppression and the lensing anomaly was discussed in (Ashtekar et al., 2020), also in the context of LQC, and our analysis confirms the relation. The value of A_L is obtained from data by performing MCMC simulations involving the standard six free parameters, together with the lensing amplitude A_L. We repeat the analysis with the modified probability distribution obtained from LQC, using TT + *lowE* data (Aghanim, 2019), and find that the marginalized mean value of the lensing parameter is $A_L = 1.20 \pm 0.092$. This value is 3.5% smaller than the result obtained from ΛCDM. This is a modest change. However, as shown in **Figure 9**, the joint probability distribution of τ-A_L, with τ the optical depth, shows that the value of $A_L = 1$ is within 2 standard deviations, and it is in this sense that the anomaly is alleviated. It should also be noted, however, that the marginalized mean value of the χ^2 statistic, which is a measure of the difference between the predictions of the model and the data, scaled suitably by the expected error (Barlow, 1989), is larger for the modulated model by $\Delta\chi^2 = 5.29$. This lower value of the lensing parameter A_L can be explained due to the slightly larger value of τ. This is because a larger value of τ implies a slightly larger value of the scalar amplitude A_s, which in turn leads to a smaller value of A_L (Ashtekar et al., 2020).

VI DISCUSSION

The success of any theory seeking to describe the unknown rests on two criteria: it should be consistent with known facts and at the same time be able to make new predictions. Loop quantum cosmology, as an effort to extend the ΛCDM model to the Planck regime, has met the first criterion since, when combined with inflation, it is able to overcome the limitations of general relativity and to produce a nearly scale-invariant power spectrum and bispectrum for almost all scales in the CMB. As far as the second aspect is concerned, LQC predicts that, if we consider adiabatic initial conditions for perturbations before the bounce, the primordial power spectrum and bispectrum deviate from scale invariance at wavenumbers $k \lesssim k_{LQC}$. The question is whether these features occur at scales that are observable today. If this is the case, then we may keep the hope to use observations to confirm some of the predictions of LQC, and to further refine the theory. It is with this second aspect in mind that we investigate the link between the enhanced and scale-dependent perturbations generated in LQC and the CMB anomalies.

CMB anomalies, as we discussed in **section II**, include several features that have been observed, mostly at large angular scales in the CMB. The genuineness of these features is not under dispute. However, if considered individually, the p-values of these features are not small enough to unambiguously establish a statistically significant departure from the standard model. In other words, the possibility that some of these features appear in the CMB in a Universe governed by the standard ΛCDM model is not negligible. However, the fact that all these seemingly distinct features occur together in our Universe imply that we either live in a rare realization of the probability distribution of the ΛCDM model, or that new physics is needed. In this paper, we have explored the second possibility in the context of LQC.

In this scenario, the cosmic bounce modifies the initial state of the Universe from which inflation and the ΛCDM model take over. The most relevant aspect comes from the fact that the bounce generates strong correlations between the longest wavelengths we can observe in the CMB and longer, super-horizon perturbations. These correlations, although cannot be observed directly in the CMB—because they involve at least one super-horizon mode—bias the form of the observed power spectrum. This bias translates in a higher probability for certain features to be realized in our CMB. We find it interesting that such an effect can simultaneously produce a suppression and a dipolar modulation in the sky, both compatible with observations. These two features were thought to be unrelated, and LQC provides a common origin for both of them. It is important to keep in mind that the origin of the anomalies is probabilistic, and the way LQC can account for them is by modifying the probability distribution. For instance, the dipole asymmetry does not arise in LQC as the result of breaking isotropy at the fundamental level, but rather because in a non-Gaussian Universe the size of the anisotropies expected to be found by a typical observer are larger than in a Gaussian theory.

In our calculation we have adjusted a free parameter in LQC, which controls the amount of expansion accumulated from the bounce to the end of inflation. The statement is, therefore, that there exist a value of this parameter for which the observed anomalies can originate from LQC (this value is ≈71 e-folds, and it includes the expansion during both the inflationary and the pre-inflationary epochs). Our calculations also involve some approximations and limitations, and in particular we have not been able to account precisely for the effects of the oscillations in the bispectrum. It would be desirable to investigate the way these oscillations convolve with the power spectrum and transfer functions in order to understand their effect on CMB. Furthermore, the data quantifying the anomalies is limited, as it is based on simple estimators such as $S_{1/2}$ and the binned value of the dipolar amplitude $A_1(\ell)$. Additional data, for instance coming from tensor modes, would allow a more precise comparison of our ideas with observations. But in spite of these limitations, we find remarkable that the bounce of LQC

can produce effects in the CMB which are in good consonance with the observed anomalies, regarding both the order of magnitude of the amplitudes as well as their scale dependence. The possibility that the observed features are informing us about the Planck era of the cosmos is mind-blowing, and certainly deserves further attention. Our contribution should be considered as a first step in this direction.

Finally, in this work we have assumed adiabatic initial conditions for the scalar perturbations before the bounce, wherein the unmodulated primordial power spectrum generated in LQC is enhanced at super-horizon scales. There has been a proposal in LQC (Ashtekar and Gupt, 2017; Ashtekar et al., 2020) for different initial conditions, which leads to a suppressed power spectrum even before considering the non-Gaussian modulation. It would be interesting to combine both sets of ideas and compute the effect of non-Gaussian modulation in that model.

DATA AVAILABILITY STATEMENT

The original contributions presented in the study are included in the article/supplementary material, further inquiries can be directed to the corresponding author.

AUTHOR CONTRIBUTIONS

All authors listed have made a substantial, direct, and intellectual contribution to the work and approved it for publication.

FUNDING

This work is supported by the NSF CAREER grant PHY-1552603, and by the Hearne Institute for Theoretical Physics. This paper is based on observations obtained from Planck (http://www.esa.int/Planck), an ESA science mission with instruments and contributions directly funded by ESA Member States, NASA, and Canada.

ACKNOWLEDGMENTS

We have benefited from discussions with A. Ashtekar, B. Bolliet, B. Gupt, J. Olmedo, J. Pullin, and P. Singh. We also thank the referees for constructive and useful comments on the first version of this article. This research was conducted with high performance computing resources provided by Louisiana State University (http://www.hpc.lsu.edu).

REFERENCES

Ade, P. A. R. (2014). (Planck), "Planck 2013 Results. XXIII. Isotropy and Statistics of the CMB," *Astron. Astrophys* 571, A23.

Ade, P. A. R. (2016b). Planck 2015 Results. XII. Full Focal Plane Simulations," *Astron. Astrophys* 594, A12.

Ade, P. A. R. (2016a). (Planck), "Planck 2015 Results. XVI. Isotropy and Statistics of the CMB," Astron. *Astrophys* 594, A16.

Adhikari, S., Shandera, S., and Erickcek, A. L. (2016). Large-scale Anomalies in the Cosmic Microwave Background as Signatures of Non-gaussianity. *Phys. Rev. D93* 023524. , 2016 arXiv:1508.06489. doi:10.1103/physrevd.93.023524

Aghanim, N. (2018a). Planck 2018 Results. VIII. Gravitational Lensing. *Astron. Astrophys* 641, A8.

Aghanim, N., (2019). *Planck 2018 Results. V. CMB Power Spectra and Likelihoods. Astron. Astrophys* 641, A5.

Aghanim, N., (2018b). *Planck 2018 Results. VI Cosmological Parameters. Astron. Astrophys* 641, A6.

Aghanim, N., (2020). "Planck 2018 Results. I. Overview and the Cosmological Legacy of Planck," *Astron. Astrophys* 641, A1.

Agullo, I., Ashtekar, A., and Nelson, W. (2012). Quantum Gravity Extension of the Inflationary Scenario. *Phys. Rev. Lett.* 109, 251301. doi:10.1103/physrevlett.109.251301

Agullo, I., Ashtekar, A., and Nelson, W. (2013b). The Pre-inflationary Dynamics of Loop Quantum Cosmology: Confronting Quantum Gravity with Observations. *Class. Quan. Grav.* 30, 085014. doi:10.1088/0264-9381/30/8/085014

Agullo, I., and Corichi, A. (2014). "Loop Quantum Cosmology,"in *Springer Handbook of Spacetime* Editors A. Ashtekar and V. Petkov (Berlin, Heidelberg: Springer), 809–839. doi:10.1007/978-3-642-41992-8_39

Agullo, I., Kranas, D., and Sreenath, V. (2021a). Anomalies in the CMB from a Cosmic Bounce. *Gen. Relativ Gravit.* 53, 17. doi:10.1007/s10714-020-02778-9

Agullo, I., Kranas, D., and Sreenath, V. (2021b). Large Scale Anomalies in the CMB and Non-gaussianity in Bouncing Cosmologies. *Class. Quan. Grav.* 38, 065010. doi:10.1088/1361-6382/abc521

Agullo, I., and Morris, N. A. (2015). Detailed Analysis of the Predictions of Loop Quantum Cosmology for the Primordial Power Spectra. *Phys. Rev. D* 92, 124040. doi:10.1103/physrevd.92.124040

Agullo, I., Olmedo, J., and Sreenath, V. (2020a). Predictions for the Cosmic Microwave Background from an Anisotropic Quantum Bounce. *Phys. Rev. Lett.* 124, 251301. doi:10.1103/physrevlett.124.251301

Agullo, I. (2018). Primordial Power Spectrum from the Dapor-Liegener Model of Loop Quantum Cosmology. *Gen. Relativ Gravit.* 50, 91. doi:10.1007/s10714-018-2413-1

Agullo, I., and Singh, P. (2017). "Loop Quantum Cosmology," in *Loop Quan. Gravity: First 30 Years* Editors Abhay. Ashtekar and Jorge. Pullin (WSP), 183–240. doi:10.1142/9789813220003_0007

Agullo, Ivan., Ashtekar, Abhay., and Gupt, Brajesh. (2017). Phenomenology with Fluctuating Quantum Geometries in Loop Quantum Cosmology. *Class. Quant. Grav.* 34 074003, 2017 . arXiv:1611.09810. doi:10.1088/1361-6382/aa60ec

Agullo, I., Ashtekar, A., and Nelson, W. (2013a). Extension of the Quantum Theory of Cosmological Perturbations to the Planck Era. *Phys. Rev. D* 87, 043507. doi:10.1103/physrevd.87.043507

Agullo, I., Bolliet, B., and Sreenath, V. (2018). Non-Gaussianity in Loop Quantum Cosmology. *Phys. Rev.* D97 066021, 2018 . arXiv:1712.08148. doi:10.1103/physrevd.97.066021

Agullo, I. (2015). Loop Quantum Cosmology, Non-gaussianity, and CMB Power Asymmetry. *Phys. Rev.* D92 064038, 2015 . arXiv:1507.04703. doi:10.1103/physrevd.92.064038

Agullo, I., Nelson, W., and Ashtekar, A. (2015). Preferred Instantaneous Vacuum for Linear Scalar fields in Cosmological Space-Times. *Phys. Rev. D* 91, 064051. doi:10.1103/physrevd.91.064051

Agullo, I., Olmedo, J., and Sreenath, V. (2020b). Observational Consequences of Bianchi I Spacetimes in Loop Quantum Cosmology. *Phys. Rev. D* 102 (043523). arXiv:2006.01883. doi:10.1103/physrevd.102.043523

Akrami, Y., et al. (2019). *Planck 2018 Results. VII. Isotropy and Statistics of the CMB*.

Akrami, Y., (2018). *Planck 2018 Results X*. Constraints on inflation.

Akrami, Y., (2020). (Planck), "Planck 2018 Results. IX. Constraints on Primordial Non-gaussianity. *Astron. Astrophys* 641, A9.

Ashtekar, A., Gupt, B., Jeong, D., and Sreenath, V. (2020). Alleviating the Tension in the Cosmic Microwave Background Using Planck-Scale Physics. *Phys. Rev.*

Lett. 125, 051302, 2020 . arXiv:2001.11689. doi:10.1103/PhysRevLett.125.051302

Ashtekar, A., Pawlowski, T., and Singh, P. (2006b). Quantum Nature of the Big Bang. *Phys. Rev. Lett.* 96, 141301.

Ashtekar, A., Gupt, B., and Sreenath, V. (2021). Cosmic Tango between the Very Small and the Very Large: Addressing CMB Anomalies through Loop Quantum Cosmology. *Front. Astron. Space Sci.* 8, 76. doi:10.3389/fspas.2021.685288

Ashtekar, A., and Gupt, B. (2017). "Quantum Gravity in the Sky: Interplay between Fundamental Theory and Observations. *Class. Quant. Grav.* 34 014002. doi:10.1088/1361-6382/34/1/014002

Ashtekar, A., Pawlowski, T., Singh, P., and Vandersloot, K. (2007). Loop Quantum Cosmology K=1 FRW Modelsp. *hys. Rev. D* 75, 024035. doi:10.1103/physrevd.75.024035

Ashtekar, A., and Wilson-Ewing, E. (2009a). Loop Quantum Cosmology of Bianchi I Models. *Phys. Rev. D* 79, 083535. doi:10.1103/physrevd.79.083535

Ashtekar, A., Bojowald, M., and Lewandowski, J. (2003). Mathematical Structure of Loop Quantum Cosmology. *Adv. Theor. Math. Phys.* 7, 233–268. doi:10.4310/atmp.2003.v7.n2.a2

Ashtekar, A., Pawlowski, T., and Singh, P. (2006a). Quantum Nature of the Big Bang. *Phys. Rev. Lett.* 96, 141301.

Ashtekar, A., and Singh, P. (2011). Loop Quantum Cosmology: a Status Report. *Class. Quan. Grav.* 28, 213001. doi:10.1088/0264-9381/28/21/213001

Ashtekar, A., and Wilson-Ewing, E. (2009b). Loop Quantum Cosmology of Bianchi Type II Models. *Phys. Rev. D* 80, 123532. doi:10.1103/physrevd.80.123532

Banerjee, K., Calcagni, G., and Martin-Benito, M. (2012). Introduction to Loop Quantum Cosmology. *SIGMA* 8, 016. doi:10.3842/sigma.2012.016

Barlow, R. (1989). *Statistics : A Guide to the Use of Statistical Methods in the Physical Sciences*. West Sussex, England: Wiley.

Barrau, A., Bojowald, M., Calcagni, G., Grain, J., and Kagan, M. (2015). Anomaly-free Cosmological Perturbations in Effective Canonical Quantum gravityJCAP. *J. Cosmol. Astropart. Phys.* 2015, 051. doi:10.1088/1475-7516/2015/05/051

Bennett, C. L., Halpern, M., Hinshaw, G., Jarosik, N., Kogut, A., Limon, M., et al. (2003). First-Year Wilkinson Microwave Anisotropy Probe (WMAP) Observations: Preliminary Maps and Basic Results. *Astrophys J. Suppl. S* 148, 1–27. doi:10.1086/377253

Bentivegna, E., and Pawlowski, T. (2008). Anti-de Sitter Universe Dynamics in Loop Quantum Cosmology. *Phys. Rev. D* 77, 124025. doi:10.1103/physrevd.77.124025

Bojowald, M. (2001). Absence of a Singularity in Loop Quantum Cosmology. *Phys. Rev. Lett.* 86, 5227–5230. doi:10.1103/physrevlett.86.5227

Bojowald, M., and Calcagni, G. (2011). Inflationary Observables in Loop Quantum Cosmology. *JCAP* 032. doi:10.1088/1475-7516/2011/03/032

Bojowald, M., Mortuza Hossain, G., Kagan, M., and Shankaranarayanan, S. (2009). Gauge Invariant Cosmological Perturbation Equations with Corrections from Loop Quantum Gravity. *Phys. Rev.* D 7982, 043505109903. doi:10.1103/physrevd.79.043505

Bonga, B., and Gupt, B. (2016b). Phenomenological Investigation of a Quantum Gravity Extension of Inflation with the Starobinsky Potential. *Phys. Rev.*D93, 063513. doi:10.1103/physrevd.93.063513

Bonga, B., and Gupt, B. (2016a). Inflation with the Starobinsky Potential in Loop Quantum Cosmology. *Gen. Relativ Gravit.* 48, 71, 2016a . arXiv:1510.00680. doi:10.1007/s10714-016-2071-0

Castelló Gomar, L., Mena Marugán, G. A., Martín de Blas, D., and Olmedo, J. (2017). Hybrid Loop Quantum Cosmology and Predictions for the Cosmic Microwave Background. *Phys. Rev. D* 96, 103528. doi:10.1103/physrevd.96.103528

Dai, L., Jeong, D., Kamionkowski, M., and Chluba, J. (2013). The Pesky Power Asymmetry. *Phys. Rev. D* 87, 123005. doi:10.1103/physrevd.87.123005

de Blas, D. M., and Olmedo, J. (2016). Primordial Power Spectra for Scalar Perturbations in Loop Quantum Cosmology. *J. Cosmol. Astropart. Phys.* 2016, 029, 2016 . arXiv:1601.01716. doi:10.1088/1475-7516/2016/06/029

Durrer, R. (2008). *The Cosmic Microwave Background*. Cambridge: Cambridge University Press.

Elizaga Navascués, B., Marugán, G. A. M., and Thiemann, T. (2019). Hamiltonian Diagonalization in Hybrid Quantum Cosmology. *Class. Quan. Grav.* 36, 185010, 2019 . arXiv:1903.05695. doi:10.1088/1361-6382/ab32af

Fernández-Méndez, M., Mena Marugán, G. A., and Olmedo, J. (2013). Hybrid Quantization of an Inflationary Model: The Flat Case. *Phys. Rev. D* 88, 044013. doi:10.1103/physrevd.88.044013

Fixsen, D. J. (2009). "The temperature cosmic microwave background," *Astrophysical J.* 707, 916920. doi:10.1088/0004-637x/707/2/916

Mena Marugan, G. A. (2010). Loop Quantum Cosmology: A Cosmological Theory with a view. *J. Phys. Conf. Ser.* 314, 012012. doi:10.1088/1742-6596/314/1/012012

Garay, L. J., Martin-Benito, M., and Mena Marugan, G. A. (2010). Inhomogeneous Loop Quantum Cosmology: Hybrid Quantization of the Gowdy Model. *Phys. Rev. D* 82 044048. doi:10.1103/physrevd.82.044048

Gordon, C., Hu, W., Huterer, D., and Crawford, T. (2005). Spontaneous Isotropy Breaking: A Mechanism for Cmb Multipole Alignments. *Phys. Rev. D* 72, 10. doi:10.1103/physrevd.72.103002

Hajian, A., and Souradeep, T. (2003). Measuring the Statistical Isotropy of the Cosmic Microwave Background Anisotropy. *ApJ* 597, L5–L8. doi:10.1086/379757

Hinshaw, G., Banday, A. J., Bennett, C. L., Górski, K. M., Kogut, A., Lineweaver, C. H., et al. (1996). Two-Point Correlations in the [ITAL]COBE[/ITAL] DMR Four-Year Anisotropy Maps. *Astrophys. J.* 464, L25–L28. doi:10.1086/310076

Jeong, D., and Kamionkowski, M. (2012). Clustering Fossils from the Early Universe. *Phys. Rev. Lett.* 108, 251301. doi:10.1103/physrevlett.108.251301

Joshi, N., S.JhinganSouradeep, T., and Hajian, A. (2010). Bipolar Harmonic Encoding of CMB Correlation Patterns. *Phys. Rev.* D81, 083012. doi:10.1103/physrevd.81.083012

Li, B.-F., Olmedo, J., Singh, P., and Wang, A. (2020b). Primordial Scalar Power Spectrum from the Hybrid Approach in Loop Cosmologies. *Phys. Rev. D* 102, 126025. doi:10.1103/physrevd.102.126025

Li, B-F., Singh, P., and Wang, A. (2020a). Primordial Power Spectrum from the Dressed Metric Approach in Loop Cosmologies. *Phys. Rev. D* 101 086004. doi:10.1103/physrevd.101.086004

Maldacena, J. (2003). Non-gaussian Features of Primordial Fluctuations in Single Field Inflationary Models. *J. High Energ. Phys.* 2003, 013. doi:10.1088/1126-6708/2003/05/013

Martin-Benito, M., Garay, L. J., and . Mena Marugan, G. A. (2008). Hybrid Quantum Gowdy Cosmology: Combining Loop and Fock Quantizations. *Phys. Rev. D* 78 083516. doi:10.1103/physrevd.78.083516

Martín-Benito, M., Neves, R. B., and Olmedo, J. (2021). States of Low Energy in Bouncing Inflationary Scenarios in Loop Quantum Cosmology. *Phys. Rev. D* 103 123524. doi:10.1103/PhysRevD.103.123524

Martínez, F. B., and Olmedo, J. (2016). Primordial Tensor Modes of the Early UniversearXiv:1605.04293. *Phys. Rev. D* 93, 124008. doi:10.1103/physrevd.93.124008

Fernández-Méndez, M., Mena Marugán, G. A., and Olmedo, J. (2014). Effective Dynamics of Scalar Perturbations in a Flat Friedmann-Robertson-Walker Spacetime in Loop Quantum Cosmology. *Phys. Rev. D* 89, 044041. doi:10.1103/physrevd.89.044041

Navascués, B. E., and Mena Marugán, G. A. (2020). *Hybrid Loop Quantum Cosmology: An Overview*," .

Navascués, B. E., Mena Marugán, G. A., and Prado, S. (2020). Non-oscillating Power Spectra in Loop Quantum Cosmology. *Class Quant. Grav.* 38, 035001. doi:10.1088/1361-6382/abc6bb

Pawlowski, T., and Ashtekar, A. (2012). Positive Cosmological Constant in Loop Quantum Cosmology. *Phys. Rev. D* 85 064001.

Schmidt, F., and Hui, L. (2013). Cosmic Microwave Background Power Asymmetry from Non-gaussian Modulation. *Phys. Rev. Lett.* 110, 011301. doi:10.1103/PhysRevLett.110.011301

Schmidt, F., and Kamionkowski, M. (2010). Halo Clustering with Nonlocal Non-gaussianity. *Phys. Rev. D* 82, 103002. doi:10.1103/physrevd.82.103002

SchwarzSchwarz, D. J., CopiCopi, C. J., Huterer, D., and Starkman, G. D. (2016). CMB Anomalies after Planck. *Class. Quan. Grav.* 33, 184001. doi:10.1088/0264-9381/33/18/184001

Spergel, D. N., Verde, L., Peiris, H. V., Komatsu, E., Nolta, M. R., Bennett, C. L., et al. (2003). First-Year Wilkinson Microwave Anisotropy Probe (WMAP) Observations: Determination of Cosmological Parameters. *Astrophys J. Suppl. S* 148, 175–194. doi:10.1086/377226

Sreenath, V., Agullo, I., and Bolliet, B. (2019). Computation of Non-gaussianity in Loop Quantum Cosmology." in Fifteenth Marcel Grossmann Meeting on Recent Developments in Theoretical and Experimental General Relativity, Astrophysics, and Relativistic Field Theories, Rome, Italy.

Szulc, Ł. (2007). An Open FRW Model in Loop Quantum Cosmology. *Class. Quan. Grav.* 24, 6191–6200. doi:10.1088/0264-9381/24/24/003

Szulc, Ł., Kamiński, W., and Lewandowski, J. (2007). Closed Friedmann-Robertson-Walker Model in Loop Quantum Cosmology. *Class. Quan. Grav.* 24, 2621–2635. doi:10.1088/0264-9381/24/10/008

Taveras, V. (2008). Corrections to the Friedmann Equations from LQG for a Universe with a Free Scalar Field. *Phys. Rev.* D78, 064072. doi:10.1103/PhysRevD.78.064072

Weinberg, S. (2008). *Cosmology*. New York: Oxford University Press.

Wilson-Ewing, E. (2010). Loop Quantum Cosmology of Bianchi Type IX Models. *Phys. Rev. D* 82, 043508. doi:10.1103/physrevd.82.043508

Zhu, T., Wang, A., Cleaver, Gd., Kirsten, Ks., and Sheng, Q. (2017). Pre-inflationary Universe in Loop Quantum Cosmology. *Phys. Rev.* D96, 083520, 2017 . arXiv:1705.07544. doi:10.1103/physrevd.96.083520

Zhu, T., Wang, A., Kirsten, K., Cleaver, G., and Sheng, Q. (2018). Primordial Non-gaussianity and Power Asymmetry with Quantum Gravitational Effects in Loop Quantum Cosmology. *Phys. Rev. D* 97, 043501. doi:10.1103/physrevd.97.043501

Conflict of Interest: The authors declare that the research was conducted in the absence of any commercial or financial relationships that could be construed as a potential conflict of interest.

Advantages of publishing in Frontiers

OPEN ACCESS
Articles are free to read for greatest visibility and readership

FAST PUBLICATION
Around 90 days from submission to decision

HIGH QUALITY PEER-REVIEW
Rigorous, collaborative, and constructive peer-review

TRANSPARENT PEER-REVIEW
Editors and reviewers acknowledged by name on published articles

Frontiers
Avenue du Tribunal-Fédéral 34
1005 Lausanne | Switzerland

Visit us: www.frontiersin.org
Contact us: frontiersin.org/about/contact

REPRODUCIBILITY OF RESEARCH
Support open data and methods to enhance research reproducibility

DIGITAL PUBLISHING
Articles designed for optimal readership across devices

FOLLOW US
@frontiersin

IMPACT METRICS
Advanced article metrics track visibility across digital media

EXTENSIVE PROMOTION
Marketing and promotion of impactful research

LOOP RESEARCH NETWORK
Our network increases your article's readership